



A University of Sussex PhD thesis

Available online via Sussex Research Online:

<http://sro.sussex.ac.uk/>

This thesis is protected by copyright which belongs to the author.

This thesis cannot be reproduced or quoted extensively from without first obtaining permission in writing from the Author

The content must not be changed in any way or sold commercially in any format or medium without the formal permission of the Author

When referring to this work, full bibliographic details including the author, title, awarding institution and date of the thesis must be given

Please visit Sussex Research Online for more information and further details

DEVELOPMENT OF PKN2 CHEMICAL PROBES TO ENABLE DRUG DISCOVERY

FIONA SCOTT

Submitted for the degree of Doctor of Philosophy

UNIVERSITY OF SUSSEX

JUNE 2020

I hereby declare that this thesis has not been, and will not be, submitted in whole or in part to another University for the award of any other degree.

X

Acknowledgements

I would first of all like to thank my supervisors, Prof. Simon E. Ward and Prof. Antony Carr for their advice and support throughout this project. Particular thanks must also be expressed to our collaborators at the Structural Genomics Consortium, Dr. Jon Elkins and Dr. Angela Maria Fala and to Mihaela Ficu for her contributions during her MChem degree project. I am grateful to the Genome Damage student development fund for funding this work.

Thanks too, in particular, to Dr. Lewis E. Pennicott for his day-to-day insight and help in the laboratory. I'd also like to thank the other members of lab Ar319 and colleagues at the Sussex Drug Discovery Centre, past and present, for their contributions to this work and for making my time at Sussex an overall pleasant and productive learning environment.

Within Sussex, I'd also like to thank Dr. Iain Day for his support with NMR spectroscopy experiments; Dr Alaa Abdul-Sada for running mass spectrometry experiments; and Verity Holmes for use of the teaching lab's IR spectrophotometer. I'm also grateful for the companionship of Dr. Darren Bellshaw and the friendship of Dr. Sam Furfari and fellow PhD students in the School of Life Sciences – Lucas, Katie, Ryan, Tori, James, Thalia and Rebecca, to name just a few. Thanks also to Dr. Katy Petherick for public engagement opportunities outside of the lab to communicate my enthusiasm for drug discovery to the public. Outside of the campus bubble, I'm grateful to the many friends I made in Brighton, particularly my family away from home at Holland Road Baptist Church for enduring the highs and lows of this PhD with me.

I would not have been able to start this project had it not been for the NHS staff at Whitefriars and Abingdon Surgeries, the Queen Elizabeth University Hospital, and the Cancer Research UK Beatson Institute for their prompt delivery of my treatment for thyroid cancer. Thanks also to the Sussex Cancer Centre and Macmillan Horizon Centre for their ongoing support during my aftercare in Brighton.

To those who also faced cancer before and during this PhD: my late Grandma Rena; Oliver Gill, whose passing prompted me to look into medicinal chemistry courses; Gill Bellshaw, who is now thankfully on the other side of treatment, and Dr. Becky Laidlaw who is sadly no longer with us.

Finally, a huge thank you to my family: mum, dad, Hilary, Irene and Martyn. Thank you for your limitless support during this degree in so many ways I cannot begin to list them. Thank you all.

Abstract

Kinase drug discovery has been a relatively successful endeavour: since the approval of imatinib in 2001, another 51 kinase inhibitors have been approved for treating patients by targeting these signalling proteins when they are implicated in disease. That said, more than 80% of the near 600 human protein kinases lack suitably potent and selective compounds to validate their role in biology.

The limited availability of such compounds is reflected in research output where a lot of the published work on kinases has been done on a relatively small number of targets. This thesis work is part of a collaborative effort with the Structural Genomics Consortium to provide suitable chemical probes for the, so-called, “dark kinome” to find the drug targets of the future. The aim of this PhD project was to develop a suitable chemical probe for a relatively understudied kinase, protein kinase N2 (PKN2). PKN2 is an AGC kinase that has reported roles in cell cycle, adhesion and transport amongst others. It has also been postulated as a target of interest in several cancers, heart failure and inflammation, but currently lacks selective inhibitors to convincingly validate its role in these various diseases.

The European Molecular Biology Laboratory (EMBL) ChEMBL database literature screen has record of 1200 compounds from across the literature with biological activity data against PKN2. Following a triage of the data, three relatively small but potent PKN2 inhibitors were identified (**10**, **11** and **12**). The Structure Activity Relationships of these compounds were explored by synthesis of a chemical library resulting in three series of compounds. The potencies and selectivities of these compounds within the PKN kinase family were evaluated using TR-FRET assay experiments. Selectivity within the wider kinome was investigated using the commercial DiscoverX KINOMEScan® panel containing nearly 500 kinases.

This work showed it is possible to potently and selectively drug PKN2 within the PKN kinase family and the wider kinome. One compound (**187**) shows $K_i = 2.7$ nM *in vitro* potency towards PKN2, 5-fold selectivity for PKN2 over PKN1 and inhibits just 9/400 wild-type kinases in the DiscoverX screen above 70%. This compound was further optimised to yield a compound (**312**) with PKN2 $K_i = 6.7$ nM with 18-fold selectivity over PKN1 – with wider selectivity data pending at time of writing. This is a major step towards delivering a suitable probe for this relatively neglected kinase to validate its potential as a new drug target.

Abbreviations

3D	three dimensional
Ac	acetyl
AcOH	acetic acid
AGC	PKA-, PKG- and PKC-like
Ala	alanine amino acid residue
AML	acute myeloid leukaemia
Ar	non-specific aromatic group
Arg	arginine amino acid residue
Asp	aspartate amino acid residue
ATP	adenosine triphosphate
AurA	aurora A kinase
BCR-ABL	breakpoint cluster region-Abelson murine leukaemia viral oncogene
BET	bromodomain and extra terminal protein
BINAP(±)	2,2'-bis(diphenylphosphino)-1,1'-binaphthyl
Bn	benzyl
Boc	<i>tert</i> -butoxycarbonyl protecting group
BRET	bioluminescence resonance energy transfer
Bu	butyl
CAMK	Ca ²⁺ /calmodulin-dependent protein kinase
cAMP	cyclic adenosine monophosphate
Cas9	caspase 9
Cdc25	cell division cycle 25 phosphatase
CDD	computational drug design
CDI	1,1'-carbonyldiimidazole
CDK2	cyclin dependent kinase 2
CDK7	cyclin-dependent kinase 7
cDNA	complementary DNA
cGMP	cyclic guanosine monophosphate
CHEK2	checkpoint kinase 2
ChEMBL	EMBL chemical database
CIT	Citron Rho-interacting kinase

CK1	casein kinase 1
CMGC	CDK, MAPK, GSK3 and CLK-like kinase
CML	chronic myeloid leukaemia
COSY	correlation spectroscopy
CRISPR	clustered regularly interspaced short palindromic repeats
Da	dalton
dba	dibenzylideneacetone
DCM	dichloromethane
DFG	aspartate-phenylalanine-glycine motif
DIPEA	<i>N,N</i> -diisopropylethylamine
DMAP	4-dimethylaminopyridine
DMF	<i>N,N</i> -dimethylformamide
DMSO	dimethyl sulfoxide
DMSO- <i>d</i> ₆	deuterated DMSO
DNA	deoxyribonucleic acid
dppf	1,1'-ferrocenediyl-bis(diphenylphosphine)
DYRK	dual specificity tyrosine phosphorylation regulated kinase
EDC	<i>N</i> -(3-dimethylaminopropyl)- <i>N</i> '-ethylcarbodiimide
EDC·HCl	<i>N</i> -(3-dimethylaminopropyl)- <i>N</i> '-ethylcarbodiimide hydrochloride
EMBL	European Molecular Biology Laboratory
Eq.	equivalent
ERK	extracellular signal-regulated kinases
Et	Ethyl
EtOH	Ethanol
Eu	Europium
FAK	focal adhesion kinase
FDA	US Food and Drug Agency
FLT3	fms-like tyrosine kinase 3
FRET	fluorescence resonance energy transfer
G-loop	glycine-rich loop
Glu	glutamine amino acid residue
GSK3β	glycogen synthase kinase 3 beta
GTP	guanine triphosphate
H2B	histone 2B

HASPIN	histone H3 associated protein kinase
HATU	hexafluorophosphate azabenzotriazole tetramethyl uronium
HDAC	histone deacetylase
hERG	human Ether-à-go-go-Related Gene
HIPK	homeodomain-interacting protein kinase
HM	hydrophobic motif
HMBC	heteronuclear multiple-bond correlation spectroscopy
HOBt	hydroxybenzotriazole
HRMS	high resolution mass spectrometry
HSQC	heteronuclear single quantum correlation spectroscopy
Hz	hertz
IC ₅₀	half maximal inhibitory constant
<i>i</i> -Pr	<i>isopropyl</i>
IR	infrared spectroscopy
JNK1	c-Jun <i>N</i> -terminal kinases
K_d	dissociation constant
K_i	inhibitory constant
KIT	KIT Proto-Oncogene, Receptor Tyrosine Kinase
L	non-specific ligand
LCMS	liquid chromatography mass spectrometry
Leu	leucine amine acid residue
LIMK1	LIM kinase 1
Lys	lysine amino acid residue
M	molar
m/z	mass:charge ratio
MAPK	mitogen activated kinases
Me	methyl
MEK5	mitogen activated protein kinase
MELK	maternal embryonic leucine zipper kinase
MET	tyrosine-protein kinase Met
MHz	megahertz
MINK1	misshapen-like kinase 1
MM	multiple myeloma
MOE	Molecular Operating Environment software

mRNA	messenger RNA
mTOR	mammalian target of rapamycin
mv	microwave
NanoBRET	Nano bioluminescence resonance energy transfer
NaOH	sodium hydroxide
<i>n</i> -BuLi	<i>n</i> -butyl lithium
nM	nanomolar
NMR	nuclear magnetic resonance
NOESY	nuclear Overhauser effect spectroscopy
<i>n</i> -Pr	<i>n</i> -propyl
NS5B	nonstructural protein 5B
Nu	nucleophile
p38	mitogen-activated protein kinases
PAINs	pan-assay interference compounds
Pak2	p21 (RAC1) Activated Kinase 2
PAK6	p21-activated kinases
PARP	poly-ADP ribose polymerase
Pd	palladium
Pd-118	[1,1'-Bis(di-tert-butylphosphino)ferrocene]dichloropalladium(II)
PDB	protein databank
PDK1	Pyruvate Dehydrogenase Kinase 1
Ph	phenyl
PI3K	phosphoinositide 3-kinase
PI3Ka	Phosphoinositide 3-kinases A
PIF	PDK1 Interacting Fragment
PIM1	Proto-oncogene serine/threonine-protein kinase
PKA	protein kinase A/cAMP-dependent kinase
PKA	protein kinase A
PKB	protein kinase B
PKC	protein kinase C
PKD	protein kinase D
PKG	cGMP-dependent kinase
PKIS	Protein Kinase Inhibitor Set
PKIS2	Expanded Protein Kinase Inhibitor Set

PKN	protein kinase N
PKN1	protein kinase N1
PKN2	protein kinase N2
PKN γ	protein kinase N γ
PLK	polo-like kinase
P-loop	activation loop
PPh ₃	triphenylphosphine
ppm	parts per million
PR	polymerase chain reaction
PRK	PKC-related kinase
PRKCL2	protein kinase C-like kinase 2
PRO2042	protein kinase 2042
py	pyridyl
qPCR	quantitative polymerase chain reaction
R	non-specific alkyl group
R ¹ and R ²	non-specific alkyl groups that are different from each other
RIPK2	Receptor-interacting serine/threonine-protein kinase 2.
RNA	ribonucleic acid
RNAi	RNA interference
ROCK1	rho-associated, coiled-coil-containing protein kinase
RSK1	ribosomal S6 kinase
RT	room temperature
S6K	Ribosomal protein S6 kinase beta-1
SAR	structure activity relationship
SCX	strong cation exchange
SDDC	Sussex Drug Discovery Centre
SGC	Structural Genomics Consortium
siRNA	small interfering RNA
S _N 2	type 2 nucleophilic substitution
S _N Ar	nucleophilic aromatic substitution
SRPK1	Serine/arginine-rich protein-specific kinase
STE	<i>Sacharomyces cerevisiae</i> -derived kinase
STK17A	serine threonine kinase 17A
STK7	serine threonine kinase 7

T	temperature
T3P	propylphosphonic acid anhydride
TBD	1,5,7-triazabicyclo[4,4,0]dec-5-ene
<i>t</i> -Bu	<i>tert</i> -butyl
TEA	triethylamine
TFA	trifluoroacetic acid
THF	tetrahydrofuran
THP	tetrahydropyran
TK	tyrosine kinase
TKL	tyrosine kinase-like
TLC	thin layer chromatography
TNBC	triple negative breast cancer
TR-FRET	time resolved fluorescence resonance energy transfer
Tyr	tyrosine amino acid residue
UV	ultraviolet
Val	valine amino acid residue
VEGFR2	vascular endothelial growth factor
δ	NMR chemical shift (ppm)/partial charge
ΔG	change in Gibbs Free Energy
ΔH	change in enthalpy
ΔS	change in entropy
μM	micromolar
σ	standard deviation

Index of Figures

Figure 1.1 Target-based vs. probe-based discovery process sequences ³	1
Figure 1.2 Staurosporine (1) ⁹	2
Figure 1.3 LY294002 (2) ¹²	3
Figure 1.4 Plot of kinase target vs number of PubMed literature search hits ²⁵	4
Figure 1.5 Chemical structures of (+)-JQ-1 and optimised molibresib	5
Figure 1.6 Exemplar conformational changes in a protein induced by phosphorylation ³⁶	6
Figure 1.7 General kinase topology with ATP in the binding site ⁴⁰	7
Figure 1.8 Overview of type I–IV kinase inhibitor classes ¹⁴	8
Figure 1.9 Illustration of ATP (6) binding to a length of peptide representing the hinge region of a kinase <i>via</i> hydrogen bonding interactions (shown in red) and vacant hydrophobic regions in the kinase active site outlined ⁴⁰	8
Figure 1.10 Imatinib, the first approved kinase inhibitor (9) ³⁶	8
Figure 1.11 Location of PKN2 and related PKN kinases within the human kinome phylogenetic tree highlighted in red. Illustration reproduced courtesy of Cell Signalling Technology, Inc. ⁵³ ..	10
Figure 1.12 A) AGC kinase family within the human kinome; B) evolution tree within the AGC kinase family. PLK and Aurora pseudo-kinases appear in grey ⁴¹	10
Figure 1.13 PRK2 with some annotated structural features (4CRS) ⁶³	11
Figure 1.14 Compounds 10, 11 and 12 selected from the ChEMBL screen ^{103–106}	17
Figure 2.1 Original compound for series A ¹⁰⁹	18
Figure 2.2 Chemical structure of benzimidazole-containing FDA-approved kinase inhibitors ⁴⁶ ..	18
Figure 2.3 ATP (6) structure	19
Figure 2.4 Analogues of 10 by varying pyridyl function	23
Figure 2.5 Excerpt of ¹ H NMR spectrum of compound 56	25
Figure 2.6 ¹ H NMR spectra of compounds 60 and 67 with peaks corresponding to methyl groups circled in blue	28
Figure 2.7 Structures of a selection of benzimidazole analogues prepared that lack an amide ..	30
Figure 2.8 Summary of Series A compounds synthesised	33
Figure 2.9 Overview of TR-FRET experiment	34
Figure 2.10 Labelled X-Ray Crystal Structure of PKN2 (PDB code 4CRS)	36
Figure 2.11 Benzimidazole ligand interacting with the hinge region of CK1GS (PDB code 4HGS);	36

Figure 2.12 Benzimidazole ligand interacting with the hinge region of PIM1 (PDB code 5KGD);	37
Figure 2.13 Benzimidazole ligand interacting with the hinge region of PKA-S6K1 complex (PDB code 4C35)	37
Figure 2.14 PKN2 hinge region interacting with docked 4-pyridyl nitrogen of 1	38
Figure 2.15 Compound 10 docked into PKN2 using MOE software	38
Figure 2.16 SAR summary for Series A based on compound 10	39
Figure 3.1 Original compound for series B.....	40
Figure 3.2 Sunitinib (97)	40
Figure 3.3 Structures of compounds 11, 114 and 115 with selected ¹ H NMR chemical shift values highlighted in ppm	44
Figure 3.4 Alkylated analogues 120–125 prepared in Series B library	45
Figure 3.5 Summary of SAR explored around compound 11.....	48
Figure 3.6 Overview of TR-FRET LanthaScreen™ Eu Kinase Binding Assay ¹⁴⁰	51
Figure 3.7 Bar graph of SelectScreen kinase panel targets against % inhibition for compound 114 assayed at 1 μM	52
Figure 3.8 Bar graph of SelectScreen kinase panel targets against % inhibition for compound 121 assayed at 1 μM	52
Figure 3.9 Overview of KINOMEscan® Competitive Binding Assay using DNA-tagged Kinases ¹⁴²	53
Figure 3.10 Labelled phylogenetic kinome trees highlighting the remaining % of immobilised ligand on each kinase for compounds 11 (left) and 120 (right) assayed at 1 μM in KINOMEscan® experiment. Kinase sub-family classifications are colour coded.	54
Figure 3.11 Bar graph showing where PKN2 sits in the top 24 kinases inhibited by compound 11 in the DiscoverX KINOMEscan® experiment assayed at 1 μM.....	55
Figure 3.12 7 Bar graph showing where PKN2 sits in the top 24 kinases inhibited by compound 120 in the DiscoverX KINOMEscan® experiment assayed at 1 μM.....	56
Figure 3.13 Crystal structure of compound 11 in CDK7 (PDB code 4F9B). Image prepared using Schrodinger Maestro (v 2020.1). PKN2 hinge in yellow, N-domain in blue.....	57
Figure 3.14 Series B analogue compounds successfully docked into PKN2	57
Figure 3.15 PKN2 hinge region interacting with lactam of compound 111.....	58
Figure 3.16 Distribution of binding modes in cross docking experiment with compound 11....	59
Figure 3.17 Distribution of binding modes in cross docking experiment with compound 120..	59
Figure 3.18 SAR explored around compound 11. *Indicates loss of both amide N-H and pyrrole N-H results in loss of activity, but this is not the case in the absence of one or other	60

Figure 4.1 Labelled structure of compound 12 ^{103,106}	61
Figure 4.2 Quinazoline- and quinoxaline-containing FDA approved inhibitors ⁴⁶	62
Figure 4.3 Quinoline- and isoquinoline-containing FDA approved kinase inhibitors	63
Figure 4.4 Observed ¹ H chemical shifts of aromatic protons in pyridine (160), ¹²⁷ 152 and 156	65
Figure 4.5 Exemplar ¹ H NMR showing the change in relative chemical shift and integration of aromatic peaks between intermediates 152 (left) and 156 (right)	66
Figure 4.6 Predicted structure (172) after reaction of lactone 166 with ammonia (left), actual structure of 167 (right) with molecular weights listed	69
Figure 4.7 ¹ H NMR of lactam 167 highlighting ABq peaks indicating degree of saturation in product.....	70
Figure 4.8 Series 1 compounds synthesised with 2,7-naphthyridine core	75
Figure 4.9 Quinazoline-containing intermediates and yields	76
Figure 4.10 Zoomed portion of NOESY NMR spectrum for compound 202 highlighting correlation between methylamine proton (H ^A) and 9-C proton (H ^E) in red	77
Figure 4.11 Aromatic region of ¹ H NMR spectra for compounds 12 and 220. Correlation from COSY NMR shown with coloured lines.....	79
Figure 4.12 Chloroisoquinoline intermediates 228–232 prepared via S _N Ar transformation.....	80
Figure 4.13 Zoomed portion of NOESY NMR spectrum for compound 232 highlighting correlation between methylamine proton (H ^B) and 9-C proton (H ^A) in red	80
Figure 4.14 Comparison of relative literature 1-position and 3-position ¹³ C NMR shift values for protons in quinazoline (247), isoquinoline (248) and quinoline (249) ¹⁵⁶	83
Figure 4.15 Comparison of aromatic regions of ¹ H NMR spectra for compounds 12, 220, 233 and 245	84
Figure 4.16 3'-Pyridyl analogues of compounds 220 and 222	85
Figure 4.17 Piperidine-, piperazine- and morpholine-containing analogues 262–265 with yields for S _N Ar, Suzuki (and for 264, Boc—deprotection) steps, respectively	86
Figure 4.18 Compounds 266 and 267, with reported yields for S _N Ar and Suzuki steps, respectively	87
Figure 4.19 Quinazoline and pyrimidine core match pairs	89
Figure 4.20 Comparison of aromatic region of ¹ H NMR spectra for compounds 12 and 287	90
Figure 4.21 Structures of 2,6-naphthyridine analogues with electron-withdrawing modifications with yields for S _N Ar and Suzuki steps, respectively	91
Figure 4.22 <i>N</i> -substituted analogues of 290 with yields for S _N Ar and Suzuki steps, respectively	92

Figure 4.23 Analogues of 290 with additional alkyl groups and yields for S_NAr , Suzuki and Boc-deprotection steps, respectively.....	93
Figure 4.24 Pyrrolidine analogues of 290 with yields for S_NAr , Suzuki and Boc-deprotection steps, respectively.....	94
Figure 4.25 Zoomed aliphatic region of COSY NMR spectrum for compound 312 showing two ring systems (red and blue) and their corresponding protons on structure of 312.	94
Figure 4.26 SAR explored around compound 12	95
Figure 4.27 Kinome selectivity of compound 191 @ 1 μ M.....	108
Figure 4.28 Bar graph showing where PKN2 sits in the top 24 kinases inhibited by compound 191 @ 1 μ M in the DiscoverX KINOMEScan [®] experiment dosed at 1 μ M. PKN2 highlighted in green.	108
Figure 4.29 Kinome selectivity of compound 220 @ 1 μ M	109
Figure 4.30 Kinome selectivity of compound 222 @ 1 μ M.....	109
Figure 4.31 Kinome selectivity of compound 187 @ 1 μ M.....	110
Figure 4.32 Bar graph showing where PKN2 sits in the top 24 kinases inhibited by compound 187 in the DiscoverX KINOMEScan [®] experiment dosed at 1 μ M. PKN2 highlighted in green.	110
Figure 4.33 Compound 314 interacting with hinge region (mint green) of PKC η (PDB code 3TXO). ¹⁶⁰ Figure made with Schrodinger Maestro 19-4.	112
Figure 4.34 Geminal dimethyl analogue of 12	112
Figure 4.35 Compounds successfully docked via one binding constraint	113
Figure 4.36 PKN2 hinge region (yellow) with compounds 2, 315–317 stacked. Figure made with Schrodinger Maestro 19-4.	113
Figure 4.37 Overlay of compound 318 in PKN2 from single and zero constricted experiments interacting with hinge (lime green) of PKN2. Figure made with Schrodinger Maestro 19-4. ...	114
Figure 4.38 Distribution of binding modes in cross-docking experiment with compound 191	115
Figure 4.39 Distribution of binding modes in cross docking experiment with compound 220	115
Figure 4.40 Distribution of binding modes in cross docking experiment with compound 222	116
Figure 4.41 Distribution of binding modes in cross docking experiment with compound 187	116
Figure 4.42 Crystal structure of PKN2 co-crystallised with compound 187 with zoomed section on binding site showing key interactions with residues. Figure produced by Angela Fala using MOE.	117
Figure 4.43 Alignment of PKN2 crystal structures with ATP γ S and compound 187 bound and zoomed sections of individual binding sites and key residues highlighted. Figure produced by Angela Fala using MOE.....	118

Figure 4.44 Compounds 264, 275 and 312's SAR can be rationalised with the crystal structure of 187 in PKN2.....	119
Figure 4.45 SAR summary regarding compound 12	119
Figure 4.46 Optimisation of compound 12 to compound 312	120
Figure 5.1 Compounds 10, 11 and 12 selected from the ChEMBL screen with reported potencies and selectivities ^{103–106}	121

Index of Schemes

Scheme 1.1 Mechanism of serine phosphorylation event	6
Scheme 1.2 Representation of the two-stage mechanism of activation of PKN2 ⁴¹	12
Scheme 2.1 CDI amide coupling conditions to 17 ¹¹⁶	19
Scheme 2.2 CDI amide coupling mechanism ¹¹⁷	20
Scheme 2.3 Nitro-reduction conditions using sodium dithionite ¹¹⁸	20
Scheme 2.4 The conversion of 22 to 25 ^{104,120}	21
Scheme 2.5 General HATU coupling mechanism ¹¹⁷	21
Scheme 2.6 Acid-catalysed cyclisation conditions to form benzimidazole 10 ¹⁰⁴	22
Scheme 2.7 Proposed mechanism for the acid-catalysed cyclisation of 25 to benzimidazole 10	22
Scheme 2.8 Analogues of 10 that could not be prepared thought due to possible hydrogen bonding interactions (in red)	24
Scheme 2.9 Failed preparation of analogues 47, 50 and 53 due to unprotected amines (highlighted in blue) ¹²⁰	24
Scheme 2.10 Synthesis to benzimidazole 56 from commercially available <i>O</i> -phenylenediamine (54) ^{104,120}	25
Scheme 2.11 Synthesis summary of methylated analogues 60 and 63 by usual chemistry procedures ^{104,116,118,120}	26
Scheme 2.12 Synthetic scheme to dimethylated analogue 67 ^{104,120,123}	26
Scheme 2.13 T3P-facilitated amide coupling mechanism ¹²⁴	27
Scheme 2.14 TBD-facilitated amide coupling general mechanism ¹²⁵	28
Scheme 2.15 Unsuccessful attempts at producing benzimidazole 78 from benzimidazole 77..	29
Scheme 2.16 Synthesis to 78 from 4-amino-3-nitrobenzamide	29
Scheme 2.17 Unsuccessful attempts of preparing 4-amino analogue of 10 ¹¹⁸	30
Scheme 2.18 Synthesis of Br-containing analogue 92 ^{104,116,118,126}	31
Scheme 2.19 <i>N</i> -Alkylation attempts to benzimidazole 93 ¹²⁸	32
Scheme 3.1 Synthesis to 11	41
Scheme 3.2 Mechanism for addition condensation step to form compound 11	41
Scheme 3.3 Preparations of pyridyl analogues of 11	43
Scheme 3.4 Syntheses to compounds 114 and 115	44
Scheme 3.5 Boc deprotection mechanism ¹¹⁷	44
Scheme 3.6 Synthesis to compounds 120-125	45

Scheme 3.7 Alkylation conditions used to synthesise compounds 126 and 127 ¹³⁸	46
Scheme 3.8 Alkylation mechanism involving sodium hydride and alkyl halides	46
Scheme 3.9 Attempts to alkylate the lactam N-H of 125 ¹³⁸	47
Scheme 3.10 Chemistry used to incorporate an additional aromatic group at the 6-position ^{105,139}	48
Scheme 4.1 Amide coupling conditions to form 152 ¹⁰⁶	63
Scheme 4.2 Proposed mechanism for amide coupling under ethyl chloroformate conditions to compound 152	64
Scheme 4.3 Methylation conditions for preparation of intermediate 156 ¹⁰⁶	64
Scheme 4.4 Proposed mechanism for methylation step to 156	64
Scheme 4.5 Acylation of 156 to form ketone 162 ¹⁰⁶	66
Scheme 4.6 Proposed mechanism for acylation step to form 162	67
Scheme 4.7 Cyclisation conditions to form lactone 166 ¹⁰⁶	67
Scheme 4.8 Conditions for converting lactone 162 to lactam 166 ¹⁰⁶	68
Scheme 4.9 Proposed mechanism for the conversion of lactone 166 to lactam 167	69
Scheme 4.10 Conditions for bromination/chlorination of lactam 167 ¹⁰⁶	70
Scheme 4.11 Proposed mechanism of chlorination by POBr ₃ /POCl ₃ to form 181	70
Scheme 4.12 Conditions for S _N Ar to prepare penultimate intermediate 183 ¹⁰⁶	71
Scheme 4.13 Proposed mechanism for S _N Ar transformation to form 183	71
Scheme 4.14 De-protection conditions to prepare compound 12 ¹⁰⁶	72
Scheme 4.15 General scheme for initial analogue synthesis for series 1	72
Scheme 4.16 Preparation of compound 187 from 174 ¹⁰⁶	73
Scheme 4.17 Conditions for S _N Ar involving chloride 174 and piperidine (188) to make compound 189 ¹⁰⁶	73
Scheme 4.18 S _N Ar and reductive amination conditions attempted to form 191 and 192 respectively ^{106,149}	74
Scheme 4.19 S _N Ar conditions to prepare 193 ¹⁰⁶	74
Scheme 4.20 General synthetic route to quinazoline analogues ^{150,151}	75
Scheme 4.21 Resonance structures with nucleophilic attack mechanistic pathways proposed for the 1-chlorine (red/pink) and 3-chlorine (blue)	76
Scheme 4.22 General mechanism for a Suzuki coupling ¹⁵⁴	77
Scheme 4.23 Final quinazoline match pairs with yields for Suzuki and Boc-deprotection steps	78
Scheme 4.24 Synthetic route to isoquinoline analogues ^{151,155}	79
Scheme 4.25 Isoquinoline analogues with yields for Suzuki and Boc-deprotection steps	82
Scheme 4.26 Attempted and optimised synthetic routes to compound 108	82

Scheme 4.27 Mechanism for Buchwald-Hartwig Amination ¹⁵⁸	83
Scheme 4.28 Attempted syntheses of 272 and 275	87
Scheme 4.29 Attempted synthesis to 279	88
Scheme 4.30 Syntheses to 281 and 283	88
Scheme 4.31 Synthetic route for preparing 2,6-naphthyridine analogues	90
Scheme 5.1 Attempted optimisation of compound 10	122
Scheme 5.2 Attempted optimisation of compound 11	122
Scheme 5.3 Optimisation of compound 12 to yield compounds 187 and 312.....	123

Index of Tables

Table 2.1 Summary of reaction conditions attempted to make amide 25 ^{104,120}	21
Table 2.2 Summary of Suzuki conditions attempted on bromine-containing intermediates	31
Table 2.3. Structure activity relationships for benzimidazoles binding to PKN2 and PKN1. Calculated K_i values for PKN2 and PKN1 are shown in μM . The assay Z' factor was $0.7 < Z' < 0.9$; $n = 2$	34
Table 3.1 TR-FRET bioanalysis of series B compounds for PKN2 and PKN1 with calculated K_i nM potency; Z value $> 0.70 < 0.90$; $n = 2$	49
Table 4.1 Suzuki optimisation summary with most successful conditions highlighted in green	81
Table 4.2 Structure activity relationships for 2,7-naphthyridine-containing compounds binding to PKN2 and PKN1. Calculated K_i values for PKN2 and PKN1 are shown in nM. The assay Z' factor was $0.7 < Z' < 0.9$; $n = 2$	96
Table 4.3 Structure activity relationships for ethylene diamine-containing compounds binding to PKN2 and PKN1. Calculated K_i values for PKN2 and PKN1 are shown in nM. The assay Z' factor was $0.7 < Z' < 0.9$; $n = 2$	97
Table 4.4 Structure activity relationships for piperazine-containing compounds binding to PKN2 and PKN1. Calculated K_i values for PKN2 and PKN1 are shown in nM. The assay Z' factor was $0.7 < Z' < 0.9$; $n = 2$	98
Table 4.5 Structure activity relationships for pyridyl-containing compounds binding to PKN2 and PKN1. Measured IC_{50} values and corresponding calculated K_i values for PKN2 and PKN1 are shown in nM. The assay Z' factor was $0.7 < Z' < 0.9$; $n = 2$	99
Table 4.6 Structure activity relationships for a selection of series C compounds binding to PKN2 and PKN1. Calculated K_i values for PKN2 and PKN1 are shown in nM. The assay Z' factor was $0.7 < Z' < 0.9$; $n = 2$	100
Table 4.7 Structure activity relationships for quinazoline compounds binding to PKN2 and PKN1. Calculated K_i values for PKN2 and PKN1 are shown in nM. The assay Z' factor was $0.7 < Z'$ < 0.9 ; $n = 2$	101
Table 4.8 Structure activity relationships for quinazoline- and pyrimidine-containing compounds binding to PKN2 and PKN1. Calculated K_i values for PKN2 and PKN1 are shown in nM. The assay Z' factor was $0.7 < Z' < 0.9$; $n = 2$	102
Table 4.9 Structure activity relationships for isoquinoline- and quinoline-containing compounds binding to PKN2 and PKN1. Calculated K_i values for PKN2 and PKN1 are shown in nM. The assay Z' factor was $0.7 < Z' < 0.9$; $n = 2$	102

Table 4.10 Structure activity relationships for <i>N</i> -alkylated compounds binding to PKN2 and PKN1. Calculated K_i values for PKN2 and PKN1 are shown in nM. The assay Z' factor was $0.7 < Z' < 0.9$; $n = 2$	103
Table 4.11 Structure activity relationships for 2,6-naphthyridine-containing compounds binding to PKN2 and PKN1. Calculated K_i values for PKN2 and PKN1 are shown in nM. The assay Z' factor was $0.7 < Z' < 0.9$; $n = 2$	104
Table 4.12 Structure activity relationships for 2,6-naphthyridine-containing compounds binding to PKN2 and PKN1. Calculated K_i values for PKN2 and PKN1 are shown in nM. The assay Z' factor was $0.7 < Z' < 0.9$; $n = 2$	105
Table 4.13 Structure activity relationships for 2,6-naphthyridine-containing compounds binding to PKN2 and PKN1. Calculated K_i values for PKN2 and PKN1 are shown in nM. The assay Z' factor was $0.7 < Z' < 0.9$; $n = 2$	107

Table of Contents

Chapter 1 Introduction	1
1.1 Chemical Probes.....	1
1.2 Kinase Drug Discovery.....	5
1.3 Structural Features of Protein Kinase N 2.....	9
1.4 Functional Roles of PKN2	13
1.4.1 Physiological Roles of PKN2	13
1.4.2 Pathological Roles of PKN2	15
1.5 Project Aims	16
Chapter 2 Series A – Benzimidazoles	18
2.1 Hit Origin	18
2.2 Chemistry	19
2.2.1 Synthesis of original hit.....	19
2.2.2 Preparation of analogues.....	23
2.3 Biological evaluation	33
2.3.1 TR-FRET	33
2.4 Computational Studies.....	36
2.4.1 Benzimidazole kinase ligands in the Protein Data Bank	36
2.4.2 Docking Experiments	37
2.5 Chapter 2 Summary	39
Chapter 3 Series B – Pyrrolopyridinone	40
3.1 Hit Origin	40
3.2 Chemistry	41
3.2.1 Synthesis of original hit.....	41
3.2.2 Preparation of analogues.....	42
3.3 Biological evaluation	49
3.3.1 TR-FRET	49
3.3.2 Kinome Selectivity Evaluation.....	51
3.4 Computational chemistry.....	56
3.4.1 Pyrrole-containing ligands in the Protein Data Bank	56
3.4.2 Docking Experiments	57
3.5 Chapter 3 Summary	59

Chapter 4 Series C – Naphthyridines, Quinazolines and Isoquinolines	61
4.1 Hit Origin	61
4.2 Chemistry	63
4.2.1 Synthesis of original hit.....	63
4.2.2 Preparation of analogues	72
4.3 Biological evaluation	96
4.3.1 TR-FRET	96
4.3.2 Kinome Selectivity Evaluation.....	107
4.4 Computational chemistry.....	111
4.4.1 Similar ligands in the Protein Data Bank.....	111
4.4.2 Docking Experiments	112
4.5 Crystallography	117
4.6 Chapter 4 Summary	119
Chapter 5 Conclusions and Future Work	121
Chapter 6 Experimental Methods.....	124
6.1 Chemistry	124
6.1.1 Preparation of compounds described in Chapter 2	125
6.1.2 Preparation of compounds described in Chapter 3	162
6.1.3 Preparation of compounds described in Chapter 4.....	178
6.2 Biology.....	307
6.2.1 Cloning, protein expression and purification.....	307
6.2.2 Binding Displacement Assay	308
Chapter 7 Bibliography	310
Appendices.....	324
Appendix 1 DiscoverX Panel Results.....	324
Appendix 2 Crystal structures used in X-Docking Studies.....	356

Chapter 1 Introduction

1.1 Chemical Probes

Chemical probes, also known as chemical tools, are selective small molecules designed to enable scientists to solve mechanistic biological questions. Drug molecules, on the other hand, are designed with the aim of producing a desired clinical response.¹ Chemical probes thus need not possess all of the desirable physiochemical properties of a drug candidate (e.g. off-target hERG inhibition, bioavailability and metabolic stability)² but often make excellent starting points for drug discovery programmes to facilitate the elucidation and validation of disease pathways.

Chemical probes are designed to modulate the function of a protein, nucleic acid or other biomolecule. They are used in combination with genetic approaches such as small interfering RNAs (siRNA) and CRISPR-Cas9 methods to validate that the intended change in the biochemical pathway elicits a particular biological response e.g. inhibition of a particular protein halts proliferation of a specific cancer cell line.³

A good quality probe enables the further understanding of both physiological and pathological pathways. They can also enable drug discovery programmes because probes can confirm whether a potential drug target is involved in disease or not and can be used to set up assay experiments.

The general characteristics of a good quality chemical probe have been summarised in multiple reviews^{1–3} which suggest using the following guiding parameters: a suitable probe must have less than 100 nM *in vitro* potency at the target protein; have at least 30-fold selectivity over sequence related proteins of the same target family; be profiled against an “industry standard” panel of pharmacologically relevant off-target proteins; and less than 1 μ M *in cellular* potency. They also suggest a complementary inactive analogue that can be used as a negative control compound.⁴

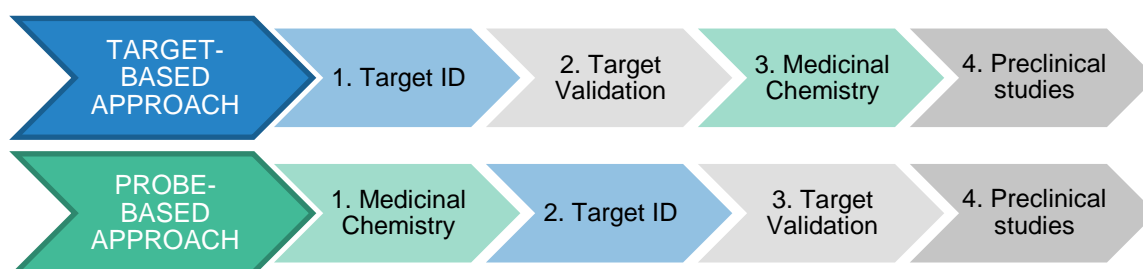


Figure 1.1 Target-based vs. probe-based discovery process sequences³

The conventional series of events in a drug discovery programme involve identifying a drug target and validating that target with biogenetic techniques before carrying out iterative rounds of medicinal chemistry to optimise a candidate before pre-clinical studies (Figure 1.1). This can be referred to as “target-based discovery”.

This sequence of processes outlined in the top schematic in Figure 1.1 can be reordered to form a so-called “probe-based discovery” strategy, whereby the bulk of the medicinal chemistry happens first. Once a suitably selective and potent probe is made, it can be used in combination with biogenetic techniques to facilitate target identification and validation before entering preclinical studies.

Genetic tools such as RNA interference (RNAi)^{5,6} have transformed how we modify genes and the protein functions they code for. While useful techniques, they have some disadvantages compared to small molecule inhibitors. For example, generation of knockdown cell lines is generally a time consuming process. The removal of one gene can sometimes cause another gene to upregulate and mask the effect of the initial gene knockdown. Sometimes it is not possible to achieve full gene knockdown e.g. when using conditional genetic techniques. The delivery of nucleic acids into cells can also be more challenging than dosing with small molecules in solution. Off-target effects, known as the “interferon response” can occur due to the cell detecting the presence of certain nucleic acids.

Additionally, changes in transcription levels of messenger RNA (mRNA) do not always correlate with the amount of expressed protein in a cell⁷ and removing a protein altogether is not always equivalent to inhibiting one with a small molecule. When dealing with multifunctional proteins, certain ligands may only modulate a portion of that protein and inhibit one of multiple functions, whereas RNAi-facilitated gene silencing removes the entire protein which is different to pharmacological intervention *via* an inhibitor compound.⁸ Having a biochemical technique to complement siRNA-based validation techniques can save time and resources in the long-term when seeking drug candidates of the future.

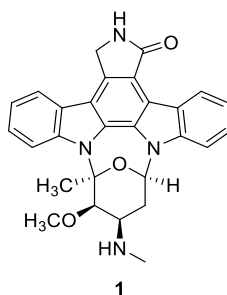
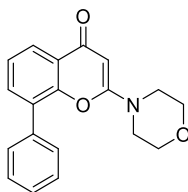


Figure 1.2 Staurosporine (1)⁹

Probes should be of high selectivity and potency as the use of low-quality probes can lead to misleading conclusions. For example, staurosporine (**1**) (Figure 1.2) is a natural product derived from bacteria¹⁰ that, while initially reported as a selective protein kinase C (PKC) inhibitor, has proven to be a pan-kinase inhibitor so it not useful for defining pathways involving more than one kinase.¹¹ That said, promiscuous probes like staurosporine are still used incorrectly in tens of thousands of studies¹ to explore specific mechanistic questions, although its use as a control compound remains appropriate when comparing it with other kinase inhibitors.



2

Figure 1.3 LY294002 (**2**)¹²

Similarly, LY294002 (**2**) (Figure 1.3) was described as a selective phosphoinositide 3-kinase (PI3K) inhibitor in 1994¹² which was later disproven¹³ and, whilst better PI3K inhibitors have since been synthesised and characterised,¹⁴ the compound still features in over 1200 publications from the last five years alone according to a PubMed search for “LY294002 and PI3 kinase” in March 2020.¹⁵

Selectivity is not the defining characteristic of a poor chemical probe. Other features such as the appearance of chemically reactive motifs (e.g. acrylates and multiple halides) or molecular fragments known as pan-assay interference compounds (PAINS)¹⁶. These can give rise to false positives across common biochemical assays can be missed by researchers who do not have a background in chemistry or a research group that lacks the input of a synthetic or medicinal chemist.¹⁻³

The reasons why low quality probes continue to be used can be put down to any number of factors, from commercial vendors choosing to omit up to date information about their products in their catalogues and websites to unsuspecting clients; to a lack of chemistry support within a research team who might otherwise spot issues with a probe.¹

Resources such as the Protein Kinase Inhibitor Sets (PKIS/PKIS2)^{17,18}, Chemical Probes Portal¹⁹ and Structural Genomics Consortium Probes Database⁴ have been created as peer-reviewed information deposits in order to combat the wave of poor quality probe use in academia. Various review articles¹⁻³ have been written specifically warning against the use of deficient probes.

The authors' motives behind these articles were to ensure time and resources are not wasted in progressing drug discovery projects that may ultimately fail if the underlying biology is not sufficiently well understood. Drug discovery projects developed in academic labs frequently fail when they reach *in vivo* studies²⁰ because the move from a relatively simple *in vitro* model to a more complex *in vivo* model often reveals a lack of selectivity for a given compound.^{1–3,21–23}

If high quality tools are available, research into the proteins they target is more likely to be carried out, and thus the development of new chemical tools is vital in drug discovery research.^{1,24} Figure 1.4 plots the number of PubMed²⁵ literature search hits found in April 2019 for over 500 human protein kinases. The skewed results show that a lot of published work is carried out on a very small number of kinases. This is likely due to there being more information available about the pathways that small number of kinases are involved in and an unavailability of reagents (e.g. inhibitors, genetic tools, modified cell lines) for the majority of those kinases.

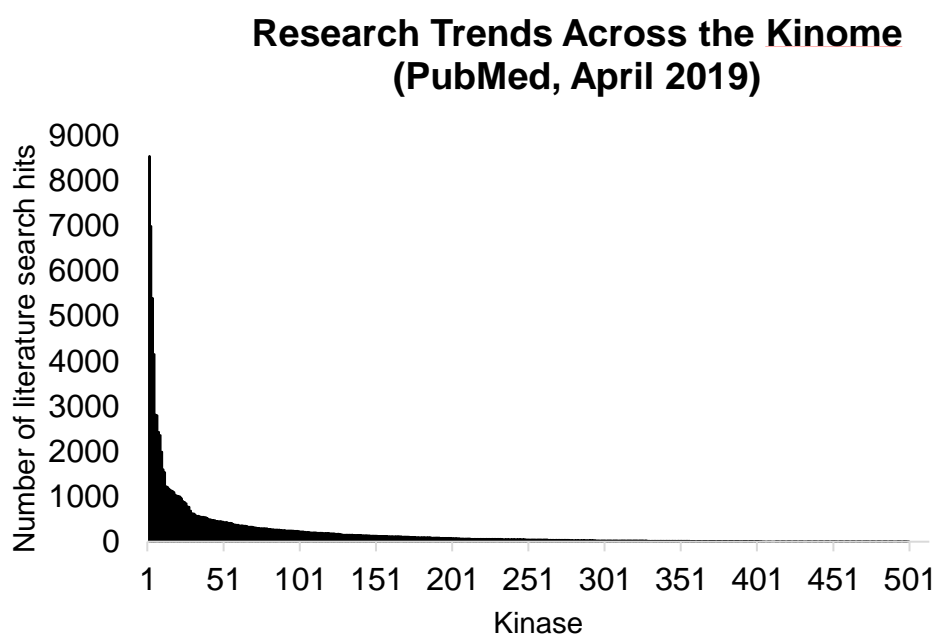


Figure 1.4 Plot of kinase target vs number of PubMed literature search hits²⁵

An example of a high impact probe is the bromodomain extra terminal motif (BET) inhibitor (+)-JQ-1 (**3**) (Figure 1.5). A collaboration between James E. Bradner of Harvard and the Structural Genomics Consortium's University of Oxford team began in January 2010 and resulted in the development of compound **3** which was published in *Nature* in December of that same year, as it was recognised as a first-in-class selective BET inhibitor.²⁶

Following this publication, compound **3** was distributed to over 100 laboratories who requested use of the compound and in 2011 alone, links were established between this bromodomain and

acute myeloid leukaemia (AML)²⁷ and multiple myeloma²⁸ (MM) cancers. A slightly modified version of this compound, molibresib (**4**) (Figure 1.5), then entered first-in-human studies in 2012.²⁹ This series of events covered just over two years from lab to patient which shows the potential power good chemical probes can have in accelerating the drug discovery process. Usually this process can take several years.

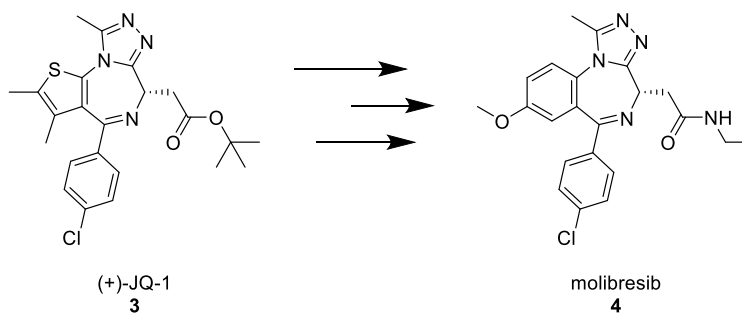


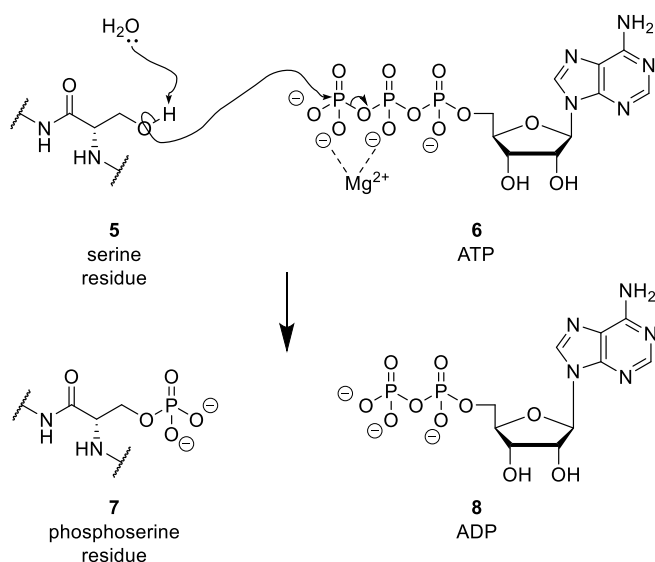
Figure 1.5 Chemical structures of (+)-JQ-1 and optimised molibresib

Other examples of high quality probes that catalysed research areas in the past include the mTOR allosteric inhibitor, rapamycin;¹ liver X receptor- α/β agonist, GW683965;³⁰ GNF-5, an allosteric inhibitor of kinase breakpoint cluster region-Abelson murine leukaemia viral oncogene (BCR-ABL);³¹ and BET bromodomain inhibitors I-BET and PFI-1.²³

1.2 Kinase Drug Discovery

Achieving selectivity across the 518 known human protein kinases³² continues to present a significant challenge to drug discovery scientists working on projects involving these cell signalling proteins.³³ At present, less than 20% of the human kinome is believed to have been investigated with small molecule inhibitors (Figure 1.4) and an even smaller fraction of those compounds meet the previously described criteria⁴ for being used as chemical probes.³⁴

Protein kinases facilitate the transfer of a phosphate group from adenosine triphosphate (ATP) (**6**) to a specific hydroxyl-containing amino acid residue (serine (**5**)/threonine/tyrosine) in a target protein substrate. Scheme 1.1 outlines a general mechanism for this catalytic biotransformation.³⁵



Scheme 1.1 Mechanism of serine phosphorylation event

The addition of a negatively charged phosphate to a protein often induces a conformational change in the shape of the protein³⁶ which can activate or deactivate that protein's function (Figure 1.6). Protein kinases are thus involved in many signalling pathways, as are phosphatase enzymes which carry out the reverse process of dephosphorylation.³⁵ The protein kinases can in general be divided into those that phosphorylate serine or threonine residues, and those that phosphorylate tyrosine residues, along with a small number of dual-specificity kinases as well as a number of further sub-categories such as histidine and lipid kinases.³⁷

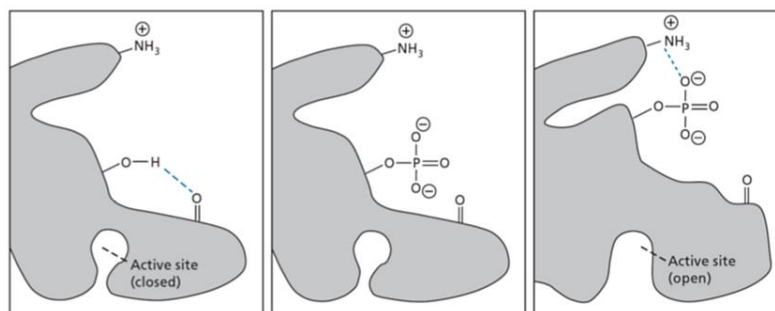


Figure 1.6 Exemplar conformational changes in a protein induced by phosphorylation³⁶

Until the 1950s, casein, phosvitin and a few other related proteins involved in embryonic development were the only known phosphoproteins. Following work on better understanding the action of glycogen phosphorylase, the discovery of *c*-AMP dependent protein kinase (PKA) by Walsh *et al.* in 1968³⁸ gave rise to rapid discovery of many distinct kinase proteins involved in cell signalling processes.³⁹

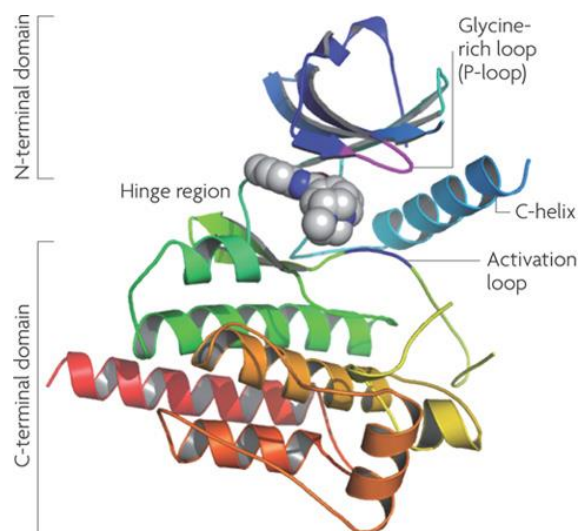


Figure 1.7 General kinase topology with ATP in the binding site⁴⁰

A typical structure of a protein kinase contains several characteristics (Figure 1.7) such as a large C-terminal domain which mainly consists of α -helices and a smaller N-terminal domain which possesses a 5-stranded β -sheet.⁴¹ Between the N- and C-domains lies a cleft which is the site where ATP binds. This binding site is covered by a glycine-rich activation loop (P-loop/G-loop),⁴² a relatively unstructured length of peptide chain that lies outside the active site and distinguishes between serine/threonine and tyrosine residues on protein substrates. The start of the activation loop is marked by the DFG motif, a characteristic trio of aspartate (D), phenylalanine (F) and glycine (G) amino acid residues.³⁷

The aspartate coordinates with a Mg^{2+} ion which holds the β - and γ -phosphates of ATP in place to aid phosphate transfer (Scheme 1.1).^{43,44} The conformation of this loop, and the orientation of the DFG-aspartate residue indicates whether the kinase is in its active (DFG-D_{in}) or inactive (DFG-D_{out}) state and usually converts between the two *via* the phosphorylation/dephosphorylation of one or more residues on this loop.^{43,45,46}

Figure 1.8 outlines the four main sub-types of kinase inhibitor. Type I inhibitors bind to the ATP site of an active (DFG-D_{in}) kinase, while type II inhibitors fit into the ATP site, such that the kinase is in its inactive conformation (DFG-D_{out}). Type III and type IV inhibitors bind allosterically to other regions of the kinase.^{47,48}

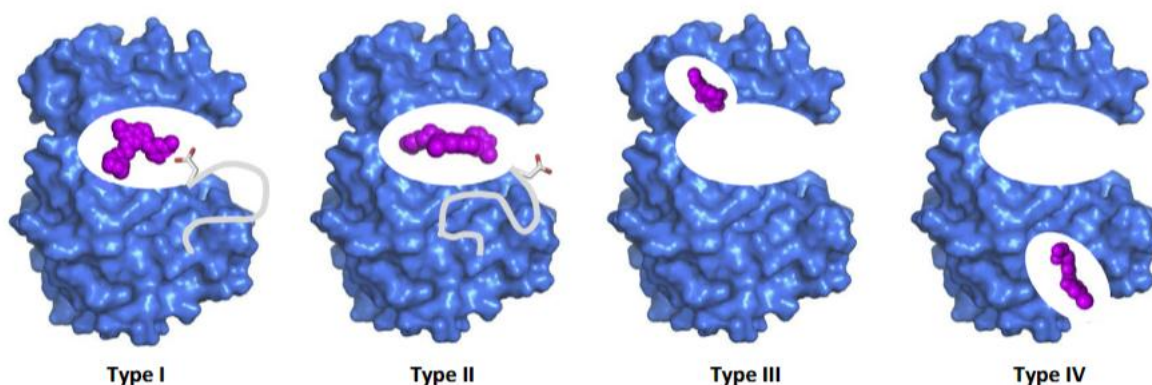


Figure 1.8 Overview of type I-IV kinase inhibitor classes¹⁴

This project involved isosteric inhibitors that target the ATP-site. The precise type I/II inhibition is unknown due to a lack of crystallographic information. Selectivity is harder to achieve with ATP-isosteric inhibitors over allosteric inhibitors because ATP is the common substrate across all kinases, although it is generally thought that it is possible to achieve selective type I/II inhibition by taking advantage of unoccupied hydrophobic spaces within the ATP-binding site (Figure 1.9).⁴⁰

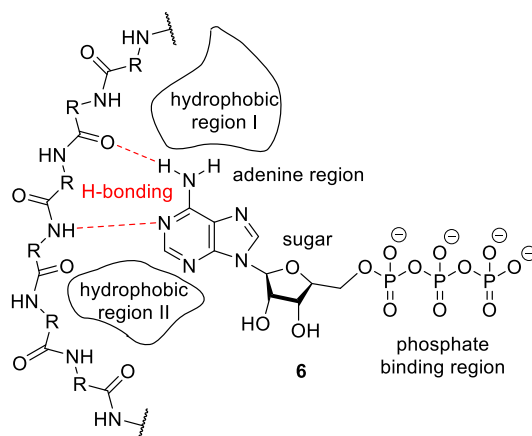


Figure 1.9 Illustration of ATP (6) binding to a length of peptide representing the hinge region of a kinase via hydrogen bonding interactions (shown in red) and vacant hydrophobic regions in the kinase active site outlined⁴⁰

The approval of imatinib (9) (Figure 1.10),⁴⁹ the first FDA-approved kinase inhibitor, in 2001 was a milestone event in kinase drug discovery history. It primarily targets a tyrosine kinase called BCR-ABL which is particularly prevalent in chronic myeloid leukaemia (CML), making it a first-in-class monogenic cancer drug.

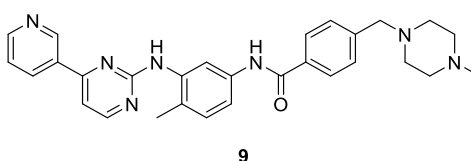


Figure 1.10 Imatinib, the first approved kinase inhibitor (9)³⁶

Since then, a further 51 kinase inhibitors have been approved by the FDA for treating cancers and other autoimmune, cardiovascular, inflammatory and nervous system diseases.⁴⁶ Bringing over fifty drugs to market around a particular drug class in twenty years shows just how fruitful pursuing kinases has been for academic and industrial drug discovery laboratories.

That said, the 52 approved kinase inhibitors do not cover 52 distinct kinases. Only 20 kinases are primarily targeted by these drugs while a further 15–20 targets are currently under investigation in clinical trials.⁴⁶ This constitutes less than 10% of the human kinome which comprises 518 kinases. The reasons for this include well intentioned efforts to bring through second- and third-line treatment options in the event of drug resistance, but also because it is easier to develop marginally improved drugs for established and well-studied targets.⁴⁶ While such admirable efforts give more options to patients with diseases that involve this sub-set of well-studied kinases, there are still many hundreds of kinases with poorly understood roles in both physiological and pathological biology.⁵⁰

It has been estimated that less than 4% of the human genome⁵¹ has suitable tools available for probing the roles of proteins coded for within the genome. Within that, 2% of all coding genes in the human genome are linked to protein kinases.⁵² Less than 20% of those kinases³⁴ have suitably selective and potent inhibitors. Up to a third of drug discovery efforts are carried out on kinase proteins but only a select number of those signalling enzymes. New chemical entities are needed to probe the, so-called, “dark kinome” in order to find processes that can be targeted to treat diseases in the future.^{33,34,46,50}

1.3 Structural Features of Protein Kinase N 2

Protein kinase N 2 (PKN2) (Figure 1.7) is one of the relatively understudied kinases of the so-called “dark kinome”. In the above PubMed literature search from April 2019 (Figure 1.4), only 24 literature hits were found with PKN2 in the title compared to the many thousands of papers published about more readily researched kinases like PKA, BCR-ABL and PI3K kinases.²⁵

PKN2 is an AGC serine/threonine protein kinase (Figure 1.11). Of the 518 known protein kinases in the human kinome (Figure 1.11),³² 61 protein kinases and 2 pseudo-kinases are classified as AGC kinases. The term “AGC” arises from the similarity in structure between the *c*-AMP-dependent kinase, (PKA), the *c*-GMP-dependent kinase (PKG) and the protein kinase C (PKC) families.

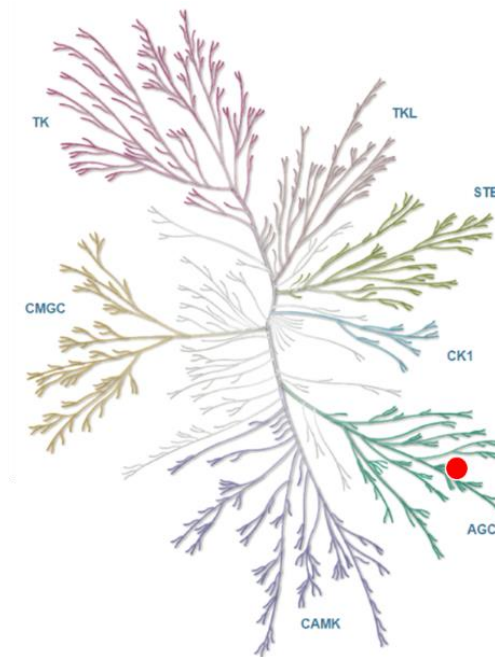


Figure 1.11 Location of PKN2 and related PKN kinases within the human kinome phylogenetic tree highlighted in red. Illustration reproduced courtesy of Cell Signalling Technology, Inc.⁵³

PKN2 falls into the PKN/PRK sub-family (Figure 1.12), closely related to the PKC sub-family, and is one of three homologues (PKN1/2/3).⁵⁴ It has a number of pseudonyms: Protein-Kinase C-Related Kinase 2 (PRK2), Protein Kinase C-like 2 (PRKCL2), Cardiolipin-Activated Protein Kinase, PRO2042, STK7, PAK2.⁵⁵

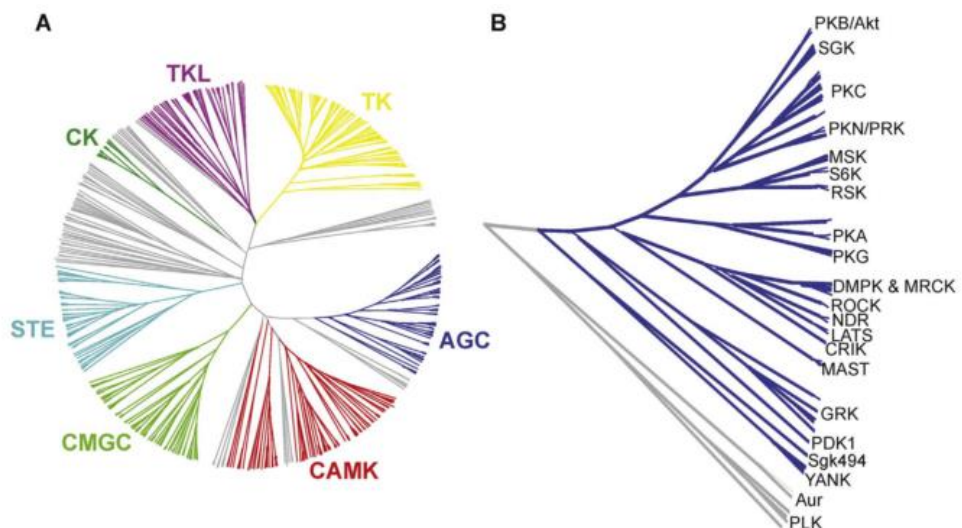


Figure 1.12 A) AGC kinase family within the human kinome; B) evolution tree within the AGC kinase family. PLK and Aurora pseudo-kinases appear in grey⁴¹

In 1994 Palmer *et al.*⁵⁶ carried out a polymerase chain reaction (PCR) based screening of two complementary deoxyribonucleic acid (cDNA) libraries derived from human monoblastoid U937 cells which led to the discovery of PKN2. Redundant oligonucleotide primers that correspond to the catalytic domain of PKC (a highly conserved region across AGC kinases) were used to identify the protein. Mukai *et al.*⁵⁷ also isolated PKN cDNA from a human hippocampal cDNA library in the same year. Following this a number of groups have isolated and sequenced PKN2 and its other isoforms.^{58,59}

PKN2's catalytic domain shares 87% sequence similarity with PKN1, 70% with PKN3⁶⁰ and 50% with PKC⁶¹ kinases. There is less chain similarity in the *N*-terminal regions (48% between PKN1/2 and 40% between PKN2/3). Other AGC kinases, e.g. the ROCK sub-family possess a 34% similarity in chain sequence to PKN2.⁶⁰

PKN1 is the most studied of the three PKN kinases. In the protein data base (PDB) there are six crystal structures of PKN1 domains available (4OTD, 4OTG, 4OTH, 4OTI, 2RMK, 4NKG) with different ligands bound. Meanwhile, there is only one structure of the PKN2 kinase domain bound to ATP γ S (4CRS) (Figure 1.13) and none available of PKN3. PKN3 is less well understood and it is found in fewer tissues than PKN1 and PKN2.⁶²

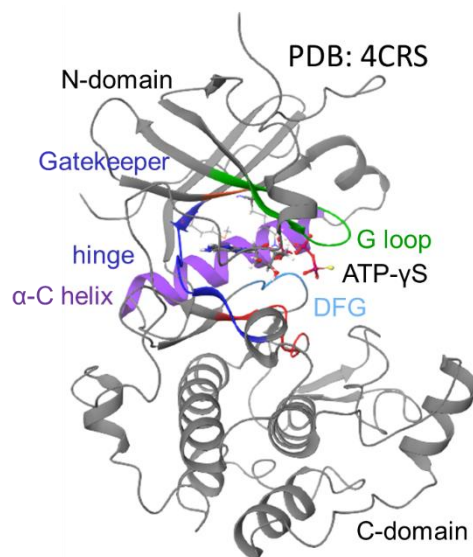


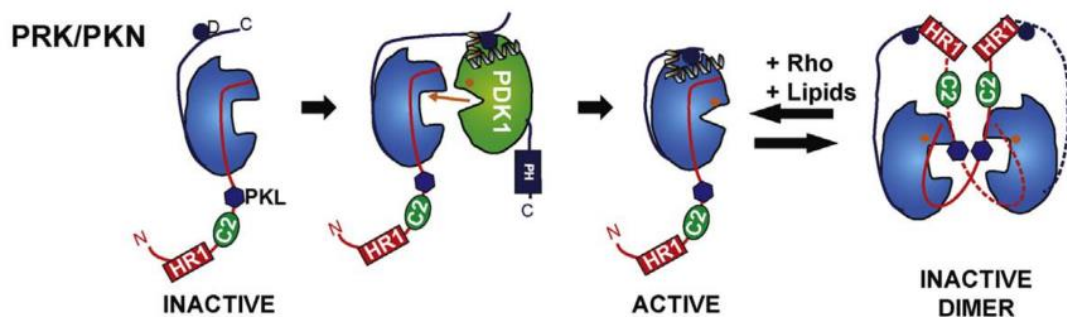
Figure 1.13 PRK2 with some annotated structural features (4CRS)⁶³

The above mentioned X-ray crystal structure of PKN2 (Figure 1.13) shows that ATP- γ -S, an analogue of ATP, interacts with the hinge region (blue) of PKN2 *via* two hydrogen bonds: with the primary amine of the adenine acting as a hydrogen bond donor to an alanine residue (Ala684) and the 1-nitrogen as a hydrogen bond acceptor with a tyrosine (Tyr739).

The C-terminus of most AGC kinases contains two specific phosphorylation sites: the hydrophobic motif (HM) that binds in a groove on the N-terminal lobe of the kinase and a turn/zipper motif.⁴¹ AGC kinases possess a hydrophobic region of six amino acids between the C-terminus and the catalytic core. The hydrophobic motif follows the general sequence pattern F/Y-X-X-F/Y-S/T/D/C-F-Y (where X represents any amino acid residue). The activation loop is phosphorylated by an upstream AGC kinase, PDK1 (Scheme 1.2) while another kinase phosphorylates the HM. The HM is also referred to as the PDK1 Interacting fragment/peptide (PIFtide). Secondly, there is the turn/zipper motif which has various roles in different AGC kinases. In PKN2 it carries the HM over to the PIF pocket and also enables the release of PKN2 when it is docked with PDK1.^{54,41}

The hydrophobic motif is connected to the, so-called, “PIF pocket”, a conserved allosteric site in the small lobe which interacts with the PIFtide of PDK1 and other kinases in order to regulate ATP-binding, activity and substrate interaction.⁶⁴ The PIFtide/PIF pocket complementarity allows PKN2 to self-inhibit itself by forming dimers/oligomers. This is thought to be a unique inhibition mechanism compared to the rest of the AGC family and a two-step mechanism has been suggested (Scheme 1.2).^{54,41}

First of all, once synthesised, PKN2 needs to be phosphorylated by PDK1 and does so by interacting with the upstream kinase. The turn-motif is phosphorylated and this process releases PKN2 from PDK1. Next, the phosphorylated PKN2 in its active state can be deactivated by forming a dimer with another PKN2 protein. The inter-molecular inhibition can be reversed through the binding of lipid/Rho-activators which stabilise the active monomer state of PKN2.^{41,54,64–67}



Scheme 1.2 Representation of the two-stage mechanism of activation of PKN2⁴¹

1.4 Functional Roles of PKN2

1.4.1 Physiological Roles of PKN2

PKN2 is activated by PDK1 and Rho GTPases. It has reported functionality in regulation of cytoskeleton, migration, cell adhesion, embryonic development, cell cycle, apoptosis and DNA translation regulation.⁶⁸ It is found in the cell nucleus, cytosol, cytoskeleton and plasma membrane.⁵⁵ This is a seemingly diverse set of proposed physiological roles which requires a good quality chemical probe to verify. Generally, genetic methods have been mainly used to postulate these functions of PKN2 so far and are detailed below.

PKN2 and Rho

The Rho family are a set of signalling G proteins, forming part of the Ras superfamily and act as molecular switches. Mukai *et al.*⁶⁹ in 1996 expressed PKN kinases with Rho in bovine brain membrane cells, COS-7 and Swiss 3T3 cell lines to investigate their dependency on each other for cell signalling. In the same year, Watanabe *et al.*⁷⁰ published similar work correlating PKN2 to Rho using a yeast two hybrid system, a common genetic technique for detecting interacting proteins in living yeast cells.^{71,72}

Flynn *et al.*⁷³ later reported that Rho and another kinase, phosphoinositide-dependent kinase-1 (PDK1) were involved in the activation of PKN2. They expressed kinase domains of PKN2 as well as PKN1 and monitored the phosphorylation rates in the presence of wild-type and mutant forms of Rho, PKN2 and PDK1 to establish structural areas of importance to function. They also used PI3K inhibitor LY294002 (**2**) to confirm this relationship because of PI3K's link to PKB and other AGC kinases but did not use any other inhibitors in their study.

Cytoskeleton regulation and cell migration

Regarding work carried out on investigating PKN2's role in cytoskeleton regulation, Vincent *et al.*⁷⁴ published work in 1997 where they made microinjections of wild-type and mutant forms of PKN2 into different cell lines to see what effect addition of the kinase had on actin microfilament arrangement. They also transfected cDNA fragments into cells and their findings were a probable but indefinite correlation between PKN2 and Rho on microfilament organisation. No inhibitors were used in this work.

In 2000, Dong *et al.*⁷⁵ used a yeast two-hybrid genetic system to find proteins that interacted with PDK1. This was to better understand how PDK1 responds to insulin-controlled signals regarding actin cytoskeleton arrangement. They also carried out pull down experiments in rat cell lines to investigate the effect of deleting PKN2. In their phosphorylation studies, cells were treated with insulin, but no small molecules were used.

Bourguignon *et al.*⁷⁶ later transfected cDNA fragments correlating to PKN2 and used wound healing assays to measure the effect certain proteins like PKN2 had on cell migration in astrocytes, specialised glial cells that support neuron cells in the central nervous system.³⁵ No compound inhibitors were used in this study.

RNAi techniques were used by Wallace *et al.*⁷⁷ in 2011 to deplete PKN2 in bronchial epithelial cells and found the cells were unable to form apical junctions – specific cytoskeleton structures formed as a result of communication between cell signalling proteins and cytoskeletal components, known as cell polarisation. They also introduced a mutated form of PKN2 into the cell line by transfecting mRNAs to ensure PKN2 was a direct target of RhoA within the Rho family.

Cell adhesion

Calautti *et al.*⁷⁸ published work in 2002 on the interaction between Fyn, a tyrosine kinase, and Rho and PKN2. The proteins were believed to be involved in adhesion between keratinocyte cells in the outer layers of the skin. They created a PKN2 expressing adenovirus that could be added to cells to induce over expression of PKN2. Mutant forms of Rho were also transfected into cells to see if PKN2 interacted with only wild-type Rho. PKN2 did not interact with the mutant form of Rho. No inhibitors were used in this study.

Embryonic development

Work by Quétier *et al.*⁷⁹ sought to remove PKN2 from mouse embryos using gene knockdown techniques. The embryos did not survive this gene deletion experiment. They also used a conditional genetic knockdown technique that involved dosing improved Cre recombinase (iCre) treated cells with tamoxifen in order to induce loss of PKN2 and saw a similar essential role of the kinase in embryonic development.

Cell cycle

Misaki *et al.*⁸⁰ used recombinant viruses like Calautti *et al.* to introduce additional PKN2 into HeLa cells. They also used microinjection techniques as well. Their aim was to investigate the effect PKN2 had on the activity of Wee1 kinase and cell division cycle 25 (Cdc25), a dual-specificity phosphatase, during mitosis – the most common form of cell division.³⁵ PKN2 did not enhance Wee1 activity but was shown to phosphorylate Cdc25, both *in vitro*.

Apoptosis

PKN2 has also been linked to apoptosis, programmed cell death.³⁵ In 1998, Takahashi *et al.*⁸¹ used DNA plasmids and mutagenesis recombinant caspase enzymes to investigate if PKN kinases were activated during apoptosis. Koh *et al.*⁸² later used yeast two-hybrid assays and PKN2 hybrids to investigate similar roles of the kinase in programmed cell death. The substrates used

in their work were histone 2B (H2B) and tumour necrosis factor, the latter used to induce apoptosis and linked PKN2 to PI3K, but no small molecules were used to probe the role of PKN2.

Transcriptional regulation

In 2005, Chang *et al.* carried out an expression screen by transfecting DNA constructs into cell lines in order to find kinases that phosphorylated histone deacetylase (HDAC) enzymes and found PKN2 might be an activator of this class of protein. HDACs catalyse the removal of acetyl groups from lysine residues residing in histone and other proteins involved in control of DNA expression.⁸³

Harrison *et al.*⁸⁴ later demonstrated in 2010 that PKN2 phosphorylates HDAC5 by using DNA transfection methods into heart tissue and carrying out phosphorylation studies. No compounds were used to validate the interaction of these proteins.

1.4.2 Pathological Roles of PKN2

PKN2 has been linked to multiple cancer sub-types, namely prostate,⁸⁵ colon,⁸⁶ head,⁸⁷ neck⁸⁷ and breast^{88,89} cancers. It has other reported roles in inflammation,⁹⁰ hepatitis C⁹¹ and cardiovascular processes,⁹² all of which will be summarised below.

Prostate cancer

With regards to PKN2's role in prostate cancers, O'Sullivan *et al.*⁸⁵ reported in 2015 that PKN1 and PKN2 were potential mediators in the release of prostanoids, eicosanoid compounds related to prostaglandins involved in the body's pain response. Prostanoids specifically control constriction of blood vessels (vasoconstriction),³⁵ a notable response in certain prostate cancers.⁸⁵ O'Sullivan *et al.*⁹³ later reported in 2017 that they had found that PKN2 may form a complex with T prostanoid receptors in prostate cancer progression. Yang *et al.*⁹⁴ also reported in 2017 that PKN2 was involved in prostate motility pathways and influences differentiation of prostate cell types.

Colon cancer

In 2018, Cheng *et al.*⁸⁶ reported that PKN2 was involved in signalling pathways for the transformation of macrophage cells into their pathogenic form, known as polarisation.⁹⁵ This polarisation process is involved in the progression of colon cancer. They found that there was high expression of PKN2 in early stage colon cancer cells but that as the disease progressed, the presence of PKN2 reduced tumour-associated macrophage association and overall tumour growth.⁸⁶

Head and neck cancer

While smokers are predominantly prone to lung cancers,⁹⁶ Rajagopalan *et al.*⁸⁷ reported in 2018 that smokers prone to head and neck cancers following long-term exposure to cigarette smoke possessed high levels of PKN2 across a panel of cell lines that had been exposed to cigarette smoke for twelve months. They depleted PKN2 in those cell lines and found that doing so reduced the rate of colony formation, cell invasion and migration.

Breast cancer

Most recently, PKN2's role in triple negative breast cancer (TNBC) has been postulated by Patel *et al.*⁸⁹ in 2020 building on previous work by Lin *et al.*⁸⁸ They found that depleting PKN1 and PKN2 in mouse and human TNBC cells reduced the rate of cell proliferation and growth of spheroid tumours. High PKN2 expression is correlated to poor patient outcome and has also been reported to support the growth of this sub-type of breast cancer – known to be particularly difficult to treat due to a lack of hormone receptors on the cancer cells' surface.⁹⁷

Hepatitis C and inflammation

Outside of cancer, PKN2 also shows promise as an anti-viral target due to its role in phosphorylating and activating NS5B, a RNA polymerase with a crucial role in the Hepatitis C disease pathway.^{91,98} The kinase also has other potential roles in inflammation due to the reported role PKN1 and PKN2 have in phosphorylating the pyrin inflammasome following activation by arachidonic acid.^{90,99,100} In the study carried out by Park *et al.*⁹⁹ staurosporine and PKC412, referred to as “potent PKN inhibitors” in their study, were used. Both of these compounds may be potent but they are not selective PKN inhibitors^{9,101} and could have given misleading results about the precise roles of PKN kinases in these processes.

Heart failure

Finally, in the area of cardiovascular function, PKNs have been linked to signalling processes during heart formation and dysregulation in certain cardiac pathologies but these relationships were deemed by the authors to be less well understood than those of their closely related homologues, PKC proteins.^{92,102} In the Sakaguchi study,¹⁰² PKN1/2 were not directly inhibited. Instead a Rho inhibitor was used to halt the phosphorylation of the PKNs by inhibiting the upstream Rho protein that would otherwise activate the PKNs.

1.5 Project Aims

The main aim of the project was to deliver a high-quality chemical probe that showed sufficient potency and selectivity for PKN2 within the PKN kinase family and wider kinome to facilitate validation of its role in physiological and pathological biochemical pathways. The parameters set for the probe were those suggested by the Structural Genomics Consortium⁴ whereby an ideal

probe should exhibit less than 100 nM IC₅₀ *in vitro* potency; at least 30-fold selectivity over other kinases; less than 1 μ M IC₅₀ *in cellulo* potency and have a suitable inactive analogue for use as a control compound.

Three literature compounds (**10**, **11** and **12**) (Figure 1.14) were selected in-house from a data triage of 1200 compounds reported in the literature as inhibitors of PRK2. The ChEMBL literature database¹⁰³ was used to find these compounds through a search for compounds with known bioactivities against PKN2, which were then ranked by their potency.

Compounds **10–12** were selected for their high potency and promising initial selectivity, with the exception of **12** due to lack of available data against other kinase targets. Each series will be discussed in a separate results chapter which will cover the similarities of the compounds to existing FDA-approved kinase inhibitors; synthesis of those initial hits and subsequent analogues for structural activity relationship (SAR) studies as well as the biological evaluation of the resulting compound libraries. The rationalisation of the compounds' biological activity using computational drug design (CDD) methods will also be discussed.

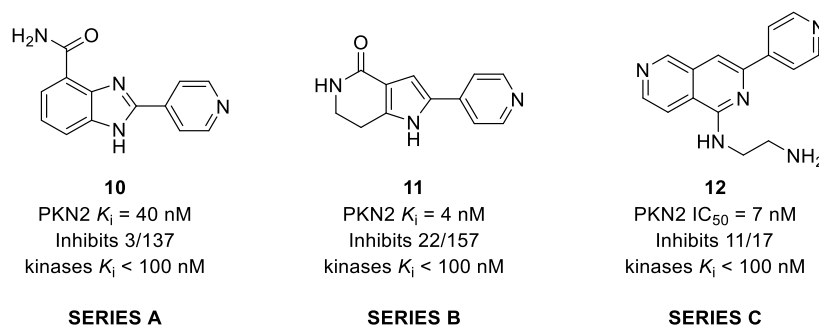


Figure 1.14 Compounds **10**, **11** and **12** selected from the ChEMBL screen^{103–106}

This project was carried out in collaboration between SDDC and GDSC at University of Sussex and the SGC in order to add a PKN2 probe to their database.⁴ Work was carried out by the SGC between University of Oxford, UK and University of Campinas, Brazil to develop TR-FRET biochemical assay methods for these compounds against PKN2 and PKN1. Compounds with promising potency and selectivity between the two PKN kinases were sent for wider kinome screening *via* the commercial KINOMEScan® platform.¹⁰⁷ The SGC also carried out crystallographic studies to obtain a structure of PKN2 with an inhibitor bound at the ATP site.

Chapter 2 Series A – Benzimidazoles

This chapter seeks to outline the work carried out in optimising compound **10**, a benzimidazole (Figure 2.1). The chemistry used to prepare this compound and other analogues will be discussed as well as the biological evaluation of the inhibitory potencies of those compounds against PKN2 and other kinases. Attempts to rationalise said biological activity using computational studies will also be outlined. Most of the work covered in this chapter was recently published in the journal *Bioorganic and Medicinal Chemistry Letters*.¹⁰⁸

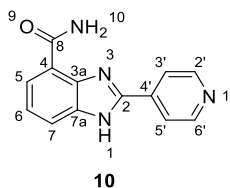


Figure 2.1 Original compound for series A¹⁰⁹

2.1 Hit Origin

Benzimidazoles are popular scaffolds in medicinal chemistry.¹¹⁰ Two of the current list of 52 FDA-approved kinase inhibitors, abemaciclib (**13**) and binimetinib (**14**) (Figure 2.2), contain benzimidazoles while thirteen others contain similar 6,5-aromatic heterocycles.⁴⁶

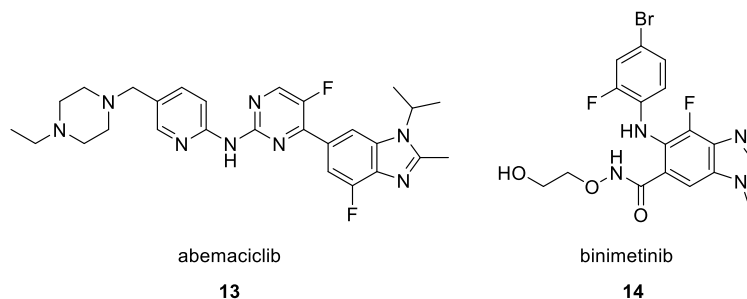


Figure 2.2 Chemical structure of benzimidazole-containing FDA-approved kinase inhibitors⁴⁶

Benzimidazoles are bioisosteres of the adenine portion of ATP (**6**) (Figure 2.3), the common phosphate-transferring molecule of kinases, making it a common motif explored in kinase inhibitor design.¹¹¹ The combination of the hydrogen bond donor and accepting nitrogen atoms allows for multiple interactions within the kinase hinge region and the fused benzene ring incorporated into the structure can potentially form hydrophobic and π - π stacking intermolecular interactions with pockets within the catalytic site.

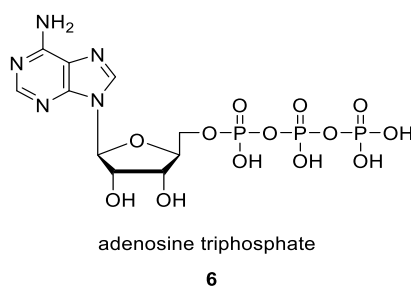
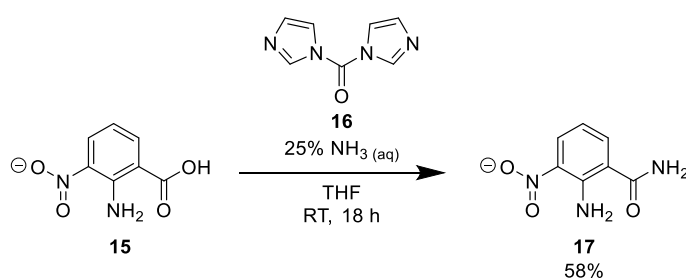


Figure 2.3 ATP (**6**) structure

One such benzimidazole was identified in the previously described triage of 1200 compounds in the ChEMBL database reported to have biological activities against PKN2. Compound **10** (Figure 2.1) was initially developed as a PARP inhibitor,^{104,112–115} but was shown to be more potent towards PKN2 than its intended target in a published kinase panel screen of Abbott's compound library.¹⁰⁹ The benzimidazole core is linked to a 4'-pyridyl ring at the 2-position and a primary amide at the 4-position. It was deemed an attractive starting point for a selective PKN2 probe because of its low reported potency of K_i 40 nM against PKN2 and in terms of selectivity, inhibited only PKN1 and CLK4 with K_i values below 100 nM out of 137 kinases with reported bioactivities.¹⁰⁹

2.2 Chemistry

2.2.1 Synthesis of original hit

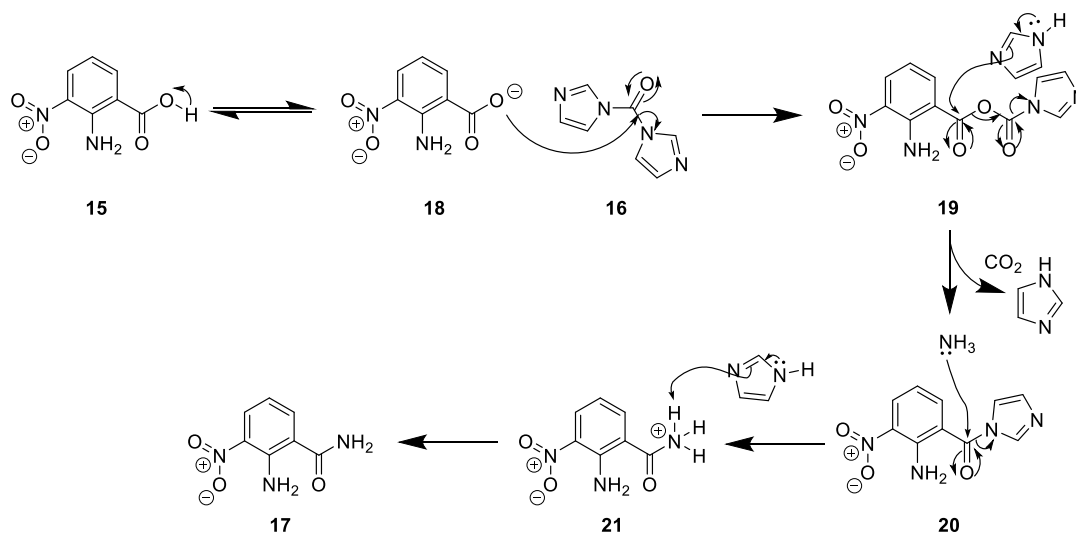


Scheme 2.1 CDI amide coupling conditions to **17**¹¹⁶

Compound **10** was successfully synthesised using a 4-step synthesis. First, 2-amino-3-nitrobenzoic acid (**15**) underwent an amide coupling with ammonia using 1,1'-carbonyldiimidazole (CDI) (**16**) as a coupling reagent (Scheme 2.1). Scheme 2.2 proposes a mechanism for the transformation.

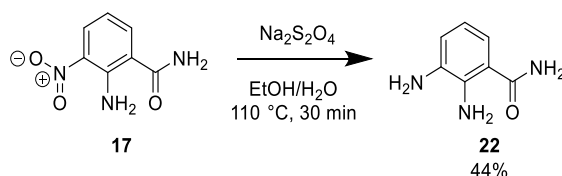
Deprotonation of the acid function forms a nucleophile (**18**) that attacks the carbonyl of the CDI (**16**), resulting in the loss of imidazole. This imidazole then attacks the carbonyl adjacent to the

benzene ring (**19**) which in turn eliminates carbon dioxide and another equivalent of imidazole. The combination of imidazole being a good leaving group and that the carbonyl carbon (**20**) is now sufficiently delta positive means that carbon undergoes nucleophilic attack by ammonia, and, for a third time, loss of imidazole occurs to yield intermediate **21**. Finally, this imidazole deprotonates the nitrogen to form amide **17**.



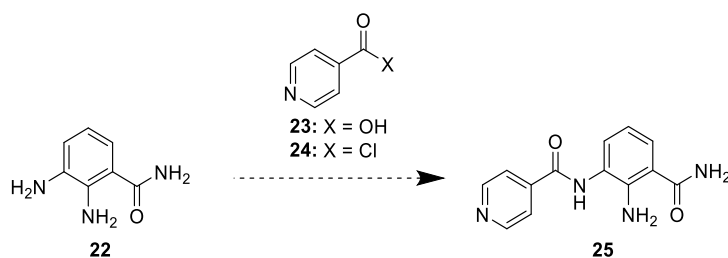
Scheme 2.2 CDI amide coupling mechanism¹¹⁷

Yields for this reaction typically ranged from 32–58% and usually two crops of amide **17** were isolated by filtration. The second batch was isolated from the filtrate after being left overnight to further crystallise. Typically, orange crystals formed.



Scheme 2.3 Nitro-reduction conditions using sodium dithionite¹¹⁸

Next, the nitro-functionality of **17** was reduced to form dianiline **22** using sodium dithionite (Scheme 2.3).¹¹⁸ It was found that 10 equivalents of the reducing agent were required for full conversion due to the tendency of sodium dithionite to degrade upon heating in aqueous solutions.¹¹⁹ Following work-up with ethyl acetate extraction and flash chromatography, dianiline **22** was isolated in 44% yield. This was thought to be due to the slow elution from the column during purification. The drop in yield was taken into account in later attempts of this step by carrying it out at larger scale to ensure enough of this key dianiline intermediate was isolated to get to the end of the synthesis.

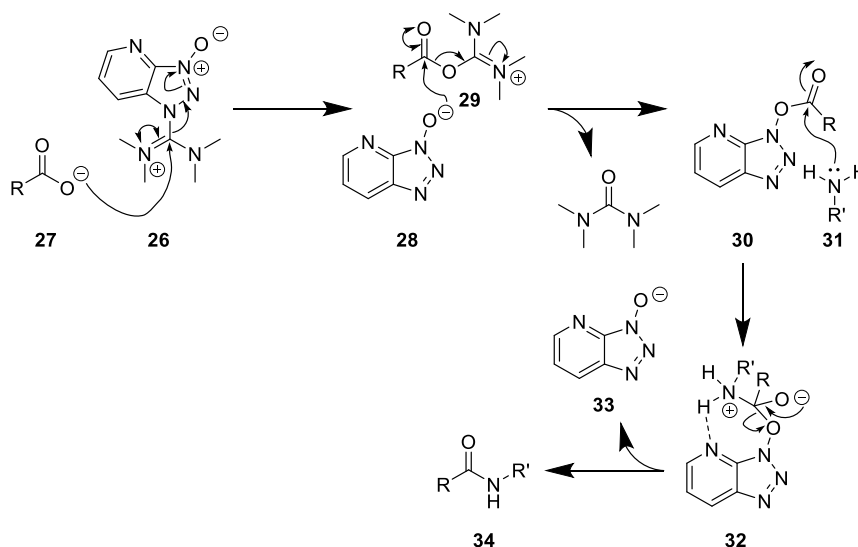
Scheme 2.4 The conversion of **22** to **25**^{104,120}

The third step of the synthesis in the literature procedure¹⁰⁴ called for isonicotinic acid (**23**) to be coupled with **22** in the presence of TEA and DMAP (Scheme 2.4). This was attempted twice with no success. Converting **23** to the corresponding acid chloride (**14**) and then using the same conditions was also unsuccessful when trying to make amide **25**. Table 2.1 summarises the chemistry attempted.

Table 2.1 Summary of reaction conditions attempted to make amide **25**^{104,120}

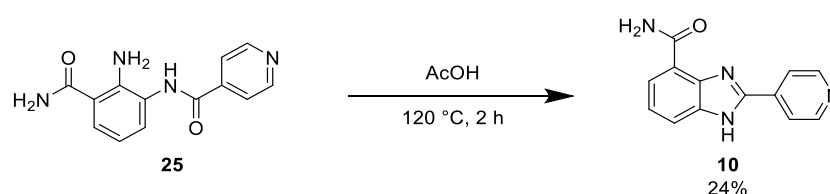
Coupling partner	Other reagents	Solvent	Temperature	Time	Yield
23	TEA, DMAP	THF	RT	18 h	0%
24	TEA, DMAP	THF	RT	2 h	0%
23	HATU, DIPEA	DCM	RT	18 h	99%

HATU-facilitated coupling conditions¹²⁰ using intermediate **22**, isonicotinic acid (**23**), HATU (**26**) and *N,N*-diisopropylethylamine (DIPEA) were successful, isolating amide **25** in quantitative yields. Scheme 2.5 outlines the mechanism for an amide bond formation using HATU (**26**) as a coupling agent.

Scheme 2.5 General HATU coupling mechanism¹¹⁷

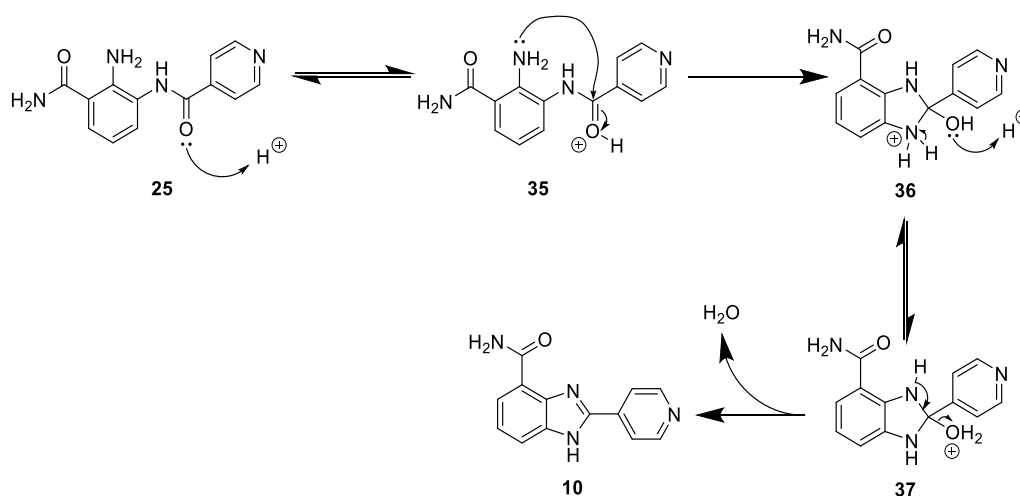
Once the acid is deprotonated (**27**), it can attack the δ^+ iminium carbon of the HATU (**26**) adjacent to three nitrogens. The resulting azabenzotriazole (**28**) can then attack the δ^+ carbon of the carbonyl of intermediate **29** to activate the acid group, such that amine **31** can then act as a nucleophile to attack the activated ester (**30**). The zwitterionic intermediate (**32**) is stabilised by a hydrogen bonding interaction between an N-H and nitrogen acceptor within the HATU-acid-amine tetrahedral intermediate which breaks down to again release azabenzotriazole (**33**) as a side product to give the amide product (**34**).

It was found in most cases that amide **25** and its derivatives could simply be isolated from the reaction mixture by filtration and the crude carried forward without further purification. This was done because in some first attempts, carrying out aqueous work-up to isolate **25** proved difficult – up to a litre of solvent was required to dissolve/transfer around 100 mg product resulting in very low yields in one attempt. For derivative amide intermediates that did not precipitate out of the reaction mixture standard work-up and purification practices were used to isolate the intermediate.



Scheme 2.6 Acid-catalysed cyclisation conditions to form benzimidazole **10**¹⁰⁴

The benzimidazole product (**10**) was formed by stirring amide **25** in acetic acid with heating (Scheme 2.6). Scheme 2.7 outlines a possible mechanism.



Scheme 2.7 Proposed mechanism for the acid-catalysed cyclisation of **25** to benzimidazole **10**

Activation of amide **25** *via* reversible protonation of the carbonyl oxygen sufficiently polarises the carbonyl bond such that the free primary aniline attacks the δ^+ carbon of intermediate **35**. The resulting intramolecular bond formation yields cationic intermediate **36**. The hydroxyl group picks up an additional proton to promote water loss from intermediate **37** to give benzimidazole **10**.

For the majority of analogues, the reaction was complete within a couple of hours and observable by TLC and LCMS analysis. The reaction mixture was concentrated and directly purified by flash chromatography to remove any residual starting material and acetic acid. Compound **10** was successfully isolated in 24% yield.

The isolation procedure was optimised which removed the need for a column in most cases. Instead, the acidic reaction mixture was neutralised by adding saturated aqueous sodium hydrogen carbonate which caused the product to precipitate out of solution. This was isolated by filtration and dried in a vacuum oven overnight to yield the benzimidazole. When preparation of **10** was repeated, e.g. for preparing *N*-alkylated analogues, isolation by this method increased the reaction yield from 24% to 60%. Occasionally the isolated product required further purification *via* flash column chromatography, as outlined in individual procedures in the experimental section which resulted in lower yields as expected.

^1H NMR confirmed the amide **25** had been converted to benzimidazole **10** because one of the two N-H peaks had disappeared from the spectra and characteristic singlet peaks for benzimidazole exchangeable N-H proton were observed around δ 7.84.

2.2.2 Preparation of analogues

Pyridyl variation

It was hypothesised that the 4'-pyridyl function was the hinge-binder in **10** so initial efforts were made to vary this ring. Three analogues with the nitrogen in the 3'-position (**38**), addition of another nitrogen with a 5'-pyrimidine (**39**) and incorporating an adjacent electron-donating methoxy group (**40**) were successfully prepared using the above synthesis by varying the acid used in the HATU coupling step (Figure 2.4).¹²⁰

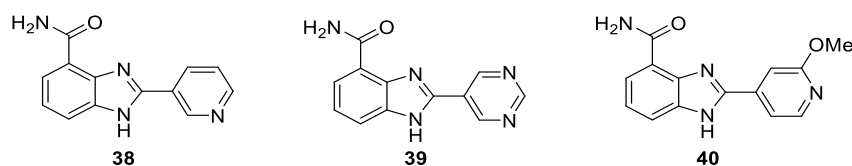
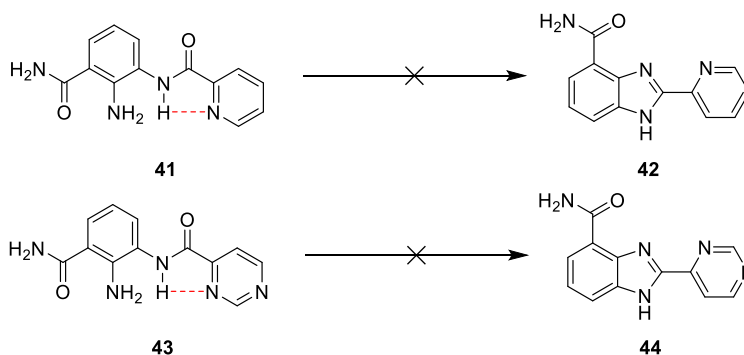


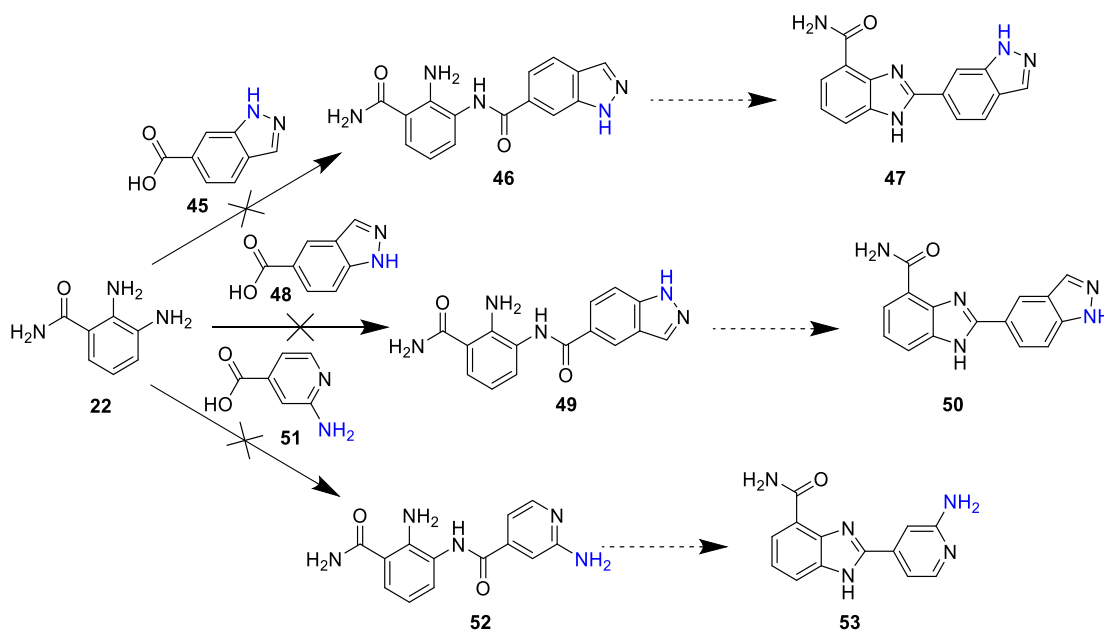
Figure 2.4 Analogues of **10** by varying pyridyl function

The 2'-pyridyl (**42**) and 6'-pyrimidine (**44**) analogues (Scheme 2.8) proved difficult to prepare in the final step. This was thought to be due to a potential intramolecular hydrogen bond as shown in Scheme 2.8. Heating both reactions to 150 °C and further to 200 °C in the microwave for 30 minutes to disrupt those intramolecular bonds did not force the reaction to completion which suggests this is not why the reaction did not progress. It may be possible that the *ortho* azo nitrogen has an inductive effect making the amide less susceptible to reaction.



Scheme 2.8 Analogues of 10 that could not be prepared thought due to possible hydrogen bonding interactions (in red)

Other attempts to exchange the six-membered ring with other heterocycles such as indazoles (**47/50**) or an amino-pyridine (**53**) were unsuccessful (Scheme 2.9). This was thought to be due to unprotected amines in the reaction mixture which were also reacting with the acids during the amide coupling step. Protection of the free N-H in the indazole-5-carboxylic acid (**45**) and indazole-6-carboxylic acid (**48**) starting materials with Boc¹²¹ and THP¹²² protecting groups was attempted but was unsuccessful at the purification stage.

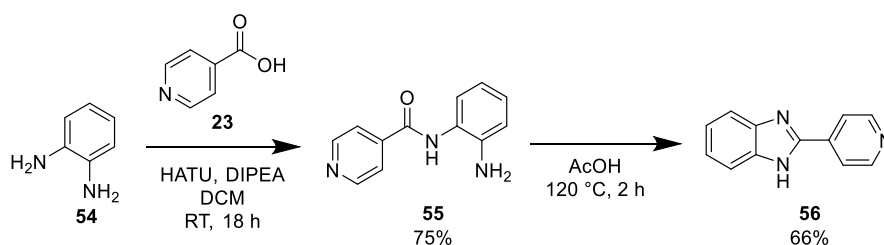


Scheme 2.9 Failed preparation of analogues 47, 50 and 53 due to unprotected amines (highlighted in blue)¹²⁰

Amide variation

Another region of interest for SAR in **10** was the amide. Generating amide libraries is generally straightforward when a fairly short synthesis has been established. Ideally, the amide should be varied at the end of the synthetic route, but this protocol often required the amide to be formed in the first step before nitro-reduction steps. Due to its relatively short length of four steps and reproducibility it was decided to stick with the existing method and the amide was introduced at the beginning of the synthesis.

Benzimidazole **56** which lacked the amide moiety was successfully synthesised using commercially available *O*-phenylenediamine (**54**) with notably higher yields than the typical 25% yield for isolating **10** (Scheme 2.10).



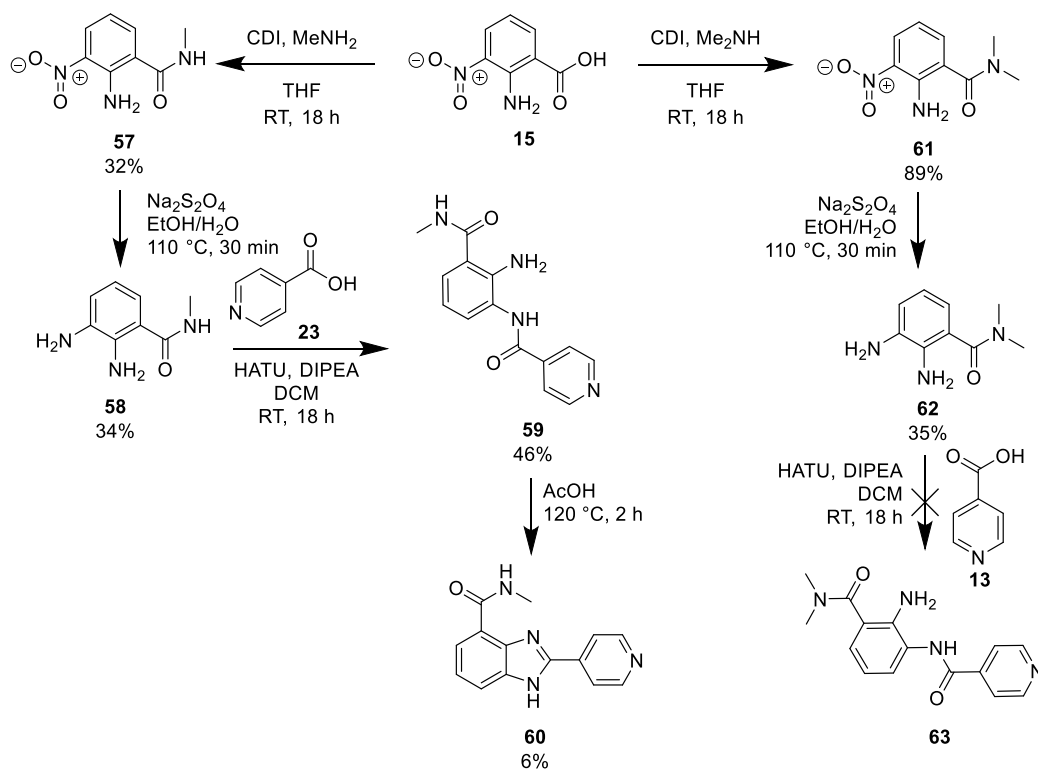
Scheme 2.10 Synthesis to benzimidazole **56** from commercially available *O*-phenylenediamine (**54**)^{104,120}

Removing the amide completely changed the ¹H NMR aromatic region. Instead of the usual two doublets and triplets observed denoting the three aromatic protons of the benzimidazole in different environments, three peaks, two integrating to one proton (either side of the exchangeable N-H hence the slightly different magnetic environments) and one integrating to two were seen due to the increased symmetry in this analogue (Figure 2.5).



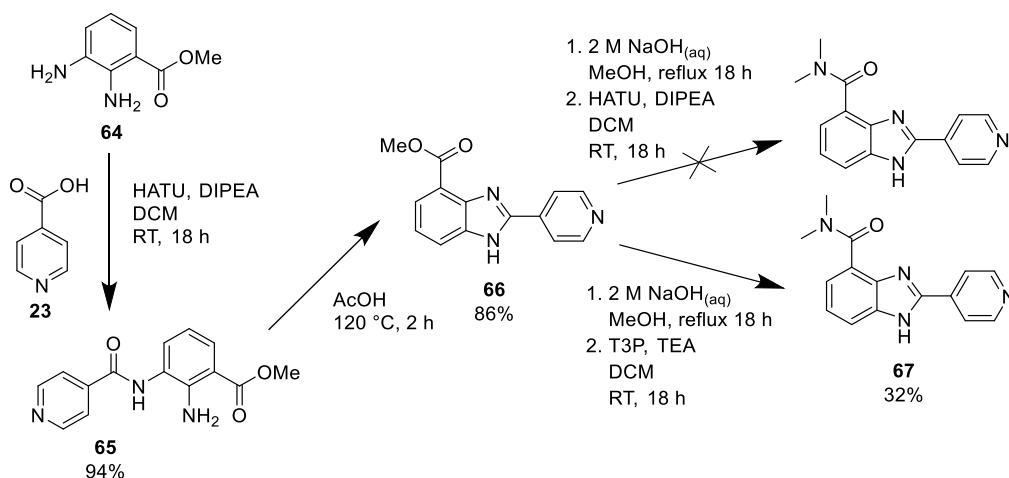
Figure 2.5 Excerpt of ¹H NMR spectrum of compound **56**

The mono-methylated (**60**) and di-methylated (**67**) amide derivatives were attempted by coupling methylamine/dimethylamine in the first step of the synthesis outlined in Scheme 2.11. The mono-methylated analogue (**60**) was prepared in 6% yield in the final step. It was not possible to sufficiently purify amide **63** for taking to the last step of the synthesis.



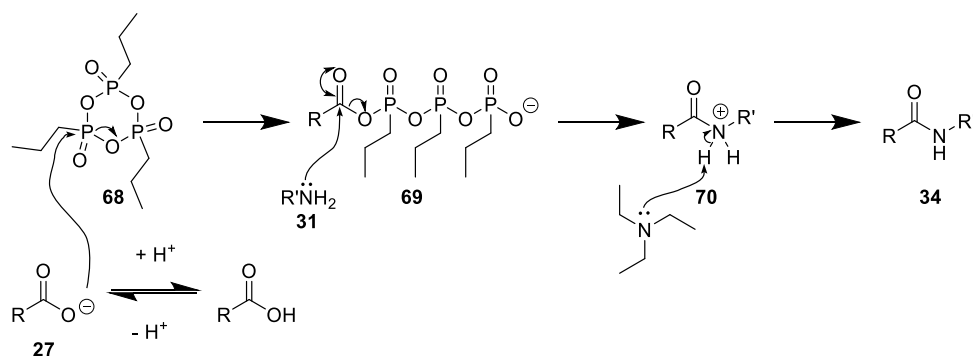
Scheme 2.11 Synthesis summary of methylated analogues **60** and **63** by usual chemistry procedures^{104,116,118,120}

In the initial CDI amide coupling step, it was particularly difficult to remove the imidazole, even after purification by column chromatography. Intermediates **57** and **61** were taken through without further purification, and this did not seem to severely affect later steps.



Scheme 2.12 Synthetic scheme to dimethylated analogue **67**^{104,120,123}

Synthesising the corresponding 4-methyl ester benzimidazole analogue (**66**) and cleaving that ester with 2 eq. 2 M aqueous sodium hydroxide solution, followed by coupling dimethylamine *via* HATU coupling conditions was also unsuccessful. Substituting the 2 M dimethylamine in THF solution for the chloride salt did not cause the reaction to progress either. Using propylphosphonic acid anhydride (T₃P, **68**) allowed the dimethylated amide analogue (**67**) to be isolated in 32% yield (Scheme 2.12). T₃P (**68**) is a cyclic trimer which activates carboxylic acids for reactions with amines, as outlined in the mechanism in Scheme 2.13.



Scheme 2.13 T₃P-facilitated amide coupling mechanism¹²⁴

Upon deprotonation, nucleophile **27** cleaves the T₃P (**68**) ring *via* nucleophilic attack of one of the phosphonate groups. The diffuse nature of the electron distribution in phosphorus and strength of the P=O bond means the P-O bond is directly cleaved *cf.* a carbonyl-based substitution. Species **69** has a sufficiently activated ester to react with amine **31** to produce cationic intermediate **70**, whose charge is neutralised *via* deprotonation by triethylamine to form the amide product (**34**).

Confirmation of the mono- (**60**) and di-methylated (**67**) versions of **10** were confirmed by observation of the expected larger masses (m/z 253 and 267, respectively *cf.* 239) and appearance of additional peaks in the aliphatic region of their ¹H NMR spectra (Figure 2.6). For compound **60**, an additional singlet integrating to three protons was observed at δ 3.02 ppm while two additional singlet peaks appeared in the ¹H NMR spectrum of **67**, both integrating to three protons each, at δ 3.11 and 2.87 ppm. Two peaks arise due to the relative rigidity around the C-N amide bond due to the adjacent electron-withdrawing carbonyl in a relatively polar solvent, DMSO-*d*₆ (ΔG^\ddagger rotation of C-N in dimethylacetamide in DMSO = 76.5 kJ mol⁻¹).¹¹⁷ Additional carbon peaks were also observed in both compounds' respective ¹³C NMR spectra.

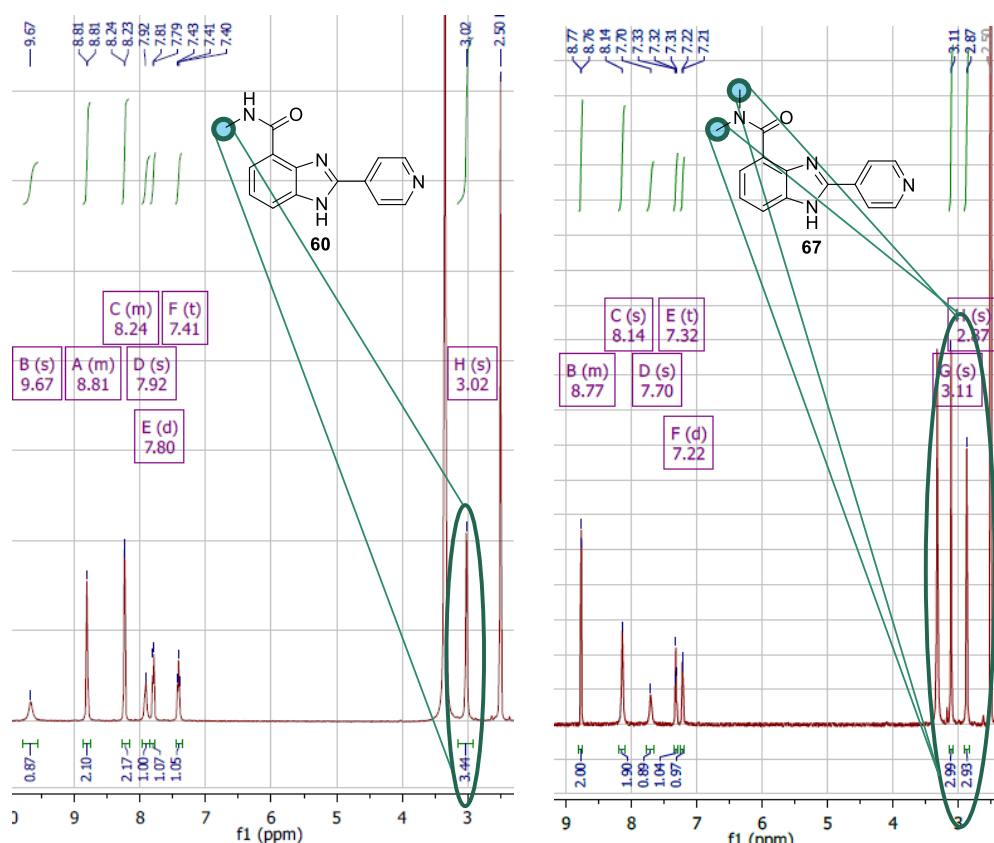
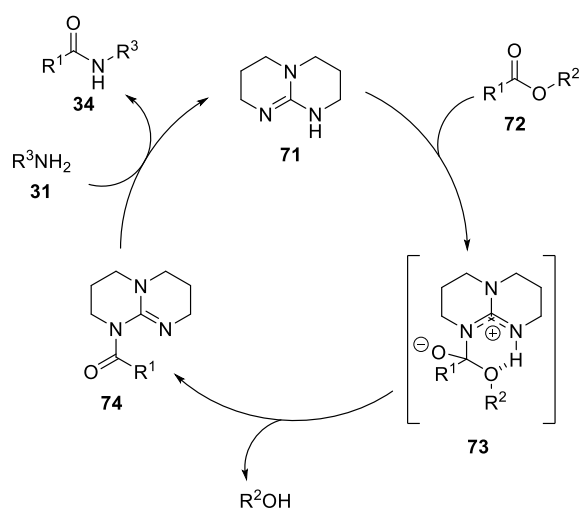
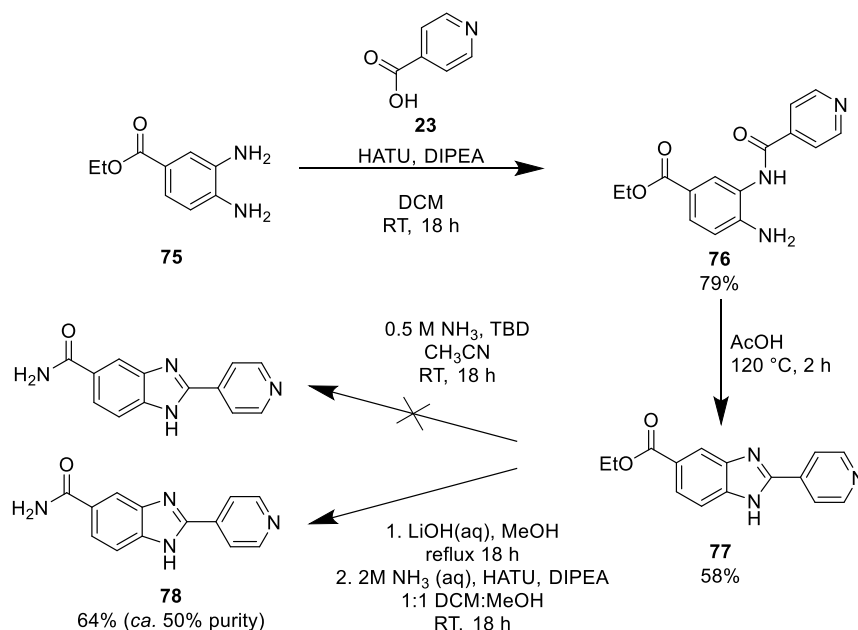


Figure 2.6 ^1H NMR spectra of compounds **60** and **67** with peaks corresponding to methyl groups circled in blue

Varying the position of the branching amide (**78**) was attempted using a similar synthetic strategy (Scheme 2.15) with the corresponding benzimidazole with a 5-ethyl ester (**62**) but the product could not be cleanly isolated. An in-house procedure using 1,5,7-triazabicyclo[4,4,0]dec-5-ene (TBD) (**71**) (for mechanism see Scheme 2.14) or HATU (**26**) coupling agents to form the 5-position amide yielded no product or product of a low purity, respectively (Scheme 2.15).

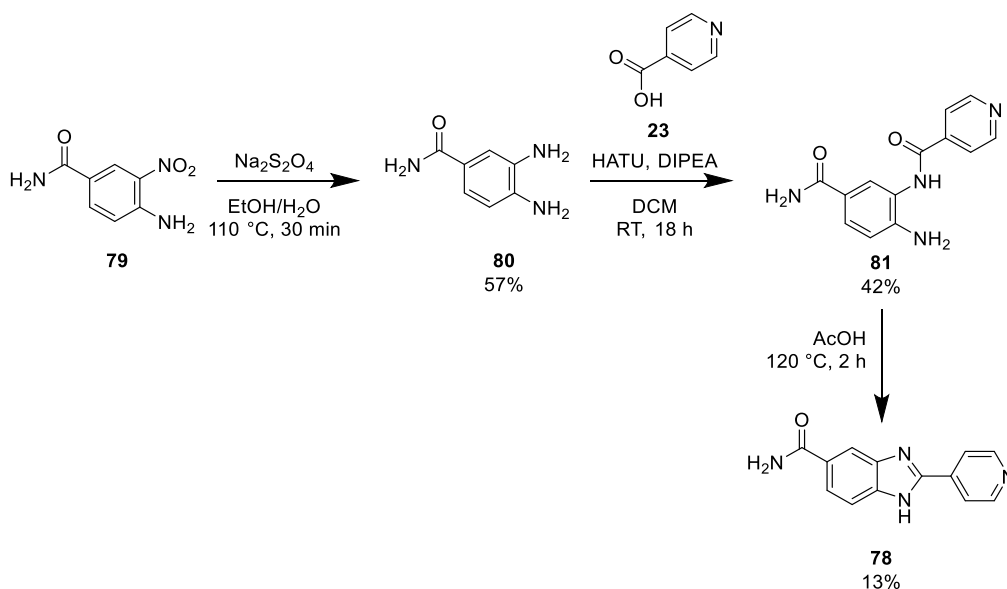


Scheme 2.14 TBD-facilitated amide coupling general mechanism¹²⁵



Scheme 2.15 Unsuccessful attempts at producing benzimidazole **78 from benzimidazole **77****

The 5-ethyl ester benzimidazole (**77**) was tested as an analogue in its own right but unfortunately converting the ester to an amide as per **67**, did not yield the desired product (**78**) in sufficient yield and purity. Instead, the compound was made using the usual original route (Scheme 2.16) from commercially available 4-amino-3-nitrobenzamide (**79**) in order to deliver compound **78** in 13% yield but of sufficient purity for biological evaluation.



Scheme 2.16 Synthesis to **78 from 4-amino-3-nitrobenzamide**

It was possible to exchange the primary amide for other functional groups using various commercially available di-anilines and nitro-anilines. In total, five other analogues (Figure 2.7)

were prepared with ester (**66** and **77**), cyano (**83**), and nitro (**82** and **84**) moieties vectoring from the 4- or 5-position of the benzimidazole.

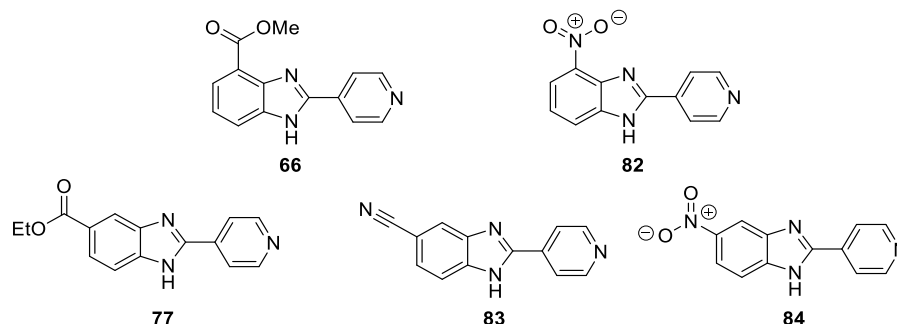
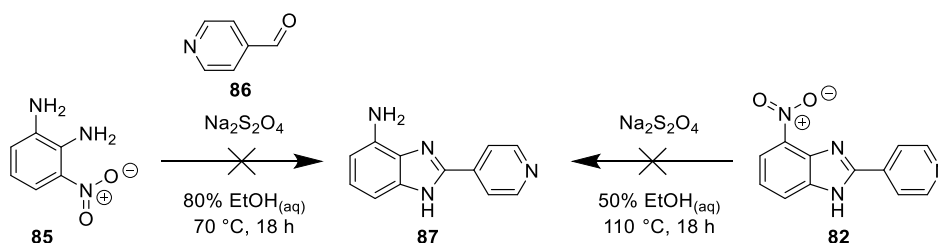


Figure 2.7 Structures of a selection of benzimidazole analogues prepared that lack an amide

Appearance of a strong peak at 2216 cm^{-1} in the IR spectrum confirmed the presence of a nitrile group in benzimidazole **83**, as well as a peak in the ^{13}C NMR spectrum at 120.9 ppm in lieu of the usual carbonyl peak observed around $\delta\ 160\text{--}220\text{ ppm}$. Similarly, the loss of carbonyl signals in ^{13}C NMR and IR spectra for nitro-containing analogues **82** and **84** helped to conclude the preceding amide intermediates had fully cyclised to the respective benzimidazoles. For the derivatives containing esters, **66** and **77**, two peaks attributed to carbonyl carbons were observed for the penultimate amide intermediates in the ^{13}C NMR spectra.

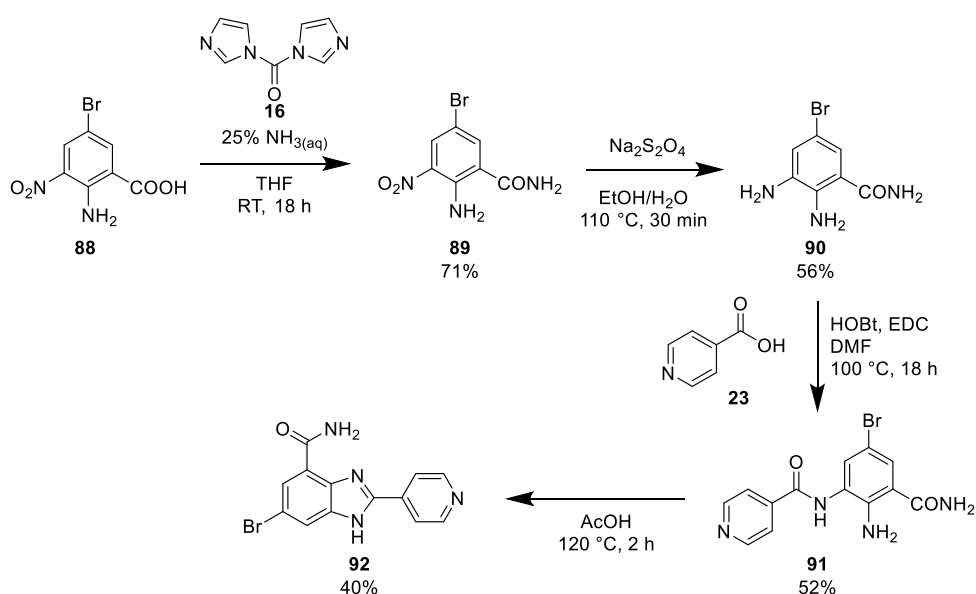
Attempts were made to produce the 4-amino derivative of **10** (**87**) in order to see what difference was made by removing the hydrogen bond acceptor but keeping the two donors. First, a one-pot cyclisation-reduction test reaction was carried out using 3-nitrobenzene-1,2-diamine (**85**), 4-pyridinecarboxaldehyde (**86**) and sodium hydrosulfite but even with 30 equivalents of the sodium hydrosulfite, the reaction did not go to completion. Similarly, reducing the nitro-containing match pair (**82**) using sodium hydrosulfite was unsuccessful as neither starting material nor product mass ions could be observed in the LCMS spectrum (Scheme 2.17).



Scheme 2.17 Unsuccessful attempts of preparing 4-amino analogue of **10**¹¹⁸

Additional ring systems

In an attempt to explore building off the 6-position of this set of compounds, a bromine moiety was introduced at the 6-position to facilitate Suzuki coupling of aromatic groups. The key bromine-containing benzimidazole (**92**) was successfully synthesised from commercially available 2-amino-5-bromo-3-nitrobenzoic acid (**88**) (Scheme 2.18). Alternative amide coupling conditions using HOBt and EDC¹²⁶ instead of HATU¹²⁰ were required for the penultimate step. Appearance of two peaks in mass spectrometry experiments of m/z [M+H] and [M+H+2] in a 1:1 ratio indicated the presence of the bromine atom across the synthesis.¹²⁷



Scheme 2.18 Synthesis of Br-containing analogue **92**^{104,116,118,126}

Unfortunately, various Pd-catalysed couplings were tried with bromo-containing intermediates **88**, **89** and **90** but none resulted in a successful reaction. The conditions are summarised in Table 2.2. It is thought that the free N-H in the benzimidazole was interfering with the catalytic cycle and would need protecting in order to carry out such steps.

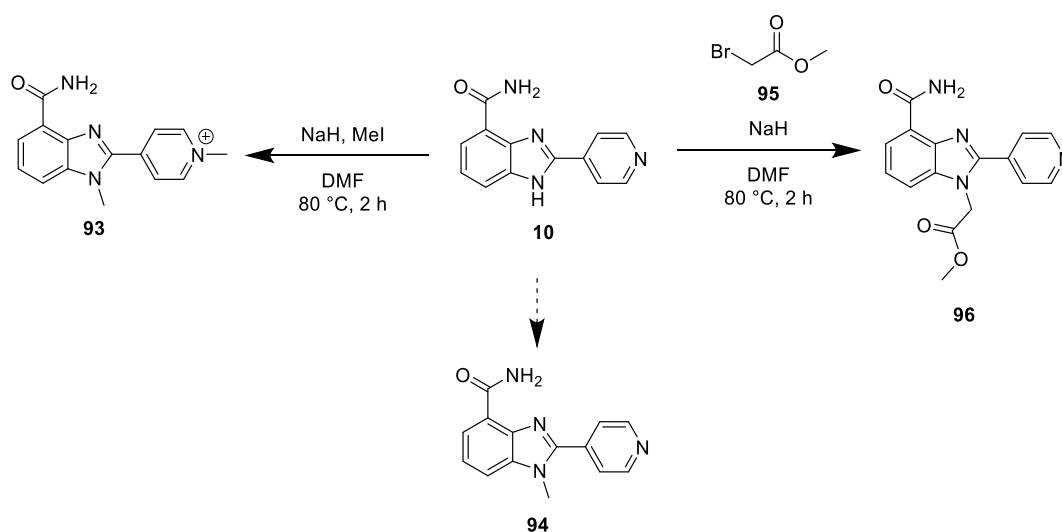
Table 2.2 Summary of Suzuki conditions attempted on bromine-containing intermediates

Starting material	Catalyst	Solvent system	Temp.	Time	Heating method	Product m/z in LCMS?
88	Pd(dppf)Cl ₂ ·CH ₂ Cl ₂	3:1 dioxane:water	100 °C	4 h	Hot plate	No
88	Pd(dppf)Cl ₂ ·CH ₂ Cl ₂	3:1 dioxane:water	100 °C	1.5 h	Microwave	No
89	Pd(dppf)Cl ₂ ·CH ₂ Cl ₂	3:1 dioxane:water	100 °C	1.5 h	Microwave	No
90	Pd-118	4:1 acetonitrile:water	100 °C	1.5 h	Microwave	No
90	Pd(PPh ₃) ₂ Cl ₂	4:1 acetonitrile:water	100 °C	18 h	Hot plate	No

Alkylation of benzimidazole

Attempts were also made to cap the benzimidazole N-H of **10** (**94**) using typical methylating conditions¹²⁸ using sodium hydride as a base and methyl iodide as the source of the methyl group (Scheme 2.19). Despite numerous attempts and careful execution of the reaction under inert conditions, the dimethylated salt (**93**) seemed to form preferentially leaving unreacted starting material rather than reacting once with the benzimidazole N-H to form desired compound **94**. Instead, it is believed that the 4'-pyridyl nitrogen was the next likely position at which the methyl iodine would react. The observation was of m/z 268 in the reaction's LCMS profile instead of the desired m/z 253 expected for a compound of 252 Da, as was the appearance of two methyl peaks in the ^1H NMR spectrum.

One of the literature sources¹²⁸ for the alkylation reaction showed a variety of alkyl groups being substituted at the N-H centre of a benzimidazole. Unfortunately, the paper only gave experimental data for the combination of methyl bromoacetate (**95**) with the benzimidazole (**96**), and not simply methyl iodide, although it was implied that the chemistry had been used to produce the equivalent analogue. The chemistry was repeated using the methyl bromoacetate and the ester-capped benzimidazole (**96**) was successfully isolated (Scheme 2.19).



Scheme 2.19 N-Alkylation attempts to benzimidazole **93**¹²⁸

Compound **96** is not an ideal match pair with **10** because the ester is a larger point change than that of a simple methyl group. It was still tested in the biochemical assay to compare with **10** in the absence of the simpler methylated analogue (**94**).

Overall, these methods provided a relatively straight forward way to synthesise fifteen benzimidazoles for exploring the SAR around compound **10** (Figure 2.8). But the library is relatively narrow in scope and it was unfortunate that the other planned 2'-position aryl, 6-

position aryl-coupled and 1-position *N*-methylated analogues could not be synthesised within the timeframe dedicated to this series.

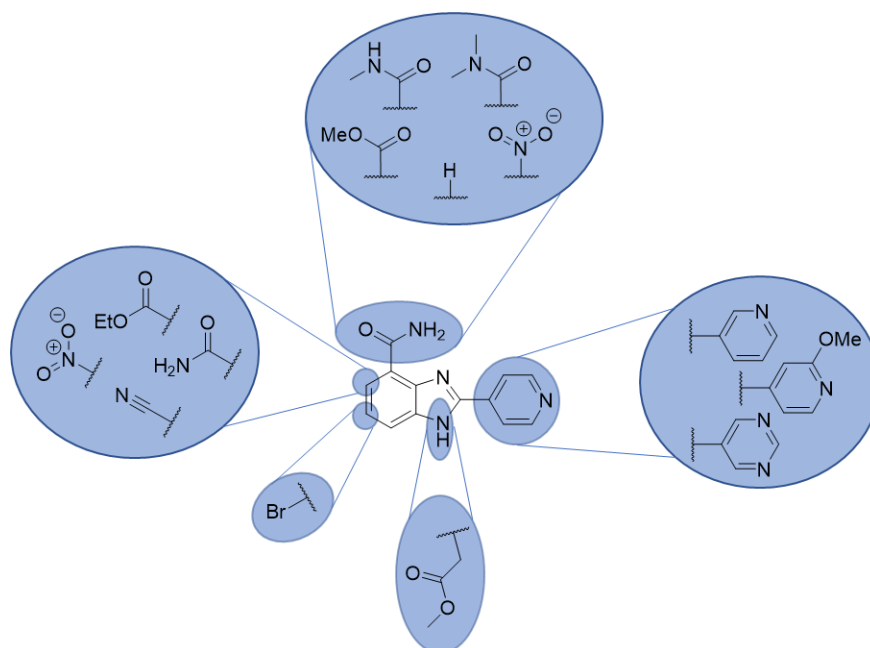


Figure 2.8 Summary of Series A compounds synthesised

2.3 Biological evaluation

2.3.1 TR-FRET

This project is being carried out in collaboration with the Structural Genomics Consortium, who agreed to test the compounds synthesised against PKN1 and PKN2 in a binding-displacement assay using a time resolved fluorescence resonance energy transfer (TR-FRET) assay readout. The assay work described below was carried out by Dr. Angela Maria Fala at the State University of Campinas, Brazil.

The assay is based on the displacement of a fluorescent tracer molecule from the ATP binding site of a kinase (Figure 2.9). When the fluorescent tracer molecule is bound to the kinase there is a TR-FRET signal due to an energy transfer from a europium- or terbium-cryptate FRET donor that is attached to the kinase *via* the high affinity streptavidin-biotin interaction. In the presence of an inhibitor that binds to the same site in the kinase, the TR-FRET signal is non-existent.

Varying concentrations of inhibitors (typically 50 μ M to 0.85 nM over 12 data points) were added to displace the Kinase Tracer 236 (Thermofisher) from the ATP binding site and decrease the FRET signal from Streptavidin bound to the biotin tag in the C-terminal of the kinase. IC₅₀ values are measured for the specific inhibitor and *K_i* values are calculated using the Cheng Prusoff equation¹²⁹ and the previously determined dissociation constant (*K_d*) of the tracer. The IC₅₀ value

is the half-maximal inhibitory concentration.⁸ Staurosporine, a commonly used pan kinase inhibitor,⁹ was used as an assay control.

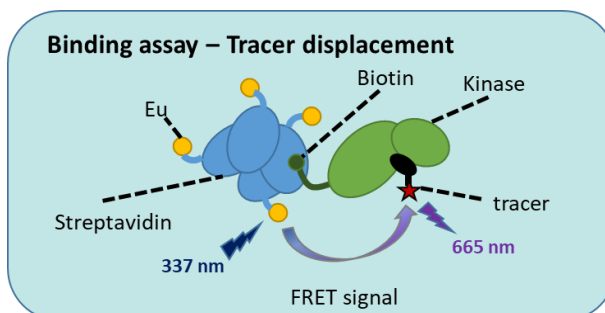
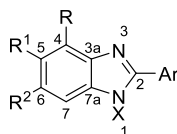


Figure 2.9 Overview of TR-FRET experiment

Two biological replicates of the experiments were carried out in triplicate. The data was normalised to 0–100% inhibition values and fitted to a four-parameter dose-response curve using GraphPad 7 Software (version 7.04). The results of the TR-FRET assay for this series are summarised in Table 2.3. K_i values are given in micromolar concentration (μM).

Table 2.3. Structure activity relationships for benzimidazoles binding to PKN2 and PKN1. Calculated K_i values for PKN2 and PKN1 are shown in μM . The assay Z' factor was $0.7 < Z' < 0.9$; $n = 2$.



#	R	R ¹	R ²	X	Ar	PKN2	PKN1
						K_i (μM)	K_i (μM)
10	CONH ₂	H	H	H	4-py	0.03	0.54
96	CONH ₂	H	H		4-py	2.69	25.9
38	CONH ₂	H	H	H	3-py	8.19	32.5
39	CONH ₂	H	H	H	5-pyrimidine	23.8	67.7
40	CONH ₂	H	H	H	3-methoxy-4-py	6.90	30.2
60	CONHMe	H	H	H	4-py	1.06	5.20
67	CONMe ₂	H	H	H	4-py	19.4	27.8
78	H	CONH ₂	H	H	4-py	8.11	48.8
56	H	H	H	H	4-py	3.85	22.4
82	NO ₂	H	H	H	4-py	1.25	28.9
66	COOMe	H	H	H	4-py	15.6	19.1
77	H	COOEt	H	H	4-py	21.1	27.8
83	H	C≡N	H	H	4-py	2.51	18.9
84	H	NO ₂	H	H	4-py	12.9	53.7
92	CONH ₂	H	Br	H	4-py	0.08	2.19

Benzimidazole **10** was confirmed as an inhibitor of PKN2 (K_i 30 nM) with 18-fold selectivity over PKN1 (K_i 540 nM). Capping the benzimidazole N-H (**96**) resulted in loss of activity. As discussed

previously, this is not as useful a point change as a simple methylated benzimidazole would have given but it potentially suggests that this group is too large for binding or that removing the basicity of that nitrogen is detrimental for bioactivity, or that N-H is needed for binding.

The 4'-pyridyl appears to be the hinge-binding motif of the molecule because exchanging it for the 3'-pyridyl (**38**) or a 5'-pyrimidine (**39**) results in a large drop in the IC₅₀. Similarly, introducing a methoxy-group at the 3-position (**40**) reduced the activity of the compound, likely due to disrupting steric access to the 4'-pyridyl nitrogen.

The primary amide also proved to be an essential component of the compound because the methylated (**60**) and dimethylated (**67**) analogues were less potently active than the original compound (**10**). A crystal structure would assist in determining whether the methyl groups cause steric hindrance with the kinase pocket. A similar result was observed in the analogue that removed the amide altogether (**56**) showing that the carbonyl hydrogen bond acceptor was also required.

The amide was moved to the adjacent 5-position (**78**) and despite this small structural change there was a large loss of bioactivity, likely due to the different conformation of the amide moiety. Similarly, exchanging the amide at the 4-position for a nitro (**82**) or methyl ester (**66**), or an ethyl ester (**77**), nitrile (**83**) or nitro (**84**) group at the 5-position, resulted in loss of activity.

Compound **92** was the only analogue of **10** that had relatively potent inhibition against PKN2. Introduction of a bromine atom at the 6-position was not a significant structural change and resulted in a nearly equipotent compound (K_i 80 nM). That said, a great loss of activity was observed for PKN1 (K_i 2.19 μ M) which meant the compound was 27-fold selective for PKN2 over PKN1, despite the overall loss in potency. The larger size of the bromine atom, in addition to its weak electron-withdrawing effects, must have slightly disrupted the binding mode of the benzimidazole.

2.4 Computational Studies

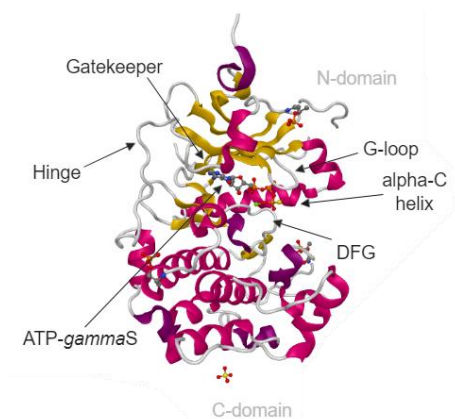


Figure 2.10 Labeled X-Ray Crystal Structure of PKN2 (PDB code 4CRS)

One X-ray crystal structure of PKN2 (Figure 2.10) was deposited in the PDB in 2014 which allowed computational studies to be carried out in order to complement and rationalise the previously discussed biological results. It suggests that ATP- γ -S, an analogue of ATP, interacts with the hinge region of PKN2 *via* two hydrogen bonds: primary amine of the adenine function acting as a H-bond donor to an alanine residue (Ala684) and the 1-nitrogen as a hydrogen bond acceptor with tyrosine (Tyr739).

2.4.1 Benzimidazole kinase ligands in the Protein Data Bank

A search for kinase ligands containing pyridyl benzimidazoles and benzimidazoles was carried out in the PDB and three crystal structures were found (Figure 2.11–2.13) that could be used to hypothesise the binding mode of **10**. The crystal structures were imported into Schrodinger Maestro (version 2018-1)¹³⁰ and prepared using the Protein Preparation application to set parameters such as missing residues.

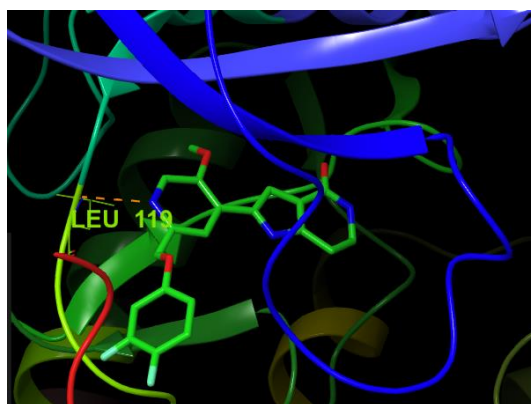


Figure 2.11 Benzimidazole ligand interacting with the hinge region of CK1GS (PDB code 4HGS);

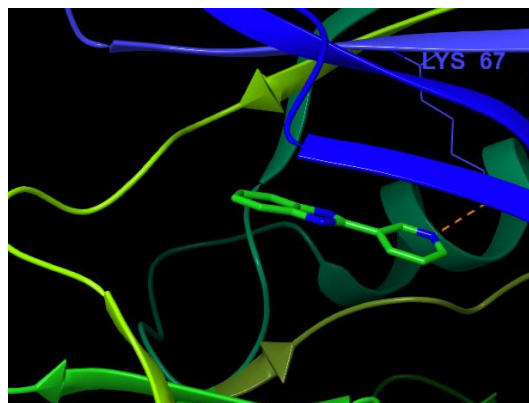


Figure 2.12 Benzimidazole ligand interacting with the hinge region of PIM1 (PDB code 5KGD);

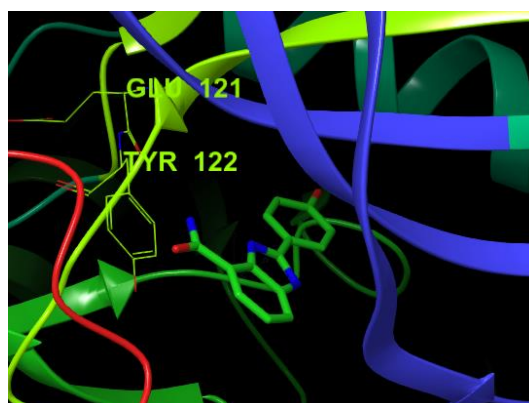


Figure 2.13 Benzimidazole ligand interacting with the hinge region of PKA-S6K1 complex (PDB code 4C35)

Figure 2.11 shows a benzimidazole similar to **10** that binds to a leucine residue (Leu119) within the hinge region of kinase CK1GS through a hydrogen bond between the 4'-pyridyl nitrogen acceptor and an amide N-H donor. In Figure 2.12, a benzimidazole with a 3'-pyridyl function (*cf.* **38** and **56**) does not interact with the hinge of the kinase in structure 5KGD. Instead the 3'-pyridyl nitrogen of the ligand forms a hydrogen bond with the N-H of a lysine residue (Lys67). Figure 2.13 is a crystal structure of a PKA-S6K1 complex with a benzimidazole that contains a primary amide like that of **10**. The amide points towards the hinge region of the kinase, particularly in the direction of a glutamine (Glu121) and tyrosine (Tyr122) residue.

2.4.2 Docking Experiments

All of the aforementioned benzimidazole compounds based around compound **10**, including those that could not be synthesised, were docked into a prepared receptor grid defined in the hinge region of the existing structure of PKN2 (4CRS) using Schrodinger Maestro's Receptor Grid Generator application¹³⁰ by the author. The ligands were prepared in all possible conformations using the Schrodinger LigPrep function. Three docking studies were run with varying levels of constraints added, in terms of hydrogen bonding interactions that had to be met:

1. Ala684 and Tyr739 both interact with the ligand
2. Either Ala684/Tyr739 interact with the ligand
3. No constraints

Only one series A compound was successfully docked into the protein across these three experiments. The 5-amide analogue (**78**) which suggested the amide formed hydrogen bonds with Ala740 and Glu738 (Figure 2.14).

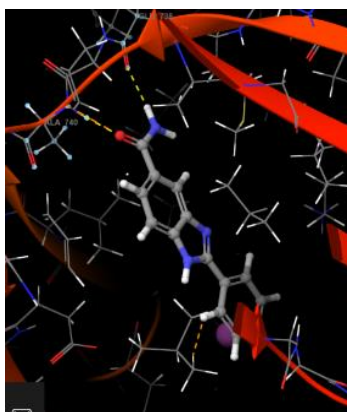


Figure 2.14 PKN2 hinge region interacting with docked 4-pyridyl nitrogen of **1**

This unfortunately does not correlate with biological data as this compound was shown to be relatively inactive compared to **10** and any experimentally potent compounds could not be docked in this particular experiment. Dr. Ben Wahab, a computational chemist, ran repeat docking experiments instructing the compounds to bind with the hinge *via* the 4'-pyridyl and obtained similar results with biologically inactive compounds being docked in the ATP site. Thus, it was deemed that the 4CRS crystal structure was not representative of PKN2 under physiological conditions and these computational chemistry experiments could not add value to the experimental data obtained for the project thus far.

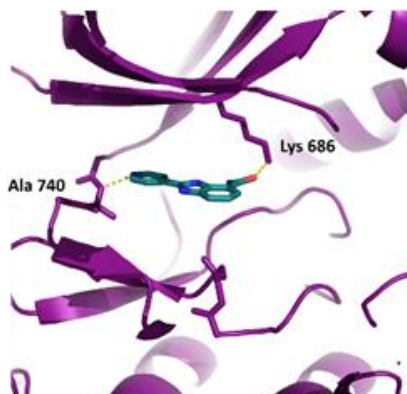


Figure 2.15 Compound **10** docked into PKN2 using MOE software

Further docking experiments carried out by Dr. Angela Maria Fala at the SGC using MOE software successfully docked **10** into PKN2 (Figure 2.15). The binding mode suggests the pyridine portion of the compound interacts with an alanine residue in the hinge region (Ala740) and the primary amide has another key, but different, interaction with a lysine residue (Lys686). This docking experiment was only carried out on a small number of compounds for use in publications associated with this series so it is unclear whether this computational method would have been of use for directing medicinal chemistry efforts if it had been more complementary to the experimental data obtained for this series.

2.5 Chapter 2 Summary

This portion of work focused on optimising benzimidazole **10**, a repurposed PARP inhibitor that showed affinity for PKN2. The compound was re-synthesised using a four-step synthesis and was confirmed as an inhibitor of PKN2 with K_i 30 nM and 18-fold selectivity over PKN1 (K_i 540 nM). Subsequent analogues were prepared to explore SARs between portions of the compound e.g. the primary amide, 4'-pyridyl which were deemed critical for potent binding to PKN2 (Figure 2.16). The necessity of the benzimidazole N-H could not be determined from the analogues synthesised.

In total 15 compounds were isolated and unfortunately none, with the exception of **92** improved on the PKN2/1 selectivity of the original compound (27-fold *cf.* 18-fold). Additionally, attempts to use computer assisted docking did not match experimental data so it was not extensively used to guide chemistry efforts for this series. A short communication of this work has been published in the journal Bioorganic and Medicinal Chemistry Letters.¹⁰⁸

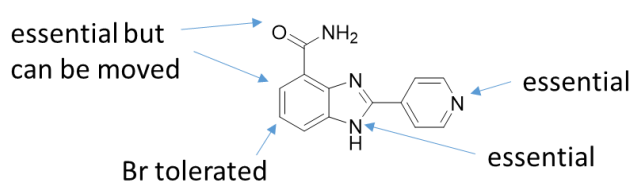


Figure 2.16 SAR summary for Series A based on compound **10**

Chapter 3 Series B – Pyrrolopyridinone

This chapter seeks to outline the work carried out in optimising compound **11**, a pyrrolopyridinone (Figure 3.1). The chemistry used to prepare this compound and other analogues will be discussed as well as the biological evaluation of the inhibitory potencies of those compounds against PKN2 and other kinases. Attempts to rationalise said biological activity using computational studies will also be outlined.

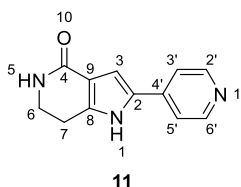


Figure 3.1 Original compound for series B

3.1 Hit Origin

6,7-Dihydro-5H-pyrrolo[3,2-c]pyridin-4-one (**11**) (Figure 3.1) was identified as a potent PKN2 inhibitor ($K_i = 4 \text{ nM}$)¹⁰⁵ via a ChEMBL¹⁰³ data mining effort as described in Section 2.1. It was previously made for research efforts developing inhibitors for various kinases such as CDKs¹³¹⁻¹³⁵ and MK-2.¹⁰⁵ According to the ChEMBL database, it inhibits 22 out of 157 kinases with a K_i less than 100 nM, including PKN2. This reasonable selectivity and high potency made it a good starting point for a developing a more selective PKN2 inhibitor.

The pyrrolopyridinone structure is particularly unusual, exhibited by the observation that none of the current 52 FDA-approved kinase inhibitors possess the core within their structures, although sunitinib (**97**), a multi-receptor tyrosine kinase inhibitor, contains a pyrrole ring (Figure 3.2). Unfortunately, most pyrrole-containing motifs are classified as pan-assay interference compounds (PAINS)¹⁶ due to their tendency to interfere with bioassays because they are easily oxidizable and can act as nucleophiles. Pyrroles also contain a relatively acidic proton ($pK_a \approx 16.5$ ¹¹⁷) which can react with weak basic reagents used in assay protocols. It was hoped that suitable modifications could be made to **11** to improve its properties as a PKN2 chemical probe.

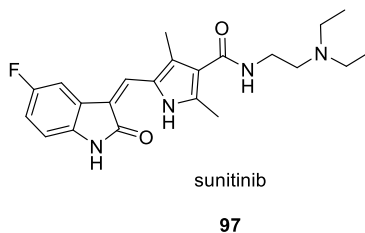
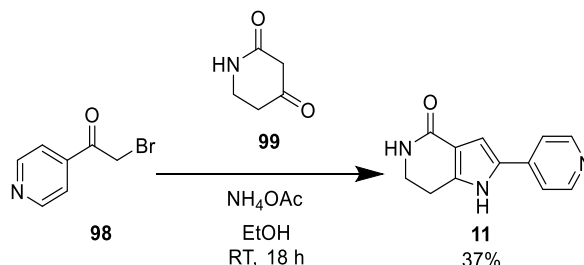


Figure 3.2 Sunitinib (**97**)

Work on this series was carried out in part by a University of Sussex MChem student, Mihaela Paula-Ficu, as part of her dissertation research project.

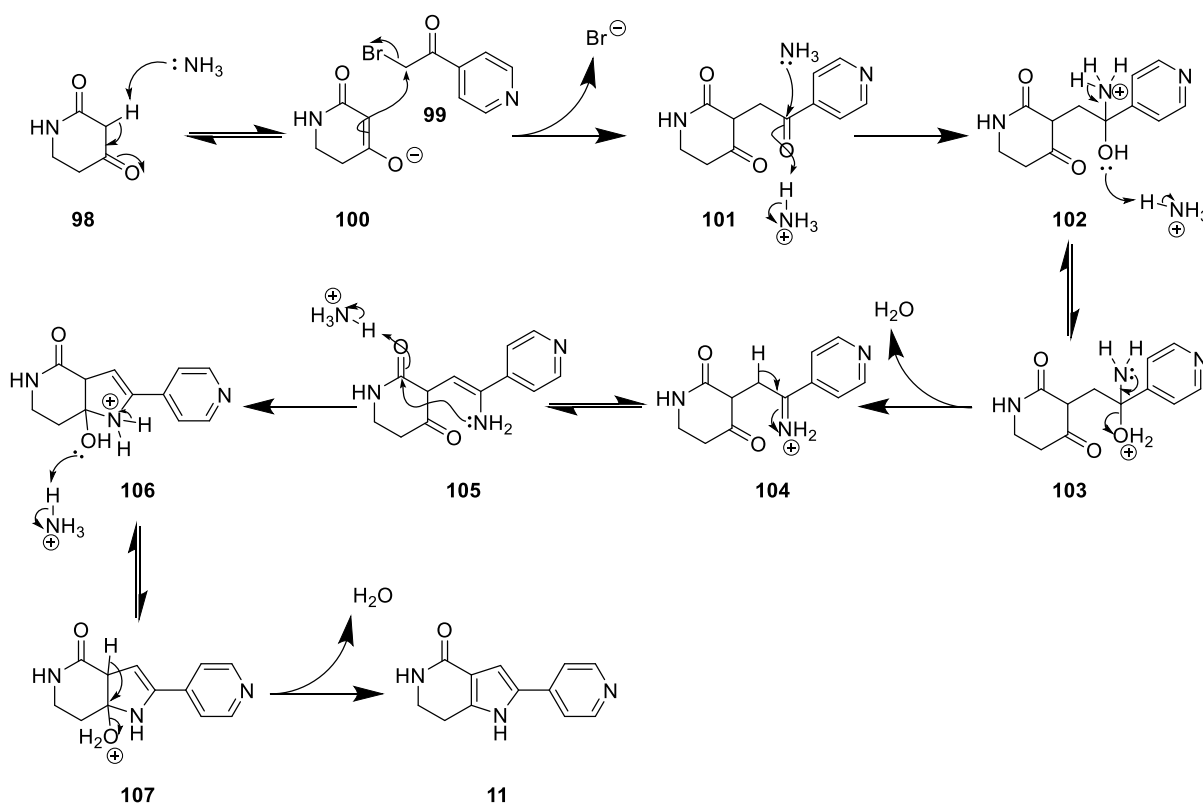
3.2 Chemistry

3.2.1 Synthesis of original hit



Scheme 3.1 Synthesis to **11**

4-(Bromoacetyl)pyridine (**98**) and piperidin-2,4-dione (**99**) were stirred in ethanol with ammonium acetate at room temperature (Scheme 3.1) to make compound **11**. The reaction involves a nucleophilic addition step followed by enamine formation then a dehydration reaction (see Scheme 3.2 for mechanism).



Scheme 3.2 Mechanism for addition condensation step to form compound **11**

First, acetate deprotonates a relatively acidic proton from piperidin-2,4-dione ($\text{pK}_a \approx 10^{136}$) (**98**). The resulting enolate (**100**) attacks **99** via the α -carbon to displace the bromoketone bromine atom to form intermediate **101**. Ammonia then attacks the carbonyl carbon adjacent to the

pyridyl to form charged intermediate **102**. Loss of water from **103** encourages the formation of iminium **104** and subsequent proton exchange yields enamine **105**. Upon activation of the ketone carbonyl by protonation, enamine **105** cyclises at this carbon to form species **107** which, upon loss of another molecule of water, yields pyrrolopyridinone **11**.

While the original procedure¹⁰⁵ stated the reaction would be complete after an hour, it was found that leaving the reaction to stir overnight at room temperature improved the reaction profile, with a higher percentage of the product observed in a sample taken from the reaction mixture by LCMS. Following aqueous work-up and purification, compound **11** was successfully isolated in 28% yield (*cf.* 71% reported yield¹⁰⁵). LCMS indicated a mixture of intermediate **106** and product **11** tended to form. Attempts to improve the conversion to **11** such as changing the solvent; order of addition and/or adding a catalytic quantity of concentrated hydrochloric acid to encourage the loss of water from **106** *via* **107** did not improve on the reaction yield.

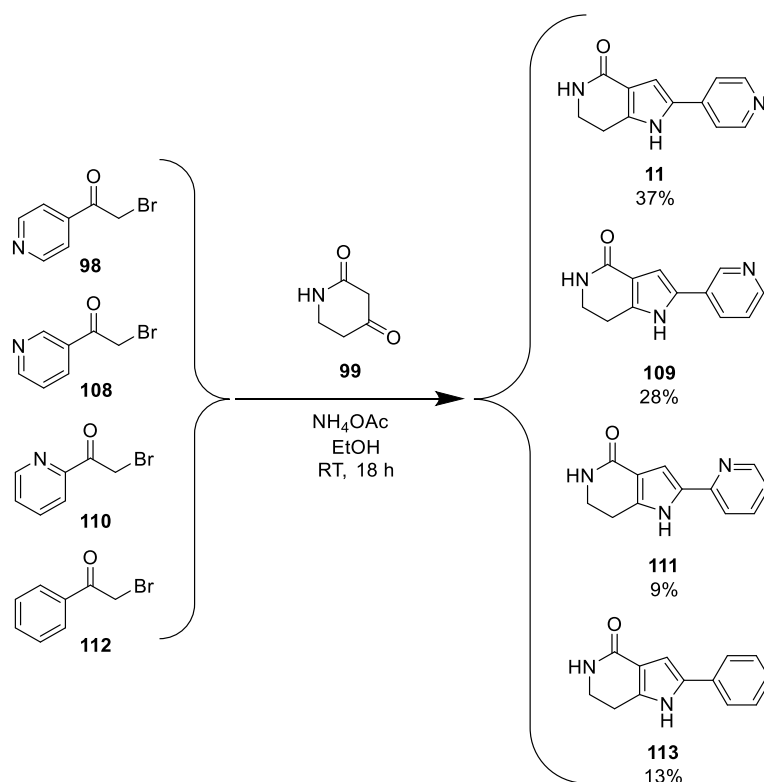
Despite the fairly poor yield for a one-step synthesis, the affordability of the commercial starting materials meant suitable quantities of the product could be isolated if carried out at sufficient scale. The reaction was repeated at 2 g scale to afford 598 mg (37%) of **11** for preparing analogues

LCMS (*m/z* 214) and ¹H NMR confirmed formation of the product. The same pair of doublets in the aromatic region correlate to the 4'-pyridyl ring were observable for **11** as in **10** as well as two broad N-H singlets at δ 11.95 and 7.08 ppm for the pyrrole and amide protons; a sharper singlet at δ 7.00 ppm for the 3-position C-H and two upfield triplet/multiplet peaks each integrating to two protons for the aliphatic protons at the 6- and 7-positions.

3.2.2 Preparation of analogues

Pyridyl variation

The first analogues of **11** that were prepared were variants at the pyridyl portion of the molecule because compound **11** has a similar general shape to benzimidazole **10** and the 4'-pyridyl group was critical for activity in series A. The 3'- (**109**) and 2'-pyridyl (**111**) derivatives were successfully prepared (in 28% and 9% yields, respectively) using the corresponding α -haloketones (Scheme 3.3) (**108** and **110**, respectively). Preparation of the aryl-derivative (**113**) using phenacyl bromide (**112**) enabled the synthesis of **113** in 13% yield.

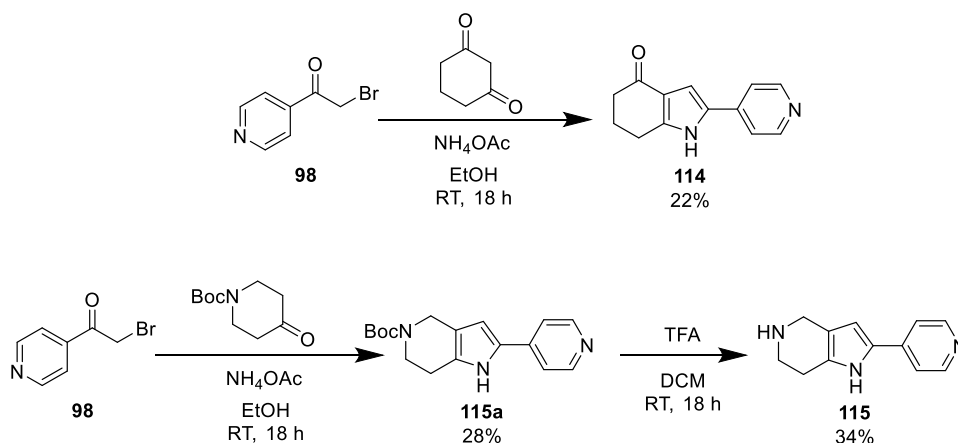


Scheme 3.3 Preparations of pyridyl analogues of 11

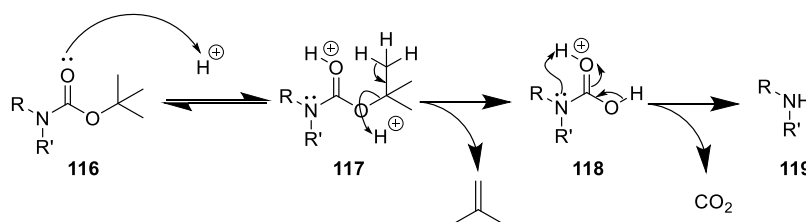
The aromatic regions of the ^1H NMR spectra for these compounds were used to distinguish between the analogues. The aromatic region of the original hit (**11**) contained two doublets due to the symmetrical 4'-pyridyl ring, while **109** had four peaks integrating to four protons in total – a singlet, two doublets and a double doublet. The 2'-pyridyl moiety of compound **111** was identifiable by a doublet and two multiplets with a similar combined integration of four protons and, finally, the phenyl derivative (**113**) had the characteristic doublet and two triplets that represent the five benzene hydrogens.

Lactam variation

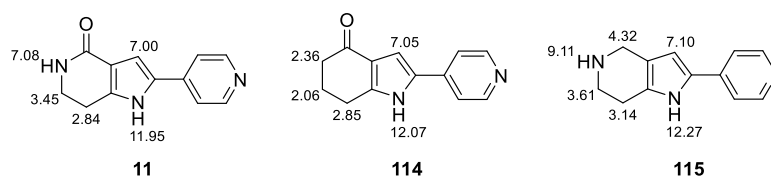
It was possible to modify individual components of the amide by exchanging piperidin-2,4-dione for 1,3-cyclohexanedione and *tert*-butyl 4-oxopiperidine-1-carboxylate to produce the cycloketone (**114**) and cyclo-amine (**115**), respectively (Figure 3.3).

Scheme 3.4 Syntheses to compounds **114** and **115**

Typical Boc-deprotection conditions were used to give **115** by stirring the protected analogue of the compound (**115a**) in trifluoroacetic acid (TFA) (see Scheme 3.5 for mechanism). Activation of the carbamate carbonyl oxygen of **116** by acidified protonation encourages the loss of a proton from the *tert*-butyl group of **117**. This subsequently triggers the loss of isobutene from **117** and carbon dioxide from **118** to yield the unprotected amine (**119**).¹¹⁷

Scheme 3.5 Boc deprotection mechanism¹¹⁷

Alongside expected changes in the mass observed in the LCMS and HRMS spectra, ¹H NMR was used to confirm the structural changes from the lactam in **11** to the ketone (**114**) and cyclic amine (**115**) (Figure 3.3).

Figure 3.3 Structures of compounds **11**, **114** and **115** with selected ¹H NMR chemical shift values highlighted in ppm

The loss of the amide N-H peak at δ 9.11 ppm from the ¹H NMR spectrum for **11** indicated that only the C=O was present in **114**. Similarly, the appearance of a new aliphatic C-H peak integrating to two hydrogens at δ 4.32 ppm in the ¹H NMR confirmed the removal of the nitrogen in **114**. An additional peak was also observed in the ¹³C NMR spectrum which corresponds to the additional carbon atom.

When characterising compound **115**, a lack of C=O peaks in the IR spectra and ^{13}C NMR were observed. Additionally, the N-H peak in the ^1H NMR shifted from δ 7.08 to 9.11 ppm and a new peak was present at δ 2.36 ppm which correlated to the other aliphatic hydrogens (by COSY NMR) confirmed the isolation of compound **115** as a TFA salt.

Alkylation of pyrrole

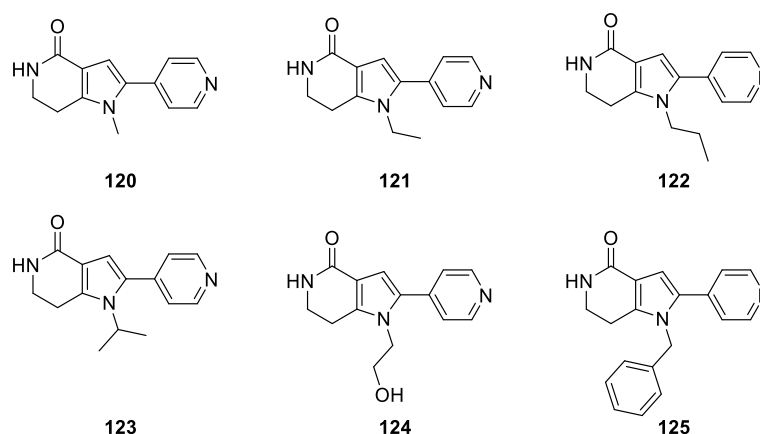
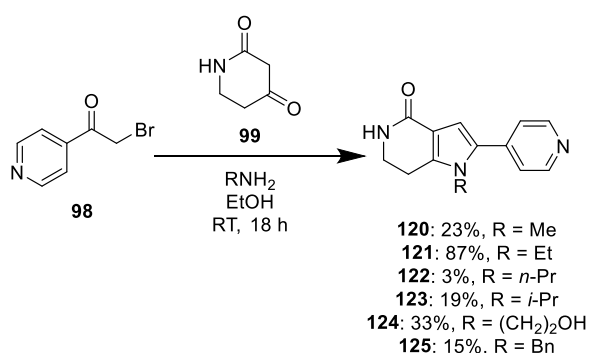


Figure 3.4 Alkylated analogues 120–125 prepared in Series B library

Replacing ammonium acetate with an alkyl amine enabled simple alkylation of the pyrrole N-H (Scheme 3.6) without having to carry out traditional alkylation reactions with air-sensitive agents such as sodium hydride.¹³⁷ Methyl (**120**), ethyl (**121**), *n*-propyl (**122**) and *i*-propyl (**123**) groups were easily introduced to cap the N-H from their respective amines, either added neat or in combination with acetic acid in order to mimic the ammonium acetate used to prepare compound **11**.



Scheme 3.6 Synthesis to compounds 120-125

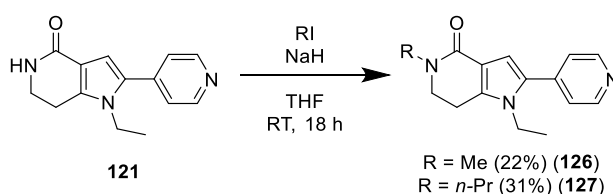
Additional peaks in the higher end of the aliphatic region of ^{13}C and ^1H NMR spectra were used to confirm the incorporation of the alkyl groups, as well as an expected increase in molecular weight observed by LCMS. In all cases, the N-H peak observed at δ 11.95 in the ^1H NMR spectrum for **11** disappeared due to a lack of hydrogen present at that 1-position nitrogen.

Similarly, it was possible to introduce a terminal alcohol (**124**) by using ethanolamine. A new peak was observed at δ 4.98 in the ^1H NMR spectrum due to the hydroxyl proton present in the molecule.

In order to observe the effect of incorporating a bulky aromatic group into the compound, benzyl amine was used to make compound **125**. Three new peaks were observed in the aromatic region at δ 7.32, 7.25 and 7.15 ppm collectively integrating to the five protons present in the benzyl group, as well as a new peak in the aliphatic region integrating to two protons at δ 5.05.

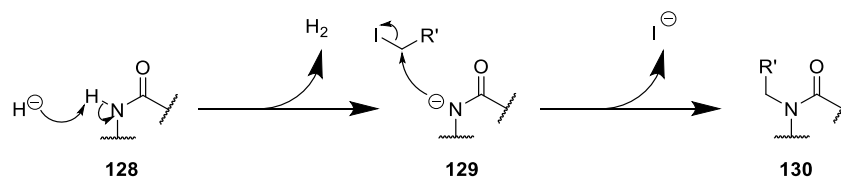
Alkylation of lactam

It was also possible to further alkylate the amide portion of **121** by using a combination of sodium hydride and alkyl iodides to produce the methyl- (**126**) and *n*-propyl-capped (**127**) amides, respectively (Scheme 3.7).¹³⁸ ^1H NMR confirmed alkylation at this centre because the amide N-H peak at δ 7.08 disappeared and new aliphatic peaks appeared corresponding to their respective methyl and *n*-propyl moieties.



Scheme 3.7 Alkylation conditions used to synthesise compounds **126** and **127**¹³⁸

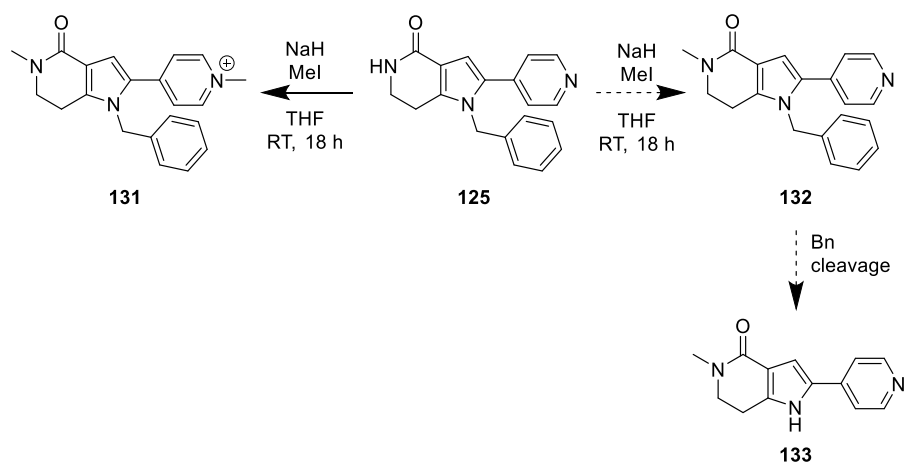
Scheme 3.8 outlines the mechanism of this chemical transformation. The hydride anion deprotonates amide **128** which allows resulting nucleophile **129** to attack the alkyl halide's α -carbon displacing the iodide *via* a $\text{S}_{\text{N}}2$ mechanism. This converts the secondary amide to a tertiary amide (**130**).



Scheme 3.8 Alkylation mechanism involving sodium hydride and alkyl halides

The same chemistry was deployed to try and synthesise a derivative of **11** with a free pyrrole N-H and a methylated amide (**133**) (Scheme 3.9) by methylating **125** to form **132** and then remove the benzyl group to yield the free pyrrole (**133**). Similar to the issues experienced with alkylation reactions for series 2 in section 2.2, carrying out this reaction produced a product with m/z 332 $[\text{M} + \text{CH}_3]^+$, instead of m/z 318 $[\text{M} + \text{H}]^+$. This was presumed to be the methyl iodide reacting at

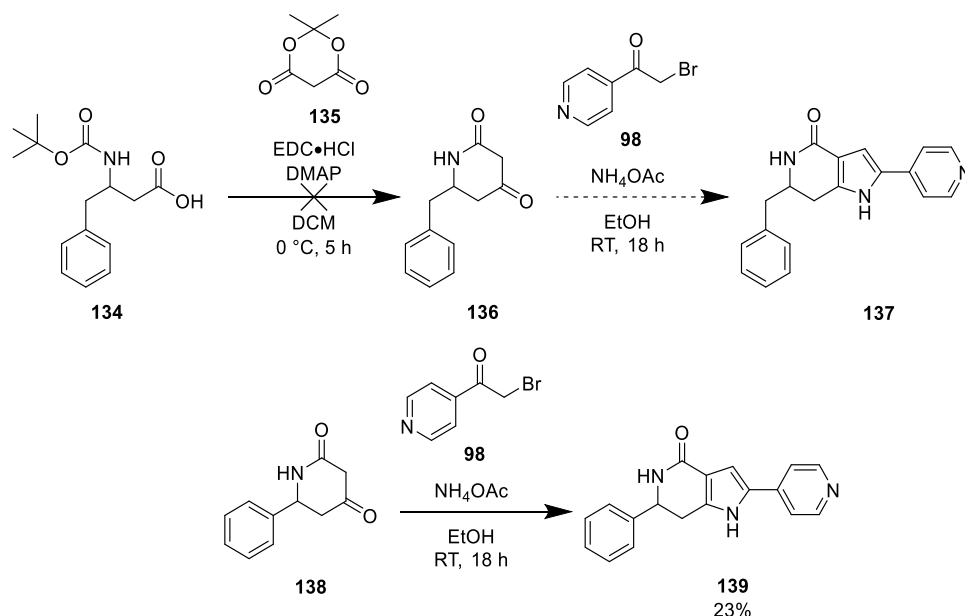
the 4'-pyridyl nitrogen as well as the amide (**131**). Care was taken to ensure stoichiometric quantities of sodium hydride and methyl iodide were slowly added at low temperature but after multiple attempts, this analogue was abandoned due to time constraints to focus on other aspects of the project.



Scheme 3.9 Attempts to alkylate the lactam N-H of **125**¹³⁸

Additional ring systems

Simultaneous attempts were made to introduce a benzyl or phenyl group at the 6-position of the lactam ring with varying success (Scheme 3.10). 3-(*Tert*-Butoxycarbonylamino)-4-phenylbutanoic acid (**134**) was combined with 2,2-dimethyl-1,3-dioxane-4,6-dione (**135**) using *N*-(3-dimethylaminopropyl)-*N'*-ethylcarbodiimide hydrochloride (EDC·HCl) as a coupling agent¹³⁹ to produce compound **136**, but this reaction was abandoned because the product could not be sufficiently purified and the latter, phenyl-containing analogue (**138**) was successfully isolated by another method which was being carried out in parallel.



Scheme 3.10 Chemistry used to incorporate an additional aromatic group at the 6-position^{105,139}

More success was had using the phenyl-containing equivalent, commercially available 6-phenylpiperidine-2,4-dione (**138**) using the original chemistry route,¹⁰⁵ and **139** was isolated in 23% yield. The disappearance of one of the four aliphatic C-H peaks, replaced by three additional peaks in the aromatic region in the ¹H NMR, confirmed the isolation of **139**. The benzyl analogue (**137**) was not reattempted because **139** was deemed a suitable match pair for **11** that had an additional aromatic ring incorporated into its structure at that particular vector. If the compound had particularly promising bioactivity, synthesis of the single enantiomers would have been attempted, but this was not the case.

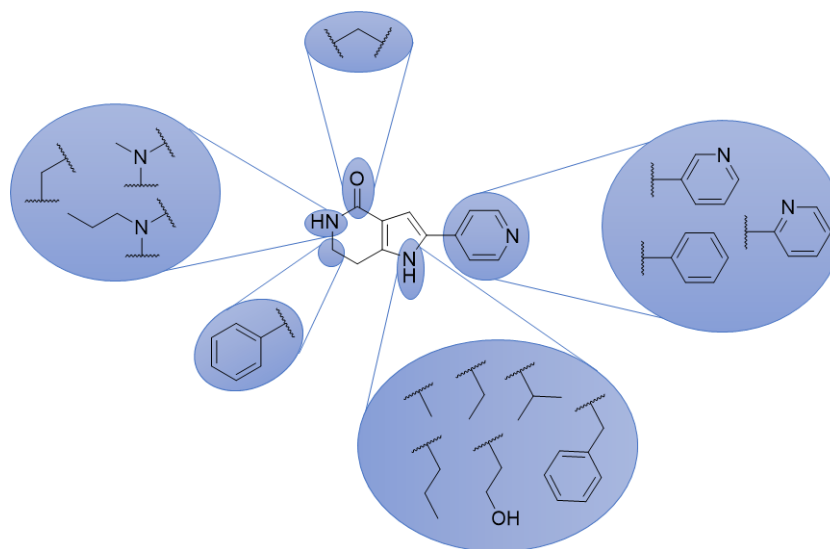


Figure 3.5 Summary of SAR explored around compound **11**

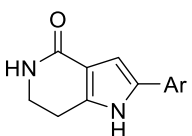
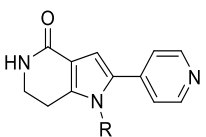
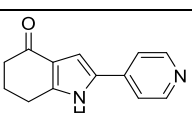
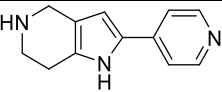
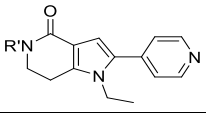
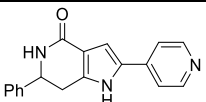
In total, fourteen analogues of **11** were prepared (Figure 3.5). It was possible to remove portions of the amide, manoeuvre the pyridyl nitrogen, as well as remove the pyridyl nitrogen all together. The pyrrole and amide nitrogen atoms were capped with various small alkyl groups, and it was also possible to introduce additional benzyl and phenyl groups at the 1- and 6- positions respectively.

3.3 Biological evaluation

3.3.1 TR-FRET

The compounds were sent for biological evaluation at the SGC using the TR-FRET assay previously described in Section 2.3. Table 3.1 summarises the calculated K_i values for PKN1 and 2. K_i values were calculated as before using the Cheng-Prusoff equation.¹²⁹

Table 3.1 TR-FRET bioanalysis of series B compounds for PKN2 and PKN1 with calculated K_i nM potency; Z value > 0.70 < 0.90; n = 2

Structure			PKN2	PKN1
			<i>K_i</i> (nM)	<i>K_i</i> (nM)
Ar				
11		4-py	8	156
109		3-py	1616	10267
111		2-py	45120	144757
113		Ph	62225	16487
R				
120		Me	129	2275
121		Et	8	108
122		<i>n</i> -Pr	7	64
123		<i>i</i> -Pr	73	922
124		(CH ₂) ₂ OH	15	222
125		Bn	323	1529
R'				
114		-	33	653
115		-	1123	10140
126		Me	178	4780
127		<i>n</i> -Pr	1296	14125
139		-	27	260

Compound **11** was confirmed as an inhibitor of PKN2 with $K_i = 8$ nM against PKN2 and 20-fold selectivity over PKN1. An ideal molecule should have at least 30-fold selectivity over other kinases, so this was a promising start to have this level of selectivity in the original compound⁴

Much like series 2, altering the 4'-pyridyl by either moving (**109/111**) or removing (**113**) the nitrogen resulted in the largest loss of potency across the series. This suggests the hinge region of the kinase specifically interacts with this portion of the molecule.

When the pyrrole N-H bond was replaced by a *N*-methyl group (**115**), there was a 16-fold decrease in potency for PKN2. However, when an ethyl (**121**) or *n*-propyl (**122**) group was added, these compounds were equipotent with **11**; however there was a decrease in selectivity between PKN2/PKN1 – 14-fold and 9-fold for compounds **121** and **122**, respectively. This suggests that the pyrrole N-H is not as well tolerated in PKN1 and is not essential for binding in PKN2 either. Removing this hydrogen bond donor increases the compounds' affinities for PKN1 which is undesirable for a PKN2 chemical probe within the context of this project.

As the substituent became bulkier, this effect was lost: the isopropyl (**123**) and benzyl (**125**) analogues resulted in 9-fold and 40-fold less potent compounds, respectively.

Extending the hydrogen bond donor by replacing the ammonia source with ethanolamine (**124**) halved the potency of the compound, and slightly reduced the selectivity between PKN2/PKN1 from 20-fold to 15-fold.

Removing the carbonyl group from the amide (**115**) resulted in 140-fold loss in potency. This indicates the hydrogen bond acceptor forms a more important interaction within PKN2 than the hydrogen bond donor with regards to the amide N-H portion of **11**. On the other hand, removing the amide N-H (**114**), only resulted in a negligible 4-fold loss of potency towards PKN2, but held the 20-fold selectivity between PKN2 and PKN1.

Capping the amide and pyrrole nitrogen atoms (**126** and **127**) resulted in larger losses of potency. This dissuaded any further attempts to build off that particular vector because this structural change was detrimental to the compound's ability to bind to PKN2.

Introducing the additional phenyl group (**139**) resulted in a slight 3-fold reduction in potency for PKN2 and effectively halved the selectivity of the compound between PKN2/1 to 10-fold, down from 20-fold. This implies that the bulky phenyl group can be accommodated within the PKN2 pocket.⁴

In summary, it was possible to synthesise two equipotent PKN2 inhibitor analogues (**121** and **122**) with PKN2 K_i values matching that of **11**. However, the selectivity of 20-fold between PKN2 and PKN1 for **11** could not be improved upon in compounds **121** and **122**. All other compounds resulted in loss of potency. Attempts to remove hydrogen bond donors and acceptors generally resulted in loss of potency and selectivity, most notably altering the 4'-pyridyl portion of the compound, suggesting this is where the compound interacts with the hinge of the kinase.

3.3.2 Kinome Selectivity Evaluation

Due to the promising *ca.* 18-20-fold PKN2/1 selectivity of analogues **114** and **121**, these two compounds were sent for wider kinome selectivity analysis by the commercial Thermo Fisher Scientific SelectScreen Kinase Profiling Service. The compounds are dosed at a single 1 μ M dose in a LanthaScreen™ Eu Kinase TR-FRET Binding Assay (Figure 3.6) across a selected panel of kinases.¹⁴⁰ The 50 kinase panel used was mostly composed of other AGC kinases and particularly undesirable off-target kinases such as GSK3 β which is involved in energy metabolism and neurological processes.¹⁴¹

Briefly, an ATP-competitive Alexa Fluor™ tracer, is attached to the kinase of choice. This conjugate binding is detected by the addition of a europium-labelled anti-tag antibody. The interaction is observed by a resulting FRET signal. When the tracer is displaced by a more competitive inhibitor, there is a reduction in this signal readout.¹⁴⁰

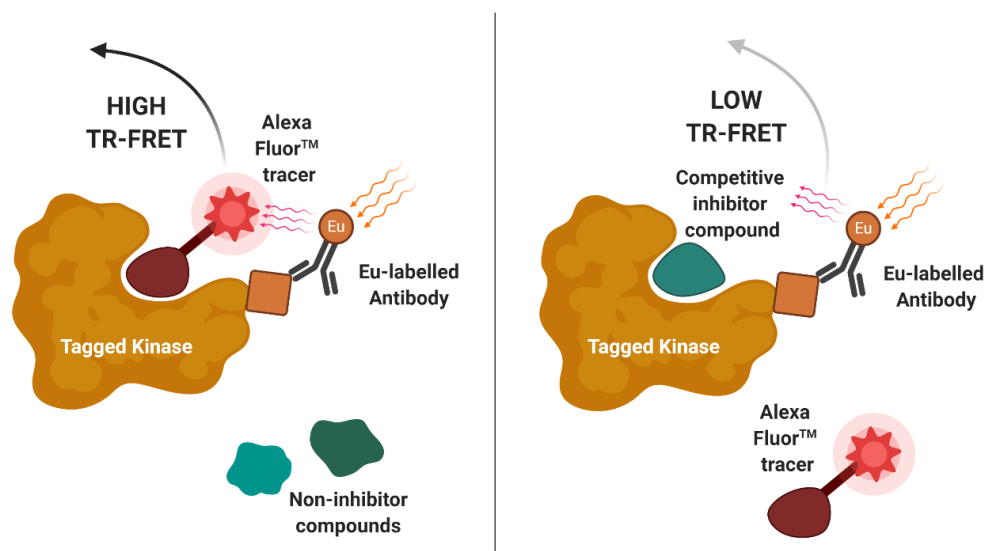


Figure 3.6 Overview of TR-FRET LanthaScreen™ Eu Kinase Binding Assay¹⁴⁰

Figure 3.7 and Figure 3.8 show % inhibition values for those 50 kinases for compounds **114** and **121** dosed at 1 μ M. Compound **114** was shown to inhibit 6/50 kinases above 75%, with PKN2

ranking the highest in terms of potency, along with CDK8, GSK3 β , PRKG2, STK17A and DYRK1A. It also inhibited three other kinases above 50% (MINK1, ROCK1 and RIPK2) (Figure 3.7).

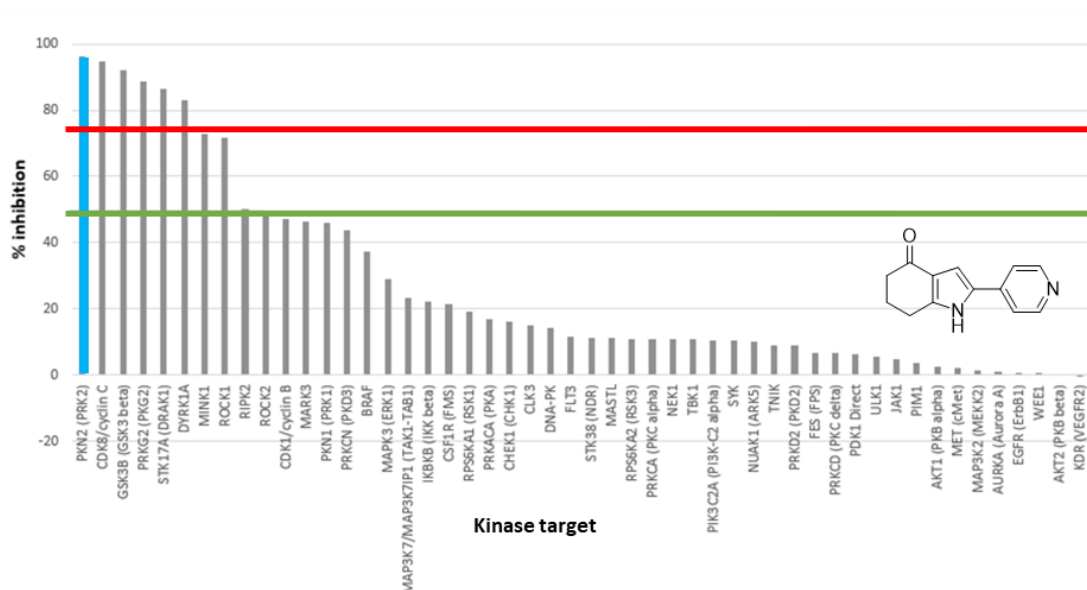


Figure 3.7 Bar graph of SelectScreen kinase panel targets against % inhibition for compound 114 assayed at 1 μ M

On the other hand, compound **121**, the ethylated analogue of **11**, was more selective. It inhibited five kinases (CDK8, GSK3 β , PKN2, PRKG2 and STK17A) above 75% and two others, DYRK1A and MINK1 \geq 50%. While PKN2 is not the most inhibited target by compound **121** – in this case it is CDK8 – the same kinases appear in the top tier of targets inhibited by both compounds (Figure 3.8).

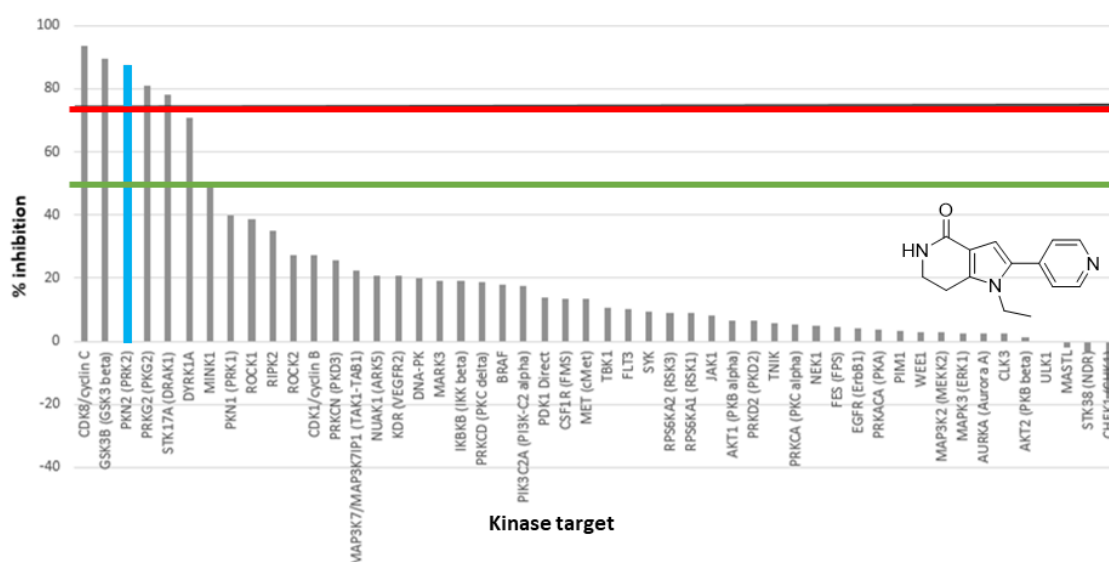


Figure 3.8 Bar graph of SelectScreen kinase panel targets against % inhibition for compound 121 assayed at 1 μ M

This drop in potency across the majority of targets for **121** is thought to be due to the loss of the pyrrole N-H hydrogen bond donor. While this did not prove to be useful for achieving PKN2/1 selectivity, at least across this particular kinase panel, it had a more dramatic effect in reducing potency across the wider kinome.

The original compound (**11**) and the 1-*N*-methylated analogue (**120**) were also sent for wider kinome selectivity analysis *via* the commercial KINOMEScan® panel provided by DiscoverX. At the time of testing (Q4 2018), the KINOMEScan®¹⁰⁷ panel was composed of 469 kinases, comprised of 400 wild types and 69 mutants. This number has since increased to 489 kinase targets and it provides a good indicator of how the compound behaves across around 80% of the human kinome. The full results from this kinase panel can be found in the Appendix 1.

The experiment involves a competition binding-assay (Figure 3.9). Firstly, DNA-tagged kinases are mixed with test compound and a known ligand immobilised on a solid support. After equilibration, the solid support is washed to remove unbound kinase. Test compounds that bind to the kinase compete with the immobilised ligand and if sufficiently potent and present at high enough concentration are able to prevent kinase binding to the immobilised ligand. This reduces the quantity of kinase on the solid bead support. If a compound does not bind well to a kinase, that kinase remains on the solid support. qPCR is then used to quantify the associated DNA-label of the kinases left on the support. A “hit” compound is defined as one where the kinase level remaining is lower than that of the DMSO control sample.

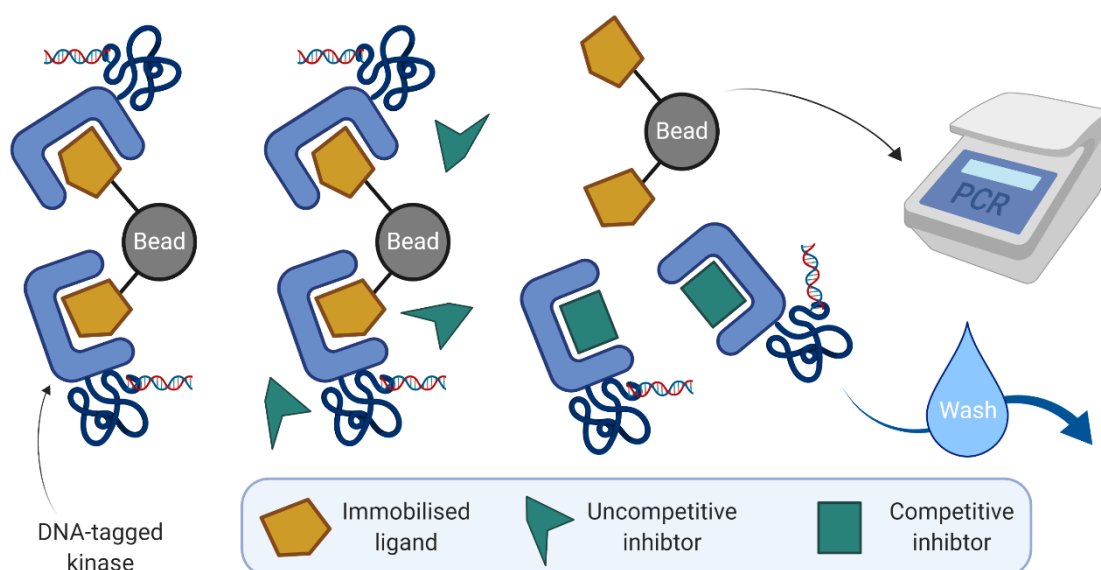


Figure 3.9 Overview of KINOMEScan® Competitive Binding Assay using DNA-tagged Kinases¹⁴²

Compound **11** was shown to bind relatively potently (i.e. > 70%) to 20 out of the 400 wild-type kinases while **120** was similarly selective, inhibiting 19 kinases to the same extent. Figure 3.10 summarises these data for compounds **11** and **120**.

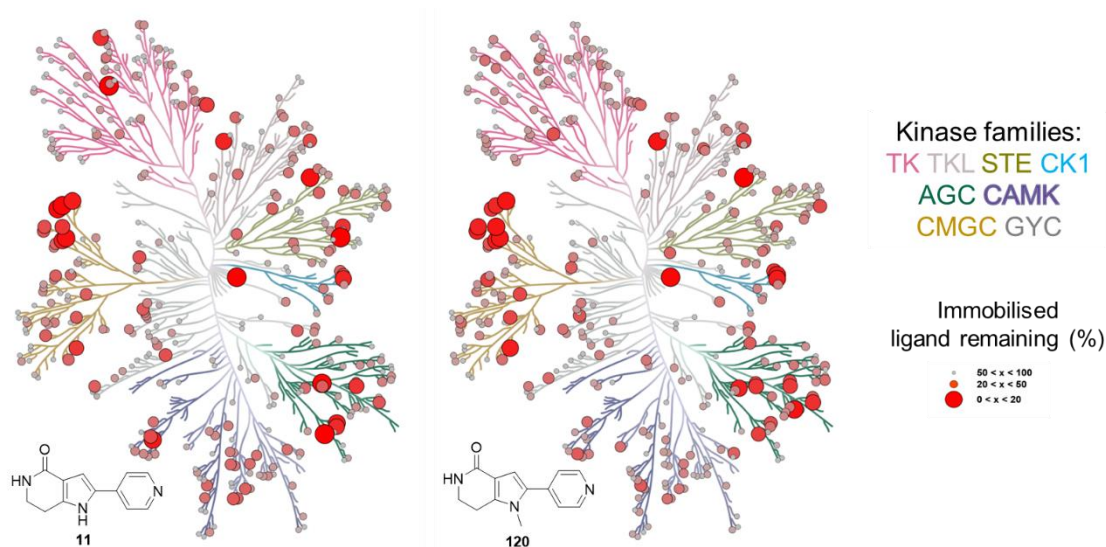


Figure 3.10 Labelled phylogenetic kinome trees highlighting the remaining % of immobilised ligand on each kinase for compounds **11** (left) and **120** (right) assayed at 1 μ M in KINOMEScan[®] experiment. Kinase sub-family classifications are colour coded.

Alkylating the pyrrole N-H (**120**) appears to reduce potency for tyrosine kinases (TK, in pink); CAMK kinases (purple); and ROCK kinases within the AGC kinase family (green). See the kinome phylogenetic trees in Figure 1.11 and Figure 1.12 for sub-classes within kinase families.

Generally, compounds **11** and **120** inhibit PKN2 and a few other AGC kinases (green), such as the PKC sub-family. This is understandable given the structural similarity of these kinases. The compounds also inhibit some CK1 kinases (blue), STE kinases (olive), CMGC kinases (mustard), in particular, the DYRK sub-family, and non-classified kinases like FLT3 (centre of the tree). Figure

3.11

and

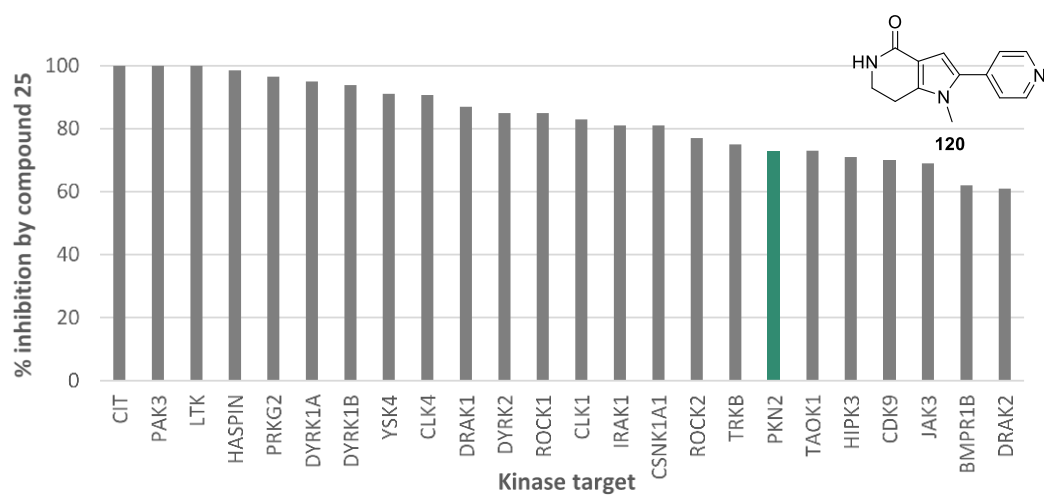


Figure 3.12 detail the 24 kinase targets inhibited the most by compounds **11** and **120**, including PKN2.

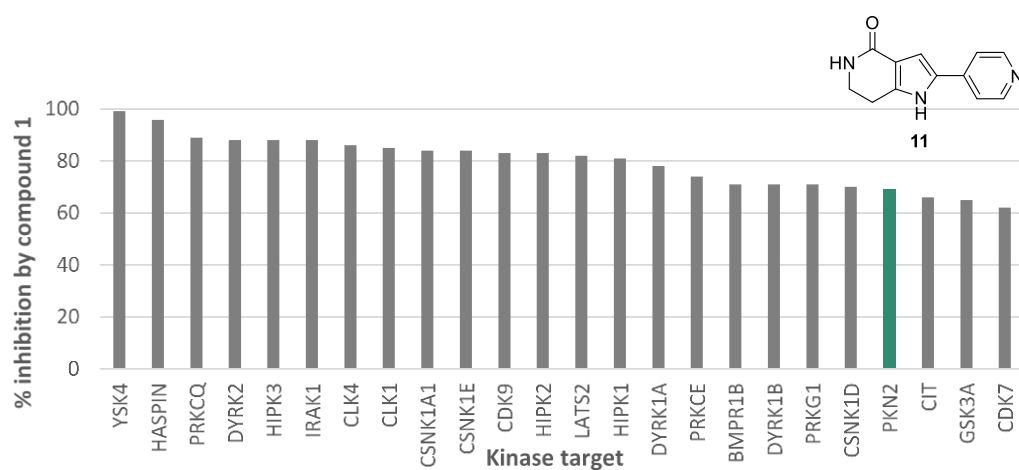


Figure 3.11 Bar graph showing where PKN2 sits in the top 24 kinases inhibited by compound **11** in the DiscoverX KINOMEscan® experiment assayed at 1 μ M

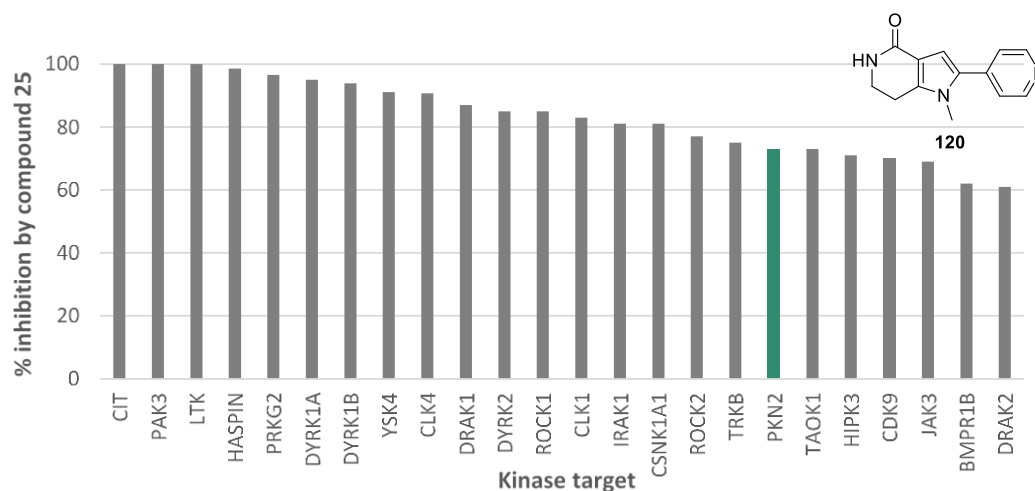


Figure 3.12 7 Bar graph showing where PKN2 sits in the top 24 kinases inhibited by compound 120 in the DiscoverX KINOMEscan® experiment assayed at 1 μ M

The change in kinome selectivity is too small to say that the capping of the N-H significantly changes the selectivity profile of the compound, as there are often false positives in these single point experiments. Hits are usually confirmed by carrying out further K_d experiments on a selected number of targets. Such experiments were not carried out for compounds **11** and **120** in this series because they were not deemed the most selective compounds in this overall work (see Chapter 4). That said, it was encouraging to see that these two compounds only affect around 5% of the human kinome potentially in this effort to find a selective probe for PKN2.

3.4 Computational chemistry

3.4.1 Pyrrole-containing ligands in the Protein Data Bank

There is one example of compound **11** bound to a kinase in the PDB (Figure 3.13). Crystal structure 4F9B suggests that the 4'-pyridyl of **11** points towards a tyrosine residue (Tyr136) within the hinge region of cyclin-dependent kinase 7 (CDK7). It also shows the lactam oxygen interacting with a neighbouring lysine residue (Lys90). This binding conformation agrees with the experimental data for **11** against PKN2 that shows the largest loss of potency across the series was when the 4'-pyridyl motif was altered, suggesting this interaction is key for binding. CDK7 is one of the targets shown to bind to **11** in Figure 3.11.

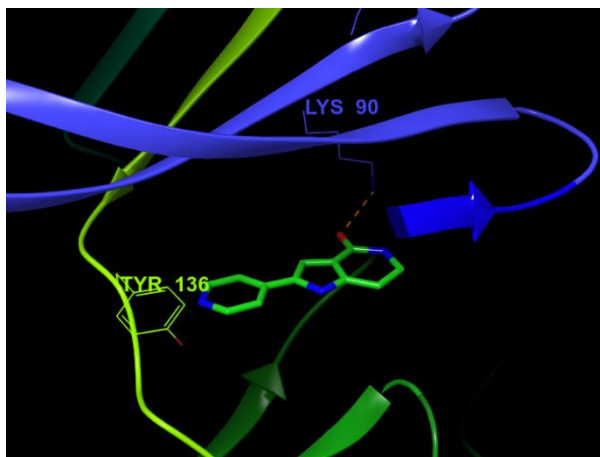


Figure 3.13 Crystal structure of compound **11** in CDK7 (PDB code 4F9B). Image prepared using Schrodinger Maestro (v 2020.1). PKN2 hinge in yellow, N-domain in blue.

3.4.2 Docking Experiments

Single Target Docking

The majority of synthesised series B compounds along with a series of hypothetical derivatives were docked into PKN2 as previously described in section 2.4 by the author. The 2'-pyridyl analogue (**111**) and the ethylated derivative of the same compound (**140**) (Figure 3.14) were the only two of the compound set that were successfully docked into PKN2 with the two previously described binding constraints enforced. No compounds docked with one or no constraints were applied.

Both compounds were shown to interact with the hinge region of PKN2 *via* the lactam moiety (Figure 3.15), as seen for Series A in the previous chapter. This does not correlate with the TR-FRET data as **111** was shown to be over 5000-fold less potent than compound **11**. Additionally, compound **114** which contained a ketone instead of a lactam showed potency towards PKN2 so this does not explain that retainment of potency.

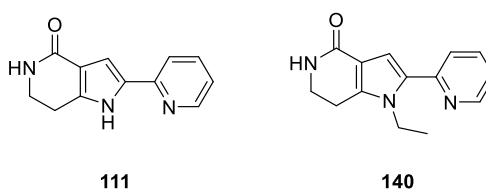


Figure 3.14 Series B analogue compounds successfully docked into PKN2

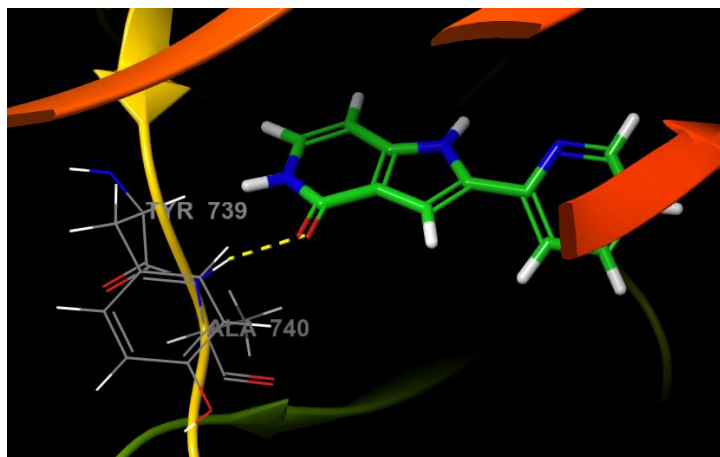


Figure 3.15 PKN2 hinge region interacting with lactam of compound 111

Multi-Target Docking

After analysing the KINOMEScan[®] selectivity data regarding compounds **11** and **120**, the two compounds were applied to a cross docking experiment using the XGlide application in Schrodinger (version 2019.1).^{130,143} Cross docking involves docking one compound against multiple targets rather than the more common docking experiments involving multiple compounds docked into a single protein. The proteins, ligands and receptor grids were prepared using the same methods as described previously in chapter 2. Two studies were carried out:

1. Compounds **11** and **120** were docked into the binding pockets of a selection of physiologically relevant kinase crystal structures (PI3Ka, ROCK1, GSK3, VEGFR2, JNK1, p38, AurA, MELK, FLT3, PKN2) that were structurally similar to PKN2 – as evaluated by a BLAST protein sequence alignment.
2. Compounds **11** and **120** were docked into a selection of physiologically relevant kinase crystal structures (CHEK2, RSK1 (Kin. Dom.1-N-terminal), LIMK1, CDK2, FAK, PIK3CA (H1047Y), PAK6, MET (M1250T), PIM2, MELK, ERK5/MAPK7, KIT (L576P)) from the DiscoverX KINOMEScan[®] panel that all six compounds (two from series B, four from series C) inhibited above 90%.

A full list of the crystal structures used can be found in Appendix 2. The outcome of the docking experiments across the 24 targets as well as the motif of the compound that interacted with the hinge of the respective kinases were logged and summarised in the pie charts below (Figure 3.16 and Figure 3.17). For the original compound (**11**) (Figure 3.16), there was a roughly equal number of poses where the compounds orientated either the 4'-pyridyl or the lactam portion of the compound towards the hinge, which does not provide a convincing hypothesis for either binding mode. It may be that these two hinge motifs mean the compound has multiple binding

conformations. This contradicts the experimentally observed TR-FRET data, which suggests the pyridyl is far more important for binding than the lactam.

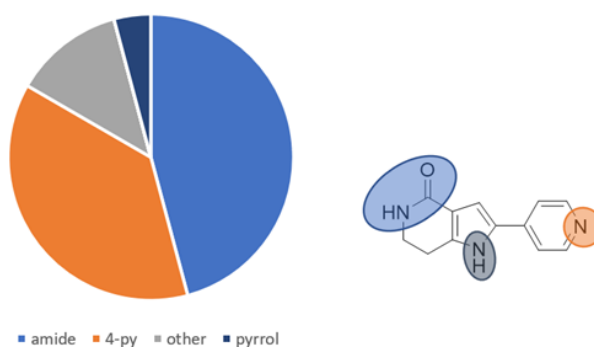


Figure 3.16 Distribution of binding modes in cross docking experiment with compound 11

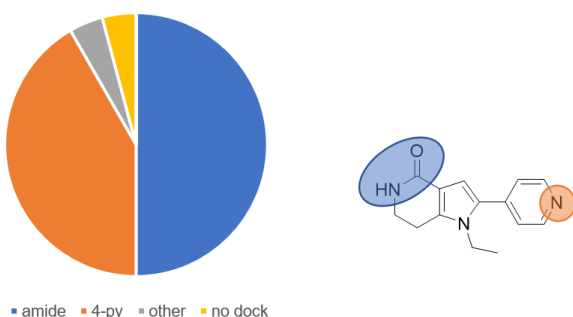


Figure 3.17 Distribution of binding modes in cross docking experiment with compound 120

These inconclusive results suggest using computational methods to justify the binding hypothesis of this set of compounds is not a suitable method to use for this series because of the ambiguous binding modes that the compound can adopt *via* the lactam or 4'-pyridyl. Experimentally, removal of the amide portion of compound **11** was less detrimental to binding compared to the 4'-pyridyl.

Unfortunately, the Glide dock used to rationalise the experimental data did not match up with that observed in the TR-FRET assay. Removing one of the hydrogen-bond forming motifs from the compound resulted in loss of potency and selectivity, so it was not possible to force the compound to bind in a single conformation in order to achieve selectivity within the kinase. As a result, docking experiments across PKN2 and other kinases give ambiguous binding poses because the compound set contains multiple functional groups that mimic ATP in a kinase active site.

3.5 Chapter 3 Summary

Fifteen compounds were successfully synthesised in series B, based on a previously developed MAPK inhibitor (**11**) that showed high affinity for PKN2 (Figure 3.18). Compared to series A, this

series of pyrrolopyridinones proved to be a more promising set of compounds in terms of their potency and selectivity towards PKN2, PKN1 and the wider kinome.

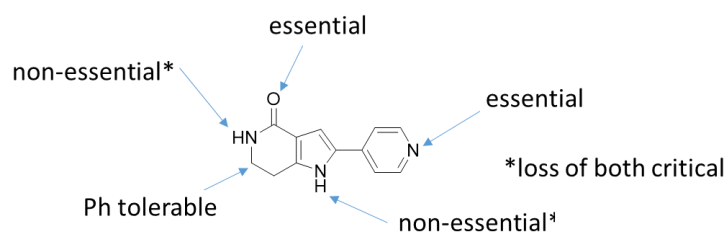


Figure 3.18 SAR explored around compound 11. *Indicates loss of both amide N-H and pyrrole N-H results in loss of activity, but this is not the case in the absence of one or other

The best compound was once again the original hit, **11**, with $K_i = 8$ nM for PKN2 and with 20-fold selectivity over PKN1. It was also found to inhibit 19 other kinases above a nominal threshold of 70% in the commercial KINOMEScan® of 400 distinct kinase targets. Two equipotent compounds (**120** and **121** which capped the pyrrole N-H with ethyl and *n*-propyl groups respectively) were not as selective as **11** against PKN1, despite improved selectivity within the context of the wider kinome.

Attempts to alter the pyridyl, lactam and pyrrole portions of the compound resulted in loss of potency and/or selectivity between the PKNs. Interestingly, the alkylated derivatives of **11** showed slightly better selectivity within the wider kinome, likely due to the lack of hydrogen bond donor by loss of the pyrrole N-H, but this was not enough to significantly improve on the existing compound.

Computational studies of series B compounds yielded results which did not line up with experimental data. Cross docking compounds **11** and **120** across multiple kinases yielded ambiguous results which did not give any decisive rationale for the binding mode of this set of compounds.

Chapter 4 Series C – Naphthyridines, Quinazolines and Isoquinolines

This chapter seeks to outline the work carried out in optimising compound **12**, a 2,7-naphthyridine (Figure 4.1). The chemistry used to prepare this compound and other analogues will be discussed as well as the biological evaluation of the inhibitory potencies of those compounds against PKN2 and other kinases. IUPAC numbering will not be used for this series to allow for consistent numbering across the different ring systems used. Attempts to rationalise the biological activity using computational studies will also be outlined. This series proved to be the most productive in terms of the optimised chemical route and biological activity of the compounds. Thus this chapter constitutes the majority of the work involved in this project.

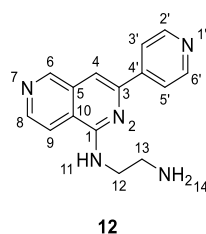


Figure 4.1 Labelled structure of compound **12**^{103,106}

4.1 Hit Origin

Compound **12** (Figure 4.1) was identified in the previously described ChEMBL data mining effort¹⁰³ as a potent inhibitor of PKN2 (PKN2 IC₅₀ 7 nM). This compound comes from work¹⁰⁶ carried out to identify an inhibitor of protein kinase D (PKD), and was likely not further developed by the researchers involved due to its poor selectivity profile.

In terms of selectivity, this compound had not been tested against as many targets as the lead compounds of the previous chapters. Compound **12** is only reported to inhibit eleven out of seventeen other kinases with IC₅₀ potency below 100 nM according to ChEMBL.¹⁰³ The low PKN2 potency of **12** made this compound an attractive starting point for tuning in PKN selectivity in order to produce a high quality probe for validating PKN2 as a potential drug target.

Naphthyridines are 6,6-heterocycles composed of two fused aromatic rings made up of eight carbons and two nitrogen atoms with the nitrogen atoms distributed across the rings. While none of the current FDA-approved inhibitors contain the 2,7-naphthyridine core of **12**, other similar *N*-containing fused heterocycles feature on the list of approved drugs (Figure 4.2).

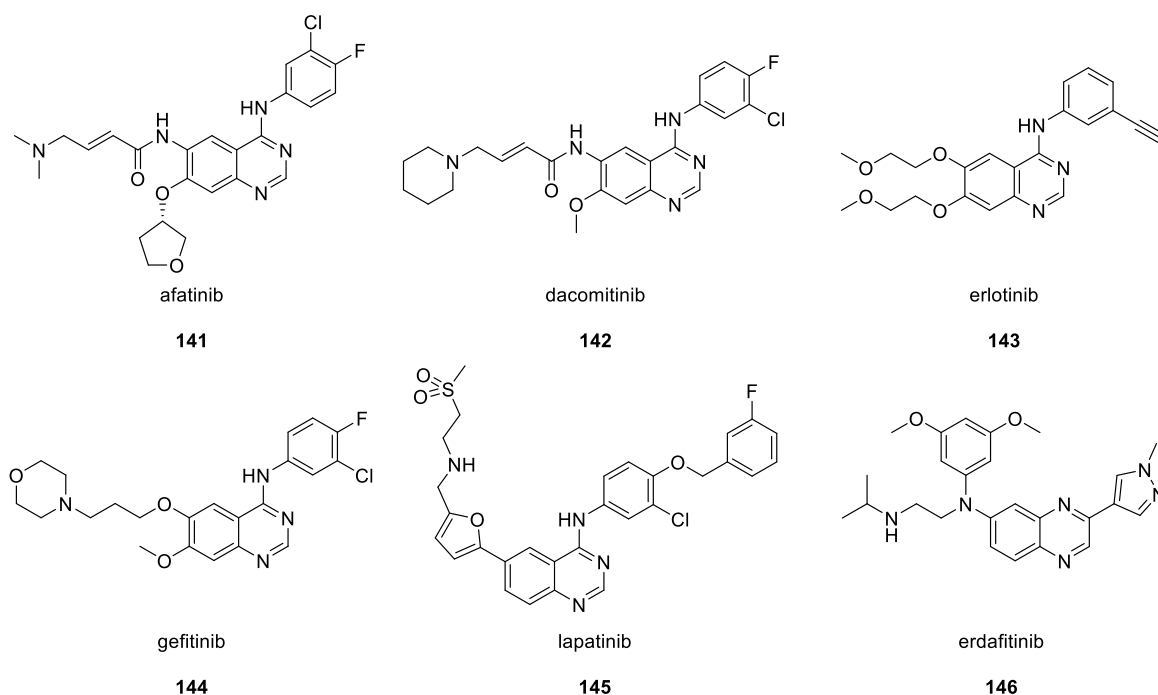


Figure 4.2 Quinazoline- and quinoxaline-containing FDA approved inhibitors⁴⁶

Quinazolines are isomers of naphthyridines and have the two nitrogen atoms on only one of the rings, whereas as naphthyridines have one nitrogen on each ring. They are particularly common within the current list of 52 FDA-approved kinase inhibitors, likely due to their ability to mimic the hydrogen bond donor/acceptor motif of the adenine portion of ATP (Figure 2.3). Five drugs – afatinib (**141**), dacomitinib (**142**), erlotinib (**143**), gefitinib (**144**), lapatinib (**145**) possess a quinazoline core. Erdafitinib (**146**) contains a closely related quinoxaline core (Figure 4.2).

Quinolines and isoquinolines are bioisosteres for naphthyridines and quinazolines but only possess one nitrogen atom in their heterocycle. Three approved kinase inhibitor drugs contain a quinoline motif, bosutinib (**147**), lenvatinib (**148**) and neratinib (**149**), while netarsudil (**150**) contains an isoquinoline core (Figure 4.3).

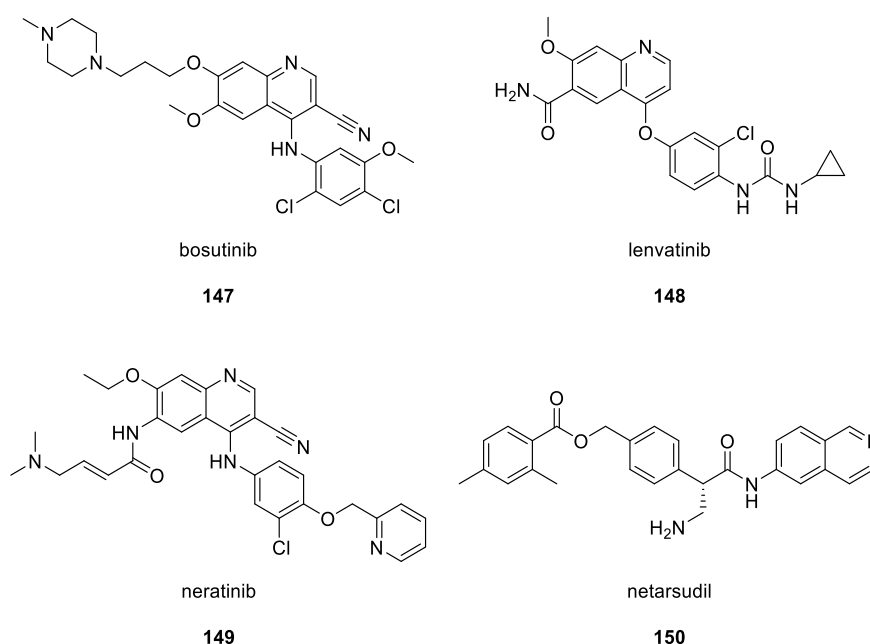
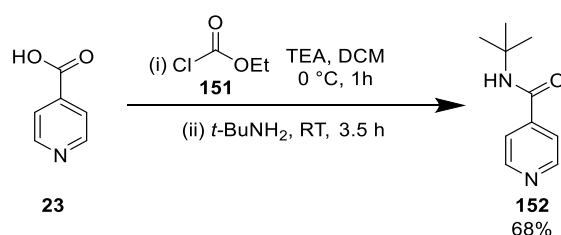


Figure 4.3 Quinoline- and isoquinoline-containing FDA approved kinase inhibitors

4.2 Chemistry

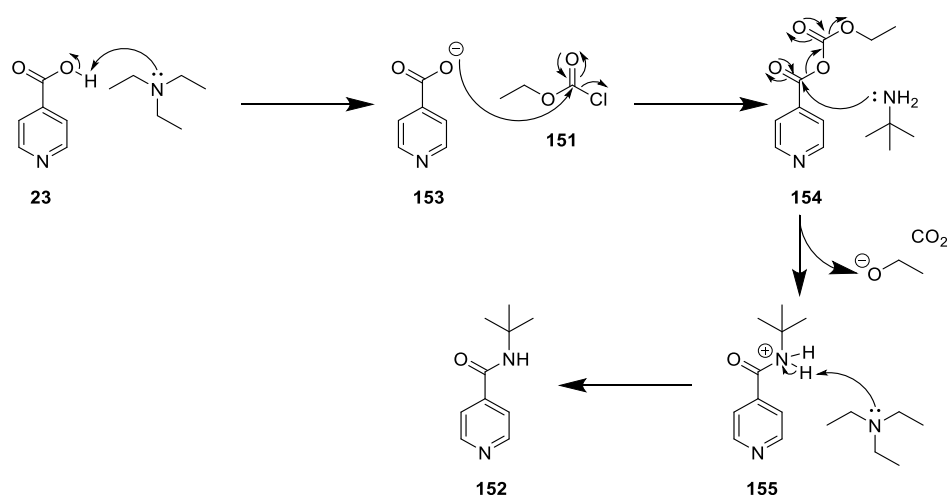
4.2.1 Synthesis of original hit

The initial hit, compound **12**, was synthesised by the same 8-step synthesised used by Meredith *et al.*¹⁰⁶ First, isonicotinic acid (**23**) underwent an amide coupling with *tert*-butyl amine using ethyl chloroformate (**151**) under basic conditions (Scheme 4.1). The best attempt of this reaction yielded amide **152** in 68% yield.



Scheme 4.1 Amide coupling conditions to form **152**¹⁰⁶

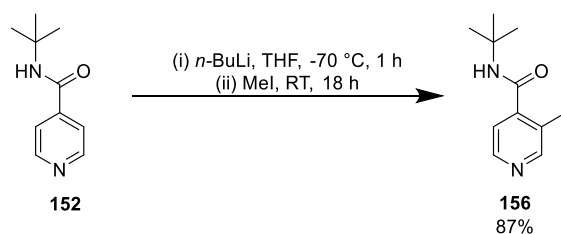
A proposed mechanism for this step is outlined in Scheme 4.2. First, triethylamine (TEA) deprotonates the isonicotinic acid (**23**) then resulting nucleophile **153** attacks the carbonyl carbon of ethyl chloroformate (**151**), with the loss of a chloride leaving group. The mixed anhydride intermediate (**154**) is now susceptible to nucleophilic attack by *tert*-butylamine, with loss of carbon dioxide and ethoxide. A final deprotonation of **155** by TEA yields the amide (**152**).



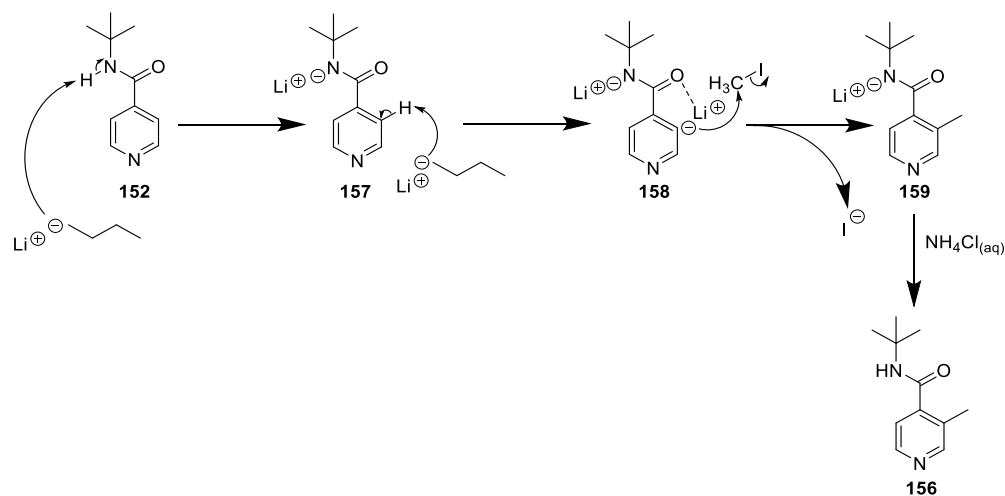
Scheme 4.2 Proposed mechanism for amide coupling under ethyl chloroformate conditions to compound **152**

The presence of the *tert*-butyl amide moiety in **152** was confirmed by two singlets in the ^1H NMR, one occurring at δ 1.47 ppm integrating to the nine protons in the *tert*-butyl group and one at δ 5.98 ppm, integrating to the hydrogen in the amide. The desired mass ion (m/z 179.1 $[\text{M}+\text{H}]^+$) was also observed by LCMS (LCQ).

Compound **152** was methylated to form intermediate **156** (Scheme 4.3) using strong base *n*-butyl lithium (*n*-BuLi) to deprotonate one of the carbon atoms positioned *ortho* to the amide. Scheme 4.4 outlines the mechanism for this transformation.



Scheme 4.3 Methylation conditions for preparation of intermediate **156**¹⁰⁶



Scheme 4.4 Proposed mechanism for methylation step to **156**

A minimum of two equivalents of *n*-BuLi were required because the more acidic amide N-H proton ($pK_a \approx 20$)¹¹⁷ preferentially deprotonates over one of the pyridyl protons ($pK_a \approx 35$)¹⁴⁴ to give **157**. The directed *ortho* metalation mechanism encourages the electrophile to attach exclusively to the *ortho*-carbon because of the coordination with the amide carbonyl group. Methyl iodide provides the methyl source for the product and was added after dianion **158** formed at low temperature. Following quenching of species **159** with aqueous ammonium chloride solution and purification, amide **156** was isolated in 87% yield.

¹H NMR was used to determine whether **152** had been methylated at the 3-position (**156**) over the 2-position, relative to the pyridyl nitrogen. The ¹H NMR of **152**, the starting material, included two doublets, each integrating to two protons (Figure 4.4), representing the pairs of protons in the symmetrical ring. The chemical shift values of **152** are higher than the equivalent values of the reference ¹H chemical shift values of pyridine (**160**) due to the electron-withdrawing amide.¹²⁷ The two equivalent peaks of product **156** appear slightly lower than the starting material and pyridine due to increased electron shielding by addition of an electron donating methyl group to the aromatic ring.

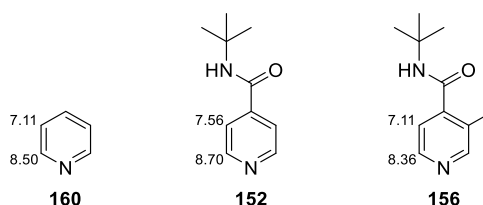


Figure 4.4 Observed ¹H chemical shifts of aromatic protons in pyridine (**160**),¹²⁷ **152** and **156**

Additionally, a new singlet integrating to three protons at δ 2.37 indicated the introduction of a methyl group to molecule **156**. The relative integration of the doublet with the higher chemical shift to the doublet with the lower chemical shift increased from 1:1 in **152** to 2:1 in **156**. This meant there was only one proton *ortho* to the amide as the other had been methylated, and two *meta*-protons, confirming the formation of **156** (Figure 4.5).

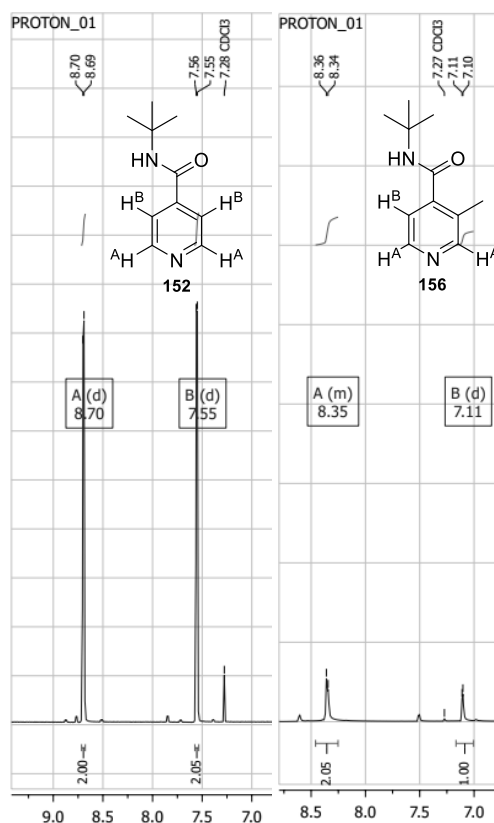
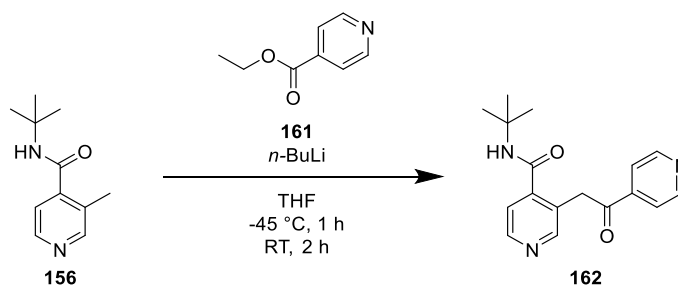
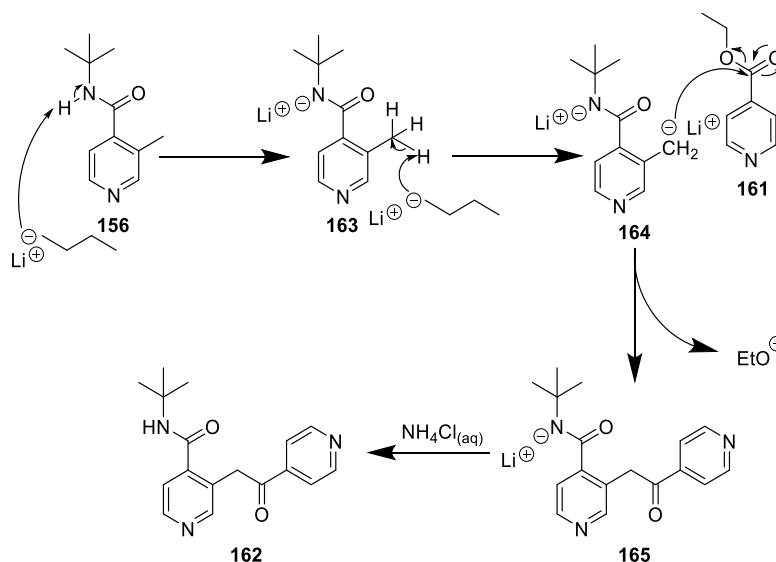


Figure 4.5 Exemplar ^1H NMR showing the change in relative chemical shift and integration of aromatic peaks between intermediates **152** (left) and **156** (right)

n-BuLi was also used in the third step to deprotonate the new methyl carbon to allow a displacement reaction to take place between **156** and ethyl isonicotinate (**161**) (Scheme 4.5). Scheme 4.6 outlines the mechanism to compound **162**.



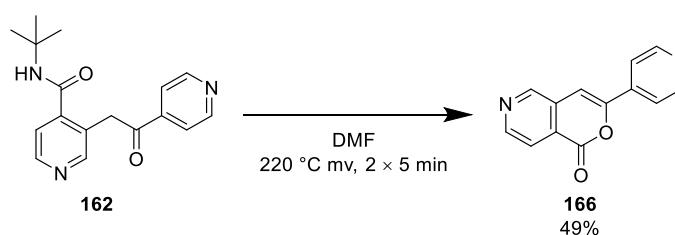
Scheme 4.5 Acylation of **156** to form ketone **162**¹⁰⁶



Scheme 4.6 Proposed mechanism for acylation step to form 162

Similar to the previous step, 2.1 equivalents of *n*-BuLi were required to form dianion **164** so that the methyl anion could form after the amide proton was removed (**163**) and attack the carbonyl of ethyl isonicotinate (**161**) to form intermediate **165**, with loss of ethoxide. Quenching and purification of the reaction mixture yielded ketone **162** in 55% yield.

The formation of two new correlating doublets in the aromatic region of the ^1H NMR confirmed the introduction of a second pyridyl moiety to the molecule, as did LCMS where a mass ion of m/z 298.04 $[\text{M}+\text{H}]^+$ was observed which conformed to the product **162**'s molecular weight of 297.



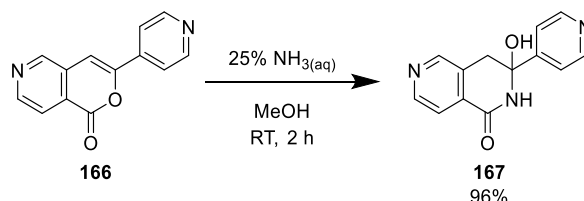
Scheme 4.7 Cyclisation conditions to form lactone 166¹⁰⁶

Next, ketone **162** underwent a cyclisation reaction by being heated in the microwave (mv) in DMF at 220 °C (Scheme 4.7). The product, lactone **166**, precipitated out in solution as a pale pink solid. Reheating the filtrate caused more product to precipitate but the combined yield of this step could not be pushed beyond 49%. The formation of product **166** was confirmed by the correct mass ion (m/z 225 $[\text{M}+\text{H}]^+$) by LCMS (LCQ). By ^1H NMR, the loss of the aliphatic C-H peaks in the ^1H NMR and observation of six peaks instead of five in the aromatic region of the spectrum also confirmed the product had formed.

The mechanism for this particular step could not be fully elucidated. It is unusual in that it involves the loss of a bulky *tert*-butyl amine group, by definition a poor leaving group. That said, the reaction is taking place under harsh conditions (220 °C, microwave heating) so any *tert*-butyl amine lost from the compound would be expected to boil off from the reaction mixture, which may drive the transformation but this reaction was carried out in a sealed microwave tube so this is not the case. This reaction is thought to be less feasible if the amide and ketone functions were in separate molecules. As this is an intramolecular cyclisation, reactions that aren't usually energetically favourable can become more so when brought into closer proximity. The change in enthalpy (ΔH) will be roughly the same for **162** and **166** and intramolecular reactions do not result in a negative change in entropy (ΔS). The reaction is also carried out at high temperature (T) which increases the product value of $T\Delta S$. This means overall, the change in Gibbs Free Energy (ΔG), defined as,

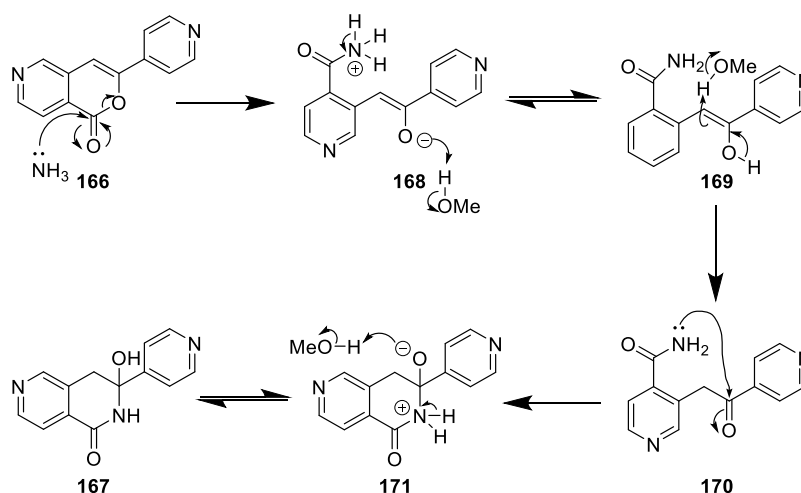
$$\Delta G = \Delta H - T\Delta S$$

will result in a negative value so the equilibrium of the reaction will preferentially lean towards the product **166** over intermediate **162**.^{117,145}



Scheme 4.8 Conditions for converting lactone **162** to lactam **166**¹⁰⁶

Conversion of lactone **166** to lactam **167** was achieved by stirring **166** in an excess of ammonia in methanol for 2 h (Scheme 4.8) and isolating the product by filtration in 96% yield. Scheme 4.9 outlines the mechanism.



Scheme 4.9 Proposed mechanism for the conversion of lactone **166** to lactam **167**

Ammonia attacks at the carbonyl carbon of **166** to hydrolyse the ester. After a series of reversible proton exchanges, the newly formed primary amide nitrogen in **170** acts as a nucleophile to attack the resulting ketone within its structure to form the hydroxyl-containing amide intermediate (**167**).

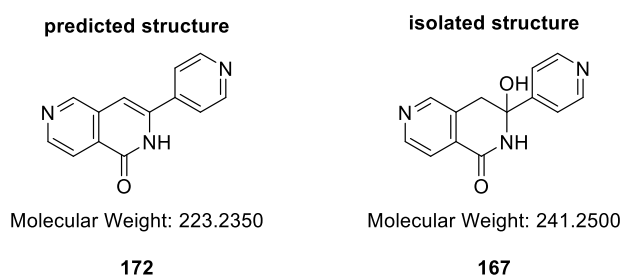


Figure 4.6 Predicted structure (**172**) after reaction of lactone **166** with ammonia (left), actual structure of **167** (right) with molecular weights listed

Initially it was thought a fully unsaturated intermediate (**172**) formed (Figure 4.6) but ^1H NMR showed a set of ABq peaks¹²⁷ in the aliphatic region between δ 3.0–3.5 ppm, indicating the presence of two diastereotopic protons belonging to a saturated carbon within the molecule (Figure 4.7). This and the mass ion by LCMS being m/z 242 $[\text{M}+\text{H}_2\text{O}]^+$ instead of m/z 224 $[\text{M}+\text{H}]^+$ were used to deduce that the hydroxy-containing product (**167**) with a molecular weight of 241 had formed instead of **172**.

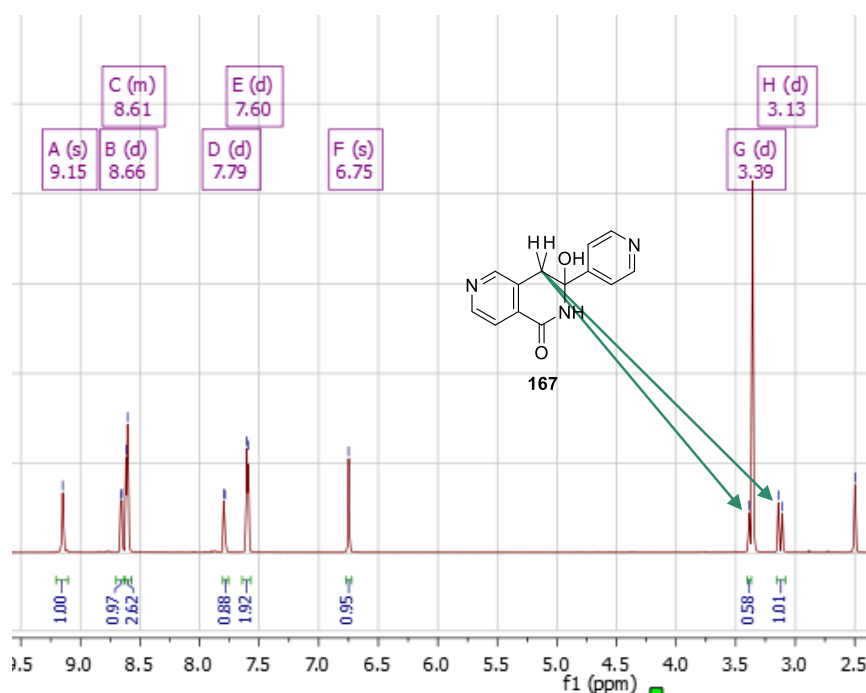
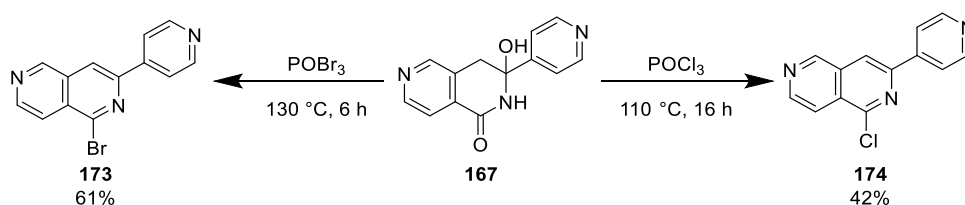
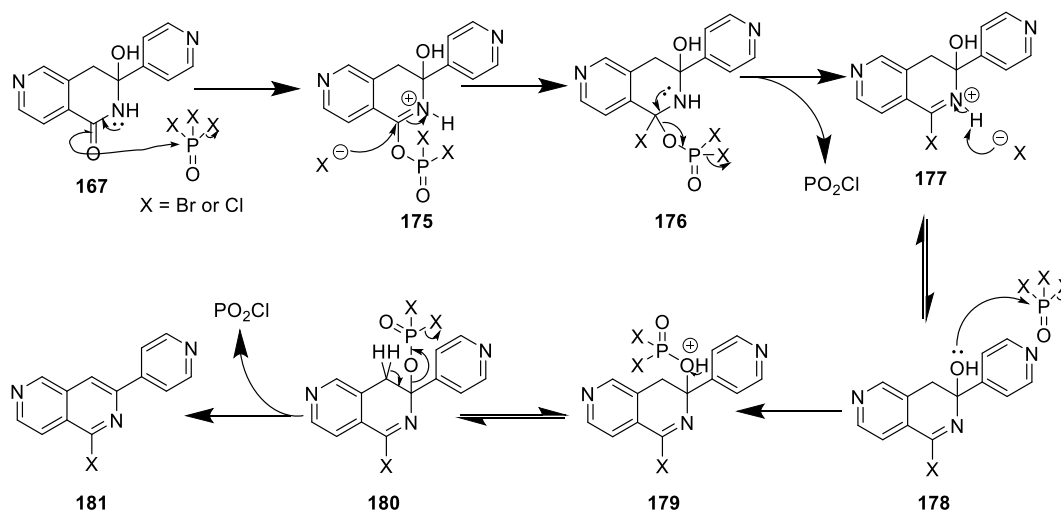


Figure 4.7 ^1H NMR of lactam **167** highlighting ABq peaks indicating degree of saturation in product

The formation of the key bromide/chloride naphthyridine intermediates **173** and **174** was achieved by heating **167** in neat phosphoryl bromide/chloride ($\text{POBr}_3/\text{POCl}_3$), followed by quenching and isolation by flash chromatography (Scheme 4.10). Both were prepared because Meredith *et al.*¹⁰⁶ who originally made the compound used the bromide for the preparation of **12** and the chloride for other derivatives. A mechanism is outlined in Scheme 4.11.



Scheme 4.10 Conditions for bromination/chlorination of lactam **167**¹⁰⁶



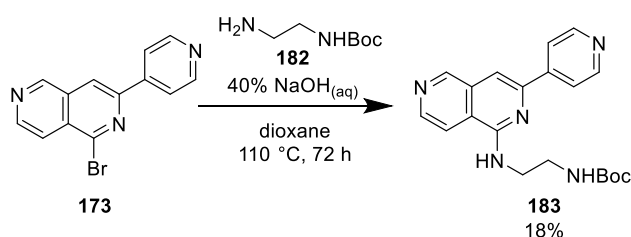
Scheme 4.11 Proposed mechanism of chlorination by $\text{POBr}_3/\text{POCl}_3$ to form **181**

The lone pair on the amide nitrogen of **167** delocalises to encourage a C-O carbonyl bond to break to form a new O-P bond with the corresponding phosphoryl halide, displacing a halide anion. The diffuse nature of the p-orbitals in phosphorus and the high strength of a P=O bond (575 kJ mol^{-1})¹¹⁷ means there is no breaking and reforming of the P-O bond, as would otherwise be seen in a carbonyl under nucleophilic attack. The halide anion can then attack species **175** to yield intermediate **176** where loss of a phosphinic halide results in intermediate **177**. Following deprotonation of **177**, the hydroxyl group oxygen lone pair of **178** acts as a nucleophile to attack another phosphoryl halide molecule to give species **179**. Loss of a proton from **180** to restore aromaticity drives loss of another phosphinic halide to yield product **181**.

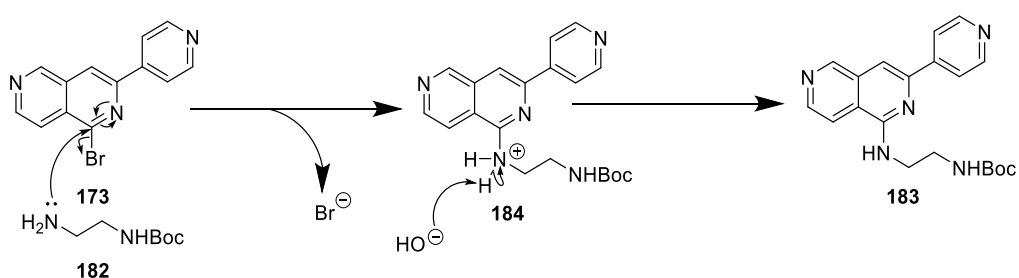
This step usually led to a significant drop in yield (typical yields 30–61%) which was undesirable at this point in the synthesis. The largest scale attempt of the synthesis started with 5 g isonicotinic acid yet only 484 mg of **174** was isolated after six steps.

The ^1H NMR was consistent with that expected for the product because the amide N-H, hydroxyl and aliphatic ABq peaks of the starting material disappeared and six aromatic peaks remained. The LCMS (LCQ) spectra also exhibited the expected 1:1 and 3:1 splitting pattern for **173** and **174** with the relative abundances ^{79}Br and $^{81}\text{Br}/^{35}\text{Cl}$ and ^{37}Cl isotopes respectively.^{146,147}

Bromide **173** was used to prepare the intermediate **183**, the penultimate intermediate to make **12**, by undergoing a nucleophilic aromatic substitution ($\text{S}_{\text{N}}\text{Ar}$) reaction with the Boc-protected ethylenediamine (**182**), heated in dioxane for 72 h (Scheme 4.12). **183** was isolated in 18% yield despite being left for the allotted time (*cf.* 71% reported yield¹⁰⁶). Scheme 4.13 proposes a general mechanism for this $\text{S}_{\text{N}}\text{Ar}$ transformation.



Scheme 4.12 Conditions for $\text{S}_{\text{N}}\text{Ar}$ to prepare penultimate intermediate **183**¹⁰⁶



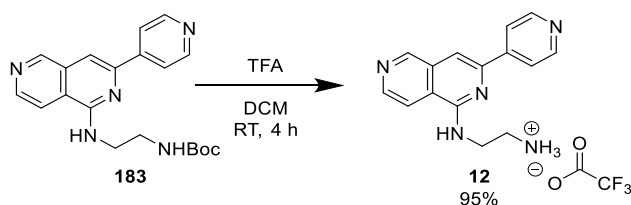
Scheme 4.13 Proposed mechanism for $\text{S}_{\text{N}}\text{Ar}$ transformation to form **183**

The lone pair associated with the unprotected nitrogen in Boc-ethylene diamine (**182**) attacks the δ^+ carbon of **173**, displacing a bromide anion and shuffling electrons between that carbon and the adjacent nitrogen. The presence of the sodium hydroxide in the reaction deprotonates resulting intermediate **184** to yield product **183**.

^1H NMR confirmed introduction of the Boc-protected ethylene diamine moiety to **173** by the appearance of two triplet peaks in the aliphatic region which each integrated to two protons as well as a further upfield singlet integrating to nine protons, representing the nine *tert*-butyl protons in the Boc-group.

In later attempts of this synthesis, the chloride (**174**) was used to prepare analogues of **12** because the chloride intermediate is more reactive than the bromide and thus required less harsh conditions.¹⁴⁸

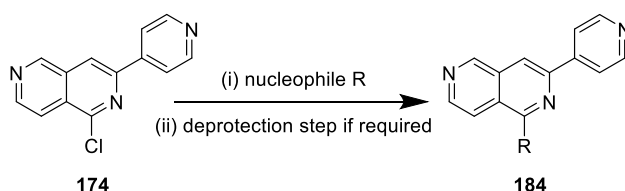
Compound **12** was prepared by removal of the protecting group from the terminal amine by stirring **183** in trifluoroacetic acid (TFA), as shown in Scheme 4.14. The mechanism for this transformation was previously described in section 3.1.1. **12** was isolated in 95% yield as the trifluoroacetate salt. Disappearance of the singlet integrating to nine protons indicated the removal of the Boc-group. The multiplicity of the two aliphatic peaks changed from two triplets seen for **183** to a triplet and quadruplet because of the different number of protons adjacent to the ethylene carbons.



Scheme 4.14 De-protection conditions to prepare compound **12**¹⁰⁶

4.1.2 Preparation of analogues

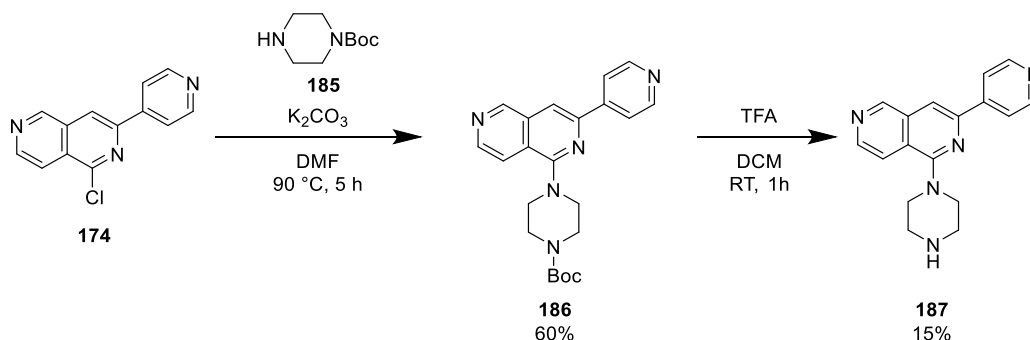
Amine variation



Scheme 4.15 General scheme for initial analogue synthesis for series 1

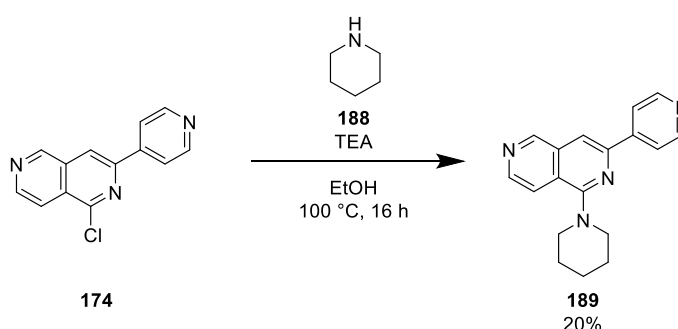
Four other amines were coupled with **174** to identify the SAR relating to the free-moving ethyl amine (Scheme 4.15). **187** was prepared with the two nitrogens fixed in position by stirring **174**

with Boc-protected piperazine (**185**) in DMF at 90 °C for 5 h. After work-up and purification the Boc-group was removed by stirring the intermediate in TFA. Compound **187** was isolated as the trifluoroacetate salt and then converted to the equivalent free base by purification through an SCX cartridge by elution with methanol then 2 M NH₃ in methanol (Scheme 4.16). The appearance of two singlets in the aliphatic region, each integrating to 4 protons confirmed the introduction of the piperazine function to the compound, as did the new broad singlet at δ 9.09 integrating to one proton, indicative of the presence of a secondary amine.



Scheme 4.16 Preparation of compound **187** from **174**¹⁰⁶

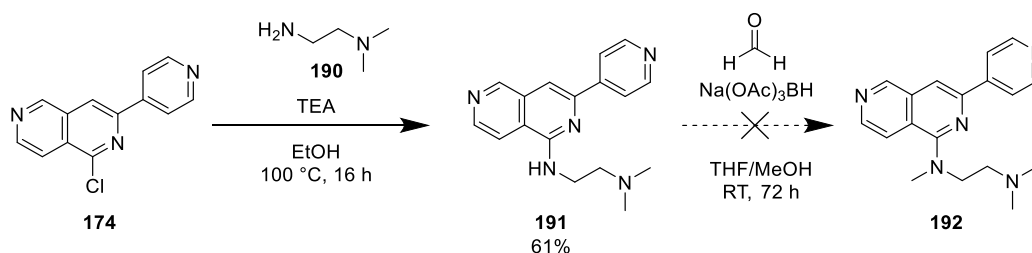
The terminal nitrogen was also removed in the preparation of analogue **189** by introducing piperidine (**188**) to the molecule (Scheme 4.17). The appearance of three multiplets, two integrating to 4 protons and one integrating to two protons between δ 1.51–3.50 ppm confirmed the piperidine group had successfully coupled with the naphthyridine. The correct mass ion (m/z 291.33) was observed by LCMS (LCQ) corresponding to the molecular weight of the compound (290.36).



Scheme 4.17 Conditions for S_NAr involving chloride **174** and piperidine (**188**) to make compound **189**¹⁰⁶

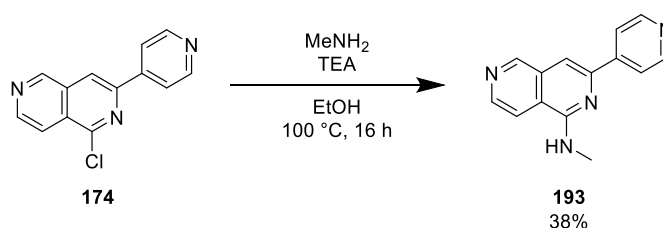
Further questions can be answered about how the two amino groups are involved in binding by methylation of the nitrogen atoms to see if removing hydrogen-bond donors affects how the compound fits into the active site. The analogue with the dimethylated terminal nitrogen (**191**) was successfully isolated in 61% yield but attempts to fully methylate both basic nitrogens by

reductive amination of **191** to make **192** were unsuccessful (Scheme 4.18). The lack of peak corresponding to -NH_2 compared to the ^1H NMR spectrum for **12** and the appearance of a singlet at δ 2.24 ppm integrating to six protons confirmed formation of product **191**.



Scheme 4.18 $\text{S}_{\text{N}}\text{Ar}$ and reductive amination conditions attempted to form **191** and **192** respectively^{106,149}

Another analogue of **12** where the ethylene diamine moiety is truncated to a methyl group was successfully prepared by reacting **174** with methyl amine, isolating **193** in 38% yield (Scheme 4.19).



Scheme 4.19 $\text{S}_{\text{N}}\text{Ar}$ conditions to prepare **193**¹⁰⁶

This initial set of five 2,7-naphthyridine compounds (Figure 4.8) provided some useful point changes around the amine region of the molecule. Due to the length of the synthesis (7–8 steps), it was decided to investigate whether the naphthyridine core could be replaced in order to simplify and shorten the synthetic route to access other analogues. This is because any changes to the pyridyl portion of the compound had to be introduced at the third step, while any change to the amine portion required sufficient quantities of an intermediate made using six chemical transformations. There were no suitable intermediates available from commercial vendors with this naphthyridine core.

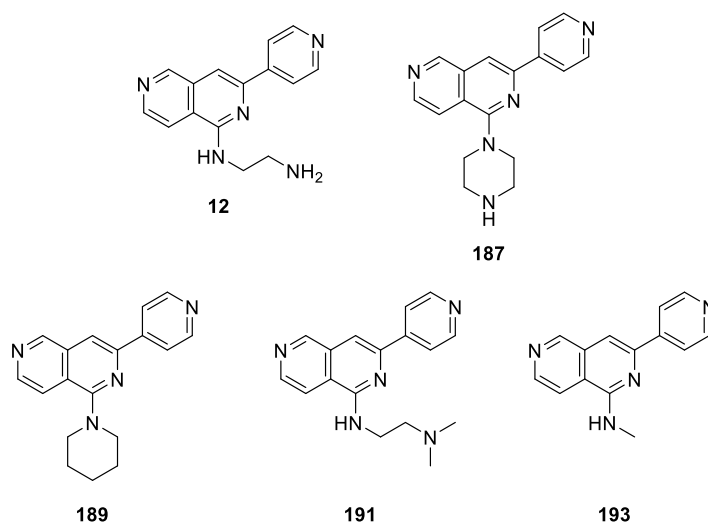
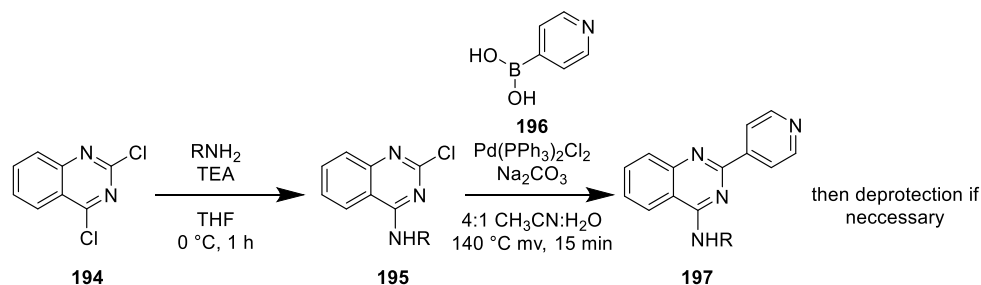


Figure 4.8 Series 1 compounds synthesised with 2,7-naphthyridine core

Quinazoline analogues

A quinazoline core was chosen to explore and compare with the 2,7-naphthyridine core of **12** due to the commercial availability of 1,3-dichloroquinazoline (**194**) in order to optimise the length of the synthesis – the 2,6-naphthyridine equivalent is not commercially available. This enabled the rapid generation of quinazoline-containing analogues *via* S_NAr and Suzuki coupling steps (Scheme 4.20).



Scheme 4.20 General synthetic route to quinazoline analogues^{150,151}

The first step involved S_NAr coupling conditions that coupled methylamine to 1,3-dichloroquinazoline (**194**), summarised in Scheme 4.20.¹⁵⁰ These conditions were transferable for all five amines previously used and a set of chloroquinazoline intermediates (**198–202**) were synthesised (Figure 4.9).

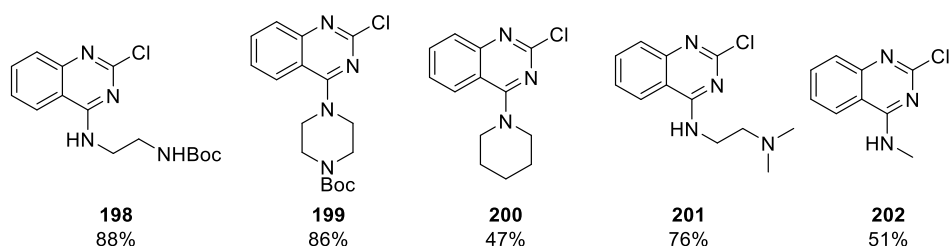
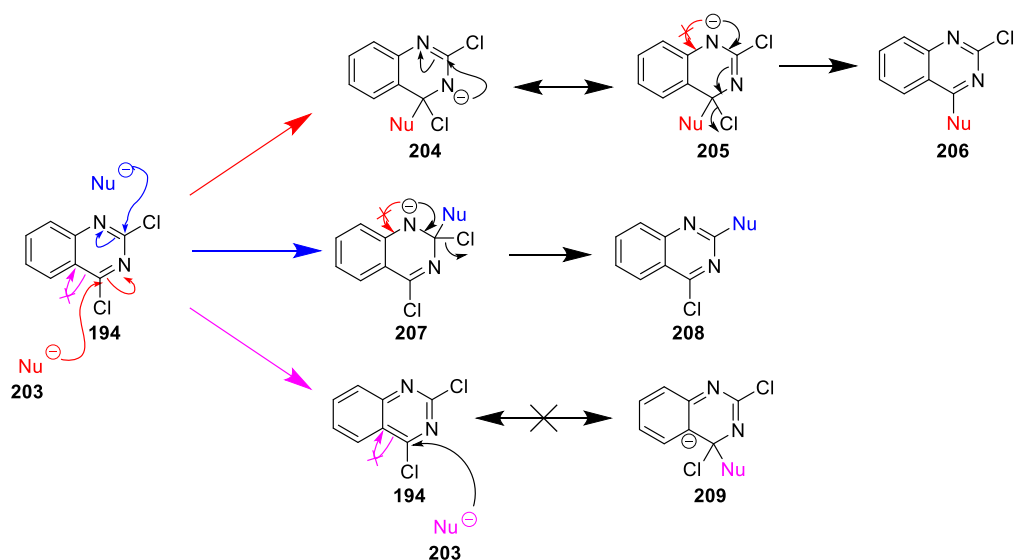


Figure 4.9 Quinazoline-containing intermediates and yields

The amines are believed to selectively attack at the 1-position chlorine of **194** due to the stabilising resonance effects of the tetrahedral intermediate that forms. Scheme 4.21 shows the possible resonance forms that can potentially arise by nucleophilic attack at the 1-position (red/pink) and the 3-position (blue). More resonance forms exist for the intermediate that occurs from addition at the 1-position (**204–206**). This means this intermediate is more stable and thus formed selectively over a 3-substituted product.



Scheme 4.21 Resonance structures with nucleophilic attack mechanistic pathways proposed for the 1-chlorine (red/pink) and 3-chlorine (blue)

NOESY NMR was used to check the amine substituted with the desired chlorine of **194**. An exemplar spectrum of **202** (Figure 4.10) shows correlation between the methylamine N-H and the 9-position hydrogen on the quinazoline ring, indicating the amine had substituted at the 1-position. If it had substituted at the 3-position, no correlation with the aromatic protons would have been observed because of the nitrogen atoms at the 2- and 4-positions.

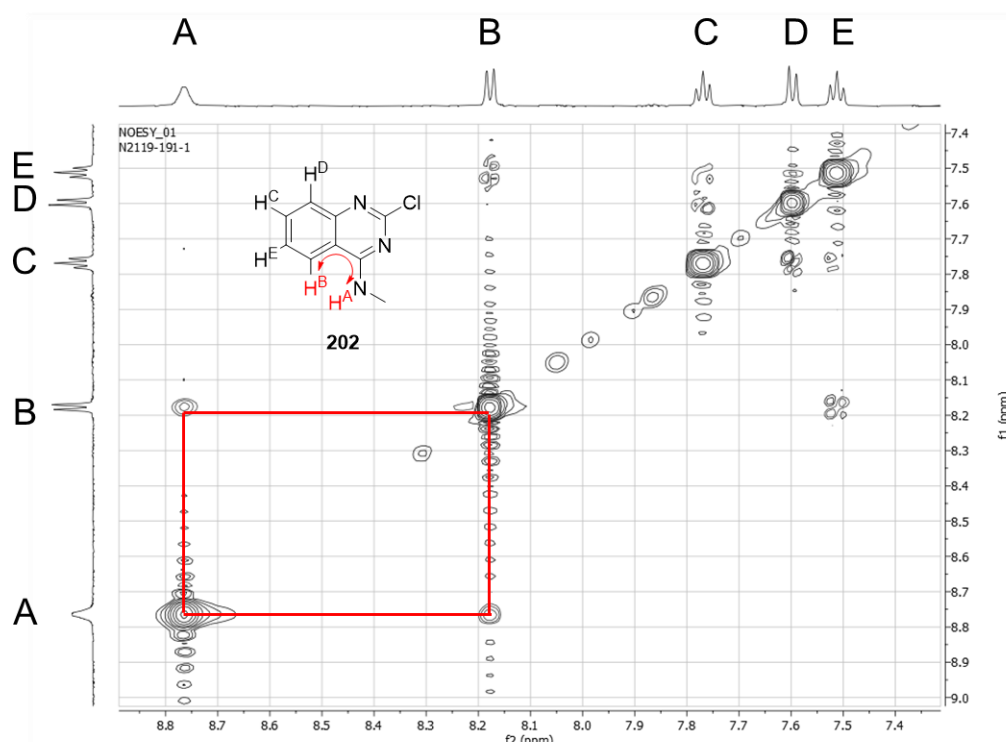
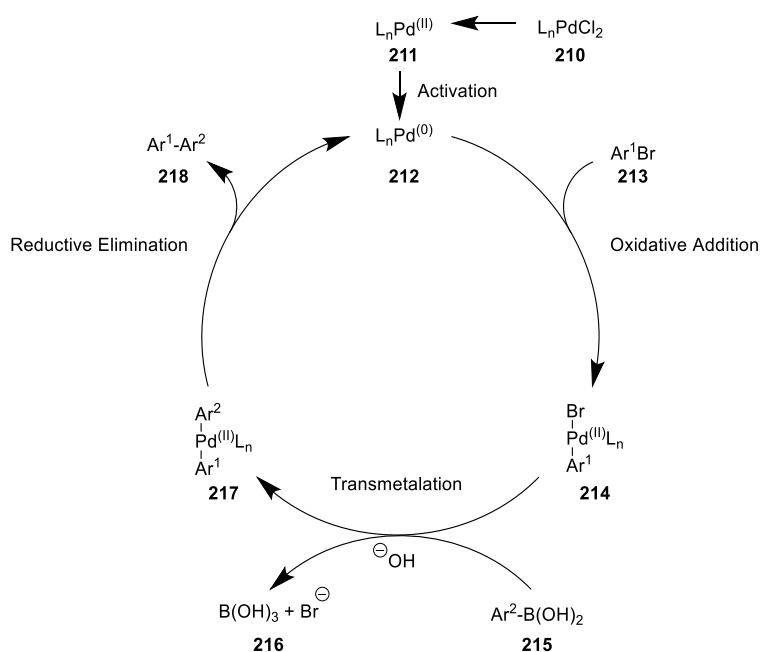


Figure 4.10 Zoomed portion of NOESY NMR spectrum for compound **202** highlighting correlation between methylamine proton (H^A) and 9-C proton (H^E) in red

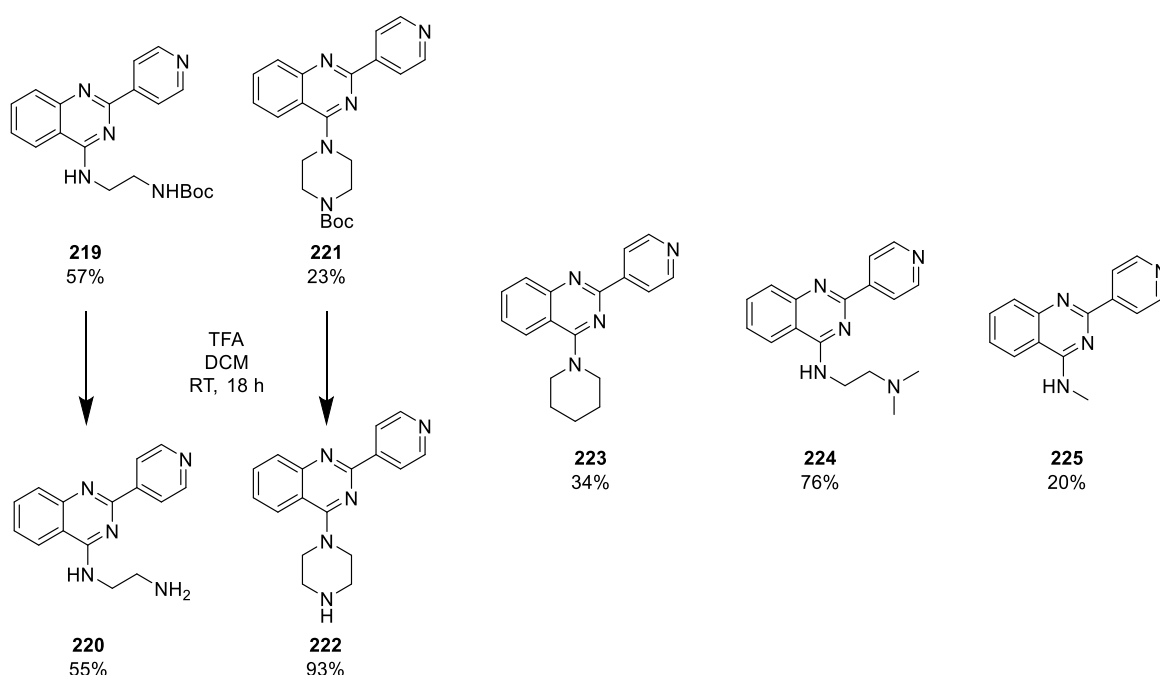
Palladium-catalysed couplings¹⁵² are one of the most commonly used transformations in medicinal chemistry.¹⁵³ Such couplings are used to form carbon-carbon bonds between aryl rings. Some Suzuki conditions (Scheme 4.20)¹⁵¹ were found to efficiently introduce the pyridyl moiety to intermediates **198–202**. Scheme 4.22 outlines a typical mechanism for a Suzuki reaction.



Scheme 4.22 General mechanism for a Suzuki coupling¹⁵⁴

Following activation of the palladium catalyst (**210**) to yield a Pd(0) source (**212**), the palladium is oxidised by donating two electrons to form a new Pd-C bond with the aryl group of an aryl halide, e.g. an aryl bromide (**213**). After formation of **214**, transmetalation occurs which transfers a second nucleophilic aryl group from a boronic acid (**215**) to the palladium (**217**). Reductive elimination from the palladium yields the combined aryl groups (**218**) and regenerates the palladium (**212**) ready to be used again in this catalytic transformation.^{152,154}

A set of Suzuki conditions using (dppf)₂PdCl₂ found in the literature did not work when first attempted. Conditions that are commonly used in-house²¹ with a different catalyst, Pd(PPh₃)₂Cl₂, were more successful to prepare compounds **220** and **222–225** (Scheme 4.23).



Scheme 4.23 Final quinazoline match pairs with yields for Suzuki and Boc-deprotection steps

¹H NMR was used to distinguish between the 2,7-naphthyridine and quinazoline cores. For the former, two singlets and two multiplets were typically observed (e.g. **12** in Figure 4.11) while for a quinazoline core, two triplets and two doublets were observed instead due to all four aromatic protons being on the same ring adjacent to one another (e.g. **220** in Figure 4.11). COSY and NOESY NMR were used to fully assign the intermediates and final products.

In some cases the ¹H NMR peaks of aromatic C-Hs overlapped, and the COSY NMR was sufficiently ambiguous that it was difficult to confirm which aromatic protons were which. Such compounds have been assigned as fully as possible in the experimental section.

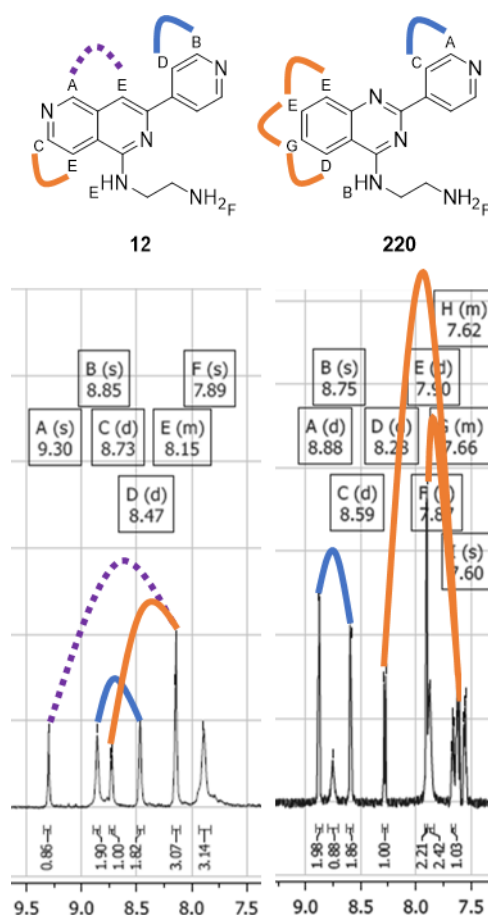
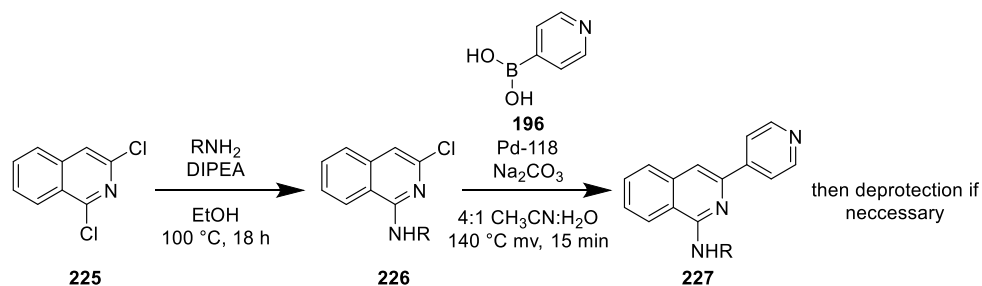


Figure 4.11 Aromatic region of ^1H NMR spectra for compounds **12** and **220**. Correlation from COSY NMR shown with coloured lines.

Isoquinoline analogues

The $\text{S}_{\text{N}}\text{Ar}$ conditions¹⁵⁰ used to prepare chloroquinazolines **198–202** were unsuccessful in the preparation of isoquinoline match pairs, likely due to the less electrophilic nature of the isoquinoline ring so harsher conditions were required.



Scheme 4.24 Synthetic route to isoquinoline analogues^{151,155}

An alternative set of conditions¹⁵⁵ (Scheme 4.24) where the 1,3-dichloroisoquinoline (**225**) was heated overnight at 100 °C instead of 1 h at 0 °C were found to be successful and used to bring through the equivalent five isoquinoline-containing intermediates (**228–232**) in good yield (Figure 4.12).

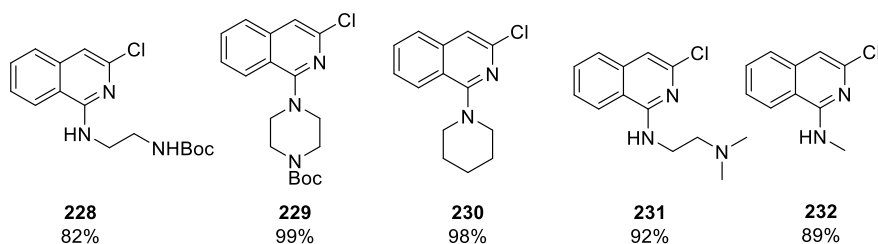


Figure 4.12 Chloroisoquinoline intermediates 228–232 prepared via S_NAr transformation

NOESY NMR was again used to confirm that the amine had displaced the desired 1-chlorine over the 3-chlorine. Figure 4.13 shows a zoomed NOESY NMR spectrum for compound **232**. The correlation between peaks A and B confirm that the amine coupled at the 1-position. Had the amine substituted at the 3-position, correlation would be observed between peaks B and F, which is not the case.

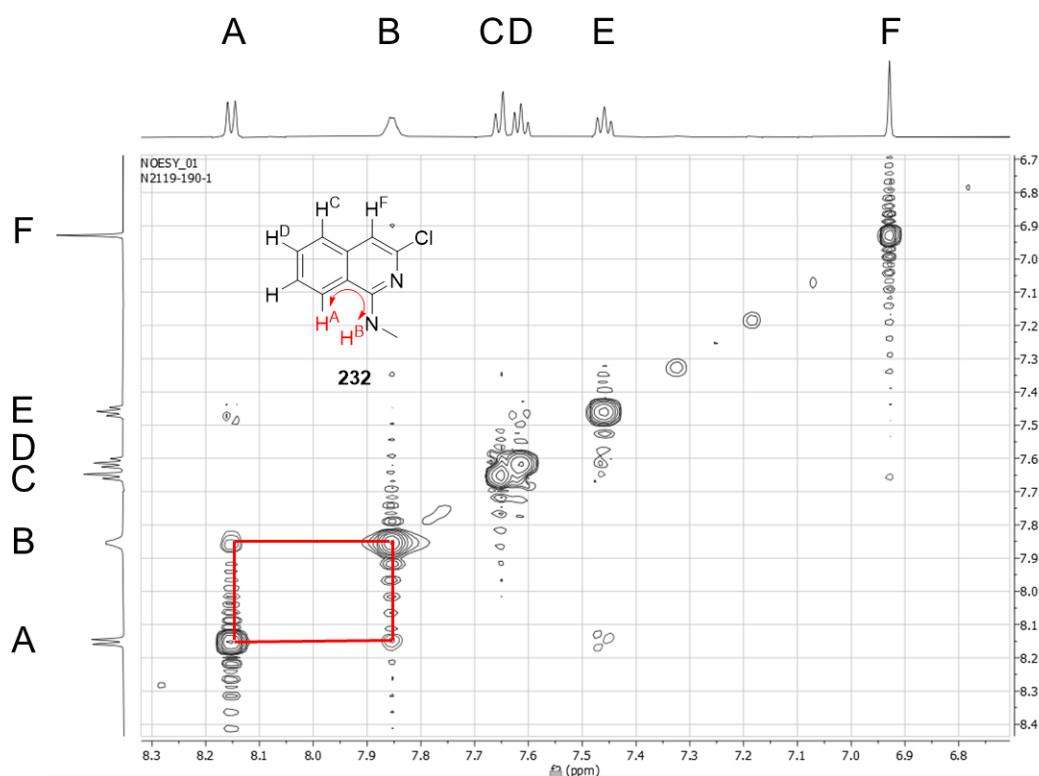
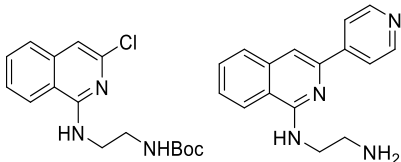
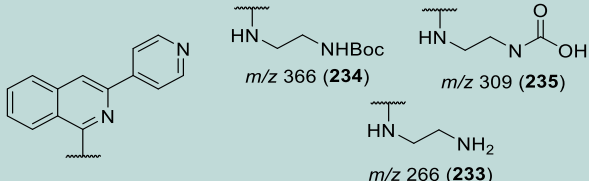


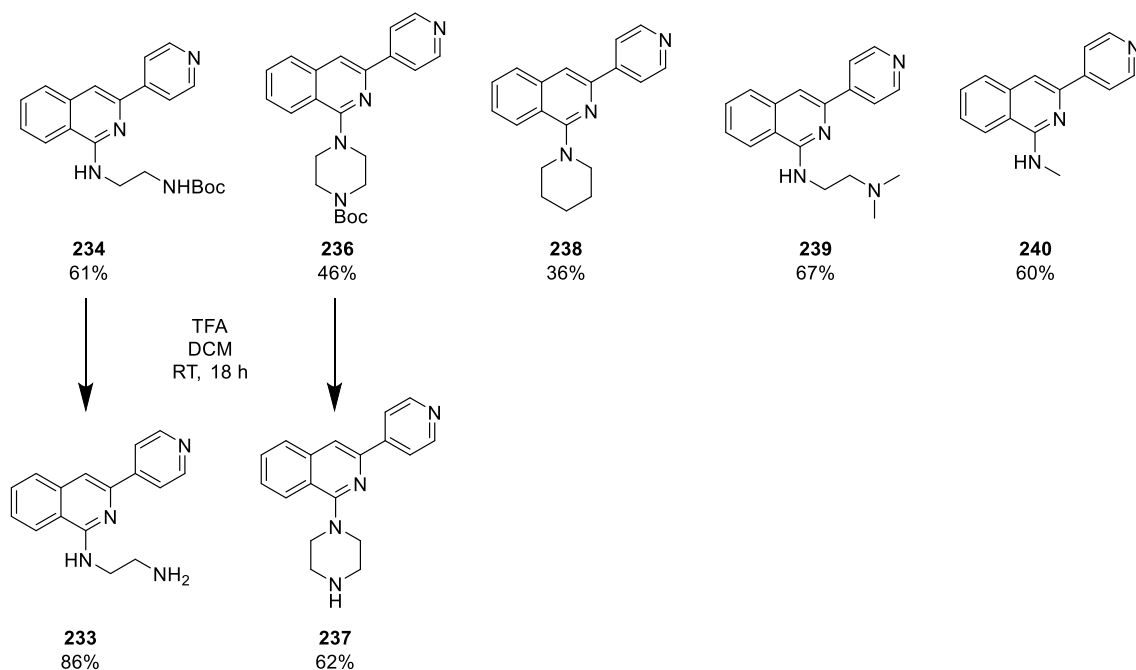
Figure 4.13 Zoomed portion of NOESY NMR spectrum for compound **232** highlighting correlation between methylamine proton (H^B) and 9-C proton (H^A) in red

The Suzuki conditions used for the quinazoline analogues in Scheme 4.20 did not work for preparing the equivalent isoquinoline intermediates. A small reaction condition screen was set up whereby 50 mg scale reactions were run with different Pd-catalysts. The reactions were followed by LCQ LCMS (Table 4.1). Microwave and hotplate heating methods were compared as were time (15 minutes vs. overnight) and temperature (140 °C and 100 °C) parameters.

Table 4.1 Suzuki optimisation summary with most successful conditions highlighted in green

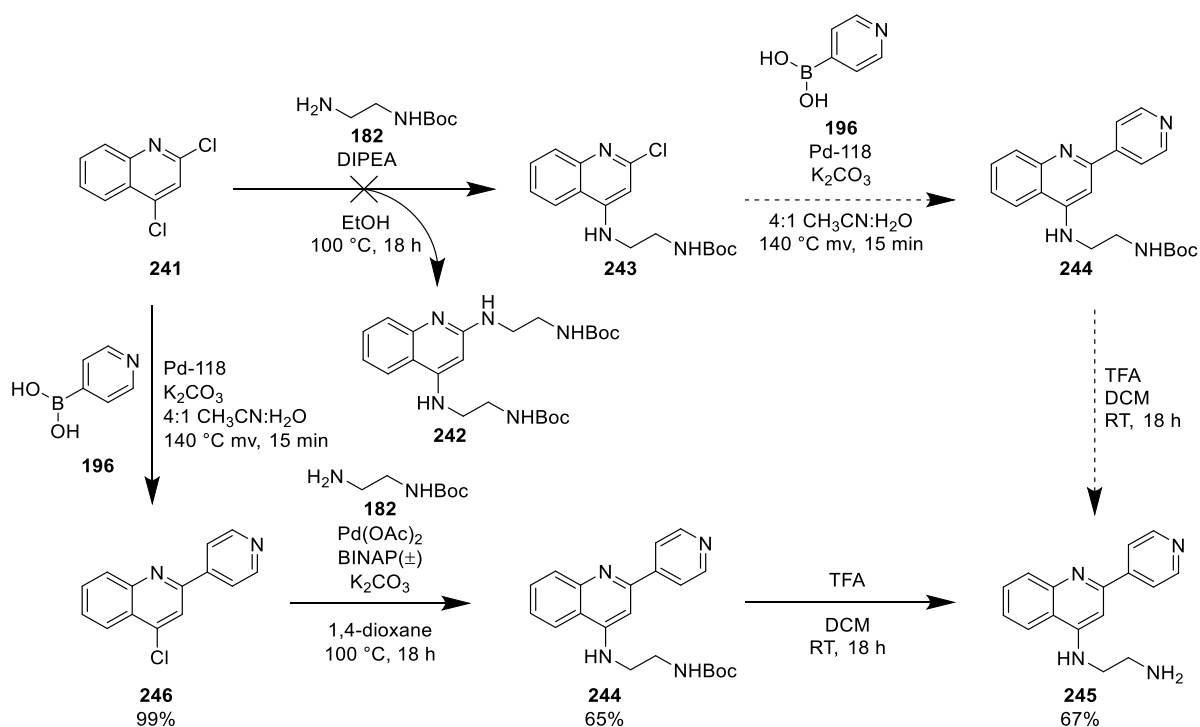
Catalyst	Reaction Time	Temp.	Heating apparatus	Observed <i>m/z</i> values (LCQ LCMS) and predicted products formed
Pd(dba) ₂	15 min	140 °C	Microwave	 <i>m/z</i> 322/324 (228) <i>m/z</i> 266 (233)
Pd(dppf) ₂ Cl ₂	15 min	140 °C	Microwave	<i>m/z</i> 322/324 (228) and 266 (233)
Pd-118	15 min	140 °C	Microwave	 <i>m/z</i> 366 (234) <i>m/z</i> 309 (235) <i>m/z</i> 266 (233)
Pd(PPh ₃) ₄	15 min	140 °C	Microwave	<i>m/z</i> 322/324 (228) and 266 (233)
Pd(dba) ₂	overnight	100 °C	Hot plate	<i>m/z</i> 322/324 (228) and 366 (234)
Pd(dppf) ₂ Cl ₂	overnight	100 °C	Hot plate	<i>m/z</i> 322/324 (228) and 266 (233)
Pd-118	overnight	100 °C	Hot plate	<i>m/z</i> 366 (234), 309 (235) and 266 (233)
Pd(PPh ₃) ₄	overnight	100 °C	Hot plate	Indecipherable mixture of compounds

It was found that Pd-118 was a suitable replacement for Pd(PPh₃)Cl₂ and facilitated the synthesis of compounds **234–240** (Scheme 4.25). Again, intermediates were deprotected using TFA where necessary (**95** and **97**).



Scheme 4.25 Isoquinoline analogues with yields for Suzuki and Boc-deprotection steps

To compare the removal of the 2-nitrogen from the quinazoline core, the 4-quinoline derivative of **12** and **233** (**245**) was attempted. Unfortunately using the previously successful synthetic route of reactions did not work because the disubstituted product (**242**) formed in the S_NAr step (LCMS m/z 446 with no chlorine splitting pattern instead of 321/323). The reaction was repeated with a 1:1 ratio of 1,3-dichloro-4-quinoline and ethylene diamine (normally an excess of amine was still added) but a mixture of unreacted starting material (**241**) and compound **242** formed.



Scheme 4.26 Attempted and optimised synthetic routes to compound 108

This was thought to be due to the difference in reactivity of the relative 1- and 3-position carbon atoms of the quinazoline (**247**), isoquinoline (**248**) and quinoline (**249**) rings due to the electronic effects affected by the relatively more electronegative nature of nitrogen (3.04)¹¹⁷ compared to carbon (2.55)¹¹⁷ atoms (Figure 4.14.). Carbons adjacent to nitrogens are more susceptible to nucleophilic attack whereas the 1-carbon of **249** is only adjacent to other carbons atoms, making it less delta positive for attracting a nucleophile.

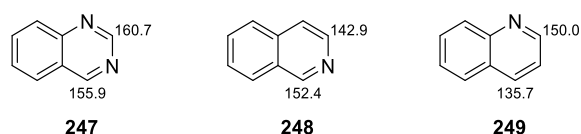
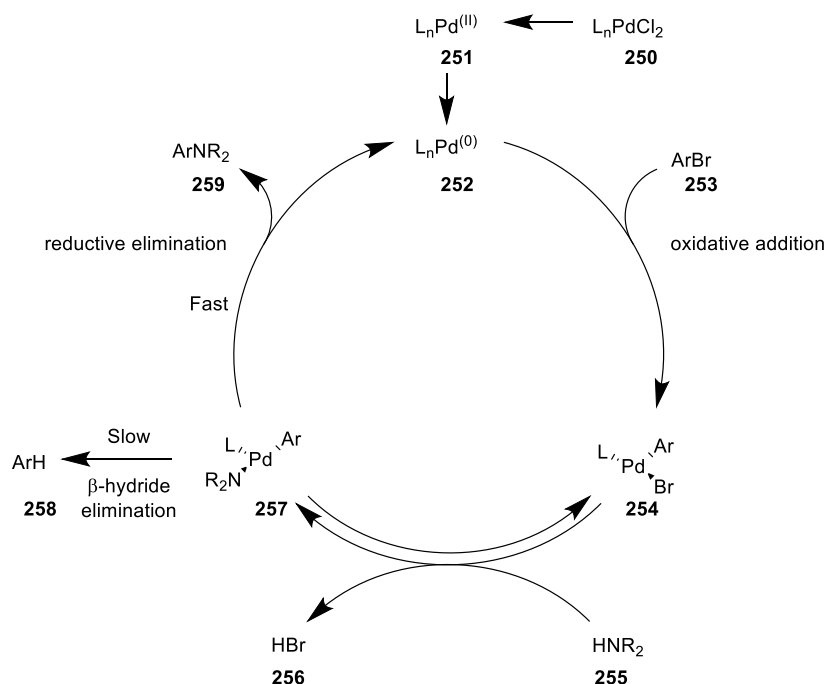


Figure 4.14 Comparison of relative literature 1-position and 3-position ¹³C NMR shift values for protons in quinazoline (**247**), isoquinoline (**248**) and quinoline (**249**)¹⁵⁶

Instead, the Suzuki step was attempted first. This successfully introduced the pyridyl group in place of the 3-position chlorine to make **246** in near quantitative yield. The amine (**182**) was successfully coupled to **246** through Buchwald Hartwig coupling conditions¹⁵⁷ and removal of the Boc-group yielded compound **245** in 43% yield across three steps.

Scheme 4.27 outlines the mechanism for the Buchwald-Hartwig transformation. Oxidative addition of an aryl bromide (**253**) to a Pd(0) complex (**252**), followed by coordination of an amine (**255**) catalyses the reductive elimination of the N-coupled aryl group (**259**).



Scheme 4.27 Mechanism for Buchwald-Hartwig Amination¹⁵⁸

There were observable general differences between the ^1H NMR spectra when comparing the 2,6-naphthyridine (e.g. **12**) and its quinazoline (**220**), isoquinoline (**233**) and quinoline (**245**) match pairs (Figure 4.15). Due to the lack of nitrogen in the left fused ring of **220**, **233** and **245**, additional correlation is seen between four aromatic protons instead of just two in **1** (orange). In **1**, two singlets and two doublets were observed while for **220**, **233** and **245**, two doublets and two triplets were generally observed. For **233** and **245** an additional singlet was observed compared to **220** because of the removal of the nitrogen.

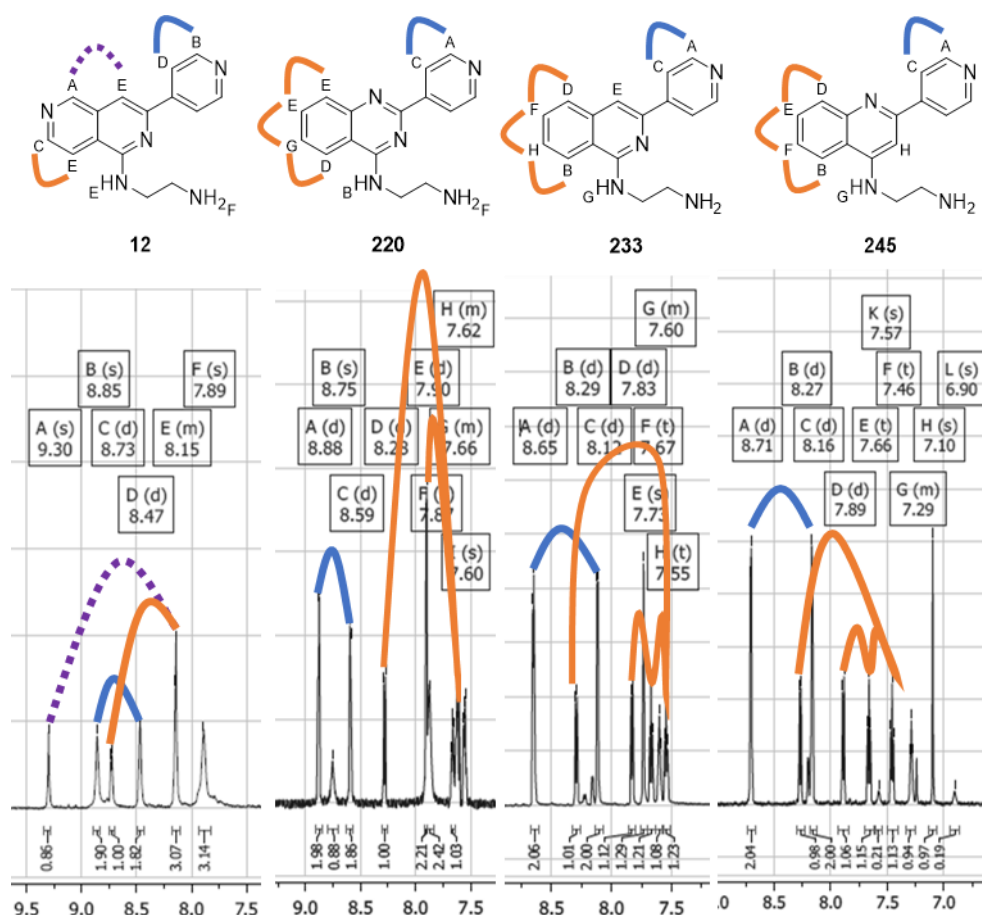


Figure 4.15 Comparison of aromatic regions of ^1H NMR spectra for compounds **12**, **220**, **233** and **245**

Pyridyl variation

When TR-FRET evaluation of the aforementioned 2,7-naphthyridine, quinazoline, isoquinoline and quinoline compounds confirmed it was possible to retain potency for PKN2 for certain core and amine combinations (see Section 4.3.1), further structural changes were made to the compound set. The next region of SAR investigation focused on the 4'-pyridyl moiety within compound **12**.

Due to the slightly shorter $\text{S}_\text{N}\text{Ar}$ reaction time for the quinazoline (1 h) compared to the isoquinoline series (overnight), the quinazoline series was used to observe this structural point

change. The 3'-pyridyl analogues of **220** (**260**) and **222** (**261**) were prepared using the chemistry described in Scheme 4.20 but 3-pyridylboronic acid was used instead of 4-pyridylboronic acid (**196**) Figure 4.16. For **260**, the yields of the Suzuki and deprotection steps were 46% and 86%, respectively and for **261** the transformations yielded 37% and 86% of product, respectively.

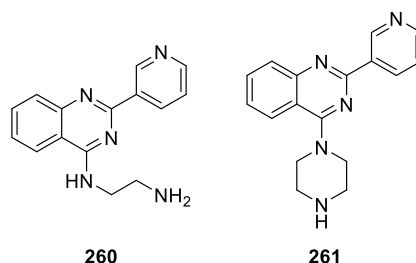


Figure 4.16 3'-Pyridyl analogues of compounds **220** and **222**

^1H NMR was used to confirm the 3'-pyridyl analogues had been prepared. Instead of observing two doublets to reflect the symmetrical nature of the four 4'-pyridyl protons, four peaks each integrating to a single proton correlated to the unsymmetrical nature of a 3'-pyridyl motif. For **260**, this was observable as a singlet at δ 9.61; two doublets at δ 8.75 and δ 8.68 ppm; and a fourth peak overlapping with other aromatic peaks associated with the quinazoline structure between δ 7.58–7.45 ppm.

Similarly, for the piperazine match-pair (**261**), two multiplets were observed at δ 9.66–9.54 and 7.62–7.50 ppm, as well as two double triplets at δ 8.76 and 8.70 ppm. Each peak corresponded to a single proton within the 3'-pyridyl structure and COSY NMR was used to assign the pyridyl hydrogens of compounds **260** and **261**.

Further amine variation

Similar to above, the quinazoline core was primarily used to further explore changes to the amine portion of compound **220** due to the relatively short reaction time. Larger structural changes were made to compound **220** by introduction of a morpholine ring (**262**) and extending beyond the ethylene diamine function by addition of a piperidine (**263**), piperazine (**264**) and morpholine ring (**265**) at the end of the two carbon chain (Figure 4.17).

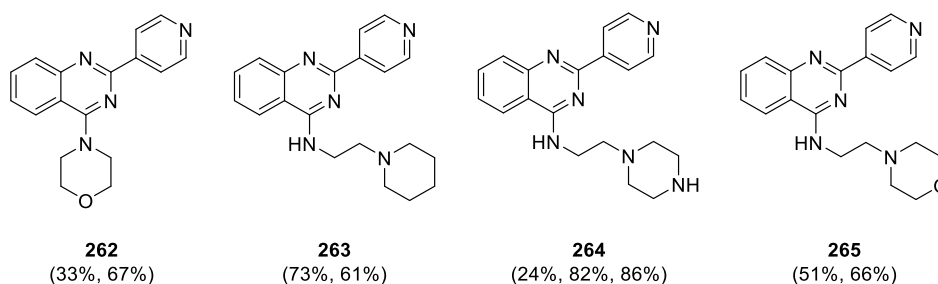


Figure 4.17 Piperidine-, piperazine- and morpholine-containing analogues **262–265** with yields for S_NAr , Suzuki (and for **264**, Boc—deprotection) steps, respectively

For morpholine analogue **262**, a shift in the positions of the aliphatic 1H NMR peaks was observed compared to **222** containing a piperazine ring. Two overlapping doublets, giving the appearance of a double doublet was observed at δ 3.86 ppm compared to the two distinct triplet peaks observed at δ 3.94 and 3.23 ppm for compound **222**. There was also no N-H peak in the 1H NMR spectrum of **262**.

For the extended amines (**263–265**) on the other hand, additional peaks were observed in the 1H NMR spectrum to the two ethylene diamine peaks each integrating to two protons. Three additional broad singlets were observed at δ 2.48, 1.50 and 1.38 ppm with integrations of four, four and two protons respectively in the 1H NMR spectrum for **263**. The lack of multiplicity is thought to be due to the relative flexibility of the piperidine ring system.

For **264**, there were only two broad singlets each integrating to four protons at 2.75 and 2.48 and while no N-H peak was observable in the 1H NMR, LCMS analysis gave m/z 335 for **264**, corresponding to a molecular weight of 334. A similar 1H NMR spectrum was observed for **265** but a higher m/z of 336 was observed in the LCMS spectrum, indicating the presence of an oxygen instead of a nitrogen in **265**.

This chemistry was also utilised to prepare pyrrolidine (**266**) and dimethylamine (**267**) analogues of **220** (Figure 4.18). For **266**, a broad singlet and a multiplet were observed in the 1H NMR spectrum at δ 4.00 and 2.08–1.93 ppm respectively. Both peaks integrated to four protons each, confirming reduction in ring size compared to piperidine-containing analogue **223**. In the 1H NMR spectrum for compound **267**, a singlet integrating to six protons at δ 3.46 indicated the dimethylamine had been successfully coupled to the quinazoline ring.

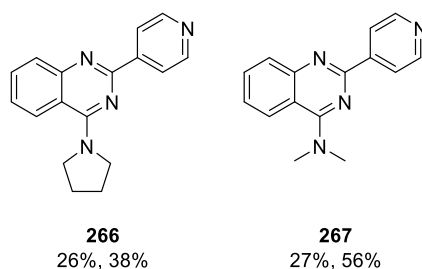
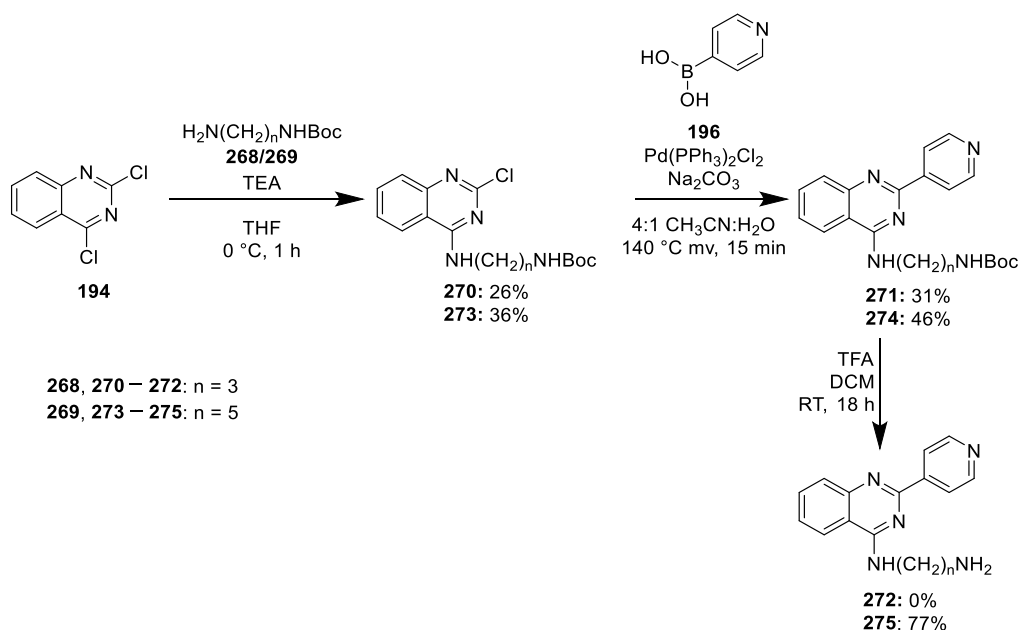


Figure 4.18 Compounds 266 and 267, with reported yields for S_NAr and Suzuki steps, respectively

Attempts to extend the ethylene diamine chain resulted in the synthesis of compound **275** with five carbon atoms between the two amine functions. The propylene analogue (**272**) was prepared in part, but purification of **271** proved difficult partly due to its solubility (it could not be dissolved in DCM, methanol, ethyl acetate, DMSO and combinations of these solvents) and it was of insufficient purity to carry out the final deprotection step. Scheme 4.28 summarises the attempted syntheses of the two compounds.



Scheme 4.28 Attempted syntheses of 272 and 275

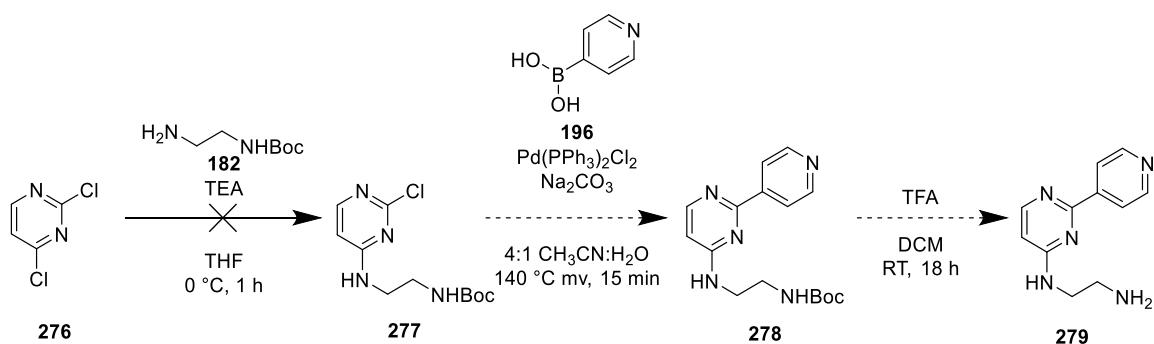
The synthesis of **272** was later reattempted but was abandoned due to time constraints within the project. Isolation of only compound **275** was deemed a suitable matched pair for comparing the bioactivity of a compound with an extended chain against **220** in the absence of **272**.

Removal of phenyl ring

Attempts to synthesise respective pyrimidine and pyridine analogues of **220** and **222** without a fused benzene ring proved unsuccessful. An exemplar scheme of the chemistry intended to make **279** is summarised in Scheme 4.29. Solubility was the main issue in trying to make these.

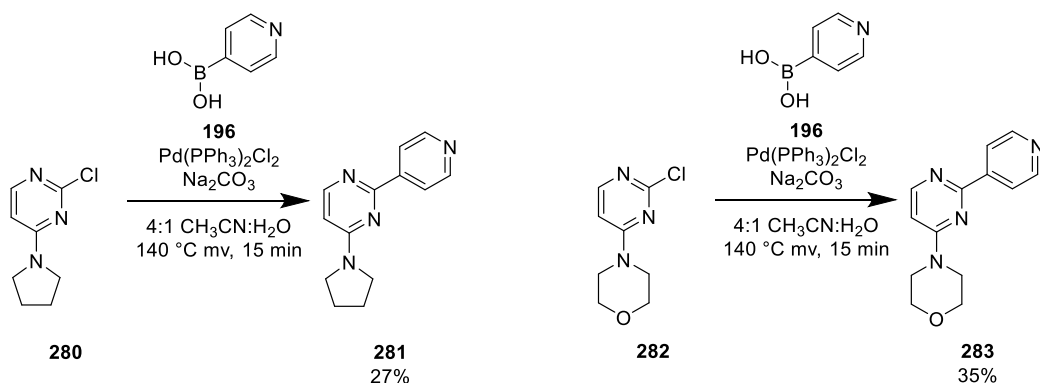
The formed products preferred to dissolve in the aqueous phase rather than the organic phase, even when using a polar 2:1 chloroform:propan-2-ol solvent mixture as the organic phase so compound **277** could not be isolated. Thin Layer Chromatography (TLC) analysis of the reaction mixture also indicated flash column chromatography would not be a suitable method to purify this reaction mixture due to the polarity of the reaction and the number of other closely running side products.

Any samples of **277** and similar analogues that were isolated were not of sufficient quantity or purity to carry forward in the synthesis. A 250 mg sample of an unprotected version of **277** was purchased and while the Suzuki transformation was successful by LCMS, the compound could not be isolated, again due to its solubility. Purchasing larger quantities of this intermediate was not economically viable so the synthesis of other possible analogues was investigated.



Scheme 4.29 Attempted synthesis to 279

Instead, a comparison was made between two matched pairs where an already substituted intermediate was available commercially, to check the Suzuki chemistry worked. These were the pyrrolidine and morpholine containing entities which were made from commercially available 2-chloro-4-(1-pyrrolidinyl)pyrimidine (**280**) and 4-(2-chloro-4-pyrimidinyl)morpholine (**282**) which only required a single Suzuki reaction step to make products **281** and **283**, respectively (Scheme 4.30).



Scheme 4.30 Syntheses to 281 and 283

The ^1H NMR profiles of **281** and **283** were similar to their quinazoline, counterparts **266** and **262** respectively, but there were two fewer aromatic peaks due to the removal of the benzene ring. While the yields were relatively low, sufficiently pure sample was prepared in quantities adequate for use in the TR-FRET assay.

While it would have been useful to have prepared the ethylene diamine and piperazine analogues, these compounds should provide a useful matched pair with **262** and **266** to see what effect removing the phenyl ring from the quinazoline has on the potency against PKN2 (Figure 4.19).

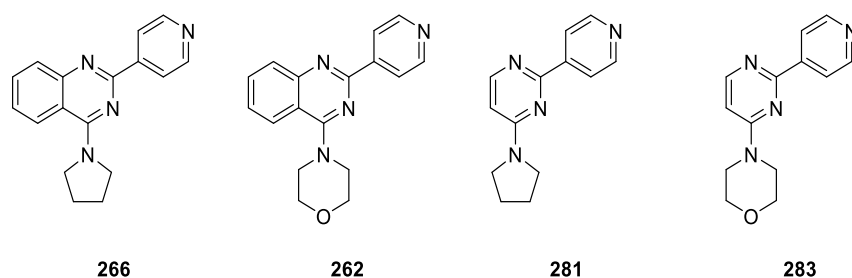


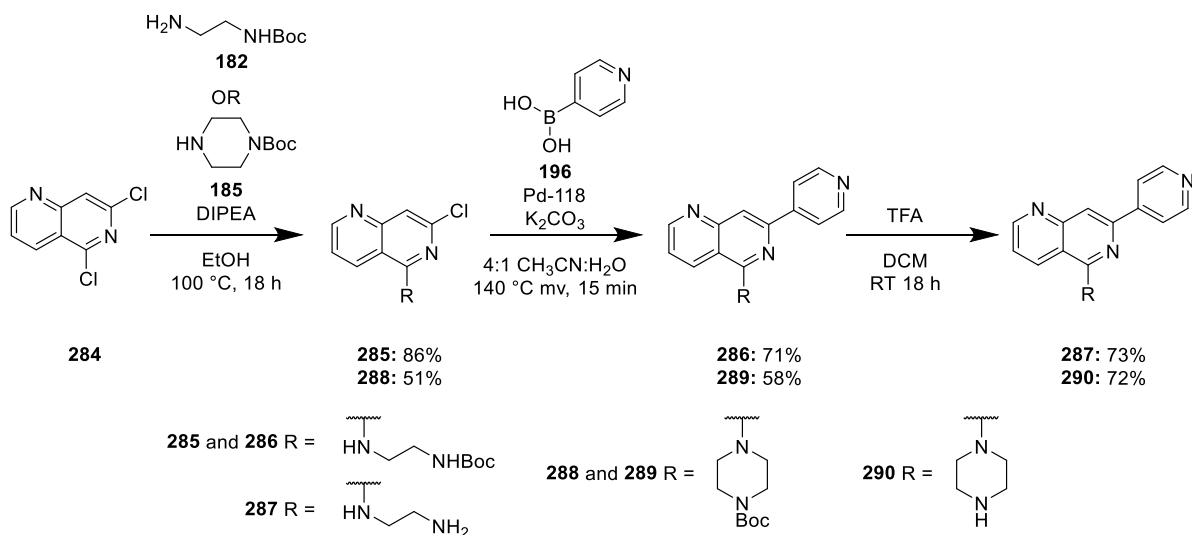
Figure 4.19 Quinazoline and pyrimidine core match pairs

Returning to a naphthyridine core

After receiving kinome selectivity data on 2,7-naphthyridines **187**, **191** and quinazolines **220** and **222** (see section 4.3.2), the 2,7-naphthyridine core was shown to have better selectivity across the human kinome than the quinazoline cores. This was a disappointing result because quinazoline-containing compounds like **220** had a shorter synthetic route (2–3 steps) than the other three compounds (7–8 steps).

It was decided to return to a naphthyridine core to see what effect shifting the 7-nitrogen to the 6-position had on potency and selectivity because of the commercial availability of 1,3-dichloro-2,6-naphthyridine (**284**). If these compounds exhibited similar PKN2/1 selectivity, the 2,6-naphthyridine core would be used to prepare further analogues with finer structural changes made in order to further optimise a chemical probe for PKN2.

Scheme 4.31 outlines the $\text{S}_{\text{N}}\text{Ar}$, Suzuki and deprotection chemistry conditions used to produce the 2,6-naphthyridine analogues of **12** and **187–287** and **290**, respectively. These conditions were the same used for preparing isoquinoline analogues.



Scheme 4.31 Synthetic route for preparing 2,6-naphthyridine analogues

The general changes in ^1H NMR splitting pattern observed going from a 2,7- to a 2,6-naphthyridine were loss of a singlet peak and the gain of a triplet/multiplet peak correlating to two other peaks as there were now three aromatic protons adjacent to one another. Figure 4.20 gives an example comparison between the spectra of compounds **12** and **287**. Correlation was generally observable between aromatic hydrogens at the 7- and 8-positions as well as the pyridyl hydrogens.

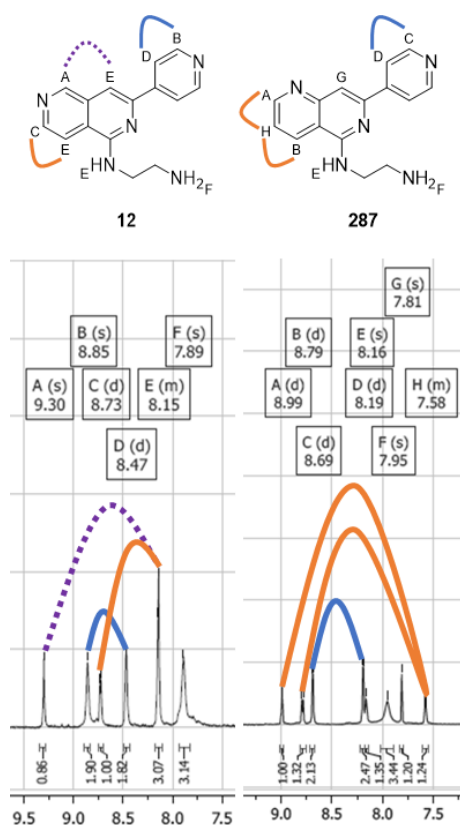


Figure 4.20 Comparison of aromatic region of ^1H NMR spectra for compounds **12** and **287**

Finer structural changes to piperazine

Potency for PKN2 and selectivity against PKN1 were retained for compounds **287** and **290** which indicated the 2,6-naphthyridine core was suitable to use (see Section 4.3.1). This resulted in the rapid synthesis of analogues related to **290**, due to the high kinome selectivity of its 2,7-naphthyridine analogue, **187**.

The analogues in Figure 4.21 contain electron-withdrawing groups adjacent to one of the basic nitrogen atoms. **286** and **289** are Boc-protected intermediates produced during the synthesis of **287** and **290** while compounds **291** and **292** contain less bulky amide groups. **293** contains a lactam moiety and **294** is a *N*-methylated derivative of **293**. These were prepared using commercially available amides which were coupled using the same S_NAr conditions outlined in Scheme 4.31. The reaction yields when preparing these analogues were generally high (70–100%) due to the removed basicity of one of the amines present which made purification by flash column chromatography on acidic silica gel relatively straightforward.

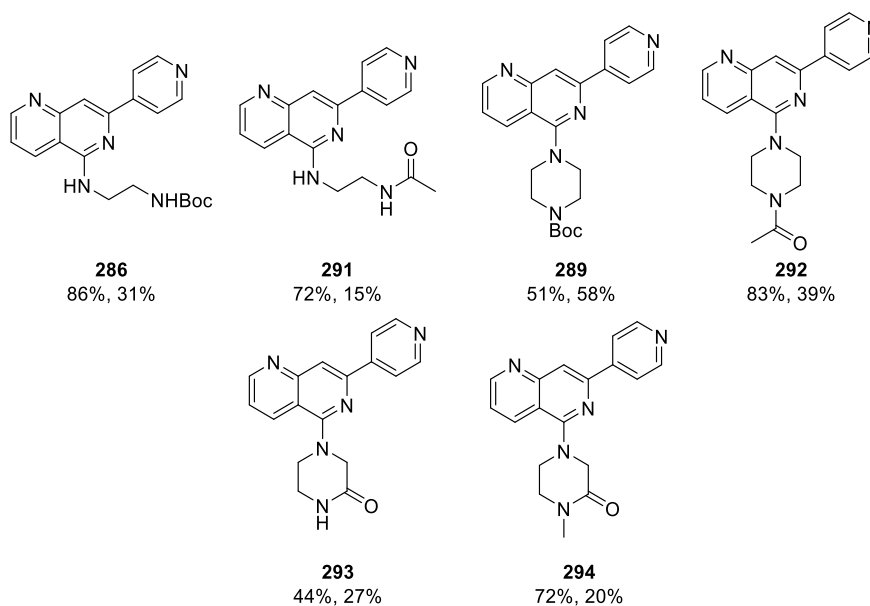


Figure 4.21 Structures of 2,6-naphthyridine analogues with electron-withdrawing modifications with yields for S_NAr and Suzuki steps, respectively

It was also relatively simple to produce alkylated analogues of **290** using the same chemistry with commercially available piperazines, removing the need for an alkylation step. The methyl (**295**), *iso*-propyl (**296**) and phenyl (**297**) capped piperazine analogues (Figure 4.22) were prepared using the previously described S_NAr and Suzuki chemistry in Scheme 4.31.

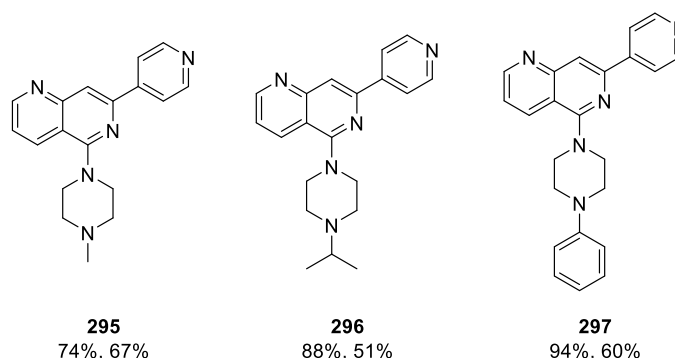


Figure 4.22 *N*-substituted analogues of **290** with yields for S_NAr and Suzuki steps, respectively

1H NMR spectra for these compounds lacked an N-H peak and gained peaks associated with the alkyl species capping the piperazine, in addition to the usual pairs of peaks observed for the piperazine protons. Generally, these compounds required a more polar solvent system during flash column chromatography purification, typically dichloromethane:methanol over petroleum ether:ethyl acetate because of their increased polarity compared to the compounds in Figure 4.21.

Similarly, it was also possible to investigate the addition of branching moieties on the piperazine carbons (Figure 4.23). A series of mono- and di-methylated piperazines (**298–302** and **306–307**) were attempted and all but one were successfully isolated. A suitably pure sample of the opposite diastereoisomer of **298** was not successfully isolated within the timeframe of the project but it was thought the difference in bioactivity would be negligible given the small size of the methyl group.

It was possible to introduce a geminal dimethyl group next to the N-H (**307**) but not adjacent to the 2,6-naphthyridine ring, likely due to steric hindrance occurring during the S_NAr step. Similarly, **306** was successfully prepared using *tert*-butyl (2*R*,6*S*)-2,6-dimethylpiperazine-1-carboxylate but a similar reaction using *tert*-butyl (3*R*,5*S*)-3,5-dimethylpiperazine-1-carboxylate with the two methyl groups on the carbons nearest the naphthyridine was unsuccessful. Larger *isopropyl* (**303**), *isobutyl* (**304**) and *benzyl* (**305**) groups were also introduced to the terminal end of the piperazine ring to compare with **290** using commercially available amines with the alkyl groups already substituted onto the piperazine ring. It was also possible to substitute the piperazine for a simple bicycle in **308** using commercial reagent (1*R*,4*R*)-5-Boc-2,5-diazabicyclo[2.2.1]heptane.

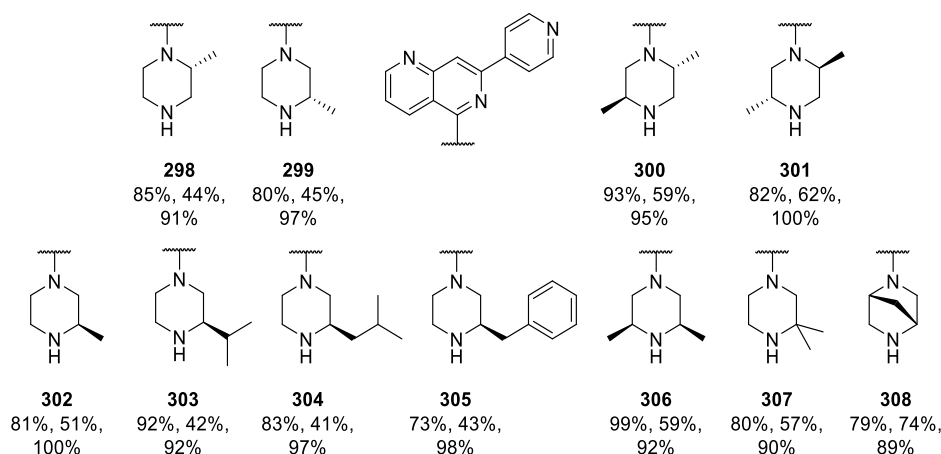


Figure 4.23 Analogues of 290 with additional alkyl groups and yields for S_NAr , Suzuki and Boc-deprotection steps, respectively

The observable changes in the 1H NMR spectra for these compounds was generally in the lower shift aliphatic region. One or more of the piperazine C-H peaks would either disappear or would half in size corresponding to the loss of piperazine protons that had been substituted by alkyl groups. New peaks would be observed corresponding to the group introduced to the ring. Little difference was seen in chemical shift between diastereoisomers e.g. for **298** and **299**, a methyl-related peak was observed at δ 1.31 and 1.17 ppm, respectively. At times due to overlapping peaks and overall flexibility of the ring system, it was difficult to fully assign peaks due to the appearance of broad singlets and these have been assigned as far as possible in the experimental section.

Converting the flexible ethylene diamine of **12** to a relatively more rigid piperazine ring (**187**) was one example of restricting the relative position of the terminal hydrogen bond donating N-H to the naphthyridine core. Other rigidified ring systems involving Boc-protected amino pyrrolidines were reacted with **284** using the usual chemistry in Scheme 4.31 to yield compounds **309–312** (Figure 4.24) in addition to bicycle **308** shown in Figure 4.23. It was possible to verify the incorporation of these ring systems into the compound using COSY NMR which showed how the aliphatic C-H protons correlated to the various amine groups.

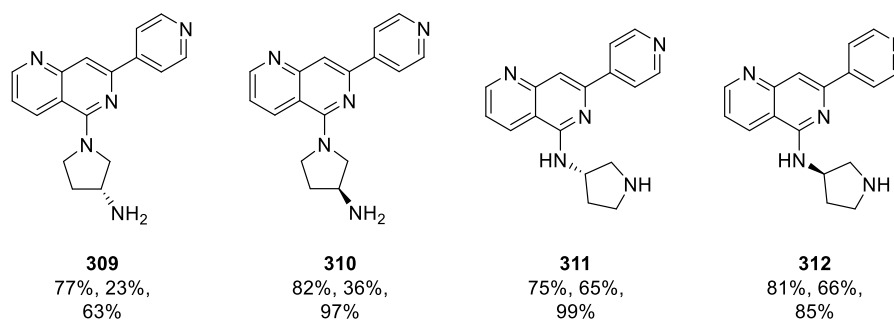


Figure 4.24 Pyrrolidine analogues of 290 with yields for S_NAr , Suzuki and Boc-deprotection steps, respectively

For example, in the aliphatic region of the COSY NMR for compound **312** (Figure 4.25), two connected ring systems could be elucidated, starting from tertiary proton 12, in order to distinguish between the less polar 16-C protons and the slightly more polar C-15/13 protons. The C-15/13 protons which were adjacent to the pyrrolidine N-H meaning they had a higher δ value than peaks corresponding to 16-C protons which were between two carbon atoms. Two sets of peaks were observable for protons 13, 15 and 16 because each carbon was bound to two protons, each in distinct magnetic environments.

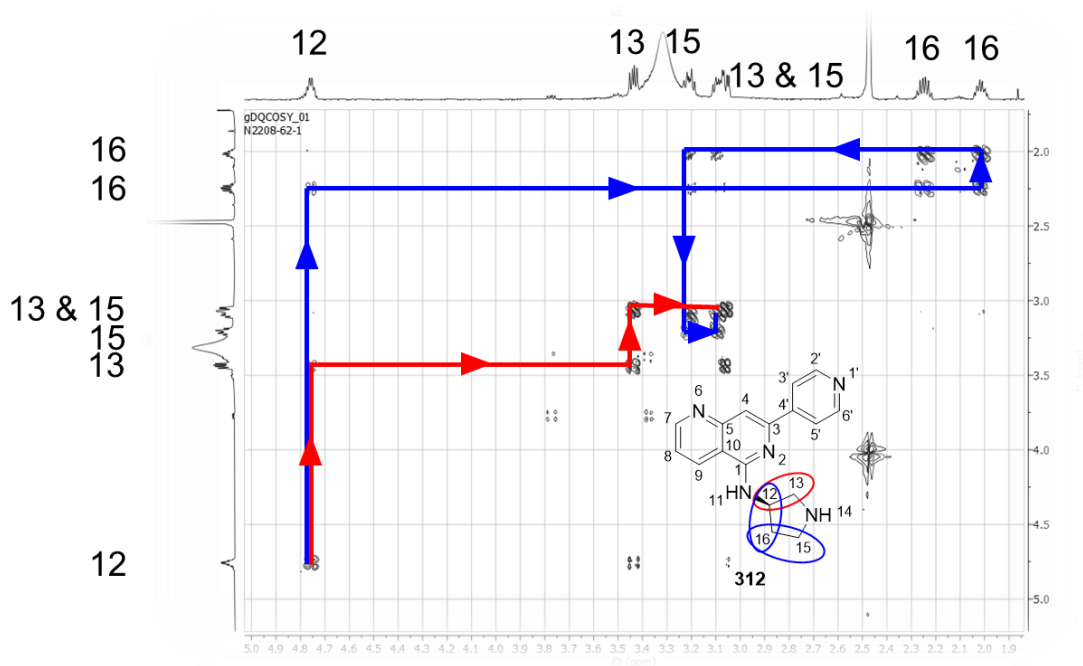


Figure 4.25 Zoomed aliphatic region of COSY NMR spectrum for compound **312** showing two ring systems (red and blue) and their corresponding protons on structure of **312**.

Unexplored SAR

Beyond the 2,6-naphthyridine core chemistry work, no other cores were explored. This was due to the general unavailability of equivalent commercial reagents possessing chlorines at the 1-, 3- and other positions, that would have otherwise facilitated efficient synthesis of modular

compounds. A small number of compounds do exist as commercial agents but were not available in quantities that were useful for the previously described syntheses. It would have otherwise been interesting to investigate the effect of growing off other vectors within the compounds, for example, the 5–8-positions on the naphthyridine ring, on the activity of the compound against PKN2.

In total, 52 analogues of compound **12** were prepared (Figure 4.26), most using an optimised synthetic route by altering the central core of the molecule. Naphthyridine, quinazoline and isoquinoline cores were reacted with amines and boronic acids in order to vary the modular components of compound **12**, primarily focusing on the amine moiety at the 1-position of the central core of the molecule.

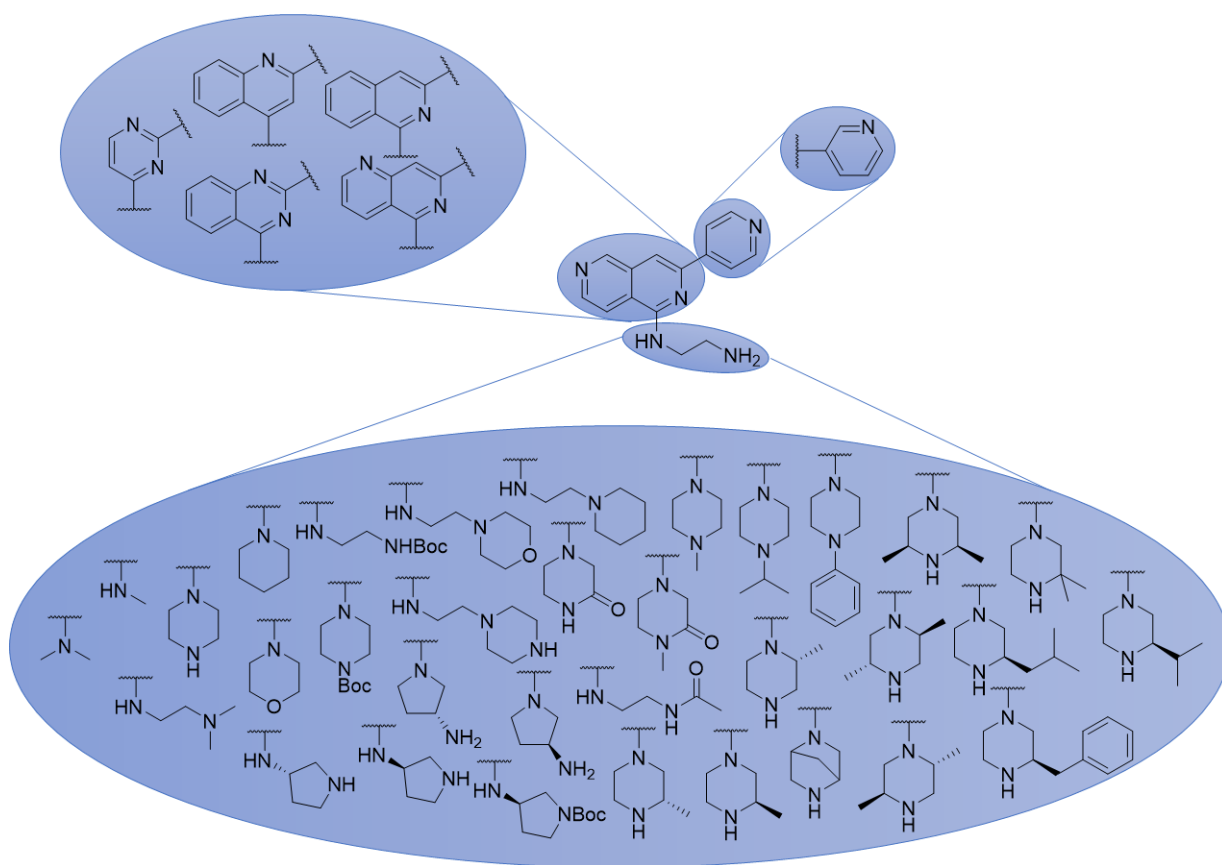


Figure 4.26 SAR explored around compound **12**

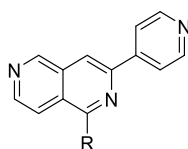
4.3 Biological evaluation

4.3.1 TR-FRET

The compounds were tested by the SGC using the commercial TR-FRET technology assay previously described in section 2.3.1. Due to the size of compound library compared to Series A and Series B, similar chemical species have been grouped into individual results tables to outline the SAR explored around compound **12**. Some of the TR-FRET measurements are missing for PKN1. This is due to a lack of sufficiently purified PKN1 protein at the time of testing.

Compound **12** was confirmed to be a potent inhibitor of PKN2 ($K_i = 12$ nM), however exhibited only 5-fold selectivity over PKN1. Table 4.2 shows that these particular variations of the amine at the 1-position of **12** largely retain potency for PKN2 but can tune selectivity between PKN2 and PKN1. Rigidifying the ethylene diamine group to a piperazine (**187**) also shows a gain in potency although no improvement on selectivity. Removing the terminal N-H of **187** in piperidine analogue **189** results in a negligible doubling of potency. Capping the primary amine in **12** with two methyl groups in **191** suggests the presence of a terminal primary amide is not essential for binding in PKN2 but is more desirable for achieving potency in PKN1. Finally, removal of most of the amine to a methylamine moiety in **193** results in a large loss in potency suggesting the terminal nitrogen in **12**, **187** and **191** is important for binding to PKN2.

Table 4.2 Structure activity relationships for 2,7-naphthyridine-containing compounds binding to PKN2 and PKN1. Calculated K_i values for PKN2 and PKN1 are shown in nM. The assay Z' factor was $0.7 < Z' < 0.9$; $n = 2$.

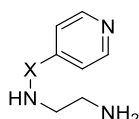


#	R	PKN2 K_i (nM)	PKN1 K_i (nM)
12		12	56
187		2.7	15
189		25	140
191		14	120
193	-NHMe	5400	23000

Table 4.3 compares the different central cores investigated compared to compound **1**. Switching to a 2,6-naphthyridine (**287**) from a 2,7-naphthyridine (**12**) has little impact on potency, but PKN2/1 selectivity improves slightly from 5-fold (**12**) to 12-fold. This improvement drove the decision to focus on making 2,6-naphthyridines in the latter stages of the project.

Switching to the quinazoline core (**220**) results in a slight loss of potency (3-fold) but also improves the PKN2/1 selectivity (16-fold). This suggests the 6-position nitrogen in the naphthyridine ring is not essential for PKN2 binding if it can be moved or removed. **233**, the isoquinoline derivative of **12** has similar potency and selectivity to **12** (7-fold). The 4-isoquinoline (**245**), on the other hand, results in 34-fold loss of potency for PKN2 highlighting the importance of having a nitrogen at the 2-position in the central core of this set of compounds.

Table 4.3 Structure activity relationships for ethylene diamine-containing compounds binding to PKN2 and PKN1.
Calculated K_i values for PKN2 and PKN1 are shown in nM. The assay Z' factor was $0.7 < Z' < 0.9$; $n = 2$.



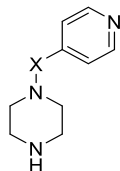
#	X	PKN2 K_i (nM)	PKN1 K_i (nM)
12		12	56
287		11	130
220		30	480
233		8.4	58
245		410	4600

A similar comparison is made between piperazine-containing analogues in Table 4.4. Switching to the 2,6-naphthyridine (**290**) compared to the 2,7-naphthyridine (**187**) results in a slight 7-fold loss of potency but maintains selectivity between PKN2 and PKN1 (7-fold *cf.* 6-fold for **187**). Due to the promising wider kinome selectivity of **187** (see Section 4.3.2), the medicinal chemistry moved towards a focused library around piperazine- and 2,6-naphthyridine-containing compounds, as outlined in the latter portion of section 4.2.

A quinazoline core with both nitrogen atoms on the one ring (**222**) slightly reduced the potency of the compound for PKN2 by 10-fold but maintained PKN2/1 selectivity at 7-fold difference in K_i between the two kinases. Isoquinoline **237**, on the other hand, had a less drastic effect on potency compared to **222** but reduced the selectivity to 3-fold, less than that of **12**. As with the

ethylene diamine library above in Table 4.3, the naphthyridine cores are advantageous over quinazoline and isoquinoline cores for these compounds.

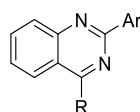
Table 4.4 Structure activity relationships for piperazine-containing compounds binding to PKN2 and PKN1.
Calculated K_i values for PKN2 and PKN1 are shown in nM. The assay Z' factor was $0.7 < Z' < 0.9$; $n = 2$.



#	X	PKN2 K_i (nM)	PKN1 K_i (nM)
187		2.7	15
290		19	135
222		32	210
237		8.4	28

Table 4.5 compares the bioactivities of quinazolines **220** and **222** with their 3'-pyridyl matched pairs, **260** and **261**, respectively, as well as their preceding Boc-protected intermediates (**219** and **221**, respectively). Both Boc-protected analogues result in large loss of potency indicating the importance of the free terminal basic amine in **220** and **222**. Similarly, compounds **260** and **261** indicate that the 3'-pyridyl is detrimental to PKN2 potency, as has been the case for compounds in Series B and Series C, suggesting it may be interacting with the hinge region of PKN2. For this reason, no further changes were made to the pyridyl region of the series.

Table 4.5 Structure activity relationships for pyridyl-containing compounds binding to PKN2 and PKN1. Calculated K_i values for PKN2 and PKN1 are shown in nM. The assay Z' factor was $0.7 < Z' < 0.9$; $n = 2$.

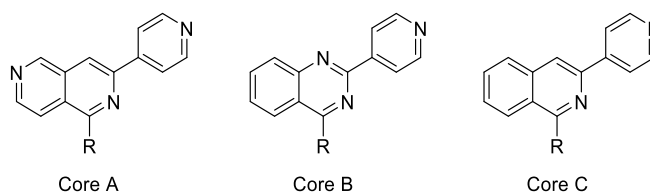


#	Ar	R	PKN2 K_i (nM)	PKN1 K_i (nM)
220	4'-py		30	480
260	3'-py		35000	-
119	4'-py		99763	-
222	4'-py		32	210
261	3'-py		4000	15000
221	4'-py		31549	31548

Table 4.6 shows the data in preceding tables combined with the other quinazoline and isoquinoline derivatives of the initial five compounds isolated containing the 2,7-naphthyridine core. It appears that removing or moving the 7-nitrogen atom from **12** and **220** has a generally negligible effect on the potency of the quinazoline and isoquinoline analogues but when the amine is neither ethylene diamine or piperazine, there is loss of potency when the core changes to a quinazoline or isoquinoline.

For piperidine containing compounds, there is 125-fold and 917-fold loss of potency when moving from the 2,7-naphthyridine (**189**) to the quinazoline (**223**) or isoquinoline (**238**) core, respectively. This suggests **189** is not binding *via* the pyridyl group but in another conformation, which is no longer possible by removal of the 7-nitrogen. For **193**, a truncated version of **12**, there is loss of activity across the three cores. Compound **267**, the dimethyl derivative of **225** shows similar inactivity compared to **220** indicating it is the loss of the terminal amine has a larger effect on potency than whether the nitrogen attached to the 1-position of the core has a hydrogen bond donor. The 2,6-naphthyridine analogues containing piperidine, methylamine and *N,N*-dimethylethylene diamine were not synthesised due to a focus on piperazine-based analogues.

Table 4.6 Structure activity relationships for a selection of series C compounds binding to PKN2 and PKN1.
 Calculated K_i values for PKN2 and PKN1 are shown in nM. The assay Z' factor was $0.7 < Z' < 0.9$; $n = 2$.



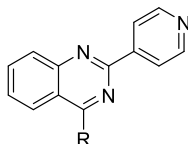
#	Core	R	PKN2 K_i (nM)	PKN1 K_i (nM)
12	A		12	56
220	B		30	480
233	C		8.4	58
187	A		2.7	15
222	B		32	210
237	C		8.4	28
189	A		25	140
223	B		1500	13000
238	C		11000	36000
193	A	-NHMe	5400	23000
225	B		1200	4800
240	C		600	2600
267	B	-NMe ₂	1400	7000
191	A		14	120
224	B		520	5200
239	C		251	tbc

Table 4.7 compares quinazoline **220** with attempts to extend the ethylene diamine moiety. Removing the terminal nitrogen with a piperidine ring (**263**) results in 83-fold loss of PKN2 potency due to steric effects or loss of the hydrogen bond donor N-H. Attaching a piperazine ring (**264**) on the other hand, which effectively extends the terminal hydrogen bond donating N-H by a length of three atoms, results in a smaller 13-fold loss of potency. This suggests a terminal hydrogen bond donor (e.g. N-H) protruding away from the central core of the compound is beneficial for binding to PKN2. Meanwhile, capping with a morpholine (**265**) results in a greater 230-fold drop in K_i showing an oxygen atom is not a suitable replacement for the secondary amine.

Extending the carbon chain to five atoms in compound **275** results in 4-fold loss of potency towards PKN2. This suggests there is an optimal distance for either a N-H or -NH₂ to occupy within the PKN2 site. Retrospectively, it was disappointing that the propylene diamine analogue (**273**) could not be isolated for reasons previously described as this finer point change would

have been interesting to investigate given the result for its pentylene derivative. None of these compounds improved on compound **220**.

Table 4.7 Structure activity relationships for quinazoline compounds binding to PKN2 and PKN1. Calculated K_i values for PKN2 and PKN1 are shown in nM. The assay Z' factor was $0.7 < Z' < 0.9$; $n = 2$.



#	R	PKN2 K_i (nM)	PKN1 K_i (nM)
220		30	480
263		2500	16000
264		390	2100
265		6900	36000
275		130	820

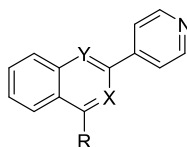
Table 4.8 shows the effect of removing the phenyl ring from the quinazoline structure. As previously described in section 4.2.2, it was not possible to isolate the ethylene diamine- or piperazine-containing analogues with a pyrimidine core due to the polarity of the S_NAr reaction product. Instead, intermediates containing already substituted pyrimidine rings with morpholine (**283**) and pyrrolidine (**281**) functions were used because they only required a Suzuki step to get to the product. When compared with the quinazoline counterparts (**262** and **266** respectively), loss of potency is observed between **262/283** and **262/266**. It can be postulated that a similar loss of activity would be observed for an ethylene diamine analogue like **220** confirming the importance of the second ring for PKN2 potency.

Table 4.8 Structure activity relationships for quinazoline- and pyrimidine-containing compounds binding to PKN2 and PKN1. Calculated K_i values for PKN2 and PKN1 are shown in nM. The assay Z' factor was $0.7 < Z' < 0.9$; $n = 2$.

#	Structure	R	PKN2 K_i (nM)	PKN1 K_i (nM)
262			1200	7500
266			2100	18000
283			5100	42000
281			14000	7100000

Table 4.9 shows the full set of compounds synthesised with an isoquinoline and quinoline core. As previously discussed, the piperidine (**238**), *N,N*-dimethyl ethylene diamine (**239**) and methylamine (**240**) analogues exhibit a loss of potency with this core, unlike their 2,7-naphthyridine counterparts (see Table 4.6), as does removing the basicity of the terminal ethylene diamine (**234**) or piperazine (**236**) nitrogen by use of the carbamate in the Boc protecting group. For completeness, **245**, the quinoline analogue of **12** was also synthesised and was 48-times less potent than the isoquinoline **233** and the original compound, **12** ($K_i = 12$ nM).

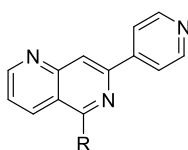
Table 4.9 Structure activity relationships for isoquinoline- and quinoline-containing compounds binding to PKN2 and PKN1. Calculated K_i values for PKN2 and PKN1 are shown in nM. The assay Z' factor was $0.7 < Z' < 0.9$; $n = 2$.



#	X	Y	R	PKN2 K_i (nM)	PKN1 K_i (nM)
233	N	C-H		8.4	58
234				25060	79245
237				8.4	28
236				99763	199054
238				11000	36000
239				251	tbc
240			-NHMe	600	2600
245	C-H	N		4100	4600

The library becomes more focused beyond this point, predominantly around 2,6-naphthyridine- and piperazine-containing compounds, with reference to **290**. Table 4.10 details the three compounds isolated that capped the piperazine N-H using a methyl (**295**), *isopropyl* (**296**) and phenyl (**297**) groups. **295** was 4-times less potent than **290**; and as group size increased, loss in potency also increased. In terms of selectivity, **295** and **296** have comparable PKN2/1 selectivity *cf.* **290** and the selectivity of **297** is irrelevant given its drop in potency for PKN2. This set of results indicates capping the terminal N-H of the piperazine is undesirable for achieving PKN2 potency and selectivity.

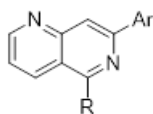
Table 4.10 Structure activity relationships for *N*-alkylated compounds binding to PKN2 and PKN1. Calculated K_i values for PKN2 and PKN1 are shown in nM. The assay Z' factor was $0.7 < Z' < 0.9$; $n = 2$.



#	R	PKN2 K_i (nM)	PKN1 K_i (nM)
290		19	135
295		83	410
296		130	760
297		18000	190000

Analogues were prepared that sought to remove basicity from the terminal primary amine in compound **287** and the secondary amine in the piperazine ring of **290** (Table 4.11). Addition of a carbamate (**286** and **289**) or acetate (**291** and **292**) group resulted in loss of potency. Swapping the piperazine ring for a piperazinone (**293**) and methylating the N-H of the oxopiperazine (**294**) also decreased the activity of the compound compared to **290** (PKN2 $K_i = 19$ nM).

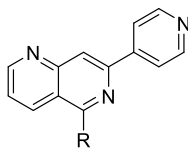
Table 4.11 Structure activity relationships for 2,6-naphthyridine-containing compounds binding to PKN2 and PKN1. Calculated K_i values for PKN2 and PKN1 are shown in nM. The assay Z' factor was $0.7 < Z' < 0.9$; $n = 2$.



#	R	PKN2 K_i (nM)	PKN1 K_i (nM)
286		7925	19906
291		1500	6900
292		1991	31548
289		12000	29000
293		730	15000
294		2800	23000

Table 4.12 shows structural changes made elsewhere on the piperazine ring. Compound **298** is equipotent with **290** with little improvement on PKN2/1 selectivity. Diastereoisomers **299** and **302** are roughly similar in their potency and selectivity. Thus the same result could be expected for the diastereoisomer of **298**.

Table 4.12 Structure activity relationships for 2,6-naphthyridine-containing compounds binding to PKN2 and PKN1. Calculated K_i values for PKN2 and PKN1 are shown in nM. The assay Z' factor was $0.7 < Z' < 0.9$; $n = 2$.



#	R	PKN2 K_i (nM)	PKN1 K_i (nM)
290		19	135
298		18	170
299		29	310
302		36	420
303		360	1400
304		32	150
305		300	1000
307		18	190
300		15	130
301		590	2500
306		64	680

Increasing the protruding alkyl group from a methyl (**302**) to an *isopropyl* (**303**) group reduces PKN2 potency by 10-fold while, surprisingly, the slightly larger *isobutyl* (**304**) group is equipotent with **302** but is less selective between PKN2 and PKN1. The *i*-butyl group potentially accommodates a cavity in the ATP binding site of PKN2 better than an *i*-propyl group does. The benzylated analogue (**305**) on the other hand, is 16-fold less potent than **290**.

Incorporating a second additional methyl group into the piperazine ring gave different results. When present on the same carbon in a geminal arrangement (**307**), PKN2 potency was comparable to **290** and there was a slight improvement in selectivity from 7-fold to 10-fold.

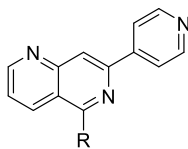
Diastereoisomers **300** and **301** gave different results based on the 3D conformation of the two methyl groups spaced three carbons apart in a trans conformation. Compound **300** had similar potency and selectivity *cf.* **290** but **301** was 31-fold less potent than **290** towards PKN2. This suggests the space the piperazine ring occupies is relatively small but can accommodate two methyl groups branching from the ring if they are in the right conformation.

Moving the methyl groups slightly closer together in a symmetrical *cis*-conformation adjacent to the amine (**306**) resulted in 3-fold loss of PKN2 potency but PKN2/1 selectivity increased from 7-fold to 10-fold compared to **290**.

Table 4.13, the last of TR-FRET results, details the potencies of the fused ring systems synthesised compared to the flexible terminal amine in **12** and **287**. Bicycle **308** is 12-fold less potent than **287**. Pyrrolidines **309** and **310** are 3–4 times less potent than **287** with similar selectivity over PKN1. Reversing the branched pyrrolidine such that the branching amine is coupled with the 2,5-naphthyridine core gave more contrasting results: **311** was 20-fold less potent towards PKN2 but its diastereoisomer **312** nearly doubled the potency towards PKN2. It also exhibited 18-fold selectivity over PKN1, the highest of any compound in this series.

The Boc-protected version of **312**, compound **313** was also tested and was shown to be 1000-fold less active towards PKN2 than **312** like other Boc-containing compounds. In combination with **312**, it provides a useful matched pair for use as a control in target validation experiments.

Table 4.13 Structure activity relationships for 2,6-naphthyridine-containing compounds binding to PKN2 and PKN1. Calculated K_i values for PKN2 and PKN1 are shown in nM. The assay Z' factor was $0.7 < Z' < 0.9$; $n = 2$.



#	R	PKN2 K_i (nM)	PKN1 K_i (nM)
287		11	130
290		19	135
308		130	970
309		48	680
310		28	320
311		200	3000
312		6.7	120
313		7400	19000

4.3.2 Kinome Selectivity Evaluation

Compounds **187**, **191**, **220**, and **222** were sent for screening against the DiscoverX kinase panel previously described in Section 3.3.2. These compounds were picked for their reasonable potency and selectivity for PKN2 over PKN1 – using a single run of TR-FRET data which differed slightly from the averaged data in the section 4.3.1. Figure 4.27–Figure 4.31 show the inhibited kinases on the kinome phylogenetic tree with varying sizes of circle, corresponding to percentage inhibition by the compound. These will be discussed in order of increasing PKN2 selectivity. The full data can be viewed in Appendix 1.

Figure 4.27 and shows that 1 μ M concentration of compound **191** inhibits 4 out of 400 distinct kinase targets above a nominal threshold of 70%. Unfortunately, PKN2 does not feature in that set of four kinases. Instead it is the 24th most inhibited kinase from the panel used in this experiment (Figure 4.28). The kinases that were inhibited by **191** were ROCK1, ROCK2, HASPIN and YSK4. ROCK kinases lie within the AGC family and share structural similarity with PKNs, so it is not surprising that compound **191** inhibits these kinases. It should be noted that false positives are possible in this experiment given the single dose and vast quantity of targets.

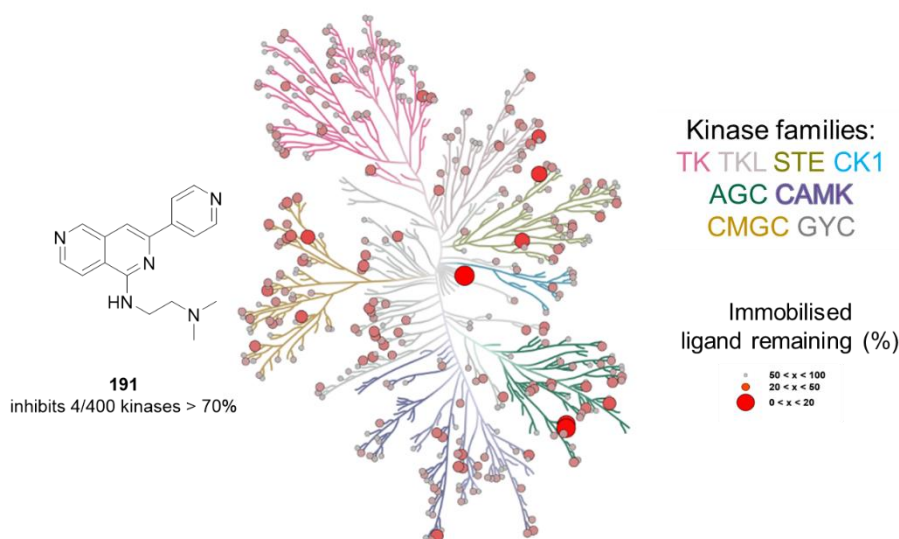


Figure 4.27 Kinome selectivity of compound 191 @ 1 µM

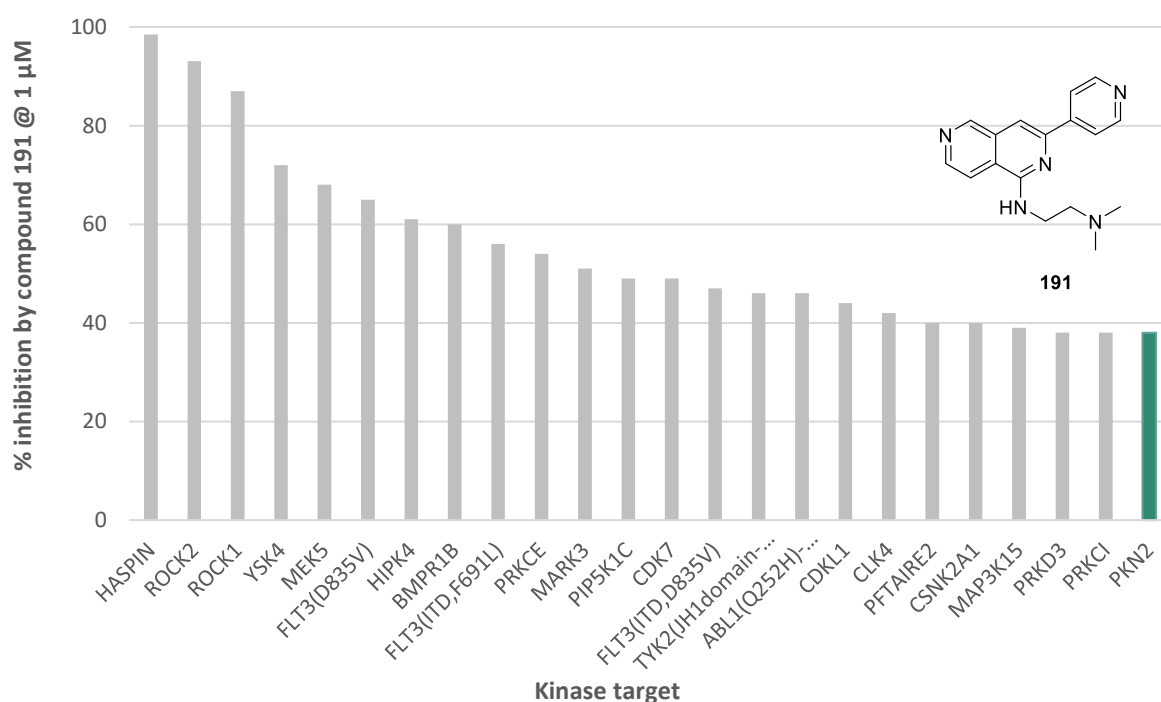


Figure 4.28 Bar graph showing where PKN2 sits in the top 24 kinases inhibited by compound 191 @ 1 µM in the DiscoverX KINOMEScan® experiment dosed at 1 µM. PKN2 highlighted in green.

A small number of large red spots in Figure 4.29 suggests **220** has a similar selectivity profile to compound **191**. **220** was shown to inhibit 2 out of 400 targets in this experiment, neither of which were PKN2. PKN2 is ranked 176th in terms of the most inhibited kinase in this set, while HASPIN and FLT3 kinases have the lowest % of immobilised ligand remaining in the experiment. The AGC family is highlighted in green and some degree of inhibition but nothing that suggests the compound is particularly selective for PKNs.

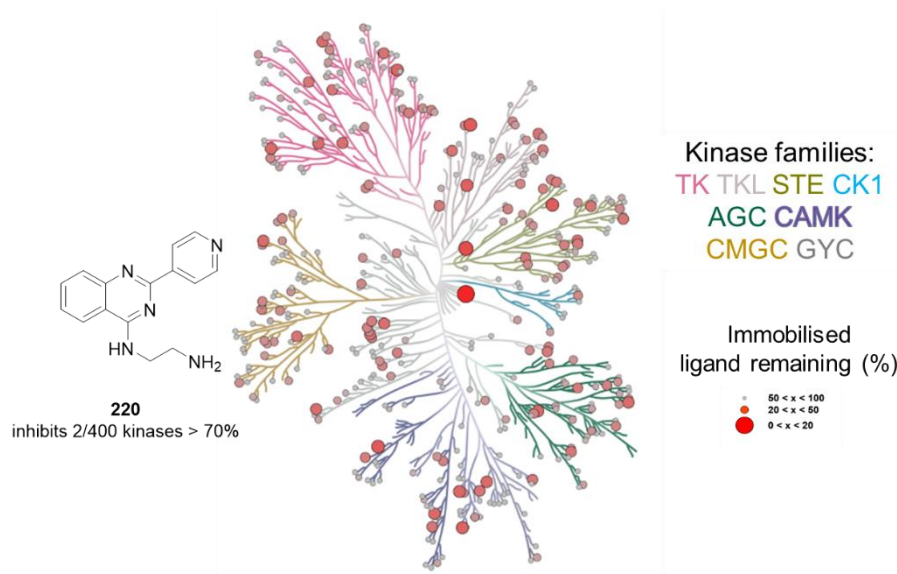


Figure 4.29 Kinome selectivity of compound 220 @ 1 μ M

Similarly, compound **222** in Figure 4.30 appears to not inhibit any of the kinases in this experiment above the nominal threshold of 70% when dosed at 1 μ M. PKN2 was ranked 176th out of 469 wild-type and mutant kinase domains used in the experiment. AMPK- α is the most inhibited kinase but only had a measured inhibition of 56% when dosed with 1 μ M **222**. While some binding is observed predominantly in the mustard yellow CMGC branch of the kinome, this shows this compound would not be ideal as a tool compound for PKN2. This discrepancy compared to the TR-FRET will be discussed further below.

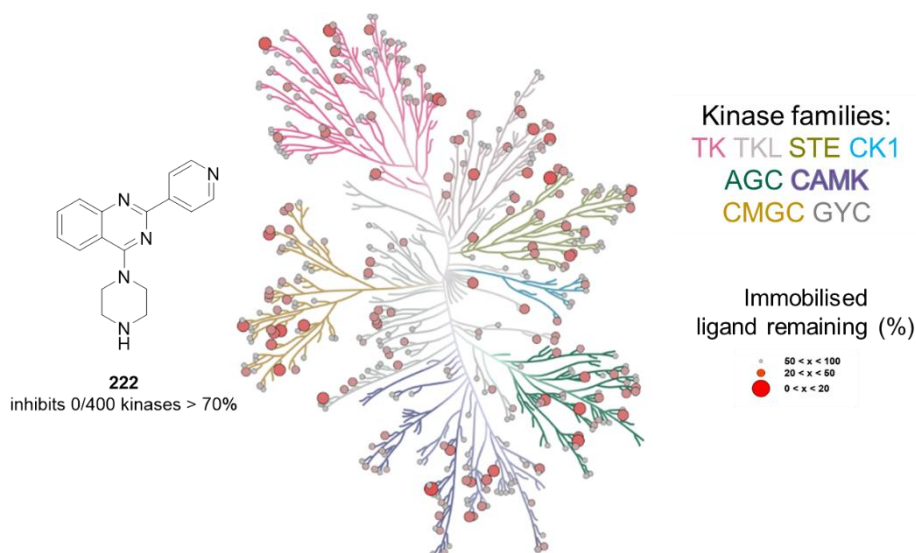


Figure 4.30 Kinome selectivity of compound 222 @ 1 μ M

The most promising result for this experiment regards compound **187**. In Figure 4.31, **187** is shown to have bound potently (indicated by large red circles) to several AGC kinases located on

the green branch of the kinome phylogenetic tree. Specifically, **187** was shown to bind to 9 out of 400 kinase targets above 70% inhibition.

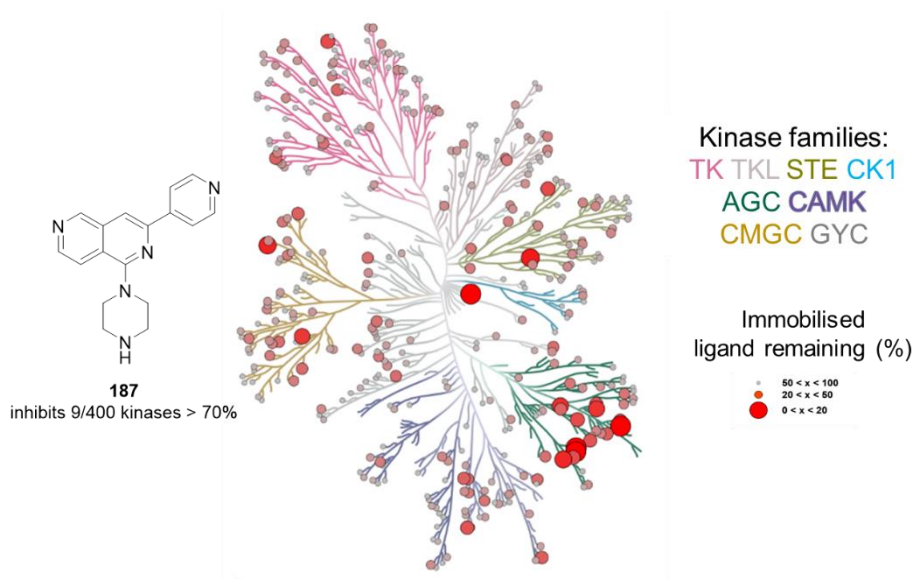


Figure 4.31 Kinome selectivity of compound **187** @ 1 μ M

The other kinases more potently inhibited by this compound were ROCK1, ROCK2 and HASPIN as seen for compounds **191** and **220** as well as PRKCE, MEK5, HIPK2, CIT and PRKG2. Some activity is also seen in the DYRK regions of the mustard yellow branches of the CMGC kinase family. Activity across the AGC kinase family is to be expected for a compound designed to target an AGC kinase.

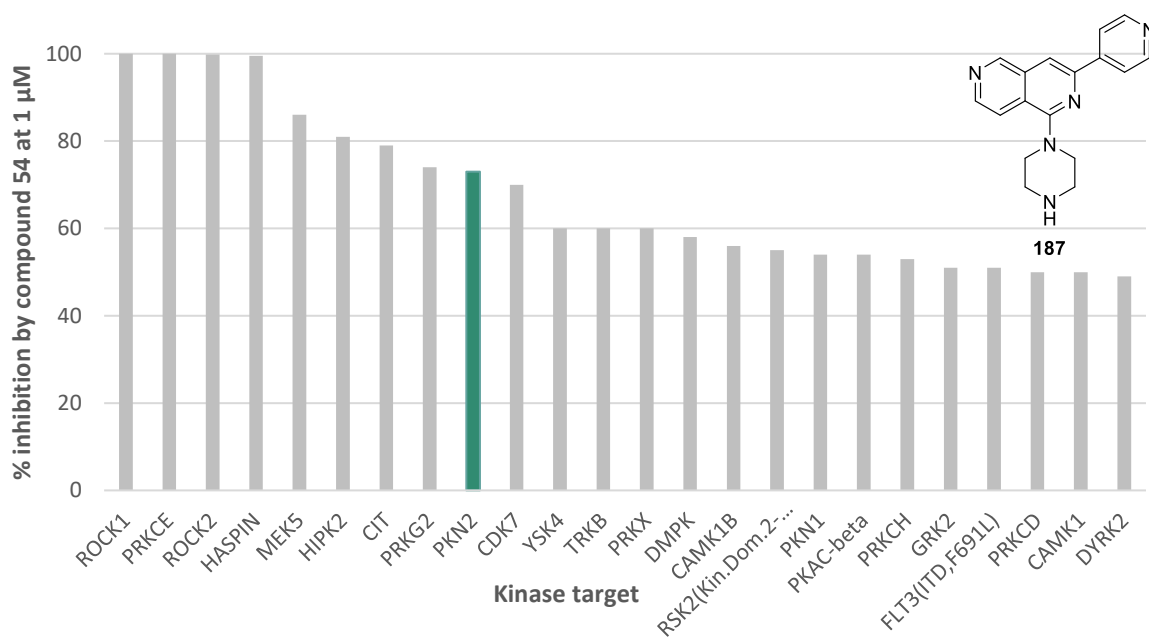


Figure 4.32 Bar graph showing where PKN2 sits in the top 24 kinases inhibited by compound **187** in the DiscoverX KINOMEScan[®] experiment dosed at 1 μ M. PKN2 highlighted in green.

DiscoverX data often contains false positives because testing these four compounds at single dose concentration (1 μ M) against over 400 kinases resulted in over 1600 data points. Perceived “hits” from a DiscoverX selectivity screen are usually followed up by testing the top hits from the KINOMEscan® in a dose-response measurement in order to obtain IC₅₀ values for the off-targets as well as the desired targets. This work has not been completed for these compounds thus far.

There is also the possibility of false negatives, as seen here for compounds **57**, **80** and **82** which appeared to be potent PKN2 inhibitors by the TR-FRET assay but not by the KINOMEscan®. An example of such an inhibitor is the SPHINX31 SRPK1 inhibitor.¹⁵⁹ The DiscoverX SRPK1 assay showed other SRPK1 inhibitors to be potent but not SPHINX31. It may be possible that certain inhibitors bind along with the immobilised ligand but generally these discrepancies have not been rationalised. The TR-FRET experiment is a more reliable method for showing compounds bind to PKN2 and PKN1 and this kinase panel screen is more useful as a general guide about selectivity.

After receiving these data, the decision was taken to focus on further optimising **187**, the most potent and selective of these four compounds. Attempts were made to investigate if returning to the 2,7,naphthyridine could be avoided because of the length of the synthetic route.

The 2,6-naphthyridine analogue (**290**) showed similar potency and PKN2/1 selectivity to **187** as previously described and a library of compounds related to **290** were prepared to see if the wider kinome selectivity could be maintained, or even improved upon with this small structural change.

4.4 Computational chemistry

4.4.1 Similar ligands in the Protein Data Bank

In the PDB there is one example of a similar compound bound to PKC η (Figure 4.33), a geminal dimethyl analogue of **12** (**314**) (Figure 4.34). The pyridyl nitrogen of this compound, is shown to interact with the N-H of a valine residue (Val436) *via* a hydrogen bonding interaction in crystal structure 3TXO in Protein Kinase C- η (PKC η). Given the general similarity of PKC kinases to PKN kinases, this supports the pyridyl-based binding hypothesis associated with this series of compounds.

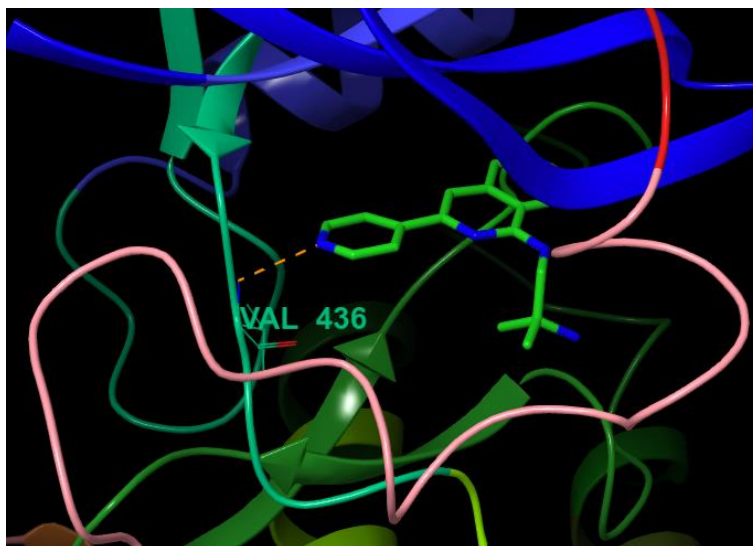


Figure 4.33 Compound 314 interacting with hinge region (mint green) of PKC η (PDB code 3TXO).¹⁶⁰ Figure made with Schrodinger Maestro 19-4.

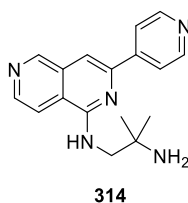


Figure 4.34 Geminal dimethyl analogue of 12

Searches for similar pyridine-containing structures with 2,6-naphthyridine, quinazoline, isoquinoline and quinoline cores yielded no hits. More crystal structures with these core heterocycles are deposited in the PDB e.g. 533 structures co-crystallised with quinazoline-containing ligands, but these lacked the experimentally determined essential pyridyl ring also needed for binding in this series of compounds.

4.4.2 Docking Experiments

A selection of synthesised and hypothetical Series C compounds were docked into PKN2 as previously described in section 2.4 by the author. While in the previous two chapters, experimentally inactive compounds were docked and *vice versa*, more compounds from this series were successfully docked by this method.

Figure 4.35 shows five compounds (**12**, **315–318**) that were successfully docked into the ATP binding site of PKN2 with one of the two bonding constraints applied regarding the alanine (Ala740) and Tyrosine (Tyr739) residues shown to form hydrogen bonds with ATP- γ S in a structure of PKN2 (PDB code 4CRS).

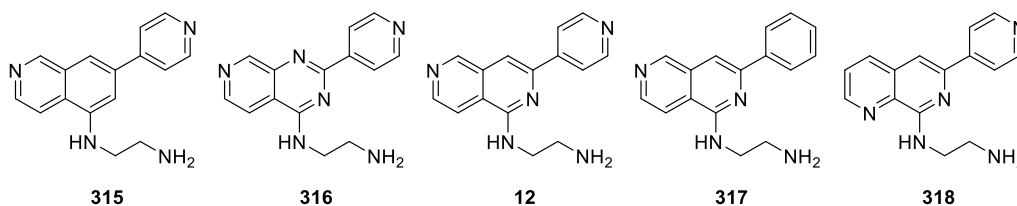


Figure 4.35 Compounds successfully docked via one binding constraint

Unfortunately, the compounds did not correspond to the experimentally elucidated bonding hypothesis. Compounds **12** and **315–317** were shown to interact with Ala740 within the kinase hinge region (yellow) *via* the 7-position nitrogen hydrogen bond acceptor. None of the compounds bound *via* the 4'-position nitrogen acceptor in the pyridyl ring (Figure 4.36).

Compound **318** is the phenyl derivative of **12**. While this was not synthesised, the 3'-pyridyl quinazoline analogue (**260**) was shown to be experimentally inactive in section 4.3.1. It is assumed a phenyl group would have given a similar result, as per the set of series B compounds synthesised in section 3.3.1.

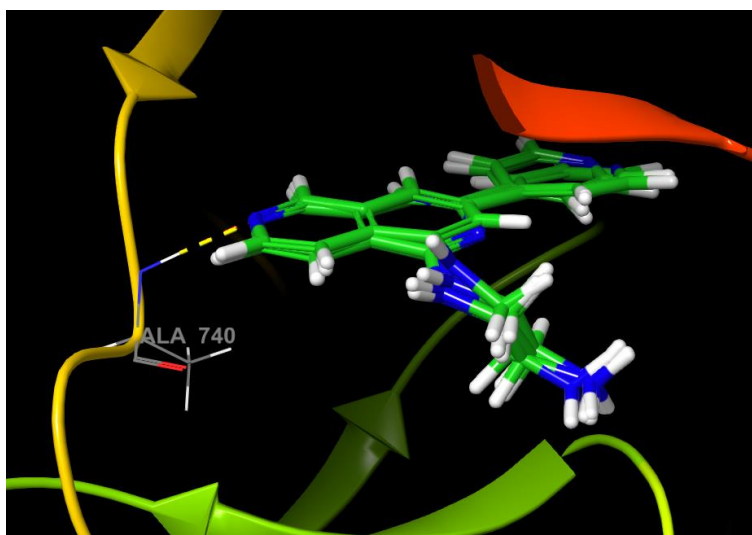


Figure 4.36 PKN2 hinge region (yellow) with compounds **2**, **315–317** stacked. Figure made with Schrodinger Maestro 19-4.

The theoretical 2,9-naphthyridine (**318**), which was not synthesised, was the only one of this set of compounds shown to bind *via* the 4'-pyridyl to Ala740 within the hinge of PKN2 (yellow) (Figure 4.37). Compound **318** does not have a nitrogen at the 7-position like the other four compounds in Figure 4.35 which may be why the 4'-pyridyl nitrogen became the preferential hinge binder.

Figure 4.37 shows an overlay of the two docked binding poses of compound **318** in the constrained and unconstrained docking experiments. There is little change in the overall

positioning of the compound. An additional interaction is shown whereby the terminal amine forms a hydrogen bond with an aspartate (Asp 744) residue in the C-domain of the kinase. It may be possible that the piperazine N-H of **54** and the pyrrolidine N-H of **167** occupy more desirable orientations to interact with this residue.

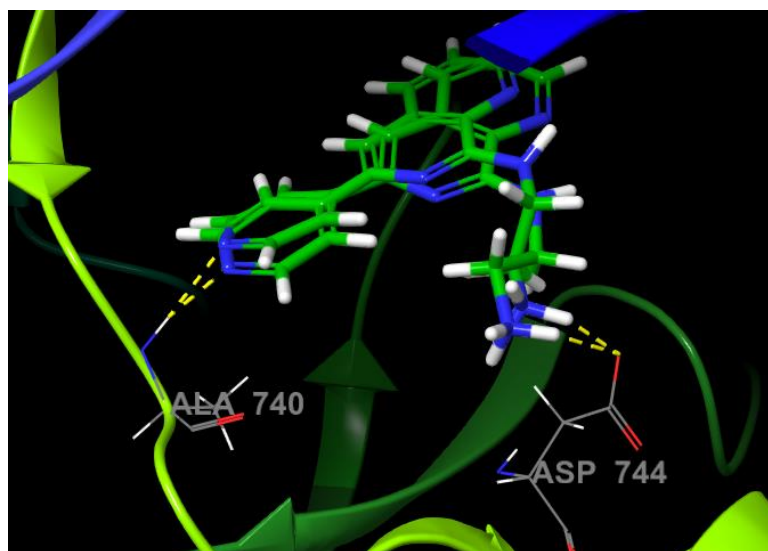


Figure 4.37 Overlay of compound **318** in PKN2 from single and zero constricted experiments interacting with hinge (lime green) of PKN2. Figure made with Schrodinger Maestro 19-4.

Generally, it is difficult to carry out docking studies without a crystal structure containing a molecule from the same series of compounds because a kinase conformation usually changes when it is inhibited by ATP-competitive ligands. Using this crystal structure of PKN2 as the basis for the docking model did not correlate that with experimental data but assuming the binding conformation of **318** was correct, it was possible to justify some of the experimental changes in SAR. Many of the compounds that proved to be active by biochemical assay were not successfully docked into the protein.

Cross-docking experiments

Following return of the DiscoverX data for compounds **187**, **191**, **220** and **222**, these compounds underwent similar cross docking experiments described in section 3.4.2. As per the series B compounds, ambiguous binding modes were observed for the compounds across the different kinase targets, fully outlined in Appendix 2.

When compound **191** was docked across the two kinase sets with high inhibition in the DiscoverX screen and had structural similarity to PKN2 (Figure 4.38), two thirds of the docking experiments were ambiguous (grey), in that the compound did not bind to the hinge region or bound *via* an unusual conformation such as the aliphatic amine. This was expected as the crystal

structures chosen for the various kinases in this cross-docking study contained a variety of chemotypes of ligands that were not necessarily naphthyridine-based.

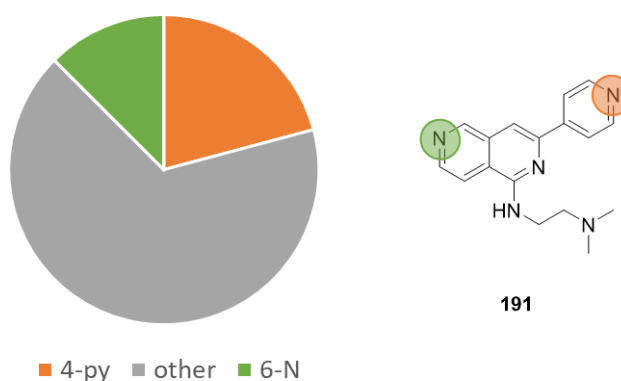


Figure 4.38 Distribution of binding modes in cross-docking experiment with compound 191

Of the successful cross-docking experiments, just over half bound to the hinge *via* the 4'-pyridyl nitrogen (orange) while the remaining cases bound *via* the nitrogen at the 6-position (green) in the naphthyridine ring. These are the two most expected binding conformations for this compound so although only a third of the kinases successfully accommodated the compound using this method, it highlights the ambiguity in potential binding mode.

All of the docking experiments using compound **220** were successful (Figure 4.39). Just under half of those showed the compound bound to the kinase *via* the 4'-pyridyl (orange) of those that successfully docked into their respective kinases.

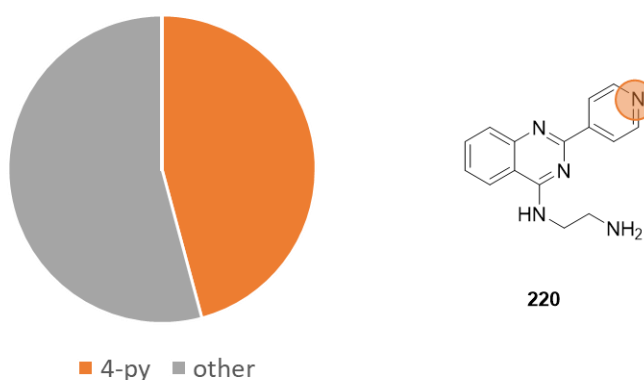


Figure 4.39 Distribution of binding modes in cross docking experiment with compound 220

The other binding conformations were classified as "other" (grey), meaning the compound either bound elsewhere in the kinase or they bound *via* the amine or other portion of the molecule in an inconsistent way. This suggests that removing the 6-nitrogen from compound **12** to the 4-position removes the ability of the compound to bind to the kinase in the alternative conformation seen for compound **12**.

Compound **222** is the piperazine analogue of **220**. While there was a small number of cases where the compound did not dock (yellow), around a quarter docked *via* the 4'-pyridyl nitrogen (orange). There was a case where the 4-position nitrogen in the quinazoline core interacted with the hinge (blue), but this was not seen across other kinases. The majority of binding modes were unclassifiable (Figure 4.40).

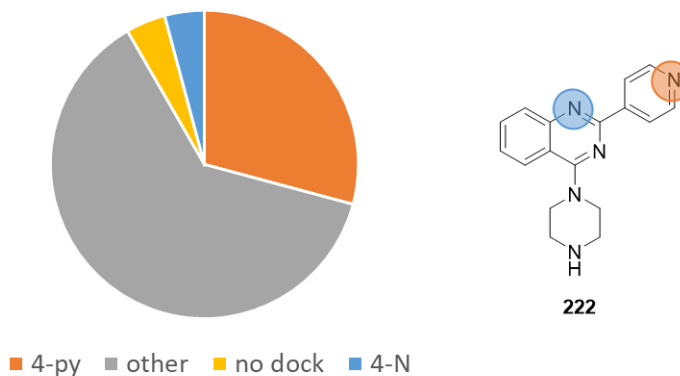


Figure 4.40 Distribution of binding modes in cross docking experiment with compound **222**

Finally, for compound **187**, the 2,7-naphthyridine equivalent of **222** showed similar ambiguous binding modes seen for the other compounds (Figure 4.41). In this case, half of the docking experiments showed the kinases forming hydrogen bonding interactions with the 6-position nitrogen (green) and around just under a quarter of cases with the 4'-pyridyl nitrogen (orange).

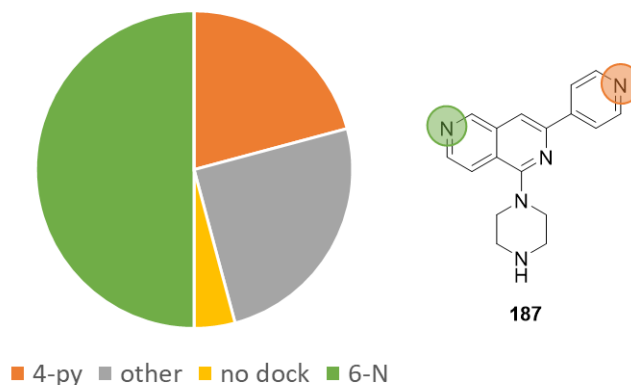


Figure 4.41 Distribution of binding modes in cross docking experiment with compound **187**

The cross docking studies suggest 2,7-naphthyridine-containing compounds have more possible binding conformations than quinazoline and isoquinoline cores. This is thought to be due to having a nitrogen on both rings within the central heterocycle core of the molecule. These studies suggest it be possible to reduce binding ambiguity by removing this nitrogen through the use of an alternative heterocycle like a quinazoline or isoquinoline. Reducing the number of ATP-like motifs in a compound is a reasonable strategy to prevent the compounds binding to more

kinases. There was also an instance where the dock was unsuccessful (yellow) and around a quarter of cases where the compound bound to the kinase in other ways (grey) such as the piperazine interacting with the hinge over the aromatic rings.

Overall, the docking experiments did show that the compounds bound *via* the pyridyl ring (orange) in some, but not all cases. While ambiguous binding modes outside of the hinge region were the most common binding type, it was possible to see the effect removing the 6-nitrogen had on forcing the binding conformation towards the pyridyl-led interaction. Unfortunately removing this nitrogen did not improve the selectivity experimentally so a nitrogen is required in that region for PKN2 potency.

Due to the inconclusive nature of the docking experiments, with multiple binding modes suggested, computational docking was not deemed a suitable tool using this particular model for guiding chemistry for this series of molecules. Experimental results showed that loss of the 4'-pyridyl ring resulted in the greatest loss of potency, suggesting this hydrogen bond acceptor at this particular arrangement was involved in the key interaction with the kinase hinge.

4.5 Crystallography

Dr. Angela Fala (SGC) managed to successfully co-crystallise compound **187** with PKN2 (Figure 4.42). This is the first crystal structure of PKN2 bound to a non-ATP-type ligand. Compared to the existing structure of PKN2 bound to ATPyS (PDB code: 4CRS), the structure of PKN2 with **187** bound shows that it binds to the hinge region of the PKN2 *via* the 4'-pyridyl nitrogen which forms a hydrogen bond with an alanine residue (Ala740). The 7-nitrogen also forms a hydrogen bond with a lysine in the N-terminal region (Lys686). The aromatic rings lie parallel to each other but the piperazine extends almost perpendicular to the naphthyridine ring to make an interaction with an aspartate residue (Asp786).

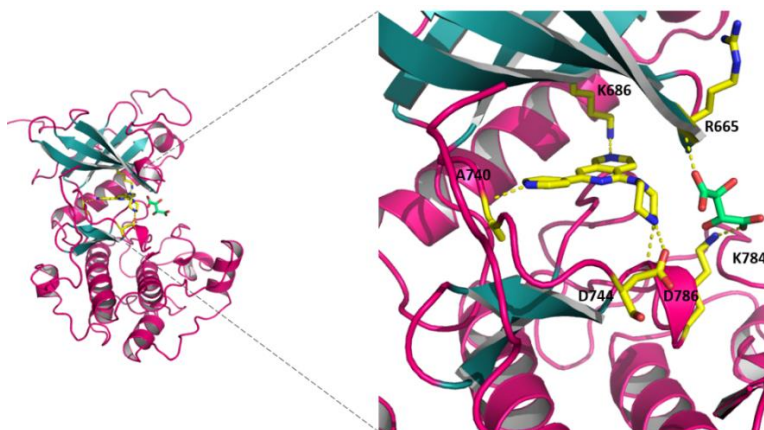


Figure 4.42 Crystal structure of PKN2 co-crystallised with compound **187** with zoomed section on binding site showing key interactions with residues. Figure produced by Angela Fala using MOE.

Figure 4.43 shows the aligned PKN2 structures and highlights the binding sites of the two structures individually. It appears that Asp744 interacts with both a hydroxyl group in the sugar portion of ATP and with the piperazine N-H. The 5-nitrogen and 4-amino functions of the adenine portion of ATP form an acceptor donor motif with the hinge of the motif while compound **187** only requires a single hydrogen bonding interaction with an alanine residue in the hinger (A/Ala740). The lysine residue that interacts with the 7-nitrogen of **187** also interacts with the central phosphate group in ATP. The lack of disparity between the two structures in the hinge region suggests that compound **187** occupies a similar space to ATP in that it mimics three key interactions with PKN2. A tartrate molecule has also crystallised with the structure and interacts with lysine (Lys/K784) and arginine (Arg/R665) residues at the exterior of the PKN2 ATP site due to the conditions used to grow the crystal (see section 6.2.3).

While the docking studies discussed in section 4.4.2 did not show this binding conformation for compound **12**, a 2,9-naphthyridine analogue (**318**) did occupy the ATP site of PKN2 in a similar orientation, with the 4'pyridyl nitrogen forming a hydrogen bond with the alanine (Ala740) residue in the hinge and the terminal amine with an aspartate residues Asp744 and Asp786. Docking studies should be reattempted using this new crystal structure to see if compound **12** and other 2,7- and 2,6-naphthyridine analogues dock into the kinase with a similar conformation as **318**.

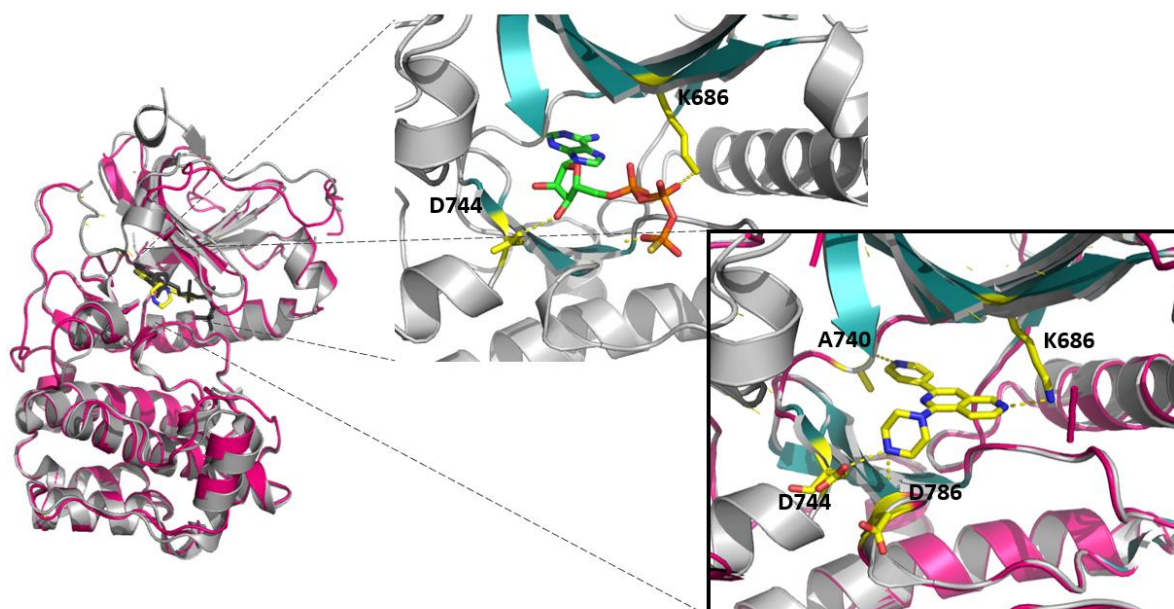


Figure 4.43 Alignment of PKN2 crystal structures with ATP γ S and compound **187** bound and zoomed sections of individual binding sites and key residues highlighted. Figure produced by Angela Fala using MOE.

Crystallisation studies with compound **312** are underway but it is possible to postulate that the branched pyrrolidine in **312** provides a more optimal angle for the terminal amine to protrude away from the naphthyridine ring to form a stronger interaction with aspartate residue (Asp744). Compounds with longer amine branches such as **264** and **275** may be too large to form an ideal interaction with this residue (Figure 4.44).

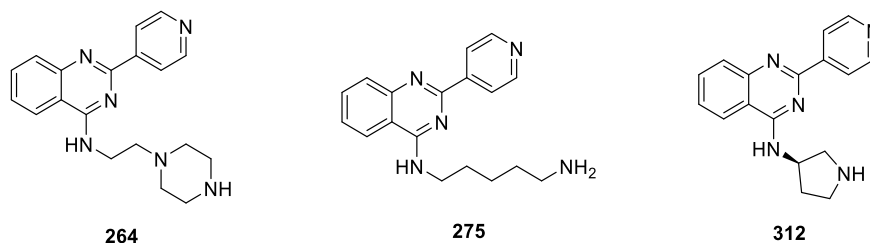


Figure 4.44 Compounds **264**, **275** and **312**'s SAR can be rationalised with the crystal structure of **187** in PKN2

The attainment of this crystal structure confirms the importance of the pyridyl ring and the necessary inclusion of a second nitrogen in the central ring across this series of compounds. It can be proposed that the quinazoline and isoquinoline analogues could not participate in the same hydrogen bonding interaction with Lys686 but were still able to occupy the ATP site, taking advantage of nearby hydrophobic residues to accommodate the less polar fused phenyl ring.

4.6 Chapter 4 Summary

Series C proved to be the most successful of the three series of compounds for optimising a PKN2 chemical probe. The original hit, a reported PKC/PKD inhibitor,^{106,161} was synthesised *via* an 8-step synthesis and was confirmed as a potent inhibitor of PKN2 (K_i 12 nM) but had only 5-fold selectivity over PKN1. Exchanging the core, amine and pyridyl rings established the 6/7-position nitrogen and pyridyl ring were required for potency and selectivity (Figure 4.45) and confirmed a shorter chemical route could be used to make an optimised compound using a 2,6-naphthyridine instead of a 2,7-naphthyridine.

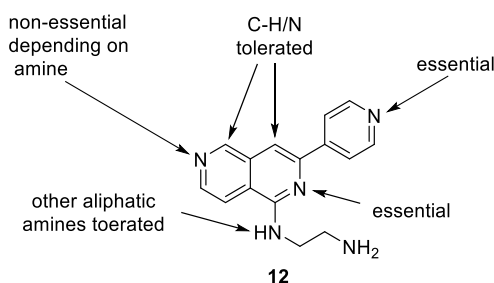


Figure 4.45 SAR summary regarding compound **12**

Piperazine analogue **187** was shown to inhibit 9/400 kinases above 70% when dosed at 1 μ M in the commercial DiscoverX scheme but had the same 5-fold selectivity as **12** (PKN2 K_i 2.9 nM,

PKN1 K_i 15 nM). Further optimisation of this compound led to compound **312** (Figure 4.46), whereby the fused pyrrolidine system improved the potency to PKN2 K_i 6.7 nM and the selectivity to 18-fold over PKN1. Further kinome selectivity studies on **312** are currently pending. Compound **313**, the Boc-protected analogue of **312** also serves as a suitable inactive probe for use in experimental controls.

While computational studies could not fully rationalise compound **12**'s potency for PKN2 or other kinases, crystallographic studies around this series yielded the first crystal structure of PKN2 with a non-ATP analogue ligand bound. The structure confirmed the binding mode of compound **187** with the 4'-pyridyl binding with the hinge of the compound and other critical SAR for further compound optimisation.

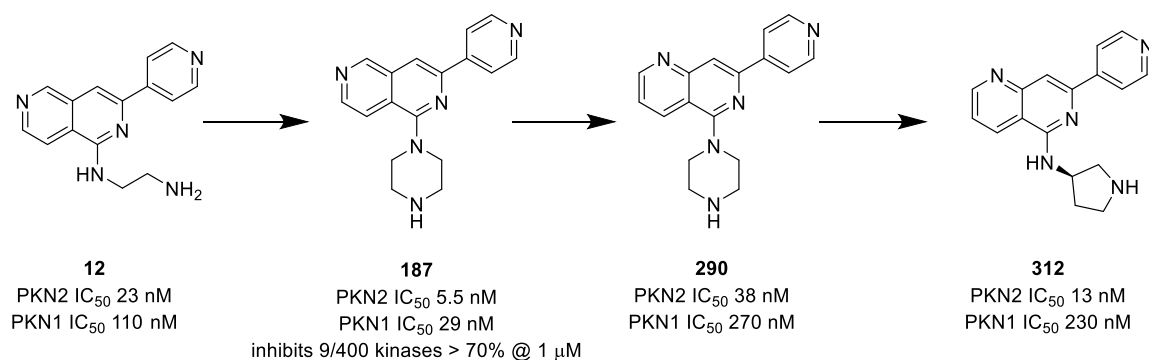


Figure 4.46 Optimisation of compound **12** to compound **312**

Chapter 5 Conclusions and Future Work

Chemical probes are drug-like compounds used in early-stage drug discovery projects. They are designed to be sufficiently potent and selective against a desired biological target, usually a protein, in order to answer mechanistic questions in physiological and pathological biology. While kinase drug discovery has impressively brought 52 drugs to market over the past 20 years, more than 80% of the, so called, “dark kinome” lacks good quality small molecule inhibitors.

PKN2 is one of those understudied kinases with several postulated roles across normal cell biology, from cytoskeleton regulation to cell cycle amongst others. The AGC kinase is of interest as a potential drug target for its apparent role in several sub-types of cancer, inflammation and heart failure.

This PhD project sought to repurpose and optimise existing kinase inhibitors identified from a ChEMBL literature screen. The main aim was to investigate where it was possible to achieve potency and selectivity with one or more of the compounds within the PKN sub-family and wider human kinome through a collaboration with the SGC.

A triage of 1200 reported PKN2 inhibitors resulted in the prioritisation of three potent compounds (**10**, **11** and **12**) (Figure 5.1). This thesis aimed to outline the work undertaken to synthesise these compounds, confirm their bioactivities as inhibitors of PKN2, and explore SAR in order to improve on their selectivity for PKN2 over PKN1 and the wider kinome.

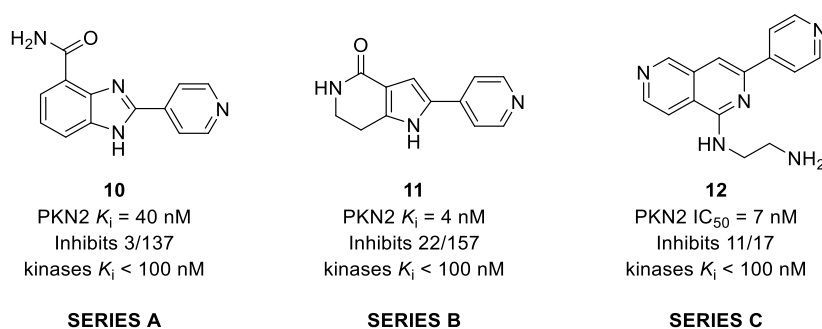
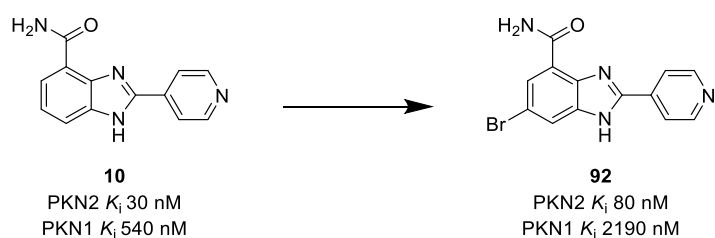


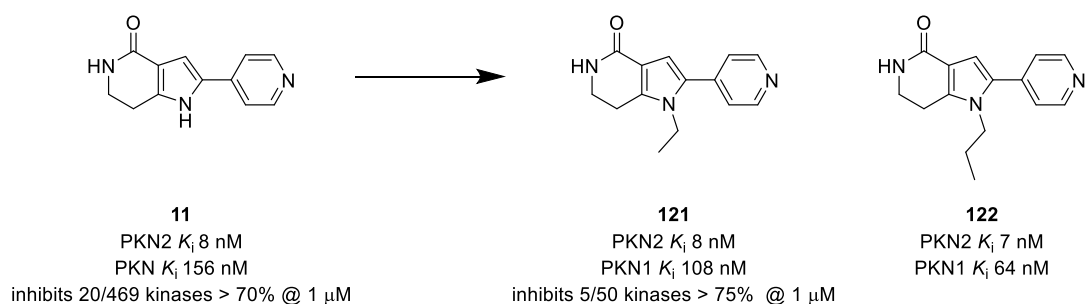
Figure 5.1 Compounds **10**, **11** and **12** selected from the ChEMBL screen with reported potencies and selectivities^{103–106}

Chapter 2 summarised work concerning series A, around benzimidazole **10**, synthesised in four steps. It was not possible to improve on the original compound's potency but a more selective (27-fold) analogue (**92**), containing a bromine at the 6-position, was successfully isolated and tested against PKN2 and PKN1 along with the other compounds in series A using a TR-FRET assay (Scheme 5.1).



Scheme 5.1 Attempted optimisation of compound 10

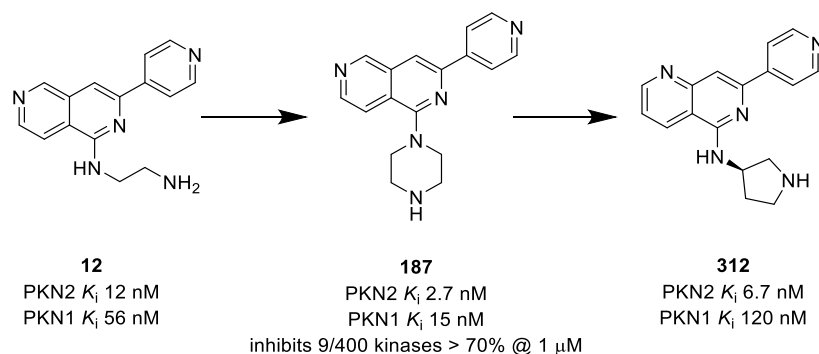
Chapter 3 focused on series B, based around pyrrolopyridinone **11**. This compound was successfully made in a one-step addition-condensation reaction, with additional conditions used to alkylate the various free N-H bonds present in the compound. Two equipotent compounds, **121** and **122**, were made by alkylating the pyrrole N-H with ethyl and *n*-propyl respectively, but they were less selective over PKN1 *cf.* **11** (Scheme 5.3).



Scheme 5.2 Attempted optimisation of compound 11

When these compounds were tested in focused (50 kinases) and diverse (469 wild-type and mutant) kinase panels for their selectivity, it was found that alkylating the pyrrole N-H improved some degree of selectivity across the kinome because of the lost hydrogen bond donor, but the compounds of series B did not prove to be the most selective series.

Chapter 4 discusses the most promising of the three series, series C. The starting compound, **12**, a 2,7-naphthyridine was successfully synthesised using a previously reported 8-step synthesis. Exchanging the 2,7-naphthyridine for other *N*-containing-fused heterocycles optimised the synthesis to 2–3 steps, depending on if the amine coupled at the 1-position required deprotection or not. **12** was confirmed as a potent but relatively unselective PKN2 inhibitor. Close analogue, **187**, containing a piperazine moiety had improved potency and was shown to inhibit only 9/469 wild-type and mutant kinases above 70% at 1 μ M in the commercial DiscoverX panel.



Scheme 5.3 Optimisation of compound 12 to yield compounds 187 and 312

This result was used to guide further chemistry around 2,6-naphthyridine compounds containing rigidified amines and the best compound of the series was compound **312**, with K_i 6.7 nM potency for PKN2 and 18-fold selectivity over PKN1. While this compound has the desired *in vitro* potency (< 100 nM), its selectivity falls short (30-fold) and its *in cellulo* activity is still to be tested. Despite this, it provides a significant step towards a good quality PKN2 chemical probe.

Computational studies generally did not add value to the experimental work. This was primarily because the only crystal structure available of PKN2 available had an ATP-like ligand which meant the kinase was not in the conformation it would otherwise be in if bound to a more similar chemotype of ligand. Towards the end of this work, a structure of PKN2 in an alternative conformation co-crystallised with **187** was successfully produced by Dr. Angela Fala and provides a useful tool for further exploring how to drug this kinase.

In specific terms of future work, knowing the wider selectivity of **92** and **312** will help to direct future chemistry efforts. The new crystal structure can be used for fully rationalising the SAR of the series C compounds synthesised thus far and can provide the basis for docking studies to support and guide future compound design and syntheses. Further characterisation of these probes and their ability to engage with PKN2 in cells using target engagement assays such as NanoBRET would also be beneficial.

Previous research carried out on PKN2 has, for the most part, utilised genetic tools and techniques to elucidate the function of this kinase. This work is believed to be the first concerted effort to design small molecule inhibitors specifically for PKN2, as oppose to serendipitously finding potent and selective PKN2 inhibitors while targeting other kinases. The work around the three series of compounds has shown it is indeed possible to drug PKN2 with a reasonable degree of selectivity over its close homologue PKN1 and the wider human kinome. 121 novel compounds were synthesised as part of this project. If an appropriate probe can be developed, it will be possible to validate whether PKN2 could be a useful drug target of the future.

Chapter 6 Experimental Methods

6.1 Chemistry

All commercial reagents were purchased from Sigma-Aldrich, Alfa Aesar, Apollo Scientific, Fisher Scientific, Fluorochem, Tokyo Chemical Industry or Manchester Organics and were of the highest available purity. Unless otherwise stated, chemicals were used as supplied without further purification. Anhydrous solvents were purchased from Acros (AcroSeal™) or Sigma-Aldrich (SureSeal™) and were stored under nitrogen. Anhydrous solvents and reagents were used as purchased. Petroleum ether refers to the fraction with a boiling point between 40 °C and 60 °C.

Reactions were magnetically stirred and monitored by liquid chromatography mass spectrometry (LCMS) or thin layer chromatography (TLC) using aluminium-supported thin layer chromatography sheets with Merck silica gel 60 F254. For TLC, the eluent was as stated (where this consisted of more than one solvent, the ratio is stated as volume: volume). Visualisation was by absorption of UV light (λ_{max} 254 or 365 nm).

Flash column chromatography was carried out using either: commercial pre-packed silica columns from Biotage (SNAP and Zip), Isco (RediSep), Grace (Reveleris) or filled with Merck silica gel 60 (40-63 μm); C18 silica (Biotage SNAP KP-C18-HS, Grace Reveleris C18); amino silica (Biotage SNAP KP-NH or Grace Reveleris Amino) on an ISCO Combiflash R_f or a Biotage Isolera Prime.

¹H and ¹³C NMR spectra were recorded at 500 or 600 MHz on a Varian VNMRS 500/600 MHz spectrometer (at 30 °C), using residual isotopic solvent as an internal reference. The chemical shift data for each signal are given as δ in units of parts per million (ppm). Each spectrum is corrected to the appropriate solvent reference; δ (CHCl₃) = 7.27/77 ppm or δ (DMSO) = 2.50/39.52 ppm for ¹H/¹³C NMR respectively. The multiplicity of each δ signal is indicated by: s (singlet); br s (broad singlet); d (doublet); t (triplet); q (quartet); or m (multiplet). The number of protons (n) for a given resonance signal is indicated by nH. Coupling constants (*J*) are quoted in Hz and are recorded to the nearest 0.1 Hz. Identical proton coupling constants (*J*) are averaged in each spectrum and reported to the nearest 0.1 Hz. The coupling constants are determined by analysis using MestreNova version 10 software.

LCMS (LCQ) data was recorded on a Waters 2695 HPLC using a Waters 2487 UV detector and a Thermo LCQ ESI-MS. Samples were eluted through a Phenomenex Luna 3 μ C18 50 mm \times 4.6 mm column, using water and acetonitrile acidified by 0.1% formic acid at 1.5 mL/min and detected at 254 nm.

LCMS (MDAP) data was recorded on a Shimadzu Prominence Series coupled to a LCMS-2020 ESI and EI mass spectrometer. Samples were eluted through a Phenomenex Gemini 5 μ C18 110 Å 250 mm \times 4.6 mm column, using water and acetonitrile acidified by 0.1% formic acid at 1 mL/min and detected at 254 nm.

High resolution mass spectrometry: HRMS data (ESI⁺) was recorded on Bruker Daltonics, Apex III, ESI source: Apollo ESI with methanol as spray solvent. Only molecular ions, fractions from molecular ions and other major peaks are reported as mass/charge (m/z) ratios.

Known intermediates have previous literature referenced where available and were only characterised by ¹H NMR, LCMS and HRMS when ionisation by MDAP/LCQ LCMS was not possible. Final compounds and novel intermediates were further characterised, as follows.

R_f values were obtained *via* Thin Layer Chromatography, as previously described.

Infra-red spectra were recorded on a Perkin Elmer FT-IR Spectrum One spectrometer as a neat sample. Absorption maxima are reported in wavenumber (cm⁻¹). Distinguishable and significant absorptions were recorded in wave numbers (cm⁻¹), with key stretches identified in brackets.

Melting points were recorded using a Fisherbrand™ Digital Melting Point Apparatus with samples in 2 mm glass capillary tubes.

6.1.1 Preparation of compounds described in Chapter 2

*General Method A (CDI amide coupling)*¹¹⁶

1,1'-Carbonyldiimidazole (CDI) (**16**) (1 eq.) was added portion-wise to the corresponding benzoic acid (1 eq.) in tetrahydrofuran (20 mL/g) at room temperature. The reaction mixture was heated to reflux for 30 min to facilitate the coupling of the CDI (**16**) to the acid, allowed to cool and then the corresponding amine (1.1 eq.) was added in one portion. The reaction was stirred at room temperature overnight resulting in the formation of an orange suspension. The product was isolated as per specification.

*General Method B (nitro reduction)*¹¹⁸

The corresponding nitroaniline (1 eq.) was added to 50% aqueous ethanol (5 mL/g) at room temperature and heated to reflux. Sodium dithionite (10 eq.) was added portion-wise. The reaction was heated under reflux for 30 min. TLC confirmed consumption of starting material (100% ethyl acetate, UV). The cooled reaction mixture was extracted four times with ethyl

acetate (4×10 mL/g) and the combined organic phases were dried over MgSO_4 , filtered and concentrated under reduced pressure. The product was isolated as per specification.

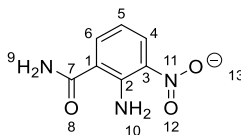
General Method C (HATU amide coupling)¹²⁰

The corresponding dianiline (1 eq.), the corresponding aromatic acid (1.1 eq.), HATU (1.1 eq.) and *N,N*-diisopropyl-ethylamine (2 eq.) in dichloromethane (2 mL/g) was stirred overnight at room temperature. The product was isolated as per specification.

General Method D (acid-catalysed cyclisation)¹⁰⁴

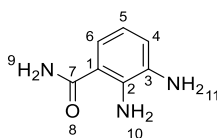
The corresponding amide (1 eq.) was dissolved in acetic acid (excess *ca.* 140 eq.) and heated to 120 °C. The reaction was monitored by TLC and after 1.5 h, all of the starting material had been consumed. The product was isolated as per specification.

2-Amino-3-nitro-benzamide (17)^{162–164}



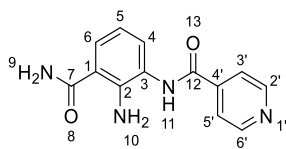
Compound **17** was prepared *via* General Method A using 2-amino-3-nitro-benzoic acid (**10**) (10 g, 54.91 mmol) and 13.4 M aqueous ammonia solution (41 mL, 549.1 mmol). The reaction mixture was filtered giving 2-amino-3-nitro-benzamide (**17**) (2.24 g, 21%) as a fine orange solid. The filtrate was partially concentrated under reduced pressure, left overnight and a further crop of 2-amino-3-nitro-benzamide (**17**) (3.91 g, 37% yield) was isolated by filtration as a fine orange solid.

^1H NMR (500 MHz, $\text{DMSO}-d_6$) δ 8.47 (s, 2H, H-9), 8.25–8.07 (m, 2H, H-4 and H-10), 8.01–7.86 (m, 1H, H-6), 7.62 (s, 1H, H-10), 6.67 (t, $J = 7.4\text{Hz}$, 1H, H-5); HRMS m/z (ESI⁺) [Found: 204.0382, $\text{C}_7\text{H}_7\text{N}_3\text{O}_3\text{Na}$ requires $(\text{M}+\text{Na})^+$ 204.1390]; LCMS (MDAP) $R_t = 24.9$ min (Ana 9–95), not ionisable by LCQ/MDAP LCMS.

2,3-Diaminobenzamide (22)^{165–167}

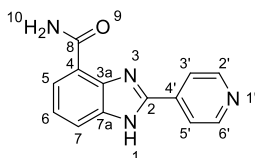
Compound **22** was prepared *via* General Method B using 2-amino-3-nitro-benzamide (**17**) (6 g, 31.47 mmol). The crude was purified *via* flash column chromatography (100 g silica, ethyl acetate:methanol, 100:0 to 90:10) to give 2,3-diaminobenzamide (**22**) (2.21 g, 44%) as a light brown solid.

¹H NMR (500 MHz, DMSO-*d*₆) δ 7.63 (s, 1H, H-10), 7.00 (s, 1H, H-10), 6.90 (d, *J* = 8.0 Hz, 1H, H-6), 6.62 (d, *J* = 7.5 Hz, 1H, H-4), 6.35 (t, *J* = 7.7 Hz, 1H, H-5), 6.08 (s, 2H, H-9), 4.63 (s, 2H, H-11); HRMS *m/z* (ESI⁺) [Found: 174.0638, C₇H₉N₃ONa requires (M+H)⁺ 174.1560]; LCMS (MDAP) Rt = 19.3 min (Ana 9–95), not ionsable by LCQ/MDAP LCMS.

***N*-(2-Amino-3-carbamoyl-phenyl)pyridine-4-carboxamide (25)**

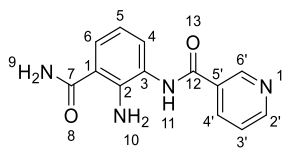
Compound **25** was prepared *via* General Method C using 2,3-diaminobenzamide (**22**) (150 mg, 0.94 mmol) and isonicotinic acid (128 mg, 1.04 mmol). The reaction mixture was filtered giving *N*-(2-amino-3-carbamoyl-phenyl)-pyridine-4-carboxamide (**25**) (245 mg, 96%) as an off-white solid.

^1H NMR (500 MHz, $\text{DMSO}-d_6$) δ 9.91 (s, 1H, H-11), 8.77 (d, $J = 5.3$ Hz, 2H, H-2'and H-6'), 7.91 (d, $J = 5.5$ Hz, 2H, H-3'and H-5'), 7.87 (s, 1H, H-10), 7.53 (d, $J = 7.9$ Hz, 1H, H-6), 7.26 (d, $J = 7.6$ Hz, 1H, H-4), 7.23 (s, 1H, H-10), 6.57 (t, $J = 7.8$ Hz, 1H, H-5), 6.52 (s, 2H, H-9); HRMS m/z (ESI $^+$) [Found: 256.9010, $\text{C}_{13}\text{H}_{12}\text{N}_4\text{O}_2$ requires (M) $^+$ 256.2595]; LCMS (LCQ) Rt = 0.8 min (4 min method), not ionisable by LCQ/MDAP LCMS.

2-(4-Pyridyl)-1*H*-benzimidazole-4-carboxamide (10)^{109,112,114,115,168}

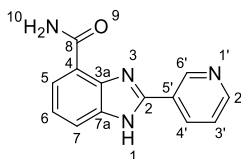
Compound **10** was prepared *via* General Method D using *N*-(2-amino-3-carbamoyl-phenyl)pyridine-4-carboxamide (**25**) (330 mg, 1.29 mmol). The reaction mixture was concentrated under reduced pressure to give a pale yellow crude solid (37 mg). The crude was purified *via* flash column chromatography (11 g amino silica, ethyl acetate:methanol, 100:0 to 85:15) to give 2-(4-pyridyl)-1*H*-benzimidazole-4-carboxamide (**10**) (193 mg, 60%) as a yellow solid.

R_f 0.50 (9:1 ethyl acetate:methanol); MP > 250 °C; ν_{\max} (thin film)/cm⁻¹ 3347 (N-H, b), 1650 (C=O, s), 1609 (C=C, s), 756 (N-H, s); ¹H NMR (500 MHz, DMSO-*d*₆) δ 9.19 (s, 2H, H-10), 8.80 (d, J = 4.3 Hz, 2H, H-2' and H-6'), 8.19 (d, J = 4.3 Hz, 2H, H-3' and H-5'), 7.91 (d, J = 7.3 Hz, 1H, H-7), 7.84 (s, 1H, H-1), 7.81 (d, J = 7.9 Hz, 1H, H-5), 7.41 (t, J = 7.7 Hz, 1H, H-6); ¹³C NMR (126 MHz, DMSO-*d*₆) δ 170.8 (C-7), 166.5 (C-3a), 151.0 (C-2' and C-6'), 150.0 (C-4'), 136.7 (C-2), 123.9 (C-7), 123.6 (C-5), 123.2 (C-6), 121.2 (C3' and C-5'), 116.4 (C-7a); HRMS m/z (ESI⁺) [Found: 239.0924, C₁₃H₁₀N₄O requires (M+H)⁺ 239.0927]; LCMS (LCQ) R_t = 0.6 min (4 min method), not ionisable by LCQ.

***N*-(2-Amino-3-carbamoyl-phenyl)pyridine-3-carboxamide**

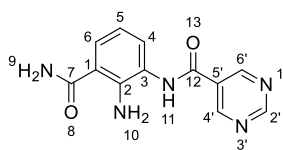
The intermediate was prepared *via* General Method C using 2,3-diaminobenzamide (**22**) (150 mg, 0.94 mmol) and nicotinic acid (128 mg, 1.04 mmol). *N*-(2-Amino-3-carbamoyl-phenyl)pyridine-3-carboxamide (229 mg, 85%) was isolated by filtration as a light brown solid.

R_f 0.66 (9:1 ethyl acetate:methanol); m.p. 170–174 °C; 3441 (N-H, m), ν_{\max} (thin film)/ cm^{-1} 3355 (N-H, s), 3173 (C-H, m), 1643 (C=O, s), 1517 (N-H/C-C, s); ^1H NMR (500 MHz, $\text{DMSO}-d_6$) δ 9.84 (s, 1H, H-11), 9.16 (s, 1H, H-6'), 8.78–8.70 (m, 1H, H-2'), 8.33 (d, $J = 7.8$ Hz, 1H, H-4'), 7.88 (s, 1H, H-10), 7.60–7.47 (m, 2H, H-6 and H-3'), 7.27 (d, $J = 7.4$ Hz, 1H, H-4), 7.23 (s, 1H, H-10), 6.56 (m, 3H, H-5 and 2 \times H-9); ^{13}C NMR (126 MHz, $\text{DMSO}-d_6$) δ 171.7 (C-7), 164.9 (C-12), 152.4 (C-2'), 149.4 (C-6'), 146.1 (C-5'), 136.0 (C-4'), 131.1 (C-4), 130.58 (C-1), 127.6 (C-3'), 124.2 (C-2), 123.8 (C-6), 115.9 (C-3), 114.3 (C-5); HRMS m/z (ESI $^+$) [Found: 257.1032, $\text{C}_{13}\text{H}_{12}\text{N}_4\text{O}_2$ requires (M+H) $^+$ 257.1033]; LCMS (LCQ) Rt = 0.6 min (4 min method), m/z (ESI $^+$) 257.08 (M+H) $^+$.

2-(3-Pyridyl)-1*H*-benzimidazole-4-carboxamide (38)^{112,115,169}

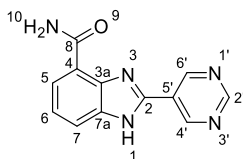
Compound **38** was prepared *via* General Method D using *N*-(2-Amino-3-carbamoyl-phenyl)pyridine-3-carboxamide (179 mg, 0.70 mmol). The reaction mixture was concentrated under reduced pressure to give a pale-yellow crude solid (37 mg). The crude was purified *via* flash column chromatography (11 g amino silica, ethyl acetate:methanol, 100:0 to 90:10) to give 2-(3-pyridyl)-1*H*-benzimidazole-4-carboxamide (**38**) (45 mg, 26%) as an off-white solid.

R_f 0.29 (9:1 ethyl acetate:methanol); m.p. 293–295 °C; ν_{\max} (thin film)/cm⁻¹ 2998 (C-H, b), 1685 (C=O, s), 1634 (C=C, s), 3376 (C-N, s), 1120 (C-N, s); ¹H NMR (500 MHz, DMSO-*d*₆) δ 13.62 (s, 1H, H-1), 9.42 (s, 1H, H-6'), 9.29 (s, 1H, H-10), 8.72 (d, J = 7.1 Hz, 1H, H-7), 8.59 (d, J = 7.1 Hz, 1H, H-5), 7.94–7.87 (d, J = 7.9 Hz, 1H, H-2'), 7.83 (s, 1H, H-10), 7.78 (d, J = 7.5 Hz, 1H, H-4'), 7.62 (t, J = 7.5 Hz, 1H, H-6), 7.38 (t, J = 7.0 Hz, 1H, H-5'); ¹³C NMR (126 MHz, DMSO-*d*₆) δ 166.0 (C-8), 151.1 (C-7), 149.6 (C-7a), 147.9 (C-6'), 141.3 (C-3a/4), 135.3 (C-2), 134.4 (C-5), 125.3 (C-5'), 124.1 (C-6), 123.2 (C-2'), 122.8 (C-3'), 115.2 (C-4'), C-4/3a peak missing; HRMS m/z (ESI⁺) [Found: 239.0924, C₁₃H₁₀N₄O requires (M+H)⁺ 239.0927]; LCMS (LCQ) R_t = 0.6 min (4 min method), m/z (ESI⁺) 239.0 (M+H)⁺.

***N*-(2-Amino-3-carbamoyl-phenyl)pyrimidine-5-carboxamide**

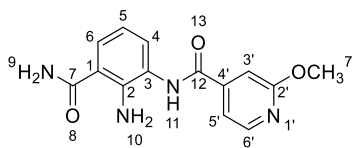
The intermediate was prepared *via* General Method C using 2,3-diaminobenzamide (**22**) (150 mg, 0.94 mmol) and pyrimidine-5-carboxylic acid (117 mg, 0.94 mmol). *N*-(2-amino-3-carbamoyl-phenyl)pyrimidine-5-carboxamide (240 mg, 94%) was isolated by filtration as a pale brown solid. The crude was taken on without further purification.

R_f 0.72 (9:1 ethyl acetate:methanol); m.p. 171–173 °C; ν_{\max} (thin film)/cm⁻¹ 3427 (N-H, m), 3213 (C-H/N-H, br), 1355 (C=O, s), 1502 (C-H, m), 713 (N-H, s); ¹H NMR (500 MHz, DMSO-*d*₆) δ 10.09 (s, 1H, H-11), 9.34 (s, 1H, H-2'), 9.32 (s, 2H, H-4' and H-6'), 7.89 (s, 1H, H-10), 7.54 (d, J = 7.4 Hz, 1H, H-6), 7.28 (d, J = 7.1 Hz, 1H, H-4), 7.23 (s, 1H, H-10), 6.64 (s, 2H, H-9), 6.57 (t, J = 7.4 Hz, 1H, H-5); ¹³C NMR (126 MHz, DMSO-*d*₆) δ 171.6 (C-7), 163.2 (C-12), 160.4 (C-2'), 156.8 (C-4' and 6'), 146.1 (C-2), 131.1 (C-4), 128.6 (C-5'), 127.8 (C-6), 123.6 (C-3), 115.7 (C-1), 114.2 (C-5); HRMS m/z (ESI⁺) [Found: 280.0812, C₁₂H₁₁N₅NaO₂ requires (M+H+Na)⁺ 280.0805]; LCMS (LCQ) Rt = 0.7 min (4 min method), m/z (ESI⁺) 257.98 (M+H)⁺.

2-Pyrimidin-5-yl-1*H*-benzimidazole-4-carboxamide (39)

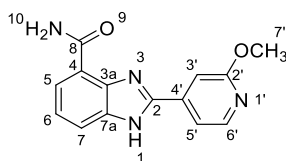
Compound **39** was prepared *via* General Method D using *N*-(2-amino-3-carbamoyl-phenyl)-pyrimidine-5-carboxamide (140 mg, 0.54 mmol). The reaction mixture was concentrated under reduced pressure and was purified *via* flash column chromatography (11 g amino silica, ethyl acetate:methanol 100:0 to 85:15) to give 2-pyrimidin-5-yl-1*H*-benzimidazole-4-carboxamide (**39**) (90 mg, 66%) as a yellow solid.

R_f 0.51 (9:1 ethyl acetate:methanol); m.p. > 300 °C; ν_{\max} (thin film)/cm⁻¹ 3308 (N-H, br), 3218 (N-H, br), 1650 (C=O, m), 1559 (aromatic C-C, s), 718 (N-H, s); ¹H NMR (500 MHz, DMSO-*d*₆) δ 9.57 (s, 2H, H-4' and H-6'), 9.30 (s, 1H, H-2'), 9.09 (s, 2H, H-10), 7.90 (d, J = 7.3 Hz, 1H, H-5), 7.84–7.72 (m, 2H, H-1 and H-7), 7.37 (t, J = 7.7 Hz, 1H, H-6); ¹³C NMR (151 MHz, DMSO-*d*₆) δ 166.0 (C-8), 158.7 (C-2'), 154.8 (C-4' and 6'), 146.9 (C-2), 140.0 (C-3a), 136.5 (C-4), 123.8 (C-7), 123.1 (C-5), 122.5 (C-6), 122.2 (C-7a), 116.1 (C-5'); HRMS m/z (ESI⁺) [Found: 262.0705, C₁₂H₉N₅NaO requires (M+H+Na)⁺ 262.0699]; LCMS (LCQ) Rt = 0.6 min (4 min method), m/z (ESI⁺) 239.99 (M+H)⁺.

***N*-(2-Amino-3-carbamoyl-phenyl)-2-methoxy-pyridine-4-carboxamide**

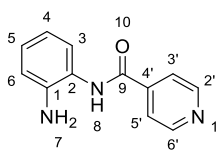
The intermediate was prepared *via* General Method C using 2,3-diaminobenzamide (**22**) (150 mg, 0.94 mmol) and 2-methoxyisonicotinic acid (159 mg, 1.04 mmol). *N*-(2-Amino-3-carbamoyl-phenyl)-2-methoxy-pyridine-4-carboxamide (242 mg, 81%) was isolated by filtration as a pale brown solid.

R_f 0.77 (9:1 ethyl acetate:methanol); m.p. 282–284 °C; ν_{\max} (thin film)/cm⁻¹ 3424 (N-H, w), 3330 (N-H, br), 1639 (C=O, s), 1520 (C-H, m); ¹H NMR (500 MHz, DMSO-*d*₆) δ 9.84 (s, 1H, H-11), 8.33 (d, J = 5.3 Hz, 1H, H-6'), 7.87 (s, 1H, H-10), 7.53 (d, J = 8.0 Hz, 1H, H-4), 7.48 (d, J = 5.3 Hz, 1H, H-5), 7.37 (s, 1H, H-3'), 7.27–7.18 (m, 2H, H-10 and H-6), 6.57 (t, J = 7.8 Hz, 1H, H-5), 6.51 (s, 2H, H-9), 3.91 (s, 3H, H-7'); ¹³C NMR (126 MHz, DMSO-*d*₆) δ 171.6 (C-7), 164.5 (C-12), 147.7 (C-6'), 145.8 (C-2), 145.2 (C-2'), 130.8 (C-4), 127.7 (C-6), 124.0 (C-1), 116.1 (C-4'), 115.6 (C-5'), 114.4 (C-5), 109.5 (C-3'), 53.9 (C-7'), C-3 peak missing; HRMS m/z (ESI⁺) [Found: 309.0963, C₁₄H₁₄N₄NaO₃ requires (M+H+Na)⁺ 309.0958]; LCMS (LCQ) Rt = 0.6 min (4 min method), m/z (ESI⁺) 286.96 (M+H)⁺.

2-(2-Methoxy-4-pyridyl)-1*H*-benzimidazole-4-carboxamide (40)

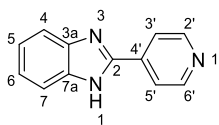
Compound **40** was prepared *via* General Method D using *N*-(2-amino-3-carbamoyl-phenyl)-2-methoxy-pyridine-4-carboxamide (190 mg, 0.66 mmol). The reaction mixture was concentrated under reduced pressure. The crude was purified *via* flash column chromatography (11 g amino silica, ethyl acetate:methanol, 100:0 to 90:10) to give 2-(2-methoxy-4-pyridyl)-1*H*-benzimidazole-4-carboxamide (**40**) (152 mg, 81%) as a pale yellow solid.

R_f 0.34 (100% ethyl acetate); m.p. 290–293 °C; ν_{\max} (thin film)/cm⁻¹ 3459 (N-H, w), 3170 (N-H, br), 3135 (N-H, br), 1667 (C=O, s), 736 (N-H, s); ¹H NMR (500 MHz, DMSO-*d*₆) δ 13.64 (s, 1H, H-1), 9.22 (s, 1H, H-10), 8.35 (d, J = 4.7 Hz, 1H, H-6'), 7.91 (d, J = 6.7 Hz, 1H, H-5), 7.83 (s, 1H, H-1), 7.82–7.76 (m, 2H, H-7 and H-5'), 7.61 (s, 1H, H-3'), 7.40 (t, J = 7.3 Hz, 1H, H-6), 3.92 (s, 3H, H-7'); ¹³C NMR (126 MHz, DMSO-*d*₆) δ 166.3 (C-8), 164.8 (C-2'), 149.7 (C-2), 148.5 (C-6'), 141.5 (C-3a), 139.6 (C-4'), 135.6 (C-4), 124.0 (C-5), 123.7 (C-6), 123.4 (C-7a), 115.9 (C-7), 114.8 (C-5'), 108.0 (C-3'), 54.0 (C-7'); HRMS m/z (ESI⁺) [Found: 291.0857, C₁₄H₁₂N₄NaO₂ requires (M+H+Na)⁺ 291.0852]; LCMS (LCQ) Rt = 0.6 min (4 min method), m/z (ESI⁺) 269.01 (M+H)⁺.

***N*-(2-Aminophenyl)pyridine-4-carboxamide (**55**)**

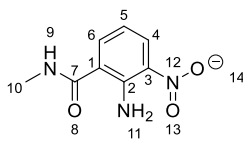
Intermediate **55** was prepared *via* General Method C using *O*-phenylenediamine (**54**) (100 mg, 0.92 mmol) and isonicotinic acid (**23**) (125 mg, 1.02 mmol). The reaction mixture was filtered giving *N*-(2-aminophenyl)pyridine-4-carboxamide (**55**) (156 mg, 75%) as an off-white solid.

^1H NMR (500 MHz, $\text{DMSO}-d_6$) δ 9.90 (s, 1H, H-8), 8.76 (d, $J = 4.6$ Hz, 2H, H-2' and H-6'), 7.89 (d, $J = 4.6$ Hz, 2H, H-3' and H-5'), 7.16 (d, $J = 7.6$ Hz, 1H, H-3), 6.99 (t, $J = 7.5$ Hz, 1H, H-5), 6.78 (d, $J = 7.9$ Hz, 1H, H-6), 6.59 (t, $J = 7.4$ Hz, 1H, H-4), 5.01 (s, 2H, H-7); LCMS (LCQ) $R_t = 0.7$ min (4 min method), m/z (ESI $^+$) 214.11 (M+H) $^+$.

2-(4-Pyridyl)-1*H*-benzimidazole (56)^{170–172}

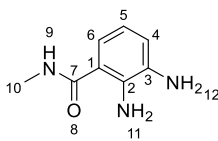
Compound **56** was prepared *via* General Method D using *N*-(2-aminophenyl)pyridine-4-carboxamide (**54**) (100 mg, 0.47 mmol). TLC (9:1 ethyl acetate:methanol) showed reaction was complete after 2 h. The reaction mixture was concentrated under reduced pressure to give an off-white solid (181 mg). The crude was purified by flash column chromatography (5 g amino silica, ethyl acetate:methanol, 100:0 to 90:10) to give 2-(4-pyridyl)-1*H*-benzimidazole (**56**) (64 mg, 66%) as a white solid.

R_f 0.51 (9:1 ethyl acetate:methanol); m.p. 212–214 °C; ν_{\max} (thin film)/cm⁻¹ 3249 (br, NH), 3066 (m, aromatic CH), 1642 (m, C=C), 1509 (s, aromatic CH), 1066 (s, C-N), 656 (s, N-H)¹H NMR (500 MHz, DMSO-*d*₆) δ 13.28 (s, 1H, H-1), 8.76 (d, J = 5.7 Hz, 2H, H-2' and H-6'), 8.10 (d, J = 5.8 Hz, 2H, H-3' and H-5'), 7.73 (s, 1H, H-5/8), 7.61 (s, 1H, H-8/5), 7.27 (s, 2H, H-6 and H-7); ¹³C NMR (126 MHz, DMSO-*d*₆) δ 150.5 (C-2' ad C-6'), 148.8 (C-2), 143.6 (C-7a), 137.1 (C-4'), 135.0 (C-3a), 123.5 (C-6), 122.2 (C-5), 120.3 (C-3' and C-5'), 119.4 (C-7), 111.8 (C-4).; HRMS m/z (ESI⁺) [Found: 196.0871, C₁₂H₁₀N₃ requires (M+H)⁺ 196.0869]; LCMS (LCQ) R_t = 0.6 min (4 min method), m/z (ESI⁺) 196.27 (M+H)⁺.

2-Amino-*N*-methyl-3-nitro-benzamide (57)

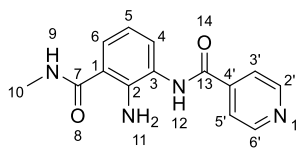
Intermediate **57** was prepared *via* General Method A using 2-amino-3-nitro-benzoic acid (**15**) (2 g, 10.98 mmol) and 13.4 M aqueous methylamine (6 mL, 12.08 mmol). The reaction mixture was concentrated under reduced pressure. The crude was purified *via* flash column chromatography (30 g silica, petroleum ether:ethyl acetate, 1:0 to 0:1) to give a 1:2 mixture of 2-amino-*N*-methyl-3-nitro-benzamide (**57**) (2.00 g, 32%) and imidazole. The product was carried forward without further purification.

^1H NMR (500 MHz, CDCl_3) δ 8.25 (d, J = 8.5 Hz, 1H, H-4), 8.21 (s, 2H, H-11), 7.67 (d, 1H, H-6), 6.60 (t, J = 8.0 Hz, 1H, H-5), 2.99 (d, J = 4.7 Hz, 3H, H-10); LCMS (LCQ) R_t = 0.8 min (4 min method), m/z (ESI $^+$) 195.92 (M+H) $^+$.

2,3-Diamino-*N*-methyl-benzamide (58)

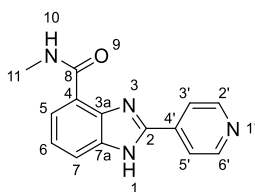
Intermediate **(58)** was prepared *via* General Method B using 2-amino-*N*-methyl-3-nitrobenzamide (**57**) (1 g, 5.12 mmol). The crude was purified *via* flash column chromatography (10 g silica, ethyl acetate:methanol, 100:0 to 90:10) to give 2,3-diamino-*N*-methyl-benzamide (**58**) (357 mg, 34%) as a yellow oil.

^1H NMR (500 MHz, CDCl_3) δ 7.58 (s, 1H, H-9), 7.03 (s, 1H, H-11), 6.88 (d, $J = 7.9$ Hz, 1H, H-6), 6.77–6.68 (m, 1H, H-4), 6.64 (s, 1H, H-11), 6.55 (t, $J = 7.8$ Hz, 1H, H-5), 5.15 (s, 2H, H-12), 2.89 (d, $J = 4.8$ Hz, 3H, H-10); LCMS (LCQ) $R_t = 0.5$ min (4 min method), m/z (ESI $^+$) 195.92.

***N*-[2-Amino-3-(methylcarbamoyl)phenyl]pyridine-4-carboxamide (**59**)**

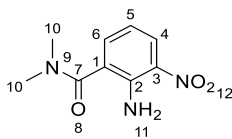
Intermediate **59** was prepared *via* General Method C using 2,3-diamino-*N*-methyl-benzamide (**58**) (140 mg, 0.85 mmol) and isonicotinic acid (**23**) (115 mg, 0.93 mmol). *N*-[2-Amino-3-(methylcarbamoyl)-phenyl]pyridine-4-carboxamide (**59**) (123 mg, 46%) was isolated by filtration as an off-white solid.

R_f 0.62 (9:1 ethyl acetate:methanol); m.p. 299–300 °C; ν_{\max} (thin film)/cm⁻¹ 3407 (N-H, br) 3309 (N-H, m), 3229 (N-H, br), 1625 (C=O, m), 1639 (C=O, s), 1406 (aromatic C-C, s), 714 (N-H, s); ¹H NMR (500 MHz, DMSO-*d*₆) δ 9.93 (s, 1H, H-12), 8.77 (d, J = 5.2 Hz, 2H, H-2' and H-6'), 8.33 (s, 1H, H-9), 7.91 (d, J = 5.3 Hz, 2H, H-3' and H-5'), 7.44 (d, J = 7.5 Hz, 1H, H-6), 7.26 (d, J = 7.3 Hz, 1H, H-4), 6.60 (t, J = 7.6 Hz, 1H, H-5), 6.35 (s, 2H, H-11), 2.75 (d, J = 4.3 Hz, 3H, H-10); ¹³C NMR (126 MHz, DMSO-*d*₆) δ 169.2 (C-7), 164.0 (C-12), 150.1 (C-2' and C-6'), 144.9 (C-2), 141.6 (C-4'), 130.2 (C-4), 126.4 (C-6), 123.52 (C-1), 121.8 (C-3' and 5'), 116.6 (C-3), 114.2 (C-5), 26.1 (C-10); HRMS m/z (ESI⁺) [Found: 293.1015, C₁₄H₁₄N₄NaO₂ requires [M+H+Na]⁺ 293.1009]; LCMS (LCQ) Rt = 0.6 min (4 min method), m/z (ESI⁺) 271.05 (M+H)⁺.

***N*-Methyl-2-(4-pyridyl)-1*H*-benzimidazole-4-carboxamide (60)**

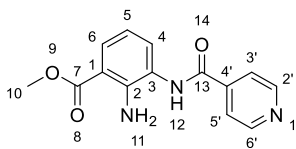
Compound **60** was prepared *via* General Method D using 2,3-diamino-*N*-methyl-benzamide (**59**) (100 mg, 0.37 mmol). The reaction mixture was concentrated under reduced pressure. The crude was purified *via* flash column chromatography (11 g amino silica, ethyl acetate:methanol, 100:0 to 90:10) to give *N*-methyl-2-(4-pyridyl)-1*H*-benzimidazole-4-carboxamide (**60**) (11 mg, 6%) as a pale yellow solid.

R_f 0.21 (100% ethyl acetate); m.p. >300 °C; ν_{\max} (thin film)/cm⁻¹ 3170 (N-H, br), 1648 (C=O, s), 1608 (aromatic C=C, s), 1526 (aromatic C-H, m), 1501 (aromatic C-C), 750 (N-H, s); ¹H NMR (500 MHz, DMSO-*d*₆) δ 13.76 (s, 1H, H-1), 9.67 (s, 1H, H-10), 8.95–8.70 (m, 2H, H-2' and H-6'), 8.30–8.17 (m, 2H, H-3' and H-5'), 7.92 (s, 1H, H-7), 7.80 (d, J = 7.8 Hz, 1H, H-5), 7.41 (t, J = 7.5 Hz, 1H, H-6), 3.02 (s, 3H, H-11); ¹³C NMR (151 MHz, DMSO-*d*₆) δ 164.9 (C-8), 150.6 (C-2' and C-6'), 149.4 (C-2), 140.7 (C-3a), 136.1 (C-4'), 135.3 (C-4), 123.4 (C-6), 123.3 (C-7), 122.8 (C-7a), 120.8 (C-3' and C-5'), 115.3 (C-5), 26.2 (C-11); HRMS m/z (ESI⁺) [Found: 275.0912, C₁₄H₁₂N₄NaO requires (M+H+Na)⁺ 275.0903]; LCMS (LCQ) Rt = 0.7 min (4 min method), m/z (ESI⁺) 253.16 (M+H)⁺.

2-Amino-*N,N*-dimethyl-3-nitro-benzamide (61)

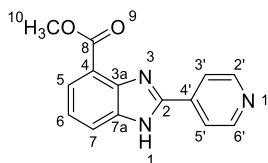
Intermediate **61** was prepared *via* General Method A using 2-amino-3-nitro-benzoic acid (**15**) (2.00 g, 10.98 mmol) and 13.4 M aqueous dimethylamine (6.6 mL, 13.33 mmol). The crude was purified by flash column chromatography (30 g silica, petroleum ether:ethyl acetate, 1:0 to 0:1) to give a 3:1 mixture of 2-amino-*N,N*-dimethyl-3-nitro-benzamide (**61**) (2.72 g, 89%) and imidazole side product from the 1,1'-carbonyldiimidazole. The product was carried forward without further purification.

^1H NMR (500 MHz, CDCl_3) δ 8.15 (d, $J = 8.5$ Hz, 1H, H-4), 7.32 (d, $J = 7.0$ Hz, 1H, H-6), 6.85 (s, 2H, H-11), 6.68 (t, $J = 7.9$ Hz, 1H, H-5), 3.05 (s, 3H, H-10), 3.04 (s, 3H, H-10); LCMS (LCQ) $R_t = 0.6$ min (4 min method), m/z (ESI $^+$) 209.91 (M+H) $^+$.

Methyl 3-amino-2-(pyridine-4-carbonyl-amino)benzoate (65)

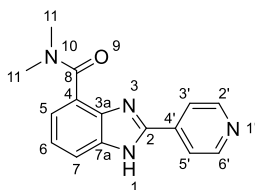
Intermediate **65** was prepared *via* General Method C using 2,3-diaminobenzoic acid methyl ester (**64**) (2 g, 1.20 mmol) and isonicotinic acid (**23**) (163 mg, 1.32 mmol). The reaction mixture was concentrated under reduced pressure and water (100 mL) was added to the residue. The aqueous solution was extracted three times with ethyl acetate (3 × 100 mL). The combined organic phases were dried over MgSO₄, filtered and concentrated under reduced pressure to give an orange oil (692 mg). The crude was purified *via* flash column chromatography (24 g silica, ethyl acetate:methanol, 100:0 to 90:10) to give methyl 3-amino-2-(pyridine-4-carbonylamino)benzoate (**65**) (3.42 g, 94%) as an orange oil which crystallised upon standing to form a pale orange solid. The product was taken forward without further purification.

¹H NMR (500 MHz, DMSO-*d*₆) δ 9.99 (s, 1H, H-7), 8.78 (d, *J* = 4.4 Hz, 2H, H-2' and H-6'), 7.92 (d, *J* = 4.4 Hz, 2H, H-3' and H-5'), 7.74 (d, *J* = 8.0 Hz, 1H, H-4), 7.37 (d, *J* = 7.4 Hz, 1H, H-6), 6.63 (d, *J* = 8.6 Hz, 3H, H-10), 3.82 (s, 3H, H-14); HRMS *m/z* (ESI⁺) [Found: 272.0200, C₁₄H₁₃N₃O₃ requires (M+H)⁺ 271.2708]; LCMS (LCQ) Rt = 0.8 min (7 min method), *m/z* (ESI⁺) 272.02 (M+H)⁺.

Methyl 2-(4-pyridyl)-1*H*-benzimidazole-4-carboxylate (66)

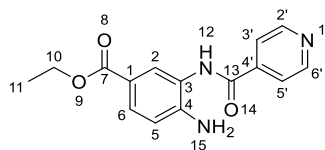
Compound **66** was prepared *via* General Method D using methyl 2-amino-3-(pyridine-4-carbonylamino) benzoate (**65**) (139 mg, 0.51 mmol). The reaction mixture was concentrated under reduced pressure. The crude was purified *via* flash column chromatography (11 g amino silica, ethyl acetate:methanol, 100:0 to 90:10) to give methyl 2-(4-pyridyl)-1*H*-benzimidazole-4-carboxylate (**66**) (118 mg, 86%) as a pale yellow solid.

R_f 0.24 (100% ethyl acetate); m.p. 85–87 °C; ν_{\max} (thin film)/cm⁻¹ 3447 (N-H, br), 3206 (N-H, br), 1619 (C=O, s), 1509 (aromatic C-H, s), 1479 (aliphatic C-H, m), 1464 (aliphatic C-H, s), 674 (N-H, s); ¹H NMR (500 MHz, DMSO-*d*₆) δ 8.76 (d, J = 4.2 Hz, 2H, H-2' and H-6'), 8.26 (d, J = 4.1 Hz, 2H, H-3' and H-5'), 8.01 (d, J = 7.8 Hz, 1H, H-7), 7.88 (d, J = 7.3 Hz, 1H, H-5), 7.37 (t, J = 7.5 Hz, 1H, H-6), 3.97 (s, 3H, H-10); ¹³C NMR (126 MHz, DMSO-*d*₆) δ 165.6 (C-8), 151.0 (C-2), 150.2 (C-2' and C-6'), 143.6 (C-4), 136.7 (C-4'), 135.4 (C-3a), 125.4 (C-5), 123.8 (C-7), 122.1 (C-6), 121.5 (C-3' and C-5'), 115.4 (C-7a), 52.2 (C-10); HRMS m/z (ESI⁺) [Found: 276.0746, C₁₄H₁₁N₃NaO₂ requires [M+Na]⁺ 276.0743]; LCMS (LCQ) Rt = 0.7 min (7 min method), m/z (ESI⁺) 254.0 (M+H)⁺.

***N,N*-Dimethyl-2-(4-pyridyl)-1*H*-benzimidazole-4-carboxamide (67)**¹²³

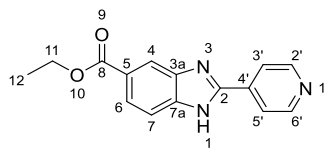
2 M aqueous sodium hydroxide solution (9 mL, 17.93 mmol) was added to methyl 2-(4-pyridyl)-1*H*-benzimidazole-4-carboxylate (**66**) (2.39 g, 8.97 mmol) in methanol (1 mL). The resulting mixture was refluxed at 100 °C overnight. The mixture was concentrated under reduced pressure and sodium 2-(4-pyridyl)-1*H*-benzimidazole-4-carboxylate (3.38 g) was taken forward without further purification. Triethylamine (1 mL, 7.66 mmol), 2 M dimethylamine (0.19 mL, 0.38 mmol) in tetrahydrofuran, sodium 2-(4-pyridyl)-1*H*-benzimidazole-4-carboxylate (100 mg, 0.38 mmol) and 50% propylphosphonic anhydride in ethyl acetate (0.34 mL, 1.15 mmol) were stirred together in *N,N*-dimethylformamide (5 mL) at RT overnight. The reaction mixture was concentrated under reduced pressure and the resulting crude yellow mixture (734 mg) was purified *via* flash column chromatography (30 g silica, ethyl acetate:methanol, 100:0 to 90:10) to give *N,N*-dimethyl-2-(4-pyridyl)-1*H*-benzimidazole-4-carboxamide (**67**) (34 mg, 32%) as an off-white solid.

R_f 0.38 (9:1 dichloromethane:methanol); m.p. 234–236 °C; ν_{\max} (thin film)/cm⁻¹ 3258 (N-H, br), 3054 (C-H, w), 2956 (C-H, w), 1604 (C=C, s), 1440 (C-H); ¹H NMR (600 MHz, DMSO-*d*₆) δ 13.34 (s, 1H, H-1), 8.92–8.59 (m, 2H, H-2' and H-6'), 8.14 (s, 2H, H-3' and H-5'), 7.70 (s, 1H, H-7), 7.32 (t, J = 7.5 Hz, 1H, H-6), 7.22 (d, J = 7.2 Hz, 1H, H-5), 3.11 (s, 3H, H-11), 2.87 (s, 3H, H-11); ¹³C NMR (151 MHz, DMSO-*d*₆) δ 168.8 (C-8), 150.9 (C-2' and C-6'), 150.0, 140.4, 137.3 (C-3' and C-5'), 135.5, 128.8, 123.7, 121.1, 113.1, 38.8 (C-11), 35.0 (C-11), insufficient sample quantity to obtain good quality HSQC and HMBC NMR; HRMS m/z (ESI⁺) [Found: 267.1241, C₁₅H₁₅N₄O requires (M+H)⁺ 267.1240]; LCMS (LCQ) Rt = 0.6 min (4 min method), m/z (ESI⁺) 267.0 (M+H)⁺.

Ethyl 4-amino-3-(pyridine-4-carbonyl-amino)benzoate (76)

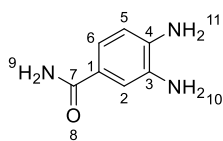
Intermediate **76** was prepared *via* General Method C using ethyl 3,4-diaminobenzoate (**75**) (100 mg, 0.55 mmol) and isonicotinic acid (**23**) (75 mg, 0.61 mmol). The reaction mixture was concentrated under reduced pressure and water (5 mL) was added to the residue. The aqueous solution was extracted three times with ethyl acetate (3 × 5 mL). The combined organic phases were dried over MgSO₄, filtered and concentrated under reduced pressure to give an orange oil (191 mg). The crude was purified *via* flash column chromatography (12 g silica, ethyl acetate:methanol, 100:0 to 90:10) to give ethyl 4-amino-3-(pyridine-4-carbonyl-amino)benzoate (**76**) (151 mg, 91%) as a pale orange solid.

R_f 0.63 (9:1 ethyl acetate:methanol); m.p. 132–135 °C; ν_{max} (thin film)/cm⁻¹ 3439 (N-H, w), 3208 (aromatic C-H, m), 1629 (C=O, s), 1606 (C=O, s), 1530 (aromatic C-H, m), 1498 (aliphatic C-H, s), 763 (N-H, s); ¹H NMR (500 MHz, DMSO-*d*₆) δ 9.92 (s, 1H, H-12), 8.77 (d, *J* = 4.2 Hz, 2H, H-2' and H-6'), 7.91 (d, *J* = 4.4 Hz, 2H, H-3' and H-5'), 7.75 (s, 1H, H-2), 7.61 (d, *J* = 8.5 Hz, 1H, H-6), 6.77 (d, *J* = 8.5 Hz, 2H, H-5), 5.93 (s, 2H, H-15), 4.22 (q, *J* = 7.1 Hz, 2H, H-10), 1.42–0.97 (m, 3H, H-11); ¹³C NMR (126 MHz, DMSO-*d*₆) δ 165.6 (C-13), 164.3 (C-7), 150.1 (C-2' and C-6'), 148.6 (C-4), 141.5 (C-4'), 129.1 (C-2), 128.8 (C-6), 121.8 (C-3' and C-5'), 120.9 (C-3), 116.3 (C-1), 114.5 (C-5), 59.8 (C-10), 14.3 (C-11); HRMS *m/z* (ESI⁺) [Found: 308.1007, C₁₅H₁₅N₃NaO₃ requires (M+Na)⁺ 308.1006]; LCMS (LCQ) Rt = 0.6 min (4 min method), *m/z* (ESI⁺) 286.1 (M+H)⁺.

Ethyl 2-(4-pyridyl)-1*H*-benzimidazole-5-carboxylate (77**)**^{173,174}

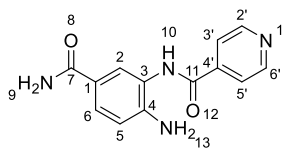
Compound **77** was prepared *via* General Method D using ethyl 4-amino-3-(pyridine-4-carbonyl-amino) benzoate (130 mg, 0.46 mmol). The reaction mixture was concentrated under reduced pressure to give an off-white solid (170 mg). The crude was purified *via* flash column chromatography (5 g amino silica, ethyl acetate:methanol, 100:0 to 90:10) to give ethyl 2-(4-pyridyl)-1*H*-benzimidazole-5-carboxylate (**77**) (50 mg, 58%) as a white solid.

R_f 0.42 (100% ethyl acetate); m.p. degrades > 240 °C; ν_{\max} (thin film)/cm⁻¹ 3246 (N-H, m, br), 3067 (aromatic C-H, m, br), 2843 (aliphatic C-H, w), 1642 (C=O, m), 1509 (aromatic C-H, s), 1472 (aliphatic C-H, m), 750 (N-H, s); ¹H NMR (500 MHz, DMSO-*d*₆) δ 8.72 (d, J = 4.7 Hz, 2H (H-2' and H-6')), 8.24 (s, 1H, H-4), 8.16 (d, J = 4.9 Hz, 2H, H-3' and H-5'), 7.80 (d, J = 8.4 Hz, 1H, H-6), 7.69 (d, J = 8.4 Hz, 1H, H-7), 4.32 (q, J = 7.0 Hz, 2H, H-11), 1.34 (t, J = 7.1 Hz, 3H, H-12); ¹³C NMR (126 MHz, DMSO-*d*₆) δ 166.5 (C-8), 153.5 (C-2), 150.3 (C-2' and C-6'), 144.3 (C-7a), 141.1 (C-5), 138.3 (C-4'), 123.1 (C-3a), 122.7 (C-6), 120.7 (C-3' and C-5'), 118.0 (C-4), 115.4 (C-7), 60.3 (C-11), 14.3 (C-12); HRMS m/z (ESI⁺) [Found: 290.0904, C₁₅H₁₃N₃NaO₂ requires (M+Na)⁺ 290.0900]; LCMS (LCQ) Rt = 0.6 min (4 min method), m/z (ESI⁺) 268.15 (M+H)⁺.

3,4-Diaminobenzamide (80)

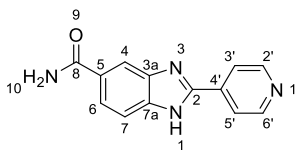
Intermediate **80** was prepared *via* General Method B using 4-amino-3-nitrobenzamide (**79**) (500 mg, 2.76 mmol). 3,4-Diaminobenzamide (249 mg, 57%) was isolated as an off-white solid.

^1H NMR (600 MHz, $\text{DMSO-}d_6$) δ 7.36 (s, 1H, H-9), 7.05 (s, 1H, H-2), 6.97 (d, J = 8.0 Hz, 1H, H-6), 6.69 (s, 1H, H-9), 6.45 (d, J = 8.0 Hz, 1H, H-5), 4.92 (s, 2H, H-10), 4.49 (s, 2H, H-11); HRMS m/z (ESI^+) [Found: 152.0900, $\text{C}_7\text{H}_{10}\text{N}_3\text{O}$ requires ($\text{M}+\text{H}$) $^+$ 151.1665]; LCMS (LCQ) R_t = 0.5 min (4 min method), m/z (ESI^+) 152.07 ($\text{M}+\text{H}$) $^+$.

***N*-(2-Amino-5-carbamoyl-phenyl)pyridine-4-carboxamide (**81**)**

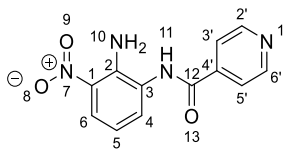
Intermediate **81** was prepared *via* General Method C using 3,4-diaminobenzamide (**80**) (196 mg, 1.3 mmol) and isonicotinic acid (**23**) (176 mg, 1.43 mmol). The reaction mixture was filtered giving *N*-(2-amino-3-carbamoyl-phenyl)-pyridine-4-carboxamide (**81**) (299 mg, 96%) as an off-white solid.

R_f 0 (9:1 dichloromethane:methanol); m.p. degrades > 220 °C; ν_{\max} (thin film)/cm⁻¹ 3343 (N-H, br), 3190 (N-H, br), 1672 (C=O, s), 1606 (C-C aromatic, s), 1393 (C-C aromatic, s), 835 (N-H, m), 690 (N-H, s), 675 (N-H, s); ¹H NMR (500 MHz, DMSO-*d*₆) δ 9.91 (s, 1H, H-10), 8.77 (d, J = 5.3 Hz, 2H, H-2' and H-6'), 7.91 (d, J = 5.5 Hz, 2H, H-3' and H-5'), 7.87 (s, 1H, H-9), 7.53 (d, J = 7.9 Hz, 1H, H-6), 7.26 (d, J = 7.6 Hz, 1H, H-2), 7.23 (s, 1H, H-9), 6.57 (t, J = 7.8 Hz, 1H, H-5), 6.52 (s, 2H, H-13); ¹³C NMR (151 MHz, DMSO-*d*₆) δ 167.6 (C-11), 164.2 (C-7), 150.2 (C-2' and C-6'), 146.9 (C-1), 141.6 (C-4'), 127.8 (C-3), 127.1 (C-4), 121.8 (C-3' and C-5'), 121.3 (C-5), 120.9 (C-6), 114.3 (C-2); HRMS m/z (ESI⁺) [Found: 257.1036, C₁₃H₁₃N₄O₂ requires (M+H)⁺ 257.1033]; LCMS (LCQ) Rt = 0.5 min (4 min method), m/z (ESI⁺) 257.02 (M+H)⁺.

2-(4-Pyridyl)-1*H*-benzimidazole-5-carboxamide (78)

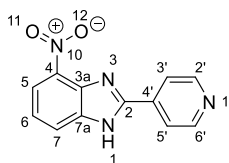
Compound **78** was prepared *via* General Method D using *N*-(2-aminophenyl)-pyridine-4-carboxamide (**81**) (30 mg, 0.12 mmol). The reaction mixture was concentrated under reduced pressure to give a pale yellow crude solid (27 mg). The crude was purified *via* flash column chromatography (11 g amino silica, ethyl acetate:methanol, 100:0 to 85:15) to give 2-(4-pyridyl)-1*H*-benzimidazole-5-carboxamide (**12**) (4 mg, 13%) as a yellow solid.

R_f 0.14 (9:1 dichloromethane:methanol); m.p. 210–213; ν_{\max} (thin film)/ cm^{-1} 3179 (N-H, br), 1670 (C=O, s), 1606 (C-C aromatic, s), 1392 (C-C aromatic, s), 697 (N-H, s), 674 (N-H, s); ^1H NMR (500 MHz, $\text{DMSO}-d_6$) δ 9.19 (s, 2H, H-10), 8.80 (d, $J = 4.3$ Hz, 2H, H-2' and H-6'), 8.19 (d, $J = 4.3$ Hz, 2H, H-3' and H-5'), 7.91 (d, $J = 7.3$ Hz, 1H, H-7), 7.84 (s, 1H, H-1), 7.81 (d, $J = 7.9$ Hz, 1H, H-5), 7.41 (t, $J = 7.7$ Hz, 1H, H-6); ^{13}C NMR insufficient quantities; HRMS m/z (ESI $^+$) [Found: 261.0741, $\text{C}_{13}\text{H}_{10}\text{N}_4\text{NaO}$ requires (M+H) $^+$ 261.0747]; LCMS (LCQ) Rt = 0.46 min (4 min method), m/z (ESI $^+$) 239.22 (M+H) $^+$.

***N*-(2-Amino-3-nitro-phenyl)pyridine-4-carboxamide**

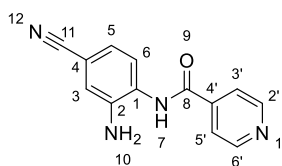
The intermediate was prepared *via* General Method C using 3-nitrobenzene-1,2-diamine (200 mg, 1.31 mmol) and isonicotinic acid (**23**) (177 mg, 1.44 mmol). The reaction mixture was filtered and *N*-(2-amino-3-nitro-phen-yl)pyridine-4-carboxamide (360 mg, 28%) was isolated as a brown solid. The product was taken forward without further purification.

R_f 0.77 (9:1 ethyl acetate:methanol); m.p. 206–208 °C; ν_{\max} (thin film)/cm⁻¹ 3450 (N-H, w), 3323 (N-H, br), 3256 (N-H, br), 1663 (C=O, m), 1525 (aromatic C-H, s), 738 (C-N, s); ¹H NMR (500 MHz, DMSO-*d*₆) δ 10.13 (s, 1H, H-11), 8.79 (s, 2H, H-2' and H-6'), 8.01 (d, J = 7.8 Hz, 1H, H-4), 7.94 (s, 2H, H-3' and H-5'), 7.54–7.43 (m, 1H, H-6), 7.28 (s, 2H, H-10), 6.75–6.63 (m, 1H, H-5); ¹³C NMR (126 MHz, DMSO-*d*₆) δ 164.7 (C-12), 150.0 (C-2' and C-6'), 142.6 (C-2), 141.2 (C-4'), 134.8 (C-6), 131.7 (C-1), 125.8 (C-3), 124.3 (C-4), 121.9 (C-3' and C-5'), 114.3 (C-5); HRMS m/z (ESI⁺) [Found: 259.0815, C₁₂H₁₁N₄O₃ requires (M+H)⁺ 259.0826]; LCMS (LCQ) R_t = 0.6 min (4 min method), m/z (ESI⁺) 259.09 (M+H)⁺.

4-Nitro-2-(4-pyridyl)-1H-benzimidazole (82)

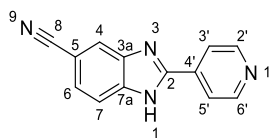
Compound **82** was prepared *via* General Method D using *N*-(2-amino-3-nitro-phenyl)pyridine-4-carboxamide (150 mg, 0.55 mmol mg). The reaction mixture was concentrated under reduced pressure to give a pale yellow solid (114 mg). The crude was purified *via* flash column chromatography (4.7 g amino silica, ethyl acetate:methanol, 100:0 to 90:10) to give 4-nitro-2-(4-pyridyl)-1H-benzimidazole (**14**) (46 mg, 33%) as an orange solid.

R_f 0.43 (100% ethyl acetate); m.p. 257–259 °C; ν_{\max} (thin film)/ cm^{-1} 1613 (m, C=C), 1510 (m,), 1481 (m, aromatic C-H), 1342 (s, N-O), 1300 (s, N-O), 806 (m, C-H), 728 (s, C-H); ^1H NMR (500 MHz, $\text{DMSO}-d_6$) δ 8.79 (d, $J = 4.1$ Hz, 2H, H-2' and H-6'), 8.29 (d, $J = 4.1$ Hz, 2H, H-3' and H-5'), 8.18 (m, 2H, H-4 and H-6), 7.47 (t, $J = 7.0$ Hz, 1H, H-5); ^{13}C NMR insufficient resolution in 10,000 scan experiment; HRMS m/z (ESI $^+$) [Found: 263.0531, $\text{C}_{12}\text{H}_8\text{N}_4\text{NaO}_2$ requires (M+H) $^+$ 263.0539]; LCMS (LCQ) Rt = 0.8 min (4 min method), m/z (ESI $^+$) 241.16 (M+H) $^+$.

***N*-(2-Amino-5-cyano-phenyl)pyridine-4-carboxamide**

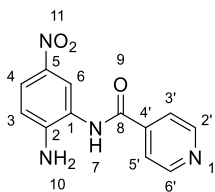
The intermediate was prepared *via* General Method C using 3,4-diaminobenzonitrile (100 mg, 0.75 mmol) and isonicotinic acid (**23**) (102 mg, 0.83 mmol). The reaction mixture was filtered and *N*-(2-amino-5-cyano-phenyl)pyridine-4-carboxamide (114 mg, 57%) was isolated as a brown solid.

^1H NMR (500 MHz, $\text{DMSO}-d_6$) δ 9.96 (s, 1H, H-7), 8.77 (d, J = 4.2 Hz, 2H, H-2' and H-6'), 7.90 (d, J = 4.4 Hz, 2H, H-3' and H-5'), 7.55 (s, 1H, H-3), 7.38 (d, J = 8.1 Hz, 1H, H-6), 6.81 (d, J = 8.4 Hz, 1H, H-5), 6.15 (s, 2H, H-10); LCMS (LCQ) R_t = 0.5 min (4 min method); HRMS m/z (ESI $^+$) [Found: 499.1607, $(\text{C}_{13}\text{H}_{10}\text{N}_4\text{O})_2\text{Na}$ requires (dimer + Na) $^+$ 499.4805; LCMS (LCQ) R_t = 0.5 min (4 min method), m/z (ESI $^+$) 239.09 (M+H) $^+$].

2-(4-Pyridyl)-1H-benzimidazole-5-carbonitrile (83)

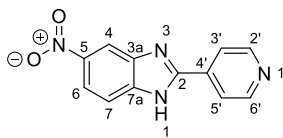
Compound **83** was prepared *via* General Method D using *N*-(2-amino-5-cyano-phenyl)pyridine-4-carboxamide (90 mg, 0.38 mmol). The reaction mixture was concentrated under reduced pressure to give an off-white solid (103 mg). The crude was purified *via* flash column chromatography (4.7 g amino silica, ethyl acetate:methanol, 100:0 to 90:10) to give 2-(4-pyridyl)-1H-benzimidazole-5-carbonitrile (**83**) (28 mg, 34%) as a pale pink solid.

R_f 0.70 (9:1 ethyl acetate:methanol); m.p. sublimes $> 260\text{ }^{\circ}\text{C}$; ν_{\max} (thin film)/ cm^{-1} 3352 (N-H, br), 2217 (C \equiv N, m), 1611 (C=C, s), 1536 (aromatic C-H, m), 798 (C-N, s); ^1H NMR (500 MHz, DMSO- d_6) δ 8.79 (d, $J = 4.1\text{ Hz}$, 2H, H-2' and H-6'), 8.23 (s, 1H, H-4), 8.11 (d, $J = 4.1\text{ Hz}$, 2H, H-3' and H-5'), 7.81 (d, $J = 8.1\text{ Hz}$, 1H, H-7), 7.65 (d, $J = 8.1\text{ Hz}$, 1H, H-6); ^{13}C NMR (151 MHz, DMSO- d_6) δ 151.8 (C-2), 150.2 (C-2' and C-6'), 141.3 (C-3a), 139.4 (C-7a), 136.1 (C-4'), 125.7 (C-7), 120.9 (C-8), 120.3 (C-3' and C-5'), 119.2 (C-6), 115.9 (C-5), 104.5 (C-4); HRMS m/z (ESI $^+$) [Found: 221.0817, $\text{C}_{13}\text{H}_9\text{N}_4$ requires (M+H) $^+$ 221.0822]; LCMS (LCQ) $R_t = 0.6\text{ min}$ (4 min method), m/z (ESI $^+$) 221.35 (M+H) $^+$.

***N*-(2-Amino-5-nitro-phenyl)pyridine-4-carboxamide**

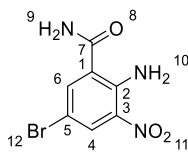
The intermediate was prepared *via* General Method C using 4-nitro-*O*-phenylene-diamine (150 mg, 0.98 mmol) and isonicotinic acid (**23**) (133 mg, 1.08 mmol). The reaction mixture was filtered and *N*-(2-amino-5-nitro-phenyl)-pyridine-4-carboxamide (146 mg, 52%) was isolated as a brown solid. The product was taken forward without further purification.

R_f 0.74 (9:1 ethyl acetate:methanol); m.p. 209–211 °C; ν_{\max} (thin film)/cm⁻¹ (bond, s) 3437 (N-H, w), 3342 (N-H, br), 3195 (N-H, br), 1626 (C=O, s), 1518 (aromatic C-H, s); ¹H NMR (500 MHz, DMSO-*d*₆) δ 10.03 (s, 1H, H-7), 8.88–8.70 (m, 2H, H-2' and H-6'), 8.12 (s, 1H, H-6), 8.00–7.86 (m, 3H, H-4, H-3' and H-5'), 6.80 (d, J = 8.9 Hz, 1H, H-3), 6.70 (s, 2H, H-10); ¹³C NMR (126 MHz, DMSO-*d*₆) δ 164.6 (C-8), 150.9 (C-2), 150.1 (C-2' and C-6'), 141.3 (C-4'), 135.2 (C-5), 124.0 (C-4), 124.0 (C-6), 121.9 (C-3' and C-5'), 120.5 (C-1), 113.8 (C-3); HRMS m/z (ESI⁺) [Found: 257.0670, C₁₂H₉N₄O₃ requires (M-H)⁺ 257.0680]; LCMS (LCQ) Rt = 0.5 min (4 min method), m/z (ESI⁺) 259.07 (M+H)⁺.

5-Nitro-2-(4-pyridyl)-1H-benzimidazole (84)

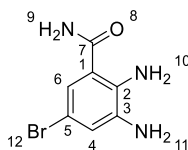
Compound **84** was prepared *via* General Method D using *N*-(2-amino-5-nitro-phenyl)-pyridine-4-carboxamide (117 mg). The reaction mixture was concentrated under reduced pressure to give an off-white solid (130 mg). The crude was purified *via* flash column chromatography (4.7 g amino silica, ethyl acetate:methanol, 100:0 to 90:10) to give 5-nitro-2-(4-pyridyl)-1H-benzimidazole (**84**) (63 mg, 0.24 mmol, 58%) as a pale orange solid.

R_f 0.24 (100% ethyl acetate); sublimes $> 265\text{ }^{\circ}\text{C}$; ν_{max} (thin film)/ cm^{-1} 3109 (br, N-H), 1614 (m, C=C), 1519 (m, N-O), 1474 (m, aromatic C-H), 1339 (s, N-O), 1312 (s, N-O) 823 (m, N-H), 738 (s, N-H); ^1H NMR (500 MHz, $\text{DMSO}-d_6$) δ 8.81 (d, $J = 4.9\text{ Hz}$, 2H, H-2' and H-6'), 8.54 (s, 1H, H-4), 8.17 (d, $J = 8.9\text{ Hz}$, 1H, H-6), 8.12 (d, $J = 4.8\text{ Hz}$, 2H, H-3' and H-5'), 7.83 (d, $J = 8.8\text{ Hz}$, 1H, H-7); ^{13}C NMR insufficient resolution in 10,000 scan experiment; HRMS m/z (ESI $^+$) [Found: 241.0721, $\text{C}_{12}\text{H}_9\text{N}_4\text{O}_2$ requires (M+H) $^+$ 241.0720]; LCMS (LCQ) $R_t = 0.6\text{ min}$ (4 min method), m/z (ESI $^+$) 241.15 (M+H) $^+$.

2-Amino-5-bromo-3-nitro-benzamide (89)

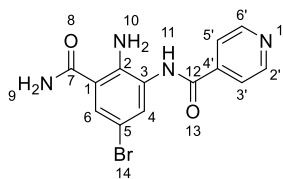
Intermediate **89** was prepared *via* General Method A using 2-amino-5-bromo-3-nitrobenzoic acid (**88**) (900 mg, 3.45 mmol) and 13.4 M aqueous ammonia solution (2.6 mL, 34.48 mmol). The reaction mixture was filtered giving 2-amino-5-bromo-3-nitro-benzamide (**89**) (330 mg, 35%) as a fine orange solid. The filtrate was partially concentrated under reduced pressure, left overnight and a further batch of the product (**89**) (150 mg, 16%) was isolated by filtration.

^1H NMR (500 MHz, DMSO- d_6) δ 8.49 (s, 2H, H-9), 8.29 (d, J = 2.3 Hz, 1H, H-4), 8.27 (s, 1H, H-10), 8.08 (d, J = 2.3 Hz, 1H, H-6), 7.76 (s, 1H, H-10); LCMS (MDAP) R_t = 1.9 min (Ana 5-95 in 5 min), m/z (ESI $^+$) 257.80 and 259.80 ($M+H$) $^+$.

2,3-Diamino-5-bromo-benzamide (90)

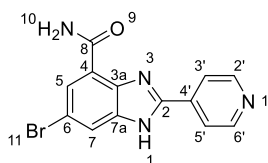
Intermediate **90** was prepared *via* General Method B using 2-amino-5-bromo-3-nitro-benzamide (**89**) (150 mg, 0.55 mmol). 2,3-Diamino-5-bromo-benzamide (**90**) (69 mg, 52%) was isolated as a pale-yellow solid.

^1H NMR (500 MHz, $\text{DMSO-}d_6$) δ 7.74 (s, 1H, H-10), 7.11 (s, 1H, H-10), 7.03 (s, 1H, H-6), 6.73 (s, 1H, H-4), 6.23 (s, 2H, H-9), 4.99 (s, 2H, H-11); HRMS m/z (ESI $^+$) [Found: 251.9743 [Br-79] and 253.9722 [Br-81], $\text{C}_7\text{H}_8\text{BrN}_3\text{ONa}$ ($\text{M}+\text{Na}$) $^+$ requires 253.0516]; LCMS (MDAP) R_t = 25.1 min (Ana 5–95 in 20 min), not ionisable by MDAP/LCQ LCMS.

***N*-(2-Amino-5-bromo-3-carbamoyl-phenyl)pyridine-4-carboxamide (**91**)**¹²⁶

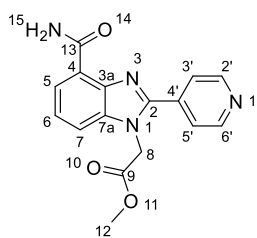
2,3-Diamino-5-bromo-benzamide (**90**) (750 mg, 3.26 mmol), isonicotinic acid (**23**) (401 mg, 3.26 mmol), 1-hydroxybenzotriazole hydrate (HOBt) (582 mg, 3.8 mmol) and *N*-(3-dimethylaminopropyl)-*N'*-ethylcarbodiimide hydrochloride (EDC-HCl) (750 mg, 3.91 mmol) in DMF (7 mL) were stirred overnight at 100 °C. The reaction was allowed to cool to room temperature and saturated aqueous Na₂CO₃ was added until effervescence ceased (*ca.* 10–15 mL). A brown precipitate formed. The mixture was filtered, and the collected solids were dried in a vacuum oven overnight. The resulting brown solid (825 mg) was purified *via* flash column chromatography (40 g silica, ethyl acetate:methanol, 100:0 to 90:10) to give *N*-(2-amino-5-bromo-3-carbamoyl-phenyl)pyridine-4-carboxamide (**91**) (825 mg, 52%) as a pale yellow solid.

*R*_f 0.64 (9:1 dichloromethane:methanol); m.p. > 300 °C; *v*_{max} (thin film)/cm⁻¹ 3349 (br, N-H), 3156 (br, N-H), 1649 (s, C=O), 1599 (aromatic C-H) 1533 (aromatic C-H), 1041 (m, C-N); ¹H NMR (600 MHz, DMSO-*d*₆) δ 9.95 (s, 1H, H-11), 8.78 (d, *J* = 4.6 Hz, 2H, H-2' and H-6'), 8.20 (s, 1H, H-10), 8.00 (s, 1H, H-10), 7.90 (d, *J* = 4.0 Hz, 2H, H-3' and H-5'), 7.71 (s, 1H, H-6), 7.46 (s, 1H, H-4), 6.66 (s, 2H, H-9); ¹³C NMR (151 MHz, DMSO-*d*₆) δ 170.3 (C-7), 165.0 (C-12), 151.1 (C-1), 150.5 (C-2' and C-6'), 145.3 (C-3), 141.7 (C-4'), 133.0 (C-4), 129.7 (C-6), 125.5 (C-2), 122.3 (C-3' and C-5'), 104.3 (C-5); LCMS (LCQ) *R*_t = 0.6 min (4 min method); HRMS *m/z* (ESI⁺) [Found: 317.0038 (product cyclised to **92** on column), C₁₃H₁₁BrN₄O₂ requires (*M*)] 335.1556]; LCMS (LCQ) *R*_t = 0.6 min (4 min method), *m/z* (ESI⁺) 317.16 [⁷⁹Br], 318.15 [⁸¹Br] (product cyclised to **92** on column), 334.97 [⁷⁹Br], 336.98 [⁸¹Br] (*M*+H)⁺.

6-Bromo-2-(4-pyridyl)-1H-benzimidazole-4-carboxamide (92)

Compound **92** was prepared *via* General Method D using *N*-(2-amino-5-bromo-3-carbamoyl-phenyl)pyridine-4-carboxamide (300 mg). The reaction mixture was neutralised to pH 8 with saturated aqueous sodium carbonate and the resulting suspension was filtered. The collected solids were dried in a vacuum oven overnight to yield 6-bromo-2-(4-pyridyl)-1H-benzimidazole-4-carboxamide (**92**) (300 mg, 100%) as a pale brown solid.

R_f 0.54 (9:1 ethyl acetate:methanol); m.p. > 300 °C; ν_{\max} (thin film)/cm⁻¹ 3344 (N-H, m), 3175 (aromatic C-H, m), 1669 (C=O, s), 1603 (C=C, s), 1409 (aromatic C-C, m), 793 (N-H, s); ¹H NMR (600 MHz, DMSO-*d*₆) δ 10.09 (d, J = 4.2 Hz, 1H, H-10), 8.59–8.44 (m, 2H, H-2' and H-6'), 8.13 (d, J = 6.0 Hz, 2H, H-3' and H-5'), 7.69 (s, 1H, H-5), 7.57 (s, 1H, H-7), 7.45 (d, J = 3.6 Hz, 1H, H-10); ¹³C NMR (151 MHz, DMSO-*d*₆) δ 175.1 (C-8), 167.5 (C-6), 159.5 (C-2), 150.1 (C-2' and C-6'), 149.9 (C-4), 145.4 (C-3a), 143.5 (C-4'), 122.3 (C-5), 122.1 (C-7), 121.4 (C-3' and C-5'), 110.5 (C-7a); HRMS m/z (ESI⁺) [Found: 338.9859, C₁₃H₉BrN₄O requires (M+H)⁺ 338.9826]; LCMS (MDAP) R_t = 2.9 min (Ana 5–95 over 5 minutes), m/z (ESI⁺) 316.850 [⁷⁹Br], 318.8 [⁸¹Br] (M+H)⁺.

Methyl 2-[4-carbamoyl-2-(4-pyridyl)benzimidazol-1-yl]acetate (96)¹⁷⁵

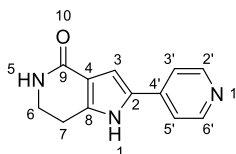
To a solution of 2-(4-pyridyl)-1*H*-benzimidazole-4-carboxamide (**10**) (50 mg, 1 eq.) in *N,N*-dimethylformamide (1 mL) was added methyl bromoacetate (**95**) (0.03 mL, 1.5 eq.) and sodium hydride (10 mg, 2 eq.). The reaction mixture was stirred at 80 °C for 2 h. The reaction mixture was concentrated under reduced pressure and chloroform (5 mL) was added. The mixture was extracted five times with water (5 × 2 mL). The organic phase was dried over MgSO₄, filtered and concentrated under reduced pressure before being recrystallised from cyclohexane to give methyl 2-[4-carbamoyl-2-(4-pyridyl)-benzimidazol-1-yl]acetate (**96**) (22 mg, 34%) as an orange solid.

¹H NMR (600 MHz, DMSO-*d*₆) δ 9.03 (s, 1H, H-15), 8.81 (d, *J* = 5.5 Hz, 2H, H-2' and H-6'), 7.98 (d, *J* = 7.5 Hz, 1H, H-5), 7.92 (d, *J* = 8.1 Hz, 1H, H-7), 7.85 (s, 1H, H-15), 7.80 (d, *J* = 5.6 Hz, 2H, H-3' and H-5'), 7.48 (t, *J* = 7.8 Hz, 1H, H-6), 5.45 (s, 2H, H-8), 3.67 (s, 3H, H-12); LCMS (MDAP) *R*_t = 0.7 min (Ana 5–95 in 5 minutes); HRMS *m/z* (ESI⁺) 311.1011 (M+H)⁺, calculated MW for C₁₆H₁₄N₄O₃ 310.3068.

6.1.2 Preparation of compounds described in Chapter 3

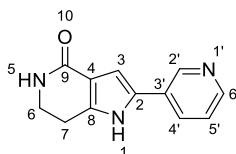
*indicates compounds synthesised by Mihaela Paula-Ficu

2-(4-Pyridyl)-1,5,6,7-tetrahydropyrrolo[3,2-*c*]pyridin-4-one (**11**)¹⁰⁵



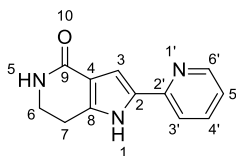
A mixture of 4-(bromoacetyl)pyridine hydrobromide (**98**) (2.00 g, 7.12mmol), piperidin-2,4-dione (**99**) (1.21 g, 10.68 mmol) and ammonium acetate (2.19 g, 28.47 mmol) in ethanol (30 mL) was stirred at room temperature overnight. A red solution formed. LCMS analysis of the reaction mixture showed the desired product ion peak (m/z 214) was the major component of the reaction mixture. The reaction mixture was concentrated under reduced pressure to give an orange/red residue (1.06 g). The crude was purified by flash column chromatography (70 g silica, dichloromethane:methanol 100:0 to 90:10) to give 2-(4-pyridyl)-1,5,6,7-tetrahydropyrrolo-[3,2-*c*]pyridin-4-one (830 mg, 52%) (**11**) as a pale orange solid.

R_f 0.38 (9:1 dichloromethane:methanol); m.p. degrades > 190 °C; ν_{\max} (thin film)/ cm^{-1} 3242 (N-H, m), 2929 (C-H, w), 1634 (C=O, s), 1604 (C=N, s), 1520 (aromatic C=C, m), 1157 (C-N, m); ^1H NMR (500 MHz, $\text{DMSO-}d_6$) δ 11.94 (s, 1H, H-5), 8.47 (d, J = 4.9 Hz, 2H, H-2' and H-6'), 7.60 (d, J = 4.9 Hz, 2H, H-3' and H-5'), 7.09 (s, 1H, H-1), 7.01 (s, 1H, H-3), 3.43–3.38 (m, 2H, H-6), 2.84 (t, J = 6.7 Hz, 2H, H-7); ^{13}C NMR (126 MHz, $\text{DMSO-}d_6$) δ 164.8 (C-9), 150.0 (C-2' and C-6'), 139.0 (C-4), 138.8 (C-4'), 128.4 (C-2), 117.5 (C-3' and C-5'), 115.7 (C-8), 106.3 (C-3), 40.1 (C-6), 21.9 (C-7); HRMS m/z (ESI⁺) [Found: 214.0977, $\text{C}_{12}\text{H}_{12}\text{N}_3\text{O}$ requires (M+H)⁺ 214.0975]; LCMS (LCQ) R_t = 0.4 min (4 min method), m/z (ESI⁺) 214.26 (M+H)⁺.

2-(3-Pyridyl)-1,5,6,7-tetrahydropyrrolo[3,2-c]pyridin-4-one (109)

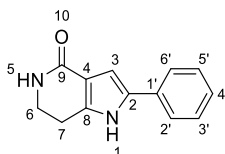
A mixture of piperidin-2,4-dione (**99**) (339 mg, 3 mmol), ammonium acetate (617 mg, 8 mmol) and 3-(bromoacetyl)pyridine hydrobromide (**108**) (400 mg, 2 mmol) in ethanol (5 mL) was stirred at room temperature overnight. A red solution formed. LCMS analysis of the reaction mixture showed the desired product ion peak (m/z 214) was the major component of the reaction mixture. The reaction mixture was concentrated to dryness under reduced pressure to give an orange/red residue (1.40 g). The crude was purified by flash column chromatography (11 g amino silica, ethyl acetate:methanol 100:0 to 90:10) to give a mixture of product and impurity (83 mg). The residue was purified a second time by flash column chromatography (5 g amino silica, ethyl acetate:methanol 100:0 to 9:1) to give 2-(3-pyridyl)-1,5,6,7-tetrahydropyrrolo[3,2-c]pyridin-4-one (**109**) (41 mg, 9%) as a yellow foam.

R_f 0.12 (9:1 ethyl acetate:methanol); m.p. degrades > 200 °C; ν_{\max} (thin film)/ cm^{-1} 3441 (N-H, w, br), 3202 (aromatic C-H, m, br), 1619 (C=O, s), 1509 (aromatic C-H, s), 1475 (aliphatic C-H, m), 776 (N-H, s); ^1H NMR (500 MHz, $\text{DMSO}-d_6$) δ 11.79 (s, 1H, H-5), 8.89 (s, 1H, H-2'), 8.36 (d, $J = 3.6$ Hz, 1H, H-6'/4'), 7.99 (d, $J = 8.0$ Hz, 1H, H-4'/6'), 7.37 (dd, $J = 7.9, 4.8$ Hz, 1H, H-5'), 7.02 (s, 1H, H-1), 6.83 (s, 1H, H-3), 3.43–3.37 (m, 2H, H-6), 2.82 (t, $J = 6.8$ Hz, 2H, H-7); ^{13}C NMR (126 MHz, $\text{DMSO}-d_6$) δ 165.0 (C-9), 146.7 (C-6'), 144.9 (C-2'), 138.0 (C-4), 130.4 (C-4'), 128.1 (C-3'), 128.0 (C-2), 123.7 (C-5'), 115.3 (C-8), 104.3 (C-3), 40.2 (C-6), 21.9 (C-7); HRMS m/z (ESI $^+$) [Found: 214.0979, $\text{C}_{12}\text{H}_{12}\text{N}_3\text{O}$ requires (M+H) $^+$ 214.0975]; LCMS (LCQ) $R_t = 0.5$ min (7 min method), m/z (ESI $^+$) 214.22 (M+H) $^+$.

2-(2-Pyridyl)-1,5,6,7-tetrahydropyrrolo[3,2-c]pyridin-4-one (111)

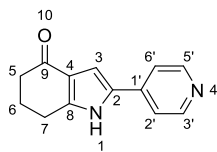
A mixture of piperidin-2,4-dione (**99**) (60 mg, 0.53 mmol), ammonium acetate (110 mg, 1.42 mmol) and 2-bromo-1-pyridin-2-ylethanone (**110**) (71 mg, 0.36 mmol) in ethanol (2 mL) was stirred at room temperature for overnight. A red solution formed. LCMS analysis of the reaction mixture showed the desired product ion peak (m/z 214) was the major component of the reaction mixture. The reaction mixture was concentrated to dryness under reduced pressure to give an orange/red residue (435 mg). The crude was purified by flash column chromatography (12 g silica, dichloromethane:methanol 100:0 to 90:10) to give 2-(2-pyridyl)-1,5,6,7-tetrahydropyrrolo-[3,2-c]pyridin-4-one (55 mg, 28%) as a pale pink solid.

R_f 0.80 (9:1 dichloromethane:methanol); m.p. 271–273 °C; ν_{\max} (thin film)/ cm^{-1} 3248 (N-H, m, br), 3065 (aromatic C-H, m, br), 2842 (aliphatic C-H, w, br), 1642 (C=O, s), 1508 (aromatic C-H, s), 775 (N-H, s); ^1H NMR (500 MHz, $\text{DMSO}-d_6$) δ 11.85 (s, 1H, H-5), 8.48 (d, J = 4.4 Hz, 1H, H-6'), 7.74 (s, 2H, H-4' and H-5'), 7.20–7.10 (m, 1H, H-3'), 7.03 (s, 1H, H-1), 6.99–6.91 (m, 1H, H-3), 3.47–3.32 (m, 2H, H-6), 2.81 (t, J = 6.6 Hz, 3H, H-7); ^{13}C NMR (126 MHz, $\text{DMSO}-d_6$) δ 165.2 (C-9), 150.3 (C-2'), 148.7 (C-6'), 138.3 (C-4), 136.8 (C-4'), 131.1 (C-2), 120.8 (C-3'), 118.1 (C-5'), 115.3 (C-8), 105.3 (C-3), 40.2 (C-6), 22.0 (C-7); HRMS m/z (ESI⁺) [Found: 214.0978, $\text{C}_{12}\text{H}_{12}\text{N}_3\text{O}$ requires (M+H)⁺ 214.0975]; LCMS (LCQ) R_t = 0.5 min (4 min method), m/z (ESI⁺) 214.23 (M+H)⁺.

2-Phenyl-1,5,6,7-tetrahydropyrrolo[3,2-c]pyridin-4-one (113)¹⁰⁵

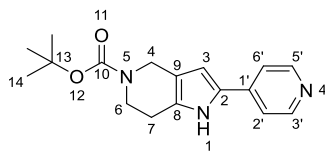
A mixture of piperidin-2,4-dione (**99**) (341 mg, 3.01 mmol), ammonium acetate (620 mg, 8.04 mmol) and phenacyl bromide (**112**) (400 mg, 2.01 mmol) in ethanol (6mL) was stirred at room temperature overnight. A yellow solution formed. LCMS analysis confirmed product formation (m/z 213). The solution was concentrated under reduced pressure to give an orange residue (1.59 g). The crude was purified by flash column chromatography (30 g silica, dichloromethane:methanol, 1:0 to 9:1) and dried under vacuum to give 2-phenyl-1,5,6,7-tetrahydropyrrolo[3,2-c]pyridin-4-one (**113**) (60 mg, 13%) as a yellow glass.

R_f 0.64 (9:1 ethyl acetate:methanol); m.p. 109–111 °C; ν_{\max} (thin film)/cm⁻¹ 3204 (N-H, br), 1621 (C=O, s), 1505 (aromatic C-H, s), 1448 (aliphatic C-H, m), 755 (N-H, s); ¹H NMR (500 MHz, DMSO-*d*₆) δ 11.62 (s, 1H, H-5), 7.63 (d, J = 7.6 Hz, 2H, H-2' and H-6'), 7.35 (t, J = 7.3 Hz, 2H, H-3' and H-5'), 7.17 (t, J = 7.1 Hz, 1H, H-4'), 6.97 (s, 1H, H-1), 6.67 (s, 1H, H-3), 3.39–3.35 (m, 2H, H-6), 2.81 (t, J = 6.5 Hz, 2H, H-7); ¹³C NMR (126 MHz, DMSO-*d*₆) δ 165.3 (C-9), 137.2 (C-8), 132.3 (C-1'), 131.1 (C-2), 128.8 (C-3' and C-5'), 125.9 (C-4'), 123.4 (C-2' and C-6'), 115.0 (C-3), 103.0 (C-4), 40.3 (C-6), 21.9 (C-7); HRMS m/z (ESI⁺) [Found: 213.1022, C₁₃H₁₃N₂O requires (M+H)⁺ 213.1022]; LCMS (LCQ) Rt = 0.6 min (4 min method), m/z (ESI⁺) 213.16 (M+H)⁺.

2-(4-Pyridyl)-1,5,6,7-tetrahydroindol-4-one (114)*

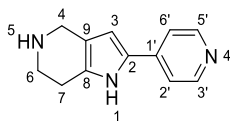
A mixture of 4-(bromoacetyl)pyridine hydrobromide (**98**) (200 mg, 0.71 mmol), 1,3-cyclohexanedione (120 mg, 1.07 mmol) and ammonium acetate (220 mg, 2.85 mmol) in ethanol (3 mL) was stirred at room temperature for 18 hours. LCMS indicated product formation (m/z 213). The reaction mixture was concentrated under reduced pressure, and the resulting dark red residue (536 mg) was purified by flash column chromatography (12 g silica, dichloromethane:methanol, 1:0 to 9:1). The desired fractions were collected to yield 2-(4-pyridyl)-1,5,6,7-tetrahydroindol-4-one (**114**) (35 mg, 22%) as a yellow solid.

R_f 0.49 (dichloromethane:methanol, 9:1); m.p. sublimated at 200–203 °C; ν_{\max} (thin film)/ cm^{-1} 3242 (N-H, m), 2929 (C-H, w), 1634 (C=O, s), 1604 (C=N, s), 1520 (aromatic C=C, m), 1157 (C-N, m); ^1H NMR (500 MHz, $\text{DMSO}-d_6$) δ 12.07 (1H, s, H-1), 8.51 (2H, d, $J = 4.6$ Hz, H-2' and H-6'), 7.64 (2H, d, $J = 5.1$ Hz, H-3' and H-5'), 7.05 (1H, s, H-3), 2.85 (2H, t, $J = 6.3$ Hz, H-7), 2.36 (2H, t, $J = 6.3$ Hz, H-5), 2.06 (2H, q, $J = 6.3$ Hz, H-6); ^{13}C NMR (126 MHz, $\text{DMSO}-d_6$) δ 192.8 (C-4), 150.0 (C-2' and C-6'), 146.5 (C-8), 138.5 (C-4'), 129.4 (C-2), 121.2 (C-9), 117.8 (C-3' and C-5'), 105.0 (C-3), 37.7 (C-5), 23.4 (C-6), 22.2 (C-7); HRMS m/z (ESI⁺) [Found: 213.1022, $\text{C}_{13}\text{H}_{13}\text{N}_2\text{O}$ requires (M+H)⁺ 213.1022]; LCMS (LCQ) R_t = 0.4 min (4 min method), m/z (ESI⁺) 213.28 (M+H)⁺.

Tert*-Butyl 2-(4-pyridyl)-1,4,6,7-tetrahydropyrrolo[3,2-*c*]pyridine-5-carboxylate (**115a**)

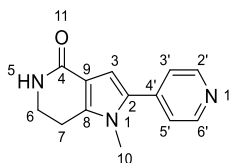
A mixture of 4-(bromoacetyl)pyridine hydrobromide (**98**) (100 mg, 0.36 mmol), *tert*-butyl 4-oxopiperidine-1-carboxylate (106 mg, 0.53 mmol) and ammonium acetate (110 mg, 1.42 mmol) in ethanol (1.5 mL) was stirred at room temperature for 18 hours. The brown mixture was concentrated under reduced pressure and the residue (273 mg) was purified by flash column chromatography (20 g silica, dichloromethane:methanol, 1:0 to 9:1) to yield the *tert*-butyl 2-(4-pyridyl)-1,4,6,7-tetrahydropyrrolo[3,2-*c*]pyridine-5-carboxylate (**115a**) (32 mg, 28%) as a yellow solid.

R_f 0.58 (dichloromethane:methanol, 9:1); m.p. 145–175 °C; ν_{\max} (thin film)/ cm^{-1} 3088 (N-H, w), 2979 (C-H, w), 1684 (C=O, s), 1632 (C=N, s), 1523 (aromatic C=C, s), 1234 (C-O, s), 1152 (C-N, s); ^1H NMR (600 MHz, $\text{DMSO-}d_6$) δ 11.37 (1H, s, H-1), 8.41 (2H, d, J = 4.6 Hz, H-2' and H-6'), 7.48 (2H, d, J = 5.1 Hz, H-3' and H-5'), 6.61 (1H, s, H-3), 4.32 (2H, s, H-4), 3.62 (2H, t, J = 5.2 Hz, H-6), 2.66 (2H, t, J = 5.2 Hz, H-7), 1.42 (9H, s, H-14); ^{13}C NMR (151 MHz, $\text{DMSO-}d_6$) δ 172.0 (C-10), 149.8 (C-2' and C-6'), 139.4 (C-8), 129.0 (C-4'), 127.4 (C-2), 116.9 (C-3' and C-5'), 105.4 (C-3), 90.2 (C-9), 78.8 (C-12), 40.1 (C-4), 39.9 (C-6), 28.1 (C-13, C-14 and C-15), 21.0 (C-7); HRMS m/z (ESI⁺) [Found: 300.1698, $\text{C}_{17}\text{H}_{22}\text{N}_3\text{O}_2$ requires (M+H)⁺ 300.1707]; LCMS (LCQ) R_t = 0.4 min (4 min method), m/z (ESI⁺) 300.01 (M+H)⁺.

2-(4-Pyridyl)-4,5,6,7-tetrahydro-1H-pyrrolo[3,2-c]pyridine; 2,2,2-trifluoroacetic acid (115)*

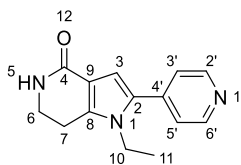
A solution of *tert*-butyl 2-(4-pyridyl)-1,4,6,7-tetrahydropyrrolo[3,2-c]pyridine-5-carboxylate (26 mg, 0.09 mmol) in dichloromethane (1.5 mL) was cooled to 0 °C and trifluoro acetic acid (0.3 mL, 3.92 mmol) was added dropwise. The resulting mixture was stirred at 0 °C for 3 hours and then was allowed to warm to room temperature. The yellow mixture was dissolved in methanol (3 mL), concentrated under reduced pressure, washed with diethyl ether and dried in a vacuum oven overnight to yield 2-(4-pyridyl)-4,5,6,7-tetrahydro-1H-pyrrolo[3,2-c]pyridine; 2,2,2-trifluoroacetic acid (**115**) (10 mg, 34%) as a dark-yellow solid.

R_f 0 (9:1 dichloromethane:methanol); m.p. 197–205 °C; ν_{\max} (thin film)/cm⁻¹ 3066 (N-H, w), 3009 (C-H, w), 1670 (C=O, s), 1628 (C=N, s), 1519 (aromatic C=C, s), 1381 (C-F, m); 1182 (C-N, s); 1122 (C-O, s); ¹H NMR (600 MHz, DMSO-*d*₆) δ 12.27 (1H, s, H-1), 9.11 (2H, s, H-5), 8.65 (2H, d, *J* = 6.0 Hz, H-2' and H-6'), 7.97 (2H, d, *J* = 6.0 Hz, H-3' and H-5'), 7.13 (1H, s, H-3), 4.16 (2H, s, H-4), 3.45–3.42 (2H, m, H-6), 2.97 (2H, t, *J* = 5.2 Hz, H-7); ¹³C NMR (151 MHz, DMSO-*d*₆) δ 142.3 (C-2' and C-6'), 131.9 (C-8), 126.6 (C-4'), 118.0 (C-3' and C-5'), 113.9 (C-2), 111.6 (C-3), 109.5 (C-9), 40.9 (C-4), 40.7 (C-6), 19.9 (C-7); HRMS *m/z* (ESI⁺) [Found: 200.1180, C₁₂H₁₄N₃ requires (M+H)⁺ 200.1182]; LCMS (LCQ) *Rt* = 0.4 min (4 min method), *m/z* (ESI⁺) 200.13 (M+H)⁺.

1-Methyl-2-(4-pyridyl)-6,7-dihydro-5H-pyrrolo[3,2-c]pyridin-4-one (120)¹⁰⁵

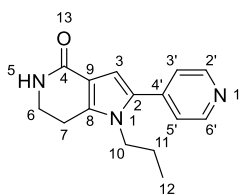
4-(Bromoacetyl)pyridine hydrobromide (**98**) (200 mg, 0.71 mmol), piperidin-2,4-dione (**99**) (121 mg, 1.07 mmol) and 8 M methylamine in ethanol (0.36 mL, 2.85 mmol) were stirred in ethanol (3 mL) at room temperature overnight. LCMS analysis indicated formation of the product (m/z 228). The reaction mixture was concentrated under reduced pressure. The crude was dissolved in saturated aqueous Sodium hydrogen carbonate (20 mL) and extracted three times with 2:1 chloroform:propan-2-ol (3 × 25 mL). The organic phases were combined, dried over MgSO_4 , filtered and concentrated under reduced pressure. The crude was purified by flash chromatography (5 g silica, dichloromethane:methanol, 100:0 to 90:10) to give 1-methyl-2-(4-pyridyl)-6,7-dihydro-5H-pyrrolo[3,2-c]pyridin-4-one (**120**) (39 mg, 23%) as a brown solid.

R_f 0.71 (dichloromethane:methanol, 9:1); m.p. decomposed at 210–214 °C; ν_{max} (thin film)/ cm^{-1} 3197 (N-H, m), 3061 (C-H, w), 1644 (C=O, s), 1599 (C=N, s), 1497 (aromatic C=C, s), 1165 (C-N, m); ^1H NMR (500 MHz, $\text{DMSO}-d_6$) δ 8.60–8.52 (m, 2H, H-2' and H-6'), 7.52–7.45 (m, 2H, H-3' and H-5'), 7.09 (s, 1H, H-N-5), 6.64 (s, 1H, H-3), 3.42 (td, J = 6.9, 2.5 Hz, 2H, H-6), 3.34 (s, 3H, H-11), 2.86 (t, J = 6.9 Hz, 2H, H-7); ^{13}C NMR (126 MHz, $\text{DMSO}-d_6$) δ 164.6 (C-4), 149.8 (C-2' and C-6'), 140.2 (C-8), 139.2 (C-4'), 131.5 (C-2), 121.8 (C-3' and C-5'), 114.3 (C-9), 107.8 (C-3), 39.8 (C-6), 32.5 (C-10), 21.2 (C-7); HRMS m/z (ESI⁺) [Found: 228.1126, $\text{C}_{13}\text{H}_{14}\text{N}_3\text{O}$ requires (M+H)⁺ 228.1131]; LCMS (LCQ) Rt = 0.4 min (4 min method), m/z (ESI⁺) 228.27 (M+H)⁺.

1-Ethyl-2-(4-pyridyl)-6,7-dihydro-5H-pyrrolo[3,2-c]pyridin-4-one (121)¹⁰⁵

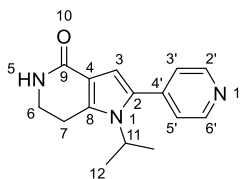
4-(Bromoacetyl)pyridine hydrobromide (**98**) (3 g, 10.68 mmol), piperidin-2,4-dione (**99**) (1.81 g, 16.02 mmol) and 70% ethylamine solution (2.8 mL, 42.71 mmol) in water were stirred in ethanol (45 mL) at room temperature overnight. LCMS (LCQ) indicated product formation (m/z 242). The reaction mixture was concentrated under reduced pressure and saturated aqueous Sodium hydrogen carbonate (240 mL) was added. The mixture was extracted six times with dichloromethane (6 × 240 mL). The combined organic phases were dried over MgSO_4 , filtered and concentrated under reduced pressure to give 1-ethyl-2-(4-pyridyl)-6,7-dihydro-5H-pyrrolo[3,2-c]pyridin-4-one (**121**) (2.37 g, 87%) as an orange solid.

R_f 0.42 (dichloromethane:methanol, 9:1); m.p. decomposed at 186–190 °C; ν_{max} (thin film)/ cm^{-1} 3189 (N-H, m), 2966 (C-H, m), 1654 (C=O, s), 1598 (C=N, s), 1496 (aromatic C=C, s), 1164 (C-N, m); ^1H NMR (600 MHz, $\text{DMSO}-d_6$) δ 8.59 (d, J = 4.3 Hz, 2H, H-2' and H-6'), 7.44 (d, J = 4.5 Hz, 2H, H-3' and H-5'), 7.08 (s, 1H, H-5), 6.59 (s, 1H, H-3), 4.05 (q, J = 6.2, 5.6 Hz, 2H, H-10), 3.48–3.38 (m, 2H, H-6), 2.96–2.84 (m, 2H, H-7), 1.19 (t, J = 6.9 Hz, 3H, H-11); ^{13}C NMR (151 MHz, $\text{DMSO}-d_6$) δ 164.6 (C-4), 150.0 (C-2' and C-6'), 139.5 (C-8), 139.4 (C-4'), 130.8 (C-2), 122.0 (C-3' and C-5'), 114.6 (C-9), 108.2 (C-3), 40.0 (C-6), 39.2 (C-10), 21.1 (C-7), 16.0 (C-11); HRMS m/z (ESI⁺) [Found: 242.1289, $\text{C}_{14}\text{H}_{16}\text{N}_3\text{O}$ requires (M+H)⁺ 242.1288]; LCMS (LCQ) R_t = 0.4 min (4 min method), m/z (ESI⁺) 242.19 (M+H)⁺.

1-Propyl-2-(4-pyridyl)-6,7-dihydro-5H-pyrrolo[3,2-c]pyridin-4-one (122)*

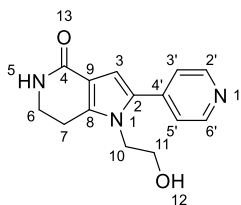
A mixture of 4-(bromoacetyl)pyridine hydrobromide (**98**) (200 mg, 0.71 mmol), piperidin-2,4-dione (**99**) (121 mg, 1.07 mmol) and propylamine (0.23 mL, 2.85 mmol, 4.0 eq.) in ethanol (3 mL) was stirred at room temperature for 18 h. The reaction mixture was concentrated under reduced pressure. The residue (503 mg) was dissolved in saturated aqueous Sodium hydrogen carbonate (20 mL) and extracted with dichloromethane (5 x 25 mL). The organic components were combined, dried over MgSO_4 , filtered and concentrated under reduced pressure. The crude product (113 mg) was washed with ethyl acetate (2 mL) to give 1-propyl-2-(4-pyridyl)-6,7-dihydro-5H-pyrrolo[3,2-c]pyridin-4-one (**122**) (33 mg, 17%). The remaining filtrate was concentrated under reduced pressure and purified by flash column chromatography (4 g silica, ethyl acetate:methanol, 1:0 to 8:2). The fractions containing the product were combined, concentrated under reduced pressure, washed with ethyl acetate (1 mL) and heated to 100 °C causing a solid to precipitate. The mixture was filtered to yield a second crop of 1-propyl-2-(4-pyridyl)-6,7-dihydro-5H-pyrrolo[3,2-c]pyridin-4-one (**122**) (5 mg, 3%).

R_f 0.71 (ethyl acetate:methanol, 1:1); m.p. 171–175 °C; ν_{max} (thin film)/ cm^{-1} 3207 (N-H, w), 2962 (C-H, w), 1655 (C=O, s), 1598 (C=N, s), 1498 (aromatic C=C, s), 1163 (C-N, m); ^1H NMR (600 MHz, $\text{DMSO}-d_6$) δ 8.58 (2H, d, $J = 5.2$ Hz, H-2' and H-6'), 7.44 (2H, d, $J = 5.2$ Hz, H-3' and H-5'), 7.09 (1H, s, H-5), 6.58 (1H, s, H-3), 4.00 (2H, t, $J = 7.4$ Hz, H-10), 3.42 (2H, td, $J = 7.0, 2.1$ Hz, H-6), 2.87 (2H, t, $J = 7.0$ Hz, H-7), 1.49 (2H, h, $J = 7.4$ Hz, H-11), 0.70 (3H, t, $J = 7.4$ Hz, H-12); ^{13}C NMR (151 MHz, $\text{DMSO}-d_6$) δ 164.7 (C-4), 150.0 (C-2' and C-6'), 139.9 (C-8), 139.8 (C-4'), 131.2 (C-2), 122.0 (C-3' and C-5'), 114.4 (C-9), 108.3 (C-3), 45.8 (C-10), 40.0 (C-6), 23.6 (C-11), 21.4 (C-7), 10.7 (C-12); HRMS m/z (ESI $^+$) [Found: 256.1446, $\text{C}_{15}\text{H}_{18}\text{N}_3\text{O}$ requires (M+H) $^+$ 256.1444]; LCMS (LCQ) Rt = 0.4 min (4 min method), m/z (ESI $^+$) 256.26 (M+H) $^+$.

1-Isopropyl-2-(4-pyridyl)-6,7-dihydro-5H-pyrrolo[3,2-c]pyridin-4-one (123)

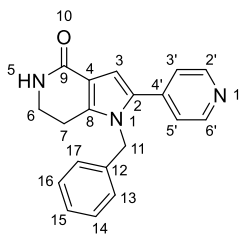
A mixture of 4-(bromoacetyl)pyridine hydrobromide (**98**) (200 mg, 0.71 mmol), piperidin-2,4-dione (**99**) (121 mg, 1.07 mmol) and isopropylamine (0.23 mL, 2.85 mmol) in ethanol (3 mL) was stirred at room temperature for 18 h. LCMS (MDAP) confirmed product formation (m/z 258). The reaction mixture was concentrated under reduced pressure and saturated aqueous sodium bicarbonate (20 mL) was added. The mixture was extracted with 2:1 chloroform:propan-2-ol (3×25 mL). The combined organic phases were dried over MgSO_4 , filtered and concentrated under reduced pressure (339 mg). The crude was purified *via* flash column chromatography (50 g silica dichloromethane:methanol, 1:0 to 9:1) to give 1-isopropyl-2-(4-pyridyl)-6,7-dihydro-5H-pyrrolo[3,2-c]pyridin-4-one (**123**) (36 mg, 19%) as a yellow solid.

R_f 0.33 (ethyl acetate:methanol, 8:2); m.p. decomposed at 266–270 °C; ν_{max} (thin film)/ cm^{-1} 3062 (N-H, w), 2347 (C-H, w), 1657 (C=O, s), 1597 (C=N, s), 1500 (aromatic C=C, s), 1165 (C-N, m); ^1H NMR (600 MHz, $\text{DMSO}-d_6$) δ 8.57 (d, $J = 6.1$ Hz, 2H, H-2' and H-6'), 7.51 (d, $J = 6.1$ Hz, 2H, H-3' and H-5'), 7.07 (s, 1H, H-5), 6.58 (s, 1H, H-3), 4.99 (t, $J = 5.3$ Hz, 1H, H-11), 4.09 (t, $J = 5.9$ Hz, 2H, H-6), 3.52 (q, $J = 5.7$ Hz, 2H, H-7), 3.41 (td, $J = 6.8, 2.5$ Hz, 3H, H-11), 2.89 (t, $J = 6.9$ Hz, 3H, H-12); ^{13}C NMR (151 MHz, $\text{DMSO}-d_6$) δ 164.5 (C-4), 149.8 (C-2' and C-6'), 140.0 (C-8), 137.8 (C-4'), 131.8 (C-2), 123.2 (C-3' and C-5'), 115.9 (C-9), 107.8 (C-3), 48.3 (C-10), 40.2 (C-6), 23.6 (C-7), 22.0 (C-11 and C-12); HRMS m/z (ESI⁺) [Found: 278.1253, $\text{C}_{15}\text{H}_{17}\text{N}_3\text{ONa}$ requires $(\text{M}+\text{Na})^+$ 278.1264]; LCMS (LCQ) $R_t = 0.4$ min (4 min method), m/z (ESI⁺) 256.24 ($\text{M}+\text{H})^+$.

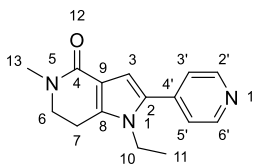
1-(2-Hydroxyethyl)-2-(4-pyridyl)-6,7-dihydro-5H-pyrrolo[3,2-c]pyridin-4-one (124)*

A mixture of 4-(bromoacetyl)pyridine hydrobromide (**98**) (100 mg, 0.36 mmol), piperidin-2,4-dion (**99**) (60 mg, 0.53 mmol) and ethanolamine (0.08 mL, 1.42 mmol) in ethanol (1.5 mL) was stirred at room temperature for 18 h. 12 M hydrochloric acid (3 drops) was added, and the reaction mixture was heated at 100 °C for 3.5 h. After cooling, the mixture was concentrated under reduced pressure. The residue (345 mg) was dissolved in saturated aqueous Sodium hydrogen carbonate (20 mL) and extracted with Dichloromethane (3 x 25 mL). The LCMS and TLC analysis of the aqueous layer indicated that a significant amount of the desired product was still present in the aqueous layer. Another extraction with a solution of 2:1 chloroform:propan-2-ol (3 x 15 mL) was performed. The organic phases were combined, dried over MgSO₄, filtered and concentrated under reduced pressure. The crude product (168 mg) was purified *via* flash column chromatography (12 g silica, dichloromethane:methanol, 1:0 to 9:1) to yield 1-(2-hydroxyethyl)-2-(4-pyridyl)-6,7-dihydro-5H-pyrrolo[3,2-c]pyridin-4-one (**124**) (32 mg, 33%) as a pale yellow solid.

R_f 0.43 (dichloromethane: methanol, 9:1); m.p. decomposed at 215–218 °C; ν_{\max} (thin film)/cm⁻¹ 3204 (O-H, br), 3044 (N-H, w), 2927 (C-H, w), 1639 (C=O, s), 1600 (C=N, s), 1501 (aromatic C=C, s), 1162 (C-N, m); ¹H NMR (400 MHz, DMSO-*d*₆) δ 8.57 (2H, d, *J* = 4.3 Hz, H-2' and H-6'), 7.53–7.48 (2H, m, H-3' and H-5'), 7.05 (1H, s, H-5), 6.58 (1H, s, H-3), 4.98 (1H, t, *J* = 5.4 Hz, H-12), 4.09 (2H, t, *J* = 5.7 Hz, H-10), 3.52 (2H, q, *J* = 5.7, 5.4 Hz, H-11), 3.41 (2H, td, *J* = 6.8, 2.5 Hz, H-6), 2.89 (2H, t, *J* = 6.8 Hz, H-7); ¹³C NMR (151 MHz, DMSO-*d*₆) δ 164.7 (C-4), 149.9 (C-2' and C-6'), 140.4 (C-8), 139.7 (C-4'), 131.5 (C-2), 122.4 (C-3' and C-5'), 114.5 (C-9), 108.2 (C-3), 60.3 (C-11), 46.9 (C-10), 40.0 (C-6), 21.7 (C-7); HRMS *m/z* (ESI⁺) [Found: 258.1241, C₁₄H₁₆N₃O₂ requires (M+H)⁺ 258.1237]; LCMS (LCQ) Rt = 0.4 min (4 min method), *m/z* (ESI⁺) 258.26 (M+H)⁺.

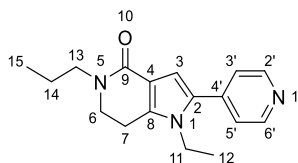


R_f 0.78 (amino silica, dichloromethane:methanol, 1:0 to 95:5); m.p. decomposed at 180–184 °C; ν_{\max} (thin film)/ cm^{-1} 3081 (N-H, w), 1647 (C=O, w), 1407 (C=C, m), 1105 (C-N, s); ^1H NMR (600 MHz, $\text{DMSO}-d_6$) δ 8.50 (d, J = 5.9 Hz, 2H, H-2' and H-6'), 7.34 (d, J = 6.0 Hz, 2H, H-3' and H-5'), 7.31 (t, J = 7.6 Hz, 2H, H-13 and H-15), 7.24 (t, J = 7.3 Hz, 1H, H-14), 7.14 (s, 1H, H-5), 6.91 (d, J = 7.4 Hz, 2H, H-12 and H-16), 6.71 (s, 1H, H-3), 5.34 (s, 2H, H-10), 3.44–3.35 (m, 2H, H-6), 2.70 (t, J = 6.8 Hz, 2H, H-7); ^{13}C NMR (151 MHz, CDCl_3) δ 166.2 (C-4), 150.3 (C-2' and C-6'), 139.7 (C-8), 139.6 (C-4'), 136.8 (C-11), 133.2 (C-2), 129.4 (C-13 and C-15), 128.1 (C-14), 125.6 (C-12 and C-16), 122.5 (C-3' and C-5'), 115.3 (C-9), 108.9 (C-3), 48.5 (C-10), 41.0 (C-6), 22.0 (C-7); HRMS m/z (ESI $^+$) [Found: 303.3630, $\text{C}_{19}\text{H}_{17}\text{N}_3\text{O}$ requires (M) $^+$ 303.3600]; LCMS (LCQ) Rt = 0.4 min (4 min method), m/z (ESI $^+$) 304.19 (M+H) $^+$.

1-Ethyl-5-methyl-2-(4-pyridyl)-6,7-dihydropyrrolo[3,2-c]pyridin-4-one (126)¹³⁷

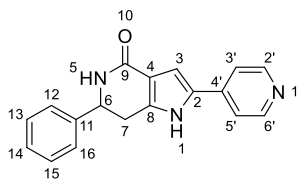
1-Ethyl-2-(4-pyridyl)-6,7-dihydro-5H-pyrrolo[3,2-c]pyridin-4-one (**121**) (100 mg, 0.41 mmol) was dissolved in *N,N*-dimethylformamide (11.5 mL), flushed with nitrogen three times and cooled to 0 °C. 60% sodium hydride (25 mg, 0.62 mmol) was added in portions at 0 °C and allowed to stir at room temperature for 15 minutes. The reaction was re-cooled to 0 °C and iodomethane (0.5 mL, 0.50 mmol) was added dropwise. The reaction mixture was stirred at room temperature overnight. LCMS indicated product formation (m/z 256). The reaction mixture was concentrated under reduced pressure and saturated aqueous sodium hydrogen carbonate (20 mL) was added. The mixture was extracted three times with 2:1 chloroform:propan-2-ol (3 × 25 mL). The combined organic phases were dried over MgSO_4 , filtered and concentrated under reduced pressure. The crude was purified *via* flash column chromatography (5 g silica, dichloromethane:methanol 1:0 to 85:15) to give 1-ethyl-5-methyl-2-(4-pyridyl)-6,7-dihydropyrrolo[3,2-c]pyridin-4-one (**126**) (24 mg, 22%) as a brown solid.

R_f 0.67 (9:1 dichloromethane:methanol); m.p. 211–213 °C; ν_{max} (thin film)/ cm^{-1} 3258 (N-H, br), 3039 (aromatic C-H, w), 2934 (aliphatic C-H, br), 2870 (C-H, br), 1632 (C=O, s), 1595 (aromatic C-H, s), 1505 (aromatic C-H, s), 1478 (aliphatic, s), 764 (N-H, s); ^1H NMR (500 MHz, $\text{DMSO}-d_6$) δ 8.58 (d, J = 5.2 Hz, 2H, H-2' and H-6'), 7.44 (d, J = 5.3 Hz, 2H, H-3' and H-5'), 6.60 (s, 1H, H-3), 4.04 (q, J = 7.2 Hz, 2H, H-11), 3.57 (t, J = 6.9 Hz, 2H, H-6), 2.98 (t, J = 6.9 Hz, 2H, H-7), 2.91 (s, 3H, H-13), 1.18 (t, J = 7.2 Hz, 3H, H-12); ^{13}C NMR (151 MHz, $\text{DMSO}-d_6$) δ 163.5 (C-9), 150.0 (C-2' and C-6'), 139.5 (C-4'), 138.6 (C-8), 131.0 (C-2), 121.9 (C-3' and 5'), 114.6 (C-4), 108.3 (C-3), 48.1 (C-6), 39.3 (C-11), 33.4 (C-13), 21.0 (C-7), 16.0 (C-12); HRMS m/z (ESI⁺) [Found: 256.1440, $\text{C}_{15}\text{H}_{18}\text{N}_3\text{O}$ requires (M+H)⁺ 256.1444]; LCMS (MDAP) R_t = 0.7 min (Ana 5-95 in 5 min), m/z (ESI⁺) 256.15 (M+H)⁺.

1-Ethyl-5-propyl-2-(4-pyridyl)-6,7-dihydropyrrolo[3,2-c]pyridin-4-one (127)

1-Ethyl-2-(4-pyridyl)-6,7-dihydro-5H-pyrrolo[3,2-c]pyridin-4-one (**121**) (100 mg, 0.41 mmol) was dissolved in *N,N*-dimethylformamide (11.5 mL), flushed with nitrogen three times and cooled to 0 °C. 60% sodium hydride (33 mg, 0.83 mmol) was added portion wise and the reaction was allowed to stir for 15 min at room temperature before being cooled to 0 °C again. 1M 1-iodopropane (0.5 mL, 0.50 mmol) in tetrahydrofuran was added dropwise and the reaction was left to stir at room temperature overnight. LCMS indicated formation of product (*m/z* 284). The reaction mixture was concentrated under reduced pressure and saturated aqueous sodium hydrogen carbonate (20 mL) was added. The mixture was extracted three times using 2:1 chloroform:propan-2-ol (4 × 25 mL). The combined organic phases were dried over MgSO₄, filtered and concentrated under reduced pressure. The crude was purified *via* flash column chromatography (5 g silica, dichloromethane:methanol 1:0 to 9:1) to give 1-ethyl-5-propyl-2-(4-pyridyl)-6,7-dihydropyrrolo[3,2-c]pyridin-4-one (**127**) (38 mg, 31%) as a yellow solid.

R_f 0.03 (9:1 dichloromethane:methanol); m.p. 139–140 °C; *v*_{max} (thin film)/cm⁻¹ 2962 (m, aliphatic C-H), 1710 (s, C=O), 1688 (s, C=C), 1644 (s, C=C), 1593 (s, aromatic C-C), 1473 (s, aliphatic C-H), 1220 (s, aliphatic C-N); ¹H NMR (600 MHz, DMSO-*d*₆) δ 8.55 (dd, *J* = 5.9, 1.6 Hz, 2H, H-2' and H-6'), 7.41 (dd, *J* = 6.0, 1.6 Hz, 2H, H-3' and H-5'), 6.56 (s, 1H, H-3), 4.01 (q, *J* = 7.2 Hz, 2H, H-11), 3.55 (t, *J* = 6.9 Hz, 2H, H-6), 3.32 (t, *J* = 6.6 Hz, 2H, H-14), 2.93 (t, *J* = 6.9 Hz, 2H, H-7), 1.49 (t, *J* = 7.3 Hz, 2H, H-13), 1.16 (t, *J* = 7.2 Hz, 3H, H-12), 0.83 (t, *J* = 7.4 Hz, 3H, H-15); ¹³C NMR (151 MHz, DMSO-*d*₆) δ 162.8 (C-4), 150.0 (C-2' and C-6'), 139.5 (C-4'), 138.5 (C-8), 131.0 (C-2), 121.9 (C-3' and C-5'), 114.9 (C-9), 108.4 (C-3), 46.8 (C-13), 46.1 (C-6), 39.2 (C-12), 21.2 (C-7), 20.6 (C-14), 16.0 (C-11), 11.3 (C-15); HRMS *m/z* (ESI⁺) [Found: 284.1758, C₁₇H₂₂N₃O requires (M+H)⁺ 284.1757]; LCMS (MDAP) *R_t* = 1.8 min (Ana 5-95 over 5 minutes), *m/z* (ESI⁺) 284.00 (M+H)⁺.

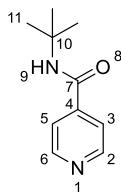
6-Phenyl-2-(4-pyridyl)-1,5,6,7-tetrahydropyrrolo[3,2-c]pyridin-4-one (139)

6-Phenylpiperidine-2,4-dione (**138**) (202 mg, 1.07 mmol), 2-bromo-1-(4-pyridyl)ethanone hydrobromide (**98**) (300 mg, 1.07 mmol) and ammonium acetate (329 mg, 4.27 mmol) were stirred in ethanol (4.5 mL) at room temperature overnight. LCMS (MDAP) indicated product formation (m/z 290). The reaction mixture was concentrated under reduced pressure and saturated aqueous sodium hydrogen carbonate (30 mL) was added. The mixture was extracted three times with 2:1 chloroform:propan-2-ol (3 \times 40 mL). The combined organic phases were dried over MgSO_4 , filtered and concentrated under reduced pressure to give a red oil (320 mg). The crude was purified *via* flash column chromatography (20 g silica, dichloromethane:methanol, 1:0 to 9:1) to give an off-white solid (102 mg). This was purified *via* SCX cartridge by elution with methanol and 2 M ammonia in methanol to give 6-phenyl-2-(4-pyridyl)-1,5,6,7-tetrahydropyrrolo[3,2-c]pyridin-4-one (**139**) (74 mg, 23%) as a pale yellow solid.

R_f 0.02 (9:1 dichloromethane:methanol); m.p. 259–260 °C; ν_{max} (thin film)/ cm^{-1} 3388 (N-H, br), 3226 (N-H, br), 3014 (aromatic C-H, w), 2979 (aliphatic C-H, w), 1690 (C=O, s), 1524 (aromatic C-H, s), 766 (N-H, s); ^1H NMR (600 MHz, $\text{DMSO}-d_6$) δ 11.87 (s, 1H, H-1), 8.50–8.44 (m, 2H, H-2' and H-6'), 7.60–7.55 (m, 2H, H-3' and H-5'), 7.42 (d, J = 1.8 Hz, 1H, H-5), 7.38 (d, J = 7.7 Hz, 2H, H-12 and H-16), 7.34 (t, J = 7.6 Hz, 2H, H-13 and H-15), 7.26 (t, J = 7.2 Hz, 1H, H-14), 7.05 (d, J = 2.4 Hz, 1H, H-3), 4.86 (td, J = 7.1, 2.0 Hz, 1H, H-6), 3.26 (dd, J = 16.2, 6.1 Hz, 1H, H-7), 2.98 (dd, J = 16.2, 7.2 Hz, 1H, H-7); ^{13}C NMR (151 MHz, $\text{DMSO}-d_6$) δ 164.8 (C-9), 149.9 (C-2' and C-6'), 142.9 (C-11), 138.8 (C-4'), 137.2 (C-8), 128.7 (C-4), 128.3 (C-13 and C-15), 127.3 (C-14), 126.4 (C-12 and C-16), 117.5 (C-3' and C-5'), 115.5 (C-2), 106.4 (C-3), 54.9 (C-6), 30.2 (C-7); HRMS m/z (ESI⁺) [Found: 290.1295, $\text{C}_{18}\text{H}_{16}\text{N}_3\text{O}$ requires (M+H)⁺ 290.1288]; LCMS (MDAP) R_t = 3.4 min (Ana 30–90 in 20 min), m/z (ESI⁺) 290.1 (M+H)⁺.

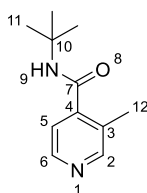
6.1.3 Preparation of compounds described in Chapter 4

*N-Tert-Butylpyridine-4-carboxamide (152)*¹⁰⁶



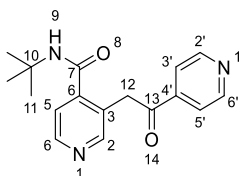
Isonicotinic acid (**23**) (5.00 g, 40.61 mmol) in dichloromethane (150 mL) was cooled to 0 °C. Triethylamine (9.06 mL, 64.98 mmol) was added dropwise maintaining the temperature between 0–5 °C. Ethyl chloroformate (**151**) (4.60 mL, 48.74 mmol) was added dropwise maintaining the temperature between 0–5 °C and then the reaction was stirred for 30 minutes at 0–5 °C. *Tert*-butylamine (5.12 mL, 48.74 mmol) was added dropwise to the reaction maintaining the temperature between 0–5 °C and then the reaction was allowed to warm up to room temperature and stirred for 3.5 hours. Water (50 mL) was added to the reaction mixture and the two resulting phases were separated. The organic phase was washed with 1 M aqueous hydrochloric acid (50 mL) and basified to pH 9 using 3.75 M aqueous sodium hydroxide (15 mL). The aqueous phase was washed twice with ethyl acetate (2 × 50 mL). The organic phases were combined, dried over MgSO₄, filtered and concentrated under reduced pressure to give *N-tert*-butylpyridine-4-carboxamide (**152**) (5.18 g, 68%) as an off-white solid.

¹H NMR (500 MHz, CDCl₃) δ 8.70 (d, *J* = 5.4 Hz, 2H, H-3 and H-5), 7.55 (d, *J* = 5.7 Hz, 2H, H-2 and H-6), 6.09 (s, 1H, H-9), 1.47 (s, 9H, 9 × H-11); LCMS (LCQ) Rt = 0.8 min (7 min method), *m/z* (APCI⁺) 179.1 (M+H)⁺.

N-Tert-Butyl-3-methyl-pyridine-4-carboxamide (156)¹⁰⁶

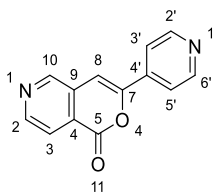
Tetrahydrofuran (250 mL) was added to *N-tert*-butylpyridine-4-carboxamide (**152**) (9.5 g, 53.3 mmol). The suspension was cooled down to -75 °C. 2 M *n*-butyl lithium (47 mL, 117.26 mmol) in hexanes was added maintaining temperature below -60 °C and the reaction was stirred for 30 min. Iodomethane (3.65 mL, 58.63 mmol) was added maintaining temperature below -60 °C. The reaction was stirred at -75 °C for 1 h. It was then allowed to warm up to room temperature and stirred overnight. The reaction mixture was quenched by addition of aqueous saturated ammonium chloride (70 mL). The reaction mixture was diluted with water (130 mL) and ethyl acetate (130 mL). The organic layer was separated, and the aqueous layer was extracted with ethyl acetate (130 mL). The combined organic phases were washed with brine (130 mL), dried over MgSO₄, filtered and concentrated under reduced pressure to give a pale orange crude solid (11.89 g). The residue was purified in two batches (*ca.* 5–6 g per column) using flash column chromatography (2 × 100 g silica, petroleum ether:ethyl acetate 20:80 to 100:00) and combined to give a 1:10 mixture (by ¹H NMR) of starting material and *N-tert*-butyl-3-methyl-pyridine-4-carboxamide (**156**) (9.90 g, 87%) as a white solid. The product was taken forward without further purification.

¹H NMR (500 MHz, CDCl₃) δ 8.38–8.30 (m, 2H, H-2 and H-6), 7.11 (d, *J* = 3.9 Hz, 1H, H-5), 5.97 (s, 1H, H-9), 2.33 (s, 3H, 3 × H-12), 1.43 (s, 9H, 9 × H-11); LCMS (MDAP) Rt = 8.5 min (Ana 5-95, 20 min method), *m/z* (ESI⁺) 193.1 (M+H)⁺.

N-Tert-Butyl-3-[2-oxo-2-(4-pyridyl)ethyl]pyridine-4-carboxamide (162)¹⁰⁶

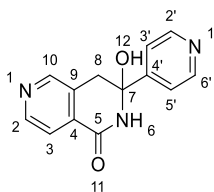
2 M *n*-butyl lithium (16 mL, 38.78 mmol) in hexanes was added to *N-tert*-butyl-3-methylpyridine-4-carboxamide (**156**) (3.55 g, 18.46 mmol) in THF (85 mL) at -45 °C (CO₂/acetonitrile bath). The resulting red reaction mixture was stirred for 1 h at -45 °C. Ethyl isonicotinate (**161**) (3.10 mL, 20.31 mmol) was added in one portion. The reaction mixture was stirred at room temperature for 2 h, upon which a mustard yellow suspension formed. TLC showed consumption of starting material (100% ethyl acetate, UV). Saturated aqueous ammonium chloride solution (50 mL) was added to quench the reaction. Ethyl acetate (85 mL) was added and a white solid precipitated out (thought to be ammonium chloride) into the separation funnel. Water (40 mL) was added which dissolved this solid. The organic and aqueous phases were separated, and the aqueous layer was washed three times with ethyl acetate (3 × 85 mL). The combined organic phases were dried over MgSO₄, filtered and concentrated under reduced pressure to give a yellow crude oil (7.05 g). The crude was purified by flash column chromatography (100 g silica, ethyl acetate:methanol, 100:0 to 90:10) to give *N-tert*-butyl-3-[2-oxo-2-(4-pyridyl)ethyl]pyridine-4-carboxamide (**162**) (2.12g, 37%) as a pale yellow foam.

¹H NMR (500 MHz, DMSO-*d*₆) δ 8.84 (m, 2H, H-2'and H-6'), 8.59–8.48 (m, 2H, H-5 and H-2), 8.14 (s, 1H, H-9), 7.91–7.83 (m, 2H, H-3'and H-5'), 7.39 (d, *J* = 4.8 Hz, 1H, H-6), 4.64 (s, 2H, H-12), 1.21 (s, 9H, 9 × H-11); LCMS (LCQ) Rt = 0.8 min (4 min method), *m/z* (APCI⁺) 298.1 (M+H)⁺.

3-(4-Pyridyl)pyrano[4,3-c]pyridin-1-one (166)¹⁰⁶

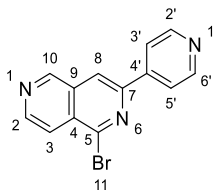
N-Tert-Butyl-3-[2-oxo-2-(4-pyridyl)ethyl]pyridine-4-carboxamide (**162**) (1.82 g, 6.12 mmol) in *N,N*-dimethylformamide (3.5 mL) was heated in a microwave at 220 °C for 2 × 10 minutes. Upon cooling, a solid precipitated out of the clear brown solution. 3-(4-Pyridyl)pyrano[4,3-c]pyridin-1-one (**166**) (695 mg, 48%) was isolated by filtration as a pale pink crystalline solid.

¹H NMR (500 MHz, DMSO-*d*₆) δ 9.09 (s, 1H, H-10), 8.83 (d, *J* = 5.1 Hz, 1H, H-2), 8.78–8.70 (m, 2H, H-2' and H-6'), 8.03 (d, *J* = 5.1 Hz, 1H, H-3), 7.91–7.74 (m, 3H, H-8, H-3' and H-5'); LCMS (LCQ) *R*_t = 0.7 min (4 min method), *m/z* (APCI⁺) 225.3 (M+H)⁺.

3-Hydroxy-3-(4-pyridyl)-2,4-dihydro-2,6-naphthyridin-1-one (167)¹⁰⁶

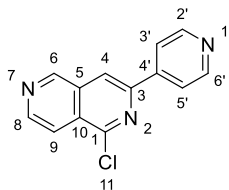
3-(4-Pyridyl)pyrano[4,3-c]pyridin-1-one (**166**) (666 mg, 2.97 mmol) in 2 M ammonia (20 mL, 40 mmol) isopropanol solution was stirred for 2 h at room temperature during which a pale yellow suspension formed. The reaction mixture was concentrated under reduced pressure to give 3-hydroxy-3-(4-pyridyl)-2,4-dihydro-2,6-naphthyridin-1-one (**167**) (626 mg, 83%) as a white solid.

¹H NMR (500 MHz, DMSO-*d*₆) δ 9.16 (s, 1H, H-6), 8.66 (d, *J* = 4.9 Hz, 1H, H-2), 8.64–8.58 (m, 3H, H-2', H-6' and H-10), 7.79 (d, *J* = 4.9 Hz, 1H, H-3), 7.60 (d, *J* = 5.9 Hz, 2H, H-3' and H-5'), 6.77 (s, 1H, H-12), 3.37, 3.13 (ABq, *J* = 12.5 Hz, 2H, 2 × H-8); LCMS (LCQ) Rt = 0.6 min (4 min method), *m/z* (APCI⁺) 242.2 (M+H)⁺.

1-Bromo-3-(4-pyridyl)-2,6-naphthyridine (173)¹⁰⁶

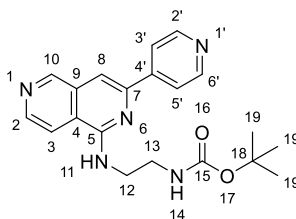
3-(4-Pyridyl)-dihydro-2,6-naphthyridin-1-one (**167**) (57 mg, 0.26 mmol) and phosphorus(V) oxybromide (183.0 mg, 0.64 mmol) were mixed and heated to 130 °C for 6 h. A yellow solid formed. The reaction mixture was cooled to room temperature and ice was added to quench the reaction. An orange solid formed. The pH was adjusted to pH 8–9 with saturated aqueous Na₂CO₃. The resulting precipitate was filtered, washed with water and dried in a vacuum oven to give 1-bromo-3-(4-pyridyl)-2,6-naphthyridine (**173**) (56 mg, 61%) as a brown solid. As per procedure, the crude was not further purified before the next reaction step.

¹H NMR (500 MHz, DMSO-d₆) δ 9.55 (s, 1H, H-10), 8.95 (s, 1H, H-8), 8.90 (d, *J* = 5.8 Hz, 1H, H-2), 8.79 (d, *J* = 5.9 Hz, 2H, H-2' and H-6'), 8.16–8.13 (m, 2H, H-3' and H-5'), 8.06 (d, *J* = 5.8 Hz, 1H, H-3); LCMS (LCQ) Rt = 0.6 min (4 min method), *m/z* (APCI⁺) 286.3 [⁷⁹Br] and 288.2 [⁸¹Br] (M+H)⁺.

1-Chloro-3-(4-pyridyl)-2,6-naphthyridine (174)¹⁰⁶

3-Hydroxy-3-(4-pyridyl)-2,4-dihydro-2,6-naphthyridin-1-one (**167**) (1.55 g, 6.42 mmol) and phosphorus(V) oxychloride (14 mL, 149.8 mmol) were mixed and heated to 80 °C for 24 h. A green-blue suspension formed. LCMS showed a mixture of mass ions corresponding to the product and the hydrolysed by-product. The reaction was heated for a further 24 h at 80 °C. The reaction mixture was concentrated under reduced pressure and warm water (50 mL at 30 °C) was added. A green/blue solution formed. NaHCO₃ was added which caused an effervescent reaction and a blue-grey gum formed. Water (100 mL) and dichloromethane (150 mL) were added and the resulting mixture was filtered. The two phases of the filtrate were separated, and the aqueous phase was extracted with more dichloromethane (50 mL). The gum that was isolated by filtration was stirred in dichloromethane (50 mL) for 10 minutes and then filtered. The combined organic phases were dried over MgSO₄, filtered and concentrated under reduced pressure to give an off-white solid crude (548 mg). The crude product was purified by flash column chromatography (12 g silica, 100:0 to 95:5) to give 1-chloro-3-(4-pyridyl)-2,6-naphthyridine (**174**) (484 mg, 30%) as an off-white solid.

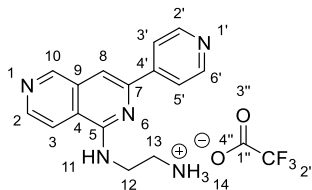
¹H NMR (500 MHz, DMSO-*d*₆) δ 9.54 (s, 1H, H-6), 8.89–8.83 (m, 2H, H-4 and H-8), 8.78–8.71 (m, 2H, H-2' and H-6'), 8.13–8.05 (m, 3H, H-9, H-3' and H-5'). LCMS (LCQ) Rt = 0.6 min (4 min method), *m/z* (ESI⁺) 242.4 [³⁵Cl] and 244.6 [³⁷Cl] (M+H)⁺.

***Tert*-Butyl-*N*-[2-[[3-(4-pyridyl)-2,6-naphthyridin-1-yl]amino]ethyl]carbamate (**183**)¹⁰⁶**

1-Bromo-3-(4-pyridyl)-2,6-naphthyridine (**173**) (45 mg, 0.16 mmol), *tert*-butyl-*N*-(2-aminoethyl)-carbamate (**182**) (37.8 mg, 0.24 mmol) and 2 M sodium hydroxide aqueous solution (1.1 mL, 2.25 mmol) in 1,4-dioxane (7 mL) was heated to 110 °C for 16 h. The reaction mixture was diluted with water (10 mL) and extracted with ethyl acetate (2 × 10 mL). The combined organic phases were dried over MgSO₄, filtered and concentrated under reduced pressure to give a yellow oil crude (198 mg). The crude was purified by flash column chromatography (4 g silica, ethyl acetate:methanol, 100:0 to 90:10) to give *tert*-butyl-*N*-[2-[[3-(4-pyridyl)-2,6-naphthyridin-1-yl]amino]ethyl]carbamate (**183**) (11 mg, 18%) as a pale yellow solid.

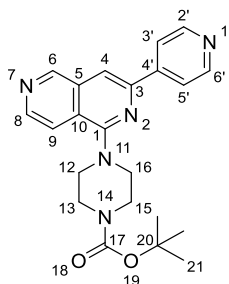
¹H NMR (500 MHz, DMSO-*d*₆) δ 9.22 (s, 1H, H-8), 8.69–8.64 (d, 2H, H-3' and H-5'), 8.62 (d, *J* = 5.7 Hz, 1H, H-3), 8.17 (d, *J* = 4.9 Hz, 2H, H-2' and H-6'), 8.10 (d, *J* = 5.8 Hz, 1H, H-2), 7.97 (t, *J* = 4.9 Hz, 1H, H-14), 7.87 (s, 1H, H-10), 7.06 (t, *J* = 5.9 Hz, 1H, H-12), 3.66 (q, *J* = 5.8 Hz, 4H, 2 × H-12 and 2 × H-13), 1.37 (s, 9H, 9 × H-19); LCMS (LCQ) Rt = 0.8 min (4 min method), *m/z* (APCI⁺) 365.8 (M+H)⁺ and 310.2 (M+H-*t*-Bu)⁺.

2-[[3-(4-Pyridyl)-2,6-naphthyridin-1-yl]amino]ethylammonium;2,2,2-trifluoroacetate
(12)^{106,161,176}



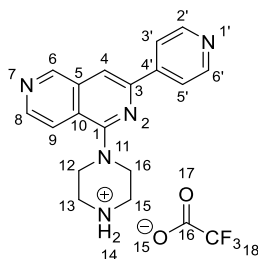
Tert-Butyl-*N*-[2-[[3-(4-pyridyl)-2,6-naphthyridin-1-yl]amino]ethyl]carbamate (**183**) (11 mg, 0.03 mmol) was stirred in trifluoroacetic acid (0.1 mL, 1.31 mmol) and dichloromethane (2.75 mL) for 10 min at 0 °C then at room temperature for 4 h. The reaction mixture was concentrated under reduced pressure to give 2-[[3-(4-pyridyl)-2,6-naphthyridin-1-yl]amino]ethylammonium;2,2,2-trifluoroacetate (**12**) (12 mg, 95%) as a yellow solid.

R_f 0.55 (1:9 methanol:dichloromethane); 180–m.p. 183 °C; ν_{\max} (thin film)/cm⁻¹ 2922 (C-H alkane, m), 2852 (C-H alkane, m), 1673 (C=C, s), 1634 (N-H, s), 1585 (N-H, m), 1540 (C-C, m), 1499 (C-H, m), 1178 (C-N, s), 1123 (C-N, s), 796 (N-H, s); ¹H NMR (500 MHz, DMSO-*d*₆) δ 9.30 (s, 1H, H-10), 8.85 (s, 2H, H-2' and H-6'), 8.73 (d, *J* = 5.8 Hz, 1H, H-2), 8.47 (d, *J* = 3.6 Hz, 2H, H-3' and H-5'), 8.19–8.09 (m, 2H, H-3 and H-8), 7.89 (s, 2H, H-14), 3.93–3.85 (m, 2H, H-12), 3.26–3.17 (m, 2H, 2 × H-13); ¹³C NMR (151 MHz, DMSO-*d*₆) δ 154.4 (C-1), 151.7 (C-6), 150.2 (C-2' and C-6'), 146.7 (C-3), 145.9 (C-4'), 144.6 (C-9), 131.9 (C-10), 121.3 (C-5), 120.5 (C-3' and C-5'), 116.1 (C-8), 105.3 (C-4), 38.9 (C-12), 38.0 (C-13); HRMS *m/z* (ESI⁺) [Found: 266.1397, C₁₅H₁₅N₅ requires (M+H)⁺ 266.1400]; LCMS (LCQ) *R*_t = 0.6 min (4 method), *m/z* (APCI⁺) 266.2 (M+H)⁺.

***Tert*-Butyl 4-[3-(4-pyridyl)-2,6-naphthyridin-1-yl]piperazine-1-carboxylate (**186**)¹⁰⁶**

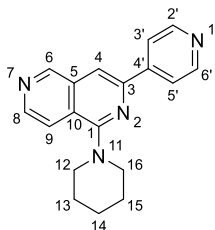
1-Boc-Piperazine (**185**) (154 mg, 0.83 mmol) and potassium carbonate (109 mg, 0.79 mmol) were added to a solution of 1-chloro-3-(4-pyridyl)-2,6-naphthyridine (**174**) (100 mg, 0.39 mmol) in *N,N*-dimethylformamide (1 mL) at room temperature. The reaction mixture was heated to 90 °C and stirred for 5 h. LCQ (LCMS) confirmed formation of the product (*m/z* 392). The reaction mixture was cooled to room temperature. Ethyl acetate (5 mL) and water (5 mL) were added and the two resulting phases were separated. The aqueous layer was extracted three times with ethyl acetate (3 × 5 mL) and the combined organic phases were dried over MgSO₄, filtered and concentrated under reduced pressure to give a solid crude residue (136 mg). The crude was purified by flash column chromatography (11 g silica, petroleum ether:ethyl acetate, 1:0 to 0:1) to give *tert*-butyl 4-[3-(4-pyridyl)-2,6-naphthyridin-1-yl]piperazine-1-carboxylate (**186**) (97 mg, 60%) as an off-white solid.

¹H NMR (500 MHz, DMSO-*d*₆) δ 9.40 (s, 1H, H-6), 8.72 (d, *J* = 5.1 Hz, 2H, H-2' and H-6'), 8.67 (d, *J* = 5.7 Hz, 1H, H-8), 8.35 (s, 1H, H-4), 8.16 (d, *J* = 5.1 Hz, 2H, H-3' and H-5'), 7.95 (d, *J* = 5.8 Hz, 1H, H-9), 3.63 (s, 4H, H-13 and H-15), 3.50 (s, 4H, H-12 and H-16), 1.44 (s, 9H, H-21).); LCMS (LCQ) *R*_t = 0.8 min (4 min method), *m/z* (APCI)⁺ 392.1 (M+H)⁺, 336.1 (M+H-*t*-Bu)⁺, 292.2 (M+H-Boc)⁺.

1-Piperazin-4-ium-1-yl-3-(4-pyridyl)-2,6-naphthyridine; 2,2,2-trifluoroacetate (187)^{106,161}

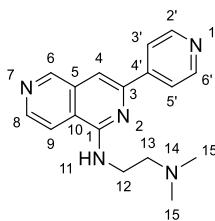
tert-Butyl 4-[3-(4-pyridyl)-2,6-naphthyridin-1-yl]piperazine-1-carboxylate (**186**) (102 mg, 0.26 mmol) was dissolved in TFA (1.0 mL, 13.06 mmol) and dichloromethane (1 mL) and stirred for 1 h at room temperature. The reaction mixture was concentrated under reduced pressure to give a crude yellow oil (239 mg). On addition of methanol (1 mL), a precipitate formed which was found to be 1-piperazin-4-ium-1-yl-3-(4-pyridyl)-2,6-naphthyridine; 2,2,2-trifluoroacetate (**187**) (17 mg, 15%) as a yellow solid.

R_f 0.73 (9:1 ethyl acetate:methanol); m.p. 253–254 °C (from methanol); ν_{\max} (thin film)/ cm^{-1} 3009 (N-H, br), 2491 (C=C, w), 1634 (C=O, s), 1505 (C-H, m), 1175 (C-N, s), 1120 (C-N, s); ^1H NMR (500 MHz, $\text{DMSO}-d_6$) δ 9.46 (s, 1H, H-6), 9.09 (s, 1H, H-14), 8.88 (d, J = 5.4 Hz, 2H, H-2' and H-6'), 8.74 (d, J = 5.7 Hz, 1H, H-9), 8.58 (s, 1H, H-4), 8.43 (d, J = 5.0 Hz, 2H, H-3' and H-5'), 8.06 (d, J = 5.7 Hz, 1H, H-8), 3.75 (s, 4H, H-12), 3.43 (s, 4H, H-13); ^{13}C NMR (126 MHz, $\text{DMSO}-d_6$) δ 159.0 (C-1), 153.4 (C-6), 147.7 (C-2' and C-6'), 145.9 (C-9), 145.1 (C-4'), 133.3 (C-10), 124.0 (C-5), 122.0 (C-3' and C-5'), 118.2 (C-8), 113.4 (C-4), 47.7 (C-12 and 16), 43.2 (C-13 and 15).; HRMS m/z (ESI⁺) [Found: 292.1548, $\text{C}_{17}\text{H}_{17}\text{N}_5$ requires (M+H)⁺ 292.1557]; LCMS (MDAP) Rt = 4.5 min (30 min method), m/z (ESI⁺) 292.2 (M+H)⁺.

1-(1-Piperidyl)-3-(4-pyridyl)-2,6-naphthyridine (189)

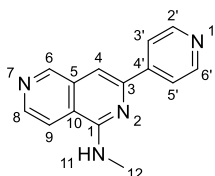
Triethylamine (0.09 mL, 0.63 mmol) was added to 1-chloro-3-(4-pyridyl)-2,6-naphthyridine (**174**) (50 mg, 0.20 mmol) in ethanol (0.60 mL) at room temperature. The reaction vessel was flushed with nitrogen gas, sealed and then piperidine (0.02 mL, 0.25 mmol) was added at room temperature. The reaction was heated to 80 °C and stirred overnight. LCMS (LCQ) confirmed formation of the product (m/z 291). The resulting red solution was concentrated under reduced pressure to give an orange solid (86 mg). Dichloromethane (10 mL) and water (10 mL) were added and the phases separated. The aqueous layer was extracted three times with dichloromethane (3 × 10 mL). The organic phases were combined, dried over MgSO_4 , filtered and concentrated under reduced pressure to give a dark red heterogeneous solid (53 mg). ^1H NMR showed a mixture of product and unreacted piperidine so the solid was dissolved in methanol (10 mL) and concentrated under reduced pressure. Toluene (10 mL) was added and the solution was concentrated under reduced pressure. The co-evaporation with toluene (10 mL) was repeated resulting in an orange solid (43 mg). Dichloromethane (5 mL) and saturated aqueous NaHCO_3 solution (5 mL) were added and the resulting phases separated. The organic phase was dried over MgSO_4 , filtered and concentrated under reduced pressure. The crude was purified by flash column chromatography (12 g silica, petroleum ether:ethyl acetate, 1:0 to 0:1) to give 1-(1-piperidyl)-3-(4-pyridyl)-2,6-naphthyridine (**189**) (12 mg, 20%) as an off-white solid.

R_f 0.70 (9:1 ethyl acetate:methanol); m.p. 150–151 °C; ν_{max} (thin film)/ cm^{-1} 3029 (aromatic C-H, w), 2936 (aliphatic C-H, m), 2853 (aliphatic C-H, w), 2820 (aliphatic C-H, w), 1600 (aromatic C-C, m), 1558 (aromatic C-C, m), 1484 (aliphatic C-H, m), 1416 (aliphatic C-H, s), 1255 (aliphatic C-N, m), 680 (alkene C-H, s); ^1H NMR (500 MHz, $\text{DMSO}-d_6$) δ 9.35 (s, 1H, H-6), 8.70 (d, J = 4.6 Hz, 2H, H-2' and H-6'), 8.64 (d, J = 5.4 Hz, 1H, H-8), 8.24 (s, 1H, H-4), 8.12 (d, J = 4.7 Hz, 2H, H-3' and H-5'), 7.83 (d, J = 5.6 Hz, 1H, H-9), 3.48 (s, 4H, H-12 and H-16), 1.78 (s, 4H, H-13 and 15), 1.72–1.61 (m, 2H, H-14); ^{13}C NMR (126 MHz, $\text{DMSO}-d_6$) δ 159. (C-1), 152.6 (C-6), 150.3 (C-2' and C-6'), 146.0 (C-3), 145.5 (C-4'), 144.5 (C-8), 133.1 (C-5), 123.3 (C-10), 120.4 (C-3' and C-5'), 117.8 (C-9), 109.8 (C-4), 51.5 (C-12), 25.5 (C-13), 24.2 (C-14); HRMS m/z (ESI⁺) [Found: 291.1614, $\text{C}_{18}\text{H}_{19}\text{N}_4$ requires (M+H)⁺ 291.1604]; LCMS (LCQ) R_t = 1.2 min (4 min method), m/z (ESI⁺) 291.3 (M+H)⁺.

***N,N'*-Dimethyl-*N*-[3-(4-pyridyl)-2,6-naphthyridin-1-yl]ethane-1,2-diamine (**191**)**

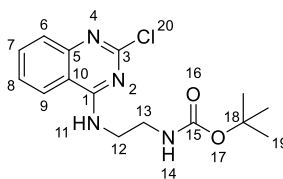
Triethylamine (0.28 mL, 2.01 mmol) and *N,N*-dimethylethylenediamine (**190**) (0.09 mL, 0.79 mmol) were added to 1-chloro-3-(4-pyridyl)-2,6-naphthyridine (**174**) (160 mg, 0.63 mmol) in ethanol (1 mL) at room temperature. The reaction was heated to 120 °C and left to stir overnight. TLC and LCMS (LCQ) showed full consumption of starting material. The reaction mixture was concentrated under reduced pressure and toluene (10 mL) was added before the reaction mixture was again concentrated under reduced pressure. This was repeated with a second portion of toluene (10 mL) to aid removal of excess *N,N*-dimethylethylenediamine (**190**). Dichloromethane (10 mL) and water (10 mL) were added to the residue and the phases separated. The aqueous phase was washed three times with dichloromethane (3 × 10 mL). The combined organic phases were dried over MgSO₄, filtered and concentrated under reduced pressure to give a crude residue (204 mg). ¹H NMR of the crude showed the product still contained excess amine. 1 M aqueous hydrochloric acid (5 mL) and ethyl acetate (5 mL) were added to the crude and the resulting phases separated. The pH was adjusted to pH 10 using saturated NaCO₃ aqueous solution (ca. 35 mL). Ethyl acetate (40 mL) was added and the resulting phases were separated. The organic phase was dried over MgSO₄, filtered and concentrated under reduced pressure to give *N,N'*-dimethyl-*N*-[3-(4-pyridyl)-2,6-naphthyridin-1-yl]ethane-1,2-diamine (**191**) (119 mg, 61%) as an off-white solid.

R_f 0.72 (9:1 ethyl acetate:methanol); m.p. 244–246 °C; ν_{max} (thin film)/cm⁻¹ 3256 (N-H, m), 3066 (aromatic C-H, w), 2977 (aliphatic C-H, w), 2766 (C-H, m), 1603 (N-H, m), 1543 (aromatic C-C, s), 684 (N-H, s); ¹H NMR (500 MHz, DMSO-*d*₆) δ 9.21 (s, 1H, H-6), 8.68 (d, *J* = 5.9 Hz, 2H, H-2' and H-6'), 8.61 (d, *J* = 5.7 Hz, 1H, H-8), 8.15–8.07 (m, 3H, H-9, H-3' and H-5'), 7.87 (t, *J* = 5.2 Hz, 1H, H-11), 7.84 (s, 1H, H-4), 3.73 (q, *J* = 6.5 Hz, 2H, H-12), 2.60 (t, *J* = 6.9 Hz, 2H, H-13), 2.24 (s, 6H, H-15); ¹³C NMR (126 MHz, DMSO-*d*₆) δ 154.3 (C-1), 151.7 (C-6), 150.2 (C-2' and C-6'), 146.9 (C-5), 146.2 (C-4'), 144.5 (C-8), 132.0 (C-3), 121.1 (C-10), 120.4 (C-3' and C-5'), 115.8 (C-9), 104.5 (C-4), 57.7 (C-13), 45.5 (C-15). C-12 peak under DMSO peak. HRMS *m/z* (ESI⁺) [Found: 294.1722, C₁₇H₂₀N₅ requires (M+H)⁺ 294.1713]; LCMS (LCQ) Rt = 0.4 min (4 min method), *m/z* (ESI⁺) 294.1 (M+H)⁺.

***N*-Methyl-3-(4-pyridyl)-2,6-naphthyridin-1-amine (193)**

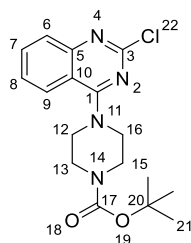
Methylamine (0.16 mL, 0.31 mmol) and triethylamine (0.14 mL, 1.01 mmol) were added to 1-chloro-3-(4-pyridyl)-2,6-naphthyridine (**174**) (80 mg, 0.31 mmol) in ethanol (1 mL) at room temperature. The reaction was heated to 120 °C and left to stir overnight. After 24 h TLC and LCMS (LCQ) showed a mixture of starting material and product so additional portions of methylamine (0.16 mL, 0.31 mmol) and triethylamine (0.14 mL, 1.01 mmol) were added. The reaction was left to stir for an additional 24 h at 120 °C, after which TLC and LCMS (LCQ) (m/z 237) confirmed complete conversion. The reaction mixture was concentrated under reduced pressure and dichloromethane (10 mL) and water (10 mL) were added. A yellow suspension formed. The mixture was concentrated under reduced pressure to remove the dichloromethane and ethyl acetate (10 mL) was added but again, the solid did not fully dissolve. The mixture was filtered, and the isolated yellow solid was found to be *N*-methyl-3-(4-pyridyl)-2,6-naphthyridin-1-amine (**193**) (30 mg, 38%).

R_f 0.65 (9:1 ethyl acetate:methanol); m.p. 260–261 °C; ν_{\max} (thin film)/cm⁻¹ 3316 (N-H, b), 2937 (aliphatic C-H, m), 1588 (N-H, s), 683 (C-H, s); ¹H NMR (500 MHz, DMSO-*d*₆) δ 9.21 (s, 1H, H-6), 8.68 (d, J = 4.5 Hz, 2H, H-2' and H-6'), 8.61 (d, J = 5.5 Hz, 1H, H-6), 8.14 (d, J = 4.6 Hz, 2H, H-3' and H-5'), 8.08 (d, J = 5.6 Hz, 1H, H-8), 8.00–7.93 (m, 1H, H-11), 7.84 (s, 1H, H-4), 3.11 (d, J = 3.5 Hz, 3H, H-12); ¹³C NMR (126 MHz, DMSO-*d*₆) δ 155.3 (C-1), 152.0 (C-6), 150.5 (C-2' and C-6'), 147.4 (C-4'), 146.7 (C-3), 145.0 (C-8), 132.3 (C-5), 121.7 (C-10), 120.9 (C-3' and C-5'), 116.1 (C-9), 104.8 (C-4), 28.4 (C-12); HRMS m/z (ESI⁺) [Found: 237.1141, C₁₄H₁₃N₄ requires (M+H)⁺ 237.1135]; LCMS (LCQ) R_t = 0.5 min (4 min method), m/z (ESI⁺) 237.3 (M+H)⁺.¹⁷⁷

***Tert*-Butyl *N*-[2-[(2-chloroquinazolin-4-yl)amino]ethyl]carbamate (**198**)**

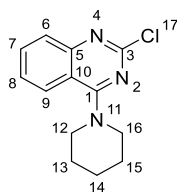
2,4-Dichloroquinazoline (**194**) (1 g, 5.02 mmol), triethylamine (1.1 mL, 7.54 mmol) and neat *tert*-butyl *N*-(2-aminoethyl)carbamate (2.4 mL, 15.07 mmol) were stirred in tetrahydrofuran (10 mL) at 0 °C for 1 h in a water/ice bath. LCMS confirmed starting material consumption and formation of product (m/z 323, 325, 267 and 269). The reaction mixture was concentrated to give a yellow oil (3.99 g). The residue was purified *via* flash chromatography (80 g silica, petroleum ether:ethyl acetate, 1:0 to 0:1) to give *tert*-butyl *N*-[2-[(2-chloroquinazolin-4-yl)amino]ethyl]carbamate (**198**) (1.50 g, 88%) as a clear colourless oil.

^1H NMR (600 MHz, $\text{DMSO-}d_6$) δ 8.77–8.68 (m, 1H, H-14), 8.23 (d, J = 8.5 Hz, 1H, H-9), 7.79 (t, J = 7.9 Hz, 1H, H-7), 7.61 (d, J = 8.6 Hz, 1H, H-6), 7.53 (t, J = 7.5 Hz, 1H, H-8), 7.03–6.94 (m, 1H, H-11), 3.58–3.51 (m, 2H, H-13), 3.24 (q, J = 6.0 Hz, 2H, H-12), 1.35 (s, 9H, H-19); LCMS (LCQ) R_t = 2.5 min (4 min method), m/z (ESI $^+$) 322.96 [^{35}Cl], 324.96 [^{37}Cl] ($\text{M}+\text{H}$) $^+$, 267.1 [^{35}Cl] and 269.1 [^{37}Cl] ($\text{M-t-Bu}+\text{H}$) $^+$.

4-(2-Chloroquinazolin-4-yl)piperazine-1-carboxylate (199)^{178–180}

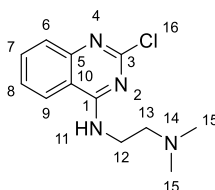
2,4-Dichloroquinazoline (**194**) (400 mg, 2.01 mmol), triethylamine (0.42 mL, 3.01 mmol) and neat 1-boc-piperazine (**185**) (1.12 g, 6.03 mmol) were stirred in tetrahydrofuran (4 mL) at 0 °C for 1 h in a water/ice bath. LCMS confirmed starting material consumption and formation of product (m/z 348, 350). The reaction mixture was concentrated to give a white solid (1.77 g). The residue was purified *via* flash chromatography (40 g silica, petroleum ether:ethyl acetate 1:0 to 0:1) to give *tert*-butyl 4-(2-chloroquinazolin-4-yl)piperazine-1-carboxylate (**199**) (637 mg, 86%) as a clear colourless oil which crystallised upon standing to form a white solid.

¹H NMR (600 MHz, DMSO-*d*₆) δ 8.07 (d, J = 8.3 Hz, 1H, H-9), 7.84 (t, J = 7.6 Hz, 1H, H-7), 7.72 (d, J = 8.4 Hz, 1H, H-6), 7.54 (t, J = 7.7 Hz, 1H, H-8), 3.87–3.81 (m, 4H, H-13 and H-15), 3.57 (s, 4H, H-12 and H-16), 1.44 (s, 9H, H-21); LCMS (LCQ) Rt = 2.47 min (4 min method), m/z (ESI⁺) 349.0 (M+H)⁺, 293.1 (M+H-*t*-Bu)⁺ and 249.2 (M+H-Boc)⁺.

2-Chloro-4-(1-piperidyl)quinazoline (200)^{181–185}

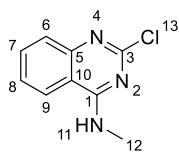
2,4-Dichloroquinazoline (**194**) (400 mg, 2.01 mmol), triethylamine (0.42 mL, 3.01 mmol) and neat piperidine (**188**) (0.6 mL, 6.03 mmol) were stirred in tetrahydrofuran (4 mL) at 0 °C for 1 h in a water/ice bath. LCMS confirmed starting material consumption and formation of product (m/z 248, 250). The reaction mixture was concentrated to give a yellow oil (775 mg). The residue was purified via flash chromatography (40 g silica, petroleum ether:ethyl acetate 1:0 to 0:1) to give a mixture of the product and the bis-substituted product. The mixed fractions containing the product were combined, concentrated and re-purified by flash column chromatography (12 g silica, petroleum ether:ethyl acetate 1:0 to 0:1) to give 2-chloro-4-(1-piperidyl)quinazoline (**200**) (247 mg, 47%) as a white solid.

^1H NMR (600 MHz, $\text{DMSO}-d_6$) δ 7.97 (d, J = 8.3 Hz, 1H, H-9), 7.81 (t, J = 7.5 Hz, 1H, H-7), 7.69 (d, J = 8.3 Hz, 1H, H-6), 7.52 (t, J = 7.9 Hz, 1H, H-8), 3.78 (s, 4H, H-12 and H-16), 1.71 (s, 6H, H-13, H-14 and H-15); LCMS (LCQ) R_t = 3.2 min (4 min method), m/z (ESI⁺) 248.3 [^{35}Cl] and 250.3 [^{37}Cl] ($\text{M}+\text{H}$)⁺.

***N*-(2-Chloroquinazolin-4-yl)-*N*',*N*'-dimethyl-ethane-1,2-diamine (**201**)**^{186–188}

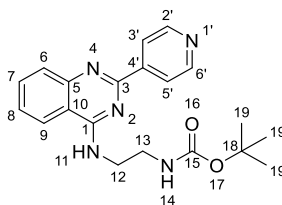
2,4-Dichloroquinazoline (**194**) (100 mg, 0.50 mmol), 2M THF *N,N*-dimethylethylenediamine (**190**) (0.06 mL, 0.55 mmol) and triethylamine (0.07 mL, 0.50 mmol) in ethanol (3.6 mL) were stirred at 0 °C for 1 h. LCMS confirmed formation of the product (*m/z* 250 and 252). The reaction mixture was diluted with water (5 mL) and extracted twice with ethyl acetate (2 × 5 mL). The combined organic phases were dried over MgSO₄, filtered and concentrated under reduced pressure to give *N*-(2-chloroquinazolin-4-yl)-*N*',*N*'-dimethyl-ethane-1,2-diamine (**201**) (74 mg, 56%) as an off-white solid.

¹H NMR (600 MHz, DMSO-*d*₆) δ 8.67 (*app. s*, 1H, H-11), 8.24 (d, *J* = 8.2 Hz, 1H, H-9), 7.79 (t, *J* = 7.7 Hz, 1H, H-7), 7.61 (d, *J* = 8.3 Hz, 1H, H-6), 7.53 (t, *J* = 7.5 Hz, 1H, H-8), 3.62 (q, *J* = 6.0 Hz, 2H, H-12), 2.54 (t, *J* = 6.5 Hz, 2H, H-13), 2.22 (s, 6H, H-15); LCMS (LCQ) Rt = 0.5 min (4 min method), *m/z* (ESI⁺) 251.1 [³⁵Cl] and 253.0 [³⁷Cl] (M+H)⁺.

2-Chloro-*N*-methyl-quinazolin-4-amine (202)^{189–197}

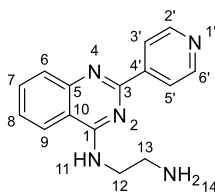
2,4-Dichloroquinazoline (**194**) (500 mg, 2.51 mmol), triethylamine (0.53 mL, 3.77 mmol) and 2 M methylamine in THF (0.71 mL, 7.54 mmol) were stirred in THF (25 mL) at 0 °C for 1 h in a water/ice bath. TLC and LCMS (LCQ) indicated product formation (m/z 194 and 196). The reaction mixture was concentrated under reduced pressure and purified *via* flash chromatography (5 g silica, petroleum ether:ethyl acetate 1:0 to 0:1) to give 2-chloro-*N*-methyl-quinazolin-4-amine (**202**) (390 mg, 76%) as a white solid.

¹H NMR (600 MHz, DMSO-*d*₆) δ 8.78 (s, 1H, H-11), 8.19 (d, J = 8.1 Hz, 1H, H-9), 7.78 (t, J = 8.2 Hz, 1H, H-7), 7.61 (d, J = 8.4 Hz, 1H, H-6), 7.53 (t, J = 8.0 Hz, 1H, H-8), 3.00 (d, J = 4.5 Hz, 3H, H-12); LCMS (LCQ) R_t = 1.25 min (4 min method), m/z (ESI⁺) 194.2 [³⁵Cl] and 196.2 [³⁷Cl] (M+H)⁺.

***Tert*-Butyl *N*-[2-[[2-(4-pyridyl)quinazolin-4-yl]amino]ethyl]carbamate (**219**)**

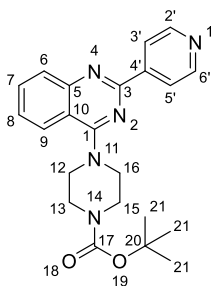
Pyridine-4-boronic acid hydrate (**196**) (36 mg, 0.29 mmol), *tert*-butyl *N*-[2-[(2-chloroquinazolin-4-yl)amino]ethyl]carbamate (**198**) (100 mg, 0.29 mmol), bis(triphenylphosphine)palladium(II) dichloride (10 mg, 0.01 mmol) and potassium carbonate (94 mg, 0.88 mmol) in 4:1 acetonitrile:water (8 mL) were degassed under a flow of nitrogen and heated in a microwave reactor at 140 °C for 15 minutes. LCMS (LCQ) confirmed reaction completion (m/z 365, 332 and 265). The reaction mixture was diluted with water (12.5 mL) and extracted twice with ethyl acetate (2 × 15 mL). The combined organic phases were dried over MgSO_4 , filtered and concentrated under reduced pressure to give a green oil (85 mg). The crude was purified *via* flash column chromatography (4 g silica, petroleum ether:ethyl acetate 1:0 to 0:1) to give *tert*-butyl *N*-[2-[[2-(4-pyridyl)quinazolin-4-yl]amino]ethyl]-carbamate (**219**) (64 mg, 57%) as a colourless glass.

R_f 0.25 (100% ethyl acetate); m.p. 152–154 °C; ν_{max} (thin film)/ cm^{-1} 3217 (N-H, br), 2936 (aliphatic C-H, m), 1708 (C=O, s), 1676 (C=C, s), 1607 (C=C, s), 764 (N-H, s); ^1H NMR (600 MHz, $\text{DMSO}-d_6$) δ 8.72 (d, J = 5.3 Hz, 2H, H-2' and H-6'), 8.52–8.46 (m, 1H, H-14), 8.39 (d, J = 5.5 Hz, 2H, H-3' and H-5'), 8.24 (d, J = 8.1 Hz, 1H, H-9), 7.82 (d, J = 3.4 Hz, 2H, H-8/7/6), 7.55 (dt, J = 7.2, 3.8 Hz, 2H, H-6/7/8 and O=PPh₃ impurity), 7.09–6.97 (m, 1H, H-11), 3.72 (q, J = 6.7, 6.0 Hz, 2H, H-13), 3.34 (d, J = 4.9 Hz, 2H, H-12), 1.35 (s, 9H, H-19). Triphenylphosphine impurity present; ^{13}C NMR (151 MHz, $\text{DMSO}-d_6$) δ 160.1 (C-15), 157.5 (C-4'), 155.8 (C-1), 150.0 (C-2' and C-6'), 149.6 (C-10), 145.9 (C-3), 133.0 (C-7), 128.0 (C-6), 126.1 (C-8), 122.8 (C-9), 121.9 (C-3' and C-5'), 114.3 (C-5), 77.7 (C-18), 40.9 (C-13), 39.0 (C-12), 28.2 (C-19).; HRMS m/z (ESI⁺) [Found: 366.1932, $\text{C}_{20}\text{H}_{24}\text{N}_5\text{O}_2$ requires (M+H)⁺ 366.1925]; LCMS (LCQ) Rt = 0.83 min (4 min method), m/z (ESI⁺) 365.96 (M+H)⁺, 310.10 (M+H-t-Bu)⁺ and 266.21 (M+H-Boc)⁺.

***N'*-[2-(4-pyridyl)quinazolin-4-yl]ethane-1,2-diamine (**220**)**¹⁹⁸

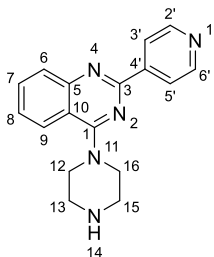
Tert-Butyl *N*-[2-[[2-(4-pyridyl) quinazolin-4-yl]amino]ethyl]carbamate (**219**) (50 mg, 0.14 mmol) was stirred in trifluoro acetic acid (0.45 mL, 5.94 mmol) and dichloromethane (2.6 mL) for 10 min at 0 °C then at room temperature for 4 h. The reaction mixture was concentrated under reduced pressure then purified *via* SCX cartridge by elution of methanol then 2 M NH₃ in methanol to give *N'*-[2-(4-pyridyl)quinazolin-4-yl]ethane-1,2-diamine (**220**) (30 mg, 77%) as a yellow solid.

R_f 0 (9:1 dichloromethane:methanol); m.p. 197–200 °C; ν_{max} (thin film)/cm⁻¹ 3284 (N-H, br), 2923 (C-H aliphatic, br), 1683 (C=O, m), 1636 (C=C, m), 1560 (N-H, m), 1525 (C-C aromatic, m), 1126 (C-N, s), 722 (N-H, s); ¹H NMR (600 MHz, DMSO-*d*₆) δ 8.88 (d, *J* = 5.8 Hz, 2H, H-2' and H-6'), 8.75 (s, 1H, H-11), 8.59 (d, *J* = 5.3 Hz, 2H, H-3' and H-5'), 8.28 (d, *J* = 8.6 Hz, 1H, H-9), 7.90 (d, *J* = 3.8 Hz, 2H, H-6/7/8), 7.87 (s, 2H, H-14), 7.68–7.64 (m, 1H, H-8/7/6), 3.96 (app. q, *J* = 6.1 Hz, 2H, H-12), 3.22 (app. q, *J* = 6.3 Hz, 2H, H-13); ¹³C NMR (151 MHz, DMSO-*d*₆) δ 160.4 (C-1), 156.3 (C-3), 148.6 (C-5), 148.1 (C-4'), 147.4 (C-2' and C-6'), 133.6 (C-7/6/8), 127.6 (C-8/7/6), 123.1 (C-3' and C-5'), 123.0 (C-9), 114.4 (C-6/7/8), 38.4 (C-12), 38.1 (C-13); HRMS *m/z* (ESI⁺) [Found: 266.1385, C₁₅H₁₆N₅ requires (M+H)⁺ 266.1400]; LCMS (LCQ) Rt = 0.38 min (4 min method), *m/z* (ESI⁺) 266.2 (M+H)⁺.

***Tert*-Butyl 4-[2-(4-pyridyl)quinazolin-4-yl]piperazine-1-carboxylate (**221**)¹⁹⁹**

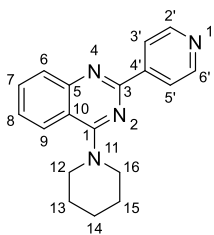
Pyridine-4-boronic acid hydrate (**196**) (35 mg, 0.29 mmol), bis(triphenylphosphine)palladium(II) dichloride (10 mg, 0.01 mmol), sodium carbonate (91 mg, 0.86 mmol) and *tert*-butyl 4-(3-chloro-1-isoquinolyl)piperazine-1-carboxylate (**199**) (100 mg, 0.29 mmol) in 4:1 acetonitrile:water (8 mL) were degassed under a flow of nitrogen and heated in a microwave reactor at 140 °C for 15 minutes. LCMS confirmed reaction completion (m/z 365, 332 and 265). The reaction mixture was diluted with water (12.5 mL) and extracted twice with ethyl acetate (2 × 15 mL). The combined organic phases were dried over MgSO₄, filtered and concentrated under reduced pressure to give a pale yellow solid (107 mg). The crude was purified *via* flash column chromatography (4 g silica, petroleum ether:ethyl acetate, 1:0 to 0:1) to give *tert*-butyl 4-[2-(4-pyridyl)quinazolin-4-yl]piperazine-1-carboxylate (**221**) (27 mg, 23%) as an off-white solid.

¹H NMR (600 MHz, DMSO-*d*₆) δ 8.76 (d, J = 4.4 Hz, 2H, H-2' and H-6'), 8.35 (d, J = 4.5 Hz, 2H, H-3' and H-5'), 8.10 (d, J = 8.1 Hz, 1H, H-9), 7.95 (d, J = 8.7 Hz, 1H, H-6), 7.88 (t, J = 7.7 Hz, 1H, H-7), 7.60 (d, J = 7.7 Hz, 2H, H-8), 3.88 (s, 4H, H-13 and H-15), 3.62 (s, 4H, H-12 and H-16), 1.44 (s, 9H, H-21); LCMS (LCQ) Rt = 0.92 min (4 min method), m/z (ESI⁺) 392.1 (M+H)⁺, 336.1 (M+H-*t*-Bu)⁺ and 292.3 (M+H-Boc)⁺.

4-Piperazin-1-yl-2-(4-pyridyl)quinazoline (222)¹⁹⁹

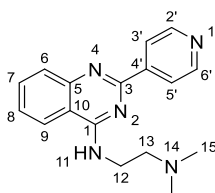
Tert-Butyl 4-[2-(4-pyridyl)quinazolin-4-yl]piperazine-1-carboxylate (**221**) (15 mg, 0.04 mmol) was dissolved in dichloromethane (1.00 mL) and trifluoro acetic acid (0.3 mL, 3.92 mmol) at 0 °C. The reaction mixture was allowed to stir for 4 h at room temperature. LCMS confirmed removal of the Boc protecting group (m/z 292). The reaction mixture was concentrated under reduced pressure to give 4-piperazin-1-yl-2-(4-pyridyl)quinazoline (**222**) (16 mg, 99%) as a brown oil.

R_f 0.08 (9:1 dichloromethane:methanol); m.p. 168–170 °C; ν_{\max} (thin film)/ cm^{-1} 3004 (C-H aromatic, br), 1673 (C=C, s), 1634 (C=C, m), 1567 (C-C aromatic, m), 1508 (C-C aromatic, m), 1431 (C-H aliphatic, m), 1180 (C-N, s), 1117 (C-N, s), 720 (N-H, s); ^1H NMR (600 MHz, $\text{DMSO}-d_6$) δ 8.92 (s, 2H, H-14), 8.89 (d, J = 5.6 Hz, 2H, H-2' and H-6'), 8.59 (d, J = 5.1 Hz, 2H, H-3' and H-5'), 8.15 (d, J = 8.3 Hz, 1H, H-6), 8.01 (d, J = 8.6 Hz, 1H, H-9), 7.94 (t, J = 7.6 Hz, 1H, H-8), 7.66 (t, J = 7.5 Hz, 1H, H-7), 4.08–3.99 (m, 4H, H-12 and H-16), 3.43–3.31 (m, 4H, H-13 and H-15); ^{13}C NMR (151 MHz, $\text{DMSO}-d_6$) δ 164.2 (C-1), 155.6 (C-3), 151.6 (C-10), 148.4 (C-2' and C-6'), 147.0 (C-3), 133.7 (C-8), 128.7 (C-9), 127.0 (C-7), 125.4 (C-6), 122.6 (C-3' and C-5'), 115.2 (C-5), 46.2 (C-12 and C-16), 42.6 (C-13 and C-15); HRMS m/z (ESI⁺) [Found: 292.1550, $\text{C}_{17}\text{H}_{18}\text{N}_5$ requires (M+H)⁺ 292.1557]; LCMS (LCQ) R_t = 0.4 min (4 min method), m/z (ESI⁺) 292.3 (M+H)⁺.

4-(1-Piperidyl)-2-(4-pyridyl)quinazoline (223)

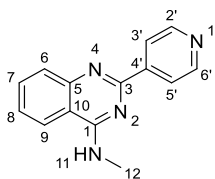
Pyridine-4-boronic acid hydrate (**196**) (47 mg, 0.38 mmol), bis(triphenylphosphine)palladium(II) dichloride (13 mg, 0.02 mmol), potassium carbonate (121 mg, 1.14 mmol) and (3*E*)-6-chloro-3-[(2*Z*)-penta-2,4-dienylidene]-2-(1-piperidyl)-4*H*-pyridine (**200**) (100 mg, 0.38 mmol) in 4:1 acetonitrile:water (8 mL) were degassed under a flow of nitrogen and heated in a microwave reactor at 140 °C for 15 minutes. LCMS confirmed reaction completion (*m/z* 365, 332 and 265). The reaction mixture was diluted with water (12.5 mL) and extracted twice with ethyl acetate (2 × 15 mL). The combined organic phases were dried over MgSO₄, filtered and concentrated under reduced pressure to give a green oil (108 mg). The crude was purified *via* flash column chromatography (4 g silica, petroleum ether:ethyl acetate 1:0 to 0:1) to give 4-(1-piperidyl)-2-(4-pyridyl)quinazoline (**223**) (40 mg, 34%) as an off-white solid.

R_f 0.47 (100% ethyl acetate); m.p. 150–151 °C; ν_{max} (thin film)/cm⁻¹ 3009 (C-H aromatic, w), 2942 (C-H aliphatic, m), 1612 (C=C, m), 1570 (C-C aromatic, m), 1504 (C-C aromatic, m), 1112 (C-N, m), 764 (N-H, s); ¹H NMR (600 MHz, DMSO-*d*₆) δ 8.75 (d, *J* = 5.8 Hz, 2H, H-2' and H-6'), 8.33 (d, *J* = 5.8 Hz, 2H, H-3' and H-5'), 8.01 (d, *J* = 8.3 Hz, 1H, H-9), 7.91 (d, *J* = 8.2 Hz, 1H, H-6), 7.85 (t, *J* = 7.6 Hz, 1H, H-7), 7.57 (t, *J* = 7.5 Hz, 1H, 8), 3.88–3.81 (m, 4H, H-12 and H-16), 1.81–1.70 (m, 6H, H-13, H-14, H-15); ¹³C NMR (151 MHz, DMSO-*d*₆) δ 164.1 (C-1), 156.3 (C-3), 151.9 (C-5), 150.2 (C-2' and C-6'), 145.4 (C-4'), 133.0 (C-7), 128.4 (C-6), 125.9 (C-8), 125.4 (C-9), 121.8 (C-3' and C-5'), 115.0 (C-10), 50.2 (C-12 and C-16), 25.5 (C-13 and C-15), 24.2 (C-14); HRMS *m/z* (ESI⁺) [Found: 291.1592, C₁₈H₁₉N₄ requires (M+H)⁺ 291.1604]; LCMS (LCQ) *R_t* = 0.7 min (4 min method), *m/z* (ESI⁺) 291.3 (M+H)⁺.

***N,N'*-Dimethyl-*N*-[3-(4-pyridyl)-2,6-naphthyridin-1-yl]ethane-1,2-diamine (**224**)**¹⁹⁹

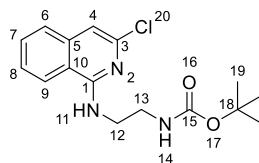
Pyridine-4-boronic acid hydrate (**196**) (74 mg, 0.60 mmol), *bis*(triphenylphosphine)palladium(II) dichloride (21 mg, 0.03 mmol), sodium carbonate (190 mg, 1.79 mmol) and *N*-(2-chloroquinazolin-4-yl)-*N,N'*-dimethyl-ethane-1,2-diamine (**201**) (150 mg, 0.60 mmol) in 4:1 acetonitrile:water (12 mL) were degassed under a flow of nitrogen and heated in a microwave reactor at 140 °C for 15 minutes. LCMS confirmed reaction completion (*m/z* 294). The reaction mixture was diluted with water (15 mL) and extracted twice with ethyl acetate (2 × 20 mL). The combined organic phases were dried over MgSO₄, filtered and concentrated under reduced pressure to give *N,N'*-dimethyl-*N*-[3-(4-pyridyl)-2,6-naphthyridin-1-yl]ethane-1,2-diamine (**224**) as a yellow solid (37 mg).

R_f 0.59 (100% ethyl acetate); m.p. 121-123 °C; *v*_{max} (thin film)/cm⁻¹ 3256 (N-H, br), 3128 (aromatic C-H, w), 3064 (aromatic C-H, w), 2972 (aliphatic C-H, w), 1583 (aromatic C-H, s), 1560 (aromatic C-H, s), 1529 (aromatic C-H, s), 1489 (aliphatic C-H, m), 758 (N-H, s), 694 (C-H, s); ¹H NMR (600 MHz, DMSO-*d*₆) δ 8.74 (d, *J* = 5.3 Hz, 2H, H-2' and H-6'), 8.42 (t, *J* = 5.4 Hz, 1H, H-11), 8.33 (d, *J* = 4.4 Hz, 2H, H-3' and H-5'), 8.27 (d, *J* = 8.2 Hz, 1H, H-9), 7.81 (d, *J* = 3.2 Hz, 2H, H-7 and H-6), 7.56 (d, *J* = 4.7 Hz, 1H, H-8), 3.80 (q, *J* = 6.5 Hz, 2H, H-12), 2.61 (t, *J* = 6.8 Hz, 2H, H-13), 2.25 (s, 6H, H-15); ¹³C NMR pending; HRMS pending; LCMS (LCQ) *R_t* = 0.4 min (4 min method), *m/z* (ESI⁺) 294.2 (M+H)⁺.

***N*-Methyl-2-(4-pyridyl)quinazolin-4-amine (225)**

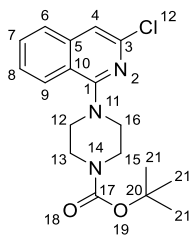
Pyridine-4-boronic acid hydrate (**196**) (95 mg, 0.77 mmol), bis(triphenylphosphine)palladium(II) dichloride (27 mg, 0.04 mmol), potassium carbonate (246 mg, 2.32 mmol) and 2-chloro-*N*-methyl-quinazolin-4-amine (**202**) (150 mg, 0.77 mmol) in 4:1 acetonitrile:water (12 mL) were degassed under a flow of nitrogen and heated in a microwave reactor at 140 °C for 15 minutes. LCMS confirmed reaction completion (m/z 237). The reaction mixture was diluted with water (20 mL) and extracted twice with ethyl acetate (2 × 25 mL). The combined organic phases were dried over MgSO_4 , filtered and concentrated under reduced pressure to give a pale yellow solid (135 mg). The crude was purified *via* flash column chromatography (5 g silica, petroleum ether:ethyl acetate 1:0 to 0:1) to give *N*-methyl-2-(4-pyridyl)quinazolin-4-amine (**225**) (39 mg, 9%) as a white solid.

R_f 0.27 (100% ethyl acetate); m.p. 237–239 °C; ν_{max} (thin film)/ cm^{-1} 3265 (N-H, br), 3132 (C-H aromatic, br), 2993 (C-H alkane, w), 1586 (C-C aromatic, s), 1562 (C-C aromatic, s), 1532 (C-C aromatic, m), 720 (N-H, s); ^1H NMR (600 MHz, $\text{DMSO}-d_6$) δ 8.73 (d, J = 5.4 Hz, 2H, H-2' and H-6'), 8.50 (m, 1H, H-11), 8.36 (d, J = 5.3 Hz, 2H, H-3' and H-5'), 8.24 (d, J = 8.1 Hz, 1H, H-9), 7.84–7.78 (m, 2H, H-6/7/8), 7.65–7.59 (m, 2H, H-7/8/6), 7.58–7.52 (m, 1H, H-8/7/6), 3.17 (d, J = 4.4 Hz, 3H, H-12); ^{13}C NMR (151 MHz, $\text{DMSO}-d_6$) δ 160.3 (C-1), 157.5 (C-3), 150.0 (C-2' and C-6'), 149.3 (C-5), 145.9 (C-4'), 132.8 (C-10), 131.4 (C-7/6/8), 128.0 (C-6/7/8), 126.2 (C-8/7/6), 122.6 (C-9), 121.8 (C-3' and C-5'), 27.6 (C-12); HRMS m/z (ESI⁺) [Found: 237.1136, $\text{C}_{14}\text{H}_{13}\text{N}_4$ requires (M+H)⁺ 237.1135]; LCMS (LCQ) R_t = 0.5 min (4 min method), m/z (ESI⁺) 237.4 (M+H)⁺.

***Tert*-Butyl *N*-[2-[(3-chloro-1-isoquinolyl)amino]ethyl]carbamate (**228**)**

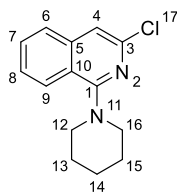
1,3-Dichloroisoquinoline (**225**) (500 mg, 2.52 mmol), 2 M *N,N*-diisopropylethylamine in THF (1.78 mL, 10.2 mmol) and *tert*-butyl *N*-(2-aminoethyl)carbamate (**182**) (2.37 mL, 15 mmol) in ethanol (18 mL) were stirred at 100 °C for 3 days. LCMS confirmed product formation (m/z 322). The reaction mixture was concentrated under reduced pressure, diluted with water (10 mL) and extracted with ethyl acetate (3 × 100 mL). The combined organic extracts were washed with water (100 mL) and brine (100 mL), dried over MgSO₄, filtered and concentrated under reduced pressure to give a yellow solid (1.95 g). The crude was purified via flash column chromatography (80 g silica, petroleum ether:ethyl acetate, 1:0 to 0:1) to give *tert*-butyl *N*-[2-[(3-chloro-1-isoquinolyl)amino]ethyl]carbamate (**228**) (703 mg, 82%) as a white solid.

¹H NMR (600 MHz, DMSO-*d*₆) δ 8.19 (d, J = 8.3 Hz, 1H, H-9), 7.83–7.76 (m, 1H, H-14), 7.67 (d, J = 7.9 Hz, 1H, H-6), 7.63 (t, J = 7.4 Hz, 1H, H-7), 6.97 (app. s, 2H, H-11 and H-8), 3.49 (q, J = 5.6 Hz, 2H, H-13), 3.23 (q, J = 6.0 Hz, 2H, H-12), 1.37 (s, 9H, H-19); LCMS (LCQ) Rt = 2.99 min (4 min method), m/z (ESI⁺) 321.87 [³⁵Cl], 323.87 [³⁷Cl] (M+H)⁺, 265.94 [³⁵Cl], 267.94 [³⁷Cl] (M+H-*t*-Bu)⁺, 222.0 [³⁵Cl] and 224.0 [³⁷Cl] (M+H-Boc)⁺.

***Tert*-Butyl 4-(3-chloro-1-isoquinolyl)piperazine-1-carboxylate (**229**)¹⁹⁸**

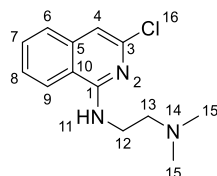
1,3-Dichloroisoquinoline (**225**) (500 mg, 2.52 mmol), *N,N*-diisopropylethylamine (1.78 mL, 10.2 mmol) and 1-Boc-piperazine (**185**) (2.82 g, 15.2 mmol) in ethanol (18 mL) were stirred at 100 °C for 3 days. TLC and LCMS showed product formation (*m/z* 247 and 249). The reaction mixture was concentrated under reduced pressure, diluted with water (10 mL) and extracted with ethyl acetate (3 × 100 mL). The combined organic extracts were washed with water (100 mL) and brine (100 mL), dried over MgSO₄, filtered and concentrated under reduced pressure to give a yellow solid (900 mg). The crude was purified *via* flash column chromatography (40 g silica, petroleum ether:ethyl acetate, 1:0 to 0:1) to give *tert*-butyl 4-(3-chloro-1-isoquinolyl)piperazine-1-carboxylate (**229**) (867 mg, 89%) as an off-white solid.

¹H NMR (600 MHz, DMSO-*d*₆) δ 8.09 (d, *J* = 8.4 Hz, 1H, H-9), 7.87 (d, *J* = 8.0 Hz, 1H, H-6), 7.74 (t, *J* = 7.5 Hz, 1H, H-7), 7.60 (t, *J* = 7.8 Hz, 1H, H-8), 7.53 (s, 1H, H-4), 3.59 (s, 4H, H-12 and H-16), 3.36–3.32 (m, 4H, H-13 and H-15), 1.44 (s, 9H, H-21); LCMS (LCQ) Rt = 0.64 min (4 min method), *m/z* (ESI⁺) 247.2 [³⁵Cl] and 249.3 [³⁷Cl] (M+H-Boc)⁺.

3-Chloro-1-(1-piperidyl)isoquinoline (230)

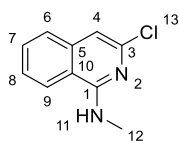
1,3-Dichloroisoquinoline (**225**) (500 mg, 2.52 mmol), *N,N*-diisopropylethylamine (1.78 mL, 10.2 mmol) and piperidine (**188**) (1.5 mL, 15.2 mmol) in ethanol (18 mL) were stirred at 100 °C for 3 days. TLC and LCMS confirmed reaction had gone to completion (m/z 245). The reaction mixture was concentrated under reduced pressure, diluted with water (10 mL) and extracted with ethyl acetate (3 × 100 mL). The combined organic extracts were washed with water (100 mL) and brine (100 mL), dried over MgSO_4 , filtered and concentrated under reduced pressure to give 3-chloro-1-(1-piperidyl)isoquinoline (**230**) (640 mg, 98%) as a pale orange solid.

^1H NMR (600 MHz, $\text{DMSO}-d_6$) δ 8.01 (d, J = 8.4 Hz, 1H, H-9), 7.85–7.81 (d, 1H, H-6), 7.71 (t, J = 7.4 Hz, 1H, H-7), 7.58 (t, J = 7.6 Hz, 1H, H-8), 7.44 (s, 1H, H-4), 3.36–3.33 (m, 4H, H-12 and H-16), 1.76 (m, H-13 and H-15), 1.65 (m, 2H, H-14); LCMS (LCQ) R_t = 0.5 min (4 min method), m/z (ESI^+) 245.3 ($\text{M}-\text{H}^+$).

***N*-(3-Chloro-1-isoquinolyl)-*N*',*N*'-dimethyl-ethane-1,2-diamine (231)**

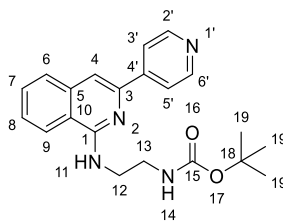
1,3-Dichloroisoquinoline (**225**) (500 mg, 2.52 mmol), *N,N*-diisopropylethylamine (1.8 mL, 10.2 mmol) and *N,N*-dimethylethylenediamine (**190**) (1.6 mL, 15 mmol) in ethanol (18 mL) were stirred at 100 °C for 3 days. LCMS confirmed product formation (m/z 250). The reaction mixture was concentrated under reduced pressure, diluted with water (10 mL) and extracted three times with ethyl acetate (3 × 100 mL). The combined organic extracts were washed with water (100 mL) and brine (100 mL), dried over MgSO_4 , filtered and concentrated under reduced pressure to give a yellow solid (1.95 g). The crude was purified *via* flash column chromatography (24 g silica, petroleum ether:ethyl acetate, 1:0 to 0:1 then ethyl acetate:methanol, 100:0 to 90:10) to give *N*-(3-chloro-1-isoquinolyl)-*N*',*N*'-dimethyl-ethane-1,2-diamine (**231**) (200mg, 30%) as a yellow oil.

^1H NMR (600 MHz, $\text{DMSO}-d_6$) δ 8.19 (dd, J = 8.5, 1.0 Hz, 1H, H-9), 7.71 (t, J = 5.5 Hz, 1H, H-11), 7.67 (dd, J = 8.3, 1.4 Hz, 1H, H-6), 7.63 (ddd, J = 8.0, 6.7, 1.1 Hz, 1H, H-7), 7.48 (ddd, J = 8.3, 6.7, 1.5 Hz, 1H, H-8), 6.94 (d, J = 0.8 Hz, 1H, H-4), 3.56 (td, J = 6.8, 5.4 Hz, 2H, H-12), 2.54–2.51 (m, 2H, H-13), 2.21 (s, 6H, H-15); LCMS (MDAP) R_t = 2.2 min (Ana 5-95 over 5 minutes), m/z (ESI $^+$) 251.0 ($\text{M}+\text{H}$) $^+$.

3-Chloro-*N*-methyl-isoquinolin-1-amine (232)¹⁵⁵

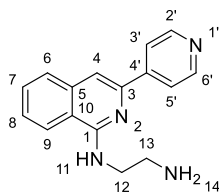
1,3-Dichloroisoquinoline (**225**) (500 mg, 2.52 mmol), 2 M methylamine in THF (1.88 mL, 15 mmol) and *N,N*-diisopropylethylamine (0.7 mL, 4.04 mmol) in ethanol (20 mL) were stirred at 100 °C overnight. LCMS showed consumption of the starting material (m/z 193 and 195). The reaction mixture was concentrated under reduced pressure, diluted with water (10 mL) and extracted with ethyl acetate (3 × 100 mL). The combined organic extracts were washed with water (100 mL) and brine (100 mL), dried over MgSO_4 , filtered and concentrated under reduced pressure to give 3-chloro-*N*-methyl-isoquinolin-1-amine (**232**) (470 mg, 92%) as a pale yellow solid.

^1H NMR (600 MHz, $\text{DMSO}-d_6$) δ 8.17 (d, J = 8.3 Hz, 1H, H-9), 7.87 (d, J = 4.3 Hz, 1H, H-11), 7.67 (d, J = 8.1 Hz, 1H, H-6), 7.63 (t, J = 7.4 Hz, 1H, H-7), 7.47 (t, J = 7.5 Hz, 1H, H-8), 6.95 (s, 1H, H-4), 2.95 (d, J = 4.4 Hz, 3H, H-12); LCMS (LCQ) R_t = 1.4 min (4 min method), m/z (ESI⁺) 193.2 [^{35}Cl] and 195.21 [^{37}Cl] ($\text{M}+\text{H}+\text{Na}$)⁺.

***Tert*-Butyl *N*-[2-[[3-(4-pyridyl)-1-isoquinolyl]amino]ethyl]carbamate (**234**)**

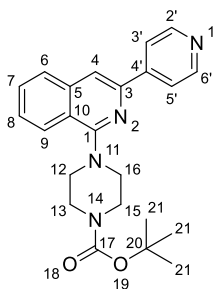
Pyridine-4-boronic acid hydrate (**196**) (54 mg, 0.44 mmol), potassium carbonate (141 mg, 1.33 mmol), bis[2-(di-*tert*-butylphosphanyl)cyclopenta-2,4-dien-1-yl]iron; dichloropalladium (14 mg, 0.02 mmol) and *tert*-butyl *N*-[2-[(3-chloro-1-isoquinolyl)amino]ethyl]carbamate (**228**) (150 mg, 0.44 mmol) in 4:1 acetonitrile: water (12 mL) were degassed under a flow of nitrogen and heated in a microwave reactor at 140 °C for 15 minutes. LCMS confirmed reaction completion (m/z 365, 332 and 265). The reaction mixture was diluted with water (3 mL) and extracted twice with ethyl acetate (2 × 4 mL). The combined organic phases were dried over MgSO_4 , filtered and concentrated under reduced pressure to give a brown oil (142 mg). The crude was purified *via* flash column chromatography (5 g silica, petroleum ether:ethyl acetate 1:0 to 0:1) to give *tert*-butyl *N*-[2-[[3-(4-pyridyl)-1-isoquinolyl]amino]ethyl]carbamate (**234**) (99 mg, 58%) as a pale orange solid.

R_f 0.73 (100% ethyl acetate); m.p. 158–160 °C; ν_{max} (thin film)/ cm^{-1} 3386 (N-H, m), 3312 (N-H, m), 2932 (C-H aliphatic, w), 1681 (C=O, s), 1542 (C-C aromatic, s), 1520 (C-C, aromatic, s), 1172 (C-N, s), 671 (N-H, m); ^1H NMR (600 MHz, $\text{DMSO}-d_6$) δ 8.64 (d, $J = 4.2$ Hz, 2H, H-2' and H-6'), 8.22 (d, $J = 8.2$ Hz, 1H, H-9), 8.16 (d, $J = 3.6$ Hz, 2H, H-3' and H-5'), 7.84 (d, $J = 7.6$ Hz, 1H, H-6), 7.75 (s, 1H, H-4), 7.71–7.61 (m, 2H, H-7 and H-14), 7.55 (t, $J = 7.8$ Hz, 1H, H-8), 7.04 (s, 1H, H-11), 3.69–3.63 (m, 2H, H-13), 3.37–3.31 (m, 2H, H-12), 1.38 (s, 9H, H-19); ^{13}C NMR (151 MHz, $\text{DMSO}-d_6$) δ 155.9 (C-15), 155.1 (C-10), 149.9 (C-2' and C-6'), 146.6 (C-4'), 145.1 (C-2), 137.2 (C-4), 130.1 (C-6), 127.5 (C-5), 126.5 (C-7), 123.0 (C-8), 120.5 (C-9), 118.1 (C-3' and C-5'), 107.0 (C-9), 77.6 (C-3), 41.3 (C-18), 39.7 (C-13), 28.2 (C-12); HRMS m/z (ESI⁺) [Found: 365.1965, $\text{C}_{21}\text{H}_{25}\text{N}_4\text{O}_2$ requires (M+H)⁺ 365.1972]; LCMS (LCQ) R_t = 0.5 min (4 min method), m/z (ESI⁺) 365.03 (M+H)⁺, 309.1 (M+H-t-Bu)⁺ and 265.2 (M+H-Boc)⁺.

***N'*-[3-(4-Pyridyl)-1-isoquinolyl]ethane-1,2-diamine (233)**¹⁶¹

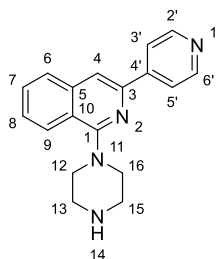
Tert-Butyl *N*-[2-[[3-(4-pyridyl)-1-isoquinolyl]amino]ethyl]carbamate (**234**) (47 mg, 0.12 mmol) was stirred in trifluoro acetic acid (0.5 mL, 6.0 mmol) and dichloromethane (1 mL) for 10 min at 0 °C then at room temperature overnight. LCMS confirmed product formation (m/z 265). The reaction mixture was concentrated under reduced pressure, purified by SCX cartridge and the product was eluted using 2 M NH₃ in methanol and concentrated under reduced pressure to give *N'*-[3-(4-pyridyl)-1-isoquinolyl]ethane-1,2-diamine (**233**) (34 mg, 100%) as a yellow solid.

R_f 0.33 (1:1 petroleum ether:ethyl acetate); m.p. 137–139 °C; ν_{\max} (thin film)/cm⁻¹ 3133 (N-H, br), 1594 (aromatic C-H, m) 1534 (aromatic C-H, s), 813 (N-H, s), 677 (C-H, s); ¹H NMR (600 MHz, DMSO-*d*₆) δ 8.65 (d, 2H, J = 5.6, H-2' and H-6'), 8.29 (d, J = 8.3 Hz, 1H, H-9), 8.12 (d, J = 5.3 Hz, 2H, H-3' and H-5'), 7.83 (d, J = 8.0 Hz, 1H, H-6), 7.73 (s, 1H, H-4), 7.67 (t, J = 7.4 Hz, 1H, H-7), 7.60 (m, 1H, H-11), 7.55 (t, J = 7.4 Hz, 1H, H-8), 3.68 (*app.* q, J = 6.1 Hz, 2H, H-12), 2.96 (t, J = 6.5 Hz, 2H, H-13), -NH₂ peak likely under water peak; ¹³C NMR (151 MHz, DMSO-*d*₆) δ 155.2 (C-1), 150.0 (C-2' and C-6'), 146.7 (C-4'), 145.0 (C-3), 137.1 (C-5), 130.2 (C-7), 127.5 (C-6), 126.5 (C-8), 123.3 (C-9), 120.4 (C-3' and C-5'), 118.3 (C-10), 107.1 (C-4), 42.5 (C-13), 39.7 (C-12); HRMS m/z (ESI⁺) [Found: 265.1440, C₁₆H₁₇N₄ requires (M+H)⁺ 265.1448]; LCMS (LCQ) R_t = 0.4 min (4 min method), m/z (ESI⁺) 265.1 (M+H)⁺.

***Tert*-Butyl 4-[3-(4-pyridyl)-1-isoquinolyl]piperazine-1-carboxylate (**236**)**

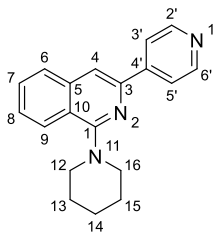
Pyridine-4-boronic acid hydrate (**196**) (53 mg, 0.43 mmol), potassium carbonate (138 mg, 1.3 mmol), bis[2-(di-*tert*-butylphosphanyl)cyclopenta-2,4-dien-1-yl]iron; dichloropalladium (14 mg, 0.02 mmol) and *tert*-butyl 4-(3-chloro-1-naphthyl)piperazine-1-carboxylate (**229**) (150 mg, 0.43 mmol) in 4:1 acetonitrile:water (12 mL) were degassed under a flow of nitrogen and heated in a microwave reactor at 140 °C for 15 minutes. LCMS confirmed reaction completion (m/z 391, 335, 291). The reaction mixture was diluted with water (20 mL) and extracted twice with ethyl acetate (2 × 25 mL). The combined organic phases were dried over MgSO_4 , filtered and concentrated under reduced pressure to give a brown solid (174 mg). The crude was purified *via* flash column chromatography (5 g silica, PE:EA, 1:0 to 0:1) to give *tert*-butyl 4-[3-(4-pyridyl)-1-isoquinolyl]piperazine-1-carboxylate (**236**) (82 mg, 46%) as a pale brown solid.

R_f 0.33 (100% ethyl acetate); m.p. 185–187 °C; ν_{max} (thin film)/ cm^{-1} 2979 (C-H aliphatic, w), 2839 (C-H aliphatic, w), 1699 (C=O, s), 1560 (C-C aromatic, m), 1411 (C-H aliphatic, s), 1248 (C-N, s), 827 (C-H, s); ^1H NMR (600 MHz, $\text{DMSO}-d_6$) δ 8.69 (d, J = 4.6 Hz, 2H, H-2' and H-6'), 8.24 (s, 1H, H-4), 8.18–8.12 (m, 3H, H-3', H-5' and H-9), 8.01 (d, J = 8.2 Hz, 1H, H-6), 7.77 (t, J = 7.8 Hz, 1H, H-7), 7.66 (t, J = 7.5 Hz, 1H, H-8), 3.64 (s, 4H, H-13 and H-15), 3.48–3.37 (m, 4H, H-12 and H-16), 1.45 (s, 9H, H-21); ^{13}C NMR (151 MHz, $\text{DMSO}-d_6$) δ 160.3 (C-17), 154.0 (C-1), 150.2 (C-2' and C-6'), 146.0 (C-4'), 144.3 (C-3), 138.4 (C-5), 130.6 (C-7), 128.2 (C-6), 127.5 (C-8), 125.4 (C-9), 120.8 (C-10), 120.5 (C-3' and C-5'), 113.0 (C-4), 79.1 (C-20), 50.8 (C-12 and C-16), 28.1 (C-21). C-13 and C-15 under solvent peak; HRMS m/z (ESI⁺) [Found: 391.2110, $\text{C}_{23}\text{H}_{27}\text{N}_4\text{O}_2$ requires (M+H)⁺ 391.2129]; LCMS (LCQ) R_t = 0.7 min (4 min method), m/z (ESI⁺) 391.10 (M+H)⁺, 335.2 (M+H-*t*-Bu)⁺ and 291.3 (M+H-Boc)⁺.

1-Piperazin-1-yl-3-(4-pyridyl)isoquinoline (237)

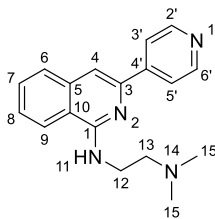
Tert-Butyl 4-[3-(4-pyridyl)-1-isoquinolyl]piperazine-1-carboxylate (**236**) (41 mg, 0.10 mmol) was stirred in trifluoro acetic acid (0.42 mL, 5.47 mmol) and dichloromethane (2.8 mL) for 10 min at 0 °C then at room temperature overnight. LCMS confirmed product formation (m/z 291). The reaction mixture was concentrated under reduced pressure, purified by SCX cartridge and the product was eluted using 2 M NH_3 in methanol then concentrated under reduced pressure to give 1-piperazin-1-yl-3-(4-pyridyl)isoquinoline (**237**) (32 mg, 62% yield) as an off-white powder.

R_f 0.07 (9:1 dichloromethane:methanol); m.p. 156-158 °C; ν_{max} (thin film)/ cm^{-1} 3247 (N-H, br), 2820 (aliphatic C-H, w), 1603 (C=C, m), 1558 (aromatic C-H, m), 1412 (aliphatic C-H, s), 827 (N-H, s), 677 (C-H, s); ^1H NMR (600 MHz, $\text{DMSO}-d_6$) δ 8.69 (d, J = 4.7 Hz, 2H, H-2' and H-6'), 8.19 (s, 1H, H-4), 8.14 (d, J = 4.7 Hz, 2H, H-3' and H-5'), 8.12 (d, J = 8.3 Hz, 1H, H-9), 7.99 (d, J = 8.1 Hz, 1H, H-6), 7.75 (t, J = 7.5 Hz, 1H, H-7), 7.64 (t, J = 7.5 Hz, 1H, H-8), 3.42 (s, 4H, H-12 and H-16), 3.06 (s, 4H, H-13 and H-15); ^{13}C NMR (151 MHz, $\text{DMSO}-d_6$) δ 160.6 (C-1), 150.2 (C-2' and C-6'), 146.0 (C-4'), 144.3 (C-5), 138.3 (C-10), 130.4 (C-7), 128.1 (C-6), 127.3 (C-8), 125.4 (C-9), 120.7 (C-3), 120.4 (C-3' and C-5'), 112.7 (C-4), 51.1 (C-12 and C-16), 44.9 (C-13 and C-15); HRMS m/z (ESI⁺) [Found: 291.1591, $\text{C}_{18}\text{H}_{19}\text{N}_4$ requires (M+H)⁺ 291.1604]; LCMS (LCQ) R_t = 0.4 min (4 min method), m/z (ESI⁺) 291.3 (M+H)⁺.

1-(1-Piperidyl)-3-(4-pyridyl)isoquinoline (238)

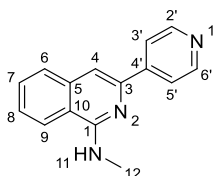
Pyridine-4-boronic acid hydrate (**196**) (75 mg, 0.61 mmol), potassium carbonate (193 mg, 1.82 mmol), bis[2-(di-*tert*-butylphosphanyl)cyclopenta-2,4-dien-1-yl]iron; dichloropalladium (20 mg, 0.03 mmol) and 3-chloro-1-(1-piperidyl)isoquinoline (**230**) (150 mg, 0.61 mmol) in 4:1 acetonitrile:water (12 mL) were degassed under a flow of nitrogen and heated in a microwave reactor at 140 °C for 15 minutes. LCMS confirmed reaction completion (m/z 290). The reaction mixture was diluted with water (20 mL) and extracted twice with ethyl acetate (2 × 25 mL). The combined organic phases were dried over MgSO_4 , filtered and concentrated under reduced pressure (150 mg). The crude was purified *via* flash column chromatography (5 g silica, petroleum ether:ethyl acetate 1:0 to 0:1) to give 1-(1-piperidyl)-3-(4-pyridyl)isoquinoline (**238**) (67 mg, 36%) as pale yellow needle crystals.

R_f 0.38 (100% ethyl acetate); m.p. 129–131 °C; ν_{max} (thin film)/ cm^{-1} 2949 (C-H aliphatic, m), 2918 (C-H aliphatic, m), 2819 (C-H aliphatic, m), 1557 (C-C aromatic, s), 1413 (C-H aliphatic, s), 825 (N-H, s); ^1H NMR (600 MHz, $\text{DMSO}-d_6$) δ 8.68 (d, $J = 5.5$ Hz, 2H, H-2' and H-6'), 8.16 (s, 1H, H-4), 8.14 (d, $J = 5.6$ Hz, 2H, H-3' and H-5'), 8.07 (d, $J = 8.3$ Hz, 1H, H-9), 7.98 (d, $J = 8.3$ Hz, 1H, H-6), 7.74 (t, $J = 7.4$ Hz, 1H, H-7), 7.64 (t, $J = 7.6$ Hz, 1H, H-8), 3.47–3.40 (m, 4H, H-12 and H-16), 1.89–1.76 (m, 4H, H-13 and H-15), 1.68 (d, $J = 5.3$ Hz, 2H, H-14); ^{13}C NMR (151 MHz, $\text{DMSO}-d_6$) δ 161.2 (C-10), 150.1 (C-2' and C-6'), 146.1 (C-4'), 144.3 (C-2), 138.3 (C-4), 130.3 (C-6), 128.0 (C-5), 127.1 (C-7), 125.4 (C-8), 120.9 (C-9), 120.4 (C-3' and C-5'), 112.2 (C-3), 52.1 (C-12 and C-16), 25.6 (C-13 and C-15), 24.4 (C-14); HRMS m/z (ESI⁺) [Found: 290.1639, $\text{C}_{19}\text{H}_{20}\text{N}_3$ requires (M+H)⁺ 290.1652]; LCMS (LCQ) $R_t = 1.9$ min (4 min method), m/z (ESI⁺) 290.4 (M+H)⁺.

***N,N'*-Dimethyl-*N*-[3-(4-pyridyl)-1-isoquinolyl]ethane-1,2-diamine (239)**

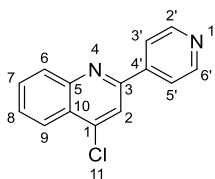
Pyridine-4-boronic acid hydrate (**196**) (74 mg, 0.60 mmol), sodium carbonate (191 mg, 1.8 mmol) and *N*-(3-chloro-1-isoquinolyl)-*N,N'*-dimethyl-ethane-1,2-diamine (**231**) (150 mg, 0.60 mmol) in 4:1 acetonitrile:water (12 mL) were degassed under a flow of nitrogen. *bis*[2-(Di-*tert*-butylphosphanyl)cyclopenta-2,4-dien-1-yl]iron; dichloropalladium (20 mg, 0.03 mmol) was added and the reaction was heated in a sealed microwave reactor vial at 140 °C in a microwave for 15 minutes. LCMS showed formation of the product (*m/z* 293). The reaction mixture was diluted with water (15 mL) and extracted twice with ethyl acetate (2 × 20 mL). The combined organic phases were dried over MgSO₄, filtered and concentrated under reduced pressure to give a brown solid (121 mg). The crude was purified *via* flash column chromatography (12 g silica, petroleum ether:ethyl acetate 1:0 to 0:1) to give *N,N'*-dimethyl-*N*-[3-(4-pyridyl)-1-isoquinolyl]ethane-1,2-diamine (**239**) (110 mg, 60%) as a pale orange solid.

R_f 0.66 (9:1 dichloromethane:methanol); m.p. 118–120 °C; *v*_{max} (thin film)/cm⁻¹ 2962 (m, aliphatic C-H), 1710 (s, C=C), 1687 (s, C=C), 1645 (s, N-H), 1594 (s, aromatic C-C), 1475 (s, aliphatic C-H), 1305 (s, aliphatic C-H), 1220 (s, aliphatic C-N), 1067 (s, aliphatic C-N); ¹H NMR (600 MHz, DMSO-*d*₆) δ 8.65 (d, *J* = 6.0 Hz, 2H, H-2' and H-6'), 8.23 (d, *J* = 8.4 Hz, 1H, H-9), 8.11 (d, *J* = 6.0 Hz, 2H, H-3' and H-5'), 7.83 (d, *J* = 8.0 Hz, 1H, H-6), 7.73 (s, 1H, H-4), 7.67 (t, *J* = 7.5 Hz, 1H, H-7), 7.54 (t, *J* = 7.2 Hz, 2H, H-8 and H-11), 3.74 (q, *J* = 6.5 Hz, 2H, H-12), 2.61 (t, *J* = 7.0 Hz, 2H, H-13), 2.25 (s, 6H, H-15); ¹³C NMR (151 MHz, DMSO-*d*₆) δ 155.1 (C-1), 150.0 (C-2' and C-6'), 146.7 (C-4'), 145.1 (C-3), 137.2 (C-5), 130.1 (C-7), 127.5 (C-6), 126.5 (C-8), 123.0 (C-9), 120.3 (C-3' and C-5'), 118.2 (C-10), 106.8 (C-4), 57.9 (C-13), 45.4 (C-15), 39.0 (C-12); HRMS *m/z* (ESI⁺) [Found: 293.1760, C₁₈H₂₁N₄ requires (M+H)⁺ 293.1761]; LCMS (MDAP) *R_t* = 0.7 min (Ana 5-95 over 5 min), *m/z* (ESI⁺) 293.1 (M+H)⁺.

***N*-Methyl-3-(4-pyridyl)isoquinolin-1-amine (240)**

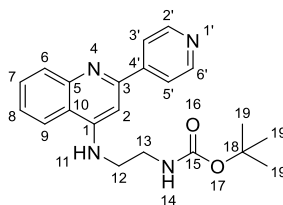
Pyridine-4-boronic acid hydrate (**196**) (91 mg, 0.74 mmol), potassium carbonate (235 mg, 2.22 mmol) and 3-chloro-*N*-methyl-isoquinolin-1-amine (**232**) (150 mg, 0.74 mmol) in 4:1 acetonitrile:water (12 mL) were degassed under a flow of nitrogen. *Bis*[2-(di-*tert*-butylphosphanyl)cyclopenta-2,4-dien-1-yl]iron; dichloropalladium (24 mg, 0.04 mmol) was added and the reaction was heated in a sealed microwave reactor at 140 °C for 15 minutes. LCMS showed formation of the product (m/z 236). The reaction mixture was diluted with water (15 mL) and extracted twice with ethyl acetate (2 × 20 mL). The combined organic phases were dried over MgSO_4 , filtered and concentrated under reduced pressure to give a brown solid (185 mg). The crude was purified *via* flash column chromatography (12 g silica, petroleum ether: ethyl acetate, 1:0 to 0:1) to give *N*-methyl-3-(4-pyridyl)isoquinolin-1-amine (**240**) (123 mg, 67%) as a pale orange solid.

R_f 0.78 (100% ethyl acetate); m.p. 168–170 °C; ν_{max} (thin film)/ cm^{-1} 3306 (N-H, br), 1595 (aromatic C-H, m), 1548 (aromatic C-H, s), 1390 (aliphatic C-H, m), 804 (N-H, s), 732 (C-H, s); ^1H NMR (600 MHz, $\text{DMSO}-d_6$) δ 8.65 (d, $J = 4.6$ Hz, 2H, H-2' and H-6'), 8.22 (d, $J = 8.2$ Hz, 1H, H-9), 8.14 (d, $J = 4.6$ Hz, 2H, H-3' and H-5'), 7.83 (d, $J = 8.0$ Hz, 1H, H-6), 7.73 (s, 1H, H-4), 7.70–7.62 (m, 2H, H-7 and H-11), 7.54 (t, $J = 7.5$ Hz, 1H, H-8), 3.11 (d, $J = 4.3$ Hz, 3H, H-12); ^{13}C NMR (151 MHz, $\text{DMSO}-d_6$) δ 156.2 (C-1), 150.4 (C-2' and C-6'), 147.2 (C-4'), 145.6 (C-3), 137.5 (C-5), 130.6 (C-7), 128.0 (C-6), 127.0 (C-8), 123.4 (C-9), 120.8 (C-3' and C-5'), 118.8 (C-10), 107.2 (C-4), 28.6 (C-12); HRMS m/z (ESI $^+$) [Found: 236.1174, $\text{C}_{15}\text{H}_{14}\text{N}_3$ requires (M+H) $^+$ 236.1182]; LCMS R_t = 0.5 min (4 min method), m/z (ESI $^+$) 236.3 (M+H) $^+$.

4-Chloro-2-(4-pyridyl)quinoline (246)¹⁹⁸

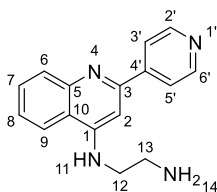
Pyridine-4-boronic acid hydrate (**196**) (124 mg, 1.01 mmol), sodium carbonate (321 mg, 3.03 mmol), 2,4-dichloroquinoline (**225**) (200 mg, 1.01 mmol) and *bis*(triphenylphosphine)-palladium(II) dichloride (35 mg, 0.0500 mmol) in 4:1 acetonitrile:water (16 mL) were de-gassed under a flow of nitrogen and heated in a microwave reactor at 140 °C for 15 minutes. LCMS indicated product formation (m/z 241 and 243). The reaction mixture was diluted with water (40 ml) and extracted twice with ethyl acetate (2 × 50 mL). The combined organic phases were dried over MgSO_4 , filtered and concentrated under reduced pressure to give 4-chloro-2-(4-pyridyl)quinoline (**246**) (310 mg, 100%) as an off-white solid. The intermediate was carried forward without further purification.

^1H NMR (600 MHz, $\text{DMSO}-d_6$) δ 8.77 (d, J = 4.2 Hz, 2H, H-2' and H-6'), 8.52 (s, 1H, H-2), 8.28–8.22 (m, 3H, H-3', H-5' and H-9), 8.20 (d, J = 8.0 Hz, 1H, H-6), 7.94 (t, J = 7.5 Hz, 1H, H-7), 7.81 (t, J = 7.4 Hz, 1H, H-8); LCMS (MDAP) R_t = 2.5 min (Ana 5-95 5 min), m/z (ESI⁺) 241.0 [^{35}Cl] and 243.0 [^{37}Cl] ($\text{M}+\text{H}$)⁺.

***Tert*-Butyl *N*-[2-[[2-(4-pyridyl)-4-quinolyl]amino]ethyl]carbamate (**244**)**

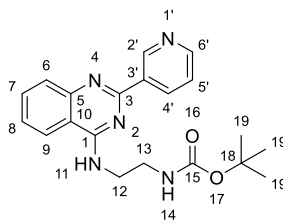
4-Chloro-2-(4-pyridyl)quinoline (**246**) (100 mg, 0.42 mmol), Potassium carbonate (1.15 g, 8.31 mmol), *tert*-butyl *N*-(2-aminoethyl)carbamate (0.13 mL, 0.83 mmol), benzyl(1-{2-[benzyl(phenyl)phosphanyl]-naphthalen-1-yl}naphthalen-2-yl)phenylphosphane (14 mg, 0.02 mmol) and palladium(II) acetate (5 mg, 0.02 mmol) in dry 1,4-dioxane (5 mL) were refluxed for 12 h under nitrogen. The reaction mixture was concentrated under reduced pressure and water (10 mL) was added. The aqueous phase was extracted three times with ethyl acetate (3 × 10 mL). The combined organic layers were dried over MgSO₄, filtered and concentrated under reduced pressure to give a brown mixture (287 mg). The crude was purified by flash column chromatography (10 g silica, petroleum ether:ethyl acetate 1:0 to 0:1) to give *tert*-butyl *N*-[2-[[2-(4-pyridyl)-4-quinolyl]amino]ethyl]carbamate (**244**) (103 mg, 65%) as a yellow foam.

R_f 0.34 (100% ethyl acetate); m.p.186–187 °C; ν_{\max} (thin film)/cm⁻¹ 3322 (br, N-H), 3144 (m, aromatic C-H), 2948 (w, aliphatic C-H), 1586 (s, aromatic C-H), 1431 (s, aliphatic C-H), 1401 (s, aliphatic C-H), 754 (s, N-H); ¹H NMR (600 MHz, DMSO-*d*₆) δ 8.70 (d, *J* = 5.3 Hz, 2H, H-2' and H-6'), 8.21 (d, *J* = 5.1 Hz, 2H, H-3' and H-5'), 8.17 (d, *J* = 8.9 Hz, 1H, H-9), 7.90 (d, *J* = 8.6 Hz, 1H, H-6), 7.67 (t, *J* = 7.3 Hz, 1H, H-7), 7.47 (t, *J* = 7.5 Hz, 1H, H-8), 7.39–7.33 (m, 1H, H-14), 7.24 (s, 1H, H-2), 7.13–7.06 (m, 1H, H-11), 3.54–3.41 (m, 2H, H-13), 3.30–3.21 (m, 2H, H-12), 1.38 (s, 9H, H-19); ¹³C NMR (151 MHz, DMSO-*d*₆) δ 156.1 (C-15), 154.1 (C-3), 151.2 (C-1), 150.0 (C-2' and C-6'), 148.2 (C-5), 147.0 (C-4'), 129.6 (C-7), 129.5 (C-6), 124.5 (C-8), 121.5 (C-9), 121.4 (C-3' and C-5'), 118.5 (C-10), 95.2 (C-2), 78.0 (C-18), 42.7 (C-13), 38.5 (C-12), 28.2 (C-19); HRMS *m/z* (ESI⁺) [Found: 365.1956, C₂₁H₂₄N₄O₂ requires (M+H)⁺ 365.1972]; LCMS (LCQ) *R_t* = 2.3 min (Ana 5-95 in 5 min), *m/z* (ESI⁺) 365.15 (M+H)⁺.

***N'*-[2-(4-pyridyl)-4-quinolyl]ethane-1,2-diamine (245)**

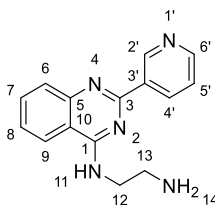
Trifluoro acetic acid (1.4 mL, 18.06 mmol) was added to *tert*-butyl *N*-[2-[[2-(4-pyridyl)-4-quinolyl]amino]ethyl]carbamate (**244**) (70 mg, 0.19 mmol) in dichloromethane (2 mL) over 10 min at 0 °C then at room temperature for 4 h. The reaction mixture was concentrated under reduced pressure, purified by SCX cartridge and the product eluted using 2 M NH₃ in methanol to give *N'*-[2-(4-pyridyl)-4-quinolyl]ethane-1,2-diamine (**245**) (36 mg, 67%) as a yellow oil.

*R*_f 0 (9:1 dichloromethane:methanol); m.p. 175–177 °C; ν_{max} (thin film)/cm⁻¹ 3400 (N-H, br), 3277 (N-H, br), 3071 (aromatic C-H, br), 1586 (aromatic C-H, s), 1531 (aromatic C-H, s), 1474 (aliphatic C-H, s), 1140 (C-N, m), 770 (N-H, s); ¹H NMR (600 MHz, DMSO-*d*₆) δ 8.71 (d, *J* = 5.3 Hz, 2H, H-2' and H-6'), 8.27 (d, *J* = 8.5 Hz, 1H, H-9), 8.16 (d, *J* = 4.9 Hz, 2H, H-3' and H-5'), 7.89 (d, *J* = 8.4 Hz, 1H, H-6), 7.66 (t, *J* = 7.6 Hz, 1H, H-7), 7.57 (s, 1H, H-14), 7.46 (t, *J* = 7.7 Hz, 1H, H-8), 7.35–7.25 (m, 1H, H-11), 7.10 (s, 1H, H-2), 6.90 (s, 1H, H-14), 3.44 (q, *J* = 6.2 Hz, 2H, H-12), 2.89 (t, *J* = 6.5 Hz, 2H, H-13); ¹³C NMR (151 MHz, DMSO-*d*₆) δ 154.1 (C-3), 151.4 (C-1), 150.1 (C-2' and C-6'), 148.2 (C-5), 147.0 (C-4'), 129.5 (C-6), 129.5 (C-7), 124.5 (C-8), 121.8 (C-9), 121.4 (C-3' and C-5'), 118.6 (C-10), 95.2 (C-2), 43.5 (C-13), 39.4 (C-12); HRMS *m/z* (ESI⁺) [Found: 265.1437, C₁₆H₁₇N₄ requires (M+H)⁺ 265.1448]; LCMS (MDAP) *R*_t = 0.7 min (Ana 5-95 in 5 minutes method), *m/z* (ESI⁺) 265.15 (M+H)⁺.

***Tert*-Butyl *N*-[2-[[2-(3-pyridyl)quinazolin-4-yl]amino]ethyl]carbamate**

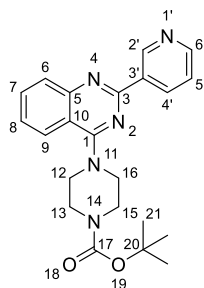
Sodium carbonate (140 mg, 1.32 mmol), *bis*[2-(di-*tert*-butylphosphanyl)cyclopenta-2,4-dien-1-yl]iron; dichloropalladium (14 mg, 0.02 mmol), *tert*-butyl *N*-[2-[(2-chloroquinazolin-4-yl)amino]ethyl]-carbamate (**198**) (150 mg, 0.44 mmol) and pyridine-3-boronic acid (54 mg, 0.44 mmol) in 4:1 acetonitrile: water (12 mL) were degassed under a flow of nitrogen and heated in a microwave reactor at 140 °C for 15 minutes. LCMS indicated product formation (*m/z* 366, 290, 265). Water (15 mL) was added and the mixture was extracted twice with ethyl acetate (2 × 20 mL). The combined organic phases were dried over MgSO₄, filtered and concentrated under reduced pressure to give a brown oil (263 mg). The crude was purified using flash column chromatography (10 g silica, petroleum ether: ethyl acetate 1:0 to 0:1) to give *tert*-butyl *N*-[2-[[2-(3-pyridyl)quinazolin-4-yl]amino]ethyl]carbamate (46 mg, 27%) as a yellow gum.

R_f 0 (9:1 dichloromethane:methanol); *m.p.* 142–144 °C; ν_{\max} (thin film)/cm⁻¹ 3296 (N-H, br), 1574 (aromatic C-H, m), 1534 (aromatic C-H, m), 1492 (aliphatic C-H, m), 765 (N-H, s); ¹H NMR (600 MHz, DMSO-*d*₆) δ 9.61 (s, 1H, H-2'), 8.75 (d, *J* = 7.9 Hz, 1H, H-4'/6'), 8.68 (d, *J* = 4.6 Hz, 1H, H-6'/4'), 8.41 (s, 1H, H-11), 8.30 (d, *J* = 8.3 Hz, 1H, H-9), 7.78 (d, *J* = 2.7 Hz, 2H, H-7/6), 7.58 – 7.45 (m, 2H, H-8 and H-5'), 3.75 – 3.67 (m, 2H, H-12), 2.93 (t, *J* = 6.5 Hz, 2H, H-13), NH₂ peak not observed; ¹³C NMR (151 MHz, DMSO-*d*₆) δ 160.0 (C-1), 157.7 (C-3), 150.7 (C-6'/4'), 149.6 (C-10), 149.3 (C-2'), 135.1 (C-4'/6'), 133.9 (C-6), 132.8 (C-5), 127.8 (C-7), 125.6 (C-8), 123.4 (C-5'), 123.0 (C-9), 114.1 (C-3'), 42.4 (C-12), 39.8 (C-13); HRMS *m/z* (ESI⁺) [Found: 266.1393, C₁₅H₁₆N₅ requires [M+H]⁺ 266.1400]; LCMS (LCQ) *R_t* = 0.4 min (4 min method), *m/z* (ESI⁺) 266.20 (M+H)⁺.

***N'*-[2-(3-Pyridyl)quinazolin-4-yl]ethane-1,2-diamine (260)**

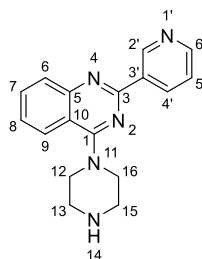
Tert-Butyl *N*-[2-[[2-(3-pyridyl)quinazolin-4-yl]amino]ethyl]carbamate (35 mg, 0.10 mmol) was stirred in dichloromethane (1 mL) and cooled to 0 °C. Trifluoro acetic acid (0.29 mL, 3.83 mmol) was added and the reaction was stirred at 0 °C for ten minutes then allowed to warm up to room temperature and stir overnight. LCMS formed (*m/z* 266). The reaction mixture was concentrated under reduced pressure and purified by SCX cartridge and eluted with 2 M NH₃ in methanol then concentrated under reduced pressure to give *N'*-[2-(3-pyridyl)quinazolin-4-yl]ethane-1,2-diamine (**260**) (23 mg, 86%) as a yellow solid.

R_f 0 (9:1 dichloromethane:methanol); m.p. 142–144 °C; ν_{max} (thin film)/cm⁻¹ 3296 (N-H, br), 1574 (aromatic C-H, m), 1534 (aromatic C-H, m), 1492 (aliphatic C-H, m), 765 (N-H, s); ¹H NMR (600 MHz, DMSO-*d*₆) δ 9.61 (s, 1H, H-2'), 8.75 (d, *J* = 7.9 Hz, 1H, H-4'/6'), 8.68 (d, *J* = 4.6 Hz, 1H, H-6'/4'), 8.41 (s, 1H, H-11), 8.30 (d, *J* = 8.3 Hz, 1H, H-9), 7.78 (d, *J* = 2.7 Hz, 2H, H-7/6), 7.58–7.45 (m, 2H, H-8 and H-5'), 3.75–3.67 (m, 2H, H-12), 2.93 (t, *J* = 6.5 Hz, 2H, H-13), NH₂ peak not observed; ¹³C NMR (151 MHz, DMSO-*d*₆) δ 160.0 (C-1), 157.7 (C-3), 150.7 (C-6'/4'), 149.6 (C-10), 149.3 (C-2'), 135.1 (C-4'/6'), 133.9 (C-6), 132.8 (C-5), 127.8 (C-7), 125.6 (C-8), 123.4 (C-5'), 123.0 (C-9), 114.1 (C-3'), 42.4 (C-12), 39.8 (C-13); HRMS *m/z* (ESI⁺) [Found: 266.1393, C₁₅H₁₆N₅ requires (M+H)⁺ 266.1400]; LCMS (LCQ) *R_t* = 0.4 min (4 min method), *m/z* (ESI⁺) 266.20 (M+H)⁺.

***Tert*-butyl 4-[2-(3-pyridyl)quinazolin-4-yl]piperazine-1-carboxylate¹⁹⁸**

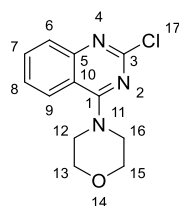
Bis(Triphenylphosphine)palladium(II) dichloride (15 mg, 0.02 mmol), sodium carbonate (137 mg, 1.29 mmol), *tert*-butyl 4-(2-chloroquinazolin-4-yl)piperazine-1-carboxylate (**198**) (150 mg, 0.43 mmol) and pyridine-3-boronic acid (53 mg, 0.43 mmol) in 4:1 acetonitrile:water (12 mL) were degassed under a flow of nitrogen and heated in a microwave reactor at 140 °C for 15 minutes. LCMS confirmed reaction completion (m/z 392, 336, 292). The reaction mixture was diluted with water (20 mL) and extracted twice with ethyl acetate (2 × 25 mL). The combined organic phases were dried over MgSO_4 , filtered and concentrated under reduced pressure to give a yellow oil (167 mg). The crude was purified *via* flash column chromatography (5 g petroleum ether:ethyl acetate 1:0 to 0:1) to give a yellow solid (76 mg) which was further purified *via* SCX cartridge by eluting with methanol then 2 M ammonia in methanol to give *tert*-butyl 4-[2-(3-pyridyl)quinazolin-4-yl]piperazine-1-carboxylate (66 mg, 37%) as an off-white solid.

^1H NMR (600 MHz, $\text{DMSO}-d_6$) δ 9.61 (d, J = 1.5 Hz, 1H, H-2'), 8.76 (dt, J = 7.9, 1.9 Hz, 1H, H-4'), 8.70 (dd, J = 4.7, 1.7 Hz, 1H, H-6'), 8.08 (d, J = 8.0 Hz, 1H, H-9), 7.92 (d, J = 8.3 Hz, 1H, H-6), 7.86 (t, J = 7.6 Hz, 1H, H-7), 7.60–7.50 (m, 2H, H-8 and H-5'), 3.89–3.82 (m, 4H, H-13 and H-15), 3.61 (s, 4H, H-12 and H-16), 1.44 (s, 9H, H-20); LCMS (LCQ) R_t = 0.8 min (4 min method), m/z (ESI⁺) 392.07 ($\text{M}+\text{H}$)⁺, 336.2 ($\text{M}+\text{H}-t\text{-Bu}$)⁺, 292.1 ($\text{M}+\text{H}-\text{Boc}$)⁺.

4-Piperazin-1-yl-2-(3-pyridyl)quinazoline (261)

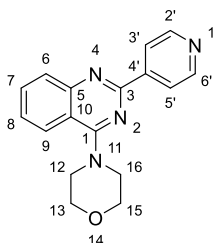
Tert-Butyl 4-[2-(3-pyridyl)quinazolin-4-yl]piperazine-1-carboxylate (50 mg, 0.13 mmol) was dissolved in dichloromethane (1 mL) and cooled to 0 °C. Trifluoro acetic acid (0.5 mL, 5.17 mmol) was added dropwise and the reaction mixture was allowed to stir at room temperature overnight. LCMS (LCQ) indicated product formation (m/z 292). The reaction mixture was concentrated under reduced pressure to give a yellow solid. The crude was purified *via* SCX cartridge by elution with methanol then 2 M ammonia in methanol to give 4-piperazin-1-yl-2-(3-pyridyl)quinazoline (**261**) (38 mg, 97%) as a yellow solid.¹⁰⁶

R_f 0.18 (9:1 dichloromethane:methanol); m.p. 182-185 °C; ν_{\max} (thin film)/ cm^{-1} 3024 (aromatic C-H, w), 2851 (aliphatic C-H, w), 1683 (aromatic C=C, m), 1562 (aromatic C-C, m), 1539 (aromatic C-C, m), 1499 (aliphatic C-H, s), 1114 (C-N, s), 768 (N-H, s); ^1H NMR (600 MHz, $\text{DMSO}-d_6$) δ 9.66–9.54 (m, 1H, H-2'), 8.76 (dt, $J = 7.9$ Hz, 1H, H-4'), 8.70 (td, $J = 4.7$ Hz, 1H, H-6'), 8.08 (d, $J = 8.2$ Hz, 1H, H-9), 7.93 (d, $J = 8.3$ Hz, 1H, H-6), 7.87 (t, $J = 7.6$ Hz, 1H, H-7), 7.62–7.50 (m, 2H, H-8 and H-5'), 3.94 (t, $J = 5.0$ Hz, 4H, H-12 and H-16), 3.23 (t, $J = 5.1$ Hz, 4H, H-13 and H-15); ^{13}C NMR (151 MHz, $\text{DMSO}-d_6$) δ 164.5 (C-1), 156.9 (C-3), 152.3 (C-5), 151.4 (C-6'), 149.7 (C-2'), 149.7 (C-3'), 135.6 (C-4'), 133.7 (C-7), 128.8 (C-6), 126.4 (C-8), 125.8 (C-9), 124.0 (C-5'), 115.2 (C-10), 48.2 (C-12 and C-16), 44.0 (C-13 and C-15); HRMS m/z (ESI⁺) [Found: 292.1560, $\text{C}_{17}\text{H}_{18}\text{N}_5$ requires (M+H)⁺ 292.1557]; LCMS (LCQ) $R_t = 0.6$ min (4 min method), m/z (ESI⁺) 292.4 (M+H)⁺.

4-(2-Chloroquinazolin-4-yl)morpholine^{181,184,185,191,200–202}

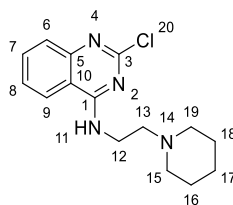
2,4-Dichloroquinazoline (**194**) (250 mg, 1.26 mmol), triethylamine (0.26 mL, 1.88 mmol) and morpholine (0.12 mL, 1.38 mmol) were stirred in THF (2.5 mL) at 0 °C for 1 h in a water/ice bath. TLC and LCMS (LCQ) indicated product formation (m/z 250 and 252). The reaction mixture was concentrated under reduced pressure and water (20 mL) was added followed by extraction twice by ethyl acetate (2 × 25 mL). The combined organic phases were dried over MgSO_4 and concentrated under reduced pressure to give a white solid (190 mg). The crude was purified by flash column chromatography (10 g silica, petroleum ether:ethyl acetate, 1:0 to 0:1) to give 4-(2-chloroquinazolin-4-yl)morpholine (114 mg, 33%) as a white solid.

^1H NMR (600 MHz, $\text{DMSO}-d_6$) δ 8.04 (d, J = 8.4 Hz, 1H, H-9), 7.82 (t, J = 7.7 Hz, 1H, H-7), 7.71 (d, J = 8.4 Hz, 1H, H-6), 7.52 (t, J = 7.6 Hz, 1H, H-8), 3.86–3.78 (m, 4H, H-13 and H-15), 3.79–3.72 (m, 4H, H-12 and H-16); LCMS (LCQ) R_t = 1.6 min (4 min method), m/z (ESI⁺) 250.3 [^{35}Cl] and 252.3 [^{37}Cl] ($\text{M}+\text{H}$)⁺.

4-[2-(4-Pyridyl)quinazolin-4-yl]morpholine (262)

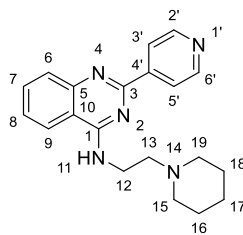
Pyridine-4-boronic acid hydrate (**196**) (69 mg, 0.56 mmol), *bis*(triphenylphosphine)palladium(II) dichloride (20 mg, 0.03 mmol), potassium carbonate (178 mg, 1.68 mmol) and 4-(2-chloroquinazolin-4-yl)morpholine (140 mg, 0.56 mmol) in 4:1 acetonitrile:water (12 mL) were degassed under a flow of nitrogen and heated in a microwave reactor at 140 °C for 15 minutes. LCMS confirmed reaction completion (*m/z* 293 and 295). The reaction mixture was diluted with water (20 mL) and extracted twice with ethyl acetate (2 × 25 mL). The combined organic phases were dried over MgSO_4 , filtered and concentrated under reduced pressure to give a pale yellow solid (135 mg). The crude was purified via flash column chromatography (5 g silica, petroleum ether: ethyl acetate, 1:0 to 0:1) to give 4-[2-(4-pyridyl)quinazolin-4-yl]morpholine (**262**) (116 mg, 67%).

R_f 0.38 (100% ethyl acetate); m.p. 157–160 °C; ν_{max} (thin film)/ cm^{-1} 3345 (N-H, br), 2951 (aliphatic C-H, w), 1688 (C=C, m), 1557 (aromatic C-H, m), 1528 (aromatic C-H, s), 1501 (aromatic C-H, s), 1492 (aliphatic C-H, s), 1114 (C-N, s), 768 (N-H, s), 674 (C-H, s); ^1H NMR (600 MHz, $\text{DMSO}-d_6$) δ 8.66 (m, 2H, H-2' and H-6'), 8.34 (m, 2H, H-3' and H-5'), 8.10 (d, J = 8.4 Hz, 1H, H-9), 7.95 (d, J = 8.3 Hz, 1H, H-6), 7.88 (t, J = 7.5 Hz, 1H, H-7), 7.59 (t, J = 7.5 Hz, 1H, H-8), 3.86 (dd, J = 20.4, 4.5 Hz, 8H, H-12, H-13, H-14 and H-15); ^{13}C NMR (151 MHz, $\text{DMSO}-d_6$) δ 164.0 (C-1), 156.2 (C-3), 151.8 (C-5), 150.2 (C-3' and C-5'), 145.2 (C-4'), 133.1 (C-7), 128.6 (C-6), 126.1 (C-8), 125.4 (C-9), 121.8 (C-2' and C-6'), 115.0 (C-10), 66.0 (C-12 and C-16), 49.6 (C-13 and C-15); HRMS *m/z* (ESI⁺) [Found: 293.1392, $\text{C}_{17}\text{H}_{17}\text{N}_4\text{O}$ requires (M+H)⁺ 293.1397]; LCMS Rt = 0.56 min (4 min method), *m/z* (ESI⁺) 293.4 (M+H)⁺.

2-Chloro-*N*-[2-(1-piperidyl)ethyl]quinazolin-4-amine

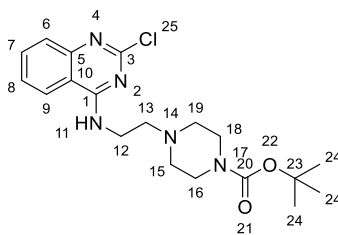
2,4-Dichloroquinazoline (**194**) (500 mg, 2.51 mmol), triethylamine (0.53 mL, 3.77 mmol) and 2-(1-piperidiny)ethanamine (1.1 mL, 7.54 mmol) were stirred in tetrahydrofuran (5 mL) at 0 °C for 1 h in a water/ice bath. TLC and LCMS (LCQ) indicated product formation (m/z 323 and 325, 269 and 267). The reaction mixture was concentrated under reduced pressure to give a colourless oil (422 mg, excess thought to be due to unreacted amine). The crude was purified by flash column chromatography (12 g silica, petroleum ether:ethyl acetate, 1:0 to 0:1) to give 2-chloro-*N*-[2-(1-piperidyl)ethyl]quinazolin-4-amine (564 mg, 73%) as a clear colourless glass.

^1H NMR (600 MHz, $\text{DMSO}-d_6$) δ 8.67 (t, $J = 5.6$ Hz, 1H, H-11), 8.22 (d, $J = 8.3$ Hz, 1H, H-9), 7.79 (t, $J = 7.7$ Hz, 1H, H-7), 7.61 (d, $J = 8.4$ Hz, 1H, H-6), 7.53 (t, $J = 7.5$ Hz, 1H, H-8), 3.62 (q, $J = 6.5$ Hz, 2H, H-12), 2.62–2.52 (m, 2H, H-13), 2.43 (s, 4H, H-15 and H-19), 1.49 (p, $J = 5.3$ Hz, 4H, H-16 and H-18), 1.41–1.33 (m, 2H, H-17); LCMS (LCQ) $R_t = 0.4$ min (4 min method), m/z (ESI $^+$) 291.2 [^{35}Cl] and 293.1 [^{37}Cl] ($\text{M}+\text{H}$) $^+$.

***N*-[2-(1-Piperidyl)ethyl]-2-(4-pyridyl)quinazolin-4-amine (263)**

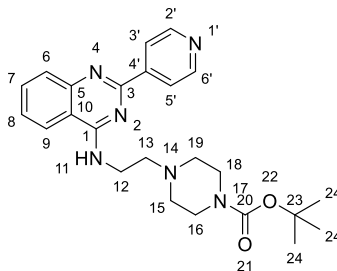
Pyridine-4-boronic acid hydrate (**196**) (60 mg, 0.49 mmol), *bis*(triphenylphosphine)palladium(II) dichloride (17 mg, 0.02 mmol), sodium carbonate (156 mg, 1.47 mmol) and 2-chloro-*N*-[2-(1-piperidyl)ethyl]-quinazolin-4-amine (150 mg, 0.49 mmol) in 4:1 acetonitrile:water (12 mL) were degassed under a flow of nitrogen and heated in a microwave reactor at 140 °C for 15 minutes. LCMS confirmed reaction completion (*m/z* 334). The reaction mixture was diluted with water (15 mL) and extracted twice with ethyl acetate (2 × 20 mL). The combined organic phases were dried over MgSO₄, filtered and concentrated under reduced pressure to give a heterogeneous mixture (215 mg). The crude was purified *via* flash column chromatography (10 g silica, petroleum ether: ethyl acetate 1:0 to 0:1) to give *N*-[2-(1-piperidyl)ethyl]-2-(4-pyridyl)quinazolin-4-amine (**263**) (105 mg, 61%) as an orange solid.

R_f 0.08 (9:1 ethyl acetate:methanol); m.p. 151–153 °C; *v*_{max} (thin film)/cm⁻¹ 3261 (N-H, br), 2932 (aliphatic C-H, m), 1588 (aromatic C-H, s), 1574 (aromatic C-H, s), 1460 (aliphatic C-H, s), 761 (N-H, s); ¹H NMR (600 MHz, DMSO-*d*₆) δ 8.74 (d, *J* = 4.8 Hz, 2H, H-2' and H-6'), 8.43 (s, 1H, H-11), 8.33 (d, *J* = 5.0 Hz, 2H, H-3' and H-5'), 8.26 (d, *J* = 8.3 Hz, 1H, H-9), 7.82 (app. d, *J* = 3.2 Hz, 2H, H-6 and H-7), 7.60–7.52 (m, 1H, H-8), 3.82 (app. s, 2H, H-12), 2.65 (app. s, 2H, H-13), 2.48 (app. s, 4H, H-15 and H-19), 1.50 (app. s, 4H, H-16 and H-18), 1.38 (app. s, 2H, H-17); ¹³C NMR (151 MHz, DMSO-*d*₆) δ 159.9 (C-1), 157.5 (C-3), 150.1 (C-2' and C-6'), 149.5 (C-5/10), 145.9 (C-4'), 132.9 (C-7), 128.1 (C-6), 126.2 (C-8), 122.7 (C-9), 121.7 (C-3' and C-5'), 114.3 (C-10/5), 57.1 (C-13), 54.1 (C-15 and C-19), 38.1 (C-12), 25.4 (C-16 and C-18), 23.8 (C-17); HRMS *m/z* (ESI⁺) [Found: 334.2018, C₂₀H₂₄N₅ requires (M+H)⁺ 334.2026]; LCMS (LCQ) *R_t* = 0.4 min (4 min method), *m/z* (ESI⁺) 334.2 (M+H)⁺.

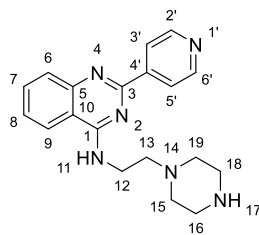
***Tert*-Butyl 4-[2-[(2-chloroquinazolin-4-yl)amino]ethyl]piperazine-1-carboxylate**

2,4-Dichloroquinazoline (**194**) (300 mg, 1.51 mmol), triethylamine (0.32 mL, 2.26 mmol) and 2-methyl-2-propanyl 4-(2-aminoethyl)-1-piperazinecarboxylate (1.04 g, 4.52 mmol) were stirred in THF (3 mL) at 0 °C for 1 h in a water/ice bath. LCMS (LCQ) indicated product formation (m/z 392 and 394). The reaction mixture was concentrated under reduced pressure and diluted with water (15 mL) and extracted twice with ethyl acetate (2 × 15 mL). The combined organic phases were dried over MgSO_4 , filtered and concentrated under reduced pressure to give a yellow oil (372 mg). The crude was purified *via* flash column chromatography (10 g silica, petroleum ether:ethyl acetate 1:0 to 0:1) to give *tert*-butyl 4-[2-[(2-chloroquinazolin-4-yl)amino]ethyl]piperazine-1-carboxylate (147 mg, 24%) as a white solid.

^1H NMR (600 MHz, $\text{DMSO}-d_6$) δ 8.69 (t, J = 5.1 Hz, 1H, H-11), 8.23 (d, J = 8.4 Hz, 1H, H-9), 7.79 (t, J = 7.6 Hz, 1H, H-7), 7.61 (d, J = 8.2 Hz, 1H, H-6), 7.53 (t, J = 7.7 Hz, 1H, H-8), 3.64 (app. q, J = 6.7 Hz, 2H, H-12), 3.29 (app. s, 4H, H-16 and H-18), 2.60 (t, J = 6.6 Hz, 2H, H-13), 2.40 (m, 4H, H-15 and H-19), 1.39 (s, 9H, H-24); LCMS (LCQ) R_t = 0.5 min (4 min method), m/z (ESI $^+$) 392.0 [^{35}Cl] and 394.2 [^{37}Cl] ($\text{M}+\text{H}$) $^+$.

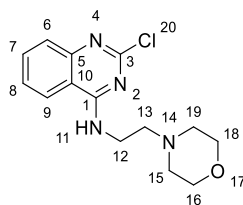


R_f 0.11 (100% ethyl acetate); m.p. 118–120 °C; ν_{max} (thin film)/cm⁻¹ 3251 (N-H, br), 2939 (aliphatic C-H, w), 1691 (C=O, m), 1586 (aromatic C-H, s), 1561 (aromatic C-H, s), 1526 (aromatic C-H, s), 1117 (C-N, s), 762 (N-H, s); ¹H NMR (600 MHz, DMSO-*d*₆) δ 8.74 (d, *J* = 5.2 Hz, 2H, H-2 and H-6'), 8.44 (t, *J* = 5.3 Hz, 1H, H-11), 8.33 (d, *J* = 5.2 Hz, 2H, H-3' and H-5'), 8.26 (d, *J* = 8.4 Hz, 1H, H-9), 7.82 (d, *J* = 3.5 Hz, 2H, H-6 and H-7), 7.56 (dd, *J* = 8.0, 3.9 Hz, 2H, H-8/7), 3.83 (q, *J* = 6.5 Hz, 2H, H-12), 3.29 (app. s, 4H, H-16 and H-18), 2.70 (t, *J* = 6.7 Hz, 2H, H-13), 2.47 (app. s, 4H, H-15 and H-19), 1.38 (s, 9H, H-23); ¹³C NMR (151 MHz, DMSO-*d*₆) δ 159.9 (C-1), 157.5 (C-3), 153.8 (C-21), 150.1 (C-2' and C-6'), 149.5 (C-5), 145.9 (C-4'), 133.0 (C-7), 131.4 (TPP/C-8), 128.8 (TPP/C-8), 128.1 (TPP/C-6), 126.2 (TPP/C-8), 122.7(C-9), 121.7 (C-3' and C-5'), 114.3 (C-10), 78.7 (C-23), 56.4 (C-13), 52.6 (C-15 and C-19), 43.9 (C-16/18), 42.6 (C-18/16), 38.1 (C-12), 28.0 (C-24), TPP = triphenylphosphine oxide impurity; HRMS *m/z* (ESI⁺) [Found: 435.2507, C₂₄H₃₁N₆O₂ requires (M+H)⁺ 435.2503]; LCMS (LCQ) Rt = 0.45 min (4 min method), *m/z* (ESI⁺) 335.15 (M+H)⁺, 379.2 (M+H-*t*-Bu)⁺, 435.1 (M+H-Boc)⁺.

***N*-(2-Piperazin-1-ylethyl)-2-(4-pyridyl)quinazolin-4-amine (264)¹⁹⁹**

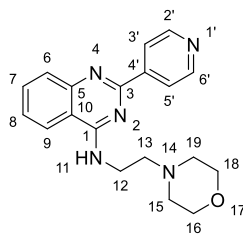
Tert-Butyl 4-[2-[[2-(4-pyridyl)quinazolin-4-yl]amino]ethyl]piperazine-1-carboxylate (90 mg, 0.21 mmol) was stirred in trifluoro acetic acid (1.49 mL, 19.47 mmol) and dichloromethane (2 mL) for 10 min at 0 °C then at room temperature for 4 h. LCMS confirmed product formation (m/z 335). The reaction mixture was concentrated under reduced pressure, purified by SCX cartridge and the product eluted using 2M NH_3 in methanol to give *N*-(2-piperazin-1-ylethyl)-2-(4-pyridyl)quinazolin-4-amine (**264**) (63 mg, 86%) as a yellow oil.

R_f 0 (9:1 dichloromethane:methanol); m.p. N/A; ν_{max} (thin film)/ cm^{-1} 3290 (N-H, br), 2940 (aliphatic C-H, br), 2826 (aliphatic C-H, br), 1579 (N-H, s), 1559 (C=C, s), 1527 (aromatic C-H), 1411 (aliphatic C-H, s), 764 (N-H, s); ^1H NMR (600 MHz, $\text{DMSO}-d_6$) δ 8.74 (d, $J = 5.3$ Hz, 2H, H-2' and H-6'), 8.47–8.37 (m, 1H, H-11), 8.33 (d, $J = 5.3$ Hz, 2H, H-3' and H-5'), 8.26 (d, $J = 8.1$ Hz, 2H, H-9/8/7/6), 7.81 (d, $J = 3.7$ Hz, 2H, H-8/7/6/9), 7.61–7.51 (m, 1H, H-7/6/9/8), 3.81 (q, $J = 6.5$ Hz, 2H, H-12), 2.75 (s, 4H, H-16 and H-18), 2.66 (t, $J = 6.7$ Hz, 2H, H-13), 2.48 (s, 4H, H-15 and H-19); ^{13}C NMR (151 MHz, $\text{DMSO}-d_6$) δ 159.9 (C-1), 157.5 (C-3), 150.1 (C-2' and C-6'), 149.5 (C-5), 146.0 (C-4'), 133.0 (C-7), 128.1 (C-6), 126.2 (C-8), 122.8 (C-9), 121.8 (C-3' and C-5'), 114.3 (C-10), 57.0 (C-13), 53.2 (C-15 and C-19), 45.0 (C-16 and C-18), 38.0 (C-12); HRMS m/z (ESI⁺) [Found: 335.1965, $\text{C}_{19}\text{H}_{23}\text{N}_6$ requires (M+H)⁺ 335.1979]; LCMS (MDAP) $R_t = 3.0$ min (Ana 30-95 in 20 min), m/z (ESI⁺) 335.0 (M+H)⁺.

2-Chloro-*N*-(2-morpholinoethyl)quinazolin-4-amine¹⁸⁶

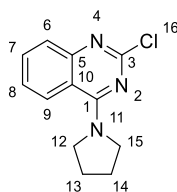
2,4-Dichloroquinazoline (**194**) (250 mg, 1.26 mmol), triethylamine (0.26 mL, 1.88 mmol) and 4-(2-amino-ethyl)morpholine (0.20 mL, 1.38 mmol) were stirred in THF (2.5 mL) at 0 °C for 1 h in a water/ice bath. TLC and LCMS indicated product formation (m/z 293 and 295). The reaction mixture was concentrated under reduced pressure and water (25 mL) was added. The mixture was extracted four times with ethyl acetate (4 x 25 mL). The combined organic phases were dried over MgSO_4 , filtered and concentrated under reduced pressure to give an orange oil (278 mg). The crude was purified *via* flash column chromatography (10 g silica, petroleum ether:ethyl acetate, 1:0 to 0:1) to give 2-chloro-*N*-(2-morpholinoethyl)quinazolin-4-amine (199 mg, 51%) as a pale orange solid.

^1H NMR (600 MHz, $\text{DMSO}-d_6$) δ 8.69 (t, $J = 5.3$ Hz, 1H, H-11), 8.23 (d, $J = 8.2$ Hz, 1H, H-9), 7.79 (t, $J = 7.6$ Hz, 1H, H-7), 7.61 (d, $J = 8.3$ Hz, 1H, H-6), 7.54 (t, $J = 7.6$ Hz, 1H, H-8), 3.64 (q, $J = 6.4$ Hz, 2H, H-12), 3.56 (t, $J = 4.2$ Hz, 4H, H-16 and H-18), 2.58 (t, $J = 6.7$ Hz, 2H, H-13), 2.46 (s, 4H, H-15 and H-19); LCMS (LCQ) $R_t = 0.44$ min (4 min method), m/z (ESI⁺) 293.1 [^{35}Cl] and 295.1 [^{37}Cl] ($\text{M}+\text{H}$)⁺.

***N*-(2-Morpholinoethyl)-2-(4-pyridyl)quinazolin-4-amine (265)**

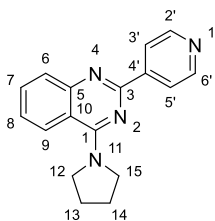
Pyridine-4-boronic acid hydrate (**196**) (63 mg, 0.51 mmol), *bis*(triphenylphosphine)palladium(II) dichloride (18 mg, 0.03 mmol), potassium carbonate (163 mg, 1.54 mmol) and 2-chloro-*N*-(2-morpholinoethyl)-quinazolin-4-amine (150 mg, 0.51 mmol) in 4:1 acetonitrile:water (12 mL) were degassed under a flow of nitrogen and heated in a microwave reactor at 140 °C for 15 minutes. LCMS confirmed reaction completion (m/z 336). The reaction mixture was diluted with water (15 mL) and extracted twice with ethyl acetate (2 × 20 mL). The combined organic phases were dried over MgSO_4 , filtered and concentrated under reduced pressure to give *N*-(2-morpholinoethyl)-2-(4-pyridyl)quinazolin-4-amine (**265**) (121 mg, 66%) as a pale yellow solid.

R_f 0.25 (9:1 ethyl acetate:methanol); m.p. 102–103 °C; ν_{max} (thin film)/ cm^{-1} 3289 (N-H, br), 3053 (aromatic C-H, w), 2948 (aliphatic C-H, w), 2854 (aliphatic C-H, w), 1583 (C=C, s), 1113 (aliphatic C-N, s), 721 (N-H, s), 694 (C-H, s); ^1H NMR (600 MHz, $\text{DMSO}-d_6$) δ 8.74 (d, J = 5.8 Hz, 2H, H-2' and H-6'), 8.46–8.40 (m, 1H, H-11), 8.33 (d, J = 5.7 Hz, 2H, H-3' and H-5'), 8.27 (d, J = 8.1 Hz, 1H, H-9), 7.82 (d, J = 4.0 Hz, 2H, H-8/7/6), 7.65–7.58 (m, 1H, H-8/7/6), 7.58–7.54 (m, 2H, H-7/6/8), 3.83 (q, J = 6.5 Hz, 2H, H-12), 3.58 (t, J = 4.6 Hz, 4H, H-16 and H-18), 2.68 (t, J = 6.9 Hz, 2H, H-13). H-15 and H-19 under solvent peak according to COSY NMR; ^{13}C NMR (151 MHz, $\text{DMSO}-d_6$) δ 159.9 (C-1), 157.5 (C-3), 150.1 (C-2' and C-6'), 149.5 (C-5), 145.9 (C-4'), 132.9 (C-8/7/6), 128.1 (C-8/7/6), 126.2 (C-8/7/6), 122.7 (C-9), 121.7 (C-3' and C-5'), 114.3 (C-10), 66.2 (C-16 and C-18), 56.9 (C-13), 53.4 (C-15 and C-19), 37.9 (C-12); HRMS m/z (ESI⁺) [Found: 336.1810, $\text{C}_{19}\text{H}_{22}\text{N}_5\text{O}$ requires (M+H)⁺ 336.1819]; LCMS (LCQ) Rt = 0.4 min (4 min method), m/z (ESI⁺) 336.3 (M+H)⁺.

2-Chloro-4-pyrrolidin-1-yl-quinazoline^{185,203–205}

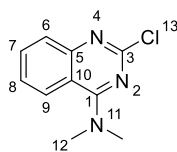
2,4-Dichloroquinazoline (**194**) (250 mg, 1.26 mmol), triethylamine (0.26 mL, 1.88 mmol) and pyrrolidine (0.11 mL, 1.38 mmol) were stirred in tetrahydrofuran (2.5 mL) at 0 °C for 1 h in a water/ice bath. TLC and LCMS (MDAP) indicated product formation (m/z 234 and 236). The reaction mixture was concentrated under reduced pressure and water (25 mL) was added. The mixture was extracted twice with ethyl acetate (2 × 25 mL). The combined organic phases were dried over MgSO_4 , filtered and concentrated under reduced pressure (227 mg). The crude was purified *via* flash column chromatography (10 g silica, petroleum ether:ethyl acetate 1:0 to 0:1) to give 2-chloro-4-pyrrolidin-1-yl-quinazoline (80 mg, 26%) as a white solid.

^1H NMR (500 MHz, $\text{DMSO}-d_6$) δ 8.31 (d, J = 8.4 Hz, 1H, H-9), 7.78 (t, J = 7.6 Hz, 1H, H-7), 7.62 (d, J = 8.3 Hz, 1H, H-6), 7.48 (t, J = 7.8 Hz, 1H, H-8), 3.88 (s, 4H, H-12 and H-15), 1.97 (s, 4H, H-13 and H-14); LCMS (MDAP) R_t = 2.1 min (Ana 5-95 in 5 min), m/z (ESI⁺) 234.05 [^{35}Cl] and 236.00 [^{37}Cl] ($\text{M}+\text{H}$)⁺.

2-(4-Pyridyl)-4-pyrrolidin-1-yl-quinazoline (266)

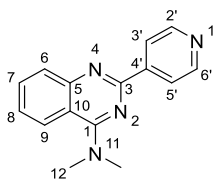
Pyridine-4-boronic acid hydrate (**196**) (42 mg, 0.34 mmol), bis(triphenylphosphine)-palladium(II) dichloride (12 mg, 0.02 mmol), potassium carbonate (142 mg, 1.03 mmol) and 2-chloro-4-pyrrolidin-1-yl-quinazoline (80 mg, 0.34 mmol) in 4:1 acetonitrile:water (6.4 mL) was degassed under a flow of nitrogen and heated in a microwave reactor at 140 °C for 15 minutes. LCMS confirmed product formation (m/z 277). Water (8 mL) was added and the reaction mixture was extracted twice with ethyl acetate (2 × 10 mL). The organic phases were combined, dried over MgSO_4 , filtered and concentrated under reduced pressure to give a white solid (62 mg). The crude was purified *via* flash column chromatography (4 g silica, petroleum ether:ethyl acetate 1:0 to 0:1) to give 2-(4-pyridyl)-4-pyrrolidin-1-yl-quinazoline (**266**) (42 mg, 38%) as a white solid.

R_f 0.72 (100% ethyl acetate); m.p. 154–156 °C; ν_{max} (thin film)/ cm^{-1} 2971 (aromatic C-H, br), 2866 (aromatic C-H, br), 1558 (aliphatic C-H, s), 1501 (aliphatic C-H, s), 1459 (aromatic C-H, s), 677 (aromatic C-H, s); ^1H NMR (500 MHz, $\text{DMSO}-d_6$) δ 8.73 (d, J = 6.0 Hz, 2H, H-2' and H-6'), 8.37–8.29 (m, 3H, H-3', H-5' and H-9), 7.88–7.75 (m, 2H, H-6 and H-7), 7.51 (t, J = 6.8 Hz, 1H, H-8), 4.00 (s, 4H, H-12 and H-15), 2.08–1.93 (m, 4H, H-13 and H-14); ^{13}C NMR (151 MHz, $\text{DMSO}-d_6$) δ 159.3 (C-3/1), 156.5 (C-1/3), 151.6 (C-5), 150.1 (C-2' and C-6'), 145.8 (C-4'), 132.5 (C-7), 128.0 (C-6), 125.9 (C-9), 125.2 (C-8), 121.8 (C-3' and C-5'), 115.2 (C-10), 50.6 (C-12 and C-15), 39.1 (C-13 and C-14); HRMS m/z (ESI⁺) [Found: 277.1442, $\text{C}_{17}\text{H}_{17}\text{N}_4$ requires (M+H)⁺ 277.1448]; LCMS (MDAP) R_t = 3.6 min (Ana 30-95 in 8 min), m/z (ESI⁺) 277.00 (M+H)⁺.

2-Chloro-*N,N*-dimethyl-quinazolin-4-amine^{195,196,212,213,197,204,206–211}

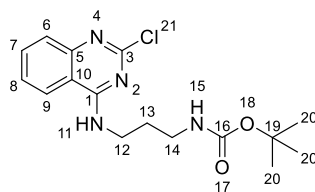
2,4-Dichloroquinazoline (200 mg, 1 mmol), triethylamine (0.21 mL, 1.51 mmol) and dimethylamine (0.55 mL, 1.11 mmol) were stirred in tetrahydrofuran (2 mL) at 0 °C for 1 h in a water/ice bath. LCMS (MDAP) indicated product formation (m/z 208 and 210). The reaction mixture was concentrated under reduced pressure and water (25 mL) was added. The mixture was extracted twice with ethyl acetate (2 × 25 mL). The combined organic phases were dried over MgSO_4 , filtered and concentrated under reduced pressure (227 mg). The crude was purified *via* flash column chromatography (10 g silica, petroleum ether:ethyl acetate 1:0 to 0:1) to give a 3:1 mixture (by ^1H NMR) of 2-chloro-*N,N*-dimethyl-quinazolin-4-amine (76 mg, 27%) and excess starting material as a white solid. The intermediate was carried forward without further purification.

^1H NMR (600 MHz, $\text{DMSO}-d_6$) δ 8.23 (d, $J = 8.5$ Hz, 1H, H-9), 7.79 (t, $J = 8.2$ Hz, 1H, H-7), 7.65 (d, $J = 8.9$ Hz, 1H, H-6), 7.48 (t, $J = 8.3$ Hz, 1H, H-8), 3.37 (s, 6H, H-12); LCMS (LCQ) $R_t = 1.8$ min (4 min method), m/z (ESI $^+$) 208.3 [^{35}Cl] and 210.3 [^{37}Cl] ($\text{M}+\text{H}$) $^+$.

***N,N*-Dimethyl-2-(4-pyridyl)quinazolin-4-amine (267)**²¹⁴

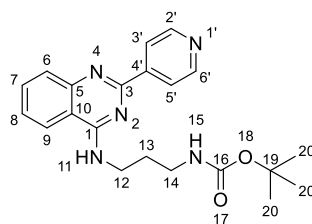
Pyridine-4-boronic acid hydrate (**196**) (36 mg, 0.29 mmol), bis(triphenylphosphine)palladium(II) dichloride (10 mg, 0.01 mmol), potassium carbonate (120 mg, 0.87 mmol) and 2-chloro-*N,N*-dimethyl-quinazolin-4-amine (60 mg, 0.29 mmol) in 4:1 acetonitrile:water (4 mL) were degassed under a flow of nitrogen and heated in a microwave reactor at 140 °C for 15 minutes. LCMS (MDAP) indicated product formation (m/z 251). Water (6 mL) was added and the mixture was extracted twice with ethyl acetate (2 × 8 mL). The organic phases were combined, dried over MgSO_4 and concentrated under reduced pressure to give a yellow oil (68 mg). The crude was purified *via* flash column chromatography (5 g silica, petroleum ether:ethyl acetate 1:0 to 0:1) to give the product contaminated with O=PPh_3 (52 mg). The product was purified *via* a SCX cartridge eluted with methanol and then 2 M ammonia in methanol to give *N,N*-dimethyl-2-(4-pyridyl)quinazolin-4-amine (**267**) (43 mg, 56%) as a brown solid.

R_f 0.36 (100% ethyl acetate); m.p. 109-111 °C; ν_{max} (thin film)/ cm^{-1} 3033 (w, aromatic C-H), 2938 (aliphatic C-H), 1680 (w, C=C), 1574 (s, aromatic C-C), 1522 (s, aromatic C-C), 1484 (aliphatic, C-H), 1029 (s, aliphatic C-N); ^1H NMR (600 MHz, $\text{DMSO}-d_6$) δ 8.74 (d, J = 6.0 Hz, 2H, H-2' and H-6'), 8.34 (d, J = 6.0 Hz, 2H, H-3' and H-5'), 8.24 (d, J = 8.4 Hz, 1H, H-9), 7.87 (d, J = 8.3 Hz, 1H, H-6), 7.82 (t, J = 8.1 Hz, 1H, H-7), 7.52 (t, J = 8.2 Hz, 1H, H-8), 3.46 (s, 6H, H-12); ^{13}C NMR (151 MHz, $\text{DMSO}-d_6$) δ 162.7 (C-1), 156.0 (C-3), 152.0 (C-5), 150.1 (C-2' and C-6'), 145.6 (C-4'), 132.6 (C-7), 128.1 (C-6), 126.2 (C-9), 125.1 (C-8), 121.8 (C-3' and C-5'), 114.7 (C-10), 41.5 (C-12); HRMS m/z (ESI^+) [Found: 251.1285, $\text{C}_{15}\text{H}_{15}\text{N}$ requires ($\text{M}+\text{H}$) $^+$ 251.1291]; LCMS (MDAP) R_t = 0.8 min (Ana 5–95 over 5 minutes), m/z (ESI^+) 251.0 ($\text{M}+\text{H}$) $^+$.

***Tert*-Butyl *N*-[3-[(2-chloroquinazolin-4-yl)amino]propyl]carbamate (**270**)**

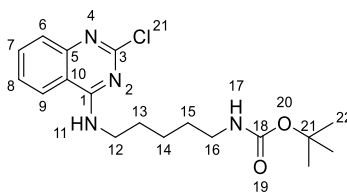
2,4-Dichloroquinazoline (**194**) (500 mg, 2.51 mmol), triethylamine (0.53 mL, 3.77 mmol) and *N*-Boc-1,3-propanediamine (**268**) (0.49 mL, 2.76 mmol) were stirred in tetrahydrofuran (5 mL) at 0 °C for 1 h in a water/ice bath. LCMS confirmed product formation (m/z 337 and 379). The reaction mixture was concentrated under reduced pressure. Water (40 mL) was added and the mixture was extracted twice with dichloromethane (2 × 50 mL). The organic phases were combined, dried over MgSO_4 , filtered and concentrated under reduced pressure to give an off-white heterogeneous mixture (280 mg). The crude was purified *via* flash column chromatography (12 g silica, petroleum ether:ethyl acetate, 1:0 to 0:1) to give *tert*-butyl *N*-[3-[(2-chloroquinazolin-4-yl)amino]propyl]carbamate (**270**) (262 mg, 26%) as an off-white foam.

^1H NMR (600 MHz, $\text{DMSO}-d_6$) δ 8.66 (t, $J = 5.3$ Hz, 1H, H-15), 8.24 (d, $J = 8.0$ Hz, 1H, H-9), 7.79 (t, $J = 8.2$ Hz, 1H, H-7), 7.61 (d, $J = 8.3$ Hz, 1H, H-6), 7.53 (t, $J = 7.6$ Hz, 1H, H-8), 6.85 (t, $J = 5.4$ Hz, 1H, H-11), 3.50 (q, $J = 6.6$ Hz, 2H, H-14), 3.02 (q, $J = 6.6$ Hz, 2H, H-12), 1.76 (q, $J = 6.9$ Hz, 2H, H-13), 1.36 (s, 9H, H-20); LCMS (LCQ) $R_t = 0.5$ min (4 min method), m/z (ESI^+) 337.02 [^{35}Cl], 339.03 [^{37}Cl] ($\text{M}+\text{H}$) $^+$, 281.13 [^{35}Cl], 283.14 [^{37}Cl] ($\text{M}+\text{H}-t\text{-Bu}$) $^+$, 237.1 [^{35}Cl] and 239.1 [^{37}Cl] ($\text{M}+\text{H}-\text{Boc}$) $^+$.

***Tert*-Butyl *N*-[3-[[2-(4-pyridyl)quinazolin-4-yl]amino]propyl]carbamate (**271**)**

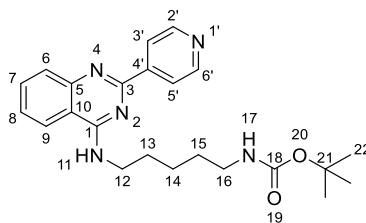
Pyridine-4-boronic acid hydrate (**196**) (55 mg, 0.45 mmol), bis(triphenylphosphine)palladium(II) dichloride (16 mg, 0.02 mmol), potassium carbonate (185 mg, 1.34 mmol) and *tert*-butyl *N*-[3-[[2-chloroquinazolin-4-yl]amino]propyl]carbamate (**270**) (150 mg, 0.45 mmol) in 4:1 acetonitrile:water (12 mL) were degassed under a flow of nitrogen and heated in a microwave reactor at 140 °C for 15 minutes. LCMS confirmed product formation (m/z 380). Water (20 mL) was added to the reaction and the mixture was extracted twice with ethyl acetate (2 × 25 mL). The combined organic phases were dried over MgSO₄, filtered and concentrated under reduced pressure to give a yellow gum (94 mg). The crude was purified *via* flash column chromatography (5 g silica, petroleum ether:ethyl acetate, 1:0 to 0:1) to give *tert*-butyl *N*-[3-[[2-(4-pyridyl)quinazolin-4-yl]amino]propyl]carbamate (**271**) (55 mg, 31%) as a yellow solid.

R_f 0.48 (100% ethyl acetate); m.p. 142–144 °C, ν_{\max} (thin film)/cm⁻¹ 3388 (N-H, br), 3226 (N-H br), 3014 (aromatic C-H, w), 2979 (aliphatic C-H, w), 1690 (C=O, s), 1524 (aromatic C-H, s), 766 (N-H, s); ¹H NMR (600 MHz, DMSO-*d*₆) δ 8.75–8.66 (d, J = 6.0 Hz, 2H, H-2' and H-6'), 8.42 (t, J = 5.6 Hz, 1H, H-15), 8.37–8.32 (d, J = 5.3 Hz, 1H, H-3' and H-5'), 8.26 (d, J = 8.2 Hz, 1H, H-9), 7.81 (d, J = 3.9 Hz, 2H, H-6 and H-7), 7.58–7.51 (m, 1H, H-8), 6.88 (t, J = 5.9 Hz, 1H, H-11), 3.69 (q, J = 6.6 Hz, 2H, H-14), 3.07 (q, J = 6.6 Hz, 2H, H-12), 1.85 (q, J = 7.0 Hz, 2H, H-13), 1.35 (s, 9H, H-20); ¹³C NMR (151 MHz, DMSO-*d*₆) δ 160.3 (C-16), 157.9 (C-3), 156.1 (C-1), 150.5 (C-2' and C-6'), 150.0 (C-5), 146.4 (C-4'), 133.4 (C-7), 128.5 (C-6), 126.6 (C-8), 123.1 (C-9), 122.2 (C-3' and C-5'), 114.7 (C-10), 77.9 (C-19), 38.9 (C-14), 38.3 (C-12), 29.5 (C-13), 28.7 (C-20); HRMS m/z (ESI⁺) [Found: 380.2094, C₂₁H₂₆N₅O₂ requires (M+H)⁺ 380.2081]; LCMS (MDAP) Rt = 7.5 min (Ana 30–90 in 20 min), m/z (ESI⁺) 380.2 (M+H)⁺.

***Tert*-Butyl *N*-[5-[(2-chloroquinazolin-4-yl)amino]pentyl]carbamate (**273**)**

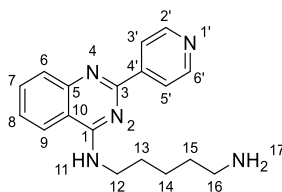
2,4-Dichloroquinazoline (**194**) (500 mg, 2.51 mmol), triethylamine (0.53 mL, 3.77 mmol) and 2-methyl-2-propanyl (5-aminopentyl)carbamate (**269**) (0.58 mL, 2.76 mmol) were stirred in tetrahydrofuran (5 mL) at 0 °C for 1 h in a water/ice bath. TLC and LCMS indicated product formation (m/z 365, 309, 265). The reaction mixture was concentrated under reduced pressure, diluted with water (25 mL) and extracted three times with 2:1 chloroform:propan-2-ol (2 × 20 mL). The combined organic phases were dried over MgSO_4 , filtered and concentrated under reduced pressure to give an off-white oil (521 mg). The crude was purified *via* flash column chromatography (12 g silica, petroleum ether:ethyl acetate, 1:0 to 0:1) to give *tert*-butyl *N*-[5-[(2-chloroquinazolin-4-yl)amino]pentyl]carbamate (**273**) (351 mg, 36%) as a colourless gum.¹⁵⁰

^1H NMR (600 MHz, $\text{DMSO}-d_6$) δ 8.70 (t, J = 5.6 Hz, 1H, H-17), 8.26 (d, J = 8.3 Hz, 1H, H-9), 7.78 (m, 1H, H-7), 7.60 (d, J = 7.2 Hz, 1H, H-6), 7.52 (m, 1H, H-8), 6.79 (t, J = 5.6 Hz, 1H, H-11), 3.48 (q, J = 6.6 Hz, 2H, H-16), 2.91 (q, J = 6.6 Hz, 2H, H-12), 1.63 (q, J = 7.4 Hz, 2H, H-15), 1.42 (p, J = 7.1 Hz, 2H, H-13), 1.35 (s, 9H, H-22), 1.34–1.28 (m, 2H, H-14); LCMS (MDAP) R_t = 19.0 min (30 min method), m/z (ESI⁺) 365.0 [^{35}Cl] and 366.9 [^{37}Cl] and (M+H)⁺.

***Tert*-Butyl *N*-[5-[[2-(4-pyridyl)quinazolin-4-yl]amino]pentyl]carbamate (**274**)**

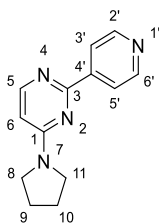
Pyridine-4-boronic acid hydrate (**196**) (51 mg, 0.41 mmol), *bis*(triphenylphosphine)palladium(II) dichloride (14 mg, 0.02 mmol), potassium carbonate (170 mg, 1.23 mmol) and *tert*-butyl *N*-[5-[[2-chloroquinazolin-4-yl]amino]pentyl]carbamate (**273**) (150 mg, 0.41 mmol) in 4:1 acetonitrile:water (12 mL) were degassed under a flow of nitrogen and heated in a microwave reactor at 140 °C for 15 minutes. LCMS indicated product formation (m/z 408). Water (15 mL) was added and the reaction mixture was extracted twice with ethyl acetate (2 × 20 mL). The combined organic phases were dried over MgSO₄, filtered and concentrated under reduced pressure to give a yellow oil (190 mg). The crude was purified *via* flash column chromatography (5 g silica, petroleum ether:ethyl acetate, 1:0 to 0:1) to give *tert*-butyl *N*-[5-[[2-(4-pyridyl)quinazolin-4-yl]amino]pentyl]carbamate (**274**) (82 mg, 46%) as a yellow solid.

R_f 0.47 (100% ethyl acetate); m.p. 110–111 °C; ν_{\max} (thin film)/cm⁻¹ 3308 (N-H, br), 1932 (aromatic C-H, w), 1682 (C=O, m), 1581 (C=C, s), 1529 (aromatic C-C, s), 1449 (aliphatic C-H, m), 1120 (C-N, s), 766 (N-H, s); ¹H NMR (600 MHz, DMSO-*d*₆) δ 8.73 (d, J = 6.1 Hz, 2H, H-2' and H-6'), 8.47 (t, J = 5.6 Hz, 1H, H-17), 8.33 (d, J = 6.0 Hz, 2H, H-3' and H-5'), 8.29 (d, J = 8.3 Hz, 1H, H-9), 7.81 (d, J = 3.8 Hz, 2H, H-6 and H-7), 7.58–7.51 (m, 1H, H-8), 6.81 (t, J = 5.6 Hz, 1H, H-11), 3.68 (q, J = 6.6 Hz, 2H, H-16), 2.93 (q, J = 6.6 Hz, 2H, H-12), 1.77–1.69 (m, 2H, H-15), 1.46 (q, J = 7.0 Hz, 2H, H-13), 1.42–1.36 (m, 2H, H-14), 1.34 (s, 9H, H-22); ¹³C NMR (151 MHz, DMSO-*d*₆) δ 159.9 (C-1), 157.5 (C-5), 155.6 (C-18), 150.1 (C-2' and H-6'), 149.5 (C-3), 146.0 (C-4'), 132.9 (C-7/6), 128.1 (C-6/7), 126.1 (C-8), 122.8 (C-9), 121.8 (C-3' and C-5'), 114.3 (C-10), 77.3 (C-21), 40.6 (C-16), 39.8 (C-12), 29.3 (C-13), 28.3 (C-22), 28.2 (C-15), 23.9 (C-14); HRMS m/z (ESI⁺) [Found: 408.2378, C₂₃H₃₀N₅O₂ requires (M+H)⁺ 408.2394]; LCMS (MDAP) R_t = 9.5 min (Ana 30–95 over 20 min), m/z (ESI⁺) 408.1 (M+H)⁺.

***N'*-[2-(4-Pyridyl)quinazolin-4-yl]pentane-1,5-diamine (275)**

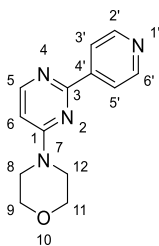
Tert-Butyl *N*-[5-[[2-(4-pyridyl)quinazolin-4-yl]amino]pentyl]carbamate (**274**) (40 mg, 0.10 mmol) was dissolved in dichloromethane (1 mL) and cooled to 0 °C. Trifluoro acetic acid (0.5 mL, 6.53 mmol) was added dropwise and the reaction mixture was allowed to stir at room temperature overnight. LCMS (MDAP) confirmed product formation (*m/z* 308). The reaction mixture was concentrated under reduced pressure and purified *via* SCX cartridge, eluting first with methanol then 2 M ammonia in methanol to give *N'*-[2-(4-pyridyl)quinazolin-4-yl]pentane-1,5-diamine (**275**) (23 mg, 77%) as an off-white solid.

R_f 0.05 (9:1 dichloromethane:methanol); m.p. 118–120 °C; ν_{max} (thin film)/cm⁻¹ 3283 (br, N-H), 2937 (m, aliphatic C-H), 1579 (s, aromatic C-C/C-N), 1557 (s, aromatic C-C/C-N), 1527 (s, aromatic C-C/C-N), 1413 (s, aliphatic C-H), 1037 (s, aliphatic C-N), 763 (s, N-H); ¹H NMR (600 MHz, DMSO-*d*₆) δ 8.73 (d, *J* = 5.7 Hz, 2H, H-2' and H-6'), 8.51 – 8.45 (m, 1H, H-11), 8.37 – 8.26 (m, 3H, H-3', H-5' and H-9), 7.83 – 7.76 (m, 2H, H-6 and H-7), 7.57 – 7.50 (m, 1H, H-8), 5.70 (s, 2H, H-17), 3.68 (q, *J* = 6.6 Hz, 2H, H-12), 2.66 (t, *J* = 7.2 Hz, 2H, H-16), 1.74 (p, *J* = 7.3 Hz, 2H, H-13), 1.53 (p, *J* = 7.3 Hz, 2H, H-15), 1.44 (q, *J* = 8.0 Hz, 2H, H-14); ¹³C NMR (151 MHz, DMSO-*d*₆) δ 159.9 (C-1), 157.4 (C-3), 150.1 (C-2' and C-6'), 149.5 (C-5/10), 146.0 (C-4'), 132.8 (C-7), 128.0 (C-6), 126.1 (C-8), 122.9 (C-9), 121.7 (C-3' and C-5'), 114.3 (C-10/5), 40.5 (C-16), 40.1 (C-12), 29.8 (C-15), 28.1 (C-13), 23.7 (C-14); HRMS *m/z* (ESI⁺) [Found: 308.1863, C₁₈H₂₂N₅ requires (M+H)⁺ 308.1870]; LCMS (MDAP) *R_t* = 1.9 min (Ana 5–95 over 5 minutes), *m/z* (ESI⁺) 308.10 (M+H)⁺.¹⁰⁶

2-(4-Pyridyl)-4-pyrrolidin-1-yl-pyrimidine (281)

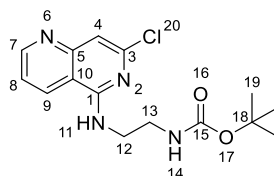
Pyridine-4-boronic acid hydrate (**196**) (100 mg, 0.82 mmol), *bis*(triphenylphosphine)-palladium(II) dichloride (29 mg, 0.04 mmol), potassium carbonate (339 mg, 2.45 mmol) and 2-chloro-4-(1-pyrrolidinyl)pyrimidine (**280**) (150 mg, 0.82 mmol) in 4:1 acetonitrile:water (12 mL) were degassed under a flow of nitrogen and heated in a microwave reactor at 140 °C for 15 minutes. LCMS indicated formation of the product (m/z 227). Water (15 mL) was added to the reaction mixture and extracted twice with ethyl acetate (2 × 20 mL). The combined organic phases were dried over $MgSO_4$, filtered and concentrated under reduced pressure. The crude was purified *via* flash column chromatography (5 g silica, petroleum ether:ethyl acetate 1:0 to 0:1) to give 2-(4-pyridyl)-4-pyrrolidin-1-yl-pyrimidine (**281**) (52 mg, 27%) as an off-white solid.

R_f 0.48 (100% ethyl acetate); m.p. 100–103 °C; ν_{max} (thin film)/ cm^{-1} 3039 (aromatic C-H, br), 2966 (aliphatic C-H, w), 2866 (aliphatic C-H, w), 1587 (aromatic C-H, s), 1541 (aromatic C-H, s), 1494 (aliphatic C-H, s), 1482 (aliphatic C-H, s), 1125 (C-N, m), 833 (aromatic C-H, s); 1H NMR (600 MHz, $DMSO-d_6$) δ 8.70 (d, J = 4.7 Hz, 2H, H-2' and H-6'), 8.31 (d, J = 6.0 Hz, 1H, H-6), 8.21 (d, J = 4.7 Hz, 2H, H-3' and H-5'), 6.53 (d, J = 6.0 Hz, 1H, H-5), 3.66 (s, 2H, H-11/8), 3.39 (s, 2H, H-8/11), 1.98 (app. d, J = 28.6 Hz, 4H, H-9 and H-10); ^{13}C NMR (151 MHz, $DMSO-d_6$) δ 284.1 (C-3), 283.0 (C-1), 278.6 (C-6), 273.7 (C-2' and C-6'), 269.1 (C-4'), 245.1 (C-3' and C-5'), 227.1 (C-5), 169.6 (C-11 and C-8), 148.7 (C-9/10), 148.0 (C-10/9); HRMS m/z (ESI⁺) [Found: 227.1284, $C_{13}H_{15}N_4$ requires (M+H)⁺ 227.1291]; LCMS (LCQ) R_t = 0.7 min (Ana 5-95 in 5 min method), m/z (ESI⁺) 227.10 (M+H)⁺.

4-[2-(4-Pyridyl)pyrimidin-4-yl]morpholine (283)

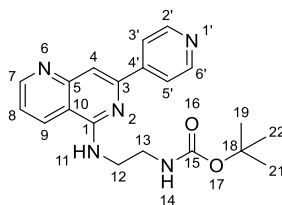
Pyridine-4-boronic acid hydrate (**196**) (92 mg, 0.75 mmol), bis(triphenylphosphine)-palladium(II) dichloride (26 mg, 0.04 mmol), potassium carbonate (312 mg, 2.25 mmol) and 4-(2-chloro-4-pyrimidinyl)morpholine (**282**) (150 mg, 0.75 mmol) in 4:1 acetonitrile:water (12 mL) were degassed under a flow of nitrogen and heated in a microwave reactor at 140 °C for 15 minutes. LCMS indicated product formation (m/z 243). Water (15 mL) was added and the reaction mixture was extracted twice with ethyl acetate (2 × 20 mL). The combined organic phases were dried over MgSO_4 , filtered and concentrated under reduced pressure to give an off-white solid (163 mg). The crude was purified *via* flash column chromatography (5 g silica, petroleum ether:ethyl acetate 1:0 to 0:1) to give 4-[2-(4-pyridyl)pyrimidin-4-yl]morpholine (**283**) (67 mg, 35%) as a pale yellow solid.

R_f 0.28 (100% ethyl acetate); m.p. 71–73 °C; ν_{max} (thin film)/ cm^{-1} 3391 (N-H, br), 2975 (aliphatic C-H, br), 2870 (aliphatic C-H, w), 1596 (aromatic C-H, s), 1542 (aromatic C-H, s), 1478 (aliphatic C-H, s), 963 (aliphatic C-H, m), 774 (N-H, s); ^1H NMR (500 MHz, $\text{DMSO}-d_6$) δ 8.71 (d, J = 5.3 Hz, 2H, H-2' and H-6'), 8.40 (d, J = 6.2 Hz, 1H, H-5), 8.20 (d, J = 5.4 Hz, 2H, H-3' and H-5'), 6.90 (d, J = 6.2 Hz, 1H, H-6), 3.72 (s, 8H, H-8, H-9, H-11 and H-12); ^{13}C NMR (151 MHz, $\text{DMSO}-d_6$) δ 161.6 (C-1), 160.5 (C-3), 156.2 (C-5), 150.2 (C-2' and C-6'), 145.1 (C-4'), 121.5 (C-3' and C-5'), 103.1 (C-6), 65.8 (C-8/9/11/12), 43.7 (C-8/9/11/12); HRMS m/z (ESI⁺) [Found: 243.1235, $\text{C}_{13}\text{H}_{15}\text{N}_4\text{O}$ requires (M+H)⁺ 243.1240]; LCMS (MDAP) R_t = 0.7 min (Ana 5-95 in 5 min method), m/z (ESI⁺) 243.10 (M+H)⁺.

***Tert*-Butyl *N*-[2-[(7-chloro-1,6-naphthyridin-5-yl)amino]ethyl]carbamate (**285**)**

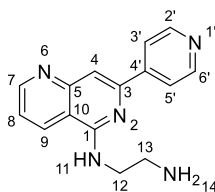
N,N-Diisopropylethylamine (0.71 mL, 4.06 mmol), *tert*-butyl *N*-(2-aminoethyl)carbamate (**182**) (0.94 mL, 5.97 mmol) and 5,7-dichloro-1,6-naphthyridine (**284**) (200 mg, 1 mmol) in ethanol (7 mL) were stirred at 100 °C overnight. LCMS confirmed product formation (m/z 323, 267, 223). The reaction mixture was concentrated under reduced pressure, diluted with water (4 mL) and extracted with ethyl acetate (3 × 40 mL). The combined organic extracts were washed with water (40 mL) and brine (40 mL), dried over MgSO_4 , filtered and concentrated under reduced pressure to give a white solid (791 mg). The crude was purified *via* flash column chromatography (20 g silica, petroleum ether:ethyl acetate, 1:0 to 0:1) to give *tert*-butyl *N*-[2-[(7-chloro-1,6-naphthyridin-5-yl)amino]ethyl]carbamate (**285**) (292 mg, 86%) as a white solid.

R_f 0.61 (100% ethyl acetate); m.p. 110–113 °C; ν_{max} (thin film)/ cm^{-1} 3387 (N-H, br), 3215 (N-H, br), 3039 (aromatic C-H, w), 2979 (aliphatic C-H), 1684 (C=O, m), 1526 (aromatic C-H), 765 (N-H, s); ^1H NMR (600 MHz, $\text{DMSO}-d_6$) δ 8.90 (dd, J = 4.4, 1.6 Hz, 1H, H-7), 8.63 (d, J = 8.4 Hz, 1H, H-9), 8.11 (t, J = 5.5 Hz, 1H, H-14), 7.49 (dd, J = 8.4, 4.3 Hz, 1H, H-8), 6.97 (s, 1H, H-4), 6.95 (t, J = 6.3 Hz, 1H, H-11), 3.50 (q, J = 6.1 Hz, 2H, H-13), 3.23 (q, J = 6.2 Hz, 2H, H-12), 1.36 (s, 9H, H-19); ^{13}C NMR (151 MHz, $\text{DMSO}-d_6$) δ 156.6 (C-15), 156.3 (C-1), 154.7 (C-7), 153.5 (C-3), 148.0 (C-10), 132.5 (C-9), 121.2 (C-8), 112.4 (C-10), 108.3 (C-4), 78.1 (C-18), 41.8 (C-13), 39.4 (C-12), 28.6 (C-19); HRMS m/z (ESI $^+$) [Found: 345.1098, $\text{C}_{15}\text{H}_{19}\text{ClN}_4\text{NaO}_2$ requires (M+H) $^+$ 345.1089]; LCMS (LCQ) R_t = 0.6 min (4 min method), m/z (ESI $^+$) 323.1 (M+H) $^+$, 267.2 (M-tBu+H) $^+$.

***Tert*-Butyl *N*-[2-[[7-(4-pyridyl)-1,6-naphthyridin-5-yl]amino]ethyl]carbamate (**286**)**

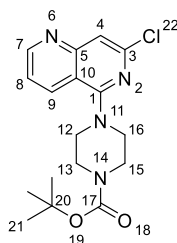
Pyridine-4-boronic acid hydrate (**196**) (57 mg, 0.46 mmol), potassium carbonate (193 mg, 1.39 mmol) and *tert*-butyl *N*-[2-[(7-chloro-1,6-naphthyridin-5-yl)amino]ethyl]carbamate (**285**) (150 mg, 0.46 mmol) in 4:1 acetonitrile:water (12 mL) were degassed under a flow of nitrogen. *bis*[2-(di-*tert*-butylphosphanyl)cyclopenta-2,4-dien-1-yl]iron; dichloropalladium (15 mg, 0.02 mmol) was added and the reaction was heated in a sealed microwave reactor at 140 °C for 15 minutes. LCMS indicated formation of the product (*m/z* 293). The reaction mixture was diluted with water (15 ml) and extracted twice with ethyl acetate (2 × 20 mL). The combined organic phases were dried over MgSO₄, filtered and concentrated under reduced pressure to give a brown gum (163 mg). The crude was purified *via* flash column chromatography (5 g silica, petroleum ether:ethyl acetate, 1:0 to 0:1) to give *tert*-butyl *N*-[2-[[7-(4-pyridyl)-1,6-naphthyridin-5-yl]amino]ethyl]carbamate (**286**) (59 mg, 31%) as a yellow solid.

R_f 0.57 (9:1 dichloromethane:methanol); m.p. 180–181 °C; ν_{max} (thin film)/cm⁻¹ 3396 (N-H, br), 3222 (N-H, br), 1977 (aliphatic C-H, m), 1688 (C=O, s), 1556 (aromatic C-H, s), 765 (N-H, s); ¹H NMR (600 MHz, DMSO-*d*₆) δ 8.96 (dd, *J* = 4.3, 1.6 Hz, 1H, H-9), 8.67 (d, *J* = 6.1 Hz, 2H, H-2' and H-6'), 8.65 (d, *J* = 8.7 Hz, 1H, H-7), 8.21 (d, *J* = 6.2 Hz, 2H, H-3' and h-5'), 7.94 (t, *J* = 5.5 Hz, 1H, H-14), 7.75 (s, 1H, H-4), 7.55 (dd, *J* = 8.3, 4.3 Hz, 1H, H-8), 7.05 (t, *J* = 5.9 Hz, 1H, H-11), 3.66 (q, *J* = 6.3 Hz, 2H, H-13), 3.35 – 3.29 (m, 2H, H-12), 1.37 (s, 9H, H-19); ¹³C NMR (151 MHz, DMSO-*d*₆) δ 155.8 (C-15), 155.8 (C-1), 154.0 (C-7), 152.7 (C-7), 150.1 (C-2' and C-6'), 149.2 (C-3), 146.1 (C-4'), 131.6 (C-9), 121.4 (C-8), 120.8 (C-3' and C-5'), 113.5 (C-10), 107.7 (C-4), 77.6 (C-18), 41.3 (C-13), 39.1 (C-12), 28.3 (C-19); HRMS *m/z* (ESI⁺) [Found: 366.1912, C₂₀H₂₄N₅O₂ requires [M+H]⁺ 366.1925]; LCMS (MDAP) *R_t* = 7.2 min (Ana 30–95 over 20 min), *m/z* (ESI⁺) 366.9 [M+H]⁺.

***N'*-[7-(4-Pyridyl)-1,6-naphthyridin-5-yl]ethane-1,2-diamine (**287**)**¹⁶¹

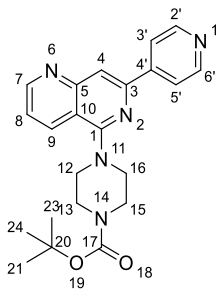
Tert-Butyl *N*-[2-[[7-(4-pyridyl)-1,6-naphthyridin-5-yl]amino]ethyl]carbamate (**286**) (50 mg, 0.14 mmol) was dissolved in dichloromethane (1 mL) and cooled to 0 °C. Trifluoro acetic acid (0.5 mL, 5.53 mmol) was added dropwise and the reaction mixture was allowed to stir at room temperature overnight. LCMS (LCQ) indicated product formation (*m/z* 266). The reaction mixture was concentrated under reduced pressure to give a yellow solid. The crude was purified *via* SCX cartridge by elution with methanol then 2 M ammonia in methanol. The resulting yellow solid (34 mg) was triturated in methanol to give *N'*-[7-(4-pyridyl)-1,6-naphthyridin-5-yl]ethane-1,2-diamine (**287**) (6 mg, 15%) as a pale yellow solid.

¹H NMR (600 MHz, DMSO-*d*₆) δ 8.99 (d, *J* = 4.0 Hz, 1H, H-7), 8.80 (d, *J* = 8.4 Hz, 1H, H-9), 8.69 (d, *J* = 5.9 Hz, 2H, H-2' and H-6'), 8.19 (d, *J* = 6.0 Hz, 2H, H-3' and H-5'), 7.98 (s, 3H, H-11 and H-14), 7.81 (s, 1H, H-4), 7.57 (dd, *J* = 8.2, 4.3 Hz, 1H, H-8), 3.90 (q, *J* = 5.7 Hz, 2H, H-12), 3.22 (t, *J* = 6.1 Hz, 2H, H-13); LCMS (MDAP) *R*_t = 0.8 min (Ana 5–95 over 5 minutes), *m/z* (ESI⁺) 266.0 (M+H)⁺. Insufficient quantities isolated for further characterisation.

***Tert*-Butyl 4-(7-chloro-1,6-naphthyridin-5-yl)piperazine-1-carboxylate (**288**)**

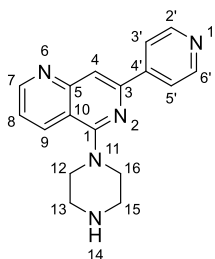
N,N-Diisopropylethylamine (0.71 mL, 4.06 mmol) 5,7-dichloro-1,6-naphthyridine (**284**) (200 mg, 1 mmol) and 1-Boc-piperazine (**185**) (1.11 g, 5.97 mmol) in ethanol (7 mL) were stirred at 100 °C overnight. LCMS confirmed product formation (m/z 349). The reaction mixture was concentrated under reduced pressure, diluted with water (4 mL) and extracted with ethyl acetate (3 × 40 mL). The combined organic extracts were washed with water (40 mL) and brine (40 mL), dried over MgSO₄, filtered and concentrated under reduced pressure to give a yellow solid (884 mg). The crude was purified *via* flash column chromatography (25 g silica, petroleum ether:ethyl acetate, 1:0 to 0:1) to give *tert*-butyl 4-(7-chloro-1,6-naphthyridin-5-yl)piperazine-1-carboxylate (**288**) (188 mg, 51%) as a white solid.

¹H NMR (600 MHz, DMSO-*d*₆) δ 9.01 (dd, J = 4.2, 1.5 Hz, 1H, H-7), 8.48 (d, J = 8.4 Hz, 1H, H-9), 7.57 (dd, J = 8.5, 4.2 Hz, 1H, H-8), 7.45 (s, 1H, H-4), 3.58 (s, 4H, H-13 and H-15), 3.47–3.41 (m, 4H, H-12 and H-16), 1.44 (s, 9H, H-21); LCMS (LCQ) R_t = 4.8 min (5 min method), m/z (ESI⁺) 349.1 (M+H)⁺, 293.2 (M+H-*t*-Bu)⁺, 249.2 (M+H-Boc)⁺.

***Tert*-Butyl 4-[7-(4-pyridyl)-1,6-naphthyridin-5-yl]piperazine-1-carboxylate (**289**)**

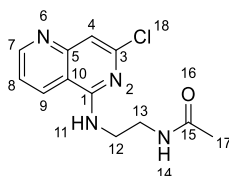
Sodium carbonate (137 mg, 1.29 mmol), *tert*-butyl 4-(7-chloro-1,6-naphthyridin-5-yl)piperazine-1-carboxylate (**288**) (150 mg, 0.43 mmol), pyridine-4-boronic acid hydrate (**196**) (53 mg, 0.43 mmol) and *bis*[2-(di-*tert*-butylphosphanyl)cyclopenta-2,4-dien-1-yl]iron;dichloropalladium (14 mg, 0.02 mmol) in 4:1 acetonitrile:water (12 mL) were degassed under a flow of nitrogen and heated in a microwave reactor at 140 °C for 15 minutes. LCMS confirmed reaction completion (m/z 392, 336, 292). The reaction mixture was diluted with water (20 mL) and extracted twice with ethyl acetate (2 × 25 mL). The combined organic phases were dried over MgSO_4 , filtered and concentrated under reduced pressure to give a brown solid (160 mg). The crude was purified *via* flash column chromatography (5 g silica, petroleum ether:ethyl acetate, 1:0 to 0:1) to give *tert*-butyl 4-[7-(4-pyridyl)-1,6-naphthyridin-5-yl]piperazine-1-carboxylate (**289**) (103 mg, 58%) as a pale brown solid.¹⁵¹

R_f 0.59 (9:1 dichloromethane:methanol); m.p. 209–210 °C; ν_{max} (thin film)/ cm^{-1} 3050 (aromatic C-H, br), 2972 (aliphatic C-H, br), 1699 (C=O, s), 1569 (aromatic C-H, s), 834 (alkene C-H, s), 767 (alkene C-H, s); ^1H NMR (600 MHz, $\text{DMSO}-d_6$) δ 9.07 (dd, $J = 4.3, 1.6$ Hz, 1H, H-9), 8.70 (d, $J = 5.8$ Hz, 2H, H-2' and H-6'), 8.52 (d, $J = 8.3$ Hz, 1H, H-7), 8.26–8.12 (m, 3H, H-3', H-5' and H-4), 7.62 (dd, $J = 8.4, 4.2$ Hz, 1H, H-8), 3.63 (s, 4H, H-13 and H-15), 3.51–3.46 (m, 4H, H-12 and H-16), 1.44 (s, 9H, H-21); ^{13}C NMR (151 MHz, $\text{DMSO}-d_6$) δ 161.1 (C-17), 155.0 (C-9), 154.4 (C-1), 153.8 (C-5), 150.7 (C-2' and C-6'), 148.5 (C-3), 145.9 (C-4'), 134.4 (C-7), 122.6 (C-8), 121.2 (C-3' and C-5'), 116.4 (C-10), 113.7 (C-4), 79.5 (C-20), 55.3 (C-13 and C-15), 51.1 (C-12 and C-16), 28.5 (C-21); HRMS m/z (ESI⁺) [Found: 392.2098, $\text{C}_{22}\text{H}_{26}\text{N}_5\text{O}_2$ requires (M+H)⁺ 392.2081]; LCMS (LCQ) R_t = 0.7 min (4 min method), m/z (ESI⁺) 392.2 (M+H)⁺, 336.2 (M+H-*t*-Bu)⁺, 292.4 (M+H-Boc)⁺.

5-Piperazin-1-yl-7-(4-pyridyl)-1,6-naphthyridine (290)

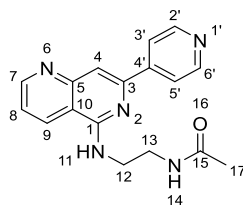
Tert-Butyl 4-[7-(4-pyridyl)-1,6-naphthyridin-5-yl]piperazine-1-carboxylate (**289**) (80 mg, 0.20 mmol) was dissolved in dichloromethane (1.5 mL) and cooled to 0 °C. Trifluoro acetic acid (0.80 mL, 8.26 mmol) was added dropwise and the reaction mixture was allowed to stir at room temperature overnight. LCMS (LCQ) indicated product formation (m/z 292). The reaction mixture was concentrated under reduced pressure to give a yellow solid. The crude was purified *via* SCX cartridge by elution with methanol then 2 M ammonia in methanol to give 5-piperazin-1-yl-7-(4-pyridyl)-1,6-naphthyridine (**290**) (45 mg, 72%) as a pale brown solid.¹⁰⁶

R_f 0.59 (9:1 dichloromethane: methanol); m.p. 147–149 °C; ν_{\max} (thin film)/ cm^{-1} 3399 (N-H, br), 1669 (C=C, m), 1597 (aromatic C-H, s), 1565 (aromatic C-H, s), 1496 (aliphatic C-H), 826 (N-H, s); ^1H NMR (600 MHz, $\text{DMSO}-d_6$) δ 9.05 (d, J = 4.3 Hz, 1H, H-9), 8.71 (d, J = 5.0 Hz, 2H, H-2' and H-6'), 8.50 (d, J = 8.4 Hz, 1H, H-7), 8.19 (d, J = 5.2 Hz, 2H, H-3' and H-5'), 8.17 (s, 1H, H-4), 7.61 (dd, J = 8.4, 4.2 Hz, 1H, H-8), 3.51 (t, J = 4.9 Hz, 4H, H-12 and H-16), 3.10 (t, J = 4.9 Hz, 4H, H-13 and H-15). N-H peak not observed; ^{13}C NMR (151 MHz, $\text{DMSO}-d_6$) δ 161.2 (C-1), 154.9 (C-9), 153.7 (C-5), 150.7 (C-2' and C-6'), 148.4 (C-3), 145.9 (C-4'), 134.4 (C-7), 122.5 (C-8), 121.1 (C-3' and C-5'), 116.4 (C-10), 113.6 (C-4), 51.1 (C-12 and C-16), 45.0 (C-13 and C-15); HRMS m/z (ESI⁺) [Found: 292.1560, $\text{C}_{17}\text{H}_{18}\text{N}_5$ requires (M+H)⁺ 292.1557]; LCMS (MDAP) R_t = 2.9 min (Ana 30–90 in 20min), m/z (ESI⁺) 292.1 (M+H)⁺.

***N*-[2-[(7-Chloro-1,6-naphthyridin-5-yl)amino]ethyl]acetamide**

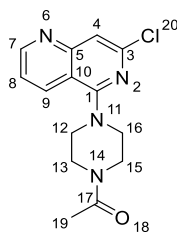
N,N-Diisopropylethylamine (1.77 mL, 10.2 mmol), 5,7-dichloro-1,6-naphthyridine (**284**) (500 mg, 2.51 mmol), and *N*-(2-aminoethyl)acetamide (1.52 g, 14.9 mmol) in ethanol (17.5 mL) were degassed under a flow of nitrogen and heated to 100 °C overnight. LCMS confirmed reaction completion (*m/z* 265.0 and 266.9). The reaction mixture was diluted with water (20 mL) and extracted twice with ethyl acetate (2 × 25 mL). The combined organic phases were dried over MgSO₄, filtered and concentrated under reduced pressure to give a yellow oil (631 mg). The crude was purified *via* flash column chromatography (5 g silica, petroleum ether:ethyl acetate, 1:0 to 0:1) to give *N*-[2-[(7-chloro-1,6-naphthyridin-5-yl)amino]ethyl]acetamide (502 mg, 72%) as an off-white solid.

R_f 0.32 (9:1 ethyl acetate:methanol); m.p. 238–240 °C; ν_{\max} (thin film)/cm⁻¹ 3270 (N-H, br), 3223 (N-H, br), 1651 (C=O, m), 1588 (aromatic C-C, s), 1332 (aliphatic C-H, s), 805 (N-H, s); ¹H NMR (600 MHz, DMSO-*d*₆) δ 8.90 (dd, *J* = 4.4, 1.6 Hz, 1H, H-9), 8.61 (dt, *J* = 8.2, 1H, H-7), 8.20 (t, *J* = 5.4 Hz, 1H, H-14), 8.04 (t, *J* = 5.7 Hz, 1H, H-11), 7.50 (dd, *J* = 8.4, 4.3 Hz, 1H, H-8), 6.97 (s, 1H, H-4), 3.51 (q, *J* = 6.3 Hz, 2H, H-13), 3.36–3.31 (m, 2H, H-12), 1.81 (s, 3H, H-17); ¹³C NMR (151 MHz, DMSO-*d*₆) δ 170.1 (C-15), 156.6 (C-1), 154.8 (C-7), 153.5 (C-5), 148.0 (C-3), 132.4 (C-9), 121.3 (C-8), 112.4 (C-10), 108.3 (C-4), 41.4 (C-13), 38.0 (C-12), 23.1 (C-17); HRMS *m/z* (ESI⁺) [Found: 287.0663, C₁₂H₁₃ClN₄NaO requires (M+H)⁺ 287.0670]; LCMS (MDAP) *R_t* = 7.8 min (Ana 30–95 over 20 min), *m/z* (ESI⁺) 264.9 [³⁵Cl] and 266.9 [³⁷Cl] (M+H)⁺.

***N*-[2-[[7-(4-Pyridyl)-1,6-naphthyridin-5-yl]amino]ethyl]acetamide (291)**

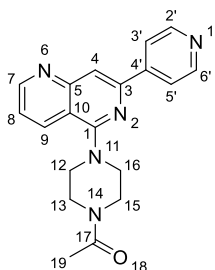
Potassium carbonate (203 mg, 1.47 mmol), pyridine-4-boronic acid hydrate (**196**) (60 mg, 0.49 mmol), *bis*[2-(di-*tert*-butylphosphanyl)cyclopenta-2,4-dien-1-yl]iron; dichloropalladium (16 mg, 0.02 mmol) and *N*-[2-[(7-chloro-1,6-naphthyridin-5-yl)amino]ethyl]acetamide (150 mg, 0.54 mmol) in 4:1 acetonitrile:water (12 mL) were degassed under a flow of nitrogen and heated in a microwave reactor at 140 °C for 15 minutes. LCMS confirmed reaction completion (*m/z* 308). The reaction mixture was diluted with water (15 mL) and extracted three times with ethyl acetate (3 × 20 mL). The combined organic phases were dried over MgSO₄, filtered and concentrated under reduced pressure to give a yellow oil (71 mg). The crude was purified *via* flash column chromatography (4 g silica dichloromethane:methanol, 1:0 to 9:1) to give *N*-[2-[[7-(4-pyridyl)-1,6-naphthyridin-5-yl]amino]ethyl]acetamide (**291**) (26 mg, 15%) as a light brown solid.

*R*_f 0.28 (9:1 dichloromethane:methanol); m.p. 273–275 °C; ν_{\max} (thin film)/cm⁻¹ 3338 (N-H, m), 3200 (aromatic C-H, br), 2997 (aliphatic C-H, br), 1671 (C=O, s), 1539 (aromatic C-C, s), 792 (N-H, m); ¹H NMR (600 MHz, DMSO-*d*₆) δ 8.96 (d, *J* = 4.0 Hz, 1H, H-7), 8.67 (d, *J* = 5.7 Hz, 2H, H-2' and H-6'), 8.65 (d, *J* = 8.5 Hz, 1H, H-9), 8.19 (d, *J* = 5.8 Hz, 2H, H-3' and H-5'), 8.06 (t, *J* = 5.3 Hz, 1H, H-14), 7.98 (t, *J* = 5.1 Hz, 1H, H-11), 7.75 (s, 1H, H-4), 7.54 (dd, *J* = 8.3, 4.2 Hz, 1H, H-8), 3.67 (q, *J* = 6.3 Hz, 2H, H-13), 3.42 (q, *J* = 6.4 Hz, 2H, H-12), 1.82 (s, 3H, H-17); ¹³C NMR (151 MHz, DMSO-*d*₆) δ 170.0 (C-15), 156.2 (C-1), 154.4 (C-7), 153.1 (C-5), 150.5 (C-2' and C-6'), 149.6 (C-3), 146.5 (C-4'), 132.0 (C-9), 121.8 (C-8), 121.1 (C-3' and C-5'), 113.9 (C-10), 108.1 (C-4), 41.4 (C-13), 38.3 (C-12), 23.2 (C-17); HRMS *m/z* (ESI⁺) [Found: 308.1499, C₁₇H₁₈N₅O requires (M+H)⁺ 308.1506]; LCMS (MDAP) *R*_t = 10.2 min (Ana 5–95 over 20 min), *m/z* (ESI⁺) 308.1 (M+H)⁺.

1-[4-(7-Chloro-1,6-naphthyridin-5-yl)piperazin-1-yl]ethanone

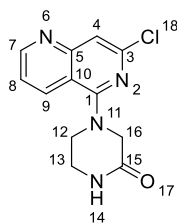
N,N-Diisopropylethylamine (0.71 mL, 4.06 mmol), 5,7-dichloro-1,6-naphthyridine (**284**) (200 mg, 1 mmol) and 1-(1-piperazinyl)ethanone (765 mg, 5.97 mmol) in ethanol (7 mL) were stirred at 100 °C overnight. LCMS indicated product formation (*m/z* 293). The reaction mixture was concentrated under reduced pressure and water (4 mL) was added. The reaction mixture was extracted three times with ethyl acetate (3 × 40 mL) and the combined organic phases were washed with water (40 mL) and brine (40 mL) before being dried over MgSO₄, filtered and concentrated under reduced pressure (321 mg). The crude was purified *via* flash column chromatography (12 g silica, dichloromethane:methanol, 1:0 to 9:1) to give 1-[4-(7-chloro-1,6-naphthyridin-5-yl)piperazin-1-yl]ethanone (256 mg, 83%) as a white solid.

R_f 0.28 (9:1 ethyl acetate:methanol); m.p. 144–146 °C; *v*_{max} (thin film)/cm⁻¹ 2998 (aliphatic C-H, w), 2850 (aldehyde C-H, m), 1630 (C=O, s), 1596 (C=C, s), 1556 (aliphatic C-C, s), 1366 (aliphatic C-H, s), 977 (aliphatic C-H, s), 874 (N-H, s); ¹H NMR (600 MHz, DMSO-*d*₆) δ 9.01 (dd, *J* = 4.2, 1.6 Hz, 1H, H-9), 8.50 (dt, *J* = 8.5, 1.2 Hz, 1H, H-7), 7.57 (dd, *J* = 8.5, 4.2 Hz, 1H, H-8), 7.45 (s, 1H, H-4), 3.68 (t, *J* = 4.6 Hz, 4H, H-12 and H-16), 3.54–3.46 (m, 2H, H-13/15), 3.43 (dd, *J* = 6.5, 3.9 Hz, 2H, H-15/13), 2.06 (s, 3H, H-19); ¹³C NMR (151 MHz, DMSO-*d*₆) δ 168.5 (C-17), 160.5 (C-1), 154.9 (C-7), 153.8 (C-5), 145.6 (C-3), 134.4 (C-9), 121.4 (C-8), 114.3 (C-10), 113.9 (C-4), 50.7 (C-13/C-15), 50.4 (C-15/C-13), 45.2 (C-12/16), 40.6 (C-16/12), 21.3 (C-19); HRMS *m/z* (ESI⁺) [Found: 313.0822, C₁₄H₁₅ClN₄NaO requires (M+H)⁺ 313.0827]; LCMS (MDAP) *R_t* = 11.6 min, (Ana 30–95 over 20 min); *m/z* (ESI⁺) 291.0 [³⁵Cl] and 292.9 [³⁷Cl] [M-H]⁺.

1-[4-[7-(4-Pyridyl)-1,6-naphthyridin-5-yl]piperazin-1-yl]ethanone (292)

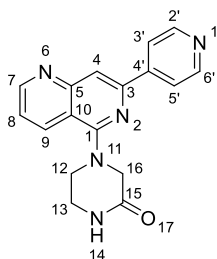
Potassium carbonate (214 mg, 1.55 mmol), pyridine-4-boronic acid hydrate (**196**) (63 mg, 0.52 mmol), *bis*[2-(di-*tert*-butylphosphanyl)cyclopenta-2,4-dien-1-yl]iron; dichloropalladium (17 mg, 0.03 mmol) and 1-[4-(7-chloro-1,6-naphthyridin-5-yl)piperazin-1-yl]ethanone (150 mg, 0.52 mmol) in 4:1 acetonitrile:water (12 mL) were degassed under a flow of nitrogen and heated in a microwave reactor at 140 °C for 15 minutes. LCMS confirmed reaction completion (m/z 334). The reaction mixture was diluted with water (20 mL) and extracted twice with ethyl acetate (2 × 25 mL). The combined organic phases were dried over $MgSO_4$, filtered and concentrated under reduced pressure (158 mg). The crude was purified *via* flash column chromatography (5 g petroleum ether:ethyl acetate, 1:0 to 0:1) to give 1-[4-[7-(4-pyridyl)-1,6-naphthyridin-5-yl]piperazin-1-yl]ethanone (**292**) (71 mg, 39%) as an off-white solid.¹⁵¹

R_f 0.23 (9:1 dichloromethane:methanol); m.p. 201–202 °C; ν_{max} (thin film)/ cm^{-1} 2923 (aliphatic C-H, w), 2853 (aliphatic C-H, m), 1647 (C=O, m), 1600 (aromatic C-C, s), 1567 (aromatic C-C, s), 818 (alkene C-H, m); 1H NMR (600 MHz, $DMSO-d_6$) δ 9.07 (dd, J = 4.2, 1.3 Hz, 1H, H-7), 8.71 (d, J = 5.9 Hz, 2H, H-2' and H-6'), 8.54 (d, J = 8.4 Hz, 1H, H-9), 8.24–8.17 (m, 3H, H-3', H-5' and H-4), 7.63 (dd, J = 8.4, 4.2 Hz, 1H, H-8), 3.79–3.68 (m, 4H, H-12 and H-16), 3.59–3.51 (m, 2H, H-13/15), 3.50–3.41 (m, 2H, H-15/13), 2.08 (s, 3H, H-19); ^{13}C NMR (151 MHz, $DMSO-d_6$) δ 168.6 (C-17), 160.6 (C-1), 154.6 (C-7), 153.3 (C-5), 150.3 (C-2' and C-6'), 148.0 (C-1'), 145.5 (C-3), 134.0 (C-9), 122.2 (C-8), 120.8 (C-3' and C-5'), 116.0 (C-10), 113.3 (C-4), 51.0 (C-13/15), 50.7 (C-15/13), 45.5 (C-12/16), 40.8 (C-16/12), 21.4 (C-19); HRMS m/z (ESI⁺) [Found: 334.1662, $C_{19}H_{20}N_5O$ requires (M+H)⁺ 334.1662]; LCMS (LCQ/MDAP) R_t = 6.9 min (Ana 30–95 over 20 min) m/z (ESI⁺) 334.1 (M+H)⁺.

4-(7-Chloro-1,6-naphthyridin-5-yl)piperazin-2-one

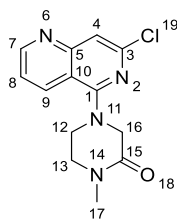
N,N-Diisopropylethylamine (0.71 mL, 4.06 mmol), 5,7-dichloro-1,6-naphthyridine (**284**) (200 mg, 1 mmol), piperazin-2-one (598 mg, 5.97 mmol) and in ethanol (7 mL) were heated at 100 °C overnight. LCMS indicated product formation (m/z 263). The reaction mixture was concentrated under reduced pressure and water (4 mL) was added. The mixture was extracted three times with ethyl acetate (3 × 40 mL) but the product was not soluble in ethyl acetate. The organic and aqueous phases were re-concentrated under reduced pressure and the remaining aqueous layer extracted with dichloromethane (3 × 40 mL). The combined organic phases were washed with water (40 mL), brine (40 mL), dried over MgSO_4 , filtered and concentrated under reduced pressure to give 4-(7-chloro-1,6-naphthyridin-5-yl)piperazin-2-one (123 mg, 44%) as an off-white solid.²¹⁵

R_f 0.23 (9:1 ethyl acetate:methanol); m.p. 210–212 °C; ν_{max} (thin film)/ cm^{-1} 3228 (N-H, br), 3052 (aromatic C-H, w), 1673 (C=O, s), 1571 (aromatic C-C, s), 1049 (C-N, s), 870 (N-H, s); ^1H NMR (600 MHz, $\text{DMSO}-d_6$) δ 9.01 (dd, J = 4.2, 1.6 Hz, 1H, H-9), 8.49 (d, J = 8.5 Hz, 1H, H-7), 8.09 (s, 1H, H-14), 7.56 (dd, J = 8.5, 4.2 Hz, 1H, H-8), 7.49–7.39 (m, 1H, H-4), 4.04 (s, 2H, H-16), 3.74 (d, J = 5.0 Hz, 2H, H-12), 3.44–3.38 (m, 2H, H-13); ^{13}C NMR (151 MHz, $\text{DMSO}-d_6$) δ 166.7 (C-15), 159.2 (C-1), 155.0 (C-7), 153.9 (C-5), 145.5 (C-3), 134.4 (C-9), 121.5 (C-10), 114.3 (C-4), 113.8 (C-8), 52.9 (C-16), 48.2 (C-12), 39.9 (C-13); HRMS m/z (ESI⁺) [Found: 285.0508, $\text{C}_{12}\text{H}_{11}\text{ClN}_4\text{NaO}$ requires (M+H)⁺ 285.0514]; LCMS (MDAP) Rt = 9.4 min (Ana 30–95 over 20 min), m/z (ESI⁺) 263.0 [^{35}Cl] and 264.7 [^{37}Cl] (M+H)⁺.

4-[7-(4-Pyridyl)-1,6-naphthyridin-5-yl]piperazin-2-one (293)

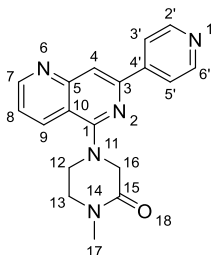
Potassium carbonate (150 mg, 1.08 mmol), pyridine-4-boronic acid hydrate (**196**) (44 mg, 0.36 mmol), *bis*[2-(di-*tert*-butylphosphanyl)cyclopenta-2,4-dien-1-yl]iron; dichloropalladium (12 mg, 0.02 mmol) and 4-(7-chloro-1,6-naphthyridin-5-yl)piperazin-2-one (100 mg, 0.36 mmol) in 4:1 acetonitrile:water (12 mL) were degassed under a flow of nitrogen and heated in a microwave reactor at 140 °C for 15 minutes. LCMS confirmed reaction completion (m/z 306). The reaction mixture was diluted with water (10 mL) and extracted twice with ethyl acetate (2 × 15 mL). The combined organic phases were dried over MgSO₄, filtered and concentrated under reduced pressure (55 mg). The crude was purified *via* flash column chromatography (4 g silica, petroleum ether:ethyl acetate, 1:0 to 0:1) to give 4-[7-(4-pyridyl)-1,6-naphthyridin-5-yl]piperazin-2-one (**293**) (31 mg, 27%) as a brown solid.¹⁵¹

R_f 0.70 (9:1 dichloromethane:methanol); m.p. 241–242 °C; ν_{\max} (thin film)/cm⁻¹ 3383 (N-H, br), 3196 (aromatic C-H, m), 3072 (aromatic C-H, m), 1662 (C=O, s), 1599 (aromatic C-C, m), 1358 (aliphatic C-H, s), 837 (N-H, s), 772 (C-H, s); ¹H NMR (600 MHz, DMSO-*d*₆) δ 9.07 (dd, J = 4.3, 1.6 Hz, 1H, H-7), 8.71 (d, 6.1 Hz, 2H, H-2' and H-6'), 8.54 (d, J = 8.3 Hz, 1H, H-9), 8.22–8.19 (m, 3H, H-13, H-14 and H-15), 8.01 (s, 1H, H-4), 7.62 (dd, J = 8.4, 4.2 Hz, 1H, H-8), 4.12 (s, 2H, H-16), 3.77 (t, J = 5.4 Hz, 2H, H-12), 3.47–3.32 (m, 2H, H-13); ¹³C NMR (151 MHz, DMSO-*d*₆) δ 167.4 (C-15), 159.2 (C-1), 154.7 (C-7), 153.4 (C-5), 150.3 (C-2' and C-6'), 147.9 (C-3), 145.3 (C-4'), 133.8 (C-9), 122.2 (C-8), 120.8 (C-3' and C-5'), 115.9 (C-10), 113.3 (C-4), 53.0 (C-16), 48.6 (C-12), 40.0 (C-13); HRMS m/z (ESI⁺) [Found: 328.1161 C₁₇H₁₅N₅NaO requires (M+Na)⁺ 328.1169]; LCMS (MDAP) R_t = 7.2 min (Ana 30–95 over 20 min), m/z (ESI⁺) 306.0 (M+H)⁺.

4-(7-Chloro-1,6-naphthyridin-5-yl)-1-methyl-piperazin-2-one

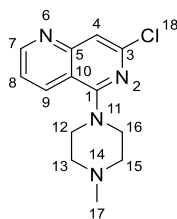
N,N-Diisopropylethylamine (0.71 mL, 4.06 mmol), 5,7-dichloro-1,6-naphthyridine (**284**) (200 mg, 1 mmol), and 1-methylpiperazin-2-one (684 mg, 5.99 mmol) in ethanol (7 mL) were stirred at 100 °C overnight. LCMS indicated product formation (m/z 276, 278). The mixture was concentrated under reduced pressure and water (4 mL) was added. The mixture was extracted four times with ethyl acetate (4 × 40 mL). The combined organic phases were washed with water (40 mL) and brine (40 mL) then dried over MgSO_4 , filtered and concentrated under reduced pressure to give an orange oil (553 mg). The crude was purified *via* flash column chromatography (12 g silica, dichloromethane:methanol, 1:0 to 9:1) to give 4-(7-chloro-1,6-naphthyridin-5-yl)-1-methyl-piperazin-2-one (212 mg, 72%) as a pale yellow solid.

R_f 0.53 (9:1 dichloromethane:methanol); m.p. 162–164 °C; ν_{max} (thin film)/ cm^{-1} 2939 (aliphatic C-H, w), 1657 (C=O, s), 1578 (aromatic C-C, s), 1346 (aliphatic C-H, s), 1071 (C-N, s), 873 (C-H, m); ^1H NMR (600 MHz, $\text{DMSO}-d_6$) δ 9.01 (dd, J = 4.2, 1.6 Hz, 1H, H-7), 8.51–8.47 (m, 1H, H-9), 7.57 (dd, J = 8.5, 4.2 Hz, 1H, H-8), 7.45 (d, J = 0.7 Hz, 1H, H-4), 4.10 (s, 2H, H-16), 3.81 (t, J = 5.4 Hz, 2H, H-12), 3.61–3.47 (m, 2H, H-13), 2.91 (s, 3H, H-17); ^{13}C NMR (151 MHz, $\text{DMSO}-d_6$) δ 165.4 (C-15), 159.3 (C-1), 155.4 (C-7), 154.2 (C-5), 145.9 (C-3), 134.6 (C-9), 121.9 (C-8), 114.5 (C-10), 114.3 (C-4), 53.5 (C-16), 48.4 (C-12), 47.6 (C-13), 33.9 (C-17); HRMS m/z (ESI $^+$) [Found: 299.0665, $\text{C}_{13}\text{H}_{13}\text{ClN}_4\text{NaO}$ requires (M+H) $^+$ 299.0670]; LCMS (MDAP) R_t = 15.6 min (Ana 5–95 over 20 min), m/z (ESI $^+$) 276.900 [^{35}Cl] and 278.850 [^{37}Cl] (M+H) $^+$.

1-Methyl-4-[7-(4-pyridyl)-1,6-naphthyridin-5-yl]piperazin-2-one (294)

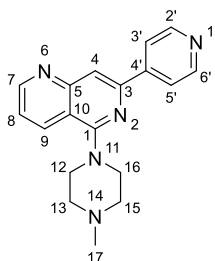
Potassium carbonate (225 mg, 1.63 mmol), pyridine-4-boronic acid hydrate (**196**) (67 mg, 0.54 mmol), *bis*[2-(di-*tert*-butylphosphanyl)cyclopenta-2,4-dien-1-yl]iron; dichloropalladium (18 mg, 0.03 mmol) and 4-(7-chloro-1,6-naphthyridin-5-yl)-1-methyl-piperazin-2-one (150 mg, 0.54 mmol) in 4:1 acetonitrile:water (12 mL) were degassed under a flow of nitrogen and heated in a microwave reactor at 140 °C for 15 minutes. LCMS confirmed reaction completion (m/z 320). The reaction mixture was diluted with water (20 mL) and extracted twice with ethyl acetate (2 × 25 mL). The combined organic phases were dried over MgSO_4 , filtered and concentrated under reduced pressure to give a yellow oil (52 mg). The crude was purified *via* flash column chromatography (4 g dichloromethane:methanol, 1:0 to 9:1) to give 1-methyl-4-[7-(4-pyridyl)-1,6-naphthyridin-5-yl]piperazin-2-one (**294**) (36 mg, 20%) as a pale brown solid.

R_f 0.62 (9:1 dichloromethane:methanol); m.p. 200–202 °C; ν_{max} (thin film)/ cm^{-1} 3029 (aromatic C-H, w), 2918 (aliphatic C-H, w), 1635 (C=O, s), 1598 (C=C, s), 1567 (aromatic C-C, s), 1076 (C-N, s); ^1H NMR (600 MHz, $\text{DMSO}-d_6$) δ 9.08 (dd, J = 4.2, 1.6 Hz, 1H, H-7), 8.71 (d, J = 5.9 Hz, 2H, H-2' and H-6'), 8.54 (d, J = 8.4 Hz, 1H, H-9), 8.22 (s, 1H, H-4), 8.20 (d, J = 6.0 Hz, 2H, H-3' and H-5'), 7.63 (dd, J = 8.4, 4.2 Hz, 1H, H-8), 4.17 (s, 2H, H-16), 3.84 (t, J = 5.5 Hz, 2H, H-13), 3.55 (t, J = 5.5 Hz, 2H, H-12), 2.91 (s, 3H, H-17); ^{13}C NMR (151 MHz, $\text{DMSO}-d_6$) δ 165.7 (C-15), 159.0 (C-1), 154.7 (C-7), 153.3 (C-5), 150.3 (C-2' and C-6'), 147.9 (C-3), 145.3 (C-4'), 133.8 (C-9), 122.3 (C-8), 120.8 (C-3' and C-5'), 115.8 (C-10), 113.4 (C-4), 53.2 (C-16), 48.6 (C-13), 47.4 (C-12), 33.4 (C-17); HRMS m/z (ESI⁺) [Found: 342.1320, $\text{C}_{18}\text{H}_{17}\text{N}_5\text{NaO}$ requires (M+H)⁺ 342.1325]; LCMS (MDAP) R_t = 9.9 min (Ana 5–95 over 20 min), m/z (ESI⁺) 320.1 (M+H)⁺.

7-Chloro-5-(4-methylpiperazin-1-yl)-1,6-naphthyridine

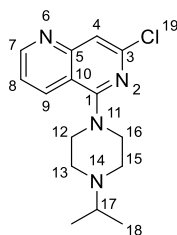
5,7-Dichloro-1,6-naphthyridine (**284**) (200 mg, 1 mmol), 1-methylpiperazine (0.66 mL, 5.97 mmol) and *N,N*-diisopropylethylamine (0.71 mL, 4.06 mmol) were stirred in ethanol (7 mL) at 100 °C overnight. LCMS confirmed formation of product (m/z 263). The reaction mixture was concentrated under reduced pressure and water was added (4 mL). The mixture was extracted three times with ethyl acetate (3 × 40 mL). The combined organic phases were washed with water (40 mL) and brine (40 mL), dried over MgSO_4 , filtered and concentrated under reduced pressure to give a brown solid (252 mg). The crude was purified *via* flash column chromatography (10 g silica, dichloromethane:methanol, 1:0 to 9:1) to give 7-chloro-5-(4-methylpiperazin-1-yl)-1,6-naphthyridine (206 mg, 74%) as an off-white solid.

R_f 0.38 (9:1 dichloromethane:methanol); m.p. 125–127 °C; ν_{max} (thin film)/ cm^{-1} 2929 (aromatic C-H, w), 2831 (aliphatic C-H, w), 2795 (aliphatic C-H, m), 1598 (aromatic C=C, m), 1557 (aromatic C-C, s), 1417 (C-H, s), 1004 (C-N, s); ^1H NMR (600 MHz, $\text{DMSO}-d_6$) δ 8.99 (dd, J = 4.2, 1.5 Hz, 1H, H-7), 8.42 (d, J = 8.5 Hz, 1H, H-9), 7.55 (dd, J = 8.5, 4.2 Hz, 1H, H-8), 7.40 (s, 1H, H-4), 3.46 (t, J = 4.9 Hz, 4H, H-12 and H-16), 2.55 (t, J = 4.9 Hz, 4H, H-13 and H-15), 2.26 (s, 3H, H-17); ^{13}C NMR (151 MHz, $\text{DMSO}-d_6$) δ 106.6 (C-1), 154.8 (C-7), 153.7 (C-5), 145.7 (C-3), 134.3 (C-9), 121.3 (C-8), 114.2 (C-10), 113.5 (C-4), 54.3 (C-13 and C-15), 50.6 (C-12 and C-16), 45.7 (C-17); HRMS m/z (ESI^+) [Found: 263.0512, $\text{C}_{13}\text{H}_{16}\text{ClN}_4$ requires ($\text{M}+\text{H}$) $^+$ 263.1058]; LCMS (LCQ) R_t = 2.4 min, (4 min method); m/z (ESI^+) 263.18 ($\text{M}+\text{H}$) $^+$.

5-(4-Methylpiperazin-1-yl)-7-(4-pyridyl)-1,6-naphthyridine (295)

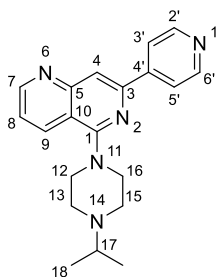
Potassium carbonate (225 mg, 1.63 mmol), pyridine-4-boronic acid hydrate (**196**) (67 mg, 0.54 mmol), *bis*[2-(di-*tert*-butylphosphanyl)cyclopenta-2,4-dien-1-yl]iron; dichloropalladium (18 mg, 0.03 mmol) and 7-chloro-5-(4-methylpiperazin-1-yl)-1,6-naphthyridine (150 mg, 0.54 mmol) in 4:1 acetonitrile:water (12 mL) were degassed under a flow of nitrogen and heated in a microwave reactor at 140 °C for 15 minutes. LCMS indicated product formation (m/z 306). The reaction mixture was diluted with water (20 mL) and extracted twice with ethyl acetate (2 × 25 mL). The combined organic phases were dried over $MgSO_4$, filtered and concentrated under reduced pressure to give a yellow oil (191 mg). The crude was purified twice *via* flash column chromatography (5 g petroleum ether:ethyl acetate, 1:0 to 0:1; then ethyl acetate:methanol, 1:0 to 9:1) to give 5-(4-methylpiperazin-1-yl)-7-(4-pyridyl)-1,6-naphthyridine (**295**) (116 mg, 67%) as a pale brown solid.

R_f 0.68 (100% ethyl acetate); m.p. 174–175 °C; ν_{max} (thin film)/ cm^{-1} 2922 (aliphatic C-H, m), 2836 (aliphatic C-H, m), 1599 (aromatic C-C, s), 1569 (aromatic C-H, s), 1443 (aliphatic C-H, s), 1007 (C-N, s); 1H NMR (600 MHz, $DMSO-d_6$) δ 9.05 (dd, J = 4.3, 1.6 Hz, 1H, H-7), 8.70 (d, J = 6.1 Hz, 2H, H-2' and H-6'), 8.46 (d, J = 8.3 Hz, 1H, H-9), 8.19 (d, J = 6.2 Hz, 2H, H-3' and H-5'), 8.15 (s, 1H, H-4), 7.60 (dd, J = 8.4, 4.2 Hz, 1H, H-8), 3.52 (t, J = 4.6 Hz, 4H, H-12 and H-16), 2.61 (t, J = 4.8 Hz, 4H, H-13 and H-15), 2.29 (s, 3H, H-17); ^{13}C NMR (151 MHz, $DMSO-d_6$) δ 160.7 (C-1), 154.4 (C-7), 153.3 (C-5), 150.3 (C-2' and C-6'), 148.0 (C-1'), 145.5 (C-3), 133.9 (C-9), 122.0 (C-8), 120.7 (C-3' and C-5'), 115.9 (C-10), 112.9 (C-4), 54.5 (C-13 and C-15), 50.6 (C-12 and C-16), 45.7 (C-17); HRMS m/z (ESI⁺) [Found: 306.1711, $C_{18}H_{20}N_5$ requires (M+H)⁺ 306.1713]; LCMS (LCQ) R_t = 7.9 min (Ana 5–95 over 20 min), m/z (ESI⁺) 306.1 (M+H)⁺.

7-Chloro-5-(4-isopropylpiperazin-1-yl)-1,6-naphthyridine

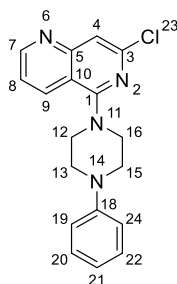
N,N-Diisopropylethylamine (0.71 mL, 4.06 mmol), 5,7-dichloro-1,6-naphthyridine (**284**) (200 mg, 1 mmol) and 1-isopropylpiperazine (765 mg, 5.97 mmol) in ethanol (7 mL) were stirred at 100 °C overnight. LCMS indicated product formation (*m/z* 291, 293). The mixture was concentrated under reduced pressure and water (4 mL) was added. The mixture was extracted four time with ethyl acetate (4 × 40 mL). The combined organic phases were washed with water (40 mL) and brine (40 mL) then dried over MgSO₄, filtered and concentrated under reduced pressure (313 mg). The crude was purified *via* flash column chromatography (12 g silica, dichloromethane:methanol, 1:0 to 9:1) to give 7-chloro-5-(4-isopropylpiperazin-1-yl)-1,6-naphthyridine (271 mg, 88%) as a yellow oil.

R_f 0.28 (9:1 ethyl acetate:methanol); m.p. N/A; ν_{max} (thin film)/cm⁻¹ 2966 (aliphatic C-H, m), 1675 (C=C, m), 1596 (aromatic C-C, s), 1555 (aromatic C-C, s), 1441 (aliphatic C-H, s), 1015 (C-N, s), 769 (C-H, s); ¹H NMR (600 MHz, DMSO-*d*₆) δ 8.98 (dd, *J* = 4.2, 1.6 Hz, 1H, H-7), 8.43 (d, *J* = 8.5 Hz, 1H, H-9), 7.54 (dd, *J* = 8.5, 4.2 Hz, 1H, H-8), 7.39 (s, 1H, H-4), 3.45 (t, *J* = 4.8 Hz, 4H, H-12 and H-16), 2.72 (p, *J* = 6.6 Hz, 1H, H-17), 2.67 (t, *J* = 4.8 Hz, 4H, H-13 and H-15), 1.02 (d, *J* = 6.5 Hz, 6H, H-18); ¹³C NMR (151 MHz, DMSO-*d*₆) δ 161.1 (C-1), 155.2 (C-7), 154.3 (C-5), 146.2 (C-3), 134.8 (C-9), 121.7 (C-8), 114.6 (C-10), 113.8 (C-4), 54.2 (C-17), 51.5 (C-12 and C-16), 48.3 (C-13 and C-15), 18.6 (C-18); HRMS *m/z* (ESI⁺) [Found: 291.1362, C₁₅H₂₀ClN₄ requires (M+H)⁺ 291.1371]; LCMS (MDAP) *R_t* = 7.1 min, (Ana 30–95 over 20 min); *m/z* (ESI⁺) 291.0 [³⁵Cl] and 293.0 [³⁷Cl] (M+H)⁺.

5-(4-Isopropylpiperazin-1-yl)-7-(4-pyridyl)-1,6-naphthyridine (296)

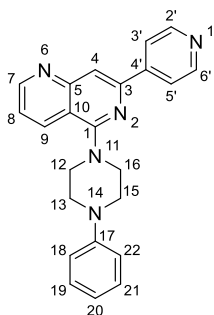
Potassium carbonate (203 mg, 1.47 mmol), pyridine-4-boronic acid hydrate (**196**) (60 mg, 0.49 mmol), *bis*[2-(di-*tert*-butylphosphanyl)cyclopenta-2,4-dien-1-yl]iron; dichloropalladium (16 mg, 0.02 mmol) and 7-chloro-5-(4-isopropylpiperazin-1-yl)-1,6-naphthyridine (150 mg, 0.49 mmol) in 4:1 acetonitrile:water (12 mL) were degassed under a flow of nitrogen and heated in a microwave reactor at 140 °C for 15 minutes. LCMS confirmed reaction completion (m/z 334). The reaction mixture was diluted with water (15 mL) and extracted twice with ethyl acetate (2 × 20 mL). The combined organic phases were dried over $MgSO_4$, filtered and concentrated under reduced pressure to give a yellow oil (167 mg). The crude was purified *via* flash column chromatography (4 g silica, dichloromethane:methanol, 1:0 to 9:1) to give 5-(4-isopropylpiperazin-1-yl)-7-(4-pyridyl)-1,6-naphthyridine (**296**) (87 mg, 51%) as an off-white solid.

R_f 0.28 (9:1 dichloromethane:methanol); m.p. 145–146 °C; ν_{max} (thin film)/ cm^{-1} 2962 (aliphatic C-H, m), 1599 (C=C, s), 1569 (aromatic C-C, s), 1328 (aliphatic C-H, s), 1118 (C-N, m), 774 (C-H, s); 1H NMR (600 MHz, $DMSO-d_6$) δ 9.04 (dd, J = 4.3, 1.6 Hz, 1H, H-7), 8.70 (d, J = 6.1 Hz, 2H, H-2' and H-6'), 8.47 (dd, J = 8.2, 1.5 Hz, 1H, H-9), 8.19 (d, J = 6.1 Hz, 2H, H-3' and H-5'), 8.14 (s, 1H, H-4), 7.60 (dd, J = 8.3, 4.2 Hz, 1H, H-8), 3.51 (app. s, 4H, H-12 and H-15), 2.73 (app. s, 2H, H-13 and H-15), 1.05 (d, J = 6.5 Hz, 7H, H-17 and H-18); ^{13}C NMR (151 MHz, $DMSO-d_6$) δ 160.7 (C-1), 154.5 (C-7), 153.3 (C-5), 150.3 (C-2' and C-6'), 148.0 (C-3), 145.5 (C-4'), 134.0 (C-9), 122.0 (C-8), 120.8 (C-3' and C-5'), 115.9 (C-10), 112.9 (C-4), 54.0 (C-17), 51.1 (C-12 and C-16), 48.0 (C-13 and C-15), 18.2 (C-18); HRMS m/z (ESI⁺) [Found: 334.2019, $C_{20}H_{24}N_5$ requires (M+H)⁺ 334.2026]; LCMS (MDAP) R_t = 5.5 min (Ana 5–95 over 20 min), m/z (ESI⁺) 334.1 (M+H)⁺.

7-Chloro-5-(4-phenylpiperazin-1-yl)-1,6-naphthyridine

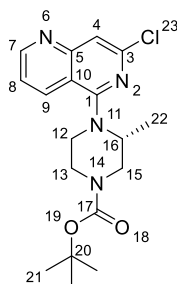
N,N-Diisopropylethylamine (0.71 mL, 4.06 mmol), 5,7-dichloro-1,6-naphthyridine (**284**) (200 mg, 1 mmol), and phenyl piperazine (972 mg, 5.99 mmol) in ethanol (7 mL) were heated at 100 °C overnight. LCMS indicated product formation (*m/z* 325). The reaction mixture was concentrated under reduced pressure and water (4 mL) was added. The mixture was extracted three times with ethyl acetate (3 × 40 mL). The combined organic phases were washed with water (40 mL), brine (40 mL), dried over MgSO₄, filtered and concentrated under reduced pressure (976 mg). The crude was purified *via* flash column chromatography (30 g silica, petroleum ether:ethyl acetate, 1:0 to 0:1) to give 7-chloro-5-(4-phenylpiperazin-1-yl)-1,6-naphthyridine (322 mg, 94%) as an orange solid.

R_f 0.78 (100% ethyl acetate); m.p. 154–155 °C; *v*_{max} (thin film)/cm⁻¹ 3044 (aromatic C-H, w), 2954 (aliphatic C-H, w), 1597 (C=C, s), 1558 (aromatic C-C, s), 1077 (C-N, s), 697 (C-H, s); ¹H NMR (600 MHz, DMSO-*d*₆) δ 9.02 (dd, *J* = 4.2, 1.4 Hz, 1H, H-7), 8.52 (d, *J* = 8.4 Hz, 1H, H-9), 7.58 (dd, *J* = 8.5, 4.2 Hz, 1H, H-8), 7.46 (s, 1H, H-4), 7.25 (t, *J* = 7.9 Hz, 1H, H-19 and H-21), 7.01 (d, *J* = 8.2 Hz, 2H, H-18 and H-22), 6.82 (t, *J* = 7.2 Hz, 1H, H-20), 3.65–3.55 (m, 4H, H-12 and H-16/H-13 and H-15), 3.44–3.36 (m, 4H, H-13 and H-15/H-12 and H-16); ¹³C NMR (151 MHz, DMSO-*d*₆) δ 160.7 (C-1), 155.0 (C-7), 153.8 (C-5), 150.9 (C-17), 145.8 (C-3), 134.5 (C-9), 129.1 (C-19 and C-21), 121.6 (C-8), 119.2 (C-20), 115.6 (C-18 and C-22), 114.4 (C-4), 113.9 (C-10), 50.7 (C-12 and C-16), 48.1 (C-13 and C-15); HRMS *m/z* (ESI⁺) [Found: 347.1032, C₁₈H₁₇ClN₄Na requires (M+H)⁺ 347.1034]; LCMS (MDAP) *R_t* = 25.1 min (Ana 30–95 over 30 min), *m/z* (ESI⁺) 326.0 [³⁵Cl] and 327.9 [³⁷Cl] (M+H)⁺.

5-(4-Phenylpiperazin-1-yl)-7-(4-pyridyl)-1,6-naphthyridine (297)

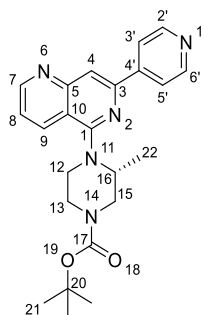
Potassium carbonate (191 mg, 1.39 mmol), pyridine-4-boronic acid hydrate (**196**) (57 mg, 0.46 mol), *bis*[2-(di-*tert*-butylphosphanyl)cyclopenta-2,4-dien-1-yl]iron; dichloropalladium (15 mg, 0.02 mmol) and 7-chloro-5-(4-phenylpiperazin-1-yl)-1,6-naphthyridine (150 mg, 0.46 mmol) in 4:1 acetonitrile:water (12 mL) were degassed under a flow of nitrogen and heated in a microwave reactor at 140 °C for 15 minutes. LCMS confirmed reaction completion (m/z 368). The reaction mixture was diluted with water (20 mL) and extracted twice with ethyl acetate (2 × 25 mL). The combined organic phases were dried over MgSO_4 , filtered and concentrated under reduced pressure (135 mg). The crude was purified *via* flash column chromatography (4 g petroleum ether:ethyl acetate, 1:0 to 0:1) to give 5-(4-phenylpiperazin-1-yl)-7-(4-pyridyl)-1,6-naphthyridine (**297**) (108 mg, 60%) as a yellow solid.

R_f 0.15 (100% ethyl acetate); m.p. 167–168 °C; ν_{max} (thin film)/ cm^{-1} 3030 (aromatic C-H, w), 1960 (aliphatic C-H, w), 1598 (C=C, s), 1570 (aromatic C-C, s), 1111 (C-N, m), 757 (C-H, s); ^1H NMR (600 MHz, $\text{DMSO}-d_6$) δ 9.08 (dd, J = 4.2, 1.7 Hz, 1H, H-7), 8.72 (d, J = 6.2 Hz, 1H, H-2' and H-6'), 8.57 (d, J = 8.3 Hz, 1H, H-9), 8.23 (d, J = 6.2 Hz, 1H, H-3' and H-5'), 8.21 (s, 1H, H-4), 7.64 (dd, J = 8.4, 4.2 Hz, 1H, H-8), 7.27 (t, J = 8.5, 7.2 Hz, 1H, H-19 and H-21), 7.04 (d, J = 7.8 Hz, 1H, H-18 and H-22), 6.83 (t, J = 7.3 Hz, 1H, H-20), 3.68 (t, J = 5.1, 4.7 Hz, 4H, H-12 and H-16), 3.46 (t, J = 5.0 Hz, 4H, H-13 and H-15); ^{13}C NMR (151 MHz, $\text{DMSO}-d_6$) δ 160.7 (C-1), 154.6 (C-7), 153.3 (C-5), 151.0 (C-17), 150.3 (C-2' and C-6'), 148.1 (C-3), 145.5 (C-4'), 134.0 (C-9), 129.0 (C-19 and C-21), 122.1 (C-8), 120.8 (C-3' and C-5'), 119.1 (C-20), 116.0 (C-10), 115.6 (C-18 and C-22), 113.2 (C-4), 50.8 (C-12 and C-16), 48.2 (C-13 and C-15); HRMS m/z (ESI $^+$) [Found: 368.1862, $\text{C}_{23}\text{H}_{22}\text{N}_5$ requires (M+H) $^+$ 368.1870]; LCMS (MDAP) R_t = 9.9 min (Ana 30–95 over 20 min), m/z (ESI $^+$) 368.0 (M+H) $^+$.

***Tert*-Butyl (3*R*)-4-(7-chloro-1,6-naphthyridin-5-yl)-3-methyl-piperazine-1-carboxylate**

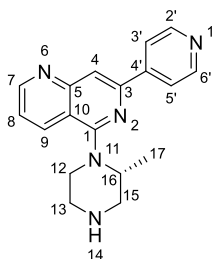
N,N-diisopropylethylamine (0.71 mL, 4.06 mmol), 5,7-dichloro-1,6-naphthyridine (**284**) (200 mg, 1 mmol) and *tert*-butyl (3*R*)-3-methylpiperazine-1-carboxylate (1.20 g, 5.99 mmol) in ethanol (7 mL) were heated at 100 °C overnight. LCMS indicated product formation (*m/z*/ 363). The reaction mixture was concentrated under reduced pressure and water (4 mL) was added. The mixture was extracted three times with ethyl acetate (3 × 40 mL). The combined organic phases were washed with water (40 mL), brine (40 mL), dried over MgSO₄, filtered and concentrated under reduced pressure to give a yellow oil (1.03 g). The crude was purified *via* flash column chromatography (30 g silica, petroleum ether:ethyl acetate, 1:0 to 0:1) to give *tert*-butyl (3*R*)-4-(7-chloro-1,6-naphthyridin-5-yl)-3-methyl-piperazine-1-carboxylate (345 mg, 85%) as a yellow solid.

R_f 0.70 (100% ethyl acetate); m.p. 101–102 °C; ν_{\max} (thin film)/cm⁻¹ 3051 (aromatic C-H, w), 2934 (aliphatic C-H, m), 1688 (C=O, s), 1597 (C=C, m), 1557 (aromatic C-C, s), 1056 (C-N, s), 771 (C-H, s); ¹H NMR (600 MHz, DMSO-*d*₆) δ 9.01 (dd, *J* = 4.2, 1.2 Hz, 1H, H-7), 8.48 (d, *J* = 8.5 Hz, 1H, H-9), 7.58 (dd, *J* = 8.5, 4.2 Hz, 1H, H-8), 7.45 (s, 1H, H-4), 4.27 (s, 1H, H-16), 3.84 (t, *J* = 15.0 Hz, 1H, H-12), 3.71 (d, *J* = 12.9 Hz, 1H, H-15), 3.41 (t, *J* = 12.4 Hz, 1H, H-13), 3.21 (dd, *J* = 13.0, 3.8 Hz, 1H, H-15), 3.06–2.91 (m, 1H, H-13), 1.42 (s, 9H, H-21), 1.28 (d, *J* = 6.7 Hz, 3H, H-22); ¹³C NMR (151 MHz, DMSO-*d*₆) δ 161.1 (C-1), 154.9 (C-7), 153.8 (C-17), 153.8 (C-5), 145.7 (C-3), 134.1 (C-9), 121.5 (C-8), 114.3 (C-10), 113.9 (C-4), 79.0 (C-20), 54.2 (C-15), 50.8 (C-12), 46.9 (C-16), 38.6 (C-13), 28.1 (C-21), 15.8 (C-22); HRMS *m/z* (ESI⁺) [Found: 385.1391, C₁₈H₂₃ClN₄NaO₂ requires (M+H)⁺ 385.1402]; LCMS (MDAP) *R_t* = 25.3 min (Ana 30–95 over 20 min), *m/z* (ESI⁺) 363.1 [³⁵Cl] and 365.0 [³⁷Cl] (M+H)⁺.

***Tert*-Butyl (3*R*)-3-methyl-4-[7-(4-pyridyl)-1,6-naphthyridin-5-yl]piperazine-1-carboxyl-ate**

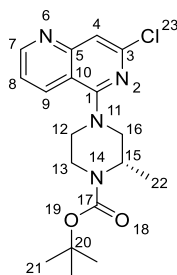
Potassium carbonate (171 mg, 1.24 mmol), pyridine-4-boronic acid hydrate (**196**) (51 mg, 0.41 mmol), *bis*[2-(di-*tert*-butylphosphanyl)cyclopenta-2,4-dien-1-yl]iron; dichloropalladium (13 mg, 0.02 mmol) and *tert*-butyl (3*R*)-4-(7-chloro-1,6-naphthyridin-5-yl)-3-methyl-piperazine-1-carboxylate (150 mg, 0.41 mmol) in 4:1 acetonitrile:water (12 mL) were degassed under a flow of nitrogen and heated in a microwave reactor at 140 °C for 15 minutes. LCMS confirmed reaction completion (*m/z* 406). The reaction mixture was diluted with water (20 mL) and extracted twice with ethyl acetate (2 × 25 mL). The combined organic phases were dried over MgSO₄, filtered and concentrated under reduced pressure (107 mg). The crude was purified *via* flash column chromatography (4 g petroleum ether:ethyl acetate, 1:0 to 0:1) to give *tert*-butyl (3*R*)-3-methyl-4-[7-(4-pyridyl)-1,6-naphthyridin-5-yl]piperazine-1-carboxylate (77 mg, 44%) as a pale orange solid.

R_f 0.15 (100% ethyl acetate); m.p. 170–172 °C; ν_{max} (thin film)/cm⁻¹ 2972 (aliphatic C-H, w), 1690 (C=O, s), 1598 (C=C, m), 1568 (aromatic C-C, m), 1025 (C-N, s), 769 (C-H, s); ¹H NMR (600 MHz, DMSO-*d*₆) δ 9.08 (dd, *J* = 4.3, 1.6 Hz, 1H, H-7), 8.71 (d, *J* = 1.6 Hz, 2H, H-2' and H-6'), 8.52 (d, *J* = 7.9 Hz, 1H, H-9), 8.23–8.19 (m, 2H, H-3' and H-5'), 8.20 (s, 1H, H-4), 7.64 (dd, *J* = 8.4, 4.2 Hz, 1H, H-8), 4.33 (s, 1H, H-16), 3.98–3.86 (m, 2H, H-12), 3.81 (d, *J* = 13.0 Hz, 1H, H-15), 3.46 (t, *J* = 12.5 Hz, 1H, H-13), 3.23 (dd, *J* = 12.9, 3.7 Hz, 1H, H-15), 3.03 (td, *J* = 12.4, 3.3 Hz, 1H, H-13), 1.44 (s, 9H, H-21), 1.34 (d, *J* = 6.7 Hz, 3H, H-22); ¹³C NMR (151 MHz, DMSO-*d*₆) δ 161.1 (C-1), 154.6 (C-7), 153.9 (C-17), 153.4 (C-5), 150.3 (C-2' and C-6'), 148.0 (C-3), 145.4 (C-4'), 133.7 (C-9), 122.1 (C-8), 120.8 (C-3' and C-5'), 116.0 (C-10), 113.2 (C-9), 79.0 (C-20), 54.7 (C-15), 50.9 (C-12), 47.0 (C-13), 28.1 (C-21), 15.8 (C-22); HRMS *m/z* (ESI⁺) [Found: 406.2230, C₂₃H₂₈N₅O₂ requires (M+H)⁺ 406.2238]; LCMS (MDAP) *R_t* = 11.0 min (Ana 30–95 over 20 min), *m/z* (ESI⁺) 406.1 (M+H)⁺.

5-[(2*R*)-2-Methylpiperazin-1-yl]-7-(4-pyridyl)-1,6-naphthyridine (298)


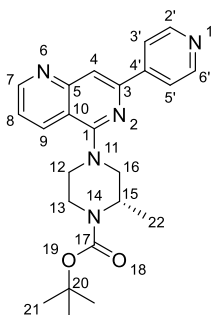
Tert-Butyl(3*R*)-3-methyl-4-[7-(4-pyridyl)-1,6-naphthyridin-5-yl]piperazine-1-carboxylate (35 mg, 0.08 mmol) was stirred in dichloromethane (1 mL) to 0 °C. Trifluoro acetic acid (0.35 mL, 4.57 mmol) was added dropwise and the reaction was stirred at room temperature for 4 h. The reaction mixture was concentrated under reduced pressure and purified *via* SCX cartridge by elution with methanol then 2 M ammonia in methanol to give 5-[(2*R*)-2-methylpiperazin-1-yl]-7-(4-pyridyl)-1,6-naphthyridine (**298**) (24 mg, 91%) as a yellow solid.

R_f 0.10 (9:1 dichloromethane:methanol); m.p. sublimates above 220 °C; ν_{\max} (thin film)/ cm^{-1} 2983 (aromatic C-H, w), 1669 (C=C, s), 1598 (aromatic C-C, s), 1464 (aliphatic C-H, m), 1058 (C-N, s), 713 (N-H, s); $^1\text{H NMR}$ (600 MHz, $\text{DMSO}-d_6$) δ 9.10–9.08 (m, 1H, H-7), 8.72 (d, J = 5.9 Hz, 2H, H-2' and H-6'), 8.59 (d, J = 8.4 Hz, 1H, H-9), 8.27 (s, 1H, H-4), 8.21 (d, J = 6.0 Hz, 2H, H-3' and H-5'), 7.65 (dd, J = 8.5, 4.3 Hz, 1H, H-8), 7.15 (s, 1H, H-14), 4.06–3.89 (m, 2H, H-13), 3.64 (s, 1H, H-16), 3.52–3.36 (m, 3H, H-12 and H-15), 3.23–3.10 (m, 1H, H-15), 1.32 (d, J = 6.5 Hz, 3H, H-17); $^{13}\text{C NMR}$ (151 MHz, $\text{DMSO}-d_6$) δ 159.9 (C-1), 154.8 (C-7), 153.2 (C-5), 149.9 (C-2' and C-6'), 147.8 (C-3), 145.8 (C-4'), 133.5 (C-9), 122.5 (C-8), 120.9 (C-3' and C-5'), 116.2 (C-10), 114.3 (C-4), 53.6 (C-13), 50.3 (C-16), 47.5 (C-12), 42.5 (C-15), 15.8 (C-17); HRMS m/z (ESI⁺) [Found: 306.1700, $\text{C}_{18}\text{H}_{20}\text{N}_5$ requires (M+H)⁺ 306.1713]; LCMS (MDAP) R_t = 6.8 min (Ana 30–95 over 20 min), m/z (ESI⁺) 305.900 (M+H)⁺.

***Tert*-Butyl (2*S*)-4-(7-chloro-1,6-naphthyridin-5-yl)-2-methyl-piperazine-1-carboxylate**

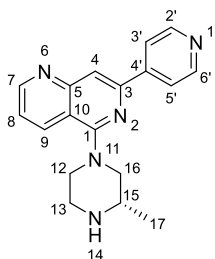
N,N-Diisopropylethylamine (0.71 mL, 4.06 mmol), 5,7-dichloro-1,6-naphthyridine (**284**) (200 mg, 1 mmol) and (*S*)-1-*N*-Boc-2-methylpiperazine (1.20 g, 5.99 mmol) in ethanol (7 mL) were heated at 100 °C overnight. LCMS indicated product formation (*m/z* 363). The reaction mixture was concentrated under reduced pressure and water (4 mL) was added. The mixture was extracted three times with ethyl acetate (3 × 40 mL). The combined organic phases were washed with water (40 mL), brine (40 mL), dried over MgSO₄, filtered and concentrated under reduced pressure to give an orange oil (920 mg). The crude was purified *via* flash column chromatography (30 g silica, petroleum ether:ethyl acetate, 1:0 to 0:1) to give *tert*-butyl (2*S*)-4-(7-chloro-1,6-naphthyridin-5-yl)-2-methyl-piperazine-1-carboxylate (365 mg, 80%) as a yellow solid.

R_f 0.70 (100% ethyl acetate); m.p. 104–106 °C; ν_{max} (thin film)/cm⁻¹ 3052 (aromatic C-H, w), 2972 (aliphatic C-H, m), 1688 (C=O, s), 1598 (C=C, m), 1577 (aromatic C-C, s), 1118 (C-N, s); ¹H NMR (600 MHz, DMSO-*d*₆) δ 9.01 (dd, *J* = 4.2, 1.3 Hz, 1H, H-7), 8.48 (d, *J* = 8.5 Hz, 1H, H-9), 7.58 (dd, *J* = 8.5, 4.2 Hz, 1H, H-8), 7.45 (s, 1H, H-4), 4.27 (s, 1H, H-15), 3.84 (t, *J* = 15.4 Hz, 2H, H-12), 3.71 (d, *J* = 13.1 Hz, 1H, H-16), 3.48–3.36 (t, *J* = 11.4 Hz, 1H, H-13), 3.20 (dd, *J* = 12.9, 3.6 Hz, 1H, H-16), 3.00 (td, *J* = 11.9, 2.8 Hz, 1H, H-13), 1.42 (s, 9H, H-21), 1.28 (d, *J* = 6.7 Hz, 3H, H-22); ¹³C NMR (151 MHz, DMSO-*d*₆) δ 161.1 (C-1), 154.9 (C-7), 153.8 (H-17), 153.8 (H-5), 145.7 (C-3), 134.1 (C-9), 121.5 (C-8), 114.3 (C-4), 113.9 (C-10), 79.0 (C-20), 54.2 (C-16), 50.8 (C-12), 46.9 (C-15), 38.6 (C-13), 28.1 (C-21), 15.8 (C-22); HRMS *m/z* (ESI⁺) [Found: 385.1390, C₁₈H₂₃ClN₄NaO₂ requires (M+H)⁺ 385.1402]; LCMS (MDAP) *R_t* = 25.3 min (Ana 5–95 over 20 min), *m/z* (ESI⁺) 363.1 [³⁵Cl] and 365.0 [³⁷Cl] (M+H)⁺.

***Tert*-Butyl (2*S*)-2-methyl-4-[7-(4-pyridyl)-1,6-naphthyridin-5-yl]piperazine-1-carboxylate**

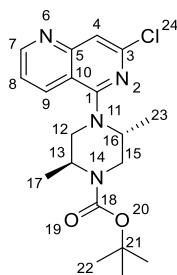
Potassium carbonate (171 mg, 1.24 mmol), Pyridine-4-boronic acid hydrate (**196**) (51 mg, 0.41 mmol), *bis*[2-(di-*tert*-butylphosphanyl)cyclopenta-2,4-dien-1-yl]iron; dichloropalladium (13 mg, 0.02 mmol) and *tert*-butyl (2*S*)-4-(7-chloro-1,6-naphthyridin-5-yl)-2-methyl-piperazine-1-carboxylate (150 mg, 0.41 mmol) in 4:1 acetonitrile:water (12 mL) were degassed under a flow of nitrogen and heated in a microwave reactor at 140 °C for 15 minutes. LCMS confirmed reaction completion (m/z 406). The reaction mixture was diluted with water (20 mL) and extracted twice with ethyl acetate (2 × 25 mL). The combined organic phases were dried over MgSO_4 , filtered and concentrated under reduced pressure (139 mg). The crude was purified *via* flash column chromatography (4 g petroleum ether:ethyl acetate, 1:0 to 0:1) give *tert*-butyl (2*S*)-2-methyl-4-[7-(4-pyridyl)-1,6-naphthyridin-5-yl]piperazine-1-carboxylate (79 mg, 45%) as a pale pink solid.

R_f 0.49 (9:1 ethyl acetate:methanol); m.p. 180–181 °C; ν_{max} (thin film)/ cm^{-1} 3030 (aromatic C-H, w), 2978 (aromatic C-H, w), 1692 (C=O, m), 1598 (C=C, s), 1569 (aromatic C-C, s); ^1H NMR (600 MHz, $\text{DMSO}-d_6$) δ 9.07 (d, J = 4.3 Hz, 1H, H-7), 8.71 (d, J = 6.2 Hz, 2H, H-2' and H-6'), 8.52 (d, J = 7.0 Hz, 1H, H-9), 8.21 (d, J = 6.3 Hz, 2H, H-3' and H-5'), 8.20 (s, 1H, H-4), 7.64 (dd, J = 8.4, 4.2 Hz, 1H, H-8), 4.33 (s, 1H, H-15), 3.96–3.87 (m, 1H, H-12), 3.81 (d, J = 12.6 Hz, 1H, H-16), 3.46 (t, J = 11.4 Hz, 1H, H-13), 3.23 (dd, J = 13.1, 4.2 Hz, 1H, H-16), 3.03 (td, J = 12.4, 3.4 Hz, 1H, H-13), 1.44 (s, 9H, H-21), 1.34 (d, J = 6.7 Hz, 3H, H-22); ^{13}C NMR (151 MHz, $\text{DMSO}-d_6$) δ 161.1 (C-1), 154.6 (C-7), 153.9 (C-17), 153.4 (C-5), 150.3 (C-2' and C-6'), 148.0 (C-3), 145.4 (C-4'), 133.7 (C-9), 122.1 (C-8), 120.8 (C-3' and C-5'), 116.0 (C-10), 113.2 (C-4), 79.0 (C-20), 54.7 (C-16), 50.9 (C-13), 47.0 (C-12), 28.1 (C-21), 15.8 (C-22); HRMS m/z (ESI^+) [Found: 406.2232, $\text{C}_{23}\text{H}_{28}\text{N}_5\text{O}_2$ requires ($\text{M}+\text{H})^+$ 406.2238]; LCMS (MDAP) R_t = 11.0 min (Ana 30–95 over 20 min), m/z (ESI^+) 406.1 ($\text{M}+\text{H})^+$.

5-[(3S)-3-Methylpiperazin-1-yl]-7-(4-pyridyl)-1,6-naphthyridine (299)


Tert-Butyl (2S)-2-methyl-4-[7-(4-pyridyl)-1,6-naphthyridin-5-yl]piperazine-1-carboxylate (30 mg, 0.07 mmol) was stirred in dichloromethane (1 mL) for 10 min at 0 °C. Trifluoro acetic acid (0.3 mL, 3.92 mmol) was added dropwise and then the reaction was stirred at room temperature for 4 h. The reaction mixture was concentrated under reduced pressure and purified *via* SCX cartridge by elution with methanol then 2 M ammonia in methanol to give 5-[(3S)-3-methylpiperazin-1-yl]-7-(4-pyridyl)-1,6-naphthyridine (**299**) (22 mg, 97%) as a yellow solid.

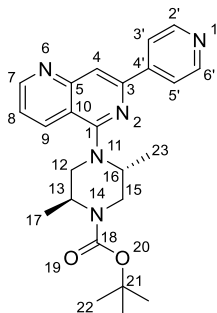
R_f 0.10 (9:1 dichloromethane:methanol); m.p. 156–158 °C; ν_{\max} (thin film)/ cm^{-1} 3352 (N-H, br), 2971 (aliphatic C-H, w), 1597 (C=C, m), 1569 (aromatic C-C, s), 1029 (C-N, s), 827 (N-H, s); ^1H NMR (600 MHz, $\text{DMSO}-d_6$) δ 9.05 (dd, J = 4.1, 1.3 Hz, 1H, H-7), 8.70 (d, J = 6.0 Hz, 2H, H-2' and H-6'), 8.51 (d, J = 8.3 Hz, 1H, H-9), 8.18 (s, 1H, H-4), 8.17 (d, J = 3.1 Hz, 2H, H-3' and H-5'), 7.61 (dd, J = 8.4, 4.2 Hz, 1H, H-8), 3.85–3.87 (m, 2H, H-12 and H-16), 3.29 (s, 1H, H-15), 3.19 (d, J = 10.1 Hz, 3H, H-12 and H-13), 2.91 (t, J = 11.7 Hz, 1H, H-16), 1.17 (d, J = 6.3 Hz, 3H, H-17); ^{13}C NMR (151 MHz, $\text{DMSO}-d_6$) δ 160.4 (C-1), 154.5 (C-7), 153.3 (C-5), 150.3 (C-2' and C-6'), 147.9 (C-3), 145.4 (C-4'), 134.0 (C-9), 122.2 (C-8), 120.7 (C-3' and C-5'), 116.0 (C-10), 113.2 (C-4), 56.0 (C-16), 50.2 (C-15), 49.7 (C-12), 44.1 (C-13), 17.7 (C-17); HRMS m/z (ESI⁺) [Found: 306.1700, $\text{C}_{18}\text{H}_{20}\text{N}_5$ requires (M+H)⁺ 306.1713]; LCMS (MDAP) R_t = 7.0 min (Ana 30–95 over 20 min), m/z (ESI⁺) 305.9 (M+H)⁺.

***Tert*-Butyl (2*S*,5*R*)-4-(7-chloro-1,6-naphthyridin-5-yl)-2,5-dimethyl-piperazine-1-carboxylate**

N,N-Diisopropylethylamine (0.71 mL, 4.06 mmol), 5,7-dichloro-1,6-naphthyridine (**284**) (200 mg, 1 mmol), and (2*S*,5*R*)-1-Boc-2,5-dimethylpiperazine (1 g, 4.67 mmol) in ethanol (7 mL) and heated to 100 °C overnight. LCMS confirmed reaction completion (m/z 377). The reaction mixture was diluted with water (4 mL) and extracted three times with ethyl acetate (3 × 40 mL). The combined organic phases were washed with water (40 mL), brine (40 mL), dried over MgSO_4 , filtered and concentrated under reduced pressure to give a brown oil (813 mg). The crude was purified *via* flash column chromatography (24 g petroleum ether:ethyl acetate, 1:0 to 0:1) to give *tert*-butyl (2*S*,5*R*)-4-(7-chloro-1,6-naphthyridin-5-yl)-2,5-dimethyl-piperazine-1-carboxylate (369 mg, 93%) as an orange solid.

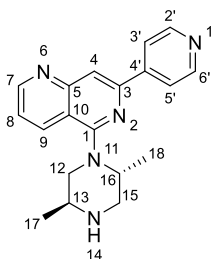
R_f 0.73 (100% ethyl acetate); m.p. 92–94 °C; ν_{max} (thin film)/ cm^{-1} 2972 (aliphatic C-H, w), 1679 (C=O, s), 1552 (aromatic C-C, s), 1364 (aliphatic C-H, s), 1130 (C-N, s), 779 (aliphatic C-H, s); ^1H NMR (600 MHz, $\text{DMSO}-d_6$) δ 8.99 (dd, J = 4.2, 1.5 Hz, 1H, H-7), 8.47 (d, J = 8.3 Hz, 1H, H-9), 7.55 (dd, J = 8.5, 4.2 Hz, 1H, H-8), 7.40 (s, 1H, H-4), 4.39–4.20 (m, 2H, H-16 and H-13), 3.71–3.59 (m, 3H, H-12 and H-15), 3.50–3.38 (m, 1H, H-12), 1.43 (s, 9H, H-22), 1.17 (d, J = 6.8 Hz, 3H, H-17), 1.05 (d, J = 6.6 Hz, 3H, H-23); ^{13}C NMR (151 MHz, $\text{DMSO}-d_6$) δ 161.0 (C-1), 155.3 (C-7), 154.7 (C-18), 154.3 (C-5), 146.1 (C-3), 134.8 (C-9), 121.7 (C-8), 114.9 (C-4), 113.8 (C-10), 79.3 (C-21), 53.2 (C-13 and C-16), 48.3 (C-12 and C-15), 16.4 (C-17), 14.2 (C-23); HRMS m/z (ESI^+) [Found: 399.1548, $\text{C}_{19}\text{H}_{25}\text{ClN}_4\text{NaO}_2$ requires ($\text{M}+\text{H}$) $^+$ 399.1558]; LCMS (MDAP) R_t = 25.7 min (Ana 5–95 over 20 min); m/z (ESI^+) 377.1 ($\text{M}+\text{H}$) $^+$.

***Tert*-Butyl (2*S*,5*R*)-2,5-dimethyl-4-[7-(4-pyridyl)-1,6-naphthyridin-5-yl]piperazine-1-carboxylate**



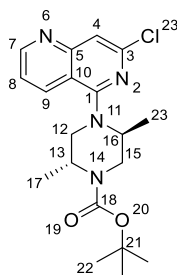
Potassium carbonate (165 mg, 1.19 mmol), pyridine-4-boronic acid hydrate (**196**) (49 mg, 0.40 mmol), *bis*[2-(di-*tert*-butylphosphanyl)cyclopenta-2,4-dien-1-yl]iron; dichloropalladium (13 mg, 0.02 mmol) and *tert*-butyl (2*S*,5*R*)-4-(7-chloro-1,6-naphthyridin-5-yl)-2,5-dimethylpiperazine-1-carboxylate (150 mg, 0.40 mmol) in 4:1 acetonitrile:water (12 mL) were degassed under a flow of nitrogen and heated in a microwave reactor at 140 °C for 15 minutes. LCMS confirmed reaction completion (m/z 420). The reaction mixture was diluted with water (20 mL) and extracted twice with ethyl acetate (2 × 25 mL). The combined organic phases were dried over MgSO_4 , filtered and concentrated under reduced pressure to give a yellow oil (167 mg). The crude was purified *via* flash column chromatography (5 g petroleum ether:ethyl acetate, 1:0 to 0:1) to give *tert*-butyl (2*S*,5*R*)-2,5-dimethyl-4-[7-(4-pyridyl)-1,6-naphthyridin-5-yl]piperazine-1-carboxylate (103 mg, 59%) as an off-white solid.

R_f 0.18 (100% ethyl acetate); m.p. 182–184 °C; ν_{max} (thin film)/ cm^{-1} 2972 (aliphatic C-H, w), 1682 (C=O, s), 1594 (C=C, s), 1478 (aromatic C-C, m), 1031 (C-N, m), 829 (N-H, s); ^1H NMR (600 MHz, $\text{DMSO}-d_6$) δ 9.05 (dd, J = 4.1, 1.3 Hz, 1H, H-9), 8.70 (d, J = 6.0 Hz, 2, H-2' and H-6'), 8.51 (d, J = 8.3 Hz, 1H, H-7), 8.19 (d, J = 6.1 Hz, 2H, H-3' and H-5'), 8.13 (s, 1H, H-4), 7.60 (dd, J = 8.4, 4.2 Hz, 1H, H-8), 4.46–4.40 (m, 1H, H-16), 4.34 (s, 1H, H-13), 3.78 (dd, J = 13.7, 3.9 Hz, 1H, H-12), 3.70 (s, 2H, H-15), 3.54 (d, J = 13.4 Hz, 1H, H-12), 1.44 (s, 9H, H-22), 1.22 (d, J = 6.7 Hz, 3H, H-17), 1.08 (d, J = 6.3 Hz, 3H, H-23); ^{13}C NMR (151 MHz, $\text{DMSO}-d_6$) δ 160.5 (C-1), 154.4 (C-7), 153.5 (C-5), 150.6 (C-18), 150.3 (C-2' and C-6'), 148.0 (C-3), 145.5 (C-4'), 134.0 (C-9), 121.9 (C-8), 121.3, 120.8 (C-3' and C-5'), 116.0 (C-10), 112.6 (C-4), 78.9 (C-21), 52.4 (C-13 and C-16), 47.9 (C-12 and C-15), 28.1 (C-22), 16.0 (C-17/23), 13.5 (C-23/17); HRMS m/z (ESI⁺) [Found: 420.2387, $\text{C}_{24}\text{H}_{30}\text{N}_5\text{O}_2$ requires (M+H)⁺ 420.2394]; LCMS (MDAP) Rt = 2.8 min (Ana 5–95 over 5 min), m/z (ESI⁺) 420.3 (M+H)⁺.

5-[(2*R*,5*S*)-2,5-Dimethylpiperazin-1-yl]-7-(4-pyridyl)-1,6-naphthyridine (300)


Tert-Butyl (2*S*,5*R*)-2,5-dimethyl-4-[7-(4-pyridyl)-1,6-naphthyridin-5-yl]piperazine-1-carboxylate (25 mg, 0.06 mmol) was stirred in dichloromethane (1 mL) and cooled to 0 °C. Trifluoro acetic acid (0.25 mL, 3.26 mmol) was added dropwise and the reaction was allowed to stir at room temperature for 4 h. The reaction mixture was concentrated under reduced pressure and purified *via* SCX cartridge by elution with methanol then 2 M ammonia in methanol to give 5-[(2*R*,5*S*)-2,5-dimethylpiperazin-1-yl]-7-(4-pyridyl)-1,6-naphthyridine (**300**) (18 mg, 95%) as a yellow solid.

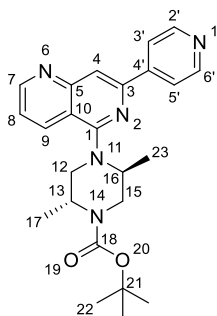
R_f 0.10 (9:1 dichloromethane:methanol); m.p. 124–125 °C; ν_{\max} (thin film)/cm⁻¹ 3288 (N-H, br), 1965 (aliphatic C-H, w), 1599 (C=C, m), 1570 (aromatic C-C, m), 1032 (C-N, s), 691 (N-H, m); ¹H NMR (600 MHz, DMSO-*d*₆) δ 9.11 (dd, J = 4.1, 1.5 Hz, 1H, H-7), 8.74–8.71 (m, 2H, H-2' and H-6'), 8.66 (d, J = 8.2 Hz, 1H, H-9), 8.38 (s, 1H, H-4), 8.22–8.16 (m, 2H, H-3' and H-5'), 7.68 (dd, J = 8.4, 4.2 Hz, 1H, H-8), 3.75 (s, 1H, H-13), 3.36 (s, 2H, H-16), 3.26 (d, J = 14.1 Hz, 2H, H-12 and H-15), 2.85 (t, J = 12.4 Hz, 1H, H-12), 2.61 (t, J = 10.4 Hz, 1H, H-15), 1.06 (d, J = 6.2 Hz, 3H, H-18), 1.03 (d, J = 6.0 Hz, 3H, H-17); ¹³C NMR (151 MHz, DMSO-*d*₆) δ 161.5 (C-1), 155.5 (C-7), 153.0 (C-5), 150.6 (C-17), 150.4 (C-2' and C-6'), 148.3 (C-3), 145.3 (C-4'), 133.5 (C-9), 123.2 (C-8), 120.7 (C-3' and C-5'), 119.3 (C-10), 115.3 (C-4), 58.9 (C-12), 56.0 (C-15), 51.1 (C-16/13), 49.8 (C-13/16), 17.5 (C-18), 15.7 (C-17); HRMS m/z (ESI⁺) [Found: 320.1857, C₁₉H₂₂N₅ requires (M+H)⁺ 320.1870]; LCMS (MDAP) R_t = 7.1 min (Ana 30–95 over 20 min), m/z (ESI⁺) 320.9 (M+H)⁺.

***Tert*-Butyl (2*R*,5*S*)-4-(7-chloro-1,6-naphthyridin-5-yl)-2,5-dimethyl-piperazine-1-carboxylate**

5,7-Dichloro-1,6-naphthyridine (**284**) (200 mg, 1 mmol), (2*R*,5*S*)-1-Boc-2,5-dimethylpiperazine hydrochloride (1.50 g, 5.97 mmol) and *N,N*-diisopropylethylamine (0.71 mL, 4.06 mmol) were stirred in ethanol (7 mL) at 100 °C overnight. LCMS indicated product formation (*m/z* 377). The reaction mixture was concentrated under reduced pressure and water (4 mL) was added. The mixture was extracted three times with ethyl acetate (3 × 40 mL). The combined organic phases were washed with water (40 mL) and brine (40 mL) and then dried over MgSO₄, filtered and concentrated under reduced pressure to give a brown mixture (569 mg). The crude was purified *via* flash column chromatography (20 g silica, petroleum ether:ethyl acetate, 1:0 to 0:1) to give *tert*-butyl (2*R*,5*S*)-4-(7-chloro-1,6-naphthyridin-5-yl)-2,5-dimethyl-piperazine-1-carboxylate (328 mg, 82%) as a yellow glass.

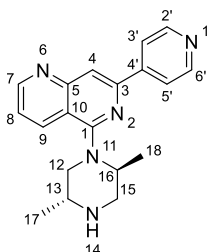
R_f 0.73 (100% ethyl acetate); m.p. 95–97 °C; ν_{max} (thin film)/cm⁻¹ 2975 (aliphatic C-H, w), 1679 (C=O, s), 1553 (aromatic C-C, s), 1488 (aliphatic C-H, m), 1031 (C-N, s), 859 (C-H, s); ¹H NMR (600 MHz, DMSO-*d*₆) δ 8.99 (dd, *J* = 4.1, 1.4 Hz, 1H, H-7), 8.47 (d, *J* = 8.3 Hz, 1H, H-9), 7.55 (dd, *J* = 8.5, 4.2 Hz, 1H, H-8), 7.40 (s, 1H, H-4), 4.32 (m, 2H, H-13 and H-16), 3.77–3.61 (m, 3H, H-12 and H-15), 3.54–3.38 (m, 1H, H-12/15), 1.43 (s, 9H, H-22), 1.17 (d, *J* = 6.8 Hz, 3H, H-17/23), 1.05 (d, *J* = 6.5 Hz, 3H, H-23/17); ¹³C NMR (151 MHz, DMSO-*d*₆) δ 160.6 (C-1), 154.8 (C-5), 154.3 (C-18), 153.9 (C-7), 145.7 (C-3), 134.4 (C-9), 121.3 (C-8), 114.5 (C-10), 113.4 (C-4), 78.9 (C-21), 52.8 (C-13 and C-16), 47.9 (C-15 and C-12), 28.1 (C-22), 16.0 (C-17/23), 13.8 (C-17/23); HRMS *m/z* (ESI⁺) [Found: 399.1546, C₁₉H₂₅ClN₄NaO₂ requires (M+H)⁺ 399.1558]; LCMS (MDAP) *R_t* = 22.9 min (Ana 30–95 over 30 min), *m/z* (ESI⁺) 377.1 [³⁵Cl] and 379.1 [³⁷Cl] (M+H)⁺.

***Tert*-Butyl (2*R*,5*S*)-2,5-dimethyl-4-[7-(4-pyridyl)-1,6-naphthyridin-5-yl]piperazine-1-carboxylate**



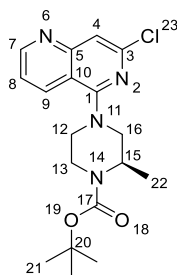
Potassium carbonate (157 mg, 1.13 mmol), pyridine-4-boronic acid hydrate (**196**) (46 mg, 0.38 mmol), *bis*[2-(di-*tert*-butylphosphanyl)cyclopenta-2,4-dien-1-yl]iron; dichloropalladium (12 mg, 0.02 mmol) and *tert*-butyl (2*R*,5*S*)-4-(7-chloro-1,6-naphthyridin-5-yl)-2,5-dimethylpiperazine-1-carboxylate (150 mg, 0.38 mmol) in 4:1 acetonitrile:water (12 mL) were degassed under a flow of nitrogen and heated in a microwave reactor at 140 °C for 15 minutes. LCMS confirmed reaction completion (m/z 420). The reaction mixture was diluted with water (20 mL) and extracted twice with ethyl acetate (2 × 25 mL). The combined organic phases were dried over MgSO_4 , filtered and concentrated under reduced pressure (163 mg). The crude was purified *via* flash column chromatography (5 g silica petroleum ether:ethyl acetate, 1:0 to 0:1) to give *tert*-butyl (2*R*,5*S*)-2,5-dimethyl-4-[7-(4-pyridyl)-1,6-naphthyridin-5-yl]piperazine-1-carboxylate (104 mg, 0.24 mmol, 62%) as an orange foam.¹⁵¹

R_f 0.18 (100% ethyl acetate); m.p. 135–137 °C; ν_{max} (thin film)/ cm^{-1} 2974 (aliphatic C-H, w), 1682 (C=O, s), 1595 (C=C, m), 1563 (aromatic C-C, s), 1055 (C-N, s), 731 (C-H, m); ^1H NMR (600 MHz, $\text{DMSO}-d_6$) δ 9.05 (dd, $J = 4.2, 1.4$ Hz, 1H, H-7), 8.70 (d, $J = 6.0$ Hz, 2H, H-2' and H-6'), 8.51 (d, $J = 8.4$ Hz, 1H, H-9), 8.19 (d, $J = 6.1$ Hz, 2H, H-3' and H-5'), 8.13 (s, 1H, H-4), 7.60 (dd, $J = 8.4, 4.2$ Hz, 1H, H-8), 4.47–4.38 (m, 1H, H-16), 4.34 (s, 1H, H-13), 3.78 (dd, $J = 13.5, 4.1$ Hz, 1H, H-12), 3.70 (s, 2H, H-15), 3.54 (dd, $J = 13.1, 1.8$ Hz, 1H, H-12), 1.44 (s, 9H, H-22), 1.21 (d, $J = 6.8$ Hz, 3H, H-17), 1.08 (d, $J = 6.4$ Hz, 3H, H-23); ^{13}C NMR (151 MHz, $\text{DMSO}-d_6$) δ 160.5 (C-1), 154.4 (C-7), 153.5 (C-5), 150.6 (C-18), 150.3 (C-2' and C-6'), 148.0 (C-3), 145.5 (C-4'), 133.9 (C-9), 121.8 (C-8), 120.7 (C-3' and C-5'), 116.0 (C-10), 112.6 (C-4), 78.9 (C-21), 52.4 (C-13 and C-16), 47.9 (C-12 and C-15), 28.1 (C-22), 16.2 (C-17), 13.5 (C-23); HRMS m/z (ESI⁺) [Found: 420.2384, $\text{C}_{24}\text{H}_{30}\text{N}_5\text{O}_2$ requires (M+H)⁺ 420.2394]; LCMS (MDAP) $R_t = 15.8$ min (Ana 5–95 over 20 min), m/z (ESI⁺) 420.2 (M+H)⁺.

5-[(2*S*,5*R*)-2,5-Dimethylpiperazin-1-yl]-7-(4-pyridyl)-1,6-naphthyridine (301)


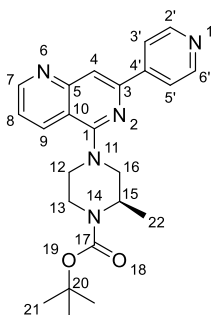
Tert-Butyl (2*R*,5*S*)-2,5-dimethyl-4-[7-(4-pyridyl)-1,6-naphthyridin-5-yl]piperazine-1-carboxylate (50 mg, 0.12 mmol) was dissolved in dichloromethane (1 mL) and cooled to 0 °C. Trifluoro acetic acid (0.5 mL, 6.68 mmol) was added dropwise and the reaction mixture was allowed to stir at room temperature overnight. LCMS (LCQ) indicated product formation (*m/z* 320). The reaction mixture was concentrated under reduced pressure to give a yellow solid. The crude was purified *via* SCX cartridge by elution with methanol then 2 M ammonia in methanol to give 5-[(2*S*,5*R*)-2,5-dimethylpiperazin-1-yl]-7-(4-pyridyl)-1,6-naphthyridine (**301**) (40 mg, 100%) as a yellow glass.

R_f 0.1 (9:1 dichloromethane:methanol); m.p. 185–186 °C; ν_{max} (thin film)/cm⁻¹ 2983 (aliphatic C-H br), 1671 (C=O, m), 1600 (C=C, m), 1570 (aromatic C-C, m), 1126 (C-N, s), 829 (N-H, s); ¹H NMR (600 MHz, DMSO-*d*₆) δ 9.17–9.08 (m, 1H, H-7), 8.74 (d, *J* = 5.6 Hz, 2H, H-2' and H-6'), 8.72 (d, *J* = 8.2 Hz, 1H, H-9), 8.44 (s, 1H, H-4), 8.20 (d, *J* = 5.7 Hz, 2H, H-3' and H-5'), 7.71 (dd, *J* = 8.4, 4.3 Hz, 1H, H-8), 3.95–3.83 (m, 1H, H-13), 3.68–3.53 (m, 1H, H-16), 3.47 (td, *J* = 13.8, 13.2, 3.0 Hz, 1H, H-12 and H-15), 3.07 (t, *J* = 11.6 Hz, 1H, H-12), 2.86 (t, *J* = 11.7 Hz, 1H, H-15), 1.18 (d, *J* = 6.5 Hz, 3H, H-18), 1.07 (d, *J* = 6.1 Hz, 3H, H-17); ¹³C NMR (151 MHz, DMSO-*d*₆) δ 161.0 (C-1), 155.3 (C-7), 153.0 (C-5), 150.5 (C-2' and C-6'), 148.4 (C-3), 145.2 (C-4'), 133.9 (C-9), 123.3 (C-8), 120.7 (C-3' and C-5'), 119.4 (C-10), 115.9 (C-4), 57.4 (C-15), 50.4 (C-16), 50.2 (C-13), 48.6 (C-12), 16.5 (C-17), 16.2 (C-18); HRMS *m/z* (ESI⁺) [Found: 320.1863, C₁₉H₂₂N₅ requires (M+H)⁺ 320.1870]; LCMS (MDAP) *R_t* = 5.5 min (Ana 5–95 over 20 min), *m/z* (ESI⁺) 320.1 (M+H)⁺.

***Tert*-Butyl (2*R*)-4-(7-chloro-1,6-naphthyridin-5-yl)-2-methyl-piperazine-1-carboxylate**

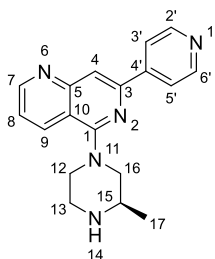
N,N-diisopropylethylamine (0.71 mL, 4.06 mmol), 5,7-dichloro-1,6-naphthyridine (**284**) (200 mg, 1 mmol) and (*R*)-*N*-Boc-2-methylpiperazine (1.20 g, 5.99 mmol) in ethanol (7 mL) were heated at 100 °C overnight. LCMS indicated product formation (*m/z* 263 and 365). The reaction mixture was concentrated under reduced pressure and water (4 mL) was added. The mixture was extracted three times with ethyl acetate (3 × 40 mL). The combined organic phases were washed with water (40 mL), brine (40 mL), dried over MgSO₄, filtered and concentrated under reduced pressure (1.03 g). The crude was purified *via* flash column chromatography (4 g silica, petroleum ether:ethyl acetate, 1:0 to 0:1) to give *tert*-butyl (2*R*)-4-(7-chloro-1,6-naphthyridin-5-yl)-2-methyl-piperazine-1-carboxylate (328 mg, 81%) as an off-white solid.

R_f 0.67 (100% ethyl acetate); m.p. 106–108 °C; ν_{\max} (thin film)/cm⁻¹ 2972 (aliphatic C-H, w), 1690 (C=O, s), 1598 (C=C, m), 1558 (aromatic C-C, s), 1471 (aliphatic C-H, m), 1024 (C-N, s), 772 (C-H, s); ¹H NMR (600 MHz, DMSO-*d*₆) δ 9.01 (dd, *J* = 4.1, 1.3 Hz, 1H, H-7), 8.48 (d, *J* = 8.5 Hz, 1H, H-9), 7.58 (dd, *J* = 8.5, 4.2 Hz, 1H, H-8), 7.45 (s, 1H, H-4), 4.27 (s, 1H, H-15), 3.84 (t, *J* = 14.8 Hz, 2H, H-12), 3.71 (d, *J* = 13.0 Hz, 1H, H-16), 3.41 (t, *J* = 12.3 Hz, 1H, H-13), 3.20 (dd, *J* = 13.1, 3.8 Hz, 1H, H-16), 3.00 (td, *J* = 12.5, 3.4 Hz, 1H, H-13), 1.42 (s, 9H, H-21), 1.28 (d, *J* = 6.7 Hz, 3H, H-22); ¹³C NMR (151 MHz, DMSO-*d*₆) δ 161.1 (C-1), 154.9 (C-7), 154.9 (C-17), 153.8 (C-5), 145.7 (C-3), 134.1 (C-9), 121.5 (C-8), 114.3 (C-4), 113.9 (C-10), 79.0 (C-20), 54.2 (C-16), 50.8 (C-12), 46.9 (C-15), 38.5 (C-13), 28.1 (C-21), 15.8 (C-22); HRMS *m/z* (ESI⁺) [Found: 385.1391, C₁₈H₂₃ClN₄NaO₂ requires (M+H)⁺ 385.1402]; LCMS (MDAP) Rt = 22.6 min (Ana 30–95 over 20 min), *m/z* (ESI⁺) 363.9 [³⁵Cl] and 365.800 [³⁷Cl] (M+H)⁺.

***Tert*-Butyl (2*R*)-2-methyl-4-[7-(4-pyridyl)-1,6-naphthyridin-5-yl]piperazine-1-carboxylate**

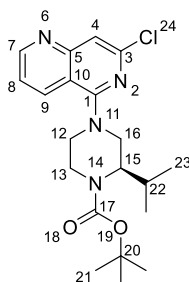
Potassium carbonate (171.4 mg, 1.24 mmol), pyridine-4-boronic acid hydrate (**196**) (51 mg, 0.41 mmol), *bis*[2-(di-*tert*-butylphosphanyl)cyclopenta-2,4-dien-1-yl]iron; dichloropalladium (13 mg, 0.02 mmol) and *tert*-butyl (2*R*)-4-(7-chloro-1,6-naphthyridin-5-yl)-2-methyl-piperazine-1-carboxylate (150 mg, 0.41 mmol) in 4:1 acetonitrile:water (12 mL) were degassed under a flow of nitrogen and heated in a microwave reactor at 140 °C for 15 minutes. LCMS confirmed reaction completion (m/z 406). The reaction mixture was diluted with water (20 mL) and extracted twice with ethyl acetate (2 × 25 mL). The combined organic phases were dried over MgSO_4 , filtered and concentrated under reduced pressure to give a brown foam (126 mg). The crude was purified *via* flash column chromatography (4 g petroleum ether:ethyl acetate, 1:0 to 0:1) to give *tert*-butyl (2*R*)-2-methyl-4-[7-(4-pyridyl)-1,6-naphthyridin-5-yl]piperazine-1-carboxylate (90 mg, 51%) as a pale pink solid.

R_f 0.48 (9:1 ethyl acetate:methanol); m.p. 181–183 °C; ν_{max} (thin film)/ cm^{-1} 2975 (aliphatic C-H, w), 1689 (C=O, s), 1598 (C=C, m), 1569 (aromatic C-C, s), 1053 (C-N, s), 769 (C-H, s); ^1H NMR (600 MHz, $\text{DMSO}-d_6$) δ 9.08–9.06 (m, 1H, H-7), 8.70 (d, J = 6.0 Hz, 2H, H-2' and H-6'), 8.52 (d, J = 8.5 Hz, 1H, H-9), 8.21 (d, J = 6.0 Hz, 2H, H-3' and H-5'), 8.20 (s, 1H, H-4), 7.64 (dd, J = 8.4, 4.2 Hz, 1H, H-8), 4.33 (s, 1H, H-15), 3.99–3.85 (m, 2H, H-12), 3.81 (d, J = 12.9 Hz, 1H, H-16), 3.46 (t, J = 12.5 Hz, 1H, H-13), 3.23 (dd, J = 13.0, 3.7 Hz, 1H, H-16), 3.03 (td, J = 12.4, 3.3 Hz, 1H, H-13), 1.43 (s, 9H, H-21), 1.34 (d, J = 6.7 Hz, 3H, H-22); ^{13}C NMR (151 MHz, $\text{DMSO}-d_6$) δ 161.1 (C-1), 154.5 (C-7), 153.9 (C-17), 153.4 (C-5), 150.3 (C-2' and C-6'), 148.0 (C-3), 145.4 (C-4'), 133.7 (C-9), 122.1 (C-8), 120.8 (C-3' and C-5'), 116.0 (C-10), 113.2 (C-4), 79.0 (C-20), 54.7 (C-16), 50.8 (C-12), 46.9 (C-15), 38.7 (C-13), 28.1 (C-21), 15.7 (C-22); HRMS m/z (ESI⁺) [Found: 406.2234, $\text{C}_{23}\text{H}_{28}\text{N}_5\text{O}_2$ requires (M+H)⁺ 406.2238]; LCMS (MDAP) R_t = 10.9 min (Ana 30–95 over 20 min), m/z (ESI⁺) 406.1 (M+H)⁺.

5-[(3R)-3-Methylpiperazin-1-yl]-7-(4-pyridyl)-1,6-naphthyridine (302)


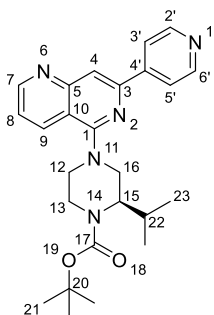
Tert-Butyl (2*R*)-2-methyl-4-[7-(4-pyridyl)-1,6-naphthyridin-5-yl]piperazine-1-carboxylate (40 mg, 0.09 mmol) was stirred in dichloromethane (1 mL) for 10 min at 0 °C. Trifluoro acetic acid (0.40 mL, 6.2 mmol) was added dropwise and the reaction mixture was stirred at room temperature for 4 h. The reaction mixture was concentrated under reduced pressure and purified *via* SCX cartridge by elution with methanol then 2 M ammonia in methanol to give 5-[(3*R*)-3-methylpiperazin-1-yl]-7-(4-pyridyl)-1,6-naphthyridine (**302**) (30 mg, 100%) as a yellow solid.

R_f 0 (9:1 dichloromethane:methanol); m.p. degrades above 200 °C; ν_{\max} (thin film)/cm⁻¹ 2988 (aliphatic C-H, w), 1598 (C=C, m), 1568 (aromatic C-C, m), 1465 (aliphatic C-H, m), 1130 (C-N, s), 722 (N-H, s); ¹H NMR (600 MHz, DMSO-*d*₆) δ 9.08 (d, J = 3.0 Hz, 1H, H-7), 8.89 (s, 1H, H-14), 8.72 (d, J = 5.2 Hz, 2H, H-2' and H-6'), 8.58 (d, J = 8.5 Hz, 1H, H-9), 8.25 (s, 1H, H-4), 8.19 (d, J = 5.1 Hz, 1H, H-3' and H-5'), 7.64 (dd, J = 7.9, 3.7 Hz, 1H, H-8), 3.98 (d, J = 9.5 Hz, 2H, H-12 and H-16), 3.63 (s, 1H, H-15), 3.52–3.36 (m, 3H, H-12 and H-13), 3.17 (t, J = 13.6 Hz, 1H, H-16), 1.31 (d, J = 5.4 Hz, 3H, H-17); ¹³C NMR (151 MHz, DMSO-*d*₆) δ 159.9 (C-1), 154.8 (C-7), 153.3 (C-5), 150.4 (C-2' and C-6'), 147.9 (C-3), 145.3 (C-4'), 134.0 (C-9), 122.5 (C-8), 120.8 (C-3' and C-5'), 116.1 (C-10), 114.1 (C-4), 53.6 (C-16), 50.3 (C-15), 47.5 (C-12), 42.5 (C-13), 15.8 (C-17); HRMS m/z (ESI⁺) [Found: 306.1702, C₁₈H₂₀N₅ requires (M+H)⁺ 306.1713]; LCMS (MDAP) R_t = 5.5 min (Ana 30–95 over 20 min), m/z (ESI⁺) 305.9 (M+H)⁺.

***Tert*-Butyl (2*R*)-4-(7-chloro-1,6-naphthyridin-5-yl)-2-isopropyl-piperazine-1-carboxylate**

N,N-Diisopropylethylamine (0.71 mL, 4.06 mmol), 5,7-dichloro-1,6-naphthyridine (**284**) (200 mg, 1 mmol) and (*S*)-1-Boc-2-isopropylpiperazine (1.37 g, 5.98 mmol) in ethanol (7 mL) were heated to 100 °C overnight. LCMS indicated product formation (m/z 391). The reaction mixture was concentrated under reduced pressure and water (4 mL) was added. The mixture was extracted three times with ethyl acetate (3 × 40 mL). The combined organic phases were washed with water (40 mL), brine (40 mL), dried over MgSO_4 , filtered and concentrated under reduced pressure to give an orange oil (805 mg). The crude was purified *via* flash column chromatography (24 g silica, petroleum ether:ethyl acetate, 1:0 to 0:1) to give *tert*-butyl (2*R*)-4-(7-chloro-1,6-naphthyridin-5-yl)-2-isopropyl-piperazine-1-carboxylate (380 mg, 92%) as a yellow solid.

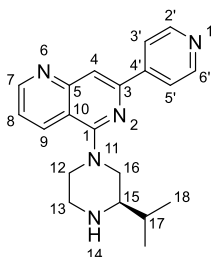
R_f 0.72 (100% ethyl acetate); m.p. 129–130 °C; ν_{max} (thin film)/ cm^{-1} 2970 (aliphatic C-H, m), 1686 (C=O, s), 1601 (C=C, m), 1561 (aromatic C-C, s), 1016 (C-N, s), 761 (C-Cl, m); ^1H NMR (600 MHz, $\text{DMSO}-d_6$) δ 8.99 (dd, $J = 4.2, 1.5$ Hz, 1H, H-7), 8.47 (d, $J = 8.7$ Hz, 1H, H-9), 7.55 (dd, $J = 8.5, 4.2$ Hz, 1H, H-8), 7.40 (s, 1H, H-4), 3.99 (d, $J = 12.7$ Hz, 1H, H-12), 3.92 (d, $J = 11.9$ Hz, 1H, H-13), 3.88 (d, $J = 12.6$ Hz, 1H, H-16), 3.79 (s, 1H, H-15), 3.26 (s, 1H, H-13), 3.14 (dd, $J = 13.6, 3.5$ Hz, 1H, H-12), 3.07 (td, $J = 12.4, 3.6$ Hz, 1H, H-16), 2.23–2.15 (m, 1H, H-22), 1.41 (s, 9H, H-21), 0.88 (d, $J = 6.6$ Hz, 3H, H-23), 0.83 (d, $J = 5.5$ Hz, 3H, H-23); ^{13}C NMR (151 MHz, $\text{DMSO}-d_6$) δ 160.8 (C-1), 154.9 (C-7), 154.1 (C-17), 153.9 (C-5), 145.7 (C-3), 134.3 (C-9), 121.3 (C-8), 114.1 (C-10), 113.5 (C-4), 78.9 (C-20), 57.6 (C-13), 56.3 (C-15), 51.5 (C-16), 49.7 (C-12), 28.0 (C-21), 26.3 (C-22), 20.1 (C-23), 18.8 (C-23); HRMS m/z (ESI⁺) [Found: 413.1704, $\text{C}_{20}\text{H}_{27}\text{ClN}_4\text{NaO}_2$ requires (M+H)⁺ 413.1715]; LCMS (MDAP) R_t = 27.3 min (Ana 5–95 over 20 min); m/z (ESI⁺) 391.1 [^{35}Cl] and 393.1 [^{37}Cl] (M+H)⁺.

***Tert*-Butyl (2*R*)-2-isopropyl-4-[7-(4-pyridyl)-1,6-naphthyridin-5-yl]piperazine-1-carboxylate**

Potassium carbonate (154 g, 1.11 mmol), pyridine-4-boronic acid hydrate (**196**) (46 mg, 0.37 mmol), *bis*[2-(di-*tert*-butylphosphanyl)cyclopenta-2,4-dien-1-yl]iron; dichloropalladium (12 mg, 0.02 mmol) and *tert*-butyl (2*R*)-4-(7-chloro-1,6-naphthyridin-5-yl)-2-isopropylpiperazine-1-carboxylate (145 mg, 0.37 mmol) in 4:1 acetonitrile:water (12 mL) were degassed under a flow of nitrogen and heated in a microwave reactor at 140 °C for 15 minutes. LCMS confirmed reaction completion (m/z 434). The reaction mixture was diluted with water (20 mL) and extracted twice with ethyl acetate (2 × 25 mL). The combined organic phases were dried over MgSO₄, filtered and concentrated under reduced pressure to give a brown oil (116 mg). The crude was purified via flash column chromatography (4 g petroleum ether:ethyl acetate, 1:0 to 0:1) to give *tert*-butyl (2*R*)-2-isopropyl-4-[7-(4-pyridyl)-1,6-naphthyridin-5-yl]piperazine-1-carboxylate (71 mg, 42%) as an off-white foam.

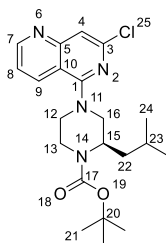
R_f 0.22 (100% ethyl acetate); m.p. 78–79 °C; ν_{\max} (thin film)/cm⁻¹ 2957 (aliphatic C-H, br), 1686 (C=O, s), 1598 (C=C, m), 1569 (aromatic C-C, s), 1103 (C-N, m), 826 (C-H, s); ¹H NMR (600 MHz, DMSO-*d*₆) δ 9.07 (dd, J = 4.2, 1.7 Hz, 1H, H-9), 8.71 (d, J = 6.2 Hz, 2H, H-2' and H-6'), 8.52 (d, J = 8.4 Hz, 1H, H-9), 8.20 (d, J = 6.2 Hz, 2H, H-3' and H-5'), 8.18 (s, 1H, H-4), 7.62 (dd, J = 8.4, 4.2 Hz, 1H, H-8), 4.06–3.93 (m, 2H, H-12 and H-13), 3.92 (d, J = 12.5 Hz, 1H, H-16), 3.86 (d, J = 10.4 Hz, 1H, H-15), 3.36 (s, 1H, H-13), 3.22 (d, J = 13.2 Hz, 1H, H-12), 3.06–2.98 (m, 1H, H-16), 2.42–2.25 (m, 1H, H-22), 1.41 (s, 9H, H-21), 0.93–0.75 (m, 6H, H-23); ¹³C NMR (151 MHz, DMSO-*d*₆) δ 161.1 (C-1), 154.6 (C-17), 153.9 (C-17), 153.4 (C-5), 150.3 (C-2' and C-6'), 148.1 (C-3), 145.4 (C-4'), 133.6 (C-9), 122.1 (C-8), 120.8 (C-3' and C-5'), 115.9 (C-10), 113.1 (C-4), 79.0 (C-20), 53.0 (C-13), 51.3 (C-15), 49.5 (C-16), 38.6 (C-12), 28.1 (C-21), 24.4 (C-22), 22.9 (C-23), 22.6 (C-23); HRMS m/z (ESI⁺) [Found: 456.2360, C₂₅H₃₁N₅NaO₂ requires (M+H)⁺ 456.2370]; LCMS (MDAP) R_t = 12.4 min (Ana 30–95 over 20 min), m/z (ESI⁺) 434.1 (M+H)⁺.

5-[(3*R*)-3-isobutylpiperazin-1-yl]-7-(4-pyridyl)-1,6-naphthyridine (303**)**



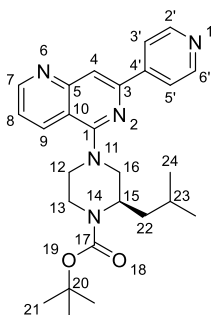
Tert-Butyl (2*R*)-2-isobutyl-4-[7-(4-pyridyl)-1,6-naphthyridin-5-yl]piperazine-1-carboxylate (50 mg, 0.11 mmol) was stirred in dichloromethane (1 mL) for 10 min at 0 °C. Trifluoro acetic acid (0.5 mL, 6.53 mmol) was added dropwise and the reaction was allowed to stir at room temperature for 4 h. The reaction mixture was concentrated under reduced pressure and purified *via* SCX cartridge by elution with methanol then 2 M ammonia in methanol to give 5-[(3*R*)-3-isobutylpiperazin-1-yl]-7-(4-pyridyl)-1,6-naphthyridine (**303**) (37 mg, 92%) as a yellow solid.

R_f 0.21 (9:1 dichloromethane:methanol); m.p. 245–247 °C; ν_{\max} (thin film)/cm⁻¹ 2960 (aliphatic C-H, w), 1597 (C=C, m), 1567 (aromatic C-C, s), 1478 (aliphatic C-H, m), 1176 (C-N, s), 723 (N-H, s); ¹H NMR (600 MHz, DMSO-*d*₆) δ 9.08 (d, J = 4.4 Hz, 1H, H-7), 8.71 (d, J = 6.2 Hz, 2H, H-2' and H-6'), 8.54 (d, J = 8.5 Hz, 2H, H-9), 8.22 (s, 1H, H-4), 8.18 (d, J = 6.2 Hz, 2H, H-3' and H-5'), 7.64 (dd, J = 8.5, 4.1 Hz, 1H, H-8), 4.06 (d, J = 14.2 Hz, 1H, H-16), 3.98 (d, J = 12.5 Hz, 1H, H-12/13), 3.57–3.54 (m, 1H, H-15), 3.49–3.37 (m, 1H, H-12/13), 3.33–3.26 (m, 2H, H-13/12) 3.13 (t, J = 12.1 Hz, 1H, H-16), 1.88–1.74 (m, 1H, H-15), 1.50 (t, J = 7.1 Hz, 1H, H-17), 0.94 (d, J = 6.5 Hz, 6H, H-18); ¹³C NMR (151 MHz, DMSO-*d*₆) δ 159.8 (C-1), 154.7 (C-7), 153.2 (C-5), 150.3 (C-2' and C-6'), 148.0 (C-3), 145.3 (C-4'), 133.8 (C-9), 122.3 (C-8), 120.8 (C-3' and C-5'), 116.0 (C-10), 113.8 (C-4), 52.3 (C-15 and C-16), 52.1 (C-13/12), 48.4 (C-12/13), 43.0 (C-12), 23.5 (C-17), 22.7 (C-18), 22.4 (C-19); HRMS m/z (ESI⁺) [Found: 348.2169, C₂₁H₂₆N₅ requires (M+H)⁺ 348.2183]; LCMS (MDAP) Rt = 10.7 min (method), m/z (ESI⁺) 348.2 (M+H)⁺.

***Tert*-Butyl (2*R*)-4-(7-chloro-1,6-naphthyridin-5-yl)-2-isobutyl-piperazine-1-carboxylate**

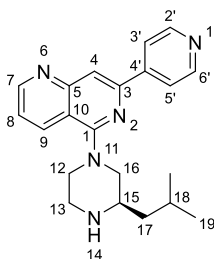
N,N-Diisopropylethylamine (0.71 mL, 4.06 mmol), 5,7-dichloro-1,6-naphthyridine (**284**) (200 mg, 1 mmol) and (*R*)-1-Boc-2-isobutylpiperazine (1.44 g, 5.95 mmol) in ethanol (7 mL) were stirred at 100 °C overnight. LCMS indicated product formation (*m/z* 405). The reaction mixture was concentrated under reduced pressure and water (4 mL) was added. The mixture was extracted three times with ethyl acetate (3 × 40 mL). The combined organic phases were washed with water (40 mL), brine (40 mL), dried over MgSO₄, filtered and concentrated under reduced pressure to give an orange oil (773 mg). The crude was purified *via* flash column chromatography (24 g silica, petroleum ether:ethyl acetate, 1:0 to 0:1) to give *tert*-butyl (2*R*)-4-(7-chloro-1,6-naphthyridin-5-yl)-2-isobutyl-piperazine-1-carboxylate (373 mg, 83%) as a yellow glass.

R_f 0.76 (100% ethyl acetate); m.p. 60–61 °C; *v*_{max} (thin film)/cm⁻¹ 2957 (aliphatic C-H, w), 1687 (C=O, s), 1598 (C=C, m), 1559 (aromatic C-C, s), 1410 (aliphatic C-H, s), 1059 (C-N, s); ¹H NMR (600 MHz, DMSO-*d*₆) δ 8.96 (s, 1H, H-7), 8.39 (d, *J* = 8.5 Hz, 1H, H-9), 7.52 (ddd, *J* = 8.4, 4.1, 1.8 Hz, 1H, H-8), 7.37 (s, 1H, H-4), 4.20 (s, 1H, H-15), 3.83 (dd, *J* = 34.5, 13.1 Hz, 2H, H-12), 3.71 (d, *J* = 13.2 Hz, 1H, H-16), 3.28 (s, 1H, H-13), 3.13 (d, *J* = 12.9 Hz, 1H, H-16), 2.97 (t, *J* = 12.2 Hz, 1H, H-13), 1.74–1.56 (m, 2H, H-22), 1.48 (s, 1H, H-23), 1.38 (s, 9H, H-21), 0.98–0.69 (m, 6H, H-24); ¹³C NMR (151 MHz, DMSO-*d*₆) δ 161.4 (C-1), 155.3 (C-7), 155.3 (C-17), 154.2 (C-5), 146.1 (C-3), 134.5 (C-9), 121.7 (C-8), 114.6 (C-4), 114.1 (C-10), 79.4 (C-20), 55.3 (C-13), 53.0 (C-16), 51.5 (C-12), 50.0 (C-15), 38.9 (C-22), 28.4 (C-21), 24.8 (C-23), 23.1 (C-24); HRMS *m/z* (ESI⁺) [Found: 427.1867, C₂₁H₂₉ClNaO₂ requires (M+H)⁺ 427.1871]; LCMS (MDAP) Rt = 27.13 min (Ana 30–95 over 20 min), *m/z* (ESI⁺) 262.950 [³⁵Cl] and 264.700 [³⁷Cl] (M+H)⁺.

***Tert*-Butyl (2*R*)-2-isobutyl-4-[7-(4-pyridyl)-1,6-naphthyridin-5-yl]piperazine-1-carboxylate**

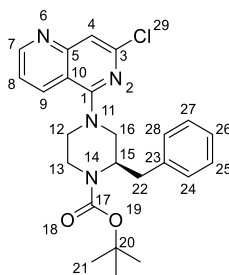
Potassium carbonate (154 mg, 1.11 mmol), pyridine-4-boronic acid hydrate (**196**) (46 mg, 0.37 mmol), *bis*[2-(di-*tert*-butylphosphanyl)cyclopenta-2,4-dien-1-yl]iron; dichloropalladium (12 mg, 0.02 mmol) and *tert*-butyl (2*R*)-4-(7-chloro-1,6-naphthyridin-5-yl)-2-isobutyl-piperazine-1-carboxylate (150 mg, 0.37 mmol) in 4:1 acetonitrile:water (12 mL) were degassed under a flow of nitrogen and heated in a microwave reactor at 140 °C for 15 minutes. LCMS confirmed reaction completion (*m/z* 448); The reaction mixture was diluted with water (20 mL) and extracted twice with ethyl acetate (2 × 25 mL). The combined organic phases were dried over MgSO₄, filtered and concentrated under reduced pressure to give a brown oil (116 mg). The crude was purified via flash column chromatography (5 g petroleum ether:ethyl acetate, 1:0 to 0:1) to give *tert*-butyl (2*R*)-2-isobutyl-4-[7-(4-pyridyl)-1,6-naphthyridin-5-yl]piperazine-1-carboxylate (71 mg, 41%) as an off-white solid.

R_f 0.22 (100% ethyl acetate); m.p. 93–95 °C; ν_{\max} (thin film)/cm⁻¹ 2970 (aliphatic C-H, br), 1685 (C=O, s), 1604 (C=C, m), 1570 (aromatic C-C, s), 1110 (C-N, s), 825 (C-H, s); ¹H NMR (600 MHz, DMSO-*d*₆) δ 9.07 (dd, *J* = 4.2, 1.4 Hz, 1H, H-7), 8.70 (d, *J* = 6.0 Hz, 2H, H-2' and H-6'), 8.50 (d, *J* = 8.3 Hz, 1H, H-9), 8.20 (d, *J* = 6.0 Hz, 2H, H-3' and H-5'), 8.18 (s, 1H, H-4), 7.63 (dd, *J* = 8.4, 4.2 Hz, 1H, H-8), 4.31 (s, 1H, H-15), 3.96 (d, *J* = 13.4 Hz, 1H, H-16), 3.93–3.85 (m, 1H, H-12/13), 3.81 (d, *J* = 13.1 Hz, 1H, H-12/13), 3.40 (s, 1H, H-16), 3.24 (d, *J* = 12.8 Hz, 1H, H-13/12), 3.02 (td, *J* = 12.4, 3.4 Hz, 1H, H-13/12), 1.78 (s, 1H, H-22), 1.60–1.50 (m, 1H, H-22), 1.50–1.43 (m, 1H, H-23), 1.42 (s, 9H, H-21), 0.93 (d, *J* = 6.6 Hz, 3H, H-24) 0.91 (d, *J* = 6.5 Hz, 3H, H-24); ¹³C NMR (151 MHz, DMSO-*d*₆) δ 161.1 (C-1), 154.6 (C-7), 154.1 (C-17), 153.4 (C-5), 150.3 (C-2' and C-6'), 148.1 (C-3), 145.4 (C-4'), 133.7 (C-9), 122.1 (C-8), 120.8 (C-3' and C-5'), 116.0 (C-10), 113.1 (C-4), 78.9 (C-20), 57.6 (C-13), 56.4 (C-16), 52.3 (C-12), 49.1 (C-15), 38.2 (C-22), 28.5 (C-21), 26.3 (C-23), 20.2 (C-24), 18.7 (C-24); HRMS *m/z* (ESI⁺) [Found: 448.2707, C₂₆H₃₄N₅O₂ requires (M+H)⁺ 448.2707]; LCMS (MDAP) *R_t* = 14.2 min (Ana 30–95 over 20 min), *m/z* (ESI⁺) 448.2 (M+H)⁺.

5-[(3*R*)-3-isopropylpiperazin-1-yl]-7-(4-pyridyl)-1,6-naphthyridine (304)


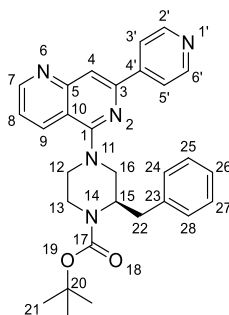
Tert-Butyl (2*R*)-2-isopropyl-4-[7-(4-pyridyl)-1,6-naphthyridin-5-yl]piperazine-1-carboxylate (46 mg, 0.11 mmol) was stirred in dichloromethane (1 mL) for 10 min at 0 °C. Trifluoro acetic acid (0.46 mL, 6.53 mmol) was added dropwise and the reaction was stirred at room temperature for 4 h. The reaction mixture was concentrated under reduced pressure and purified *via* SCX cartridge by elution with methanol then 2 M ammonia in methanol to give 5-[(3*R*)-3-isopropylpiperazin-1-yl]-7-(4-pyridyl)-1,6-naphthyridine (**304**) (36 mg, 97%) as a yellow solid.

R_f 0.21 (9:1 dichloromethane:methanol); m.p. 241–243 °C; ν_{\max} (thin film)/cm⁻¹ 2971 (aliphatic C-H, w), 1598 (C=C, s), 1567 (aromatic C-C, s), 1467 (aliphatic C-H, m), 1125 (C-N, s), 722 (N-H, s); ¹H NMR (600 MHz, DMSO-*d*₆) δ 9.08 (dd, J = 4.2, 1.7 Hz, 1H, H-7), 8.72 (d, J = 6.3 Hz, 1H, H-2' and H-6'), 8.54 (d, J = 8.4 Hz, 1H, H-9), 8.24 (s, 1H, H-4), 8.19 (d, J = 6.2 Hz, 1H, H-3' and H-5'), 7.65 (dd, J = 8.5, 4.3 Hz, 1H, H-8), 4.11 (d, J = 13.5 Hz, 1H, H-12), 4.03 (d, J = 12.9 Hz, 1H, H-12), 3.43 (t, J = 12.5 Hz, 1H, H-13), 3.38–3.35 (m, 3H, H-15 and H-16), 3.14 (t, J = 12.4 Hz, 1H, H-13), 1.97–1.89 (m, 1H, H-18), 1.07 (d, J = 6.8 Hz, 3H, H-19), 1.03 (d, J = 6.8 Hz, 3H, H-19); ¹³C NMR (151 MHz, DMSO-*d*₆) δ 159.8 (C-1), 154.7 (C-7), 153.3 (C-5), 150.3 (C-2' and C-6'), 147.9 (C-3), 145.3 (C-4'), 133.8 (C-9), 122.4 (C-8), 120.7 (C-3' and C-5'), 116.0 (C-10), 113.9 (C-4), 59.2 (C-15), 50.3 (C-12), 47.8 (C-13), 43.6 (C-16), 28.9 (C-17), 18.7 (C-18), 18.1 (C-18); HRMS m/z (ESI⁺) [Found: 334.2016, C₂₀C₂₄N₅ requires (M+H)⁺ 334.2026]; LCMS (MDAP) R_t = 9.1 min (Ana 5–95 over 20 min), m/z (ESI⁺) 334.1 (M+H)⁺.

***Tert*-Butyl (2*R*)-2-benzyl-4-(7-chloro-1,6-naphthyridin-5-yl)piperazine-1-carboxylate**

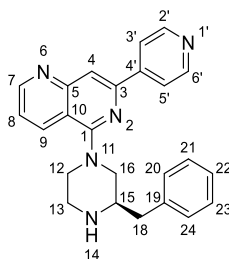
N,N-Diisopropylethylamine (0.71 mL, 4.06 mmol), 5,7-dichloro-1,6-naphthyridine (**284**) (200 mg, 1 mmol), (*R*)-1-Boc-2-benzylpiperazine (1.65 g, 5.98 mmol) in ethanol (7 mL) were heated at 100 °C overnight. LCMS indicated product formation (m/z 263). The reaction mixture was concentrated under reduced pressure and water (4 mL) was added. The mixture was extracted three times with ethyl acetate (3 × 40 mL). The combined organic phases were washed with water (40 mL), brine (40 mL), dried over MgSO_4 , filtered and concentrated under reduced pressure to give a yellow oil. The crude was purified *via* flash column chromatography to give *tert*-butyl (2*R*)-2-benzyl-4-(7-chloro-1,6-naphthyridin-5-yl)piperazine-1-carboxylate (338 mg, 73%) as an off-white solid.

R_f 0.76 (100% ethyl acetate); m.p. 63–65 °C; ν_{max} (thin film)/ cm^{-1} 2975 (aliphatic C-H, w), 1686 (C=O, s), 1597 (C=C, m), 1559 (aromatic C-C, m), 1057 (C-N, s), 697 (C-H, s); ^1H NMR (600 MHz, $\text{DMSO}-d_6$) δ 9.02 (dd, J = 4.1, 1.2 Hz, 1H, H-7), 8.55 (d, J = 8.9 Hz, 1H, H-9), 7.56 (dd, J = 8.9, 3.2 Hz, 1H, H-8), 7.46 (s, 1H, H-4), 7.26–7.18 (m, 2H, H-24 and H-28), 7.20–7.12 (m, 1H, H-26), 7.14–7.05 (m, 2H, H-25 and H-27), 4.41 (s, 1H, H-15), 3.94 (d, J = 12.1 Hz, 2H, H-12 and H-13), 3.75 (m, 1H, H-22), 3.66–3.54 (m, 1H, H-15), 3.19 (dd, J = 13.4, 3.2 Hz, 1H, H-22), 3.10 (s, 1H, H-16), 3.04 (td, J = 12.9, 3.6 Hz, 1H, H-13), 2.94–2.92 (m, 1H, H-16), 1.22 (s, 9H, H-21); ^{13}C NMR (151 MHz, $\text{DMSO}-d_6$) δ 161.0 (C-1), 155.0 (C-7), 153.8 (C-5), 153.5 (C-17), 145.7 (C-3), 138.6 (C-23), 134.3 (C-9), 129.2 (C-25 and C-27), 128.2 (C-24 and C-28), 126.1 (C-26), 121.4 (C-8), 114.4 (C-4), 113.9 (C-10), 78.8 (C-20), 53.3 (C-15), 52.1 (C-22), 51.3 (C-12), 37.9 (C-13), 35.6 (C-16), 27.8 (C-21); HRMS m/z (ESI $^+$) [Found: 461.1718, $\text{C}_{24}\text{H}_{27}\text{ClN}_4\text{NaO}_2$ requires (M+H) $^+$ 461.1715]; LCMS (MDAP) R_t = 27.3 min (Ana 5–95 over 30 min), m/z (ESI $^+$) 439.150 [^{35}Cl] 441.100 [^{37}Cl] (M+H) $^+$.

***Tert*-Butyl (2*R*)-2-benzyl-4-[7-(4-pyridyl)-1,6-naphthyridin-5-yl]piperazine-1-carboxylate**

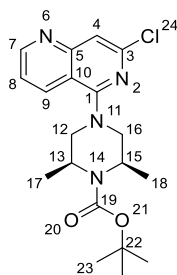
Potassium carbonate (142 g, 1.03 mmol), pyridine-4-boronic acid hydrate (**196**) (42 mg, 0.34 mmol), *bis*[2-(di-*tert*-butylphosphanyl)cyclopenta-2,4-dien-1-yl]iron; dichloropalladium (11 mg, 0.02 mmol) and *tert*-butyl (2*R*)-2-benzyl-4-(7-chloro-1,6-naphthyridin-5-yl)piperazine-1-carboxylate (150 mg, 0.34 mmol) in 4:1 acetonitrile:water (12 mL) were degassed under a flow of nitrogen and heated in a microwave reactor at 140 °C for 15 minutes. LCMS confirmed reaction completion (m/z 482). The reaction mixture was diluted with water (20 mL) and extracted twice with ethyl acetate (2 × 25 mL). The combined organic phases were dried over MgSO_4 , filtered and concentrated under reduced pressure to give a brown oil (118 mg). The crude was purified *via* flash column chromatography (4 g petroleum ether:ethyl acetate, 1:0 to 0:1) to give *tert*-butyl (2*R*)-2-benzyl-4-[7-(4-pyridyl)-1,6-naphthyridin-5-yl]piperazine-1-carboxylate (74 mg, 43%) as a yellow glass.

R_f 0.20 (100% ethyl acetate); m.p. 92–94 °C; ν_{max} (thin film)/ cm^{-1} 2973 (aliphatic C-H, w), 1685 (C=O, s), 1597 (C=C, m), 1568 (aromatic C-C, s), 1111 (C-N, s), 699 (C-H, s); ^1H NMR (600 MHz, $\text{DMSO}-d_6$) δ 9.08 (d, J = 3.9 Hz, 1H, H-7), 8.70 (d, J = 5.7 Hz, 2H, H-2' and H-6'), 8.63–8.55 (m, 1H, H-9), 8.21 (s, 1H, H-4), 8.19 (d, J = 5.4 Hz, 2H, H-3' and H-5'), 7.66–7.52 (m, 1H, H-8), 7.29–7.19 (m, 2H, H-28 and H-24), 7.19–7.14 (m, 1H, H-26), 7.15–7.08 (m, 2H, H-25 and H-27), 4.48 (s, 1H, H-15), 4.06–3.92 (m, 3H, H-12 and H-13), 3.84 (d, J = 12.9 Hz, 1H, H-22), 3.68 (t, J = 12.3 Hz, 1H, H-15), 3.27 (s, 1H, H-22), 3.19 (s, 1H, H-16), 3.05 (t, J = 11.6 Hz, 1H, H-13), 2.99 (s, 1H, H-16), 1.22 (s, 9H, H-21); ^{13}C NMR (151 MHz, $\text{DMSO}-d_6$) δ 161.5 (C-17), 155.0 (C-7), 154.0 (C-5), 153.8 (C-1), 150.7 (C-2' and C-6'), 148.5 (C-3), 145.8 (C-4'), 138.3 (C-23), 134.3 (C-9), 129.6 (C-25 and C-27), 128.6 (C-28 and C-24), 126.5 (C-26), 122.5 (C-8), 121.2 (C-3' and C-5'), 116.4 (C-10), 113.6 (C-4), 79.1 (C-20), 53.8 (C-15), 52.9 (C-22), 51.9 (C-12), 38.1 (C-13), 36.0 (C-16), 28.2 (C-21); HRMS m/z (ESI^+) [Found: 482.2551, $\text{C}_{29}\text{H}_{32}\text{N}_5\text{O}_2$ requires ($\text{M}+\text{H}$) $^+$ 482.2551]; LCMS (MDAP) R_t = 13.7 min (Ana 30–95 over 20 min), m/z (ESI^+) 482.1 ($\text{M}+\text{H}$) $^+$.

5-[(3*R*)-3-Benzylpiperazin-1-yl]-7-(4-pyridyl)-1,6-naphthyridine (305)


Tert-Butyl (2*R*)-2-benzyl-4-[7-(4-pyridyl)-1,6-naphthyridin-5-yl]piperazine-1-carboxylate (50 mg, 0.10 mmol) was stirred in dichloromethane (1 mL) for 10 min at 0 °C. Trifluoro acetic acid (0.5 mL, 6.53 mmol) was added dropwise and the reaction was stirred at room temperature for 4 h. The reaction mixture was concentrated under reduced pressure and purified *via* SCX cartridge by elution of methanol then 2 M ammonia in methanol to give 5-[(3*R*)-3-benzylpiperazin-1-yl]-7-(4-pyridyl)-1,6-naphthyridine (39 mg, 98%) as a yellow solid.

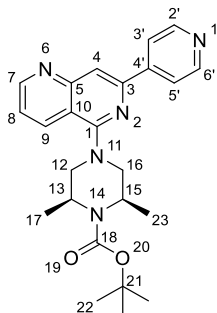
R_f 0.43 (9:1 dichloromethane:methanol); m.p. 130–132 °C; ν_{\max} (thin film)/cm⁻¹ 3034 (aromatic C-H, br), 2823 (aliphatic C-H, br), 1599 (C=C, s), 1569 (aromatic C-C, s), 1123 (C-N, s), 700 (N-H, s); ¹H NMR (600 MHz, DMSO-*d*₆) δ 9.02 (m, 1H, H-7), 8.66 (d, J = 5.7 Hz, 2H, H-2' and H-6'), 8.39 (m, 1H, H-9), 8.16 (s, 1H, H-4), 8.01 (m, 2H, H-3' and H-5'), 7.53 (s, 1H, H-8), 7.37 (t, J = 7.5, 6.3 Hz, 2H, H-20 and H-22), 7.35–7.26 (m, 3H, H-19, H-23 and H-21), 7.20 (s, 1H, H-14), 3.96 (s, 2H, H-16), 3.64 (s, 1H, H-17), 3.40 (s, 1H, H-15), 3.19 (s, 1H, H-13), 3.13 (s, 1H, H-17) 2.99 (s, 1H, H-12), 2.85 (s, 1H, H-12). Second H-13 peak under water peak; ¹³C NMR (151 MHz, DMSO-*d*₆) δ 160.0 (C-1), 154.5 (C-7), 153.4 (C-5), 150.3 (C-2' and C-6'), 147.8 (C-3), 145.3 (C-4'), 137.4 (C-18), 133.8 (C-9), 129.3 (C-19 and C-23), 128.6 (C-20 and C-22), 126.6 (C-21), 121.8 (C-8), 120.6 (C-3' and C-5'), 115.7 (C-10), 112.9 (C-4), 55.5 (C-17), 53.5 (C-16), 50.1 (C-15), 44.3 (C-13), 38.3 (C-12); HRMS m/z (ESI⁺) [Found: 382.2007, C₂₄H₂₄N₅ requires (M+H)⁺ 382.2026]; LCMS (MDAP) R_t = 10.5 min (Ana 5–95 over 20 min), m/z (ESI⁺) 382.1 (M+H)⁺.

***Tert*-Butyl (2*R*,6*S*)-4-(7-chloro-1,6-naphthyridin-5-yl)-2,6-dimethyl-piperazine-1-carboxylate**

N,N-diisopropylethylamine (0.71 mL, 4.06 mmol), 5,7-dichloro-1,6-naphthyridine (**284**) (200 mg, 1 mmol) and (2*R*,6*S*)-*tert*-butyl 2,6-dimethylpiperazine-1-carboxylate (1.28 g, 5.97 mmol) in ethanol (7 mL) were stirred overnight at 100 °C. LCMS indicated product formation (m/z 377). The reaction mixture was concentrated under reduced pressure and water (4 mL) was added. The mixture was extracted three times with ethyl acetate (3 × 40 mL) then washed with water (40 mL) and brine (40 mL). The organic phase was dried over MgSO_4 , filtered and concentrated under reduced pressure (1.04 g). The crude was purified by flash column chromatography (30 g silica, petroleum ether:ethyl acetate, 1:0 to 0:1) to give *tert*-butyl (2*R*,6*S*)-4-(7-chloro-1,6-naphthyridin-5-yl)-2,6-dimethyl-piperazine-1-carboxylate (393 mg, 99%) as a yellow crystalline solid.

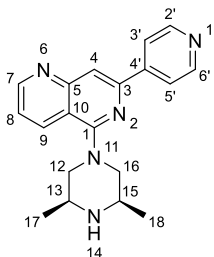
R_f 0.73 (100% ethyl acetate); m.p. 131–132 °C; ν_{max} (thin film)/ cm^{-1} 2976 (aliphatic C-H, w), 1684 (C=O, s), 1598 (C=C, m), 1560 (aromatic C-C, s), 1404 (aliphatic C-OH, s), 1036 (C-N, s), 819 (N-H, s); ^1H NMR (600 MHz, $\text{DMSO}-d_6$) δ 9.04 (dd, J = 4.2, 1.2 Hz, 1H, H-7), 8.51 (d, J = 8.5 Hz, 1H, H-9), 7.64 (dd, J = 8.5, 4.2 Hz, 1H, H-8), 7.52 (s, 1H, H-4), 4.21 (q, J = 6.6 Hz, 2H, H-13 and H-15), 3.75 (d, J = 12.8 Hz, 2H, H-12 and 16), 3.07 (dd, J = 12.8, 4.3 Hz, 2H, H-12 and 16), 1.44 (s, 9H, H-23), 1.42 (d, J = 6.8 Hz, 6H, H-17 and H-18); ^{13}C NMR (151 MHz, $\text{DMSO}-d_6$) δ 162.1 (C-1), 155.5 (C-7), 154.1 (C-5), 146.0 (C-10), 134.0 (C-8), 122.1 (C-8), 115.1 (C-4), 79.4 (C-22), 55.5 (C-12 and C-16), 47.0 (C-13 and C-15), 28.5 (C-23), 20.8 (C-17 and C-18); HRMS m/z (ESI⁺) [Found: 399.1548, $\text{C}_{19}\text{H}_{25}\text{ClN}_4\text{NaO}_2$ requires (M+H)⁺ 399.1558]; LCMS (MDAP) R_t = 24.2 min (Ana 30–95 over 20 min), m/z (ESI⁺) 377.1 [^{35}Cl] and 379.0 [^{37}Cl] (M+H)⁺.

***Tert*-Butyl (2*R*,6*S*)-2,6-dimethyl-4-[7-(4-pyridyl)-1,6-naphthyridin-5-yl]piperazine-1-carboxylate**



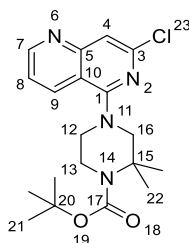
Potassium carbonate (157 mg, 1.13 mmol), pyridine-4-boronic acid hydrate (**196**) (46 mg, 0.38 mmol), *bis*[2-(di-*tert*-butylphosphanyl)cyclopenta-2,4-dien-1-yl]iron; dichloropalladium (12 mg, 0.02 mmol) and *tert*-butyl (2*R*,6*S*)-4-(7-chloro-1,6-naphthyridin-5-yl)-2,6-dimethylpiperazine-1-carboxylate (150 mg, 0.38 mmol) in 4:1 acetonitrile:water (12 mL) were degassed under a flow of nitrogen and heated in a microwave reactor at 140 °C for 15 minutes. LCMS indicated product formation (*m/z* 420). Water (15 mL) was added and the mixture was extracted twice with ethyl acetate (2 × 20 mL). The combined organic phases were dried over MgSO₄, filtered and concentrated under reduced pressure (148 mg). The crude was purified *via* flash column chromatography (5 g silica, petroleum ether:ethyl acetate, 1:0 to 0:1) to give *tert*-butyl (2*R*,6*S*)-2,6-dimethyl-4-[7-(4-pyridyl)-1,6-naphthyridin-5-yl]piperazine-1-carboxylate (99 mg, 59%) as a light brown solid.

R_f 0.18 (100% ethyl acetate); m.p. 219–220 °C; ν_{max} (thin film)/cm⁻¹ 2969 (aliphatic C-H, w), 1686 (C=O, s), 1601 (aromatic C=C, m), 1573 (aromatic C-C, m), 1364 (aliphatic C-H, s), 829 (N-H, s); ¹H NMR (600 MHz, DMSO-*d*₆) δ 9.09 (dd, *J* = 4.3, 1.5 Hz, 1H, H-7), 8.71 (d, *J* = 6.2 Hz, 2H, H-2' and H-6'), 8.56 (d, *J* = 9.0 Hz, 1H, H-9), 8.24 (s, 1H, H-4), 8.22 (d, *J* = 6.1 Hz, 2H, H-3' and H-5'), 7.68 (dd, *J* = 8.4, 4.2 Hz, 1H, H-8), 4.26 (p, *J* = 6.8 Hz, 2H, H-12 and H-16), 3.84 (d, *J* = 12.7 Hz, 2H, H-13 and H-15), 3.13 (dd, *J* = 12.8, 4.4 Hz, 2H, H-12 and H-16), 1.48 (d, *J* = 6.8 Hz, 6H, H-17 and H-23), 1.45 (s, 9H, H-22); ¹³C NMR (151 MHz, DMSO-*d*₆) δ 161.6 (C-18), 154.6 (C-7), 153.8 (C-1), 153.3 (C-5), 150.3 (C-2' and C-6'), 148.0 (C-3), 145.4 (C-4'), 133.2 (C-9), 122.3 (C-8), 120.8 (C-3' and C-5'), 116.3 (C-10), 113.7 (C-4), 78.9 (C-21), 55.3 (C-12 and C-16), 46.7 (C-13 and C-15), 28.2 (C-22), 20.5 (C-17 and C-23); HRMS *m/z* (ESI⁺) [Found: 420.2385, C₂₄H₃₀N₅O₂ requires (M+H)⁺ 420.2394]; LCMS (MDAP) *R_t* = 12.3 min (Ana 30–95 over 20 min), *m/z* (ESI⁺) 420.2 (M+H)⁺.

5-[(3*R*,5*S*)-3,5-Dimethylpiperazin-1-yl]-7-(4-pyridyl)-1,6-naphthyridine (306)


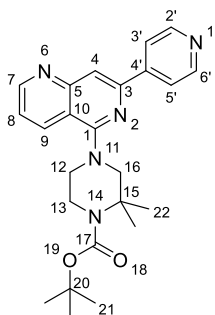
Tert-Butyl (2*R*,6*S*)-2,6-dimethyl-4-[7-(4-pyridyl)-1,6-naphthyridin-5-yl]piperazine-1-carboxylate (40 mg, 0.09 mmol) was dissolved in dichloromethane (1 mL) and cooled to 0 °C. Trifluoro acetic acid (0.4 mL, 5.17 mmol) was added dropwise and the reaction mixture was allowed to stir at room temperature overnight. LCMS indicated product formation (*m/z* 320). The reaction mixture was concentrated under reduced pressure to give a yellow solid. The crude was purified *via* SCX cartridge by elution with methanol then 2 M ammonia in methanol to give 5-[(3*R*,5*S*)-3,5-dimethylpiperazin-1-yl]-7-(4-pyridyl)-1,6-naphthyridine (**306**) (29 mg, 92%) as a yellow solid.

R_f 0.1 (9:1 dichloromethane:methanol); m.p. 168–170 °C; ν_{\max} (thin film)/cm⁻¹ 3200 (N-H, br), 2970 (aliphatic C-H, w), 1599 (C=C, s), 1570 (aromatic C-C, s), 1035 (C-N, s), 765 (N-H, s); ¹H NMR (600 MHz, CDCl₃) δ 9.02 (d, *J* = 4.1 Hz, 1H, H-7), 8.75 (d, *J* = 5.5 Hz, 2H, H-2' and H-6'), 8.37 (d, *J* = 8.4 Hz, 1H, H-9), 8.06 (d, *J* = 5.5 Hz, 2H, H-3' and H-5'), 8.04 (s, 1H, H-4), 7.46 (dd, *J* = 8.4, 4.3 Hz, 1H, H-8), 3.89 (d, *J* = 12.8 Hz, 2H, H-13 and H-15), 3.38–3.25 (m, 2H, H-12/16), 2.88 (t, *J* = 12.5 Hz, 2H, H-16/12), 1.23 (d, *J* = 6.3 Hz, 6H, H-17 and H-18); ¹³C NMR (151 MHz, DMSO-*d*₆) δ 160.7 (C-1), 154.8 (C-7), 153.7 (C-10'), 150.7 (C-2' and C-6'), 148.3 (C-3), 145.8 (C-4'), 134.5 (C-9), 122.5 (C-8), 121.1 (C-3' and C-5'), 116.4 (C-10), 113.5 (C-4), 56.4 (C-13 and C-15), 50.8 (C-12 and C-16), 18.4 (C-17 and C-18); HRMS *m/z* (ESI⁺) [Found: 320.1857, C₁₉H₂₂N₅ requires (M+H)⁺ 320.1870]; LCMS (MDAP) *R_t* = 8.8 min (Ana 5–95 over 20 min), *m/z* (ESI⁺) 320.1 (M+H)⁺.

***Tert*-Butyl 4-(7-chloro-1,6-naphthyridin-5-yl)-2,2-dimethyl-piperazine-1-carboxylate**

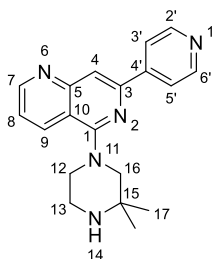
N,N-Diisopropylethylamine (0.71 mL, 4.06 mmol), 5,7-dichloro-1,6-naphthyridine (**284**) (200 mg, 1 mmol) and *tert*-butyl 2,2-dimethylpiperazine-1-carboxylate (1.28 g, 5.97 mmol) were stirred in ethanol (7mL) at 100 °C overnight. LCMS indicated product formation (m/z 377, 379). The reaction mixture was concentrated and water (4 mL) was added. The mixture was extracted three times with ethyl acetate (3 × 40 mL). The combined organic phases were washed with water (40 mL) and brine (40 mL) then dried over MgSO_4 , filtered and concentrated under reduced pressure to give a brown heterogeneous mixture (885 mg). The crude was purified *via* flash column chromatography (30 g silica, petroleum ether:ethyl acetate, 1:0 to 0:1) to give *tert*-butyl 4-(7-chloro-1,6-naphthyridin-5-yl)-2,2-dimethyl-piperazine-1-carboxylate (342 mg, 80%) as a yellow foam.

R_f 0.75 (100% ethyl acetate); m.p. 153–155 °C; ν_{max} (thin film)/ cm^{-1} 2976 (aliphatic C-H, w), 1675 (C=O, s), 1555 (aromatic C-H, s), 1401 (aliphatic C-H, s), 1068 (C-N, s), 769 (N-H, s); ^1H NMR (600 MHz, $\text{DMSO}-d_6$) δ 8.94 (dd, J = 4.2, 1.4 Hz, 1H, H-7), 8.58 (d, J = 8.6 Hz, 1H, H-9), 7.49 (dd, J = 8.5, 4.2 Hz, 1H, H-8), 7.27 (s, 1H, H-4), 3.88–3.77 (m, 2H, H-13), 3.79–3.69 (m, 2H, H-12), 3.67 (s, 2H, H-16) 1.44 (s, 9H, H-21), 1.42 (s, 6H, H-22); ^{13}C NMR (151 MHz, $\text{DMSO}-d_6$) δ 159.7 (C-17), 154.4 (C-7), 154.2 (C-1), 145.7 (C-5), 134.9 (C-9), 120.5 (C-8), 113.2 (C-10), 111.5 (C-4), 79.0 (C-20), 57.5 (C-16), 55.6 (C-15), 50.1 (C-13), 40.9 (C-12), 28.2 (C-21), 25.2 (C-22); HRMS m/z (ESI⁺) [Found: 399.1555, $\text{C}_{19}\text{H}_{25}\text{ClN}_4\text{NaO}_2$ requires (M+H)⁺ 399.1558]; LCMS (MDAP) Rt = 22.7 min, (Ana 30–95 over 20 min); m/z (ESI⁺) 377.1 [^{35}Cl] and 379.050 [^{37}Cl] (M+H)⁺.

***Tert*-butyl 2,2-dimethyl-4-[7-(4-pyridyl)-1,6-naphthyridin-5-yl]piperazine-1-carboxylate**

Potassium carbonate (165 mg, 1.19 mmol), pyridine-4-boronic acid hydrate (**196**) (49 mg, 0.40 mmol), *bis*[2-(di-*tert*-butylphosphanyl)cyclopenta-2,4-dien-1-yl]iron; dichloropalladium (13 mg, 0.02 mmol) and *tert*-butyl 4-(7-chloro-1,6-naphthyridin-5-yl)-2,2-dimethyl-piperazine-1-carboxylate (150 mg, 0.40 mmol) in 4:1 acetonitrile:water (12 mL) were degassed under a flow of nitrogen and heated in a microwave reactor at 140 °C for 15 minutes. LCMS confirmed reaction completion (m/z 420). The reaction mixture was diluted with water (15 mL) and extracted twice with ethyl acetate (2 × 20 mL). The combined organic phases were dried over MgSO_4 , filtered and concentrated under reduced pressure to give a yellow oil (147 mg). The crude was purified *via* flash column chromatography (5 g petroleum ether:ethyl acetate, 1:0 to 0:1) to give *tert*-butyl 2,2-dimethyl-4-[7-(4-pyridyl)-1,6-naphthyridin-5-yl]piperazine-1-carboxylate (101 mg, 57%) as an off-white solid.

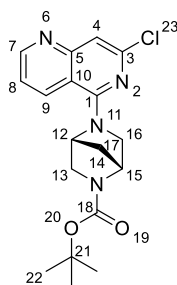
R_f 0.38 (9:1 ethyl acetate:methanol); m.p. 194–195 °C; ν_{max} (thin film)/ cm^{-1} 2967 (aliphatic C-H, w), 2880 (aliphatic C-H, w), 1694 (C=O, s), 1597 (aromatic C=C, m), 1563 (aromatic C-C, s), 832 (alkene C-H, s); ^1H NMR (600 MHz, DMSO-d_6) δ 9.02 (dd, J = 4.2, 1.6 Hz, 1H, H-7), 8.70 (d, J = 6.2 Hz, 1H, H-2' and H-6'), 8.59 (d, J = 8.4 Hz, 1H, H-9), 8.19 (d, J = 6.2 Hz, 2H, H-3' and H-5'), 8.05 (s, 1H, H-4), 7.56 (dd, J = 8.2, 4.0 Hz, 1H, H-8), 3.89 – 3.80 (m, 2H, H-12), 3.77 (t, J = 5.3 Hz, 2H, H-13), 3.74 (s, 2H, H-16), 1.53 – 1.35 (m, 15H, H-21 and H-22). ^{13}C NMR (151 MHz, CDCl_3) δ 160.5 (C-1), 155.6 (C-17), 154.3 (C-7), 154.0 (C-5), 150.5 (C-2' and C-6'), 149.2 (C-1'), 146.4 (C-3), 134.0 (C-9), 121.1 (C-3' and C-5'), 120.9 (C-8), 115.9 (C-10), 112.6 (C-4), 80.3 (C-20), 60.7 (C-16), 56.0 (C-15), 50.5 (C-12), 41.8 (C-13), 28.7 (C-21), 25.8 (C-22); HRMS m/z (ESI^+) [Found: 420.2386, $\text{C}_{24}\text{H}_{30}\text{N}_5\text{O}_2$ requires ($\text{M}+\text{H}$) $^+$ 420.2394]; LCMS (MDAP) R_t = 15.8 min (Ana 5–95 over 20 min), m/z (ESI^+) 420.2 ($\text{M}+\text{H}$) $^+$.

5-(3,3-Dimethylpiperazin-1-yl)-7-(4-pyridyl)-1,6-naphthyridine (307)

Tert-Butyl 2,2-dimethyl-4-[7-(4-pyridyl)-1,6-naphthyridin-5-yl]piperazine-1-carboxylate (50 mg, 0.12 mmol) was dissolved in dichloromethane (1 mL) and cooled to 0 °C. Trifluoro acetic acid (0.50 mL, 4.82 Mmol) was added dropwise and the reaction mixture was allowed to stir at room temperature overnight. LCMS (LCQ) indicated product formation (m/z 320). The reaction mixture was concentrated under reduced pressure to give a yellow solid. The crude was purified *via* SCX cartridge by elution with methanol then 2 M ammonia in methanol to give 5-(3,3-dimethylpiperazin-1-yl)-7-(4-pyridyl)-1,6-naphthyridine (**307**) (36 mg, 90%) as a yellow solid.

R_f 0.55 (100% ethyl acetate); m.p. 138–141 °C; ν_{\max} (thin film)/ cm^{-1} 3247 (N-H, w), 2970 (aliphatic C-H, w), 1596 (C=C, m), 1572 (aromatic C-C, s), 1020 (C-N, m), 827 (N-H, s); ^1H NMR (600 MHz, $\text{DMSO}-d_6$) δ 9.04 (dd, $J = 4.1, 1.3$ Hz, 1H, H-7), 8.70 (d, $J = 5.9$ Hz, 2H, H-2' and H-6'), 8.47 (d, $J = 8.4$ Hz, 1H, H-9), 8.18 (d, $J = 6.0$ Hz, 2H, H-3' and H-5'), 8.14 (s, 1H, H-4), 7.61 (dd, $J = 8.4, 4.2$ Hz, 1H, H-8), 3.44–3.37 (m, 2H, H-12), 3.25 (s, 2H, H-16), 3.14–3.04 (m, 2H, H-13), 1.22 (s, 6H, H-17); ^{13}C NMR (151 MHz, $\text{DMSO}-d_6$) δ 161.7 (C-1), 154.8 (C-7), 153.8 (C-5), 150.7 (C-2' and C-6'), 148.5 (C-3), 145.9 (C-4'), 134.2 (C-9), 122.4 (C-8), 121.1 (C-3' and C-5'), 116.4 (C-10), 113.3 (C-4), 61.4 (C-16), 51.8 (C-12), 51.0 (C-15), 40.7 (C-13), 25.7 (C-17); HRMS m/z (ESI $^+$) [Found: 320.1862, $\text{C}_{19}\text{H}_{22}\text{N}_5$ requires (M+H) $^+$ 320.1870]; LCMS (MDAP) R_t = 8.9 min (Ana 5–95 over 20 minutes), m/z (ESI $^+$) 320.050 (M+H) $^+$.

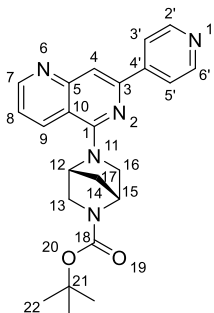
***Tert*-butyl (1*R*,4*R*)-5-(7-chloro-1,6-naphthyridin-5-yl)-2,5-diazabicyclo[2.2.1]heptane-2-carboxylate**



N,N-Diisopropylethylamine (0.71 mL, 4.06 mmol), 5,7-dichloro-1,6-naphthyridine (200 mg, 1 mmol), and *tert*-butyl 2,5-diazabicyclo[2.2.1]heptane-2-carboxylate (1.19 mg, 5.99 mmol) in ethanol (7 mL) were heated at 100 °C overnight. LCMS indicated product formation (m/z 263). The reaction mixture was concentrated under reduced pressure and water (4 mL) was added. The mixture was extracted three times with ethyl acetate (3 × 40 mL). The combined organic phases were washed with water (40 mL), brine (40 mL), dried over $MgSO_4$, filtered and concentrated under reduced pressure (123 mg) to give *tert*-butyl (1*R*,4*R*)-5-(7-chloro-1,6-naphthyridin-5-yl)-2,5-diazabicyclo[2.2.1]heptane-2-carboxylate (302 mg, 79%) as an off-white solid.²¹⁵

R_f 0.52 (100% ethyl acetate); m.p. 179–181 °C; ν_{max} (thin film)/ cm^{-1} 2980 (aliphatic C-H, w), 1686 (C=O, s), 1594 (C=C, m), 1571 (aromatic C-C, m), 1127 (C-N, m), 758 (C-H, m); 1H NMR (600 MHz, $DMSO-d_6$) δ 8.90 (d, J = 3.9 Hz, 1H, H-7), 8.53 (d, J = 8.8 Hz, 1H, H-9), 7.44 (dd, J = 8.3, 3.6 Hz, 1H, H-8), 7.14 (s, 1H, H-4), 4.98 (d, J = 18.5 Hz, 1H, H-12/15), 4.50 (d, J = 35.1 Hz, 1H, H-15/12), 4.22 (t, J = 7.7, 0.6 Hz, 1H, H-13/16), 3.59 (t, J = 8.9 Hz, 1H, H-13/16), 3.54–3.40 (m, 2H, H-16/13), 1.95 (q, J = 11.4, 10.0 Hz, 2H, H-17), 1.36 (s, 6H, H-22), 1.34 (3, 3H, H-22); ^{13}C NMR (151 MHz, $DMSO-d_6$) δ 156.3 (C-1/18), 154.2 (C-7), 153.0 (C-3), 147.2 (C-4'), 134.5 (C-9), 120.9 (C-8), 113.1 (C-10), 109.9 (C-4), 78.8 (C-21), 61.6 (C-12/15), 60.0 (C-13/16), 59.9 (C-13/16), 58.6 (C-12/15), 57.3 (C-15/12), 55.9 (C-15/12), 53.2 (C-16/13), 51.2 (C-16/13), 36.3 (C-17), 34.9 (C-17), 28.8 (C-22), C-1/18 peak missing, double peaks due to rotamers; HRMS m/z (ESI⁺) [Found: 383.1236, $C_{18}H_{21}ClN_4NaO_2$ requires (M+H)⁺ 383.1245]; LCMS (MDAP) R_t = 22.1 min (Ana 5–95 over 30 min), m/z (ESI⁺) 361.1 [^{35}Cl] and 363.0 [^{37}Cl] (M+H)⁺.

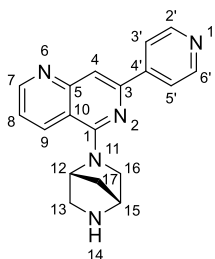
***Tert*-butyl (1*R*,4*R*)-5-[7-(4-pyridyl)-1,6-naphthyridin-5-yl]-2,5-diazabicyclo[2.2.1]heptane-2-carboxylate**



Potassium carbonate (172 mg, 1.25 mmol), pyridine-4-boronic acid hydrate (**196**) (51 mg, 0.42 mmol), *bis*[2-(di-*tert*-butylphosphanyl)cyclopenta-2,4-dien-1-yl]iron; dichloropalladium (14 mg, 0.02 mmol) and *tert*-butyl (1*R*,4*R*)-5-(7-chloro-1,6-naphthyridin-5-yl)-2,5-diazabicyclo[2.2.1]heptane-2-carboxylate (150 mg, 0.42 mmol) in 4:1 acetonitrile:water (12 mL) were degassed under a flow of nitrogen and heated in a microwave reactor at 140 °C for 15 minutes. LCMS confirmed reaction completion (*m/z* 404). The reaction mixture was diluted with water (20 mL) and extracted twice with ethyl acetate (2 × 25 mL). The combined organic phases were dried over MgSO₄, filtered and concentrated under reduced pressure (162 mg). The crude was purified *via* flash column chromatography (4 g petroleum ether:ethyl acetate, 1:0 to 0:1) to give *tert*-butyl (1*R*,4*R*)-5-[7-(4-pyridyl)-1,6-naphthyridin-5-yl]-2,5-diazabicyclo[2.2.1]heptane-2-carboxylate (130 mg, 74%) as a pale brown solid.

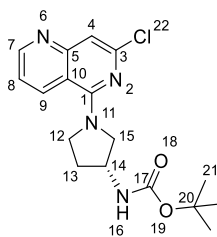
*R*_f 0.39 (9:1 ethyl acetate:methanol); *m.p.* 220–222 °C; *v*_{max} (thin film)/cm⁻¹ 2972 (aliphatic C-H, w), 1682 (C=O, s), 1594 (C=C, m), 1558 (aromatic C-C, s), 1098 (C-N, s), 771 (C-H, m); ¹H NMR (600 MHz, DMSO-*d*₆) δ 8.98 (d, *J* = 4.4 Hz, 1H, H-7), 8.70 (d, *J* = 6.2 Hz, 2H, H-2' and H-6'), 8.56 (d, *J* = 7.9 Hz, 1H, H-9), 8.16 (d, *J* = 6.3 Hz, 2H, H-3' and H-5'), 7.94 (s, 1H, H-4), 7.54–7.48 (m, 1H, H-8), 5.27–5.07 (m, 1H, H-12/15), 4.67–4.42 (m, 1H, H-15/12), 4.39–4.21 (m, 1H, H-13/16), 3.73–3.55 (m, 2H, H-16/13 and H-13/16), 3.55–3.43 (m, 1H, H-16/13), 2.05–1.96 (m, 2H, H-17), 1.37 (s, 6H, H-22), 1.32 (s, 3H, H-22); ¹³C NMR (151 MHz, DMSO-*d*₆) δ 156.7 (C-1), 156.0 (C-1), 153.9 (C-7), 153.4 (C-18), 150.6 (C-5), 149.6 (C-2' and C-6'), 147.1 (C-3), 145.7 (C-4'), 134.1 (C-9), 122.4 (C-8), 120.7 (C-3' and C-5'), 114.8 (C-10), 114.7 (C-10), 109.8 (C-4), 109.6 (C-4), 78.8 (C-21), 78.7 (C-21), 60.3 (C-12/15), 59.8 (C-13/16), 59.4 (C-12/15), 57.4 (C-15/12), 56.4 (C-15/12), 52.0 (C-16/13), 51.5 (C-16/13), 36.3 (C-17), 35.7 (C-17), 28.2 (C-22), 28.1 (C-22), double peaks due to rotamers; HRMS *m/z* (ESI⁺) [Found: 404.2079, C₂₃H₂₆N₅O₂ requires (M+H)⁺ 404.2081]; LCMS (MDAP) *R*_t = 8.4 min (Ana 30–95 over 20 min), *m/z* (ESI⁺) 404.1 (M+H)⁺.

5-[(1*R*,4*R*)-2,5-Diazabicyclo[2.2.1]heptan-2-yl]-7-(4-pyridyl)-1,6-naphthyridine (308)



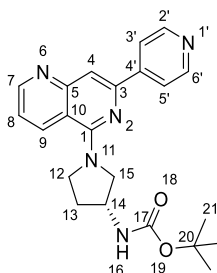
Tert-butyl (1*R*,4*R*)-5-[7-(4-pyridyl)-1,6-naphthyridin-5-yl]-2,5-diazabicyclo[2.2.1]heptane-2-carboxylate (90 mg, 0.21 mmol) was stirred in dichloromethane (1 mL) and cooled to 0 °C. Trifluoroacetic acid (0.93 mL, 12.25 mmol) was added dropwise and the reaction was allowed to stir at room temperature for 4 h. The reaction mixture was concentrated under reduced pressure and purified *via* SCX cartridge by elution with methanol then 2 M ammonia in methanol to give 5-[(1*R*,4*R*)-2,5-diazabicyclo[2.2.1]heptan-2-yl]-7-(4-pyridyl)-1,6-naphthyridine (**308**) (60 mg, 89%) as a yellow solid.

R_f 0.10 (9:1 dichloromethane:methanol); m.p. 140–141 °C; ν_{\max} (thin film)/cm⁻¹ 3279 (N-H, br), 2943 (aliphatic C-H, w), 1672 (C=C, m), 1597 (aromatic C-C, s), 1025 (C-N, s), 776 (N-H, m); ¹H NMR (600 MHz, DMSO-*d*₆) δ 8.99 (d, J = 4.2 Hz, 1H, H-7), 8.69 (d, J = 6.0 Hz, 2H, H-2' and H-6'), 8.54 (d, J = 8.5 Hz, 1H, H-9), 8.16 (d, J = 6.0 Hz, 2H, H-3' and H-5'), 7.96 (s, 1H, H-4), 7.53 (dd, J = 8.5, 4.2 Hz, 1H, H-8), 5.12 (s, 1H, H-12), 4.32 (dd, J = 9.8, 1.9 Hz, 1H, H-16), 4.17 (s, 1H, H-15), 3.70 (d, J = 9.7 Hz, 1H, H-16), 3.50 (d, J = 10.3 Hz, 1H, H-13), 3.27 (d, J = 11.3 Hz, 1H, H-13), 2.12 (d, J = 10.4 Hz, 1H, H-17), 1.89 (d, J = 10.3 Hz, 1H, H-17); ¹³C NMR (151 MHz, DMSO-*d*₆) δ 156.6 (C-1), 154.0 (C-7), 153.8 (C-5), 150.3 (C-2' and C-6'), 148.2 (C-3), 145.8 (C-4'), 133.9 (C-9), 121.1 (C-8), 120.8 (C-3' and C-5'), 114.8 (C-10), 110.0 (C-4), 58.9 (C-12), 57.9 (C-16), 57.2 (C-15), 49.8 (C-13), 35.2 (C-17); HRMS m/z (ESI⁺) [Found: 304.1539, C₁₈H₁₈N₅ requires (M+H)⁺ 304.1557]; LCMS (MDAP) R_t = 6.9 min (Ana 30–95 over 20 min), m/z (ESI⁺) 304.850 (M+H)⁺.

***Tert*-Butyl *N*-[(3*R*)-1-(7-chloro-1,6-naphthyridin-5-yl)pyrrolidin-3-yl]carbamate**

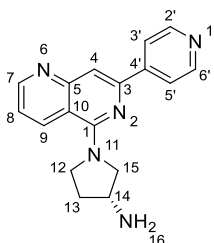
N,N-Diisopropylethylamine (0.71 mL, 4.06 mmol), 5,7-dichloro-1,6-naphthyridine (**284**) (200 mg, 1 mmol) and *tert*-butyl *N*-[(3*R*)-pyrrolidin-3-yl]carbamate (1.11 g, 5.97 mmol) in ethanol (7 mL) were stirred at 100 °C overnight. LCMS indicated product formation (m/z 349, 293, 249). The mixture was concentrated under reduced pressure and water (4 mL) was added. The mixture was extracted four times with ethyl acetate (4 × 40 mL). The combined organic phases were washed with water (40 mL) and brine (40 mL) then dried over MgSO_4 , filtered and concentrated under reduced pressure (848 mg). The crude was purified *via* flash column chromatography (30 g silica, petroleum ether:ethyl acetate, 1:0 to 0:1) to give *tert*-butyl *N*-[(3*R*)-1-(7-chloro-1,6-naphthyridin-5-yl)pyrrolidin-3-yl]carbamate (284 mg, 77%) as an off-white solid.

R_f 0.70 (100% ethyl acetate); m.p. 147–148 °C; ν_{max} (thin film)/ cm^{-1} 3211 (N-H, br), 2968 (aliphatic C-H, w), 1698 (C=O, s), 1579 (aromatic C-H, s), 1468 (aliphatic C-H, s), 876 (N-H, s); ^1H NMR (600 MHz, $\text{DMSO}-d_6$) δ 8.87 (d, J = 4.2 Hz, 1H, H-7), 8.62 (d, J = 8.6 Hz, 1H, H-9), 7.47–7.39 (m, 1, H-8), 7.23 (d, J = 5.4 Hz, 1H, H-16), 7.05 (s, 1H, H-4), 4.17–4.06 (m, 1H, H-14), 3.98 (dd, J = 11.1, 6.0 Hz, 1H, H-15), 3.91 (dt, J = 11.0, 7.2 Hz, 1H, H-12), 3.79 (ddd, J = 10.9, 7.5, 5.5 Hz, 1H, H-12), 3.61 (dd, J = 11.1, 4.5 Hz, 1H, H-15), 2.11–2.08 (m, 1H, H-13), 1.93 (m, 1H, H-13), 1.38 (s, 9H, H-21); ^{13}C NMR (151 MHz, $\text{DMSO}-d_6$) δ 156.2 (C-1), 155.2 (C-17/3), 154.4 (C-3/17), 153.8 (C-7), 146.4 (C-5), 134.9 (C-9), 119.9 (C-8), 112.8 (C-10), 108.7 (C-4), 77.9 (C-20), 56.2 (C-15), 49.8 (C-14), 49.0 (C-12), 30.5 (C-13), 28.2 (C-21); HRMS m/z (ESI⁺) [Found: 371.1240, $\text{C}_{17}\text{H}_{21}\text{ClN}_4\text{NaO}_2$ requires (M+H)⁺ 371.1245]; LCMS (LCQ) R_t = 1.4 min, (4 min method); m/z (ESI⁺) 349.1 (M+H)⁺, 293.2 (M-*t*-Bu+H)⁺ and 249.3 (M-Boc+H)⁺.

***Tert*-Butyl *N*-[(3*R*)-1-[7-(4-pyridyl)-1,6-naphthyridin-5-yl]pyrrolidin-3-yl]carbamate**

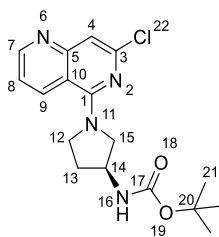
Potassium carbonate (169 mg, 1.23 mmol), pyridine-4-boronic acid hydrate (**196**) (50 mg, 0.4100mmol), *bis*[2-(di-*tert*-butylphosphanyl)cyclopenta-2,4-dien-1-yl]iron; dichloropalladium (13 mg, 0.02 mmol) and *tert*-butyl *N*-[(3*R*)-1-(7-chloro-1,6-naphthyridin-5-yl)pyrrolidin-3-yl]-carbamate (150 mg, 0.41 mmol) in acetonitrile (9.6 mL) and water (2.4 mL) were degassed under a flow of nitrogen and heated in a microwave reactor at 140 °C for 15 minutes. LCMS indicated product had formed (*m/z* 392). Water (15 mL) was added to the reaction mixture and the mixture was extracted three times with ethyl acetate (3 × 20 mL). The organic phase was dried over MgSO₄, filtered and concentrated under reduced pressure (75 mg). The crude was purified *via* flash column chromatography (4 g silica, petroleum ether:ethyl acetate 1:0 to 0:1) to give *tert*-butyl *N*-[(3*R*)-1-[7-(4-pyridyl)-1,6-naphthyridin-5-yl]pyrrolidin-3-yl]carbamate (38 mg, 23%) as a yellow gum.

¹H NMR (600 MHz, DMSO-*d*₆) δ 8.94 (dd, *J* = 4.2, 1.5 Hz, 1H, H-9), 8.68 (d, *J* = 6.0 Hz, 2H, H-2' and H-6'), 8.65 (d, *J* = 8.5 Hz, 1H, H-7), 8.16 (d, *J* = 6.0 Hz, 2H, H-3' and H-5'), 7.85 (s, 1H, H-4), 7.49 (dd, *J* = 8.5, 4.2 Hz, 1H, H-8), 7.25 (d, *J* = 6.4 Hz, 1H, H-16), 4.20–4.14 (m, 1H, H-14), 4.08 (dd, *J* = 10.9, 6.1 Hz, 1H, H-15), 4.05–4.00 (m, 1H, H-12), 3.95–3.88 (m, 1H, H-12), 3.74 (dd, *J* = 10.9, 4.5 Hz, 1H, H-15), 2.21–2.10 (m, 1H, H-13), 2.03–1.91 (m, 1H, H-13), 1.38 (s, 9H, H-21); LCMS (MDAP) *R*_t = 2.3 min (Ana 5–95 over 5 min), *m/z* (ESI⁺) 392.2 (M+H)⁺. Further characterisation pending.

(3R)-1-[7-(4-Pyridyl)-1,6-naphthyridin-5-yl]pyrrolidin-3-amine (309)

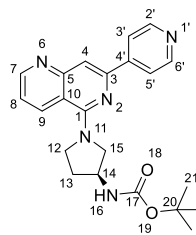
Tert-Butyl *N*-[(3*R*)-1-[7-(4-pyridyl)-1,6-naphthyridin-5-yl]pyrrolidin-3-yl]carbamate (30 mg, 0.07 mmol) was dissolved in dichloromethane (1 mL) and cooled to 0 °C. Trifluoro acetic acid (0.3 mL, 3.92 mmol) was added dropwise and the reaction mixture was allowed to stir at room temperature overnight. LCMS (LCQ) indicated product formation (*m/z* 292). The reaction mixture was concentrated under reduced pressure to give a yellow solid. The crude was purified *via* SCX cartridge by elution with methanol then 2 M ammonia in methanol to give (3*R*)-1-[7-(4-pyridyl)-1,6-naphthyridin-5-yl]pyrrolidin-3-amine (**309**) (14 mg, 63%) as a yellow solid.

R_f 0.07 (9:1 dichloromethane:methanol); m.p. 165–166 °C; ν_{max} (thin film)/cm⁻¹ 2938 (aliphatic C-H, m), 1593 (C=C, s), 1560 (aromatic C-C, s), 1410 (aliphatic C-H, s), 1032 (C-N, s), 699 (N-H, s); ¹H NMR (600 MHz, DMSO-*d*₆) δ 8.92 (d, *J* = 4.0 Hz, 1H, H-7), 8.67 (d, *J* = 5.4 Hz, 3H, H-2', H-6' and H-9), 8.14 (d, *J* = 5.6 Hz, 2H, H-3' and H-5'), 7.83 (s, 1H, H-4), 7.49 (s, 1H, H-8), 6.21 (s, 2H, H-16), 4.09 (s, 2H, H-12), 3.90 (s, 1H, H-14), 3.80 (s, 2H, H-15), 2.23 (s, 1H, H-13), 2.01 (s, 2H, H-13); ¹³C NMR (151 MHz, DMSO-*d*₆) δ 156.1 (C-1), 154.0 (C-5), 153.5 (C-7), 150.1 (C-2' and C-6'), 148.2 (C-3), 145.9 (C-4'), 134.5 (C-9), 121.3 (C-8), 120.6 (C-3' and C-5'), 114.4 (C-10), 108.8 (C-4), 55.9 (C-12), 49.8 (C-14), 48.9 (C-15), 31.2 (C-13); HRMS *m/z* (ESI⁺) [Found: 292.1549, C₁₇H₁₈N₅ requires (M+H)⁺ 292.1557]; LCMS (MDAP) *R_t* = 0.5 min (Ana 5–95 over 5 min), *m/z* (ESI⁺) 292.1 (M+H)⁺.

***Tert*-Butyl *N*-[(3*S*)-1-(7-chloro-1,6-naphthyridin-5-yl)pyrrolidin-3-yl]carbamate**

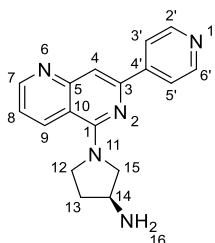
N,N-diisopropylethylamine (0.7 mL, 4.04 mmol), 5,7-dichloro-1,6-naphthyridine (**284**) (200 mg, 1 mmol) and (3*S*)-(-)-3-(*tert*-butoxycarbonylamino)pyrrolidine (1.11 g, 5.96 mmol) in ethanol (7 mL) were stirred at 100 °C overnight. LCMS indicated product formation (*m/z* 349, 293, 249). The mixture was concentrated under reduced pressure and water (4 mL) was added. The mixture was extracted four times with ethyl acetate (4 × 40 mL). The combined organic phases were washed with water (40 mL) and brine (40 mL) then dried over MgSO₄, filtered and concentrated under reduced pressure (899 mg). The crude was purified *via* flash column chromatography (25 g silica, petroleum ether:ethyl acetate, 1:0 to 0:1) to give *tert*-butyl *N*-[(3*S*)-1-(7-chloro-1,6-naphthyridin-5-yl)pyrrolidin-3-yl]carbamate (301 mg, 82%) as an off-white solid.

*R*_f 0.68 (100% ethyl acetate); m.p. 150–151 °C; *v*_{max} (thin film)/cm⁻¹ 3209 (N-H, br), 2969 (aliphatic C-H, w), 1698 (C=O, s), 1580 (aromatic C-C, m), 1438 (aliphatic C-H, s), 1246 (C-N, s), 830 (N-H, s); ¹H NMR (600 MHz, DMSO-*d*₆) δ 8.87 (dd, *J* = 5.2, 1.0 Hz, 1H, H-7), 8.62 (d, *J* = 8.6 Hz, 1H, H-9), 7.43 (dd, *J* = 8.6, 4.2 Hz, 1H, H-8), 7.23 (d, *J* = 5.8 Hz, 1H, H-16), 7.05 (s, 1H, H-4), 4.15–4.08 (m, 1H, H-14), 4.01–3.95 (m, 1H, H-15), 3.91 (dt, *J* = 10.7, 7.1 Hz, 1H, H-12), 3.83–3.75 (m, 1H, H-12), 3.61 (dd, *J* = 11.0, 4.5 Hz, 1H, H-15), 2.11 (*app. sept.*, *J* = 13.3, 7.1 Hz, 1H, H-13), 1.93 (*app. sept.*, *J* = 12.4, 6.2 Hz, 1H, H-13), 1.38 (s, 9H, H-21). ¹³C NMR (151 MHz, DMSO-*d*₆) δ 156.2 (C-1), 155.3 (C-17), 154.4 (C-5), 153.8 (C-7), 146.4 (C-3), 134.9 (C-9), 119.9 (C-8), 112.8 (C-10), 108.7 (C-4), 77.9 (C-20), 56.3 (C-15), 49.9 (C-14), 49.1 (C-12), 30.5 (C-13), 28.2 (C-21); HRMS *m/z* (ESI⁺) [Found: 371.1237, C₁₇H₂₁ClN₄NaO₂ requires (M+H)⁺ 371.1245]; LCMS (MDAP) *R*_t = 19.5 min (Ana 5–95 over 20 min), *m/z* (ESI⁺) 349.1 (M+H)⁺.

***Tert*-Butyl *N*-[(3*S*)-1-[7-(4-pyridyl)-1,6-naphthyridin-5-yl]pyrrolidin-3-yl]carbamate**

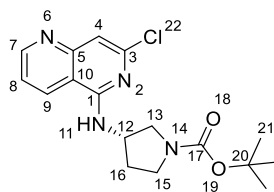
Potassium carbonate (178 mg, 1.29 mmol), pyridine-4-boronic acid hydrate (**196**) (53 mg, 0.43 mmol), *bis*[2-(di-*tert*-butylphosphanyl)cyclopenta-2,4-dien-1-yl]iron; dichloropalladium (14 mg, 0.02 mmol) and *tert*-butyl *N*-[(3*S*)-1-(7-chloro-1,6-naphthyridin-5-yl)pyrrolidin-3-yl]-carbamate (150 mg, 0.43 mmol) in 4:1 acetonitrile:water (12 mL) were degassed under a flow of nitrogen and heated in a microwave reactor at 140 °C for 15 minutes. LCMS confirmed reaction completion (*m/z* 392, 336, 292). The reaction mixture was diluted with water (20 mL) and extracted twice with ethyl acetate (2 × 25 mL). The combined organic phases were dried over MgSO₄, filtered and concentrated under reduced pressure to give a brown foam (151 mg). The crude was purified *via* flash column chromatography (4 g petroleum ether:ethyl acetate, 1:0 to 0:1) to give *tert*-butyl *N*-[(3*S*)-1-[7-(4-pyridyl)-1,6-naphthyridin-5-yl]pyrrolidin-3-yl]-carbamate (64 mg, 36%) as a pale brown solid.

*R*_f 0.13 (100% ethyl acetate); m.p. 206–208 °C; ν_{\max} (thin film)/cm^{−1} 3199 (N-H, br), 2983 (aliphatic C-H, br), 1697 (C=O, s), 1592 (aromatic C-C, m), 1067 (C-N, s), 827 (N-H, s); ¹H NMR (600 MHz, DMSO-*d*₆) δ 8.95–8.93 (m, 1H, H-7), 8.68 (d, *J* = 6.0 Hz, 2H, H-2' and H-6'), 8.65 (d, *J* = 8.5 Hz, 1H, H-9), 8.16 (d, *J* = 6.0 Hz, 2H, H-3' and H-5'), 7.85 (s, 1H, H-4), 7.49 (dd, *J* = 8.5, 4.2 Hz, 1H, H-8), 7.25 (d, *J* = 6.4 Hz, 1H, H-16), 4.20–4.13 (m, 1H, H-14), 4.11–4.05 (m, 1H, H-15), 4.05–4.00 (m, 1H, H-12), 3.95–3.88 (m, 1H, H-12), 3.74 (dd, *J* = 10.8, 4.6 Hz, 1H, H-15), 2.20–2.11 (m, 1H, H-13), 2.00–1.93 (m, 1H, H-13), 1.38 (s, 9H, H-21); ¹³C NMR (151 MHz, DMSO-*d*₆) δ 156.4 (C-1), 155.3 (C-17), 154.0 (C-7), 153.5 (C-5), 150.2 (C-2' and C-6'), 148.3 (C-3), 146.0 (C-4'), 134.5 (C-9), 120.7 (C-3' and C-5'), 120.5 (C-8), 114.4 (C-10), 108.6 (C-4), 77.9 (C-20), 56.0 (C-15), 50.0 (C-14), 49.0 (C-12), 30.7 (C-13), 28.3 (C-21); HRMS *m/z* (ESI⁺) [Found: 392.2079, C₂₂H₂₆N₅O₂ requires (M+H)⁺ 392.2081]; LCMS (MDAP) *R*_t = 13.4 min (Ana 5–95 over 20 min), *m/z* (ESI⁺) 392.2 (M+H)⁺ and 336.1 (M+H-*t*-Bu)⁺.

***Tert*-Butyl *N*-[(3*S*)-1-[7-(4-pyridyl)-1,6-naphthyridin-5-yl]pyrrolidin-3-yl]carbamate (**310**)**

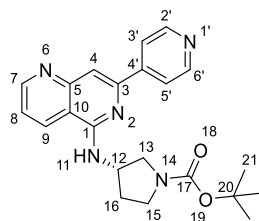
Tert-Butyl *N*-[(3*S*)-1-[7-(4-pyridyl)-1,6-naphthyridin-5-yl]pyrrolidin-3-yl]carbamate (25 mg, 0.06 mmol) was stirred in dichloromethane (0.54 mL) and cooled to 0 °C. Trifluoro acetic acid (0.25 mL, 3.26 mmol) was added dropwise and the reaction was allowed to stir at room temperature for 4 h. The reaction mixture was concentrated under reduced pressure and purified *via* SCX cartridge by elution with methanol then 2 M ammonia in methanol to give *tert*-butyl *N*-[(3*S*)-1-[7-(4-pyridyl)-1,6-naphthyridin-5-yl]pyrrolidin-3-yl]carbamate (**310**) (25 mg, 97%) as a yellow solid.

R_f 0.10 (9:1 dichloromethane:methanol); m.p. 79–80 °C; ν_{\max} (thin film)/cm⁻¹ 2937 (aliphatic C-H, w), 1592 (C=C, m), 1560 (aromatic C-C, s), 1490 (aliphatic C-H, m), 1001 (C-N, s) 697 (N-H, s); ¹H NMR (600 MHz, DMSO-*d*₆) δ 8.93 (dd, J = 4.2, 1.4 Hz, 1H, H-7), 8.69–8.66 (m, 3H, H-9, H-2' and H-6'), 8.18–8.12 (m, 2H, H-3' and H-5'), 7.84 (s, 1H, H-4), 7.49 (dd, J = 8.6, 4.2 Hz, 1H, H-8), 4.11–4.03 (m, 2H, H-15), 3.94–3.87 (m, 1H, H-14), 3.75–3.67 (m, 2H, H-12), 2.20–2.12 (m, 1H, H-13), 1.93–1.86 (m, 1H, H-13); ¹³C NMR (151 MHz, DMSO-*d*₆) δ 156.2 (C-1), 154.0 (C-5), 153.5 (C-7), 150.2 (C-2' and C-6'), 148.3 (C-3), 146.0 (C-4'), 134.5 (C-9), 120.7 (C-3' and C-5'), 120.5 (C-8), 114.4 (C-10), 108.6 (C-4), 57.1 (C-15), 50.2 (C-12), 49.0 (C-14), 32.2 (C-13); HRMS m/z (ESI⁺) [Found: 292.1545, C₁₇H₁₈N₅ requires (M+H)⁺ 292.1557]; LCMS (MDAP) R_t = 6.8 min (Ana 30–95 over 20 min), m/z (ESI⁺) 292.9 (M+H)⁺.

***Tert*-Butyl (3*S*)-3-[(7-chloro-1,6-naphthyridin-5-yl)amino]pyrrolidine-1-carboxylate**

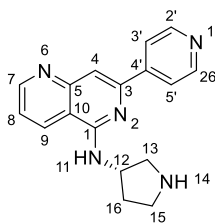
N,N-Diisopropylethylamine (0.71 mL, 4.06 mmol), 5,7-dichloro-1,6-naphthyridine (200 mg, 1 mmol) and (*S*)-3-amino-1-*N*-Boc-pyrrolidine (1.11 g, 5.97 mmol) in ethanol (7mL) were stirred at 100 °C overnight. LCMS indicated product formation (m/z 349, 293, 249). The mixture was concentrated under reduced pressure and water (4 mL) was added. The mixture was extracted four times with ethyl acetate (4 × 40 mL). The combined organic phases were washed with water (40 mL) and brine (40 mL) then dried over MgSO_4 , filtered and concentrated under reduced pressure (922 mg). The crude was purified *via* flash column chromatography (30 g silica, petroleum ether:ethyl acetate, 1:0 to 0:1) to give *tert*-butyl (3*S*)-3-[(7-chloro-1,6-naphthyridin-5-yl)amino]pyrrolidine-1-carboxylate (278 mg, 75%) as a white solid.

R_f 0.58 (100% ethyl acetate); m.p. 209–210 °C; ν_{max} (thin film)/cm⁻¹ 331 (N-H, m), 3093 (aromatic C-H, w), 2976 (aliphatic C-H, m), 1678 (C=O, s), 1576 (aromatic C-C, s), 876 (N-H, s); ¹H NMR (600 MHz, DMSO- d_6) δ 8.92 (dd, J = 4.3, 1.5 Hz, 1H, H-7), 8.78 (d, J = 8.7 Hz, 1H, H-9), 8.00 (d, J = 5.7 Hz, 1H, H-11), 7.51 (dd, J = 8.4, 4.3 Hz, 1H, H-8), 7.03 (s, 1H, H-4), 4.70–4.44 (m, 1H, H-12), 3.68 (t, J = 8.8 Hz, 1H, H-H-13), 3.53–3.41 (m, 1H, H-15), 3.42–3.31 (m, 1H, H-15), 3.29–3.21 (m, 1H, H-13), 2.30–2.09 (m, 1H, H-16), 2.09–1.87 (m, 1H, H-16), 1.40–1.33 (m, 9H, H-21); ¹³C NMR (151 MHz, DMSO- d_6) δ 155.7 (C-1), 154.4 (C-7), 153.5 (C-17), 153.0 (C-5), 147.3 (C-3), 132.3 (C-9), 120.8 (C-8), 111.9 (C-10), 108.5 (C-4), 78.3 (C-20), 51.2 (C-12), 50.7 (C-12), 50.5 (C-13), 50.4 (C-13), 44.1 (C-15), 44.0 (C-15), 30.6 (C-16), 29.8 (C-16), 28.2 (C-21). Presence of rotamers accounts for additional peaks in aliphatic region; HRMS m/z (ESI⁺) [Found: 371.1239, $\text{C}_{17}\text{H}_{21}\text{ClN}_4\text{NaO}_2$ requires (M+H)⁺ 371.1245]; LCMS (LCQ) Rt = 2.9 min, (4 min method), m/z (ESI⁺) 349.1 (M+H)⁺, 293.2 (M-*t*Bu+H)⁺ and 249.2 (M-Boc+H)⁺.

***Tert*-Butyl (3*S*)-3-[[7-(4-pyridyl)-1,6-naphthyridin-5-yl]amino]pyrrolidine-1-carboxylate**

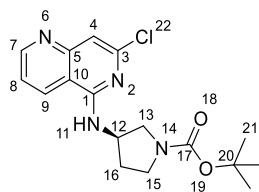
Potassium carbonate (169 mg, 1.23 mmol), pyridine-4-boronic acid hydrate (**196**) (50 mg, 0.41 mmol), *bis*[2-(di-*tert*-butylphosphanyl)cyclopenta-2,4-dien-1-yl]iron; dichloropalladium (13 mg, 0.02 mmol) and *tert*-butyl (3*S*)-3-[(7-chloro-1,6-naphthyridin-5-yl)amino]pyrrolidine-1-carboxylate (150 mg, 0.41 mmol) in 4:1 acetonitrile:water (12 mL) were degassed under a flow of nitrogen and heated in a microwave reactor at 140 °C for 15 minutes. LCMS confirmed reaction completion (*m/z* 392, 336, 292). The reaction mixture was diluted with water (20 mL) and extracted twice with ethyl acetate (2 × 25 mL). The combined organic phases were dried over MgSO₄, filtered and concentrated under reduced pressure to give a yellow oil (167 mg). The crude was purified *via* flash column chromatography (5 g petroleum ether:ethyl acetate, 1:0 to 0:1) to give *tert*-butyl (3*S*)-3-[[7-(4-pyridyl)-1,6-naphthyridin-5-yl]amino]pyrrolidine-1-carboxylate (110 mg, 65%) as an off-white solid.

*R*_f 0.38 (9:1 ethyl acetate:methanol); m.p. 120–122 °C; ν_{max} (thin film)/cm⁻¹ 3330 (N-H, br), 2974 (aliphatic C-H, w), 1668 (C=O, m), 1601 (C=C, m), 1532 (aromatic C-H, s), 1131 (C-N, m), 825 (N-H, s); ¹H NMR (600 MHz, DMSO-*d*₆) δ 9.02–8.92 (m, 1H, H-7), 8.81 (t, *J* = 6.7 Hz, 1H, H-9), 8.68 (d, *J* = 6.1 Hz, 2H, H-2' and H-6'), 8.16 (d, *J* = 6.2 Hz, 2H, H-3' and H-5'), 7.80 (s, 1H, H-4), 7.79–7.74 (m, 1H, H-11), 7.56 (dd, *J* = 8.4, 4.3 Hz, 1H, H-8), 4.89–4.69 (m, 1H, H-12), 3.91–3.67 (m, 1H, H-13), 3.57–3.44 (m, 1H, H-14), 3.46–3.33 (m, 2H, H-14), 3.35–3.31 (m, 1H, H-13), 2.35–2.21 (m, 1H, H-16), 2.17–2.00 (m, 1H, H-16), 1.53–1.31 (m, 9H, H-21); ¹³C NMR (151 MHz, DMSO-*d*₆) δ 155.4 (C-1), 154.1 (C-7), 153.6 (C-17), 152.6 (C-5), 150.1 (C-2' and C-6'), 148.9 (C-1'), 146.2 (C-3), 132.0 (C-9), 121.9 (C-8), 119.9 (C-3' and C-5'), 114.4 (C-10), 108.3 (C-4), 78.3 (C-20), 51.4 (C-12), 51.1 (C-12), 50.9 (C-13), 50.7 (C-13), 44.3 (C-14), 44.1 (C-14), 30.8 (C-16), 30.0 (C-16), 28.2 (C-21). Presence of rotamers accounts for multiple peaks; HRMS *m/z* (ESI⁺) [Found: 392.2076, C₂₂H₂₆N₅O₂ requires (M+H)⁺ 392.2081]; LCMS (MDAP) *R*_t = 8.3 min (Ana 30–95 over 20 min), *m/z* (ESI⁺) 392.1 (M+H)⁺, 336.0 (M+H-*t*-Bu)⁺, 292.0 (M+H-Boc)⁺.

7-(4-Pyridyl)-N-[(3S)-pyrrolidin-3-yl]-1,6-naphthyridin-5-amine (311)

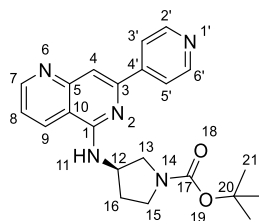
Tert-Butyl (3S)-3-[[7-(4-pyridyl)-1,6-naphthyridin-5-yl]amino]pyrrolidine-1-carboxylate (50 mg, 0.13 mmol) was dissolved in dichloromethane (1 mL) and cooled to 0 °C. Trifluoro acetic acid (0.5 mL, 5.17 mmol) was added dropwise and the reaction mixture was allowed to stir at room temperature overnight. LCMS (LCQ) indicated product formation (m/z 292). The reaction mixture was concentrated under reduced pressure to give a yellow solid. The crude was purified *via* SCX cartridge by elution with methanol then 2 M ammonia in methanol to give 7-(4-pyridyl)-N-[(3S)-pyrrolidin-3-yl]-1,6-naphthyridin-5-amine (**311**) (39 mg, 99%) as a yellow solid.

R_f 0.75 (100% ethyl acetate); m.p. 163–164 °C; ν_{\max} (thin film)/ cm^{-1} 3308 (N-H, br), 3085 (aromatic C-H, w), 2974 (aliphatic C-H, w), 1677 (C=C, m), 1588 (aromatic C-C, s), 1407 (aliphatic C-H, s), 767 (N-H, s); ^1H NMR (600 MHz, DMSO- d_6) δ 8.97 (dd, J = 4.1, 1.3 Hz, 1H, H-7), 8.78 (d, J = 8.4 Hz, 1H, H-9), 8.68 (d, J = 6.0 Hz, 2H, H-2' and H-6'), 8.15 (d, J = 6.0 Hz, 2H, H-3' and H-5'), 7.83–7.79 (m, 2H, H-11 and H-4), 7.56 (dd, J = 8.4, 4.3 Hz, 1H, H-8), 4.80 (*app.* sept, J = 5.7 Hz, 1H, H-12), 3.54 (dd, J = 11.8, 6.7 Hz, 1H, H-16), 3.23–3.12 (m, 3H, H-14 and H-16), 2.30 (h, J = 14.5, 7.4 Hz, 1H, H-13), 2.10 (*app.* sept, J = 13.1, 6.4 Hz, 1H, H-13); ^{13}C NMR (151 MHz, DMSO- d_6) δ 155.7 (C-1), 154.5 (C-7), 152.9 (C-5), 150.6 (C-2' and C-6'), 149.3 (C-3), 146.4 (C-4'), 132.4 (C-9), 121.9 (C-8), 121.1 (C-3' and C-5'), 114.0 (C-10), 108.9 (C-4), 51.5 (C-12), 50.7 (C-16), 44.6 (C-14), 30.7 (C-13); HRMS m/z (ESI $^+$) [Found: 292.1549, $\text{C}_{17}\text{H}_{17}\text{N}_5$ requires (M+H) $^+$ 292.1557]; LCMS (MDAP) Rt = 6.8 min (Ana 30–95 over 20 min), m/z (ESI $^+$) 292.0 (M+H) $^+$.

***tert*-Butyl (3*R*)-3-[(7-chloro-1,6-naphthyridin-5-yl)amino]pyrrolidine-1-carboxylate**

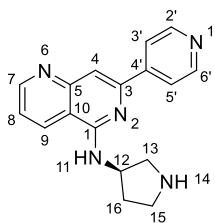
N,N-diisopropylethylamine (0.71 mL, 4.06 mmol), 5,7-dichloro-1,6-naphthyridine (200 mg, 1 mmol), and (*R*)-1-Boc-3-Aminopyrrolidine (1 mL, 5.98 mmol) in ethanol (7mL) were heated at 100 °C overnight. LCMS indicated product formation (*m/z* 349). The reaction mixture was concentrated under reduced pressure and water (4 mL) was added. The mixture was extracted three times with ethyl acetate (3 × 40 mL). The combined organic phases were washed with water (40 mL), brine (40 mL), dried over MgSO₄, filtered and concentrated under reduced pressure to give a brown mixture (931 mg). The crude was purified *via* flash column chromatography (30 g silica, petroleum ether:ethyl acetate, 1:0 to 0:1) to give *tert*-butyl (3*R*)-3-[(7-chloro-1,6-naphthyridin-5-yl)amino]-pyrrolidine-1-carboxylate (300 mg, 81%) as an off-white solid.

R_f 0.54 (100% ethyl acetate); m.p. 210–211 °C; ν_{\max} (thin film)/cm⁻¹ 3345 (N-H, br), 3075 (aromatic C-H, w), 1976 (aliphatic C-H, m), 1678 (C=O, s), 1576 (C=C, s), 1529 (aromatic C-C, s), 1111 (C-N, s), 874 (N-H, s); ¹H NMR (600 MHz, DMSO-*d*₆) δ 8.92 (dd, *J* = 4.2, 1.3 Hz, 1H, H-7), 8.78 (d, *J* = 8.0 Hz, 1H, H-9), 8.01 (d, *J* = 5.9 Hz, 1H, H-11), 7.51 (dd, *J* = 8.4, 4.3 Hz, 1H, H-8), 7.03 (s, 1H, H-4), 4.67–4.45 (m, 1, H-12), 3.74–3.58 (m, 1H, H-13), 3.51–3.40 (m, 1H, H-15), 3.39–3.31 (m, 1H, H-15), 3.28–3.21 (m, 1H, H-13), 2.25–2.15 (m, 1H, H-16), 2.07–1.92 (m, 1H, H-16), 1.40 (d, *J* = 9.0 Hz, 9H, H-21); ¹³C NMR (151 MHz, DMSO-*d*₆) δ 155.7 (C-1), 154.5 (C-7), 153.6 (C-17), 153.0 (C-5), 147.3 (C-3), 132.4 (C-9), 120.8 (C-8), 112.0 (C-10), 108.5 (C-4), 78.3 (C-20), 78.3 (C-20), 51.3 (C-12), 50.7 (C-12), 50.6 (C-13), 50.5 (C-13), 44.2 (C-15), 44.0 (C-15), 30.7 (C-16), 29.9 (C-16), 28.2 (C-21); HRMS *m/z* (ESI⁺) [Found: 371.1238, C₁₇H₂₁ClN₄NaO₂ requires (M+H)⁺ 371.1245]; LCMS (MDAP) *R_t* = 22.1 min (Ana 30–95 over 20 min), *m/z* (ESI⁺) 347.1 [³⁵Cl] and 349.0 [³⁷Cl] (M+H)⁺.

***Tert*-Butyl (3*R*)-3-[[7-(4-pyridyl)-1,6-naphthyridin-5-yl]amino]pyrrolidine-1-carboxylate (**313**)**

Potassium carbonate (169 mg, 1.23 mmol), pyridine-4-boronic acid hydrate (**196**) (50 mg, 0.41 mmol), *bis*[2-(di-*tert*-butylphosphanyl)cyclopenta-2,4-dien-1-yl]iron; dichloropalladium (13 mg, 0.02 mmol) and *tert*-butyl (3*R*)-3-[(7-chloro-1,6-naphthyridin-5-yl)amino]pyrrolidine-1-carboxylate (150 mg, 0.41 mmol) in 4:1 acetonitrile:water (12 mL) under a flow of nitrogen were heated in a microwave reactor at 140 °C for 15 minutes. LCMS confirmed reaction completion (*m/z* 392, 336, 292). The reaction mixture was diluted with water (20 mL) and extracted twice with ethyl acetate (2 × 25 mL). The combined organic phases were dried over MgSO₄, filtered and concentrated under reduced pressure to give a brown oil (141 mg). The crude was purified *via* flash column chromatography (4 g petroleum ether:ethyl acetate, 1:0 to 0:1) to give *tert*-butyl (3*R*)-3-[[7-(4-pyridyl)-1,6-naphthyridin-5-yl]amino]pyrrolidine-1-carboxylate (**313**) (117 mg, 66%) as an orange solid.

*R*_f 0.37 (9:1 ethyl acetate:methanol); m.p. 110–112 °C; *v*_{max} (thin film)/cm⁻¹ 3320 (N-H, br), 2972 (aliphatic C-H, w), 1668 (C=O, m), 1602 (C=C, m), 1575 (aromatic C-C, m), 1404 (aliphatic C-H, s), 1112 (C-N, m), 722 (N-H, m); ¹H NMR (600 MHz, DMSO-*d*₆) δ 8.98 (dd, *J* = 4.3, 1.7 Hz, 1H, H-7), 8.82 (t, *J* = 7.6 Hz, 1H, H-9), 8.69 (d, *J* = 6.2 Hz, 1H, H-2' and H-6'), 8.17 (d, *J* = 6.2 Hz, 2H, H-3' and H-5'), 7.85–7.78 (m, 2H, H-4 and H-11), 7.57 (dd, *J* = 8.4, 4.2 Hz, 1H, H-8), 4.81 (m, 1H, H-12), 3.79 (m, 1H, H-13), 3.54–3.47 (m, 1H, H-15), 3.45–3.37 (m, 1H, H-15), 3.32 (s, 1H, H-13), 2.34–2.20 (m, 1H, H-16), 2.18–2.00 (m, 1H, H-16), 1.41 (d, *J* = 16.3 Hz, 9H, H-21); ¹³C NMR (151 MHz, DMSO-*d*₆) δ 155.4 (C-1), 154.1 (C-7), 152.6 (C-5), 150.2 (C-2' and C-6'), 149.0 (C-3), 146.1 (C-4'), 132.0 (C-9), 121.4 (C-8), 120.6 (C-3' and C-5'), 113.6 (C-10), 108.3 (C-4), 78.3 (C-20), 51.4 (C-12), 51.1 (C-12), 50.9 (C-13), 50.7 (C-13), 44.3 (C-15), 44.1 (C-15), 30.8 (C-16), 30.0 (C-16), 28.2 (C-21); HRMS *m/z* (ESI⁺) [Found: 392.2079, C₂₂H₂₆N₅O₂ requires (M+H)⁺ 392.2081]; LCMS (MDAP) *R*_t = 8.2 min (method), *m/z* (ESI⁺) 392.0 (M+H)⁺.

7-(4-Pyridyl)-*N*-[(3*R*)-pyrrolidin-3-yl]-1,6-naphthyridin-5-amine (312)

Tert-Butyl (3*R*)-3-[[7-(4-pyridyl)-1,6-naphthyridin-5-yl]amino]pyrrolidine-1-carboxylate (**313**) (50 mg, 0.11 mmol) was stirred in dichloromethane (1 mL) and cooled to 0 °C. Trifluoro acetic acid (0.5 mL, 6.53 mmol) was added dropwise and the reaction was allowed to stir at room temperature for 4 h. The reaction mixture was concentrated under reduced pressure and purified *via* SCX cartridge by elution with methanol then 2 M ammonia in methanol to give 7-(4-pyridyl)-*N*-[(3*R*)-pyrrolidin-3-yl]-1,6-naphthyridin-5-amine (**312**) (30 mg, 85%) as a yellow solid.¹⁶¹

R_f 0 (9:1 dichloromethane:methanol); m.p. 156–158 °C; ν_{\max} (thin film)/cm⁻¹ 3281 (N-H, br), 2973 (aliphatic C-H, br), 1603 (C=C, m), 1575 (aromatic C-C, s), 1062 (C-N, s), 766 (N-H, s); ¹H NMR (600 MHz, DMSO-*d*₆) δ 8.96 (dd, J = 4.3, 1.5 Hz, 1H, H-7), 8.80 (d, J = 8.3 Hz, 1H, H-9), 8.69–8.66 (m, 2H, H-2' and H-6'), 8.17–8.14 (m, 2H, H-3' and H-5'), 7.84 (d, J = 5.5 Hz, 1H, H-11), 7.78 (s, 1H, H-4), 7.55 (dd, J = 8.4, 4.3 Hz, 1H, H-8), 4.81–4.75 (m, 1H, H-12), 3.46 (dd, J = 11.6, 6.5 Hz, 1H, H-16), 3.26–3.19 (m, 1H, H-15), 3.15–3.03 (m, 2H, H-15 and H-16), 2.30–2.23 (m, 1H, H-13), 2.08–2.00 (m, 1H, H-13); ¹³C NMR (151 MHz, DMSO-*d*₆) δ 155.4 (C-1), 154.1 (C-7), 152.6 (C-5), 150.2 (C-2' and C-6'), 149.0 (C-3), 146.1 (C-4'), 132.1 (C-9), 121.4 (C-8), 120.7 (C-3' and C-5'), 113.6 (C-10), 108.2 (C-4), 51.7 (C-12), 51.2 (C-16), 44.7 (C-15), 31.1 (C-13); HRMS m/z (ESI⁺) [Found: 292.1543, C₁₇H₁₈N₅ requires (M+H)⁺ 292.1557]; LCMS (MDAP) R_t = 7.1 min (Ana 30–95 over 20 min), m/z (ESI⁺) 291.90 (M+H)⁺.

6.2 Biology

The following section describes work carried out by Dr. Angela Fala.

6.2.1 Cloning, protein expression and purification

PKN2- UniProt ID Q16513 (Ser646-Cys984) and PKN1-UniProt ID Q16512 (Pro604-Cys942) were cloned fused to an N-terminal GST tag and C-terminal biotin tag attachment site (SSKGGYGLNDIFEAQKIEWHE).

Bacmid DNA containing the construct sequence was prepared from DH10Bac cells and used to transfect *Sf9* insect cells for the preparation of baculovirus. The prepared baculovirus was used to infect a new batch of *Sf9* cells cultivated in Sf-900 II SFM media (Thermo Fisher) in the presence of 20 U/mL of penicillin/streptomycin. Both proteins were expressed for 48 hours at 27°C. Additional biotin (Sigma-Aldrich) was added to the culture (200 mM/L) for biotinylation by co-expressed BirA. After incubation the cells were harvested (900 x *g*, 30 min, 4°C) and were re-suspended in lysis buffer (50 mM HEPES pH 7.5, 300 mM NaCl, 5% glycerol, 0.5 mM TCEP, 5 µL per 1 mL protease inhibitor cocktail Set III EDTA-free (Merck Millipore), frozen in liquid nitrogen and stored for later purification. The cells were thawed, re-suspended in approximately 150 mL lysis buffer, sonicated for 2 min in total (5 s ON, 10 s OFF) on ice. After sonication, the lysate was supplemented with 0.7% of Tween20 and benzonase (50 µg/100 mL of lysate) and incubated on ice for 15 min. The cell lysates were centrifuged at 50000 x *g* for 30 min at 4 °C. The supernatant was loaded on a pre-equilibrated (with lysis buffer) gravity column with 5 mL of glutathione-Sepharose resin and then purified by affinity chromatography. After loading the sample, the resin was washed with 40 CV of lysis buffer. The sample was eluted with 10 CV of lysis buffer containing 10 mM reduced glutathione. The elution fraction was concentrated to 2 mL using a 30 kDa molecular weight cut-off centrifugal concentrator (Millipore) at 4 °C and injected onto an S75 16/600 column (pre-equilibrated in 20 mM HEPES pH 7.5, 300 mM NaCl, 5% glycerol, 1 mM TCEP) at 1.0 mL/min. 1.5 mL fractions were collected and analysed on a 12% SDS-PAGE. One sample of the protein was separated to confirm its identity and the biotinylation by intact mass analysis. The main peak fractions were concentrated, and the protein was flash-frozen in a liquid nitrogen bath and stored at -80 °C until use.

6.2.2 Binding Displacement Assay

The time resolved fluorescence resonance energy transfer (TR-FRET) method was used to measure the binding of a fluorescent tracer molecule in the ATP binding site. Displacement of the tracer by varying concentrations of an inhibitor allows the IC₅₀ value for the inhibitor to be calculated. Compounds were serially diluted from 50 µM to 0.85 nM for a 12-point (1:3) in DMSO and then diluted in assay buffer (50 mM HEPES pH 7.5, 10 mM MgCl₂, 1 mM EGTA, 0.01% Brij-35). The dissociation constants of the tracer were measured for both kinases (PKN2 *K_D* = 5 ± 0.2 nM and PKN1 *K_D* = 2.8 ± 0.2 nM, Supplementary Figure 1). The final assay contained 5 nM biotinylated PKN2 or 15 nM biotinylated PKN1 ligated to streptavidin-Tb-cryptate (Cisbio), 5 nM or 2.8 nM Kinase Tracer 236 (Thermo Fisher Scientific) respectively for PKN2 and PKN1 and serial dilutions of the compounds. Final assay volume of each data point was 15 µL and final DMSO concentration was 1.25%. Black 384 well plates (Greiner) were used. The assay was incubated

at room temperature for 1 hour and then TR-FRET data was measured on a CLARIOstar Plus (BMG Labtech). Data was normalized to 0% and 100% inhibition values and fit to a four parameter dose-response binding curve in GraphPad 7 Software (version 7.04). All the points were measured in triplicate with two biological replicates. 10 μ M of Staurosporine was used as a control for 100% inhibition and calculation of the Z' value.²¹⁶

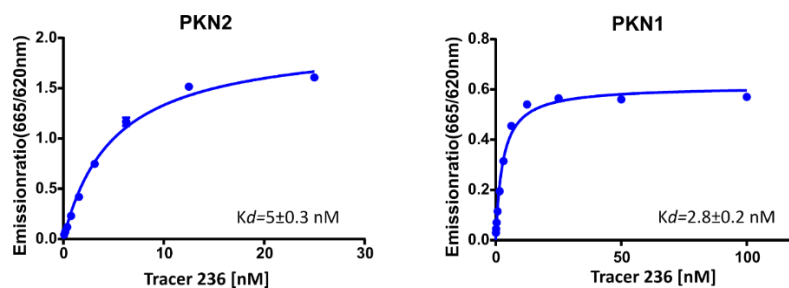


Figure S1. Determination of dissociation constant of Tracer 236 (ThermoFisher) when titrated over 5 nM of PKN2 or 15 nM of PKN1

6.2.3 Crystallography

Conditions: 2 M ammonium sulfate, 0.2 M sodium/potassium tartrate and 0.1 M of citrate pH 5.50

Chapter 7 Bibliography

1. Arrowsmith, C. H. *et al.* The promise and peril of chemical probes. *Nat. Chem. Biol.* **11**, 536–541 (2015).
2. Blagg, J. & Workman, P. Choose and Use Your Chemical Probe Wisely to Explore Cancer Biology. *Cancer Cell* **32**, 9–25 (2017).
3. Drewes, G. & Knapp, S. Chemoproteomics and Chemical Probes for Target Discovery. *Trends in Biotechnology* **36**, 1275–1286 (2018).
4. Structural Genomics Consortium. Chemical Probes. Available at: <https://www.thesgc.org/chemical-probes>. (Accessed: 12th April 2020)
5. Fire, A. *et al.* Potent and specific genetic interference by double-stranded RNA in *caenorhabditis elegans*. *Nature* **391**, 806–811 (1998).
6. Elbashir, S. M. *et al.* Duplexes of 21-nucleotide RNAs mediate RNA interference in cultured mammalian cells. *Nature* **411**, 494–498 (2001).
7. Savino, R., Paduano, S., Preianò, M. & Terracciano, R. The proteomics big challenge for biomarkers and new drug-targets discovery. *Int. J. Mol. Sci.* **13**, 13926–13948 (2012).
8. Davis, A. & Ward, S. E. (Simon E. *The handbook of medicinal chemistry : principles and practice*. (Royal Society of Chemistry, 2015).
9. Rüegg, U. T. & Gillian, B. Staurosporine, K-252 and UCN-01: potent but nonspecific inhibitors of protein kinases. *Trends Pharmacol. Sci.* **10**, 218–220 (1989).
10. S. Omura, Y. Iwai, A. Hirano, A. Nakagawa, J. Awaya, H. Tsuchiya, Y. Takahashi, R. M. A new alkaloid AM-2282 of *Streptomyces* origin: taxonomy, fermentation, isolation and preliminary characterisation. *J. Antibiot* **30**, 706–708 (1977).
11. Tamaoki, T. & Nakano, H. Potent and Specific Inhibitors of Protein Kinase C of Microbial Origin. *Bio/Technology* **8**, 732–735 (1990).
12. Vlahos, C. J., Matter, W. F., Hui, K. Y. & Brown, R. F. A specific inhibitor of phosphatidylinositol 3-kinase, 2-(4-morpholinyl)- 8-phenyl-4H-1-benzopyran-4-one (LY294002). *J. Biol. Chem.* **269**, 5241–5248 (1994).
13. Workman, P., Clarke, P. A., Raynaud, F. I. & Van Montfort, R. L. M. Drugging the PI3 kinome: From chemical tools to drugs in the clinic. *Cancer Research* **70**, 2146–2157 (2010).
14. Wu, P., Nielsen, T. E. & Clausen, M. H. FDA-approved small-molecule kinase inhibitors. *Trends Pharmacol. Sci.* **36**, 422–439 (2015).
15. LY294002 and PI3 kinase - PubMed - NCBI. Available at: <https://www.ncbi.nlm.nih.gov/pubmed>. (Accessed: 4th March 2020)
16. Baell, J. B. & Holloway, G. A. New Substructure Filters for Removal of Pan Assay Interference Compounds (PAINS) from Screening Libraries and for Their Exclusion in Bioassays. *J. Med. Chem.* **53**, 2719–2740 (2010).

17. Elkins, J. M. *et al.* Comprehensive characterization of the Published Kinase Inhibitor Set. in *Nature Biotechnology* **34**, 95–103 (Nature Publishing Group, 2016).
18. Drewry, D. H. *et al.* Progress towards a public chemogenomic set for protein kinases and a call for contributions. (2017). doi:10.1371/journal.pone.0181585
19. Chemical Probes | 'We provide the research community guidance in the selection and proper usage of chemical probes for specific protein targets.' Available at: <https://www.chemicalprobes.org/>. (Accessed: 4th March 2020)
20. Dowden, H. & Munro, J. Trends in clinical success rates and therapeutic focus. *Nature reviews. Drug discovery* **18**, 495–496 (2019).
21. Antolin, A. A. *et al.* Objective, Quantitative, Data-Driven Assessment of Chemical Probes. *Cell Chem. Biol.* **25**, 194–205.e5 (2018).
22. Retooling chemical probes. *Nat. Chem. Biol.* **6**, 157–157 (2010).
23. Bunnage, M. E., Chekler, E. L. P. & Jones, L. H. Target validation using chemical probes. *Nature Chemical Biology* **9**, 195–199 (2013).
24. Frye, S. V. *The art of the chemical probe. Nature Chemical Biology* **6**, 159–161 (2010).
25. Home - PubMed - NCBI. Available at: <https://www.ncbi.nlm.nih.gov/pubmed>. (Accessed: 4th March 2020)
26. Filippakopoulos, P. *et al.* Selective inhibition of BET bromodomains. *Nature* **468**, 1067–1073 (2010).
27. Zuber, J. *et al.* RNAi screen identifies Brd4 as a therapeutic target in acute myeloid leukaemia. *Nature* **478**, 524–528 (2011).
28. Delmore, J. E. *et al.* BET bromodomain inhibition as a therapeutic strategy to target c-Myc. *Cell* **146**, 904–917 (2011).
29. A Study to Investigate the Safety, Pharmacokinetics, Pharmacodynamics, and Clinical Activity of GSK525762 in Subjects With NUT Midline Carcinoma (NMC) and Other Cancers - No Study Results Posted - ClinicalTrials.gov. Available at: <https://clinicaltrials.gov/ct2/show/results/NCT01587703>. (Accessed: 29th February 2020)
30. Collins, J. L. *et al.* Identification of a nonsteroidal liver X receptor agonist through parallel array synthesis of tertiary amines. *J. Med. Chem.* **45**, 1963–1966 (2002).
31. Zhang, J. *et al.* Targeting wild-type and T315I Bcr-Abl by combining allosteric with ATP-site inhibitors. *Nature* **463**, 501–506 (2010).
32. G. Manning, 1, * D. B. Whyte, 1 R. Martinez, 1 T. Hunter, 2 & S. Sudarsanam 1, 3. The Protein Kinase Complement of the Human Genome. *Science (80-.)*. **298**, 1912–1934 (2002).
33. Ferguson, F. M. & Gray, N. S. Kinase inhibitors: The road ahead. *Nature Reviews Drug Discovery* **17**, 353–376 (2018).
34. Fedorov, O., Müller, S. & Knapp, S. The (un)targeted cancer kinome. *Nat. Chem. Biol.* **6**, 166–169 (2010).

35. Martin, E. & Hine, R. *A Dictionary of Biology*. (Oxford University Press, 2008). doi:10.1093/acref/9780199204625.001.0001
36. Graham L. Patrick. *An Introduction to Medicinal Chemistry*. (Oxford University Press, 2013). doi:10.1016/j.carbpol.2006.06.024
37. Fabbro, D., Cowan-Jacob, S. W. & Moebitz, H. Ten things you should know about protein kinases: IUPHAR Review 14. *Br. J. Pharmacol.* **172**, 2675–700 (2015).
38. Walsh, D. A., Perkins, J. P. & Krebs, E. G. An adenosine 3',5'-monophosphate-dependant protein kinase from rabbit skeletal muscle. *J. Biol. Chem.* **243**, 3763–3765 (1968).
39. Rebs, E. G. K. *Historical perspectives on protein phosphorylation and a classification system for protein kinases*. *Trans. R. Soc. Lond. B* **302**, (1983).
40. Sharma, S. *et al.* Design strategies, structure activity relationship and mechanistic insights for purines as kinase inhibitors. *Eur. J. Med. Chem.* **112**, 298–346 (2016).
41. Leroux, A. E., Schulze, J. O. & Biondi, R. M. AGC kinases, mechanisms of regulation and innovative drug development. *Semin. Cancer Biol.* **48**, 1–17 (2018).
42. Roskoski, R. A historical overview of protein kinases and their targeted small molecule inhibitors. *Pharmacol. Res.* **100**, 1–23 (2015).
43. Pearce, L. R., Komander, D. & Alessi, D. R. The nuts and bolts of AGC protein kinases. *Nat. Rev. Mol. Cell Biol.* **11**, 9–22 (2010).
44. Johnson, L. N. & Noble, M. E. M. Active and Inactive Protein Kinases: Review Structural Basis for Regulation. *Cell* **85**, 149–158 (1996).
45. Roskoski, R., Robert Roskoski Jr. & Roskoski, R. A historical overview of protein kinases and their targeted small molecule inhibitors. *Pharmacological Research* **100**, 1–23 (2015).
46. Roskoski, R. Properties of FDA-approved small molecule protein kinase inhibitors: A 2020 update. *Pharmacol. Res.* **152**, 104609 (2020).
47. Dar, A. C. & Shokat, K. M. The Evolution of Protein Kinase Inhibitors from Antagonists to Agonists of Cellular Signaling. *Annu. Rev. Biochem.* **80**, 769–795 (2011).
48. Gavrin, L. K. & Saiah, E. Approaches to discover non-ATP site kinase inhibitors. *MedChemComm* **4**, 41–51 (2013).
49. Druker, B. J. *et al.* Efficacy and safety of a specific inhibitor of the BCR-ABL tyrosine kinase in chronic myeloid leukemia. *N. Engl. J. Med.* **344**, 1031–7 (2001).
50. Essegian, D. J. *et al.* Abstract 5103: The dark cancer kinome - untapped opportunities for the development of novel drugs. in *Cancer Research* **79**, 5103–5103 (American Association for Cancer Research (AACR), 2019).
51. Mullard, A. A probe for every protein. *Nat. Rev. Drug Discov.* (2019). doi:10.1038/d41573-019-00159-9
52. Ogurtsov, A. Y. *et al.* Expression Patterns of Protein Kinases Correlate with Gene Architecture and Evolutionary Rates. *PLoS One* **3**, e3599 (2008).

53. Protein Kinases: Human Protein Kinases Overview | CST. Available at: <https://www.cellsignal.co.uk/contents/science-protein-kinases/protein-kinases-human-protein-kinases-overview/kinases-human-protein>. (Accessed: 4th March 2020)
54. Arencibia, J. M., Pastor-Flores, D., Bauer, A. F., Schulze, J. O. & Biondi, R. M. AGC protein kinases: From structural mechanism of regulation to allosteric drug development for the treatment of human diseases. *Biochim. Biophys. Acta - Proteins Proteomics* **1834**, 1302–1321 (2013).
55. GeneCards. Zfhx4. *LIPA GENE* 1–8 (2018). doi:10.1093/DATABASE
56. Palmer, R. H., Ridden, J. & Parker, P. J. Identification of multiple, novel, protein kinase C-related gene products. *FEBS Lett* **356**, 5–8 (1994).
57. Mukai, H. & Ono, Y. A Novel Protein Kinase with Leucine Zipper-like Sequences: Its Catalytic Domain Is Highly Homologous to That of Protein Kinase C. *Biochem. Biophys. Res. Commun.* **199**, 897–904 (1994).
58. Palmer, R. H. & Parker, P. J. Expression, purification and characterization of the ubiquitous protein kinase C-related kinase 1. *Biochem. J.* **309** (Pt 1), 315–20 (1995).
59. Oishi, K., Mukai, H., Shibata, H., Takahashi, M. & Ono, Y. Identification and Characterization of PKN β , a Novel Isoform of Protein Kinase PKN: Expression and Arachidonic Acid Dependency Are Different from Those of PKN α . *Biochem. Biophys. Res. Commun.* **261**, 808–814 (1999).
60. Bauer, A. F. *et al.* Regulation of Protein Kinase C-related Protein Kinase 2 (PRK2) by an Intermolecular PRK2-PRK2 Interaction Mediated by Its N-terminal Domain. *J. Biol. Chem.* **287**, 20590–20602 (2012).
61. Lim, W. *et al.* The very C-terminus of PRK1/PKN is essential for its activation by RhoA and downstream signaling. *Cell. Signal.* **18**, 1473–1481 (2006).
62. Mukai, H. & Ono, Y. Purification and kinase assay of PKN. *Methods Enzymol.* **406**, 234–250 (2006).
63. Mathea, S. & Knapp, S. Structure of PKN2. doi:10.2210/PDB4CRS/PDB
64. Schulze, J. O. *et al.* Bidirectional Allosteric Communication between the ATP-Binding Site and the Regulatory PIF Pocket in PDK1 Protein Kinase. *Cell Chem. Biol.* **23**, 1193–1205 (2016).
65. Palmer, R. H. *et al.* Activation of PRK1 by phosphatidylinositol 4,5-bisphosphate and phosphatidylinositol 3,4,5-trisphosphate: A comparison with protein kinase C isotypes. *J. Biol. Chem.* **270**, 22412–22416 (1995).
66. Morrice, N. A., Fecondo, J. & Wettenhall, E. H. Differential effects of fatty acid and phospholipid activators on the catalytic activities of a structurally novel protein kinase from rat liver. *FEBS Lett.* **351**, 171–175 (1994).
67. Standaert, M. *et al.* Comparative effects of GTP γ S and insulin on the activation of Rho, phosphatidylinositol 3-kinase, and protein kinase N in Rat adipocytes. Relationship to glucose transport. *J. Biol. Chem.* **273**, 7470–7477 (1998).
68. Mukai, H. The Structure and Function of PKN, a Protein Kinase Having a Catalytic

Domain Homologous to That of PKC. *J. Biochem* **133**, 17–27 (2003).

69. Amano, M. *et al.* Identification of a putative target for Rho as the serine-threonine kinase protein kinase N. *Science* **271**, 648–650 (1996).
70. Watanabe, G. *et al.* Protein kinase N (PKN) and PKN-related protein Rhophilin as targets of small GTPase Rho. *Science* **271**, 645–648 (1996).
71. Fields, S. & Song, O. K. A novel genetic system to detect protein-protein interactions. *Nature* **340**, 245–246 (1989).
72. Brückner, A., Polge, C., Lentze, N., Auerbach, D. & Schlattner, U. Yeast two-hybrid, a powerful tool for systems biology. *International Journal of Molecular Sciences* **10**, 2763–2788 (2009).
73. Flynn, P., Mellor, H., Casamassima, A. & Parker, P. J. Rho GTPase control of protein kinase C-related protein kinase activation by 3-phosphoinositide-dependent protein kinase. *J. Biol. Chem.* **275**, 11064–11070 (2000).
74. Vincent, S. & Settleman, J. The PRK2 kinase is a potential effector target of both Rho and Rac GTPases and regulates actin cytoskeletal organization. *Mol. Cell. Biol.* **17**, 2247–2256 (1997).
75. Dong, L. Q. *et al.* Phosphorylation of protein kinase N by phosphoinositide-dependent protein kinase-1 mediates insulin signals to the actin cytoskeleton. *Proc. Natl. Acad. Sci. U. S. A.* **97**, 5089–5094 (2000).
76. Bourguignon, L. Y. W., Gilad, E., Peyrolier, K., Brightman, A. & Swanson, R. A. Hyaluronan-CD44 interaction stimulates Rac1 signaling and PKN γ kinase activation leading to cytoskeleton function and cell migration in astrocytes. *J. Neurochem.* **101**, 1002–1017 (2007).
77. Wallace, S. W., Magalhaes, A. & Hall, A. The Rho target PRK2 regulates apical junction formation in human bronchial epithelial cells. *Mol. Cell. Biol.* **31**, 81–91 (2011).
78. Calautti, E. *et al.* Fyn tyrosine kinase is a downstream mediator of Rho/PRK2 function in keratinocyte cell–cell adhesion. *J. Cell Biol.* **156**, 137–148 (2002).
79. Queitier, I. *et al.* Knockout of the PKN Family of Rho Effector Kinases Reveals a Non-redundant Role for PKN2 in Developmental Mesoderm Expansion. *Cell Rep.* **14**, 440–448 (2016).
80. Misaki, K. *et al.* PKN delays mitotic timing by inhibition of Cdc25C: Possible involvement of PKN in the regulation of cell division. *Proc. Natl. Acad. Sci. U. S. A.* **98**, 125–129 (2001).
81. Takahashi, M., Mukai, H., Toshimori, M., Mlyamoto, M. & Ono, Y. Proteolytic activation of PKN by caspase-3 or related protease during apoptosis. *Proc. Natl. Acad. Sci. U. S. A.* **95**, 11566–11571 (1998).
82. Koh, H. *et al.* Inhibition of Akt and its anti-apoptotic activities by tumor necrosis factor-induced protein kinase C-related kinase 2 (PRK2) cleavage. *J. Biol. Chem.* **275**, 34451–34458 (2000).
83. Patrick, G.L. *An Introduction to Medicinal Chemistry*. (Oxford University Press, 2013).

doi:10.1016/j.carbpol.2006.06.024

84. Harrison, B. C. *et al.* Protein kinase C-related kinase targets nuclear localization signals in a subset of class IIa histone deacetylases. *FEBS Lett.* **584**, 1103–1110 (2010).
85. O’Sullivan, A. G. *et al.* Protein kinase C-related kinase 1 and 2 play an essential role in thromboxane-mediated neoplastic responses in prostate cancer. *Oncotarget* **6**, 26437–56 (2015).
86. Cheng, Y. *et al.* PKN2 in colon cancer cells inhibits M2 phenotype polarization of tumor-associated macrophages via regulating DUSP6-Erk1/2 pathway. *Mol. Cancer* **17**, 13 (2018).
87. Rajagopalan, P. *et al.* Role of protein kinase N2 (PKN2) in cigarette smoke-mediated oncogenic transformation of oral cells. *J. Cell Commun. Signal.* **12**, 709–721
88. Lin, W. *et al.* Protein kinase C inhibitor chelerythrine selectively inhibits proliferation of triple-negative breast cancer cells. *Sci. Rep.* **7**, 2022 (2017).
89. Patel, H. *et al.* Novel roles of PRK1 and PRK2 in cilia and cancer biology. *Sci. Rep.* **10**, 3902 (2020).
90. Schnappauf, O., Chae, J. J., Kastner, D. L. & Akseptijevich, I. The Pyrin Inflammasome in Health and Disease. *Front. Immunol.* **10**, 1745 (2019).
91. Kim, S.-J., Kim, J.-H., Sun, J.-M., Kim, M.-G. & Oh, J.-W. Suppression of hepatitis C virus replication by protein kinase C-related kinase 2 inhibitors that block phosphorylation of viral RNA polymerase. *J. Viral Hepat.* **16**, 697–704 (2009).
92. Marrocco, V. *et al.* PKC and PKN in heart disease. *Journal of Molecular and Cellular Cardiology* **128**, 212–226 (2019).
93. O’Sullivan, A. G., Eivers, S. B., Mulvaney, E. P. & Kinsella, B. T. Regulated expression of the TP β isoform of the human T Prostanoid receptor by the tumour suppressors FOXP1 and NKX3.1: Implications for the role of Thromboxane in Prostate Cancer. (2017). doi:10.1016/j.bbadis.2017.09.005
94. Yang, C.-S. S. *et al.* The protein kinase C super-family member PKN is regulated by mTOR and influences differentiation during prostate cancer progression. *Prostate* **77**, 1452–1467 (2017).
95. Orecchioni, M., Ghosheh, Y., Pramod, A. B. & Ley, K. Macrophage polarization: Different gene signatures in M1(Lps+) vs. Classically and M2(LPS-) vs. Alternatively activated macrophages. *Frontiers in Immunology* **10**, 1084 (2019).
96. Furrukh, M. Tobacco smoking and lung cancer: Perception-changing facts. *Sultan Qaboos University Medical Journal* **13**, 345–358 (2013).
97. Foulkes, W. D., Smith, I. E. & Reis-Filho, J. S. Triple-Negative Breast Cancer. *N. Engl. J. Med.* **363**, 1938–1948 (2010).
98. Kim, S.-J., Kim, J.-H., Kim, Y.-G., Lim, H.-S. & Oh, J.-W. Protein kinase C-related kinase 2 regulates hepatitis C virus RNA polymerase function by phosphorylation. *J. Biol. Chem.* **279**, 50031–41 (2004).
99. Park, Y. H., Wood, G., Kastner, D. L. & Chae, J. J. Pyrin inflammasome activation and

- RhoA signaling in the autoinflammatory diseases FMF and HIDS. *Nat. Immunol.* **17**, 914–921 (2016).
100. Peckham, D., Scambler, T., Savic, S. & McDermott, M. F. The burgeoning field of innate immune-mediated disease and autoinflammation. *J. Pathol.* **241**, 123–139 (2017).
 101. Stone, R. M., Manley, P. W., Larson, R. A. & Capdeville, R. Midostaurin: Its odyssey from discovery to approval for treating acute myeloid leukemia and advanced systemic mastocytosis. *Blood Adv.* **2**, 444–453 (2018).
 102. Sakaguchi, T. *et al.* Protein Kinase N Promotes Stress-Induced Cardiac Dysfunction Through Phosphorylation of Myocardin-Related Transcription Factor A and Disruption of its Interaction with Actin. *Circulation* (2019). doi:10.1161/CIRCULATIONAHA.119.041019
 103. ChEMBL. Available at: [https://www.ebi.ac.uk/chembl/g/#browse/activities/filter/molecule_chembl_id%3A\(%22CHEMBL1990482%22\) AND standard_type%3A\(%22Ki%22\)](https://www.ebi.ac.uk/chembl/g/#browse/activities/filter/molecule_chembl_id%3A(%22CHEMBL1990482%22) AND standard_type%3A(%22Ki%22)). (Accessed: 12th July 2019)
 104. White, A. W. *et al.* Resistance-Modifying Agents. 9. 1 Synthesis and Biological Properties of Benzimidazole Inhibitors of the DNA Repair Enzyme Poly(ADP-ribose) Polymerase. *J. Med. Chem.* **43**, 4084–4097 (2000).
 105. Anderson, D. R. *et al.* Pyrrolopyridine Inhibitors of Mitogen-Activated Protein Kinase-Activated Protein Kinase 2 (MK-2). *J. Med. Chem.* **50**, 2647–2654 (2007).
 106. Meredith, E. L. *et al.* Identification of orally available naphthyridine protein kinase D inhibitors. *J. Med. Chem.* **53**, 5400–5421 (2010).
 107. Davis, M. I. *et al.* Comprehensive analysis of kinase inhibitor selectivity. *Nat. Biotechnol.* **29**, 1046–1051 (2011).
 108. Scott, F. *et al.* Development of 2-(4-pyridyl)-benzimidazoles as PKN2 chemical tools to probe cancer. *Bioorganic Med. Chem. Lett.* **30**, 127040 (2020).
 109. Metz, J. T. *et al.* Navigating the kinome. *Nat. Chem. Biol.* **7**, 200–202 (2011).
 110. Velík, J. *et al.* Benzimidazole drugs and modulation of biotransformation enzymes. *Res. Vet. Sci.* **76**, 95–108 (2004).
 111. Garuti, L., Roberti, M. & Bottegoni, G. Benzimidazole Derivatives as Kinase Inhibitors. *Curr. Med. Chem.* **21**, 2284–2298 (2014).
 112. Kazuhisa, T. *et al.* Benzimidazole derivates. (2001). WO 0121615 A1
 113. Fong, P. C. *et al.* Inhibition of Poly(ADP-Ribose) Polymerase in Tumors from *BRCA* Mutation Carriers. *N. Engl. J. Med.* **361**, 123–134 (2009).
 114. Lubisch, W. *et al.* Heterocyclically substituted benzimidazoles, the production and application thereof. (2004). US 6696437 B1
 115. Kock, M., Lubisch, W. & Jentzsch, A. Use of PARP inhibitors in cosmetic preparations. (2001). WO 0182877 A2
 116. Rix, F. C., Kacker, S., Datta, S., Zhao, R. & Eswaran, V. R. Olefin polymerization catalyst

system and process for use thereof. (2005). US 7601666 B2

117. Clayden, J., Greeves, N. & Warren, S. *Organic Chemistry*. (OUP Oxford, 2012).
118. Schmidt, A. *et al.* On benzo[b][1,4]diazepinium-olates, -thiolates and -carboxylates as anti-Hückel mesomeric betaines. *Org. Biomol. Chem.* **1**, 4342–4350 (2003).
119. Lister, M. W. & Garvie, R. C. Sodium dithionite decomposition in aqueous solution and in the solid state. *Can. J. Chem.* **37**, 1567–1574 (1959).
120. Van Steijvoort, B. F., Kaval, N., Kulago, A. A. & Maes, B. U. W. Remote Functionalization: Palladium-Catalyzed C5(sp³)-H Arylation of 1-Boc-3-aminopiperidine through the Use of a Bidentate Directing Group. *ACS Catal.* **6**, 4486–4490 (2016).
121. Greene, T. W. & Wuts, P. G. M. *Protective Groups in Organic Synthesis*. *Journal of Medicinal Chemistry* **42**, (Wiley and Sons, 1999).
122. Zhan, Y., Ding, X., Wang, H., Yu, H. & Ren, F. A mild and efficient THP protection of indazoles and benzyl alcohols in water. *Tetrahedron Lett.* **59**, 2150–2153 (2018).
123. Tanaka, H. *et al.* Azole-substituted pyridine compound. (2018). EP 3418276 A1
124. Kato, D. I. *et al.* A firefly inspired one-pot chemiluminescence system using n-propylphosphonic anhydride (T3P). *Photochem. Photobiol. Sci.* **13**, 1640–1645 (2014).
125. Sabot, C., Kumar, K. A., Meunier, S. & Mioskowski, C. A convenient aminolysis of esters catalyzed by 1,5,7-triazabicyclo[4.4.0]dec-5-ene (TBD) under solvent-free conditions. *Tetrahedron Lett.* **48**, 3863–3866 (2007).
126. Yoshikawa, M. *et al.* Pyridinium cationic-dimer antimalarials, unlike chloroquine, act selectively between the schizont stage and the ring stage of *Plasmodium falciparum*. *Bioorg. Med. Chem.* **16**, 6027–6033 (2008).
127. Rodger, C. A. Spectroscopic methods in organic chemistry, fifth edition. *Concepts Magn. Reson.* **9**, 355–356 (1997).
128. Ju, A. *et al.* Identification of a Novel SHP-2 Protein Tyrosine Phosphatase Inhibitor. *Bull. Chem. Soc. Jpn.* **87**, 420–424 (2014).
129. Yung-Chi, C. & Prusoff, W. H. Relationship between the inhibition constant (KI) and the concentration of inhibitor which causes 50 per cent inhibition (I50) of an enzymatic reaction. *Biochem. Pharmacol.* **22**, 3099–3108 (1973).
130. Friesner, R. A. *et al.* Glide: A New Approach for Rapid, Accurate Docking and Scoring. 1. Method and Assessment of Docking Accuracy. *J. Med. Chem.* **47**, 1739–1749 (2004).
131. Menichincheri, M. *et al.* Cdc7 kinase inhibitors: 5-heteroaryl-3-carboxamido-2-aryl pyrroles as potential antitumor agents. 1. Lead finding. *J. Med. Chem.* **53**, 7296–7315 (2010).
132. Menichincheri, M. *et al.* First Cdc7 kinase inhibitors: pyrrolopyridinones as potent and orally active antitumor agents. 2. Lead discovery. *J. Med. Chem.* **52**, 293–307 (2009).
133. Vanotti, E. *et al.* Cdc7 kinase inhibitors: Pyrrolopyridinones as potential antitumor agents. 1. Synthesis and structure-activity relationships. *J. Med. Chem.* **51**, 487–501 (2008).

134. Montagnoli, A. *et al.* A Cdc7 kinase inhibitor restricts initiation of DNA replication and has antitumor activity. *Nat. Chem. Biol.* **4**, 357–365 (2008).
135. Vargas, B. *et al.* CDK9 inhibitors in the treatment of midline carcinoma. *J. Med. Chem.* **90**, 720–723 (2018).
136. Arnett, E. M. & Harrelson, J. A. A Spectacular Example of The Importance of Rotational Barriers: The Ionization of Meldrum's Acid. *J. Am. Chem. Soc.* **109**, 809–812 (1987).
137. Fones, W. S. The use of sodium hydride in the alkylation of N-substituted amides. *J. Org. Chem.* **14**, 1099–1102 (1949).
138. Surase, Y. B. *et al.* Identification and synthesis of novel inhibitors of mycobacterium ATP synthase. *Bioorg. Med. Chem. Lett.* **27**, 3454–3459 (2017).
139. Li, X., Taechalertrapisarn, J., Xin, D. & Burgess, K. Protein–Protein Interface Mimicry by an Oxazoline Piperidine-2,4-dione. *Org. Lett.* **17**, 632–635 (2015).
140. LanthaScreen Eu Kinase Binding Assay | Thermo Fisher Scientific - UK. Available at: <https://www.thermofisher.com/uk/en/home/industrial/pharma-biopharma/drug-discovery-development/target-and-lead-identification-and-validation/kinasebiology/kinase-activity-assays/lanthascreentm-eu-kinase-binding-assay.html>. (Accessed: 7th February 2020)
141. Khan, I., Tantray, M. A., Alam, M. S. & Hamid, H. Natural and synthetic bioactive inhibitors of glycogen synthase kinase. *European Journal of Medicinal Chemistry* **125**, 464–477 (2017).
142. KINOMEScan Assay Process -. Available at: <https://www.discoverx.com/technologies-platforms/competitive-binding-technology/kinomescan-technology-platform/kinomescan-assay-process>. (Accessed: 8th February 2020)
143. Friesner, R. A. *et al.* Extra precision glide: Docking and scoring incorporating a model of hydrophobic enclosure for protein-ligand complexes. *J. Med. Chem.* **49**, 6177–6196 (2006).
144. Bordwell, F. G. Equilibrium Acidities in Dimethyl Sulfoxide Solution. *Acc. Chem. Res.* **21**, 456–463 (1988).
145. Gibbs, J. W. A method of geometrical representation of the thermodynamic properties of substances by means of surfaces. *Trans. Connect. Acad.* **2**, 382–404 (1873).
146. Meyerson, S. Natural Abundance of Chlorine Isotopes. *Anal. Chem.* **33**, 964–964 (1961).
147. Eggenkamp, H. G. M. Summary of Methods for Determining the Stable Isotope Composition of Chlorine and Bromine in Natural Materials. in *Handbook of Stable Isotope Analytical Techniques* 604–622 (Elsevier, 2004). doi:10.1016/B978-044451114-0/50030-2
148. Sheppard, T. D. Metal-catalysed halogen exchange reactions of aryl halides. *Org. Biomol. Chem.* **7**, 1043–1052 (2009).
149. Ryneerson, K. D. *et al.* 2-Aminobenzoxazole ligands of the hepatitis C virus internal ribosome entry site. **24**, 3521–3525 (Elsevier Ltd, 2014).
150. Campbell, J. E. *et al.* Amine-substituted aryl or heteroaryl compounds as EHMT1 and

EHMT2 inhibitors. (2017). WO 181177 A1

151. Sutherlin, D. P. *et al.* Discovery of (Thienopyrimidin-2-yl)aminopyrimidines as Potent, Selective, and Orally Available Pan-PI3-Kinase and Dual Pan-PI3-Kinase/mTOR Inhibitors for the Treatment of Cancer. *J. Med. Chem.* **53**, 1086–1097 (2010).
152. Miyaura, N. & Suzuki, A. Palladium-Catalyzed Cross-Coupling Reactions of Organoboron Compounds. *Chem. Rev.* **95**, 2457–2483 (1995).
153. Roughley, S. D. & Vernalis, A. M. J. The Medicinal Chemist's Toolbox: An Analysis of Reactions Used in the Pursuit of Drug Candidates. *J. Med. Chem.* **54**, 3451–3479 (2011).
154. Lennox, A. J. J. & Lloyd-Jones, G. C. Selection of boron reagents for Suzuki-Miyaura coupling. *Chemical Society Reviews* **43**, 412–443 (2014).
155. Verheij, M. H. P. *et al.* Design, Synthesis, and Structure–Activity Relationships of Highly Potent 5-HT₃ Receptor Ligands. *J. Med. Chem.* **55**, 8603–8614 (2012).
156. Pretsch, E., Bühlmann, P. & Affolter, C. Structure Determination of Organic Compounds. *Structure Determination of Organic Compounds* (2000). doi:10.1007/978-3-662-04201-4
157. Butini, S. *et al.* Multifunctional Cholinesterase and Amyloid Beta Fibrillization Modulators. Synthesis and Biological Investigation. *ACS Med. Chem. Lett.* **4**, 1178–1182 (2013).
158. Hartwig, J. F., Richards, S., Barañ, D. & Paul, F. *Influences on the Relative Rates for C-N Bond-Forming Reductive Elimination and-Hydrogen Elimination of Amides. A Case Study on the Origins of Competing Reduction in the Palladium-Catalyzed Amination of Aryl Halides.* (1996).
159. Batson, J. *et al.* Development of Potent, Selective SRPK1 Inhibitors as Potential Topical Therapeutics for Neovascular Eye Disease. (2017). doi:10.1021/acscchembio.6b01048
160. Crunkhorn, S. Role of the Protein Data Bank. *Nat. Rev. Drug Discov.* (2019). doi:10.1038/d41573-019-00010-1
161. Van Eis, M. J. *et al.* 2,6-Naphthyridines as potent and selective inhibitors of the novel protein kinase C isozymes. *Bioorg. Med. Chem. Lett.* **21**, 7367–7372 (2011).
162. Goodman, K. B. *et al.* Development of dihydropyridone indazole amides as selective Rho-kinase inhibitors. *J. Med. Chem.* **50**, 6–9 (2007).
163. Chen, X., Jia, H., Li, Z. & Xu, X. Synthesis and nematocidal evaluation of 1,2,3-benzotriazin-4-one derivatives containing piperazine as linker against *Meloidogyne incognita*. *Chinese Chem. Lett.* **30**, 1207–1213 (2019).
164. Zhang, H. *et al.* Design, synthesis and biological activities of 2,3-dihydroquinazolin-4(1H)-one derivatives as TRPM2 inhibitors. *Eur. J. Med. Chem.* **152**, 235–252 (2018).
165. Velagapudi, U. K. *et al.* Design and Synthesis of Poly(ADP-ribose) Polymerase Inhibitors: Impact of Adenosine Pocket-Binding Motif Appendage to the 3-Oxo-2,3-dihydrobenzofuran-7-carboxamide on Potency and Selectivity. *J. Med. Chem.* **62**, 5330–5357 (2019).
166. Zhang, L.-J., Yang, K., Li, C.-Y. & Sun, Y.-Q. A simple and metal-free one-pot synthesis of

- 2-substituted-1H-4-carboxamide benzimidazole using 3,6-di(pyridin-2-yl)-1,2,4,5-tetrazine(PYTZ) as catalyst. *Chem. Pap.* **73**, 2697–2705 (2019).
167. Isbera, M., Bognor, B., Gulyes-Fekete, G., Kish, K. & Kolai, T. Syntheses of Pyrazine-, Quinoxaline-, and Imidazole-Fused Pyrroline Nitroxides. *Synthesis (Stuttg.)*. **51**, 4463–4472 (2019).
 168. Frackenpohl, J. *et al.* Use of substituted 2-amidobenzimidazoles, 2-amidobenzoxazoles and 2-amidobenzothiazoles or salts thereof as active substances against abiotic plant stress. (2015). US 2015216168 A1
 169. Xue, F., Luo, X., Ye, C., Ye, W. & Wang, Y. Inhibitory properties of 2-substituent-1H-benzimidazole-4-carboxamide derivatives against enteroviruses. *Bioorganic Med. Chem.* **19**, 2641–2649 (2011).
 170. Salehi, N. *et al.* Synthesis and biological evaluation of new N-benzylpyridinium-based benzoheterocycles as potential anti-Alzheimer's agents. *Bioorg. Chem.* **83**, 559–568 (2019).
 171. Raj, P. *et al.* Pyrophosphate Prompted Aggregation-Induced Emission: Chemosensor Studies, Cell Imaging, Cytotoxicity, and Hydrolysis of the Phosphoester Bond with Alkaline Phosphatase. *Eur. J. Inorg. Chem.* **2019**, 628–638 (2019).
 172. Onyeachu, I. B., Obot, I. B., Sorour, A. A. & Abdul-Rashid, M. I. Green corrosion inhibitor for oilfield application I: Electrochemical assessment of 2-(2-pyridyl) benzimidazole for API X60 steel under sweet environment in NACE brine ID196. *Corros. Sci.* **150**, 183–193 (2019).
 173. Moszczyzski-Patkowski, R. *et al.* Synthesis and characterization of novel classes of PDE10A inhibitors - 1H-1,3-benzodiazoles and imidazo[1,2-a]pyrimidines. *Eur. J. Med. Chem.* **155**, 96–116 (2018).
 174. Renno, T., Coste-Invernizzi, I., Giraud, S. & Lebecque, S. Benzoimidazole derivatives as anticancer agents. (2018). WO 2018054989
 175. Tsukamoto, G. *et al.* 2-Substituted azole derivatives. 1. Synthesis and antiinflammatory activity of some 2-(substituted-pyridinyl)benzimidazoles. *J. Med. Chem.* **23**, 734–738 (1980).
 176. Shaw, D. *et al.* Novel ROCK inhibitors for the treatment of pulmonary arterial hypertension. *Bioorg. Med. Chem. Lett.* **24**, 4812–7 (2014).
 177. Birkett, S. L. *et al.* Polymer conjugate comprising a bioactive agent. (2016). WO2017041142
 178. Marugan, J. J. *et al.* Evaluation of quinazoline analogues as glucocerebrosidase inhibitors with chaperone activity. *J. Med. Chem.* **54**, 1033–1058 (2011).
 179. Okubo, T. *et al.* Aminopyrrolidine compound. (2008). EP2003131
 180. Nordvall, G. & Ulrika, Y. Novel Quinazolines as 5-HT6 modulators. (2007). WO2007108744
 181. Kazemi, S. S., Keivanloo, A., Nasr-Isfahani, H. & Bamoniri, A. Synthesis of novel 1,5-disubstituted pyrrolo[1,2-: A] quinazolines and their evaluation for anti-bacterial and

- anti-oxidant activities. *RSC Adv.* **6**, 92663–92669 (2016).
182. Wynne, G. M., Moor, O. De, Johnson, P. D. & Vickers, R. Use of compounds for preparing anti-tuberculosis agents. (2010). US2010317607
 183. Fujiwara, N. *et al.* Synthesis and bioactivities of novel piperidylpyrimidine derivatives: Inhibitors of tumor necrosis factor- α production. *Bioorganic Med. Chem. Lett.* **10**, 1317–1320 (2000).
 184. Lacefield, W. B. 2-4-Diaminoquinazolines as antithrombotic agents. (1976). US 3956495
 185. Postovskii, I. Y. & Goncharova, I. N. No Title. *J. Gen. Chem. USSR* **32**, 3263–3270 (1962).
 186. Gilson, P. R. *et al.* Optimization of 2-Anilino 4-Amino Substituted Quinazolines into Potent Antimalarial Agents with Oral in Vivo Activity. *J. Med. Chem.* **60**, 1171–1188 (2017).
 187. Jiang, N. *et al.* Design, synthesis and structure-activity relationships of novel diaryl urea derivatives as potential EGFR inhibitors. *Molecules* **21**, (2016).
 188. Jiang, N. *et al.* Synthesis and biological evaluation of novel 2-(2-arylmethylene)hydrazinyl-4-aminoquinazoline derivatives as potent antitumor agents. *Eur. J. Med. Chem.* **54**, 534–541 (2012).
 189. Manetsch, R. *et al.* N2N N4-disubstituted quinazoline-2,4-diamines and uses thereof. (2019). US 10323007
 190. Fleeman, R. *et al.* Characterizing the antimicrobial activity of N2,N4-disubstituted quinazoline-2,4-diamines toward multidrug-resistant *Acinetobacter baumannii*. *Antimicrob. Agents Chemother.* **61**, (2017).
 191. Wang, S.-B. *et al.* Synthesis, biological evaluation, and physicochemical property assessment of 4-substituted 2-phenylaminoquinazolines as Mer tyrosine kinase inhibitors. *Bioorganic Med. Chem.* **24**, 3083–3092 (2016).
 192. Zhu, X. *et al.* SAR refinement of antileishmanial N2,N4-disubstituted quinazoline-2,4-diamines Dedicated to the memory of Martin John Rogers for his sincere efforts to facilitate neglected disease research, particularly in the area of drug discovery and development. *Bioorganic Med. Chem.* **23**, 5182–5189 (2015).
 193. Van Horn, K. S., Burda, W. N., Fleeman, R., Shaw, L. N. & Manetsch, R. Antibacterial activity of a series of N2, N4- disubstituted quinazoline-2,4-diamines. *J. Med. Chem.* **57**, 3075–3093 (2014).
 194. Van Horn, K. S. *et al.* Antileishmanial activity of a series of N2, N 4-disubstituted quinazoline-2,4-diamines. *J. Med. Chem.* **57**, 5141–5156 (2014).
 195. Li, X. *et al.* Modulation of chemosensory receptors and ligands associated therewith. (2008). US 2008306053
 196. Kanuma, K. *et al.* Identification of 4-amino-2-cyclohexylaminoquinazolines as metabolically stable melanin-concentrating hormone receptor 1 antagonists. *Bioorganic Med. Chem.* **14**, 3307–3319 (2006).
 197. Miki & Yamada. Fused pyrimidines. IV. The reaction of 4-alkylthio-2-chloroquinazolines with alkylamines in dimethylformamide. *Chem. Pharm. Bull.* **30**, 2313–2318 (1982).

198. Kenji, M. *et al.* Dipeptidyl peptidase IV inhibitor. (2003). EP1354882
199. Ibrahim, M. *et al.* TIE-2 modulators and methods of use. (2004). WO 200492196
200. Bodajla, M., Stankovsky, S. & Spirkova, K. SYNTHESIS OF SOME AZOLYLQUINAZOLINES. *Collect. Czechoslov. Chem. Commun.* **59**, 1463–1466 (1994).
201. Malagu, K. *et al.* The discovery and optimisation of pyrido[2,3-d]pyrimidine-2,4-diamines as potent and selective inhibitors of mTOR kinase. *Bioorganic Med. Chem. Lett.* **19**, 5950–5953 (2009).
202. Hu, H. *et al.* Design, synthesis and biological evaluation of novel thieno[3,2-d]pyrimidine and quinazoline derivatives as potent antitumor agents. *Bioorg. Chem.* **90**, (2019).
203. Yu, M. J. *et al.* Atrial Natriuretic Peptide Receptor Modulators: Effects of Disubstituted Quinazolines on Receptor Binding and in Vitro Biological Activity. *J. Med. Chem.* **33**, 348–353 (1990).
204. Morimoto, H., Sakamoto, T., Himiyama, T., Kawanishi, E. & Matsumura, T. Aromatic nitrogen-containing 6-membered ring compounds and their use. (2010). WO 201030027
205. Miki, H. & Kasahara, F. Fused Pyrimidines. III. The Reaction of 2,4-Dichloroquinazoline with N-Alkyl Cyclic Amines. *Chem. Pharm. Bull.* **30**, 3471–3475 (1982).
206. Hermann, K. & Simchen, G. Synthesis of Cyano-Substituted Heterocycles by Means of Tetraethylammonium Cyanide. *Liebigs Ann. der Chemie* 333–341 (1981).
207. Miki, H. & Yamada, J. The Reaction of 2-Chloro-4-methylthioquinazolines with Alkylamines in Dimethylformamide. *Heterocycles* **19**, 11 (1982).
208. Sekiguchi, Y. *et al.* Novel quinazoline derivatives and methods of treatment related to the use thereof. (2004). WO 200487680
209. Ili, G. J. E. *et al.* Quinazoline useful as modulators of ion channels. (2004). WO 200478733
210. Evertsson, E., Inghardt, T., Lindberg, J. & Linusson, A. Therapeutic agents II. (2005). WO 200570902
211. Kanuma, K. *et al.* Lead optimization of 4-(dimethylamino)quinazolines, potent and selective antagonists for the melanin-concentrating hormone receptor 1. *Bioorganic Med. Chem. Lett.* **15**, 3853–3856 (2005).
212. Kanuma, K. *et al.* Lead optimization of 4-(dimethylamino)quinazolines, potent and selective antagonists for the melanin-concentrating hormone receptor 1. *Bioorganic Med. Chem. Lett.* **15**, 3853–3856 (2005).
213. Holger Claus, H. & Marit, K. Imidazoquinoxaline compounds. (1994). US 5371080
214. Chen, X. *et al.* Synthesis of 4-(Dimethylamino)quinazoline via Direct Amination of Quinazolin-4(3 H)-one Using N, N -Dimethylformamide as a Nitrogen Source at Room Temperature. *Synth.* **47**, 2055–2062 (2015).
215. Verheij, M. H. P. *et al.* Design, synthesis, and structure-activity relationships of highly potent 5-HT₃ receptor ligands. *J. Med. Chem.* **55**, 8603–14 (2012).

216. Zhang, J. H., Chung, T. D. Y. & Oldenburg, K. R. A simple statistical parameter for use in evaluation and validation of high throughput screening assays. *J. Biomol. Screen.* **4**, 67–73 (1999).

Appendices

Appendix 1 DiscoverX Panel Results

Table A DiscoverX panel results for compounds 11, 120, 187, 191, 220 and 220, ranked by potency. % represents % of immobilised ligand remaining.

Compound 11		Compound 187		Compound 191		Compound 120		Compound 220		Compound 222	
Target name	% ligand remaining	Target name	% ligand remaining	Target name	% ligand remaining	Target name	% ligand remaining	Target name	% ligand remaining	Target name	% ligand remaining
PAK3	0	ROCK1	0	HASPIN	1.5	YSK4	0.8	HASPIN	21	AMPK-alpha1	44
LTK	0	PRKCE	0	ROCK2	6.9	HASPIN	4.2	FLT3 (ITD,D835V)	21	YSK4	48
CIT	0	ROCK2	0.2	ROCK1	13	PRKCQ	11	NIK	41	EPHA5	52
HASPIN	1.5	HASPIN	0.5	YSK4	28	IRAK1	12	FLT3 (D835V)	41	TRKB	53
PRKG2	3.5	MEK5	14	MEK5	32	HIPK3	12	PIP5K1C	48	JNK2	53
DYRK1A	5	HIPK2	19	FLT3 (D835V)	35	DYRK2	12	GRK2	48	ROCK2	54
DYRK1B	6.1	CIT	21	HIPK4	39	CLK4	14	MYLK	49	PRKX	54
YSK4	8.9	PRKG2	26	BMPR1B	40	CLK1	15	ANKK1	49	JAK2(JH1 domain-catalytic)	55
CLK4	9.3	PKN2	27	FLT3 (ITD, F691L)	44	CSNK1E	16	ASK2	50	GRK2	55
DRAK1	13	CDK7	30	PRKCE	46	CSNK1A1	16	LRRK2	52	CDK5	56
ROCK1	15	YSK4	40	MARK3	49	HIPK2	17	RSK2(Kin. Dom.2-C-terminal)	53	BMPR1B	56

DYRK2	15	TRKB	40	PIP5K1C	51	CDK9	17	PDGFRA	54	FLT3 (D835V)	57
CLK1	17	PRKX	40	CDK7	51	LATS2	18	MKNK1	54	CDK7	57
IRAK1	19	DMPK	42	FLT3 (ITD, D835V)	53	HIPK1	19	FLT3 (ITD, F691L)	54	CASK	57
CSNK1A1	19	CAMK1B	44	TYK2(JH1 domain-catalytic)	54	DYRK1A	22	FLT3 (R834Q)	55	NEK3	58
ROCK2	23	RSK2(Kin. Dom.2-C-terminal)	45	ABL1 (Q252H)	54	PRKCE	26	SNARK	56	HIPK2	58
TRKB	25	PKN1	46	CDKL1	56	PRKG1	29	FLT3-auto-inhibited	56	ERK2	58
TAOK1	27	PKAC-beta	46	CLK4	58	DYRK1B	29	SGK3	57	PFPK5(P. falciparum)	60
PKN2	27	PRKCH	47	PFTAIRES2	60	BMPR1B	29	LATS2	57	MEK2	60
HIPK3	29	GRK2	49	CSNK2A1	60	CSNK1D	30	CASK	57	LRRK2	60
CDK9	30	FLT3 (ITD, F691L)	49	MAP3K15	61	PKN2	31	BTK	57	BRAF (V600E)	60
JAK3(JH1 domain-catalytic)	31	PRKCD	50	PRKD3	62	CIT	34	ABL1 (M351T) -(PO4)3-	57	BRAF	60
BMPR1B	38	CAMK1	50	PRKCI	62	GSK3A	35	ABL1 (E255K) -(PO4)3-	57	MAP3K15	61
DRAK2	39	DYRK2	51	PKN2	62	CDK7	38	TRKB	58	LATS2	61
HIPK1	41	PRKD1	52	MKNK1	62	ERK8	39	SRMS	58	PRKCE	62
TTK	43	CTK	52	EIF2AK1	62	PRKG2	40	HIPK1	58	JNK3	62
NEK10	43	PRKG1	53	ABL1 (E255K) (PO4)3-	62	MINK	40	SBK1	59	S6K1	64

CSNK1E	44	FLT3 (D835V)	54	SRPK2	63	ROCK1	41	NEK3	59	MST3	64
ALK (C1156Y)	44	ALK	54	SGK2	63	PKN1	41	IKK-epsilon	60	CDK4-cyclinD1	64
HIPK2	46	CSF1R-auto-inhibited	55	IKK-alpha	63	EPHB6	43	EPHB6	60	RSK2(Kin. Dom.2-C-terminal)	65
PRKCE	47	PRKD3	57	DCAMKL1	63	CLK2	44	ABL1 (F317I) -(PO4)3-	60	NIM1	65
RSK2(Kin. Dom.2-C-terminal)	48	DCAMKL1	57	CAMKK1	63	IKK-epsilon	46	VEGFR2	61	HASPIN	65
IKK-alpha	48	CDK9	57	ABL1 (H396P) -(PO4)3-	63	PFPK5(P. falciparum)	48	TAOK1	61	BMPR2	65
PFPK5(P. falciparum)	49	NEK10	58	TYK2 (JH2 domain-pseudokinase)	64	SNARK	49	KIT-auto-inhibited	61	TYK2 (JH2 domain-pseudokinase)	66
CDK7	49	PLK3	59	PIKFYVE	64	PLK3	49	CSF1R-auto-inhibited	61	MAPKAPK5	66
PRKG1	50	JNK2	59	DYRK1A	64	GRK7	49	ALK(C1156Y)	61	EGFR (L747-S752del, P753S)	66
CDK4-cyclinD1	50	ERN1	59	RIPK5	65	DAPK3	49	ACVR1B	61	EGFR (E746-A750del)	66
PLK1	51	SgK110	60	PRKG2	65	TAOK1	51	ABL1 (F317L) -(PO4)3-	61	DDR2	66

NEK3	51	MAST1	60	MKNK2	65	TAK1	51	MAPKAPK5	62	ROCK1	67
GSK3B	51	GRK3	61	CLK1	65	PRKCH	51	IRAK1	62	SRMS	68
ERK8	51	TNNI3K	62	ULK2	66	DCAMKL1	51	CDK7	62	MKNK2	68
RPS6KA4 (Kin. Dom.2-C- terminal)	52	SRMS	62	SNRK	66	CSNK2A1	51	ABL1 (T315I)	62	FLT3 (ITD,D835V)	68
CSNK1D	52	KIT (A829P)	62	NEK7	66	EGFR (E746- A750del)	53	QSK	63	CAMK1B	68
MAP3K1	52	MAPKAPK2	62	PIK3CA (I800L)	66	GCN2 (Kin. Dom.2,S808 G)	53	ROCK2	63	FGFR1	68
CLK2	53	AKT3	62	ACVRL1	66	ABL1 (E255K)- (P04)3-	54	PFPK5(P. falciparum)	63	ALK	68
RSK3(Kin. Dom.2-C- terminal)	53	EGFR (T790M)	62	JAK2(JH1 domain- catalytic)	66	PKNB(M.tu berculosis)	54	PIK3CA (I800L)	63	ALK (C1156Y)	68
ASK2	53	DYRK1B	63	RIOK2	67	EGFR (T790M)	55	MAP4K2	63	DCAMKL1	69
CDC2L5	53	RPS6KA4 (Kin. Dom.1-N- terminal)	63	YANK1	67	GRK2	55	MINK	63	PIK3CB	69
KIT-auto- inhibited	54	VPS34	64	PLK3	67	NEK4	56	EPHB4	63	IKK-epsilon	70
SNARK	55	NIK	64	MYO3B	67	JAK3(JH1 domain- catalytic)	56	ALK	63	FLT3 (R834Q)	70
RIPK4	55	FLT3 (ITD, D835V)	64	KIT (D816H)	67	ABL1 (Y253F)- phosphoryl ated	56	RIPK5	64	FLT3 (ITD, F691L)	70

MKNK1	55	p38-gamma	65	HIPK1	67	MAP3K15	57	DCAMKL1	64	DLK	70
NIK	56	CAMKK2	65	EGFR (E746-A750del)	67	EGFR (L747-S752del, P753S)	57	BMPR1B	64	PFCDPK1(P. falciparum)	71
JAK2(JH1 domain-catalytic)	56	PIK3CA (H1047L)	66	CAMK1B	67	CSF1R-auto-inhibited	57	TAOK2	65	NIK	71
GRK2	56	GCN2 (Kin. Dom.2,S808 G)	66	ABL1-(PO4)3-	67	SGK3	58	PLK2	65	LOK	71
WNK2	57	DRAK2	66	TTK	68	p38-delta	58	MEK5	65	BUB1	71
VPS34	57	CDC2L5	66	SRMS	68	MYLK	58	MAP3K3	65	PIK3CA (Q546K)	72
ICK	57	TAK1	67	CAMKK2	68	PFCDPK1(P. falciparum)	59	ABL1 (T315I) -(PO4)3-	65	MEK5	72
ABL1 (T315I) - (PO4)3-	57	PFCDPK1(P. falciparum)	67	PFCDPK1(P. falciparum)	69	FLT3 (D835V)	59	PIK3CB	66	BTK	72
MAPKAPK5	58	MKNK2	67	MEK2	69	CDC2L5	59	ERBB3	66	RIOK2	73
BRAF	58	CDK4-cyclinD1	67	DYRK2	69	RET (V804M)	60	S6K1	67	MAP3K2	73
LATS2	58	CLK1	67	FYN	69	TSSK1B	60	SgK110	67	MEK1	73
LRRK2	59	PIK3CA (I800L)	68	ABL1-nonphosphorylated	69	EPHA4	60	MYLK2	67	JNK1	73
DCAMKL3	59	MAP3K1	68	PIK3CA (C420R)	70	ALK (C1156Y)	60	ULK3	68	WNK3	74
HPK1	60	ABL1 (E255K)-phosphorylated	68	NEK9	70	KIT-auto-inhibited	61	MTOR	68	TAOK2	74

PIP5K2C	60	BMPR1B	68	NIM1	70	RSK2(Kin. Dom.2-C-terminal)	61	PIK4CB	68	TTK	74
QSK	61	AAK1	68	MINK	70	EGFR (S752-I759del)	61	KIT (D816H)	68	SGK2	74
MYLK	61	TGFBR1	69	ALK	70	AAK1	61	EGFR (L858R, T790M)	68	RIPK4	74
FLT3 (ITD, F691L)	61	PFPK5(P. falciparum)	69	TNNI3K	71	ROCK2	62	CDKL1	68	MKNK1	74
CASK	61	STK39	70	RAF1	71	KIT (A829P)	62	WNK3	69	MINK	74
KIT (A829P)	62	SGK2	70	PIK3CA (E542K)	71	BUB1	62	TAOK3	69	JAK3(JH1 domain-catalytic)	74
BMPR2	62	KIT-auto-inhibited	70	MRCKA	71	LKB1	63	IKK-alpha	69	HIPK3	74
CAMK1B	62	MAP3K15	70	NDR1	71	MEK2	63	RSK4(Kin. Dom.1-N-terminal)	69	IRAK1	74
ABL1 (Q252H)	62	INSR	70	PLK1	72	JAK2(JH1 domain-catalytic)	63	DYRK1A	69	CSNK2A1	74
ABL1 (M351T) - (PO4)3-	62	ABL1 (Y253F) - (PO4)3-	70	PIK3CA (Q546K)	72	RPS6KA4 (Kin. Dom.2-C-terminal)	64	YSK4	70	CDKL5	74
ABL1 (H396P)- (PO4)3-	62	SNRK	71	MEK3	72	FLT3	64	TBK1	70	CDKL2	74
MEK5	63	PRKCQ	71	EGFR (L747-S752del, P753S)	72	EGFR (L861Q)	64	NIM1	70	TAK1	75

ABL1 (E255K)-(PO4)3-	63	HPK1	71	TAOK2	73	RSK3 (Kin. Dom.1-N-terminal)	65	JAK2(JH1 domain-catalytic)	70	RPS6KA4 (Kin. Dom.2-C-terminal)	75
DDR2	63	PIK3CD	71	ULK3	73	TNNI3K	65	MAP3K2	70	RSK4(Kin. Dom.1-N-terminal)	75
MINK	64	RIPK5	72	LATS2	73	EPHB3	65	CAMK1B	70	PIK3CA (C420R)	75
MKNK2	64	TAOK2	72	SGK	73	MEK1	65	EGFR (L747-S752del, P753S)	70	PKN2	75
FLT3 (ITD, D835V)	64	PRKCI	72	JNK3	73	CDK4-cyclinD3	65	ULK2	71	PCTK1	75
ABL1 (F317L)-(PO4)3	65	MKK7	72	CSNK2A2	73	PRKCI	66	NDR1	71	GRK3	75
MAP4K2	65	MYO3B	72	GRK4	73	Sgk110	66	PRKCE	71	HIPK1	75
PRKD1	66	MAP4K2	72	CSNK1G2	73	PIK3CA	66	CDKL3	71	ABL1 (T315I)-	75
MAP3K2	66	JNK3	72	CSF1R-auto-inhibited	73	NEK3	66	BMPR2	71	SGK	76
CLK3	66	HIPK1	72	ALK (L1196M)	73	EPHA6	66	PLK3	72	KIT-auto-inhibited	76
HUNK	66	JAK2(JH1 domain-catalytic)	72	CAMK1	73	MAPKAPK5	66	RIOK2	72	MKK7	76
BRAF (V600E)	66	BMX	72	p38-gamma	74	CDKL1	66	PIK3CA (E545K)	72	IKK-alpha	76
ULK2	67	ADCK3	72	NLK	74	CDK11	66	PIK3CA (C420R)	72	GRK7	76

TYK2(JH1 domain-catalytic)	67	PIK3CA	73	MST1	74	NDR1	67	PIK3CA	72	ABL1 (T315I)-(PO4)3-	76
EPHB6	67	PAK2	73	KIT-auto-inhibited	74	RIPK4	68	CSNK2A1	72	STK39	77
JNK2	67	PIK3C2G	73	MLK1	74	TTK	68	MEK2	72	TRPM6	77
ABL1-(PO4)3-	67	FYN	73	STK16	75	PRKX	68	CDK11	72	NEK11	77
SGK2	68	CDKL1	73	PFPK5(P. falciparum)	75	NEK10	68	TYK2(JH2 domain-ps.kinase)	73	NEK10	77
AAK1	68	MEK2	74	AURKB	75	DDR2	68	GRK7	73	DYRK1A	77
PFCDPK1(P. falciparum)	68	NEK3	74	BTK	75	INSR	68	JAK1(JH2 domain-ps.kinase)	73	FYN	77
PKNB(M.tuerculosis)	68	ULK2	74	IKK-beta	75	MYO3B	68	MST4	73	IRAK4	77
MEK2	68	FLT3	74	SgK110	76	DAPK2	68	DLK	73	CSF1R-auto-inhibited	77
FLT3 (D835V)	68	FGFR4	74	PIK3CB	76	CSNK1A1L	68	CTK	73	SGK3	78
CSNK1G2	68	EPHB2	74	NEK10	76	TYK2(JH1 domain-catalytic)	69	CSNK1A1	73	SgK110	78
IKK-epsilon	69	MKNK1	75	HIPK3	76	CLK3	69	BRAF(V600E)	73	ABL1 (E255K)-(PO4)3-	78
SgK110	69	PIK3CA (C420R)	75	MAP3K3	76	TGFBR1	69	CDKL5	73	MAP3K3	78
CSNK1G3	69	MARK1	75	DLK	76	AKT2	69	TYK2(JH1 domain-catalytic)	74	QSK	79

ABL1 (Y253F)-(PO4)3-	69	WNK1	76	ABL1 (T315I)-	76	ADCK4	69	TRKA	74	PLK1	79
CDK4-cyclinD3	70	TTK	76	PIK3CA (E545K)	77	ABL1 (Q252H)-	69	PIK3CA (E542K)	74	PIP5K2C	79
GSK3A	71	PLK2	76	LRRK2	77	MAPKAPK2	70	EGFR (T790M)	74	CSNK1A1	79
SRMS	71	RIPK2	76	NEK3	77	MYO3A	70	EIF2AK1	74	DYRK1B	79
WNK4	71	S6K1	76	PIK3C2G	77	STK39	70	MKK7	74	MYLK	79
ABL1 (H396P)-	71	MRCKB	76	ABL1 (H396P)-	77	PLK2	71	RIPK4	75	SBK1	80
CSF1R-auto-inhibited	71	PKNB(M.tuerculosis)	76	EGFR (L861Q)	77	RIPK2	71	VPS34	75	ZAP70	80
PLK3	72	KIT (V559D,V654A)	76	AAK1	77	MEK4	71	PLK1	75	RSK3(Kin. Dom.2-C-terminal)	80
MLCK	72	EPHA2	76	MAPKAPK5	78	DDR1	71	GRK3	75	MAP3K1	80
NIM1	72	GRK7	76	PLK2	78	HPK1	71	IKK-beta	75	MEK3	80
PIKFYVE	72	IKK-alpha	76	RSK2(Kin. Dom.1-N-terminal)	78	JAK1(JH1 domain-catalytic)	71	PCTK1	75	PIK3CA (E545A)	80
LZK	72	ALK(L1196M)	76	FLT3 (N841I)	78	CAMK1B	71	MEK3	76	KIT (D816H)	80
MEK1	72	BMPR2	76	MAP4K2	78	CSNK1G2	71	PIK3CA (E545A)	76	LRRK2 (G2019S)	80
IKK-beta	72	ZAP70	77	DMPK	78	TBK1	72	JNK1	76	KIT (A829P)	80
BUB1	72	PIK3CA (E545K)	77	BMPR2	78	STK36	72	ABL1 (F317I)-	76	VRK2	81
DAPK3	72	PIP5K1C	77	CDKL3	78	SYK	72	ERN1	76	WNK4	81
ALK	72	JNK1	77	TGFBR1	79	PIK3CG	72	ZAP70	77	VPS34	81
PKN1	73	HIPK3	77	TAOK1	79	GSK3B	72	ULK1	77	PLK3	81

PIK3CA (C420R)	73	ABL1 (T315I)-(PO4)3-	77	SBK1	79	EPHB2	73	SNRK	77	NEK4	81
PIK4CB	73	EGFR (E746-A750del)	77	STK33	79	SRPK3	73	TAK1	77	NLK	81
MST4	73	WNK3	78	RIOK1	79	CDK4-cyclinD1	73	PFCDPK1(P. falciparum)	77	NDR1	81
JNK1	73	NIM1	78	PIK3CD	79	SGK2	74	MEK1	77	CDC2L5	81
MAP3K15	73	RSK3(Kin. Dom.1-N-terminal)	78	PRKD1	79	STK35	74	MKNK2	77	CDKL1	81
ABL1 (T315I)-	73	CSNK1A1	78	JNK1	79	JNK2	74	ICK	77	PIK3CA (H1047L)	82
EGFR (T790M)	73	EPHB1	78	MARK2	79	PLK1	74	JNK2	77	RSK2(Kin. Dom.1-N-terminal)	82
FLT3-auto-inhibited	73	EPHB3	78	MYLK	79	PRKCD	74	MAP3K15	77	TYK2(JH1 domain-catalytic)	82
WNK3	74	ABL2	78	DDR2	79	JAK1(JH2 domain-ps.kinase)	74	HPK1	77	PIK3CA (E545K)	82
SGK	74	ABL1 (T315I)	78	CHEK1	79	FLT3 (ITD,F691L)	74	TRKC	78	MST4	82
ERBB4	74	PHKG2	79	EPHA8	80	BMX	74	HIPK2	78	EPHB6	82
KIT (D816H)	74	PKAC-alpha	79	EPHB2	80	BRAF(V600E)	74	RPS6KA4 (Kin. Dom.2-C-terminal)	78	ERBB2	82
PLK2	74	YANK1	79	SNARK	80	EGFR (G719C)	74	RSK2(Kin. Dom.1-N-terminal)	78	LZK	82

DLK	74	CDK4-cyclinD3	79	CAMK1D	80	RAF1	75	AURKB	78	ALK (L1196M)	82
ERBB3	74	DDR2	79	CASK	80	RIPK5	75	BRAF	78	ASK2	82
CDKL1	74	ALK (C1156Y)	79	BRAF	80	PIK3CD	75	ABL1-(PO4)3-	78	ULK3	83
CAMK2B	74	KIT (D816V)	80	ABL1 (F317I)-	80	MAP3K1	75	ABL1 (Y253F)-(PO4)3-	78	ULK2	83
TAK1	75	IRAK1	80	TAK1	81	EGFR (G719S)	75	ABL1 (H396P)-(PO4)3-	78	SNRK	83
FGFR3	75	CDKL3	80	PIK3CA (H1047L)	81	AXL	75	PRKCI	79	AURKB	83
MST1R	75	ERK8	80	PRKG1	81	BRAF	75	STK39	79	EIF2AK1	83
PIK3CA (H1047L)	75	FGFR3	80	RSK4(Kin. Dom.1-N-terminal)	81	CSNK1G3	75	WNK2	79	SIK2	83
CSNK2A1	75	CDK11	80	PDGFRA	81	ARK5	75	NEK10	79	RIPK5	84
ZAP70	76	ABL1 (Q252H)-	80	LATS1	81	ABL1-(PO4)3-	75	HIPK3	79	RET (V804L)	84
TAOK3	76	SBK1	81	ERK1	81	WNK3	76	GRK1	79	PLK2	84
SNRK	76	PIK3CG	81	EGFR (T790M)	81	RSK3(Kin. Dom.2-C-terminal)	76	OSR1	80	IKK-beta	84
RSK3(Kin. Dom.1-N-terminal)	76	MYO3A	81	EGFR L747-T751delSins	81	ROS1	76	JNK3	80	VEGFR2	85
PRP4	76	MLK2	81	CAMK4	81	PKAC-beta	76	SGK2	81	TRKA	85
MARK3	76	EPHA4	81	MEK1	82	BIKE	76	DDR2	81	CAMK1	85
p38-delta	76	EPHB4	81	PKAC-alpha	82	DAPK1	76	FLT3 (D835H)	81	CDKL3	85
PDGFRA	76	GSK3B	81	S6K1	82	FER	76	LZK	81	GRK1	85

PRKCI	76	JAK3(JH1 domain-catalytic)	81	TBK1	82	MEK5	76	SGK	81	PIK3CA (I800L)	85
DCAMKL1	76	DYRK1A	81	LOK	82	PKAC-alpha	77	ABL1 (Q252H)-(PO4)3-	81	GSK3B	86
FGFR2	76	EGFR (L747-S752del, P753S)	81	MAP4K5	82	TESK1	77	CDK4-cyclinD1	81	TAOK1	86
ACVR2B	76	CAMK4	81	FLT3-auto-inhibited	82	MAP3K2	77	ROCK1	82	ABL1 (F317L)-(PO4)3-	86
CDK8	76	CSNK1G1	81	GSK3B	82	p38-gamma	77	TGFBR1	82	ACVRL1	86
DAPK2	76	DCAMKL3	81	KIT (V559D, V654A)	82	PIK3CA (C420R)	77	TNK1	82	EGFR (T790M)	86
MEK4	77	BUB1	81	EPHA7	82	GRK4	77	EPHA5	82	ABL1 (F317I)-	86
EGFR (L858R,T790M)	77	ADCK4	81	ALK (C1156Y)	82	FGFR4	77	CDC2L5	82	TIE1	87
EPHB4	77	AXL	81	CLK3	82	FGR	77	DYRK1B	82	ULK1	87
AURKB	77	TYK2(JH2 domain-ps.kinase)	82	VEGFR2	83	CASK	77	MAP3K4	83	TGFBR1	87
PRKD3	78	RIOK2	82	TAOK3	83	ANKK1	77	ACVRL1	83	ERBB3	87
TIE1	78	SGK	82	ULK1	83	BRSK1	77	BUB1	83	FLT3 (D835H)	87
MKK7	78	PIK3CA (E545A)	82	PCTK1	83	AKT3	77	PRKX	84	ABL1 (Y253F)-(PO4)3-	87
CSNK1A1L	78	ABL1-(PO4)3-	82	EPHB1	83	RET	78	MAP3K1	84	FLT3-auto-inhibited	88

ERBB2	78	CAMK2D	82	FLT3 (D835H)	83	SNRK	78	MRCKB	84	FRK	88
GRK7	78	FRK	82	FLT3 (ITD)	83	SRMS	78	NEK4	84	PIK4CB	88
JNK3	78	PDGFRA	82	MAP3K2	83	VPS34	78	PIK3CA (Q546K)	84	PKAC-alpha	88
RPS6KA5 (Kin. Dom.2-C-terminal)	79	PDPK1	83	CAMK2B	83	GRK1	78	CAMK1	84	ADCK4	88
RSK4 (Kin. Dom.1-N-terminal)	79	RET	83	CDKL5	83	MEK6	78	CDK4-cyclinD3	84	CDK4	88
VEGFR2	79	RPS6KA5 (Kin. Dom.2-C-terminal)	83	DDR1	83	PRKD2	78	FLT3 (D835Y)	84	EPHA2	88
ACVR1B	79	GAK	83	ABL1 (Y253F)-(PO4)3-	83	ERK4	78	VRK2	85	PIK3C2G	89
ACVR2A	79	MYLK2	83	AMPK-alpha1	83	FYN	78	YANK1	85	WNK2	89
ABL1-	79	FLT3-auto-inhibited	83	WEE2	84	BTK	78	TIE2	85	IRAK3	89
TBK1	80	EGFR (L858R, T790M)	83	PYK2	84	BMPR2	78	PKN2	85	EGFR (L861Q)	89
WNK1	80	FGFR2	83	SGK3	84	BRK	78	PKNB(M.tuerculosis)	85	ICK	89
IRAK4	80	ABL1 (F317I)-(PO4)3-	83	MLCK	84	IKK-alpha	79	FGFR2	85	ABL1 (Q252H)-	89

PCTK1	80	ABL1 (F317L)- (PO4)3-	83	NIK	84	TIE1	79	PIK3C2B	85	ABL1- (PO4)3-	89
SRPK2	80	DDR1	83	PKAC-beta	84	TRKB	79	PIP5K2C	85	DMPK	89
AMPK- alpha1	80	TRPM6	84	GRK7	84	CDKL3	79	DYRK2	85	ABL1 (H396P)- (PO4)3-	89
EPHA2	80	WNK4	84	IRAK4	84	EPHA2	79	EPHA2	85	ABL1 (M351T)- (PO4)3-	89
ULK3	81	MAPKAPK5	84	ERK3	84	AURKA	79	ABL1 (F317L)-	85	TRKC	90
RIOK2	81	LATS2	84	ACVR2B	84	ACVR1B	79	PRKG2	86	MAPKAPK2	90
NEK4	81	IRAK3	84	TRKB	85	ABL1 (Q252H)- (PO4)3-	79	MARK3	86	HPK1	90
JAK1(JH2 domain- ps.kinase)	81	ERBB3	84	IRAK1	85	TIE2	80	ABL1 (Q252H)-	86	CLK2	90
LRRK2(G20 19S)	81	ERK4	84	JNK2	85	ULK2	80	KIT (A829P)	86	DAPK3	90
INSR	81	CSNK2A1	84	HCK	85	SIK2	80	NEK1	87	CAMK4	90
CDKL2	81	ABL1 (Q252H)- (PO4)3-	84	ERBB4	85	PIP5K1C	80	ABL1-	87	TLK2	91
FLT3 (R834Q)	81	CLK4	84	FLT4	85	RPS6KA4 (Kin. Dom.1-N- terminal)	80	JAK3(JH1 domain- catalytic)	87	YANK1	91
CAMK2D	81	PRKD2	85	TEC	86	p38-alpha	80	PIK3CA (H1047L)	88	PRKCI	91
CAMK4	81	VEGFR2	85	ZAP70	86	PAK3	80	RPS6KA4 (Kin.	88	SNARK	91

								Dom.1-N-terminal)			
PHKG2	82	ABL1-	85	LTK	86	ABL1 (H396P)-(PO4)3-	80	AKT3	88	ACVR1B	91
PIK3CB	82	CAMK1G	85	MST4	86	DCAMKL3	80	CDK3	88	CAMK1D	91
PIK3CD	82	PIK3CA (E542K)	85	RPS6KA4 (Kin. Dom.1-N-terminal)	86	ERBB3	80	FYN	88	MLCK	91
TRKC	82	PIKFYVE	85	SRPK3	86	IRAK3	80	MEK4	88	PKNB(M.tuerculosis)	91
NEK11	82	ABL1 (H396P)-	85	DYRK1B	86	STK16	81	INSR	89	PRP4	92
NLK	82	ABL1 (M351T)-(PO4)3-	85	EPHB6	86	WNK2	81	YSK1	89	SRC	92
ADCK4	82	PLK4	86	CAMK1G	86	PIM3	81	EGFR (S752-I759del)	89	MARK3	92
ASK1	82	RSK3 (Kin. Dom.2-C-terminal)	86	CIT	86	RIOK2	81	EPHA1	89	MEK4	92
EGFR (L861Q)	82	TAOK1	86	CSNK1E	86	RSK2 (Kin. Dom.1-N-terminal)	81	FLT3	89	PRKG2	92
ADCK3	82	MEK1	86	AURKC	86	NLK	81	RET(V804L)	90	LKB1	92
TYK2(JH2 domain-pskinase)	83	FLT3 (D835Y)	86	ARK5	86	HIPK4	81	WNK4	91	JAK1(JH2 domain-pskinase)	92
PIP5K1C	83	EGFR (L858R)	86	RSK2 (Kin. Dom.2-C-terminal)	87	CAMKK2	81	RSK3 (Kin. Dom.1-N-terminal)	91	FGR	92

RSK2 (Kin. Dom.1-N-terminal)	83	EGFR (L861Q)	86	WNK1	87	ERK3	81	TGFBR2	91	FLT3	92
MAST1	83	CDKL2	86	RET(M918T)	87	RPS6KA5 (Kin. Dom.2-C-terminal)	82	IRAK4	91	DRAK2	92
CDKL3	83	RSK1 (Kin. Dom.2-C-terminal)	87	MAPKAPK2	87	PIK3CB	82	BMPR1A	91	AKT3	92
DAPK1	83	STK16	87	PKMYT1	87	PRKD1	82	CSK	91	BIKE	92
ABL1 (F317L)-	83	RAF1	87	KIT (A829P)	87	MST1	82	AXL	91	WNK1	93
MAP3K3	84	IKK-beta	87	BRAF (V600E)	87	CHEK1	82	NLK	92	ERBB4	93
SGK3	84	LRRK2 (G2019S)	87	CSNK1G1	87	FES	82	PAK3	92	FLT4	93
TSSK3	84	LTK	87	EPHA2	87	FLT3 (R834Q)	82	PIP5K1A	92	MYLK2	93
YANK1	84	MAP4K3	87	GRK3	87	MAP4K3	82	STK16	92	PIP5K1A	93
DDR1	84	ERK1	87	RPS6KA4 (Kin. Dom.2-C-terminal)	88	AMPK-alpha1	82	NEK11	92	EGFR (G719C)	93
LOK	85	EIF2AK1	87	PIK3CA	88	ABL1 (F317I)-(PO4)3-	83	FLT3 (ITD)	92	CDK4-cyclinD3	93
PIK3CA (E545A)	85	EPHA5	87	PIK3CA (E545A)	88	PCTK1	83	LOK	92	CLK3	93
ULK1	85	EPHA6	87	RET	88	S6K1	83	MEK6	92	DCAMKL3	93
CTK	85	BRK	87	GRK2	88	PIK3CA (E545A)	84	AMPK-alpha1	92	ABL1 (F317L)-	93
GRK1	85	CDK8	87	INSR	88	PIK3CA (E545K)	84	CDK4	92	ANKK1	93

KIT (D816V)	85	CSK	87	MET	88	VEGFR2	84	FES	92	CDK3	93
CAMK1G	85	BRAF	87	ERN1	88	p38-beta	84	TSSK1B	93	TIE2	94
ABL1 (Q252H)-(PO4)3-	86	MARK4	88	BRK	88	CTK	84	MLCK	93	MAP4K2	94
ACVRL1	86	NLK	88	BUB1	88	FRK	84	MST2	93	RIPK1	94
FLT3	86	PIM3	88	CLK2	88	MLCK	84	RET	93	STK35	94
PIP5K1A	86	RSK4 (Kin. Dom.2-C-terminal)	88	CSK	88	NEK1	84	TIE1	93	TBK1	94
VRK2	87	LZK	88	ANKK1	88	CAMK4	84	LKB1	93	CSNK1G1	94
STK35	87	LOK	88	TYRO3	89	ASK1	84	PRKG1	94	ABL1 (F317I)-(PO4)3-	94
PRKCH	87	ITK	88	RSK1 (Kin. Dom.2-C-terminal)	89	ABL1 (T315I)-(PO4)3-	84	PKAC-alpha	94	TNK1	95
GRK3	87	CSNK1E	88	IGF1R	89	PRKD3	85	FLT4	94	PAK4	95
HCK	87	ERK3	88	QSK	89	SGK	85	INSRR	94	PDGFRA	95
BIKE	87	TYK2(JH1 domain-catalytic)	89	ERK8	89	PKMYT1	85	EGFR (G719S)	94	NEK5	95
TRKA	88	PIP5K1A	89	CAMK2A	89	PAK1	85	EGFR (G719C)	94	KIT (V559D,V654A)	95
PRKX	88	PIK3CA (M1043I)	89	AXL	89	NIK	85	TYRO3	95	ERK3	95
PIK3CA (Q546K)	88	GRK1	89	SIK2	90	MKNK2	85	ADCK3	95	DAPK2	95
PIM1	88	LRRK2	89	WNK3	90	MYLK2	85	PIK3CG	95	EGFR (G719S)	95

MST3	88	EGFR (S752-I759del)	89	RIOK3	90	MKK7	85	PKAC-beta	96	BRK	95
CAMK2A	88	BRSK2	89	PIM1	90	ICK	85	EPHA3	96	PKN1	96
EGFR (S752-I759del)	88	CAMK1D	89	RET(V804L)	90	MAP4K2	85	p38-beta	96	PRKD1	96
S6K1	89	ABL1 (H396P)-(PO4)3-	89	PIK3CA (M1043I)	90	GAK	85	SRPK1	97	PIP5K1C	96
MRCKB	89	RET(V804M)	90	JAK3(JH1 domain-catalytic)	90	ABL1 (M351T)-(PO4)3-	85	EGFR (E746-A750del)	97	ARK5	96
PIK3CA (E542K)	89	RSK4 (Kin. Dom.1-N-terminal)	90	OSR1	90	BMPR1A	85	MST1	97	CAMK2G	96
RIPK5	89	TGFBR2	90	PAK3	90	CSNK2A2	85	PIM3	97	MET (Y1235D)	96
MLK2	89	PLK1	90	FLT1	90	ZAK	86	TNK2	98	AMPK-alpha2	96
CDK4	89	AURKB	90	DAPK3	90	TRPM6	86	ACVR1	98	RET (M918T)	97
EPHB3	89	BRAF(V600E)	90	EGFR (G719C)	90	TYK2(JH2 domain-pskinase)	86	AURKA	98	SRPK1	97
FGR	89	EPHA3	90	EGFR (L858R, T790M)	90	YANK3	86	BLK	98	TSSK3	97
TRPM6	90	ABL1 (F317I)-	90	CSNK1A1	90	PIM1	86	ABL1 (H396P)-	98	PHKG2	97
CAMKK2	90	TIE1	91	STK36	91	LTK	86	FGR	99	KIT (D816V)	97
TAOK2	90	ULK1	91	TSSK3	91	MST4	86	WNK1	99	PHKG1	97

PIK3CA (E545K)	91	NEK2	91	PAK1	91	CAMK2G	86	ALK (L1196M)	99	EGFR (L747-T751del,Sin s)	97
PKAC-beta	91	PAK7	91	PKNB(M.tuberculosis)	91	EGFR (L747-E749del, A750P)	86	ASK1	99	EGFR (L858R, T790M)	97
TGFBR1	91	PIK3CB	91	PRKD2	91	HCK	86	BRSK1	99	FES	97
TGFBR2	91	PIK4CB	91	RIPK2	91	LOK	86	CAMK2G	99	HCK	97
CDK11	91	CHEK1	91	IRAK3	91	PDGFRA	87	YANK2	100	AKT1	97
EPHA5	91	FLT3 (N841I)	91	LYN	91	PIK3C2G	87	YANK3	100	BMX	97
ERK3	91	MLCK	91	MAP4K4	91	QSK	87	YES	100	CDK11	97
MAPKAPK2	91	MST1	91	MKK7	91	YSK1	87	ZAK	100	CSNK1E	97
BRSK1	91	CASK	91	FLT3 (D835Y)	91	NIM1	87	WEE2	100	TGFBR2	98
SBK1	92	ACVRL1	91	BIKE	91	EPHA1	87	TXK	100	RET (V804M)	98
TSSK1B	92	BMPR1A	91	CTK	91	MAK	87	WEE1	100	RSK4 (Kin. Dom.2-C-terminal)	98
MET (Y1235D)	92	STK36	92	AKT3	91	AURKC	87	TRPM6	100	MRCKA	98
PIK3CA	92	TAOK3	92	AMPK-alpha2	91	DRAK1	87	TSSK3	100	p38-beta	98
PKMYT1	92	TSSK3	92	ASK2	91	EGFR	87	TTK	100	PDGFRB	98
FLT3 (N841I)	92	SGK3	92	TNK2	92	TNK1	88	TNNI3K	100	BLK	98
EPHA1	93	EGFR	92	CDK8	92	CDKL5	88	STK33	100	ADCK3	99
FGFR3(G697C)	93	EPHB6	92	FLT3 (K663Q)	92	DRAK2	88	STK35	100	AXL	99
FLT3 (K663Q)	93	FLT3 (K663Q)	92	FLT3 (R834Q)	92	EPHB4	88	STK36	100	CAMKK1	99

GCN2 (Kin. Dom.2,S80 8G)	93	LYN	92	FRK	92	FLT3 (ITD, D835V)	88	SYK	100	CIT	99
INSRR	93	MAP3K3	92	ITK	92	MARK1	88	TEC	100	EPHB4	99
MEK6	93	MINK	92	MRCKB	92	MET (Y1235D)	88	TESK1	100	FGFR2	99
MUSK	93	MLK1	92	NEK5	92	PDGFRB	88	TLK1	100	GCN2 (Kin. Dom.2,S80 8G)	99
p38-gamma	93	p38-beta	92	STK35	92	TAOK3	88	TLK2	100	MERTK	99
PRKCD	93	PRP4	92	STK39	92	TNIK	88	TNIK	100	STK16	99
EGFR (L747-T751del,Sins)	93	ACVR1B	92	ABL2	92	ALK (L1196M)	88	SRPK2	100	YSK1	100
EIF2AK1	93	DAPK3	92	CDK3	92	CAMK1D	88	SRPK3	100	ZAK	100
ABL1 (F317I)-	93	MEK4	93	DCAMKL3	93	MKKN1	89	RSK4 (Kin. Dom.2-C-terminal)	100	WEE1	100
BMX	93	MRCKA	93	DMPK2	93	PHKG2	89	SIK	100	WEE2	100
CAMK1D	93	NEK1	93	MAP3K4	93	PIK4CB	89	SIK2	100	YANK2	100
CDK3	93	TBK1	93	PIM3	93	RET (M918T)	89	SLK	100	YANK3	100
CSNK1G1	93	WNK2	93	SRPK1	93	YANK1	89	SRC	100	YES	100
FLT3 (D835Y)	94	BRSK1	93	ACVR2A	93	ABL1 (T315I)-	89	RPS6KA5 (Kin. Dom.1-N-terminal)	100	TNK2	100
FLT4	94	CLK2	93	BMX	93	ADCK3	89	RPS6KA5 (Kin.	100	TNNI3K	100

								Dom.2-C-terminal)			
LKB1	94	CSNK2A2	93	CAMK2D	93	ALK	89	RSK1 (Kin. Dom.1-N-terminal)	100	TSSK1B	100
NEK1	94	HCK	93	CDC2L5	93	CAMKK1	89	RSK1 (Kin. Dom.2-C-terminal)	100	TXK	100
PKAC-alpha	94	MAP3K2	93	CSF1R	93	GRK3	89	RSK3 (Kin. Dom.2-C-terminal)	100	TYRO3	100
ALK (L1196M)	94	TEC	94	ABL1 (F317L)-	93	ABL1 (F317L)-(PO4)3-	89	ROS1	100	TNIK	100
RPS6KA5 (Kin. Dom.1-N-terminal)	95	SRC	94	WNK4	94	ZAP70	90	RIPK2	100	TLK1	100
BTK	96	MEK6	94	FGFR4	94	PCTK2	90	RET (V804M)	100	SYK	100
CAMK2G	96	p38-alpha	94	MAP3K1	94	RET(V804L)	90	RIOK1	100	TAOK3	100
RET (V804L)	96	PFTAIRES2	94	PIP5K2B	94	RIOK1	90	RIOK3	100	TEC	100
STK39	96	SIK2	94	RIPK1	94	RSK4 (Kin. Dom.1-N-terminal)	90	RIPK1	100	TESK1	100
STK33	97	CAMKK1	94	AURKA	94	MST3	90	PYK2	100	SRPK3	100
YSK1	97	MAP4K5	94	CSNK1A1L	94	MTOR	90	RAF1	100	STK33	100
ZAK	97	MEK3	94	DAPK1	94	MUSK	90	RET (M918T)	100	STK36	100
BRK	97	CDK3	95	FGFR2	95	ABL1-	90	PRKCH	100	RPS6KA5 (Kin.	100

										Dom.2-C-terminal)	
CDKL5	97	EGFR (L747-E749del, A750P)	95	NEK11	95	ASK2	90	PRKCQ	100	RSK1 (Kin. Dom.1-N-terminal)	100
DMPK	97	GRK4	95	PDGFRB	95	CSNK1G1	90	PRKD1	100	RSK1 (Kin. Dom.2-C-terminal)	100
EPHA4	97	PAK1	95	TLK1	95	FLT3 (D835Y)	90	PRKD2	100	RSK3 (Kin. Dom.1-N-terminal)	100
MEK3	97	PAK3	95	TNK1	95	HUNK	90	PRKD3	100	SIK	100
NDR1	97	PRKR	95	VRK2	95	MAP3K3	90	PRKR	100	SLK	100
p38-alpha	97	RSK2 (Kin. Dom.1-N-terminal)	95	WNK2	95	MLK3	90	PRP4	100	SRPK2	100
ARK5	97	BIKE	95	ERBB3	95	TAOK2	91	PRKCD	100	RPS6KA5 (Kin. Dom.1-N-terminal)	100
SIK2	98	ASK1	95	CDK5	95	RSK1 (Kin. Dom.2-C-terminal)	91	PLK4	100	RPS6KA4 (Kin. Dom.1-N-terminal)	100
PIK3CG	98	ULK3	96	ABL1 (F317L)-(PO4)3-	95	MARK4	91	PKMYT1	100	RIPK2	100
RET	98	YSK1	96	ABL1 (T315I)-(PO4)3-	95	RIOK3	91	PKN1	100	ROS1	100
CAMKK1	98	DLK	96	TIE1	96	FGFR3 (G697C)	91	PIK3CD	100	PYK2	100
CSNK2A2	98	ERBB4	96	TIE2	96	FLT1	91	PIKFYVE	100	RAF1	100

MST1	98	LKB1	96	TRKA	96	JNK1	91	PIM1	100	RET	100
MYO3A	98	PHKG1	96	YANK3	96	LIMK2	91	PIM2	100	RIOK1	100
OSR1	98	TLK1	96	YES	96	LYN	91	PIP5K2B	100	RIOK3	100
STK16	99	AMPK-alpha1	96	DRAK1	96	CSK	91	PIK3CA (H1047Y)	100	PRKG1	100
TNIK	99	CLK3	96	KIT (V559D, T670I)	96	EPHA5	91	PIK3CA (M1043I)	100	PRKR	100
ABL1 (F317I)-(PO4)3-	99	JAK1(JH2 domain-pskinase)	97	MEK4	97	LZK	92	PFTK1	100	PRKCH	100
MYO3B	99	NEK7	97	PCTK3	97	MLK2	92	PHKG1	100	PRKCQ	100
RET (V804M)	99	NEK9	97	TESK1	97	RSK4 (Kin. Dom.2-C-terminal)	92	PHKG2	100	PRKD2	100
RPS6KA4 (Kin. Dom. 1-N-terminal)	99	TNIK	97	TNIK	97	SRC	92	PIK3C2G	100	PRKD3	100
TYRO3	100	ABL1 (F317L)-	97	BLK	97	CAMK2D	92	PAK7	100	PIM3	100
WEE1	100	CAMK2G	97	BMPR1A	97	CDKL2	92	PCTK2	100	PIP5K2B	100
WEE2	100	DMPK2	97	EGFR (L747-E749del, A750P)	97	EGFR (L858R)	92	PCTK3	100	PKAC-beta	100
YANK2	100	ERBB2	97	FGR	97	EPHA3	92	PDGFRB	100	PKMYT1	100
YANK3	100	FER	97	FLT3	97	FLT4	92	PDPK1	100	PLK4	100
YES	100	IGF1R	97	LIMK2	97	JNK3	92	PFTAIRES2	100	PRKCD	100
TXK	100	STK35	98	ABL1 (M351T)-(PO4)3-	97	VRK2	93	PAK6	100	PIM2	100

TESK1	100	DAPK1	98	ABL1 (F317I)- (PO4)3-	98	FLT3 (K663Q)	93	NEK9	100	PIK3CA (E542K)	100
TIE2	100	EGFR (G719S)	98	DAPK2	98	FLT3-auto-inhibited	93	p38-alpha	100	PIK3CA (H1047Y)	100
TLK1	100	FGR	98	EPHA4	98	MARK2	93	p38-delta	100	PIK3CA (M1043I)	100
TLK2	100	PIK3CA (Q546K)	98	NEK1	98	MAST1	93	p38-gamma	100	PIK3CD	100
TNK1	100	ROS1	98	PAK4	98	PIP5K2C	93	PAK1	100	PIK3CG	100
TNK2	100	SLK	98	PCTK2	98	SLK	93	PAK2	100	PIKFYVE	100
TNNI3K	100	SNARK	98	VPS34	98	TSSK3	93	PAK4	100	PIM1	100
SYK	100	AKT1	98	PRKCD	99	DMPK2	93	NEK6	100	PIK3C2B	100
TEC	100	CDK4	98	WEE1	99	FGFR2	93	NEK7	100	PIK3CA	100
SRPK1	100	LIMK2	99	NEK4	99	ABL1 (H396P)-	93	NDR2	100	PDPK1	100
SRPK3	100	p38-delta	99	PAK7	99	ACVR1	93	NEK2	100	PFTAIR2	100
STK36	100	RPS6KA4 (Kin.Dom. 2-C-terminal)	99	PFTK1	99	ACVRL1	93	NEK5	100	PFTK1	100
SIK	100	AURKA	99	GRK1	99	LCK	94	MYLK4	100	PAK7	100
SLK	100	FES	99	JAK1(JH1 domain-catalytic)	99	SBK1	94	MYO3A	100	PCTK2	100
SRC	100	FLT3 (ITD)	99	MET (Y1235D)	99	TXK	94	MYO3B	100	PCTK3	100
RSK4 (Kin. Dom.2-C-terminal)	100	ZAK	100	EPHA1	99	FLT3 (ITD)	94	MUSK	100	PAK6	100
RIPK2	100	WEE2	100	ACVR1	99	EIF2AK1	95	MLK3	100	p38-gamma	100

ROS1	100	YANK2	100	CAMK2G	99	LRRK2	95	MRCKA	100	PAK1	100
RSK1 (Kin. Dom.1-N-terminal)	100	YANK3	100	CDC2L1	99	SRPK1	95	MST1R	100	PAK2	100
RSK1 (Kin. Dom.2-C-terminal)	100	YES	100	DRAK2	99	WNK1	95	MST3	100	PAK3	100
RIOK3	100	VRK2	100	YSK1	100	AMPK-alpha2	95	MLK1	100	p38-alpha	100
RIPK1	100	WEE1	100	ZAK	100	DMPK	95	MLK2	100	p38-delta	100
PIK3CA (M1043I)	100	STK33	100	RSK4 (Kin. Dom.2-C-terminal)	100	AURKB	96	MAP4K4	100	MTOR	100
PIM2	100	SYK	100	SIK	100	CDC2L1	96	MAP4K5	100	MUSK	100
PIM3	100	TESK1	100	SLK	100	CDK3	96	MAPKAPK2	100	MYLK4	100
PIP5K2B	100	TIE2	100	SRC	100	ERN1	96	MARK1	100	MYO3A	100
PLK4	100	TLK2	100	SYK	100	FGFR3	96	MARK2	100	MYO3B	100
PRKCQ	100	TNK1	100	TGFBR2	100	INSRR	96	MARK4	100	NDR2	100
PRKD2	100	TNK2	100	TLK2	100	KIT (V559D,V654A)	96	MAST1	100	NEK1	100
PRKR	100	TRKA	100	TRKC	100	MLK1	96	MELK	100	NEK2	100
PYK2	100	TRKC	100	TRPM6	100	PIK3CA (H1047L)	96	MERTK	100	NEK6	100
RAF1	100	TSSK1B	100	TSSK1B	100	TGFBR2	96	MET	100	NEK7	100
RET(M918T)	100	TXK	100	TXK	100	TRKA	96	MET (M1250T)	100	NEK9	100
RIOK1	100	TYRO3	100	YANK2	100	WNK4	96	MET (Y1235D)	100	OSR1	100

PHKG1	100	RSK1 (Kin. Dom.1-N-terminal)	100	RPS6KA5 (Kin. Dom.1-N-terminal)	100	CAMK2A	97	LRRK2 (G2019S)	100	MLK3	100
PIK3C2B	100	SIK	100	RPS6KA5 (Kin. Dom.2-C-terminal)	100	CAMK2B	97	LTK	100	MRCKB	100
PIK3C2G	100	SRPK1	100	RSK1 (Kin. Dom.1-N-terminal)	100	DLK	97	LYN	100	MST1	100
PIK3CA (H1047Y)	100	SRPK2	100	RSK3 (Kin. Dom.1-N-terminal)	100	KIT (D816V)	97	MAK	100	MST1R	100
PIK3CA (I800L)	100	SRPK3	100	RSK3 (Kin. Dom.2-C-terminal)	100	PIK3CA (Q546K)	97	MAP4K3	100	MST2	100
PAK7	100	RET (M918T)	100	PRKCQ	100	CAMK1G	98	KIT (V559D)	100	MAST1	100
PCTK2	100	RET(V804L)	100	PRKR	100	EGFR (L747-T751 del,Sins)	98	KIT (V559D, T670I)	100	MEK6	100
PCTK3	100	RIOK1	100	PRKX	100	KIT	98	KIT (V559D, V654A)	100	MELK	100
PDGFRB	100	RIOK3	100	PRP4	100	MST2	98	LATS1	100	MET	100
PDPK1	100	RIPK1	100	RET(V804M)	100	PIK3C2B	98	LCK	100	MET (M1250T)	100
PFTAIRES2	100	RIPK4	100	RIPK4	100	PIKFYVE	98	LIMK1	100	MLK1	100
PFTK1	100	RPS6KA5 (Kin. Dom.1-N-terminal)	100	ROS1	100	TLK2	98	LIMK2	100	MLK2	100
NEK9	100	PIM2	100	PIM2	100	ERK2	99	IRAK3	100	MAP4K3	100
p38-beta	100	PIP5K2B	100	PIP5K1A	100	MERTK	99	ITK	100	MAP4K4	100

PAK1	100	PIP5K2C	100	PIP5K2C	100	PAK2	99	JAK1(JH1 domain-catalytic)	100	MAP4K5	100
PAK2	100	PKMYT1	100	PKN1	100	PHKG1	99	KIT	100	MARK1	100
PAK4	100	PYK2	100	PLK4	100	PRP4	99	KIT (D816V)	100	MARK2	100
PAK6	100	QSK	100	PRKCH	100	ULK1	99	KIT (L576P)	100	MARK4	100
ABL2	100	ACVR1	100	ABL1 (Q252H)-(PO4)3-	100	ABL1 (F317I)-	100	AAK1	100	AAK1	100
ACVR1	100	ACVR2A	100	ACVR1B	100	ABL1 (F317L)-	100	ABL2	100	ABL1 (H396P)-	100
AKT1	100	ACVR2B	100	ADCK3	100	ABL2	100	ACVR2A	100	ABL1 (Q252H)-(PO4)3-	100
AKT2	100	AKT2	100	ADCK4	100	ACVR2A	100	ACVR2B	100	ABL1-	100
AKT3	100	AMPK-alpha2	100	AKT1	100	ACVR2B	100	ADCK4	100	ABL2	100
AMPK-alpha2	100	ANKK1	100	AKT2	100	AKT1	100	AKT1	100	ACVR1	100
ANKK1	100	ARK5	100	ASK1	100	BLK	100	AKT2	100	ACVR2A	100
AURKA	100	ASK2	100	BRSK1	100	BRSK2	100	AMPK-alpha2	100	ACVR2B	100
AURKC	100	AURKC	100	BRSK2	100	CAMK1	100	ARK5	100	AKT2	100
AXL	100	BLK	100	CDC2L2	100	CDC2L2	100	AURKC	100	ASK1	100
BLK	100	BTK	100	CDK11	100	CDK2	100	BIKE	100	AURKA	100
BMPR1A	100	CAMK2A	100	CDK2	100	CDK4	100	BMX	100	AURKC	100
BRSK2	100	CAMK2B	100	CDK4	100	CDK5	100	BRK	100	BMPR1A	100
CAMK1	100	CDC2L1	100	CDK4-cyclinD1	100	CDK8	100	BRSK2	100	BRSK1	100

CDC2L1	100	CDC2L2	100	CDK4-cyclinD3	100	CHEK2	100	CAMK1D	100	BRSK2	100
CDC2L2	100	CDK2	100	CDK9	100	CSF1R	100	CAMK1G	100	CAMK1G	100
CDK2	100	CDK5	100	CDKL2	100	DCAMKL2	100	CAMK2A	100	CAMK2A	100
CDK5	100	CDKL5	100	CHEK2	100	EGFR (L858R,T790M)	100	CAMK2B	100	CAMK2B	100
CHEK1	100	CHEK2	100	CSNK1D	100	EPHA7	100	CAMK2D	100	CAMK2D	100
CHEK2	100	CSF1R	100	CSNK1G3	100	EPHA8	100	CAMK4	100	CAMKK2	100
CSF1R	100	CSNK1A1L	100	DCAMKL2	100	EPHB1	100	CAMKK1	100	CDC2L1	100
CSK	100	CSNK1D	100	EGFR	100	ERBB2	100	CAMKK2	100	CDC2L2	100
DCAMKL2	100	CSNK1G2	100	EGFR (G719S)	100	ERBB4	100	CDC2L1	100	CDK2	100
DMPK2	100	CSNK1G3	100	EGFR (L858R)	100	ERK1	100	CDC2L2	100	CDK8	100
EGFR	100	DAPK2	100	EGFR (S752-I759del)	100	ERK5	100	CDK2	100	CDK9	100
EGFR (E746-A750del)	100	DCAMKL2	100	EPHA3	100	FAK	100	CDK5	100	CHEK1	100
EGFR (G719C)	100	DRAK1	100	EPHA5	100	FGFR1	100	CDK8	100	CHEK2	100
EGFR (G719S)	100	EGFR (G719C)	100	EPHA6	100	FLT3 (D835H)	100	CDK9	100	CLK1	100
EGFR (L747-E749del, A750P)	100	EGFR (L747-T751 del,Sins)	100	EPHB3	100	FLT3 (N841I)	100	CDKL2	100	CLK4	100
EGFR (L747-S752 del, P753S)	100	EPHA1	100	EPHB4	100	IGF1R	100	CHEK1	100	CSF1R	100

EGFR (L858R)	100	EPHA7	100	ERBB2	100	IKK-beta	100	CHEK2	100	CSK	100
EPHA3	100	EPHA8	100	ERK2	100	IRAK4	100	CIT	100	CSNK1A1L	100
EPHA6	100	ERK2	100	ERK4	100	ITK	100	CLK1	100	CSNK1D	100
EPHA7	100	ERK5	100	ERK5	100	KIT (D816H)	100	CLK2	100	CSNK1G2	100
EPHA8	100	FAK	100	FAK	100	KIT (L576P)	100	CLK3	100	CSNK1G3	100
EPHB1	100	FGFR1	100	FER	100	KIT (V559D)	100	CLK4	100	CSNK2A2	100
EPHB2	100	FGFR3 (G697C)	100	FES	100	KIT (V559D, T670I)	100	CSF1R	100	CTK	100
ERK1	100	FLT1	100	FGFR1	100	LATS1	100	CSNK1A1L	100	DAPK1	100
ERK2	100	FLT3 (D835H)	100	FGFR3	100	LIMK1	100	CSNK1D	100	DCAMKL2	100
ERK4	100	FLT3 (R834Q)	100	FGFR3 (G697C)	100	LRRK2 (G2019S)	100	CSNK1E	100	DDR1	100
ERK5	100	FLT4	100	GAK	100	MAP3K4	100	CSNK1G1	100	DMPK2	100
ERN1	100	GSK3A	100	GCN2 (Kin. Dom.2,S808 G)	100	MAP4K4	100	CSNK1G2	100	DRAK1	100
FAK	100	HIPK4	100	GSK3A	100	MAP4K5	100	CSNK1G3	100	DYRK2	100
FER	100	HUNK	100	HIPK2	100	MARK3	100	CSNK2A2	100	EGFR	100
FES	100	ICK	100	HPK1	100	MEK3	100	DAPK1	100	EGFR (L747-E749del, A750P)	100
FGFR1	100	IKK-epsilon	100	HUNK	100	MELK	100	DAPK2	100	EGFR (L858R)	100
FGFR4	100	INSRR	100	ICK	100	MET	100	DAPK3	100	EGFR (S752-I759del)	100
FLT1	100	IRAK4	100	IKK-epsilon	100	MET (M1250T)	100	DCAMKL2	100	EPHA1	100

FLT3 (D835H)	100	JAK1(JH1 domain-catalytic)	100	INSRR	100	MRCKA	100	DCAMKL3	100	EPHA3	100
FLT3 (ITD)	100	KIT	100	JAK1(JH2 domain-ps.kinase)	100	MRCKB	100	DDR1	100	EPHA4	100
FRK	100	KIT (D816H)	100	KIT	100	MST1R	100	DMPK	100	EPHA6	100
FYN	100	KIT (L576P)	100	KIT (D816V)	100	MYLK4	100	DMPK2	100	EPHA7	100
GAK	100	KIT (V559D)	100	KIT (L576P)	100	NDR2	100	DRAK1	100	EPHA8	100
GRK4	100	KIT (V559D, T670I)	100	KIT (V559D)	100	NEK11	100	DRAK2	100	EPHB1	100
HIPK4	100	LATS1	100	LCK	100	NEK2	100	EGFR	100	EPHB2	100
IGF1R	100	LCK	100	LIMK1	100	NEK5	100	EGFR (L747-E749del, A750P)	100	EPHB3	100
IRAK3	100	LIMK1	100	LKB1	100	NEK6	100	EGFR (L747-T751del,Sin s)	100	ERK1	100
ITK	100	MAK	100	LRRK2 (G2019S)	100	NEK7	100	EGFR (L858R)	100	ERK4	100
JAK1(JH1 domain-catalytic)	100	MAP3K4	100	LZK	100	NEK9	100	EGFR (L861Q)	100	ERK5	100
KIT	100	MAP4K4	100	MAK	100	OSR1	100	EPHA4	100	ERK8	100
KIT (L576P)	100	MARK2	100	MAP4K3	100	PAK4	100	EPHA6	100	ERN1	100
KIT (V559D)	100	MARK3	100	MARK1	100	PAK6	100	EPHA7	100	FAK	100
KIT (V559D,T670I)	100	MELK	100	MARK4	100	PAK7	100	EPHA8	100	FER	100

KIT (V559D,V654A)	100	MERTK	100	MAST1	100	PCTK3	100	EPHB1	100	FGFR3	100
LATS1	100	MET	100	MEK6	100	PDPK1	100	EPHB2	100	FGFR3 (G697C)	100
LCK	100	MET (M1250T)	100	MELK	100	PFTAIR2	100	EPHB3	100	FGFR4	100
LIMK1	100	MET (Y1235D)	100	MERTK	100	PFTK1	100	ERBB2	100	FLT1	100
LIMK2	100	MLK3	100	MET (M1250T)	100	PIK3CA (E542K)	100	ERBB4	100	FLT3 (D835Y)	100
LYN	100	MST1R	100	MLK2	100	PIK3CA (H1047Y)	100	ERK1	100	FLT3 (ITD)	100
MAK	100	MST2	100	MLK3	100	PIK3CA (I800L)	100	ERK2	100	FLT3 (K663Q)	100
MAP3K4	100	MST3	100	MST1R	100	PIK3CA (M1043I)	100	ERK3	100	FLT3 (N841I)	100
MAP4K3	100	MST4	100	MST2	100	PIM2	100	ERK4	100	GAK	100
MAP4K4	100	MTOR	100	MST3	100	PIP5K1A	100	ERK5	100	GRK4	100
MAP4K5	100	MUSK	100	MTOR	100	PIP5K2B	100	ERK8	100	GSK3A	100
MARK1	100	MYLK	100	MUSK	100	PLK4	100	FAK	100	HIPK4	100
MARK2	100	MYLK4	100	MYLK2	100	PRKR	100	FER	100	HUNK	100
MARK4	100	NDR1	100	MYLK4	100	PYK2	100	FGFR1	100	IGF1R	100
MELK	100	NDR2	100	MYO3A	100	RIPK1	100	FGFR3	100	INSR	100
MERTK	100	NEK11	100	NDR2	100	RPS6KA5 (Kin. Dom.1-N- terminal)	100	FGFR3 (G697C)	100	INSRR	100
MET	100	NEK4	100	NEK2	100	RSK1 (Kin. Dom.1-N- terminal)	100	FGFR4	100	ITK	100

MET (M1250T)	100	NEK5	100	NEK6	100	SIK	100	FLT1	100	JAK1(JH1 domain-catalytic)	100
MLK1	100	NEK6	100	p38-alpha	100	SRPK2	100	FLT3 (K663Q)	100	KIT	100
MLK3	100	OSR1	100	p38-beta	100	STK33	100	FLT3 (N841I)	100	KIT (L576P)	100
MRCKA	100	PAK4	100	p38-delta	100	TEC	100	FRK	100	KIT (V559D)	100
MST2	100	PAK6	100	PAK2	100	TLK1	100	GAK	100	KIT (V559D,T670I)	100
MTOR	100	PCTK1	100	PAK6	100	TNK2	100	GCN2 (Kin. Dom.2,S808G)	100	LATS1	100
MYLK2	100	PCTK2	100	PDPK1	100	TRKC	100	GRK4	100	LCK	100
MYLK4	100	PCTK3	100	PHKG1	100	TYRO3	100	GSK3A	100	LIMK1	100
NDR2	100	PDGFRB	100	PHKG2	100	ULK3	100	GSK3B	100	LIMK2	100
NEK2	100	PFTK1	100	PIK3C2B	100	WEE1	100	HCK	100	LTK	100
NEK5	100	PIK3C2B	100	PIK3CA (H1047Y)	100	WEE2	100	HIPK4	100	LYN	100
NEK6	100	PIK3CA (H1047Y)	100	PIK3CG	100	YANK2	100	HUNK	100	MAK	100
NEK7	100	PIM1	100	PIK4CB	100	YES	100	IGF1R	100	MAP3K4	100

Appendix 2 Crystal structures used in X-Docking Studies

Table B List of DiscoverX targets with corresponding physiologically relevant PDB codes used in XDocking experiments

KINASE HIT FROM DISCOVERX	PDB CODE
PI3Ka	4FA6
ROCK1	3TV7
ROCK1	3V8S
GSK3	3L1S
VEGFR2	3VHE
JNK1	4AWI
p38	5WJJ
AurA	5DN3
MELK	5K00
FLT3	4XUF
PKN2	4CRS
PKN1	4OTH
CHEK2	2CN5
RSK1(Kin.Dom.1-N-terminal)	2Z7Q
LIMK1	3S95
CDK2	4EK4
FAK	4I4E
PIK3CA(H1047Y)	4JPS
PAK6	4KS7
MET(M1250T)	4MXC
PIM2	4X7Q
MELK	5K00
ERK5/MAPK7	5O7I
KIT(L576P)	6GQJ